VNIVERSITAT DE VALÈNCIA

THE MEDIAL AMYGDALA AS A KEY NEURAL CENTRE IN MATERNAL AGGRESSION: GENETIC, NEURAL AND BEHAVIOURAL ANALYSES

2019

THE MEDIAL AMYGDALA AS A KEY NEURAL CENTRE IN MATERNAL AGGRESSION:

GENETIC, NEURAL AND BEHAVIOURAL ANALYSES

DOCTORAL THESIS

María Abellán Álvaro

VNIVERSITAT DE VALÈNCIA

Doctoral programme in Neurosciences

Supervisors

Enrique Lanuza Navarro Carmen Agustín Pavón

October 2019

THE MEDIAL AMYGDALA AS A KEY NEURAL CENTRE IN MATERNAL AGGRESSION:

GENETIC, NEURAL AND BEHAVIOURAL ANALYSIS

María Abellán Álvaro

Departamento de Biología Celular, Biología Funcional y Antropología Física

Tesis doctoral en Neurociencias

Dirigida por:

Dr. Enrique Lanuza Navarro

Dra. Carmen Agustín Pavón

VNIVERSITAT DE VALÈNCIA Facultat de Ciències Biològiques

Enrique Lanuza Navarro, Profesor Titular, y Carmen Agustín Pavón, Profesora Ayudante Doctora, ambos del Departamento de Biología Celular, Biología Funcional y Antropología Física de la Universidad de Valencia.

CERTIFICAN

que Dña. **María Abellán Álvaro**, Máster en Neurociencias por la Universitat Autònoma de Barcelona, ha realizado bajo su dirección el trabajo titulado ***"The medial amygdala as a key neural centre in maternal aggression: genetic, neural and behavioural analyses"*** para la obtención del grado de Doctora en Neurociencias.

Para que conste, en cumplimiento de la legislación, firmamos el presente certificado en Burjassot, a 30 de octubre de 2019.

Dr. Enrique Lanuza Navarro

Dra. Carmen Agustín Pavón

VNIVERSITAT DE VALÈNCIA Facultat de Ciències Biològiques

Enrique Lanuza Navarro, Associate Professor, and Carmen Agustín Pavón, Assistant Professor Doctor, both of the Department of Cell Biology, Functional Biology and Physical Anthropology of the University of Valencia.

HEREBY CERTIFY

that Ms. María Abellán Álvaro, MSc in Neurosciences at the Autonomous University of Barcelona, has conducted under their direction the work entitled ***"The medial amygdala as a key neural centre in maternal aggression: genetic, neural and behavioural analysis"*** to obtain the degree of Doctor in Neurosciences.

For the record, in compliance with the legislation, we sign this certificate in Burjassot, on October the 30th, 2019.

Dr. Enrique Lanuza Navarro

Dra. Carmen Agustín Pavón

The author of this thesis was hired with the program "Ayudas para la promoción de empleo joven e implantación de la garantía juvenil en I+D+i" (PEJ-2014-A-63220).

This work has been funded by MINECO-FEDER (BFU2016-77691- C2-1-P and C2-2-P), Generalitat Valenciana (PROMETEO2016/076) and Universitat Jaume I (UJI-B2016- 45).

"En cualquier caso, creo que la fusión de la actividad mental, sobre todo la imaginativa, con las experiencias directas constituyen la base para poder no solo acercarnos a la comprensión de la realidad natural, sino también para poder describirla y, por tanto, hacer a todos partícipes de nuestra vivencia".

Félix Rodríguez de la Fuente

"Cerrar los ojos a la naturaleza solo nos hace ciegos en un paraíso de tontos"

Jacques Y. Cousteau

"Believe nothing you hear, and only one half that you see."

Edgar Allan Poe. The System of Doctor Tarr and Professor Fether

AGRADECIMIENTOS

Bueno, ya estamos en este punto, escribiendo el último apartado de mi tesis doctoral. Llevo varios días postergando el escribir estas hojas, no sé si por miedo a poner un punto y final a este libro y a esta etapa de mi vida o porque realmente no sé cómo agradecérselo a todos los que han estado presentes en este camino. La verdad, es que nunca me han gustado las enumeraciones que se hacen en los agradecimientos, pero hace unos días me dieron la idea de no dar nombres y me parece una buena opción para no dejarme a nadie, así que lo dejo a vuestra imaginación y que cada uno se sienta identificado con la parte que más le guste o menos le disguste. Sin más preámbulo, allá vamos…

Primero que nada, tengo que dar las gracias a mis directores y jefes de los cuales he aprendido lo que realmente es la vocación por la ciencia. Ellos me han me han enseñado muchas "cosas científicas", pero con lo que realmente me quedo es con que me han permitido conocer lo que es disfrutar dedicándote a aquello que realmente amas, de verdad, espero que podáis seguir investigando en todo aquello que os motiva sin morir en el intento. Sé que os he hecho envejecer de más durante estos cuatro años, gracias por vuestra paciencia.

Obviamente no pueden faltar todos los compañeros y amigos que he hecho en el laboratorio, sois muchos, pero realmente me habéis apoyado y acompañado durante este recorrido. Pero lo que más agradezco son los momentos que me habéis dado fuera del laboratorio, las cenas en vuestra casa jugando a juegos, todo lo que me has enseñado ilustración, las clases de portugués mezclado con español que me has dado en el coche de vuelta de Castellón y la pasión por viajar y conocer Chile. No me olvido de ti, ya sabes, la que más me ha aguantado todos estos años, la que me ha enseñado a madurar con Ojete Calor, a disfrutar de los grandes placeres de no hacer nada y a valorar ante todo la tranquilidad. Porque tú tienes el poder de la risa y eso es lo que más une a las personas, realmente espero que me sigas acompañando en el resto de etapas de mi vida.

Ya sé, ya sé cómo es que no pongo a mis amigos pretesis… paciencia. Realmente me alegro mucho de que seáis tantos y de no saber cómo resumiros. Bueno, vayamos por antigüedad, primero a vosotros que os conozco desde que iba al colegio, qué sabéis más de mí que yo misma, no sé cómo agradeceros todos estos años. Sé que ahora estás en EEUU y que no vas a poder ver mi tesis, pero como quien tu ya sabes no se pierde una va a ser como si os tuviera a los dos aquí. Después del colegio llegó la Universidad y me dio la oportunidad de conocer a

gente que me abrió los ojos y que compartía conmigo muchas de mis aficiones. Te quiero dar las gracias por estar conmigo en los inicios de la tesis y por los cafés que nos echábamos en los descansos de los protocolos, siempre has estado ahí en mis altibajos y has compartido conmigo grandes momentos, espero que realmente te vaya genial con este nuevo camino que has emprendido. También estáis vosotras dos, con las que he compartido grandes momentos durante la carrera. Luego se nos unió el bombero al cual tengo que agradecer todo lo que me ha enseñado de fotografía y de observar animales. Vosotros me habéis regalado los mejores paseos de perros y descansos de la tesis junto con Falco, Gea y Ticky. Por otro lado, aunque te fuiste a Bruselas hemos compartido grandes momentos y gracias a ti hice el mejor viaje de mi vida. Y por último, aunque no menos importantes, aquellos con los que pasé mi año en Barcelona, que me hicieron sentirme realmente a gusto aunque estuviera fuera de mi casa y con los que me sigo juntando sin que pasen los años.

Mi familia, a ellos no tengo que decirles nada porque ya saben de sobra todo lo que han aguantado. A mis padres les tengo que dar las gracias porque si no fueran como son nunca hubiera estudiado Biología, gracias por inculcarme el amor por el campo y la ciencia y a hacer de esta carrera mi vocación. No he sido siempre una persona fácil, pero nunca habéis dejado de apoyarme y de acompañarme en cada paso que daba. Luego estás tu hermanito que siempre le has dado humor a mi vida y con el que no puedo imaginar ningún momento de mi vida, eres la persona con la cual cuento todos los días desde que me levanto hasta que me acuesto. También quiero acordarme de mis tios y primos que nunca han dejado de apoyarme. Por otro lado, aunque ya no están aquí quiero darles las gracias a mis abuelos que me regalaron una infancia perfecta y me ayudaron a ser la persona que soy hoy, no sabéis cuanto os hecho de menos. Por último, como dijo Konrad Lorenz "el vínculo con un perro es el más duradero de esta tierra" y por eso quiero dedicarles también parte de esta tesis a Oso y a Llauro que aunque no estuvo en el final me hizo realmente feliz durante mi adolescencia.

Y ahora quedas tú, mi sorpresa inesperada que me ha regalado grandes momentos durante esta tesis. Apareciste sin buscarte y ahora vas a quedarte una larga temporada, gracias por enseñarme a disfrutar de las pequeñas cosas y a hacer posible todo lo que siempre he querido ser y hacer. No sé bien como darte las gracias, pero sé que Runa tu y yo vamos a pasárnoslo realmente bien. En fin, para concluir me quedo con la frase de John M. Cleese, alguien que siempre me ha hecho reir: "No tienes que ser el Dalai Lama para decirle a la gente que la vida es el cambio." Así que a por la siguiente etapa.

CONTENTS

ABBREVIATIONS

GENES/PROTEINS[1]

Acox1	Acyl-Coenzyme A oxidase 1, palmitoyl
ACTH	Adrenocorticotropic hormone
Actinβ/ ACTB	Actin Beta
Adcyap1	Adenylate Cyclase Activating Polypeptide 1
Adcyap1	Adenylate cyclase activating polypeptide 1
Adra2b	Alpha 2b adrenergic receptor
Amhr2	Anti-Mullerian hormone type 2 receptor
Atf3	Activating transcription factor 3
Avp/AVP	Arginine vasopressin
Avpr1a	Arginine vasopressin receptor 1A
cFOS	Proto-oncogene c-Fos
Cga	Alpha subunit of glycoprotein hormones
Chat	Choline acetyltransferase
Chrm2	Cholinergic receptor, muscarinic 2, cardiac
Chrna2	Cholinergic receptor, nicotinic, alpha polypeptide 2 (neuronal)
Chrna6	Cholinergic receptor, nicotinic, alpha polypeptide 6
Chrnb3	Cholinergic receptor, nicotinic, beta polypeptide 3
Cis	Cytokine inducible SH2-containing protein
CRH	Corticotropin-releasing hormone
Dlk1	Delta like non-canonical Notch ligand 1
EGR	Early growth response family
Egr1	Early growth response 1
Egr2	Early growth response 2
Egr3	Early growth response 3
Egr4	Early growth response 4
ERK	Extracellular signal-regulated kinase family
ERK/MAPK	Mitogen-activated protein (MAP) kinase cascade
ESR1	Oestrogen receptor alpha
Fos/FOS	FBJ osteosarcoma oncogene
Fosb	FBJ osteosarcoma oncogene B
FSH	Follicle-stimulating hormone
Fshb	Follicle stimulating hormone beta
Gal/GAL	Galanin
Gdpd2	Glycerophosphodiester phosphodiesterase domain containing 2
Gdpd2	Glycerophosphodiester phosphodiesterase domain containing 2
Gh/GH	Growth hormone or somatotropin
Ghr	Growth hormone receptor
GHRH	Growth hormone–releasing hormone
Ghrhr	Growth hormone releasing hormone receptor
GnRH	Gonadotropin-releasing hormone
Gnrh1	Gonadotropin releasing hormone 1
Gnrhr	Gonadotropin-releasing hormone receptor
Inhbc	Inhibin beta-C
Inhbe	Inhibin beta-E
Isl1	ISL1 transcription factor, LIM/homeodomain
Itih3	Inter-alpha trypsin inhibitor, heavy chain 3
JAK/STAT	The Janus kinase/signal transducers and activators of transcription
Kdm1a	Lysine (K)-specific demethylase 1A
Lgr4	leucine-rich repeat-containing G protein-coupled receptor 4
LH	Luteinizing hormone
Lhx	LIM-homeobox family
LMW	Low-molecular-weight proteins
Msmb	Beta-microseminoprotein
MUP	Major urinary proteins
Ngfr	Nerve growth factor receptor (TNFR superfamily, member 16)
Nkx2.1	NK2 homeobox 1
Nova1	Neuro-oncological ventral antigen 1
Nr1i3	Nuclear receptor subfamily 1, group I, member 3
Nrn1	Neuritin 1
Oxt/OXT	Oxytocin
Pcyt1b	Phosphate cytidylyltransferase 1, choline, beta isoform
Pitx1	Paired-like homeodomain transcription factor 1
PL	Placental lactogens
Pmch	Pro-melanin-concentrating hormone
Pomc/POMC	Proopiomelanocortin-alpha

Pou1f1	POU domain, class 1, transcription factor 1
Prl/PRL	Prolactin
Prl2c2	Prolactin family 2, subfamily c, member 2
Prlr/PRLR	Prolactin receptor
Prop1	*Paired like homeodomain factor 1*
PSA-NCAM	Polysialylated form of the neural cell adhesion molecule
pSTAT5	Phosphorylation of STAT5
Ptgs2	Prostaglandin D2synthase
Rln3	Relaxin 3
Rxfp2	Relaxin/insulin-like family peptide receptor 2
Siglece	Sialic acid binding Ig-like lectin
SOCS	Suppressor of cytokine signaling family
Socs2	Suppressor of cytokine signaling 2
STAT	Signal Transducer and Activator of Transcription family
Stat5a	Signal transducer and activator of transcription 5A
Stat5b	signal transducer and activator of transcription 5B
Stat5b	Signal transducer and activator of transcription 5b
Tbx19	T-box 19
Th/TH	Tyrosine hydroxylase
Tpgs1	tubulin polyglutamylase complex subunit 1
TRH	Thyrotropin-releasing hormone
TRPC2	Transient receptor potential cation channel, subfamily C, member 2
Trpv1/TRPV1	Transient receptor potential cation channel, subfamily V, member 1
TSH	Thyroid-stimulating hormone
Vmn2r-ps159	Vomeronasal 2, receptor, pseudogene 159
α-MSH	Alpha -melanocyte stimulating hormones
β-MSH	Beta -melanocyte stimulating hormones
γ-MSH	Gamma-melanocyte stimulating hormones

[1]Nomenclature was based on the International Committee for Standardized Genetic Nomenclature for Mice

ANATOMICAL STRUCTURES

AAD	Dorsal part of the anterior amygdaloid area
AAV	Ventral part of the anterior amygdaloid area
AC	Anterior commissural nucleus
AC/ADP	Region of antero-dorsal preoptic nucleus and anterior commissural nucleus
Acb	Nucleus accumbens
AcbC	Core of the nucleus accumbens
ACo	Anterior cortical amygdaloid nucleus
AH	Anterior hypothalamus
AHi	Amygdalohippocampal area
AL	Nucleus of the ansa lenticularis
AOB	Accessory olfactory bulb
AOM	Anterior olfactory nucleus, medial part
AOP	Anterior olfactory nucleus, posterior part
APG	Anterior pituitary gland
Arc	Arcuate nucleus of the hypothalamus
AVPe	Anteroventral periventricular nucleus
BAOT	Bed nucleus of the accessory olfactory tract
BL	Basolateral amygdaloid nucleus
BLA	Basolateral amygdaloid nucleus, anterior
BLP	Basolateral amygdaloid nucleus, posterior
BMA	Anterior part of the basomedial amygdaloid nucleus
BMP	Basomedial amygdaloid nucleus, posterior part
BST	Bed nucleus of the stria terminalis
BSTIA	Intraamygdaloid division of the bed nucleus of the stria terminalis
BSTLP	Bed nucleus of the stria terminalis, lateral division, posterior part
BSTLV	Bed nucleus of the stria terminalis, lateral division, ventral part
BSTMA	Bed nucleus of the stria terminalis, medial division, anterior part
BSTMPI	Bed nucleus of the stria terminalis, medial division, posterointermediate part
BSTMPL	Bed nucleus of the stria terminalis, medial division, posterolateral part
BSTMPM	Bed nucleus of the stria terminalis, medial division, posteromedial part
BSTMV	Bed nucleus of the stria terminalis, medial division, ventral part
Ce	Central amygdala
CeC	Central amygdaloid nucleus, capsular part
CeL	Central amygdaloid nucleus, lateral division
CeM	Central amygdaloid nucleus, medial division
Cg	Cingulate cortex
CM	Central medial thalamic nucleus
CPu	*Caudatus putamen*
CxA	Cortex-amygdala transition zone
DEn	Dorsal endopiriform nucleus
DM	Dorsomedial hypothalamic nucleus
DP	Dorsal peduncular cortex
DpMe	Deep mesencephalic nucleus
DTT/VTT	Dorsal/Ventral *tenia tecta*
ec	External capsule
HDB	Nucleus of the horizontal limb of the diagonal band
HPA	Hypothalamic-pituitary-adrenal axis
ic	Internal capsule
IL	Infralimbic cortex
IMD	Intermediodorsal thalamic nucleus
IPAC	Interstitial nucleus of the posterior limb of the anterior commissure
LA	Lateroanterior hypothalamic nucleus
LC	*Locus coeruleus*
LGP	Lateral globus pallidus
LH	Lateral hypothalamic area
LHb	Lateral habenular nucleus
LM	Lateral mammillary nucleus
LOT	Nucleus of the lateral olfactory tract

LPB	Lateral parabrachial nucleus
LPO	Lateral preoptic area
LS	Lateral septum
LSI	Lateral septal nucleus, intermediate part
LSV	Lateral septal nucleus, ventral part
MCLH	Magnocellular nucleus of the lateral hypothalamus
MCPO	Magnocellular preoptic nucleus
MD	Mediodorsal thalamic nucleus
Me	Medial amygdala
ME	Median eminence
MeA	Anterior part of medial amygdaloid nucleus
MePD	Antero-dorsal part of medial amygdaloid nucleus
MePV	Antero-ventral part of medial amygdaloid nucleus
MGP	Medial globus pallidus
MHb	Medial habenular nucleus
MOB	Main olfactory bulb
MOE	Main olfactory epithelium
MPA	Medial preoptic area
MPB	Medial parabrachial nucleus
MPO	Medial preoptic nucleus
MPO/A	Medial preoptic region
MS	Medial septal nucleus
ns	Nigrostriatal bundle
opt	Optic tract
Pa	Paraventricular hypothalamic nucleus
PAG	Periaqueductal gray
Pe	Periventricular hypothalamic nucleus
PH	Posterior hypothalamic area
Pir	Piriform cortex
PLCo	Posterolateral cortical amygdaloid nucleus
PM	Premammillary nucleus
PMCo	Posteromedial cortical amygdaloid nucleus
PMD	Premammillary nucleus, dorsal part
PMV	Premammillary nucleus, ventral part
PP/PIL/PoT	Peripeduncular nucleus/ posterior intralaminar thalamic nucleus/ posterior thalamic nuclear group, triangular part
PPG	Posterior pituitary gland;
Prl	Prelimbic cortex
PV	Paraventricular thalamic nucleus
PVA/PVP	Paraventricular thalamic nucleus, anterior/posterior part
SCh	Suprachiasmatic nucleus
SI	Substantia innominata
SNC	Substantia nigra, compact part
SNR	Substantia nigra, reticular part
SO	Supraoptic nucleus
SuM	Supramammillary nucleus
TC	*Tuber cinereum* area
Tu	Olfactory tubercle
VDB	Nucleus of the vertical limb of the diagonal band
VEn	Ventral endopiriform nucleus
VLPO	Ventrolateral preoptic nucleus
VMH	Ventromedial hypothalamic nucleus
VMHdm	Ventromedial hypothalamic nucleus, dorsomedial area
VMHvl	Ventromedial hypothalamic nucleus, ventrolateral area
VNO	Vomeronasal organ
VP	Ventral pallidum
VTA	Ventral tegmental area
VTM	Ventral tuberomammillary nucleus
ZI	Zona *incerta*

OTHERS

AAV5	Adeno-associated virus, serotype 5
ABC	ammonium bicarbonate
CNO	Clozapine-N-oxide
DREADD	Designer receptors exclusively activated by designer drugs
FA	Formic acid
FC	Fold Change
FDR	False discovery rate
GO	Gene ontology
IQR	Interquartile range
-ir	Immunoreactive
NGS	Normal goat serum
PBS	Phosphate-buffered saline
PPD	Postpartum day
qPCR	Quantitative PCR
RIN	RNA integrity number
RNA-seq	RNA-sequencing
RQ	Relative quantification
SBN	Social brain network
SDS	Sodium dodecyl sulphate
TBS	Tris-buffered saline

ABSTRACT

In rodents, as macrosmatic animals, chemosensory processing plays an instrumental role in guiding the expression of social, sexual and maternal behaviours. Social odours and pheromones are processed by the main and the accessory olfactory systems, which information converge mainly in the medial amygdala (Me). The Me, in turn, plays a central role in the vomeronasal–sensorimotor integration that leads to specific behavioural responses such as the above-mentioned social and maternal behaviours.

Maternal behaviour comprises physiological and behavioural adaptations that help the dams to successfully raise their offspring. This behaviour is expressed in a wide range of vertebrate species and can be parsed in two main components, namely pup-directed (i.e. maternal care), and non-pup-directed behaviour as maternal aggression. Previous studies have shown that pup-sensitized virgin females, which display all pup-directed behaviours towards pups, do not show maternal aggression towards male intruders.

The main goal of this thesis is to investigate the role of Me in the control of maternal aggression and the possible adaptations that this nucleus suffers during lactation, such as changes in gene and protein expression.

The results of the experiments inducing a chemogenetic inhibition of Me showed that this nucleus is a key centre in the neural control of maternal aggression. One of the main changes in the Me of dams revealed by our RNA-seq study was an increased PRL expression. Thus, we characterized the prolactinergic (PRLergic) circuits in female brain in different physiological states. The same pattern of PRLergic immunoreactivity was present in pup-sensitized, pup-naïve virgins and lactating female mice. However, we found quantitative differences between dams and the other two groups in the supraoptic nucleus and between dams and virgin naïve females in the suprachiasmatic and the medial preoptic nucleus.

Our findings shown a widespread PRL innervation in the female mouse brain, suggesting the existence of important PRLergic pathways. In addition, these pathways suffer some adaptations during lactation. This supports a role for PRL as a neuroactive peptide, in addition to its well-documented endocrine role.

In conclusion, hormonal changes linked to pregnancy, parturition and lactation induce modifications of the socio-sexual brain network, including effects on the transcriptomic profile of the Me and the central PRLergic systems. These modifications might contribute to the expression of behaviours specifically linked to motherhood, such as maternal aggression.

GENERAL INTRODUCTION

Across the animal kingdom there are many species in which parents enhance their offspring's fitness by providing various forms of care. Among vertebrate species, almost all species of birds and mammals have parental care, which is complex and necessary for offspring survival. Mammals exhibit predominantly maternal care (about 90% of families), scarce cases of biparental care (10%) and no cases of exclusive paternal care (Gross 2005), likely because of the exclusive role of the mother in lactation. In birds, on the other hand, there are many species that present biparental care (about 90%), whereas maternal care is uncommon (8%), and paternal care is very rare (2%) (Gross 2005). In other taxa, such as fish, reptiles, amphibians, or invertebrates, parental care occurs more sporadically, is more variable, is often less complex, and it is not always expressed. In fishes, the majority of species provide no parental care at all for their young (Gross and Sargent 1985), but of those that do (about 20% of families), the majority exhibit paternal care (about 50%), followed by maternal care (30%), and biparental care (about 20%). Thus, while fishes have evolved all forms of parental care, they are especially noteworthy for their male investment (Insel and Numan 2003; Gross 2005; Kölliker et al. 2017).

The diversity in the forms of parental care is vast, ranging from the choice of oviposition sites to providing food, shelter and protection to the young. These different forms of parental care are adaptations to one or more ecological challenges and are part of the reproductive strategies of the species. The environment and the social interactions of a species determine the benefits and costs associated with parental care and, hence, the likelihood that care evolves and whether it is maintained. Evolutionary conflicts between parents and offspring, among siblings, and between parents (male and female) underlie the evolutionary maintenance of parental care (Dulac et al. 2014; Kölliker et al. 2017). These conflicts generate novel selection pressures on parental care: how much is provided, who provides it, and how it is allocated among offspring. Thus, evolution of parental care is a coevolutionary process, because parental and offspring fitness are determined not only by their respective phenotypic and genotypic characteristics, but also by the interactions between them. As a result, evolutionary trajectories of parental care traits can be diverse and complex and play an important role in the evolution of other forms of social behaviour such as eusociality (Kölliker et al. 2017) or alloparental care. Alloparental behaviour is a caregiving behaviour directed toward a conspecific infant by an individual who is not related genetically with the young, and it is performed by some species of mammals, including humans (Fleming and Rosenblatt 1974; Riedman 1982). In these cases, clearly, processes not related to the physiological events occurring during pregnancy and lactation contribute to eliciting the parental response.

COMPONENTS OF MATERNAL BEHAVIOUR

Maternal behaviour can be defined as any behaviour that the female performs to increase survival likelihood of the young (see Jay S Rosenblatt, Mayer, & Siegel, 1985). In the case of eutherian mammals, maternal behaviours are highly influenced by the degree of neonatal development after birth. Thus, it is possible to differentiate two groups of species: altricial and precocial mammals. The precocial species produce relatively independent, well-developed neonates (hystricomorph rodents, bovids, ungulates, etc), whose infants are mobile virtually from the moment of birth, whereas altricial mammals are species in which their offspring is poorly developed and are unable to move out of the nest for several days or weeks (i.e. rabbits, cricetid rodents, primates, canids, etc.) (Derrickson 1992).

Within altricial mammals, such as rats, mice, and also humans, maternal behaviours can be roughly divided into pup-directed and non-pup-directed behaviours (Insel and Numan 2003; Gammie 2005) (FIGURE 1). Pup-directed behaviours include the nursing of the pups, crouching over them to provide warmth, retrieving and grouping them into a nest and grooming and licking them, especially their anogenital region to facilitate micturition and defecation reflexes. A recent characterization of pup-directed responses by Numan & Stolzenberg (2008) has differentiated proactive maternal responses, which include pup-seeking and retrieval behaviour, and reflexive maternal responses, including those tied to proximal pup stimulation, such as nursing/crouching. Regarding non-pup directed maternal behaviours, they include the building of a nest, and the defence of the nest site against intruders (FIGURE 1).

It is important to remark that maternal behaviour has an important impact in the offspring and it will determine the future phenotype of the pups. Previous research has demonstrated that postnatal interactions of mother–offspring can persistently alter the hypothalamus–pituitary–adrenal axis (HPA) stress reactivity (Meaney 2001; Macrí et al. 2004; Coutellier et al. 2008; Vaiserman 2015), behavioural fearfulness (Denenberg et al. 1962; Meaney 2001; Coutellier et al. 2008) and social behaviour (Fleming et al. 2002; Mintz et al. 2005; Branchi et al. 2006; Coutellier et al. 2008). The impact on these developmental traits of the received maternal care is commonly inherited through epigenetic mechanisms (Weaver et al. 2004; Mychasiuk et al. 2012).

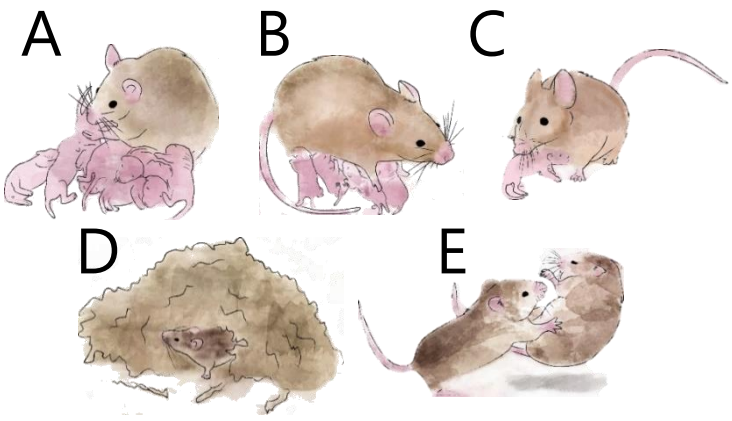

Figure 1: Maternal behaviour in rodents: Maternal behaviours can be grouped in pup-directed (upper row, A-C) or non-pup-directed (lower row, D, E). Pup-directed behaviours include licking/grooming them (A), nursing the pups (B) and looking for the pups and retrieving them into the nest (C). Maternal behaviours not directed to pups include the building of a nest area close before birth (D) and fierce territorial defence of the nest site against intruders (maternal aggression, E).

MATERNAL AGGRESSION AS A COMPONENT OF MATERNAL BEHAVIOUR

As explained before, altricial mammals give birth to very vulnerable pups, with an important lack of locomotor and sensory skills, and totally dependent on their progenitors for protection and survival. In socially living species, the interaction with conspecifics it is also a high risk for new-borns. One example is the infanticide by conspecifics, present in a wide number of mammal species. Thus, the fierce protection of offspring by their parents is a behaviour with unmistakable adaptive significance. In the species with maternal care, the loss of new-borns is a failure for female reproductive success, and thus mammalian mothers are likely to develop behavioural adaptations to prevent this event (Maestripieri 1992). In the case of maternal aggression, which is the focus of this doctoral thesis, this behavioural adaptation is a protective response in which lactating females attack intruders in order to keep them away from the nest site (Numan and Insel 2003a). This non-pup directed behaviour is well documented in rodents, carnivores, pinnipeds and nonhuman primates, but also it is present in other species (e.g. rabbits) where infanticide by conspecifics is also observed (Mykytowycz and Dudzinski 1973; Harcourt 1992; Maestripieri 1992; Lonstein and Gammie 2002; Saltzman and Maestripieri 2011). Infanticide by non-related conspecifics is probably due to the lack of ovulation during lactation, making females not available for successful mating (Marinari and Moltz 1978). Intruder males can benefit from killing non-related pups as this allows the female to return to oestrus, providing the male

an earlier opportunity for mating and thus increased reproductive success (Hrdy 1979; Labov et al. 1985; Weber and Olsson 2008).

In rodents, aggressive behaviour usually progresses from an appetitive phase that involves close investigation, to a consummatory phase that involves intense attack behaviours like biting and tussling (Chen and Hong 2018). In mice, attacks during maternal aggression may include two components: offensive and defensive attack, determined by the context and the different stimuli that elicit attack, such as the sex of the intruder (Parmigiani et al. 1988, 1998). Offensive behaviours include lateral attacks, during which the dam orients herself laterally to the intruder and often bites his back, and jump-attacks, during which the dam faces the intruder from the front, lunges towards it and bites its head or neck (Svare and Gandelman 1976a; Erskine et al. 1978; Flannelly and Flannelly 1987). Attacks are combined with other behaviours, called 'defensive' behaviours and these include rearing, arching of the back, piloerection, upright boxing, or immobility (Lonstein and Gammie 2002).

Maternal aggression varies between PPD, and the intensity of fighting in parturient animals declines as lactation advances (Svare and Gandelman 1973) (FIGURE 2). Garland & Svare, (1988) proposed that postpartum aggression in mice can be divided into three phases: 1) "Initiation phase", which comprises the first 48 hours after parturition, where an acute period of suckling stimulation is necessary for the initiation of maternal aggression. If dams do not receive suckling from young during this period or experience less than 48 hours of exposure to this stimulus, they fail to develop normal levels of aggressive behaviour (Svare and Gandelman 1976b). 2) The "mid-lactation maintenance" stage, which approximately corresponds to the middle third of the lactation period (approximately Postpartum Days (PPD) 6-12). In this phase suckling stimulation is apparently not necessary for the maintenance of aggression, since thelectomized animals continue to show normal levels of aggressive behaviour and either non-suckling or distal stimulation from the litter is sufficient to maintain the dam's behaviour (Svare and Gandelman 1976b). 3) 'Late lactational phase', during the final week of lactation, which is characterized by a decline in maternal aggression that can be accelerated in the absence of suckling. The mechanisms controlling the shifts between the suckling-dependent and suckling-independent phases have not been explained. The exposure to distal cues from pups may induce neuroendocrine or neurotransmitter changes that maintain maternal aggression during the suckling-independent mid-lactational phase (Svare and Gandelman 1973, 1976a; Svare 1977; Lonstein and Gammie 2002).

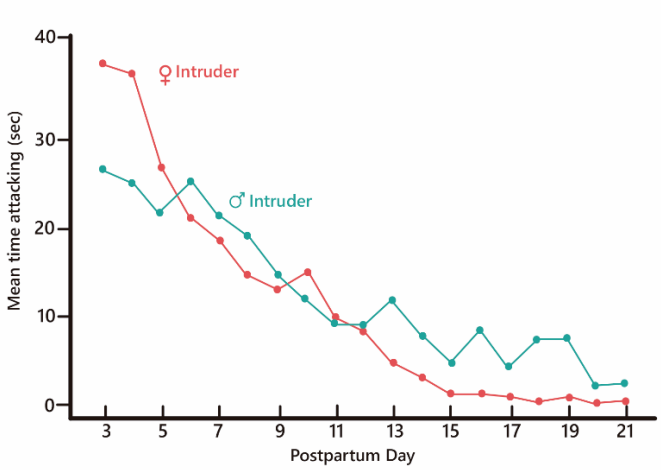

Figure 2: Mean time spent attacking by lactating mice on PPD3 to PPD21 of the lactation period. One group of females (n=5) was confronted with an adult male intruder twice daily for 3 min and another group (n=5) was presented with adult female intruder. Figure extracted from B. Svare & Gandelman, (1973).

HORMONAL BASIS OF MATERNAL AGGRESSIVE BEHAVIOUR

The endocrine system, through its secretion of hormones during pregnancy, plays an important role in stimulating maternal care at parturition in numerous species of mammals (Bridges 2015) (FIGURE 3). In mammals and other vertebrates, successful reproduction requires a broad range of adaptations in the mother. In order to meet the demands of motherhood, central homeostatic regulation must be readjusted, lactation must be established correctly and maternal behaviours must emerge. Most of these physiological and behavioural adaptations originate in changes of the brain during pregnancy, favoured by the endocrine signals of this period. These changes must be initiated before parturition and persist during postpartum periods, thus requiring the endocrine system action during late pregnancy and lactation.

The dependency on the hormonal stimulation varies, however, as a function of the species and the female's reproductive history. In rodents and ungulates hormones appear to play a more obligatory role during pregnancy and lactation, whereas in other species like non-human primates and probably women the endocrine system seems to have a modulatory role. Moreover, this dependency on endocrine stimulation is reduced as the female gains greater reproductive experience, such that multiparous females are less dependent upon hormonal regulation of maternal behaviour than nulliparous females (Bridges 2015).

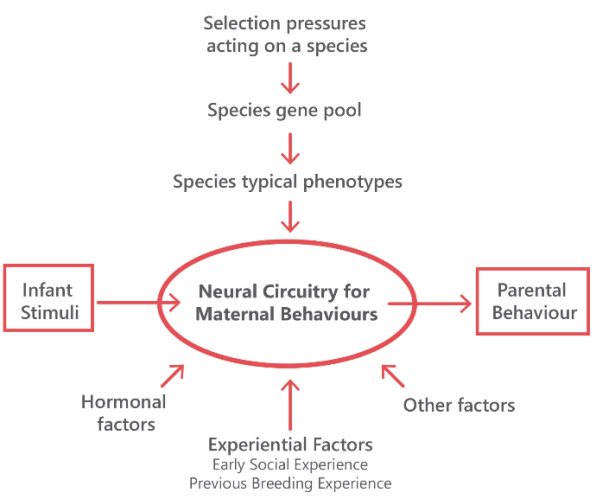

Figure 3: Scheme of how mammalian parental behaviour may have evolved. The central part of the figure represents the neural circuitry controlling parental responsiveness to infant stimuli (limbic system and hypothalamus), which is very conserved across mammalian species. These neural pathways can be influenced by genetic, hormonal, experiential, and other factors. However, as a result of different species being affected by differential natural selection pressures, what might vary among species is the degree to which this circuitry is dependent upon hormonal facilitation and whether, and to what degree, this neural network can be influenced by experiential factors during ontogeny. Adapted from Numan and Insel (2003a).

The crucial hormonal changes that occur within pregnancy include increased levels in circulating oestradiol, progesterone, and lactogenic hormones (prolactin (PRL) and placental lactogens (PL)), which secretory patterns vary during this period (FIGURE 4).

Lactogenic hormones promote mammary gland development and lactogenesis (Southard and Talamantes 1991), and are secreted from either the anterior pituitary (pituitary PRL) or the placenta (PL) throughout most of pregnancy (Freeman et al. 2000; Grattan 2001; Grattan and Kokay 2008; Bridges 2015; Bridges and Grattan 2019). During pregnancy, however, circulating PRL levels are high during early stages but drop during the second half of pregnancy (approximately from day 8-9 in mice and 10 in rats), until the moment of delivery (FIGURE 4A) (Bridges 1990; Grattan 2001; Soares 2004). Nevertheless, this suppression of hypophyseal PRL release is compensated by an alternative source of lactogenic signals: coinciding with the drop in hypophyseal PRL, the trophoblast giant cells of the placenta produce the PLs (Yamaguchi et al. 1992). These are proteins closely related in sequence to hypophyseal PRL that also bind the PRL receptor (PRLR) with high affinity (Kelly et al. 1976) and initiate the same signalling pathways (Soares et al. 1998), thus mimicking hypophyseal PRL (Linzer and Fisher 1999). Hence, they are considered functional substitutes of hypophyseal PRL during mid- and late pregnancy. Although there are different PL, the two major types are referred to as PL I and PL II (Freeman et al. 2000; Grattan 2001).

With respect to steroids, plasma oestradiol levels are low throughout the first part of pregnancy, then rise around day 16; this peak is subsequently maintained through the day of parturition. In contrast, progesterone levels are very high throughout the first part of pregnancy, with a peak on day 15, followed by a decline that becomes abrupt after day 20. Therefore, near the time of parturition (day 22) we see a reversal of the oestrogen/progesterone ratio, moving from a long period of progesterone dominance to a short period of oestradiol dominance (FIGURE 4B) (Numan and Insel 2003a; Bridges 2015).

During lactation, females display a sustained state of hyperprolactinaemia, granted by disinhibition of hypophyseal PRL release (Freeman et al. 2000; Andrews et al. 2001) in response to suckling stimulation by the pups (Freeman et al. 2000; Cservenák et al. 2010), which in turn allows lactogenesis and galactopoiesis (Freeman et al. 2000).

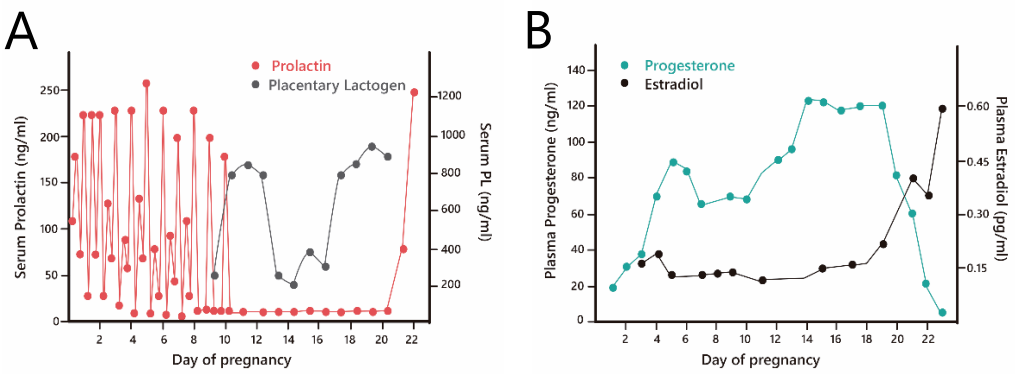

Figure 4: Hormone profiles of PRL, PL (A), oestradiol, progesterone (B) during pregnancy in the rat. The variation of these hormones is very similar in mice (Barkley et al. 1979). For abbreviations see list. Adapted from Bridges (1990).

The changes in levels of female rats hormones such as oestrogen, progesterone, and PRL through pregnancy have long been implicated in the regulation of pup retrieval (Terkel and Rosenblatt 1968). However, in the case of maternal aggression in mice, it is unclear how much hormonal changes during pregnancy and lactation contribute to the development of maternal aggression. Previous studies of the changes of aggression levels in female mice showed controversial results. Some of them demonstrated that levels of aggression in female mice are low during pregnancy and increase immediately after parturition (mainly in inbred strains) (St. John and Corning 1973). However, other studies show that aggression begins to rise during late pregnancy (mainly in outbred strains) (Noirot et al. 1975; Hedricks and Daniels 1981; Mann and Svare 1982). It is important to remark that several studies did not test the levels of aggression before parturition (Svare and Gandelman 1973; St. John and Corning 1973; Ghiraldi et al. 1993).

Regarding the possible role of the hormonal status in the display of maternal aggression during late pregnancy, previous studies have tested the implications of the increase of circulating oestrogens prior to parturition and the posterior decrease (FIGURE 4B) (Barkley et al. 1979; Bridges 2015). These studies revealed that exogenous administration of oestrogen inhibit aggression in parturient lactating mice (Gandelman 1973; Svare and Gandelman 1975). Interestingly, low levels of oestrogen due to ovariectomy can accelerate the onset of aggression independently of the young (Ghiraldi et al. 1993). This suggests that suckling is unnecessary for this process if oestrogen levels are low. In fact, suckling stimulation is needed for lactation and, consequently, for maintaining low levels of oestrogens. For these reasons this postpartum increase in aggression seems to be elicited in natural conditions by the initiation of suckling by the young (Ghiraldi et al. 1993), as it was explained before by B. Svare & Gandelman, (1973). Moreover, progesterone has no effect on maternal aggression when administered during lactation (Gandelman 1973; Svare and Gandelman 1975), but it may induce a low level of aggressive behaviour in virgin females (Mann et al. 1984). In summary, the role of oestrogens and progesterone in the onset and maintenance of maternal aggression is not clear. However, these hormones may essentially act in the periphery by promoting adequate development of nipples on which pups can suckle, thereby providing females with the critical sensory stimulation necessary for the onset of maternal aggression.

Regarding the role of PRL, studies of Broida, Michael, & Svare (1981) showed that circulating levels of PRL were not related to the initiation, maintenance, and decline of postpartum aggression in mice during lactation. Maternal aggression and circulating levels of PRL were measured in separate groups of parturient mice on PPD 0 (the day of delivery), 6, 12, or 18. The results showed that there was little correspondence between levels of the hormone in plasma and aggressive behaviour. Also, they observed no significant correlation between circulating PRL and the intensity of fighting behaviour.

All these data suggest that in mice the specific endocrine events associated with pregnancy termination may be necessary, but are not sufficient to elicit maternal aggression. Thus, the display of aggressive behaviour in dams seems to require also the integration of multisensory stimuli from pups (i.e. olfactory, auditory, visual, somatosensory, etc.) and neuronal changes occurring during pregnancy and parturition (FIGURE 3) (Okabe et al. 2012).

OLFACTORY CONTROL OF MATERNAL BEHAVIOUR

Mice and rats are macrosmatic animals, and their social behaviours are mainly guided by the detection of scent marks. Maternal commitment also requires the proper recognition and identification of the offspring (e.g. distinguishing infants from other conspecifics), which in rodents is driven mainly by chemosensory signals (Lonstein and Gammie 2002; Wyatt 2003a; Dulac et al. 2014). Also in humans, mothers are reliably able to identify their own child's odour (Porter et al. 1983; Kaitz et al. 1987) with up to about 90% accuracy in as little as 10 min after birth (Kaitz et al. 1987).

Chemosignals that give information about conspecifics are called pheromones. Pheromones were originally defined as "substances secreted to the outside by an individual and received by a second individual of the same species in which they release a specific reaction, for instance a definite behaviour [releaser pheromone] or developmental process [primer pheromone]" (Karlson and Lüscher 1959; Wyatt 2003b). The response to pheromones (at least in mammals) may vary depending on a number of factors, including the previous experience or the hormonal status of the receiver (Wyatt 2010). Wyatt, (2010) proposed an important difference between a pheromone, a molecule produced, for example, by all male mice, and a "signature mixture", an individual male's distinctive mix of molecules, which a female mouse learns and uses to recognize him as a particular individual.

In rodents, pheromones are detected by two major sensory systems: the main olfactory system and the vomeronasal system (also called accessory olfactory system) (Wyatt 2010). Briefly, the main olfactory system mainly detects air-borne volatiles, whereas the vomeronasal system seems specialised (with some exceptions) in detecting non-volatile chemicals with an intrinsic biological value (Krieger et al. 1999; Gutiérrez-Castellanos et al. 2010), such as sexual pheromones or predator-derived chemosignals. Thus, in the context of sociosexual behaviour, vomeronasal stimuli apparently trigger innate behavioural responses (Martínez-Ricós et al. 2008; Keller et al. 2009; Martínez-García et al. 2009). However, even though on anatomical grounds olfactory and vomeronasal information are processed mainly in separated structures, information from both the olfactory and vomeronasal systems should be integrated to allow the generation of a complete picture of the chemical cues present in the environment and the generation of appropriate behavioural responses (Halpern and Martínez-Marcos 2003; Boehm et al. 2005; Cádiz-Moretti et al. 2013). These types of information converge in some amygdaloid nuclei (Gutiérrez-Castellanos et al. 2010; Cádiz-Moretti et al. 2013). Therefore, chemosignals detected by both the main and accessory olfactory systems mediate sociosexual interactions, including

intersexual attraction, agonistic behaviours e.g. intermale and maternal aggression, and maternal care.

Previous studies have demonstrated that a well-functioning olfactory system is crucial for pup-directed maternal behaviour (Lévy et al. 2004; Lévy and Keller 2009). Early studies found that olfactory bulb removal totally eliminated maternal behaviour in pregnant and non-pregnant females (Gandelman et al. 1971; Zarrow et al. 1971) and could even promote cannibalism (eating her own pups) in lactating dams (Gandelman et al. 1971; Gandelman 1972). In another study, they carried out lesions of the olfactory epithelium using $ZnSO_4$ infusion into the nasal cavity and bulbectomy. Both procedures reduced nest building and resulted in a high level of cannibalism, however, the effect of bulbectomy was considerably greater. This differences between procedures can be related with the fact that females treated with $ZnSO_4$ could have retained or recovered a small degree of olfactory function (Vandenbergh 1973). In the same vein, the loss of function of the sodium channel $Nav_{1.7}$ using conditional mutants, which also causes anosmia, resulted in the lack of pup retrieval behaviour (Weiss et al. 2011).

Olfaction and maternal aggression

Olfactory cues that dams receive from intruders (and probably from pups (Okabe et al. 2013)) are also important for the maintenance of maternal aggression in mice. Olfactory bulbectomy eliminates maternal aggression in rats (Kolunie and Stern 1995) and mice (Gandelman et al. 1972). The importance of the olfactory system in maternal behaviour is also shown by transgenic mice that lack the adenylyl cyclase type 3, which are largely anosmic. These mutant mice do not exhibit maternal aggression, and also have impaired pup retrieval and nest building (Wang and Storm 2011).

In mice, it has been shown that vomeronasal organ (VNO) removal prior to mating or after parturition eliminates later maternal aggression in mice (Bean and Wysocki 1989), but does not affect other maternal behaviours (Lepri et al. 1985). Furthermore, disruption of a family of pheromone receptors in the vomeronasal organ also impairs maternal aggression in lactating mice (Del Punta et al. 2002). Likewise, when signal transduction cascade components specific of the VNO are mutated (e.g., mice that lack the Transient receptor potential cation channel, subfamily C, member 2 (TRPC2)) deficits are observed in maternal aggression and other maternal behaviours (Kimchi et al. 2007; Hasen and Gammie 2009, 2011).

In addition to pheromonal cues from pups, pheromonal cues from the intruders also influence the likelihood of maternal attack. It is known that mice are strongly territorial and males are constantly marking its territory with urine spots, especially on their boundaries, where territorial disputes with competitor males can occur. Females trespass male territorial boundaries and countermark with urine spots. Urine seems, therefore, the main vehicle for chemical advertising (Wolff and Powell 1984; Wolff 1993). In mice, two pheromonal cues promote aggressive behaviour between males: the major urinary proteins (MUPs) and unidentified molecules of low molecular weight (Chamero et al. 2007). MUPs are urinary proteins of the lipocalin family, which have an internal pocket that binds low molecular weight hydrophobic volatiles (Novotny et al. 1999). These pheromones are encoded by a cluster of >21 genes located in chromosome 4 (Hurst and Beynon 2013) and they are apparently detected by the VNO (Kaur et al. 2014). Moreover, there is a clear sexual dimorphism in urinary protein secretion in laboratory mice (Hurst 1987; Hurst and Beynon 2013). Subsequent investigations have demonstrated that the pheromone responsible for sexual attraction in female mice was a male-specific atypical MUP named *darcin* (also known as Mup20, FIGURE 5) (Roberts et al. 2010). Male soiled-bedding containing sexual chemosignals (Moncho-Bogani et al. 2002; Martínez-Ricós et al. 2007, 2008) or *darcin* by itself (Roberts et al. 2010, 2012) stimulates attraction and associative learning in female mice.

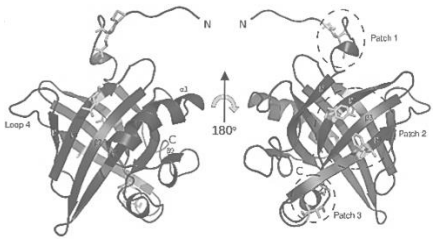

Figure 5: Three-dimensional structure of male sexual pheromone darcin (Mup 20). Adapted from Phelan et al. (2014)

Regarding the unidentified low molecular weight pheromones, they can stimulate either the VNO or both the VNO and the main olfactory ephitellium (MOE) (Chamero et al. 2007), however further studies are needed in order to know if these pheromones are related with the display of maternal aggression.

Previous research in our group has demonstrated that pup exposure is not sufficient to induce maternal aggression in virgin females (Martín-Sánchez et al. 2015b). Virgin females which have been continuously exposed to pups for 3–4 days show negligible aggressive behaviour towards intruders approaching the nest. Therefore, in our experimental conditions, pup cohabitation only induces full nest defence in females that have undergone pregnancy, parturition and lactation. In addition, these studies have also shown that the male pheromone inducing maternal

aggression in dams is *darcin*. Dams show low aggressive levels towards castrated male intruders except when they were impregnated with urine from intact males or *darcin* alone. In this case, the levels of aggression displayed by dams were comparable to those displayed against intact males. Therefore, the same chemosignal, *darcin*, promotes attraction or aggression according to female reproductive state (Martín-Sánchez et al. 2015b, a).

This thesis focuses on studying the changes that occur in the central nervous system (CNS) during pregnancy and lactation and that cause the change in the female response to male pheromones from attraction to aggression.

MATERNAL BEHAVIOUR: PHEROMONES AND SOCIAL BRAIN NETWORK

Social behaviours are under control of the so-called sociosexual brain network (SBN) (Newman 1999). The SBN is a phylogenetically old and highly conserved neural network (schematically illustrated in FIGURE 6) composed of several nodes that fulfil three main features: 1) they are known to be implicated in the regulation of various forms of social behaviour; 2) they are reciprocally interconnected (to allow for a network-type of activity); and 3) they show abundant neurons expressing gonadal steroid receptors, thus allowing a dimorphic expression of social behaviours.

The expression of a specific social or reproductive behaviour (including the different subcomponents of maternal behaviour) would be correlated not to the discrete activation of a specific nucleus or a linear circuit, but to a distinct activation pattern of the whole SBN (FIGURE 6). In addition to the SBN as the central neural circuitry of the social brain, other brain nuclei might also participate in the control of specific social behaviours. The adaptive changes in the brain of dams during pregnancy and lactation that allow them to cope to this new situation and develop successful maternal behaviours take place in the different nuclei of the SBN, where the endocrine agents act to turn the female brain into a maternal brain (Numan and Woodside 2010).

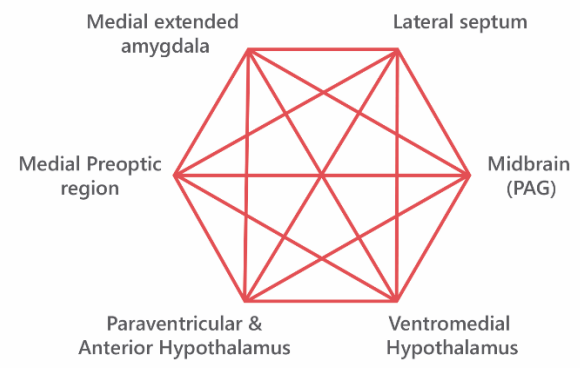

Figure 6: The social behaviour network (SBN). The network proposed by Newman, (1999) is group al the brain structures involved in the expression of every social and reproductive behaviour, including maternal behaviours. SBN is composed of six main nodes highly interconnected: the medial extended amygdala, lateral septum, medial preoptic region, paraventricular and anterior hypothalamus, ventromedial hypothalamus and midbrain areas (including the PAG). Adapted and modified from Newman (1999) and Goodson (2005). For abbreviations see list.

As mentioned before, rodents are macrosmatic animals, so the link of chemosignal detection systems and the SBN is highly important. Within the SBN, the main and accessory olfactory systems provide key sensory inputs to the medial extended amygdala node (FIGURE 6) (Newman 1999; Insel and Numan 2003; Gutiérrez-Castellanos et al. 2010; Cádiz-Moretti et al. 2013).

The amygdaloid complex is a heterogeneous structure both from the anatomical and functional points of view (Martinez-Garcia et al. 2009; Gutiérrez-Castellanos et al. 2010). Within the amygdala, we can roughly outline two functional subsystems, namely the central/basolateral subsystem and the medial/cortical subsystem involved in managing two different, but closely related, functions (Martínez-García et al. 2008; Martinez-Garcia et al. 2009). The central/basolateral subsystem coordinates innate and learned reactions of fear/anxiety/aversion or of attraction/reward-directed behaviours to virtually any stimulus (Martínez-García and Lanuza 2018). The medial/cortical subsystem is primarily involved in the coordination of species-specific behavioural responses to chemosensory stimuli (olfactory and vomeronasal) with a strong emotional component (Newman 1999; Goodson 2005; Gutiérrez-Castellanos et al. 2010). Among the secondary vomeronasal centres, the medial amygdala (Me) is a key structure in the network of neural nuclei controlling sociosexual behaviours in rodents (Newman 1999; Swann et al. 2009; Bergan et al. 2014) which forms part of the SBN. Among the SBN structures (FIGURE 6), only the Me receives convergent projections from both olfactory bulbs in mice (Cádiz-Moretti et al. 2016) and rats (Pro-Sistiaga et al. 2007). The efferent connections of the Me have been previously studied in male rats (Canteras et al. 1995), female mice (Pardo-Bellver et al. 2012) and male hamsters (Gomez and Newman 1992; Maras and Petrulis 2010). The Me is composed of anterior (MeA), posteroventral (MePV) and posterodorsal (MePD) subregions (Gomez and

Newman 1992; Canteras et al. 1995). In mice (Kang et al. 2009), but not in rats (Martinez-Marcos 2009), the MePD has also been shown to receive a direct olfactory input (FIGURE 7). These subdivision fits the pattern of expression of genes of the LIM-homeobox family (*Lhx*). Thus, the MeA expresses *Lhx5*, the MePD expresses *Lhx6*, whereas MePV is positive for *Lhx9* (Choi et al. 2005; Medina et al. 2017). These differential patterns of gene expression are related to the heterogeneous origin of the cells of the subnuclei of the Me (García-López et al. 2008) in the mouse.

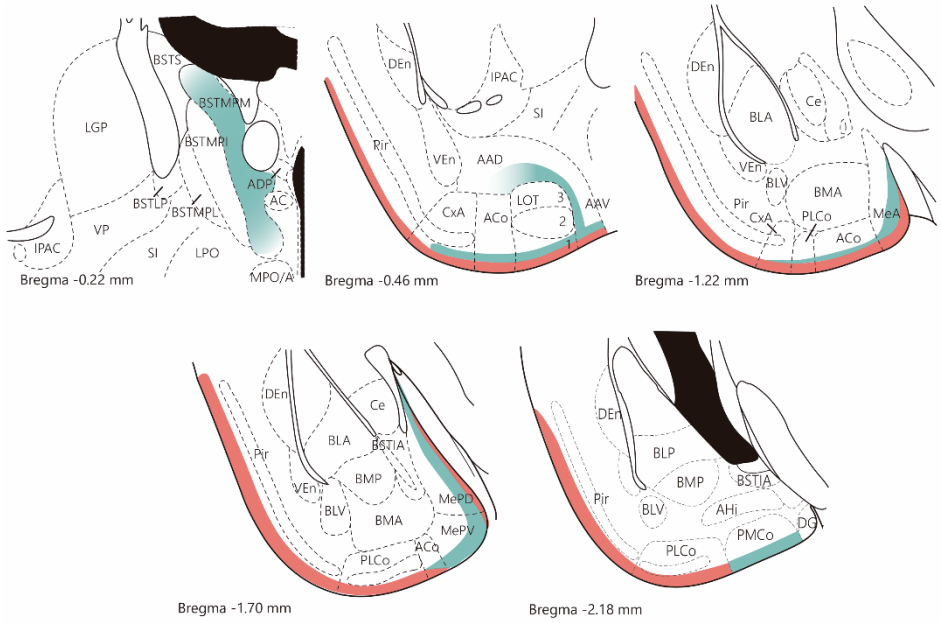

Figure 7: Schematic representation of the olfactory (in red) and vomeronasal (in blue) pathways to the cortical and extended amygdala originated, respectively, by the MOB and AOB in rodents. The segregation or integration of both types of information is indicated, delimiting the olfactory, vomeronasal, or mixed chemosensory centres of the amygdala. *The brain drawings are modified from Paxinos & Franklin, (2004). Adapted from Cádiz-Moretti et al. (2013)* For abbreviations see list.

In addition, the divisions of Me seem related to different functions and behavioural responses. Thus, the MePD (and also the posteromedial part of the medial division of the bed nucleus of the stria terminalis (BSTMPM) seems involved mainly in reproductive behaviours, whereas MePV is activated by the expression of defensive behaviours (Choi et al. 2005). Both subnuclei would elicit these behavioural responses through direct pathways to different hypothalamic centres.

Neural regulation of proactive maternal responses toward pups

A rapid onset of maternal behaviour requires an increase in approaching responses toward pups, suggesting the role of neural systems involved in motivation. Numan & Woodside (2010) proposed a functional model to explain the onset of maternal behaviours which integrates the

interaction of brain motivation systems and major SBN nodes in rats. These model shows the possible shifts between aversive or avoidance and proactive maternal responses to pups. In the avoidance pathway pup-derived chemosensory stimuli would activate the Me through the olfactory bulbs (Canteras et al. 1995; Gutiérrez-Castellanos et al. 2010; Cádiz-Moretti et al. 2016). The projections of Me to the caudal part of anterior hypothalamic nucleus (AH), and to the ventromedial nuclei of the hypothalamus (VMH) (Canteras et al. 1995; Pardo-Bellver et al. 2012) could promote pup-avoidance responses in virgin females. Experiments with excitotoxic amino acid lesions of Me show that these lesions promote maternal responsiveness in hormone-primed virgin female rats (Bridges et al. 1999). The efferences of AH and VMH target the periaqueductal gray (PAG) as a final central node (FIGURE 8) (Motta et al. 2013). Remarkably, different regions of PAG are associated with fear-related behaviours and avoidance responses and with an increase of maternal aggression toward intruder males (Lonstein and Stern 1997; Lonstein et al. 1998).

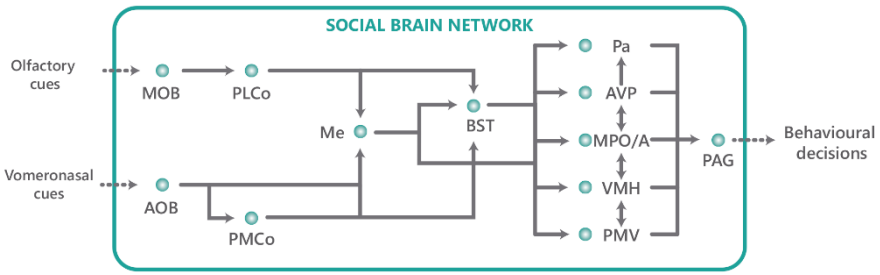

Figure 8: Schematic Representation of the Social Brain Network (SBN). Overview of key circuits and regions involved in the SBN. For abbreviations see list. Adapted from Chen and Hong (2018).

In contrast to the avoidance pathway, the pathway for proactive maternal responses is represented by the mesolimbic dopaminergic system connecting the ventral tegmental area (VTA) to the nucleus accumbens (Acb) and the ventral pallidum (VP). This pathway is likely responsible for assigning rewarding properties to pup stimuli. Numan & Woodside, (2010) postulate that dopamine release in the Acb makes VP easily excited by pup stimuli. Maternal sensitisation of virgin females, in turn, represents a progressive inhibition of the avoidance pathway, which is eventually out-weighted by attractive tendencies towards pups. The sensitization period to pups needed to display cleaning of new-borns is shorter in virgin female mice than in rats (Noirot 1972; Alsina-Llanes et al. 2015; Martín-Sánchez et al. 2015b). However, full activation of the maternal pathway is only reached in rats and mice through the endocrine events of pregnancy (Noirot 1972; Numan and Insel 2003a), for example maternal aggression is displayed only by lactating females (Martín-Sánchez et al. 2015a, b).

The central node in Numan & Woodside (2010) model, responsible for the activation or inhibition of either pathway, is the medial preoptic region (MPO/A), a component of the SBN (FIGURE 8). In lactating dams exposed to pups, GABAergic (inhibitory) neurons in the medial preoptic area (MPA) express FBJ osteosarcoma oncogene protein (FOS), a marker of neuronal activity (Lonstein and De Vries 2000). Thus, these inhibitory neural population would contribute to suppress the avoidance circuitry in primiparous female rats and mice, whereas proactive maternal responses would be activated through direct MPO/A projections to the mesolimbic dopaminergic system (Numan and Stolzenberg 2009; Numan 2014; Chen and Hong 2018). Finally, pup-derived chemo- and somatosensory inputs would reach the MPA, Acb and VP from the basolateral (BL) and basomedial (BMA) nuclei of the amygdala, which in turn receive convergent olfactory and vomeronasal inputs from the Me and piriform cortex (Pir) (Numan 2006; Numan and Stolzenberg 2009; Pardo-Bellver et al. 2012). Thereafter, the MPO/A projects to PAG in order to display maternal behaviours (Rizvi et al. 2018).

Neural substrate and neurochemical control of maternal aggression

A brain-wide neuronal activation mapping study showed that male- versus female-specific cues (i.e. pheromones) activate both distinct and shared brain regions or subregions (Kimchi et al. 2007; Kim et al. 2015; Chen and Hong 2018), raising the question of whether mating and aggression are regulated by the same or different circuits.

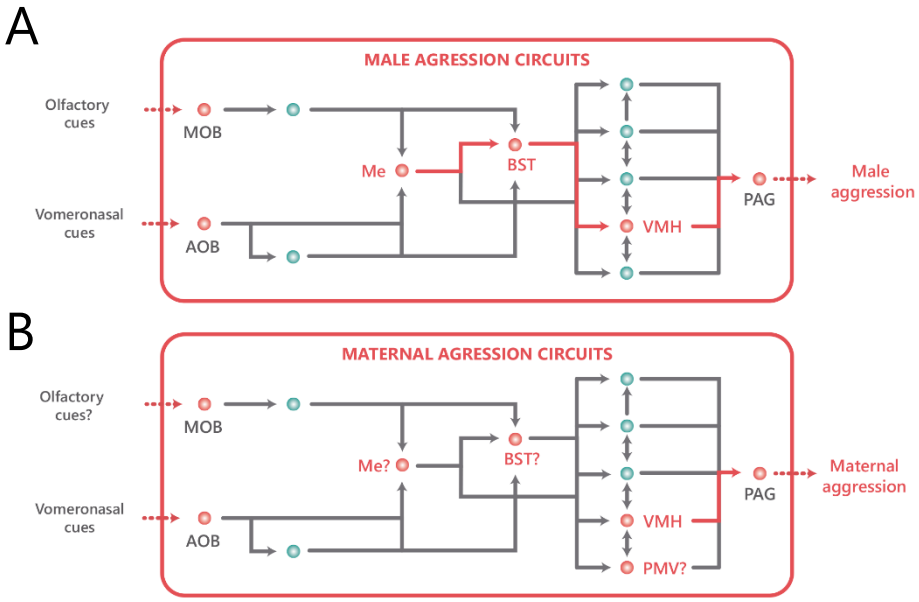

Figure 9: Representation of the Social Brain Network (SBN) nuclei involved in aggression in males and dam mice. A) Circuits involved in male B) and female aggression. Coloured nuclei and connections in red represent circuits with direct experimental evidence for the corresponding behaviour. Nuclei with question mark (?) are hypothetically involved. For abbreviations see list. Adapted from Chen and Hong (2018).

The VMH receives both direct and indirect inputs from the Me as well as inputs from BSTMPM (BNSTpr in L. Swanson (2004) nomenclature) and other brain structures involved in aggressive behaviour (FIGURE 9A AND B) (Been et al. 2019). In males, neurons in the ventrolateral area of the VMH (VMHvl) are activated during both investigation and attack of a male intruder, and they are more strongly activated by social stimuli compared to non-social ones (Lin et al. 2011). The VMHvl is highly enriched in hormone receptors, including oestrogen receptor alpha (ESR1) and progesterone receptor which co-express in nearly 100% of cells (Hashikawa et al. 2017b) making this nucleus very sensitive to ovarian hormones (Takahashi and Lisk 1985; Meisel and Sterner 1990; Lonstein and Gammie 2002). This ESR1-positive cell population plays a crucial role in the development of maternal aggression (Hashikawa et al. 2017a) and also in male aggressive behaviours (Lee et al. 2014). The PAG is thought to be a critical node for connecting the VMHvl to motor output in the spinal cord (Hashikawa et al. 2017b) (FIGURE 9A AND B). Lesions in subregions of the PAG result in increased female aggression (Lonstein and Stern 1997). The exact nature and role of these brain regions and connections in regulating aggression remains to be clarified.

Regarding the role of VMH in maternal aggression, electrolytic lesions of the ventral part of VMH in lactating rats produced a reduction in maternal aggression but not in maternal care (Hansen 1989). Recent studies using genetically defined functional manipulations were able to point the VMH and the Me as critical nuclei for eliciting aggression (FIGURE 9A AND B) (Chen and Hong 2018). Other hypothalamic areas, such as ventral premammillary nucleus (PMV) might be important for aggressive behaviour, because lesions in this centre abolish maternal aggression in rats (Motta et al. 2013) and PMV receives projections from the Me (Canteras et al. 1995; Pardo-Bellver et al. 2012).

As mentioned before, the Me receives inputs from both main olfactory and vomeronasal systems (FIGURE 8). Interestingly, recent studies in male mice shown that GABAergic neurons, but not glutamatergic neurons, in the MePD are highly activated by aggressive inter-male social interactions. Optogenetic activation of these MePD GABAergic neurons results in aggression, while silencing of this population results in termination of ongoing attack (Hong et al. 2014). In addition, other studies have suggested that a subpopulation of MePD GABAergic neurons, which expresses aromatase, is required for aggression, although chemogenetic activation of this population is unable to promote aggression (Unger et al. 2015). MePD regulates aggression through one of its downstream projection targets, the posterior portion of the bed nucleus of the stria terminalis (BST); stimulation of MePD-BST projections results in increased aggression

(Padilla et al. 2016; Yamamoto et al. 2018), however all these studies are carried out in male mice. In the case of females recent studies suggest that the aromatase-expressing MePD neurons also play a key role in the onset of maternal aggression (Unger et al. 2015) (FIGURE 8B).

Mating versus Aggression

In males, previous results showed that distinct and shared female and male interaction-evoked patterns of activation represent sex discrimination and social recognition (Kim et al. 2015), raising the question of whether mating and aggression are regulated by the same or different circuits. Interestingly, low-intensity stimulation of VMHvl ESR1 positive cells or MePD vesicular GABA transporter positive neurons leads to mounting, whereas high-intensity stimulation leads to attack, suggesting the possibility that mounting and attack could be controlled either by different subpopulations of neurons with different activation thresholds, or by the amount of neurons that are being recruited (Lee et al. 2014; Chen and Hong 2018). Within the MePD and VMHvl, the representation of male- versus female-specific cues appears to be partially distinct, both at the level of individual neurons and at the level of populations (Bergan et al. 2014; Hashikawa et al. 2017b; Li et al. 2017; Remedios et al. 2017).

Moreover, recording signals in the brains of anesthetized mice exposed to specific stimuli show that neurons in the accessory olfactory bulb (AOB) responded similarly to male and female mice, while those in the Me showed a preference for female urine in male mice, and a preference for male urine in the case of females (Bergan et al. 2014). Moreover, it seems that fractions of neurons responsive to specific conspecific cues is different in the Me of virgin males and females, demonstrating sex differences in the representation of social cues. The Me neurons can be selectively excited or inhibited in response to specific social stimuli (Li et al. 2017).

Interestingly, the VMHvl in females could be divided into two anatomically distinct subregions (medial and a lateral zone) that are differentially activated in mating and aggression and display different gene expression and axonal projection patterns (see Supplementary Figure 13 in K. Hashikawa et al., 2017). In addition, another study have identified a MePV to dorsomedial area of VMH (VMHdm) to dorsal PAG pathway that is critical for pheromone-mediated lordosis behaviour (Ishii et al. 2017). These lines of evidence suggest that the circuits for mating and attack are at least partially distinct (FIGURE 10A AND B).

All these results indicate that Me is playing a crucial role in the shift between attractive responses toward males observed in non-lactating females and the aggressive behaviour in dams. We

hypothesized that physiological and neural changes during pregnancy and lactation in the Me underlie the change from attraction towards male pheromones to aggression in response to these same chemical signals.

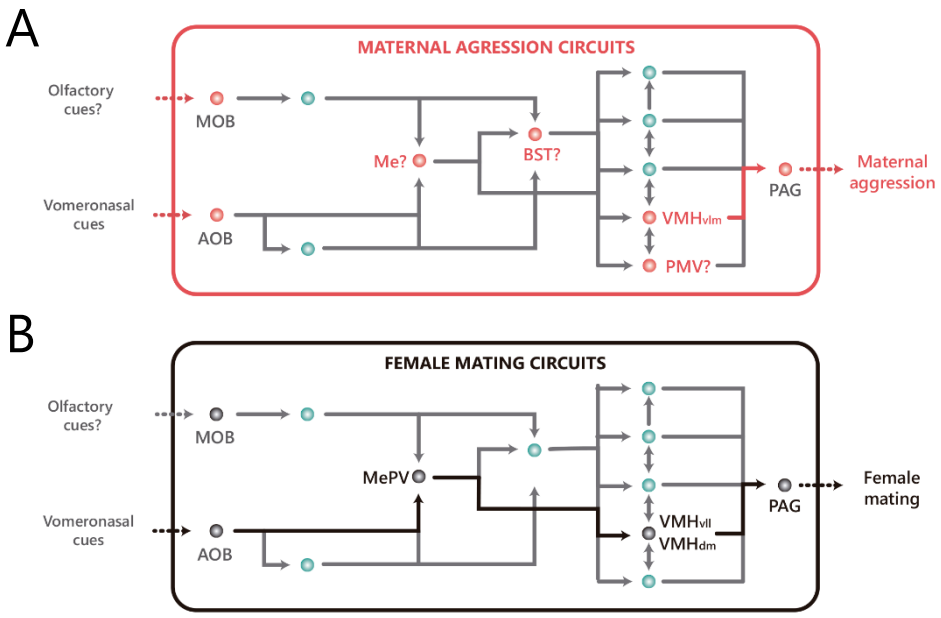

Figure 10: Representation of the Social Brain Network (SBN) nuclei involved in maternal aggression and mating in female mice. A) Circuits involved in female aggression. B) Nuclei involved in female mating. Coloured nuclei and connections in red and black represent circuits with direct experimental evidence for the corresponding behaviour. Nuclei with interrogation symbol (?) are probably involved in the behaviour but further studies are needed. For abbreviations see list. Adapted from Chen and Hong (2018).

AIMS OF THIS WORK

The present doctoral thesis aims to provide a deeper insight on the function and regulation of Me during pregnancy and lactation and its role in the display of maternal behaviours. First, we aimed to know whether Me is playing a key role in the control of maternal aggression. Afterwards, we asked what changes in gene expression take place in Me during lactation that may be involved in the display of aggressive behaviour. Since one of the main gene expression changes revealed by our study was an increased PRL expression, we characterized the prolactinergic (PRLergic) circuits in the female brain and possible changes in these circuits in dams. The specific aims of this work were:

1. Characterization of the role of Me in the expression of maternal aggression.

2. Study of changes in gene expression in Me that may underlie the shift from attractive responses in non-lactating females toward intruder males to aggressive behaviour in lactating females.

3. Characterization of the PRLergic circuits in the female brain and possible changes in these circuits in dams.

CHAPTER 1

ROLE OF MEDIAL AMYGDALA IN MATERNAL AGGRESSION

INTRODUCTION

Motherhood involves many physiological changes in the brain of females that give rise to behavioural adaptations. These changes enable the dam to cope with the new situation and improve the likelihood of offspring survival. Thus, reproductive fitness and maternal behaviour are closely related, and maternal behaviour is one of the most important social behaviours (Insel and Numan 2003; Weber and Olsson 2008).

Maternal behaviour in rodents can be parsed in those components which are directed to pups and those that are not. Pup-directed behaviours include responses and interactions with pups such as retrieval and grouping pups in nest, crouching over pups, pup-licking/grooming, and nursing. On the other hand, non-pup directed behaviours include nest building and maintenance, and maternal aggression (Gammie 2005; Weber and Olsson 2008). Maternal aggression is in fact a mechanism of defence of the offspring against intruders and has a huge adaptive value due to its direct relation to offspring survival. This is particularly true in rodents, where infanticide by non-parental conspecifics is quite common (Wolff 1985, 1993; Lonstein and Gammie 2002)

Maternal aggression, thus, also termed nest defence by some researchers, is displayed by lactating mothers and its intensity varies across the postpartum period, as pups grow old and become more independent (Svare and Gandelman 1976a; Svare 1977; Bosch 2013). Previous studies have demonstrated that most lactating mice, and rodents in general, exhibit immediate aggression toward an unfamiliar conspecific placed in the maternal home cage with the litter present (Gandelman 1972; Paul et al. 1980) or without the presence of the pups in the cage during the tests (Lonstein and Gammie 2002; Martín-Sánchez et al. 2015b). Strikingly, in laboratory mice, virgin females readily take care of the pups when they are in close contact with them (Martín-Sánchez et al. 2015b), i.e., they can perform maternal care, but they fail to display aggressive behaviours towards an intruder male (Martín-Sánchez et al. 2015a). Thus, we hypothesised that maternal aggression is more dependent on hormonal changes occurring during pregnancy and/or lactation than pup-directed behaviours, at least in laboratory mice.

In rodents, maternal aggression, and sociosexual behaviours in general, are mainly mediated by chemosensory signals. As macrosmatic animals, rodents possess highly developed olfactory and vomeronasal systems and chemosignals, pheromones and odours, are critical for intraspecies communication (Wyatt 2003a, b; Cádiz-Moretti et al. 2013). Olfactory cues may be the basis of

how dams respond to an intruder's age, sex, and reproductive status (Svare and Gandelman 1973; Lonstein and Gammie 2002). These cues can be molecules such as urinary proteins (Roberts et al. 2010), lacrimal proteins (Ishii et al. 2017; Woodson et al. 2017), etc. However, urine is usually considered the most important source of chemosignals in mice, and in fact urine marking and countermarking is highly displayed by male mice (Kaur et al. 2014). In particular, a male-specific non-volatile MUP of mass 18893Da named *darcin* elicits a female's inherent sexual attraction toward males (Roberts et al. 2010). This pheromone produces two different behavioural responses in females depending on their reproductive status. If the female mice are sexually receptive, *darcin* produces sexual attraction toward males. However, if the female is lactating, the same molecule induces aggressive behaviours against the intruder male (Martín-Sánchez et al, 2015). The changes in the behavioural responses of females likely involve plastic changes of the sociosexual brain circuits, which could be result of a mixture of endocrine agents and sensory inputs (chemosignals, nipple stimulation, etc.) acting during pregnancy, parturition and lactation (Lonstein and Gammie 2002; Martín-Sánchez et al. 2015b; Salais-López et al. 2017).

Social odours and pheromones such as *darcin* are processed by the main and the accessory olfactory systems (Xu et al. 2005; Lanuza et al. 2014; Martín-Sánchez et al. 2015a, b). Volatile compounds are primarily detected by the MOE, which projects to the main olfactory bulb (MOB), whereas non-volatile signals, including *darcin*, are preferentially processed by VNO, projecting to AOB (Wyatt 2003b; Gutiérrez-Castellanos et al. 2010, 2014). Olfactory and vomeronasal pathways run parallel and reach different areas in the amygdala, although some overlapping regions are also described (Gutiérrez-Castellanos et al. 2010; Cádiz-Moretti et al. 2013; Ennis et al. 2015). Traditionally, the structures considered as receiving only MOB projections are Pir, the olfactory tubercle (Tu), cortex-amygdala transition zone (CxA), anterior cortical amygdaloid nucleus (ACo), the nucleus of the lateral olfactory tract (LOT) and the posterolateral cortical amygdala (PLCo). On the other hand, the nuclei traditionally considered as vomeronasal recipients are the bed nucleus of the accessory olfactory tract (BAOT), the posteromedial part of the medial division of the BSTMPM, the anterior amygdaloid area, Me subdivisions (MeA and MeP) and the posteromedial cortical amygdala (PMCo). Nevertheless, the amygdala contains several associative areas where chemosensory information coming from the AOB and MOB converge, including CxA, ACo, MeA and MePD (Scalia and Winans 1975; Gutiérrez-Castellanos et al. 2010; Cádiz-Moretti et al. 2013).

The Me is probably the structure receiving the most significant convergence of direct inputs from AOB and the MOB, and in addition it projects to distinct nuclei of the hypothalamus

involved in social and defensive responses (Petrovich et al. 2001; Pardo-Bellver et al. 2012; Bergan et al. 2014; Cádiz-Moretti et al. 2016). Moreover, it plays a central role in the vomeronasal–sensorimotor transformation that leads to specific behavioural responses (Bergan et al. 2014). Thus, disruptions in signalling in the Me cause deficits in social and aggressive behaviours, and predator recognition (Ferguson et al. 2001; Li et al. 2004; Sano et al. 2013; Wang et al. 2013; Unger et al. 2015; McCarthy et al. 2017b).

In this context, our first aim is to investigate the effect of selective inactivation of Me by Designer Receptors Exclusively Activated by Designer Drugs (DREADD) to check whether it is playing a key role in the orchestration of maternal aggression. Since experiments using DREADD tools usually involve a design with intra-subject controls, i.e. first day with saline / second day with drug or viceversa in a counterbalanced order, and we know that maternal aggression levels can change across postpartum, we first explore how repeated exposure towards an intruder male can affect the aggressive behaviours of dams and pup-sensitized virgins as controls.

MATERIAL AND METHODS

EXPERIMENT 1

EFFECT OF EXPERIENCE IN AGGRESSION AND SOCIOSEXUAL SNIFFING IN VIRGIN FEMALE MICE AND DAMS

Animals

For this study, we used 16 adult females and 24 male mice (*Mus musculus*) from the CD1 strain (Janvier; Le Genest Saint-Isle, France). Animals were 8-12 weeks old and weighed between 26.8-48.5 g at the beginning of the experiments. Adult virgin females were randomly assigned to two groups: dams (n=8) and godmothers (n=8). Future dams were housed each one with a stud male during four days for mating. The day of birth was considered as PPD0. On PPD2, litters were culled to 8 pups. Regarding godmothers, they were virgin females pair-housed with dams after mating. Consequently, godmothers were continuously exposed to pups and shared maternal caregiving with the accompanying dams (Martín-Sánchez et al. 2015b). Animals were housed in cages with water and food available *ad libitum* with 12 h light: dark cycle at 22-24°C. Mice were treated according to the guidelines of the European Union Council Directive of September 22nd, 2010 (2010/63/UE). All the experimental procedures were approved by the Committee of Ethics on Animal Experimentation of the University of València.

Behavioural tests

Females were exposed during 5 minutes from PPD4-PPD6 (FIGURE 11) to a different intruder male each day, in their home cage. Pups were separated during behavioural testing to avoid any damage. Behavioural testing was video-recorded and a researcher who was blind to the experimental groups analysed number and duration of attacks, anogenital approaches and body approaches, both from female to male and from male to female. All the behavioural tests were digitally monitored and analysed using SMART 3.0 video tracking system (Panlab, Barcelona, Spain).

Statistical analyses

Statistical analyses were performed using IBM SPSS Statistics 24.0. Firstly, we checked if the data fulfilled the conditions of the ANOVA: normality (Kolmogorov–Smirnov test with Lilliefors' correction), homoscedasticity (Levene's test) and sphericity (Mauchly's test). In the case of non-normality, data was log-transformed (log [X + 1]). Data were analysed using an ANOVA of repeated measures with only DAY (PPD4, PPD5 and PPD6) as intra-subject factor. Statistically significant differences ($p \leq 0.05$) were further explored by means of post-hoc pairwise comparisons with Bonferroni's correction.

When the distribution was not normal even with the logarithmic transformation and the samples were related the non-parametric Friedman's test was used with the Wilcoxon post-hoc signed-rank test when appropriate. In the case of two non-related samples the non-parametric Mann-Whitney test was used when appropriate.

For analysis of the structure of maternal attacks, we carried out a histogram of frequencies where we used an ANOVA of repeated measures with two intrasubject variables: DAY (PPD4, PPD5 and PPD6) and RANGE of duration (0 to 1 seconds, 1 to 5 seconds and 5 to 30 seconds). The graphs were prepared using GraphPad Prism 6 Software.

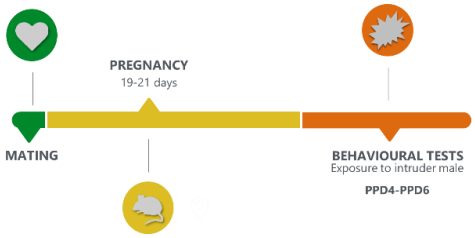

Figure 11: Repeated aggression tests timeline.

EXPERIMENT 2

EFFECT OF DREADD-INDUCED INHIBITION OF ME IN MATERNAL AGGRESSION

Animals

For this experiment we used 56 adult females and 82 adult male mice (*Mus musculus*) from CD1 strain (Janvier; Le Genest Saint-Isle, France). Animals were 8-12 weeks old and weighed between 27.8-47.9 g at the beginning of the experiments. The females were randomly assigned to four groups depending on the type of injection: DREADD+CNO (Clozapine N-oxide) injection in PPD4 (n=17), DREADD+PBS or saline injection in PPD4 (n=18), no virus + CNO injection in PPD4 (n=7) and no virus + PBS injection in PPD4 (n=7). Only animals with restricted bilateral or ipsilateral injections in Me were used in the study (see TABLE 1):

Table 1: experimental groups. Dams with restricted injections and control animals assigned to each group. IP: intraperitoneal, PBS: phosphate buffered saline, PPD4: postpartum day 4.

		STEREOTAXIC INJECTIONS	
		VIRUS	NONE
IP. INJECTIONS IN PPD4	CNO	7	9
	SALINE/ PBS	9	9

Animals were housed in cages with water and food available *ad libitum* with 12 h light: dark cycle at 22-24°C. Mice were treated according to the guidelines of the European Union Council Directive of September 22nd, 2010 (2010/63/UE). All the experimental procedures were approved by the Committee of Ethics on Animal Experimentation of the University of València.

Females were anesthetized with isoflurane (2–2.5%) in oxygen (1–1.3 l/min) (MSS Isoflurane Vaporizer, Medical Supplies and Services, UK) delivered through a mouse anaesthetic mask attached to the stereotaxic apparatus (David Kopf, 963-A, Tujunga CA, USA). For surgery, atropine was administered to prevent cardio-respiratory depression (0.05 mg/kg) and butorphanol was used as analgesia (5 mg/kg, Turbugesic, Pfizer, New York, USA), both injected subcutaneously. While the head was fixed in the stereotaxic apparatus, mice rested on a thermal blanket to keep their body temperature, and eye drops (Siccafluid, Thea S.A. Laboratories, Spain) were used to prevent eye ulceration.

An adeno-associated virus containing the Cre recombinase-independent viral construct AAV5-hSyn-HA-hM4D(Gi)-IRES-mCitrine (B. Roth's laboratory at University of North Carolina Vector Core) was used to express the modified human muscarininc inhibitory receptor (hM4Di) and the fluorescent reporter mCitrine in neurons. The virus was pressure injected bilaterally with a volume of 0.25- 0.3 µl (titter of $3.5x10^{12}$ vg/ml) per site at a rate of 0.25-0.3 µl/min. The injections were carried out using glass micropipettes (20–30 µm diameter tips), a 5 µl syringe (Hamilton, Cat# 87900) and a KDS-311 Nano Pump (KD Scientific Inc.). To avoid diffusion of the tracer along the pipette track, the micropipette tip was left in place for 10 min after finishing the injection.

Stereotaxic coordinates relative to Bregma were taken from the atlas of the mouse brain (Paxinos and Franklin 2004) and applied, using a flat skull approach, as follows: A-P: -1.5 to -1.6 mm, M-L (left hemisphere): -2 to -2.2 mm, M-L (right hemisphere): +2 to +2.2 mm and D-V: -4.7 to -5 mm. After the injection, we closed the wound with Histoacryl (Braun, Tuttlinger, Germany) and another dose of butorphanol was supplied. After surgery, we left two days of recovery before mating (FIGURE 12).

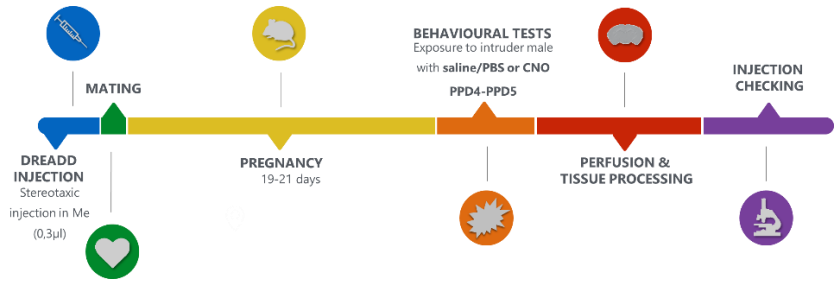

Figure 12: DREADD repeated aggression tests timeline.

Behavioural tests

After the stereotaxic injections of the viral vector, the females (operated and control) were caged with a stud male each one for four days to allow mating. Then, future dams were housed one by one until the end of the experiment. Behavioural testing started 3-4 weeks after infection with the virus (FIGURE 12). The day of birth was considered as PPD0. In addition, litters were culled to 8 pups in PPD2.

In PPD4 and PPD5, after labour, dams were exposed during 5 minutes to a different male intruder. Prior to each behavioural test, female subjects were injected intraperitoneally (ip.) with either CNO (5 mg/kg, Enzo Life Sciences, Farmingdale, NY, USA) in saline (0.9%)/PBS or vehicle 30 minutes before the test. Each female was, therefore, confronted with a male once with and once without CNO treatment, counterbalanced on consecutive days. This dose and time of administration have been previously shown to activate DREADD receptors (Guettier et al. 2009; Ray et al. 2011; Sasaki et al. 2011; Unger et al. 2015; DiBenedictis et al. 2015; McCarthy et al. 2017b) (FIGURE 12).

All the behavioural tests were video-recorded and analysed by a researcher blind to the experimental conditions. The behavioural responses analysed were number and duration of attacks, anogenital approaches and body approaches, both from female to male and from male to female. All the behavioural tests were digitally monitored and analysed using SMART 3.0 video tracking system (Panlab, Barcelona, Spain).

Histological processing and immunohistochemistry

Animals were deeply anaesthetized with an intraperitoneal injection of sodium pentobarbital (100 mg/kg, Eutanax, Laboratories Normon S.A. Madrid, Spain) and perfused transcardially with saline solution (0.9%) followed by 4% paraformaldehyde (diluted in PB 0.1M, pH 7.6). Following perfusions, brains were removed from the skulls, post fixed for 24 hours in the same fixative medium and cryoprotected in 30% sucrose in PB (0.1M, pH 7.6) at 4°C until they sank. We used a freezing microtome to obtain sagittal sections through the olfactory bulbs and frontal sections (both sections of 40 µm) through the rest of the brain. In both cases, sections were collected in four parallel series in 30% sucrose.

One series of each brain was processed for the immunohistochemical detection of mCitrine (the DREADD fluorescent reporter) in free-floating sections. To do so, endogenous peroxidase was

inactivated with 1% H_2O_2 in Tris-buffered saline (TBS) (0.05M, pH 7.6) for 30 min at room temperature. Secondly, sections were incubated in blocking solution of TBS-Tx containing 3% normal goat serum (NGS) for 2 hours at room temperature. Then, sections were sequentially incubated in: a) chicken anti-GFP (green fluorescent protein; mCitrine is a variation of GFP) (ABCAM, Cat# ab13970) diluted 1:1000 in TBS-Tx with 2% NGS 72 hours at 4°C; b) biotinylated goat anti-Chicken IgY (ABCAM, Cat# ab6876) diluted 1:200 in TBS-Tx with 2% NGS for 2 hours at room temperature; c) ABC Elite (Vector, Cat# PK-6100) diluted 1:50 in TBS-Tx for 2 hours at room temperature. Finally, the resulting peroxidase labelling was revealed with SIGMA*FAST*™ DAB (Diaminobenzidine) tablets (Sigma-Aldrich Co. LLC, Cat# D4293) dissolved in 10 ml of distilled H_2O.

Sections were mounted onto gelatinized slides, dehydrated in alcohols, cleared with xylene and cover slipped with Entellan (Merck Millipore).

Statistical analyses

Statistical analyses were carried out using IBM SPSS Statistics 24.0. First, it was checked if the data fulfilled the conditions of ANOVA: normality (Kolmogorov–Smirnov test with Lilliefors' correction), homoscedasticity (Levene's test) and sphericity (Mauchly's test) of the data. If the data did not follow a normal distribution data was log-transformed (log [X + 1]). Data were analysed using an ANOVA of repeated measures with two factors: DAY (PPD4 and PPD5) as intra-subject factor and TREATMENT (treatment in PPD4) as between-subjects' factor. Statistically significant differences ($p \leq 0.05$) were further explored by means of post-hoc pairwise comparisons with Bonferroni's correction.

RESULTS

EXPERIMENT 1

EFFECT OF EXPERIENCE IN SOCIOSEXUAL SNIFFING AND AGGRESSION IN VIRGIN FEMALE MICE AND DAMS

This experiment was designed to study the possible behavioural changes of dams and godmothers when confronted with male intruders from PPD4 to PPD6.

First, we compared maternal aggression and sociosexual behaviours (anogenital and body approaches to males) in dams and godmothers by calculating for each animal the average duration of each behaviour across the three studied PPD days.

The Mann-Whitney test for non-parametric samples revealed statistically significant differences between both groups of females in all studied behaviours: total duration of attacks (FIGURE 13A), anogenital approaches (FIGURE 13B) and body approaches (FIGURE 13C) (U = 0; p =0.001; in all the behaviours).

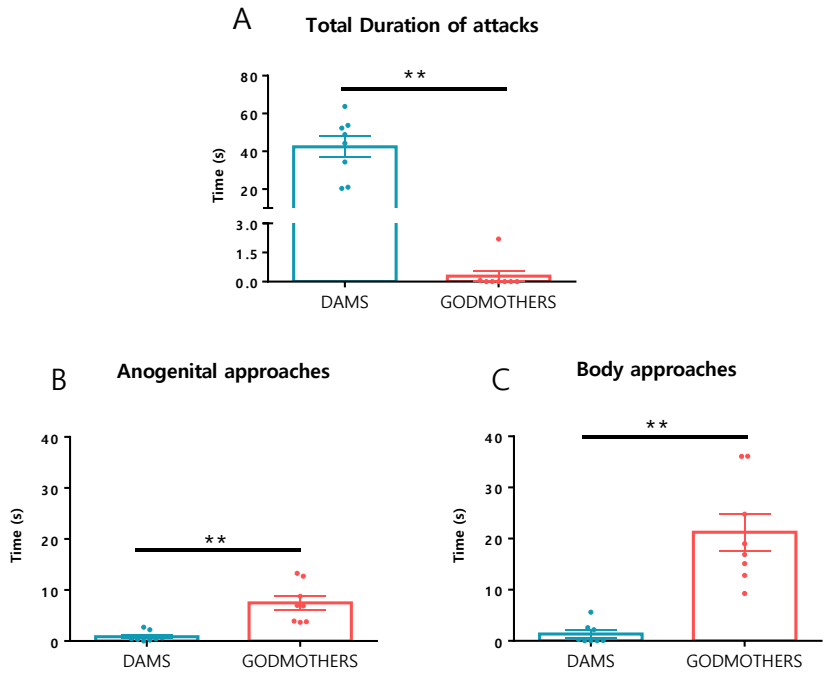

Figure 13: Levels of maternal aggression and sociosexual *behaviours were significantly different between both groups of females. A) Total duration of maternal aggression attacks was significantly different between studied groups. B) and C) Godmothers showed significantly longer duration of anogenital and body approaches to males. Data are represented as mean. ±SEM; **p< 0.01. Notice that ordinate axis scale change to show the differences between groups.*

Dams increase maternal aggression across the studied days

Regarding dams' total duration of attacks, repeated measures ANOVA showed a significant effect of DAY ($F_{2,6}$=9.988, p=0.012). Bonferroni post-hoc revealed a significant increase in the total levels of aggression between PPD4 and PPD5 (p=0.009) and significant differences between PPD4 and PPD6 (p=0.01) (FIGURE 14A).

An ANOVA of the mean duration of attacks also showed a significant effect of the factor DAY ($F_{2,6}$=10.074, p=0.012). Bonferroni post-hoc revealed significant differences between PPD4 and PPD5 (p=0.027) and between PPD4 and PPD6 (p=0.003) (FIGURE 14B).

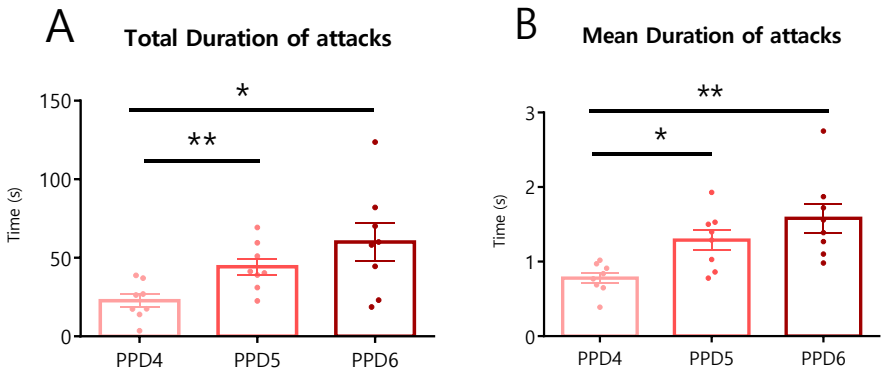

*Figure 14: Dams' levels of aggression significantly increased across testing days. A repeated measures ANOVA revealed a significant increase of the total duration of attacks performed by dams between PPD4 and PPD5 and PPD4 and PPD6 (A). Similar differences were observed in the mean duration of attacks (B). Data are represented as mean ±SEM; **p<0.01, *p<0.05.*

Regarding the latency to attack (FIGURE 15), the results of the repeated measures ANOVA of the log-transformed data showed a significant effect of the factor DAY (assuming sphericity, $F_{2,14}$=4.5, p=0.031). The Bonferroni post-hoc analysis revealed significant differences between PPD4 and PPD5 (p=0.042). Thus, dams were faster to initiate the attack during the second day of testing.

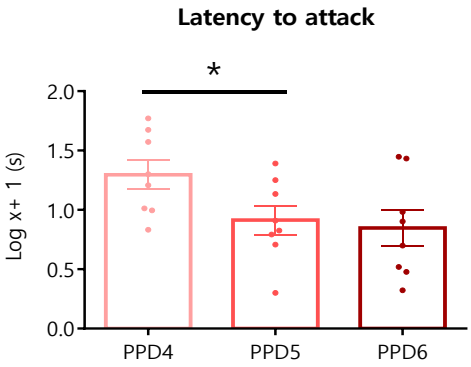

*Figure 15: The latency to first attack decreased significantly across testing days in dams. Data are log transformed and represented as mean ±SEM; *p<0.05.*

We then analysed the duration of individual attacks across PPD4 to PPD6, by classifying the attacks in three ranges: lasting <1s, between 1 and 5 s, and > 5 s. as The ANOVA revealed a significant effect of the factor RANGE ($F_{2,6}$ = 40.3, p < 0.001), as well as a significant interaction DAY × RANGE ($F_{2,6}$ =7.699, p=0.022). This interaction was further explored by analysing the simple effect of RANGE within each DAY. Bonferroni post-hoc revealed significant differences in the range of 1 to 5 seconds of attack between PPD4 and PPD6 (p=0.02) (FIGURE 16). Thus, not only dams increased the total duration of aggression across testing, but they displayed significantly more attacks of longer duration the last day of testing as compared to the first day.

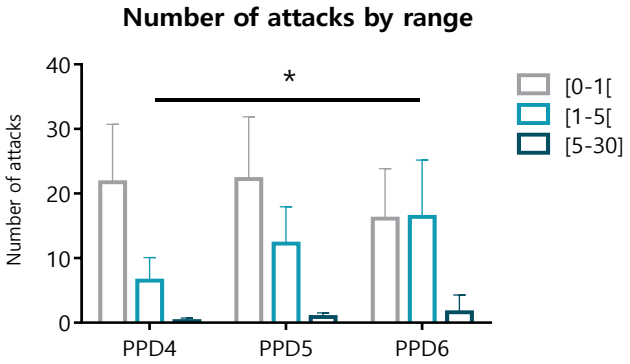

*Figure 16: The length of individual attacks increased significantly across testing days. The histogram of frequencies shows the number of attacks by range of duration (0 to 1 seconds, grey; 1 to 5 seconds, clear blue; 5 to 30 seconds, dark blue) displayed by dams (n=8) from PPD4 to PPD6. The number of attacks lasting between 1 to 5 seconds increased significantly in PPD6 as compared to PPD4. Data are represented as mean ± SD; *p<0.05.*

Dams display low levels of sociosexual sniffing

Since their aggressive behaviour was high, dams displayed very low levels of exploratory behaviour. In the case of ano-genital approaches, this decreased across testing days as aggression increased, as shown by the Friedman test for non-parametric samples ($\chi^2(2)$ =13, p=0.002). The post-hoc of Wilcoxon signed-rank tests with Bonferroni-adjusted significance level (α=0.017) revealed a trend toward significant differences between PPD4 and the other two days (p=0.018, highest than adjusted α) (FIGURE 17A).

Concerning to dams' approaches to males' body, there were no significant differences between the mean ranks of the related groups ($\chi^2(2)$ = 4.588, p=0.101) in the Friedman test (FIGURE 17B).

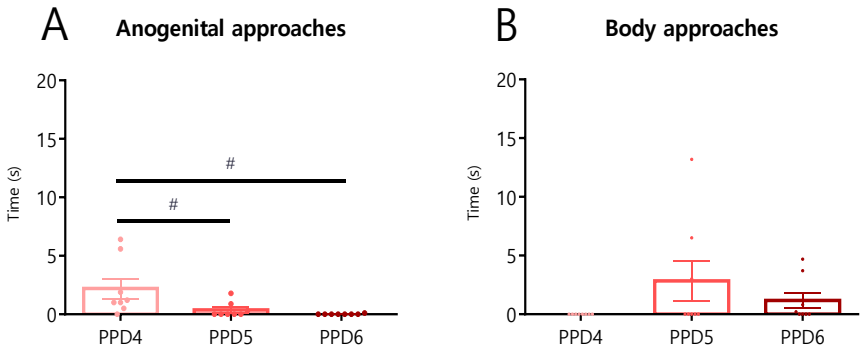

Figure 17: Dams display low levels of sociosexual behaviour across studied days. A) Anogenital approaches of dams tend to decrease between PPD4 and the other studied days. B) Body approaches did not significantly change across days. F: female; M: male. Data are represented as mean ± SEM; # p=0.018.

Godmothers do not display aggressive behaviours toward males

By contrast to dams, godmothers displayed sociosexual investigation but not maternal aggression toward males.

Regarding godmothers' aggressive behaviour, it was quite low (in fact, tending to 0), and the Friedman test for non-parametric samples did not revealed statistically significant difference between the mean ranks of the related groups ($\chi^2(2) = 0$, $p = 1$) in the total and mean duration of attacks (FIGURE 18A AND B).

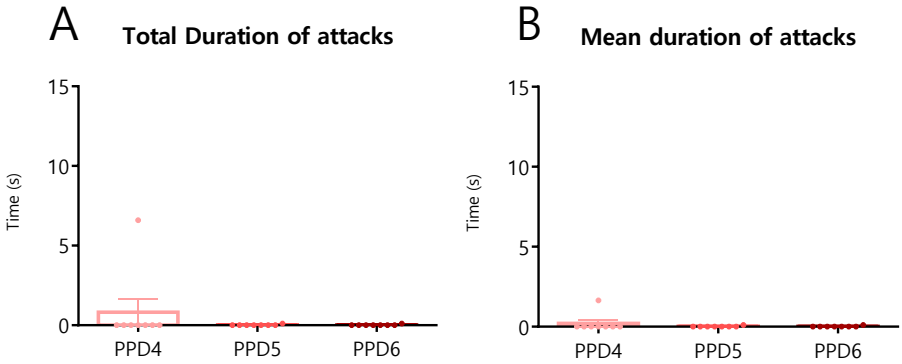

Figure 18: Godmothers did not display aggressive behaviour towards intruder males. A) Godmothers' total duration of attacks did not significantly change across days. B) The same happen with the mean duration of attacks. Data are represented as mean ± SEM. Notice that ordinate axis scale changes relative to Figure 7.

In the statistical analysis of godmothers' latency to attack, the Friedman test for non-parametric samples did not showed significant differences between the mean ranks of the related groups ($\chi^2(2) = 0.286$, $p = 0.867$) (FIGURE 19).

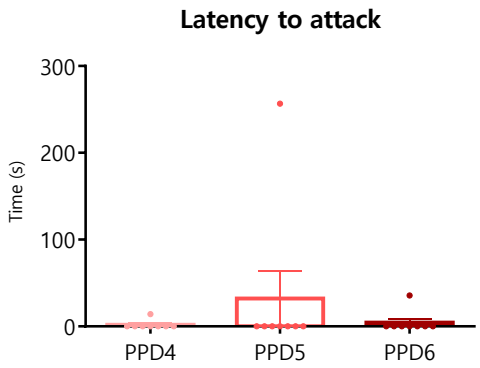

Figure 19: The latency to first attack did not change significantly across testing days in godmothers. Friedman *test did not reveal a significant difference in the latency to first attack between PPD4 and PPD6 in godmothers. Data is represented as mean ±SEM.*

Godmothers do not show significant differences in sociosexual sniffing across testing days

In the case of godmothers, neither ano-genital approaches to males ($F_{2.6}$ =0.33, p=0.967) (FIGURE 20A), nor body approaches ($F_{2.6}$ =3.537, p=0.097) (FIGURE 20B) were significantly different across testing days. Thus, sociosexual investigation of males did not change with repeated testing in godmothers.

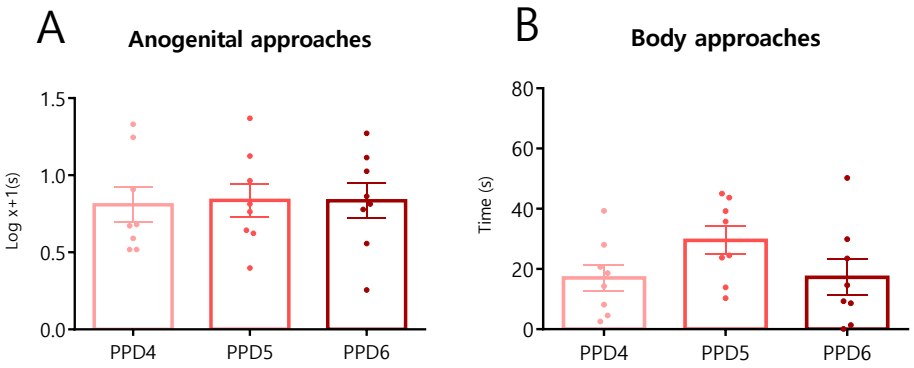

Figure 20: Godmothers showed sociosexual *interactions with intruder males, which did not change across testing days. Data are represented as mean ± SEM.*

Male sociosexual behaviours do not change across testing days

Males could spent little time displaying ano-genital approaches to lactating females, since they were extensively attacked, and the level of approaches did not differ across testing days ($\chi^2(2)$ =0,154, p=0,926) (FIGURE 21A). In addition, males could not display any investigation of the bodies of dams due to the high rate of attacks (FIGURE 21B).

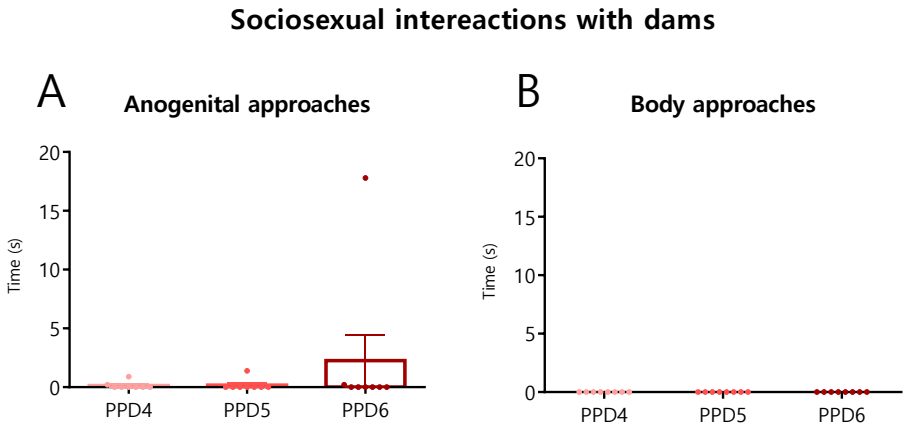

Figure 21: The behaviour of males was restricted due to the high aggression levels they suffered and did not change across sessions. Data are represented as mean ± SEM.

In the case of male ano-genital approaches to godmothers, the repeated measures ANOVA revealed a significant effect of the factor DAY ($F_{2.6}$ =7.485, p=0.023), but Bonferroni post-hoc did not show significant differences between the studied PPD (p>0.05) (FIGURE 22A). In the case of males' approaches to godmothers' body the repeated measures ANOVA revealed significant differences of the factor DAY ($F_{2.6}$ =0.845, p=0.475) but Bonferroni post-hoc did not show significant differences between the studied PPD (p>0.05) (FIGURE 22B). In conclusion, the behaviour of males did not change across testing days, and therefore the behavioural changes observed in females is unlikely to depend on how males behave.

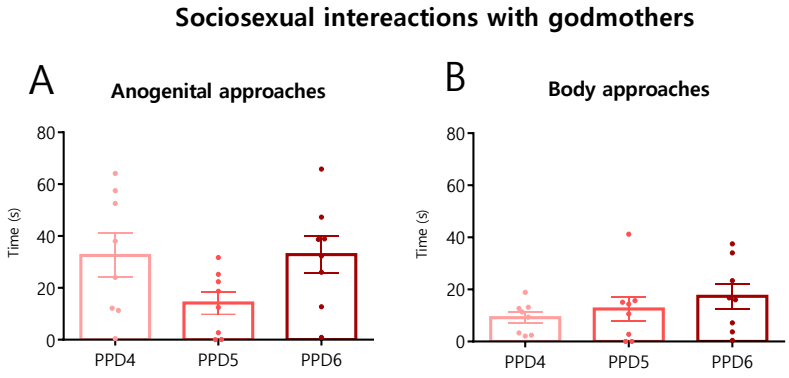

Figure 22: Males showed sociosexual *interactions with godmothers which did not vary across testing days. Data are represented as mean ± SEM.*

EXPERIMENT 2

EFFECT OF DREADD-INDUCED INHIBITION OF ME IN MATERNAL AGGRESSION

This experiment was designed to study the effect of Me inactivation in maternal aggression. Sixteen injections targeted the Me. The extent of the injection sites was considered as the area showing an intensely dark extracellular deposit of HRP reaction product (FIGURE 23).

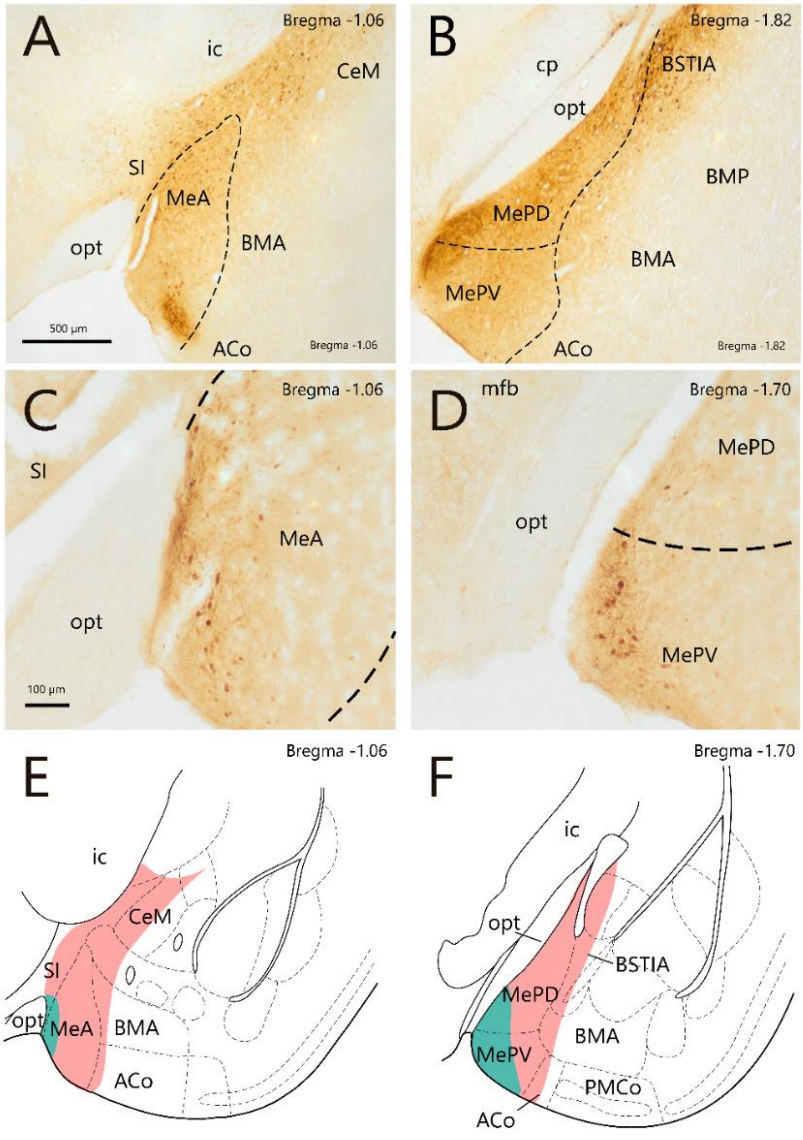

Figure 23: Injection sites in the Me showing the extent of the DREADD infections. Photomicrographs showing the rostro-caudal size of the biggest (A) and B)) and the smallest(C) and D)) injection included in the analysis. Scale bar A-B: 500 µm C-D:100 µm. E) and F) schematic reconstruction of coronal brain sections showing the extent of DREADD infections of photomicrographs A-D. Different coloured outlines represent the extent of Me infections for individual female subjects Orange: the biggest infection included in the behavioural analysis and green area: the smallest infection site. The brain drawings are modified from Paxinos & Franklin (2004). For abbreviation see list.

Regarding behavioural data, the repeated measures ANOVA of the log-transformed data of total duration of attacks showed a significant effect of the factor DAY ($F_{1,14}$= 14.416, p=0.003) and a significant interaction between the factors DAY and GROUP ($F_{1,14}$= 5.099, p=0.04) in the group with DREADD stereotaxic injections (TABLE 1). The Bonferroni post-hoc revealed a significant increase in total duration of attacks between PPD4 and PPD5 in DREADD-infected dams when CNO was injected in PPD4 (p=0.001), but not when CNO was injected on PPD5 (FIGURE 24A). Thus, although the inactivation of Me by means of DREADD/CNO was unable to block the expression of maternal aggression during the first encounter with the male intruder, Me inactivation prevented the increase in aggressive responses of dams in the second day of testing.

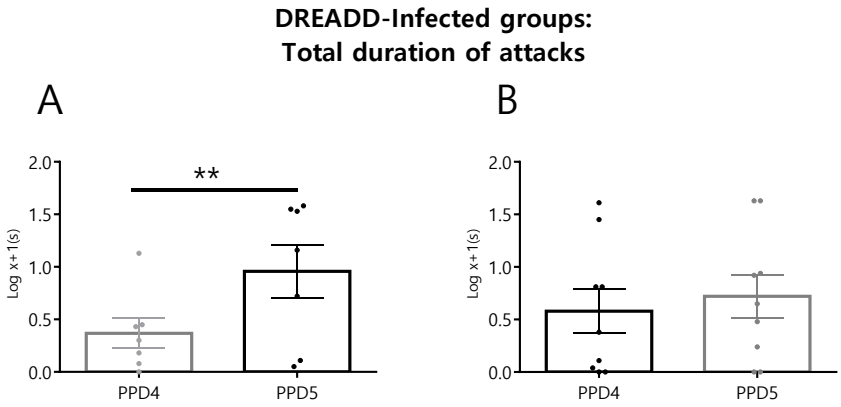

*Figure 24: Inactivation of Me blocked the increase of aggression levels during the second day of testing. A) DREADD-Injected group with CNO in PPD4. ANOVA showed significant differences between PPD4 and PPD5. B) DREADD-Injected group with CNO in PPD5. ANOVA did not reveal significant differences between studied days. Data are log transformed and represented as mean ±SEM; **p<0.01. Grey= CNO, Black=Saline/PBS.*

To discard that CNO had an effect per se, we run control groups without DREADD infection. In this case, the repeated measures of the log-transformed data of total duration of attacks revealed a significant main effect of the factor DAY ($F_{1,16}$ = 16.927, p= 0.001), and a non-significant main effect of GROUP or DAY X GROUP interaction (F < 1, p > 0.6; in both cases). The analysis of the simple effects of the factor DAY in each test showed that they were significant differences in aggression levels ($F_{1,16}$ = 16.927, p= 0.001) between the PPD4 and PPD5 (FIGURE 25A AND B). Thus, CNO injection per se did not affect maternal aggression.

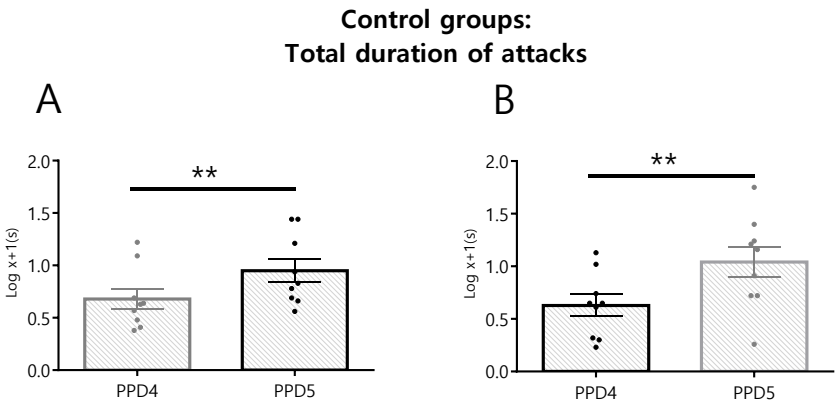

*Figure 25: CNO injection did not affect maternal aggression levels. The repeated measures ANOVA showed a significant increase of maternal aggression between PPD4 and PPD5 irrespective of the intraperitoneal injection. Control group with CNO in PPD4 (A); Control group with CNO in PPD5 (B). Data are log transformed and represented as mean ±SEM; **p<0.01. Control groups are represented with patterned column Grey= CNO, Black=Saline/PBS.*

DISCUSSION

In this study, we first characterized in depth the behavioural responses displayed by dams and pup-sensitized virgin female mice (godmothers) across three PPD days, PPD4 to PPD6, towards male intruders. Results show that the aggressive responses of dams are significantly increased across testing. Not only the average time spent by dams in attacking males was tripled from first to third day of testing, but also the duration of the individual attacks was significantly increased. By contrast, data confirmed that godmothers do not display maternal aggression, even after repeated exposure to male intruders.

Second, we tested the effect of inactivation of Me in maternal aggression by means of DREADD technology. Our results show that inactivation of Me in dams during the first day of testing do not abolish maternal aggression. However, Me inactivation during the second day of testing prevented the expected increase in aggression levels. Thus, our results reinforce the hypothesized role of Me in maternal aggression.

THE ONSET OF MATERNAL AGGRESSION NEEDS THE HORMONAL CHANGES OF PREGNANCY AND LACTATION

By contrast to dams, which readily fight an intruder male and even significantly increase aggressive behaviour across testing, godmothers were not aggressive towards males even after repeated exposure. Previously, work from our group showed that CD1 virgins sharing maternal care with dams did not attack males in a single maternal aggression test, even though they

displayed comparable, or even increased levels of pup-directed behaviours than dams (Martín-Sánchez et al. 2015b). Our current results confirm and extend these previous observations showing that godmothers do not develop maternal aggression even after a more extensive training, suggesting that, by contrast to maternal care, which can be induced by mere contact with the dam and the pups, maternal aggression needs both the physiological and hormonal changes occurring during pregnancy and/or lactation and contact with the pups.

REPEATED TESTING LEADS TO SIGNIFICANT INCREASE IN MATERNAL AGGRESSION

Our results show that the aggressive behaviour of dams increases significantly across three days of testing. This effect can be due to two non-exclusive possibilities. First, it is possible that repeated testing promotes learning, allowing the females to more readily identify the situation and improving the effectiveness of aggressive responses, and second, the hormonal profiles and/or changing pup features might modulate aggression across PPD. This latter possibility, however, is not very likely in our study, given the narrow period of our testing, from PPD4 to PPD6, during which pups are still absolutely dependant on the mother.

In this context, B. Svare & Gandelman, (1976a) tested lactating mice for aggression during 6 successive pregnancies and lactation periods, on PPD3, PPD7, PPD11, PPD15 and PPD19. They observed that aggression was very rarely displayed during pregnancy, but it appeared during PPD, and that the level of aggressiveness was similarly high during PPD3 and PPD7 and decreased as the lactation period advanced. These data showed that the highest levels of aggression are displayed during the initial period of lactation, when pups are still immobile and suckling is very frequent, as opposed to the final period of lactation, where pups start feeding by themselves, suckling is reduced and hormonal levels are returning to pre-partum levels. The fact that they did not find differences between PPD3 and PPD7 might be due to their design differing from ours in that they did not expose the dams on consecutive days. In this respect, it is also likely that we might had found that the aggression levels decrease across PPD, had we tested during the whole lactation period until weaning.

By contrast, male mice repeatedly exposed to an intruder increased the levels of aggression and decreased the latency to attack as compared to males exposed only once, although they were also tested in non-consecutive days (Parmigiani and Brain 1983). In this framework, previous studies have demonstrated that aggression between conspecifics have an important motivational component. They observed that male mice show a clear preference for aggression

only when aroused by prior aggression (Tellegen et al. 1969; Legrand 1970; Tellegen and Horn 1972). Thus, it is likely that the motivation to attack of the dams in our study is increasing across testing.

Another possibility, not excluding an increase in motivation, is the existence of a learning component in maternal aggression. In fact, in the case of sexual behaviour, it is known that receptivity, and in particular lordosis, increases with sexual experience (Thompson and Edwards 1971; Meisel and Mullins 2006; Ismail et al. 2011; McCarthy et al. 2017a). In this case, sensory cues from the male need to be integrated with the hormonal status of females to improve female receptivity (McCarthy et al. 2017b). This mechanism is likely to be similar to the one inducing an improvement in maternal aggression in lactating females.

Dams can recognize intruders by their pheromones and other cues, and they can distinguish between familiar males and females and intruders and only display attacks against the intruders (Svare and Gandelman 1976b). A previous study showed that the critical cue eliciting maternal aggression in CD1 dams is the pheromone *darcin* (Martín-Sánchez et al. 2015b), a protein found in the urine of gonadally-intact males which induces attraction and associative learning in virgin females (without pups or pregnant) and in males (Roberts et al. 2012). *Darcin* seems to activate a specific mechanism of associative learning so that instinctive attraction to spend time near this pheromone is extended both to its learned location and to airborne odours associated with the pheromone (Roberts et al. 2010). Thus, the integration of the innately aggressive-inducing (for dams) pheromone to other stimuli such as the sight or the smell of the intruder in the particular context of nest defence testing might facilitate learning and subsequently the selection and display of the appropriate behaviour.

A critical region involved both in the processing of pheromonal information and maternal aggression is the Me (Haller 2018). For example, c-FOS is increased in the Me in virgin females after exposure to male pheromones (Moncho-Bogani et al. 2005), and Me shows significantly higher c-FOS expression in lactating dams exposed to a male intruder than in virgins (Hasen and Gammie 2005). Thus, Me is a good candidate to be involved in the increase in aggression showed by experienced dams, as it is involved in the increase of lordosis in receptive females (McCarthy et al. 2017b).

Me presents feedback projections to AOB and MOB and projects to areas related with reproductive, defensive and aggressive behaviours (Pardo-Bellver et al. 2012; Cádiz-Moretti et al. 2013, 2016). Me subdivisions project to hypothalamic nuclei as AH, VMH and PMV (Van Berg et al. 1983; Fahrbach et al. 1989; Numan and Insel 2003b; Pardo-Bellver et al. 2012) and to septal regions as the ventral part (LSV) related all with defensive and aggressive behaviour (Swanson and Cowan 1979; Pardo-Bellver et al. 2012). In addition, Me presents a dense output to BST subnuclei (Pardo-Bellver et al. 2012) which play a role in different sociosexual behaviours and to MPO/A, a region related with the modulation of motivational behaviours as maternal behaviour (Chiba and Murata 1985).

The role of Me in aggression, and in maternal aggression in particular, has been studied before by Unger et al. (2015). They have proven the role of MePD aromatase neurons in the control of aggressive behaviours in male and female mice. In order to study the function of these aromatase neurons they employed a non-reversible genetic technique (cre-dependent Caspase-expressing viral vectors in cre-aromatase animals) to ablate this specific population of neurons. The bilateral ablation of MePD aromatase-expressing neurons produced a reduction of aggression events (in intermale and maternal aggression tests), but not in the total duration of attacks, suggesting that aromatase positive neurons in MePD play a role in initiating each attack event. These results suggest a common pathway in neural circuits of aggression regulated by steroid hormones (progesterone, oestradiol, etc.) and activated by different kind of stimuli. The results obtained in our study, showing that Me inactivation results in a reduction of maternal aggression in experienced dams are thus in agreement with the ones in Unger et al. (2015).

Taken together, data strongly suggest that Me is involved in controlling maternal aggression. The role of Me is likely related to the ability of the animals to process chemosensory signals of the intruders, such as *darcin*. Probably, by blocking Me activity, the relay of information to hypothalamic nuclei that trigger aggressive and motivational behaviours cannot occur (see nuclei connections in Figure 7.6 in Gutiérrez-Castellanos et al., 2010). The role of Me in mate recognition and mating behaviour in female mice (DiBenedictis et al. 2012) is consistent with the proposed role of Me in processing chemosensory signals.

As mentioned above, McCarthy et al., (2017) studied the role of Me in sexual behaviours and in the response to male chemosignals in virgin female mice. They observed that the inhibition of Me reduces the improvement in receptivity, as measured by lordosis quotient (percentage of

lordosis with respect to male mounting attempts) after a repeated exposure to a male (McCarthy et al. 2017b). This result mimics the lack of improvement of aggression after repeated exposure to a male upon inactivation of Me in dams observed in our data. The inactivation of Me is likely preventing the integration of pheromonal inputs in the sociosexual brain circuits, thereby altering the information being sent to downstream targets of the Me and affecting the control of female reproductive and maternal behaviours (Numan and Insel 2003b; Pardo-Bellver et al. 2012; Unger et al. 2015; McCarthy et al. 2017b).

METHODOLOGICAL CONSIDERATIONS

Several methodological considerations need to be taken into account with respect to the results of Experiment 2. First, we have included in our analysis dams with both ipsi and bilateral injections of DREADD, because we did not observe any statistically significant behavioural difference between these dams. This suggests that the inhibition of Me in only one hemisphere is enough to see a behavioural effect. In this respect, previous studies reported interhemispheric connections, observing that all three Me subnuclei are mainly ipsilateral but also they present few axons that cross the midline through the anterior commissure (Pardo-Bellver et al. 2012).

Second, previous studies using DREADD commonly use 2-3 weeks of recovery after viral injections, a period that ensures robust DREADD expression in most studied brain areas (Smith et al. 2016). However, in our design we injected the DREADD vector before mating, and given that pregnancy in mice takes 19-21 days, our experiments were carried out 3-4 weeks after viral injections. Anyhow, as can be appreciated in the histological figures, the expression of DREADD was detectable by means of immunohistochemistry. This, together with the behavioural effect, make us confident about the reliability of the technique.

Another aspect of DREADD technique that should be considered is the efficiency across serotypes. Here, we employed an AAV5, which is demonstrated to be very effective in the striatum, but less so in the cortex (Aschauer et al. 2013). Although, to our knowledge, there were not previous serotype efficiency studies in amygdaloid structures, previous DREADD studies in Me (McCarthy et al. 2017b) and Tu (DiBenedictis et al. 2015) they employed the same AAV5. In all, we observed a noticeable number of DREADD-infected cells (see FIGURE 23), so we are confident that inactivation of the Me was successful.

An additional concern with DREADD technology is the use of CNO, a drug that could potentially have some effects depending on the dose. First, the amount of stimulation required to elicit certain behaviours may be difficult to titrate precisely (Urban and Roth 2014). For our

experiments we employed 5 mg/kg of CNO injected 30 min prior to testing, the same dosage and time as previous study (DiBenedictis et al. 2015). Moreover, Mahler et al., (2014) tried different CNO dosage and determined that 5-10 mg/kg produces maximal behavioural effects through a number of assays, viruses, and neuronal pathways.

In addition, CNO produces behavioural effects in male Long–Evans rats due to CNO itself or to the conversion to clozapine and N-desmethylclozapine (MacLaren et al. 2016), highlighting the need to control for the effect of CNO injection in the DREADD-expressing animals. To do so, we used two groups of non-operated animals which received either CNO or saline in first or second testing days, counterbalanced. Our results show no significant differences between maternal aggression in both groups of animals, and very similar levels of aggression to DREADD-infected animals injected with saline. However, it is important to note that total duration of attack of dams in Experiment 1 (increased aggression across testing days) was higher than in Experiment 2. Thus, whereas in Experiment 1 the average duration of attack was 20 seconds in the first day of testing and 50 s in the second day of testing, in Experiment 2 these were reduced around four times on average in all groups in Experiment 2. Moreover, the duration of attack in Experiment 1 is comparable to that showed in previous experiments from our group (Martín-Sánchez et al. 2015b, a). This reduction in aggression may be in part caused by the stress provoked by handling and ip. injection, and not by surgery, since similar durations were expressed by all the groups of experiment 2. In this framework, it is not unlikely that low levels of aggression might be causing a floor effect, masking a possible further reduction in aggression provoked by DREADD inactivation during the first day of testing.

CONCLUSIONS

In summary, our results show that maternal aggressiveness during the first third of lactation increases after repeated testing. In addition, data confirm that, in mice, and at least in our experimental conditions, maternal aggression cannot be induced in pup-sensitized virgins, even when they are in continuous contact with pups (godmothers) and after extensive training. Thus, this behaviour might need the hormonal changes that take place during pregnancy and lactation, which are probably shaping the brain and preparing it for motherhood (Salais-López et al. 2017). A candidate area that might suffer these changes, as our data and previous reports suggest, is the Me. In our study, chemogenetic inhibition of Me blocked the expected increase in maternal aggression during the second day of training (FIGURE 26).

Finally, it is known that there is an important hormonal regulation which control the neuroendocrinological changes that allow maternal behaviour (Numan and Insel 2003a) and which can be acting in the Me (Salais-López et al. 2017). This hormonal regulation is likely to produce significant changes in gene expression patterns in the Me of dams, which we study in the next chapter by means of RNA-seq (RNA-sequencing) technology.

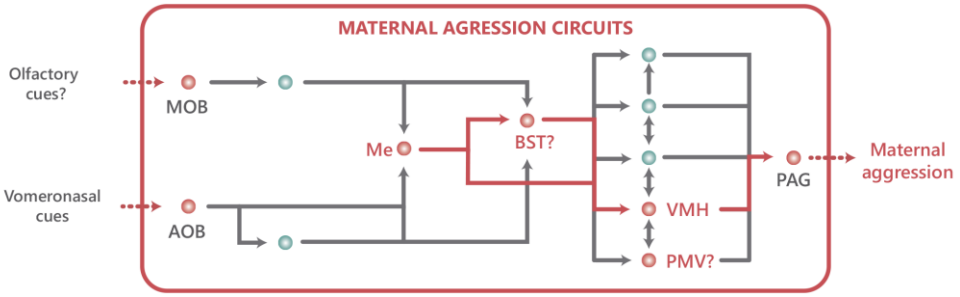

Figure 26: Representation of the Social Brain Network (SBN) nuclei involved in aggression in dam mice. Circuits involved in female maternal aggression including our recent results of Me key role in the display of this behaviour. Coloured nuclei and connections in red represent circuits with direct experimental evidence for the corresponding behaviour. Nuclei with interrogation symbol (?) are probably involved in the behaviour but further studies are needed. For abbreviations see list. Adapted from Chen and Hong (2018).

CHAPTER II

MATERNAL BEHAVIOUR AND CHANGES IN GENE EXPRESSION IN MEDIAL AMYGDALA

INTRODUCTION

As seen in Chapter I, maternal behaviour is only displayed by lactating females, even though pup sensitized females display all the rest of maternal behaviours (Lonstein and Gammie 2002; Martín-Sánchez et al. 2015b, a). Also, our results reveal that the Me plays a key role in the brain circuit mediating maternal aggression in female mice.

In general Me is implicated in the control of aggression (Koolhaas et al. 1990; Sano et al. 2013; Wang et al. 2013; Unger et al. 2015), parental care (Bridges 1996; Morgan et al. 1999; Numan and Insel 2003b; Weber and Olsson 2008), inter- sexual recognition (Ferguson et al. 2001; Moncho-Bogani et al. 2005; Bergan et al. 2014) and mating (Hari Dass and Vyas 2014), as well as in other behaviours and physiological processes. The control of these functions is carried out by different subdivisions of Me. Thus, MeA is connected with structures implicated in defensive, agonistic and reproductive behaviours (Dong and Swanson 2004), MePD with structures implicated in reproductive behaviours (Canteras et al. 1992, 1995; Simerly 2002; Pardo-Bellver et al. 2012; Cádiz-Moretti et al. 2016), and MePV with structures involved in defensive behaviours (Canteras 2002; Lonstein and Gammie 2002; Pardo-Bellver et al. 2012; Cádiz-Moretti et al. 2016).

In spite of its central position in the vomeronasal sensory pathway and its importance for social communication, little is known about the physiological changes happening in the Me during pregnancy and lactation that, potentially, could underlie the change in significance of male pheromones from attraction-inducing in virgin females to aggression-inducing in dams. Thus, in this chapter we aim at filling this gap by analysing the changes induced by motherhood in the Me transcriptome by means of RNA-seq.

MATERIAL AND METHODS

EXPERIMENT 1

RNA- SEQUENCING (RNA-SEQ) IN THE MEDIAL AMYGDALA OF DAMS AND GODMOTHERS

Animals

For this experiment, we used 20 adult mice (*Mus musculus*) from the CD1 strain (females, n=12; males, n=8, Janvier; Le Genest Saint-Isle, France). The animals were 8-12 weeks old and weighed between 27.2-49.1 g at the beginning of the experiments. Females were randomly assigned to

two groups: dams (n=6) and godmothers (n=6). The group of dams were housed individually with a stud male during four days for mating. The day of birth was considered as PPD0, and in PPD2 litters were culled to 8 pups. Godmothers were pair-housed with dams after mating. Thus, godmothers were continuously exposed to pups and they shared maternal caregiving with the accompanying dams (Martín-Sánchez et al. 2015b). Animals were housed in cages with water and food available *ad libitum* with 12 h light: dark cycle at 22-24°C. Mice were treated according to the guidelines of the European Union Council Directive of September 22nd, 2010 (2010/63/UE). All of the experimental procedures were approved by the Committee of Ethics on Animal Experimentation of the University of Valencia.

Behavioural tests and medial amygdala microdissection

All females were exposed at PPD4 or PPD5 during 5 minutes to an intruder male in their home cage. Pups were separated during behavioural testing to avoid any damage (FIGURE 27). Behavioural testing was video-recorded and a researcher who was blind to the experimental groups analysed the number and duration of attacks that females directed towards males. All the behavioural tests were digitally monitored and analysed using SMART 3.0 video tracking system (Panlab, Barcelona, Spain).

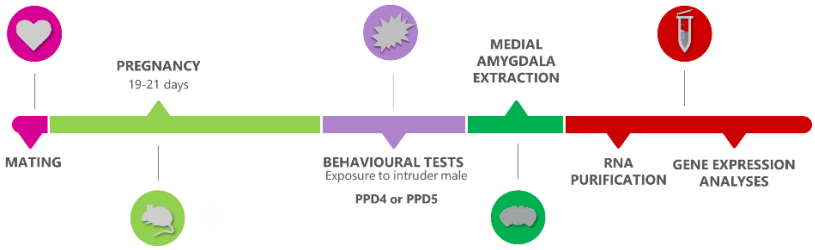

Figure 27: RNA-seq tests timeline.

At the end of the behavioural test, animals were sacrificed by cervical dislocation, between 11:00 and 12:00 am, and the brain was removed for Me microdissection (FIGURE 28A). The brain tissues were dissected rapidly in ice-cold Dulbecco's Phosphate Buffered Saline (PBS; Cat# L0615, Biowest), flash-frozen in liquid nitrogen, and maintained on dry ice until storage at –80°C (FIGURE 27). The microdissection of the Me of both hemispheres was done following histological landmarks in a 1mm-thick slice obtained by positioning the brain in a stainless-steel brain matrix with a coronal cut of 1 mm (FIGURE 28B). Then, under a stereoscopic microscope, two incisions were made, one following the optic tract (*opt*) and the other tracing an approximately dorsoventral straight line (FIGURE 28C). The approximate stereotaxic coordinates of the microdissected tissue (relative to Bregma, from the mouse brain atlas of (Paxinos and Franklin

2004), were: A-P: -0.7 mm to -2.06 mm, M-L: -2 to -2.2 mm and D-V: -4.2 mm to the ventral surface of the brain (FIGURE 28).

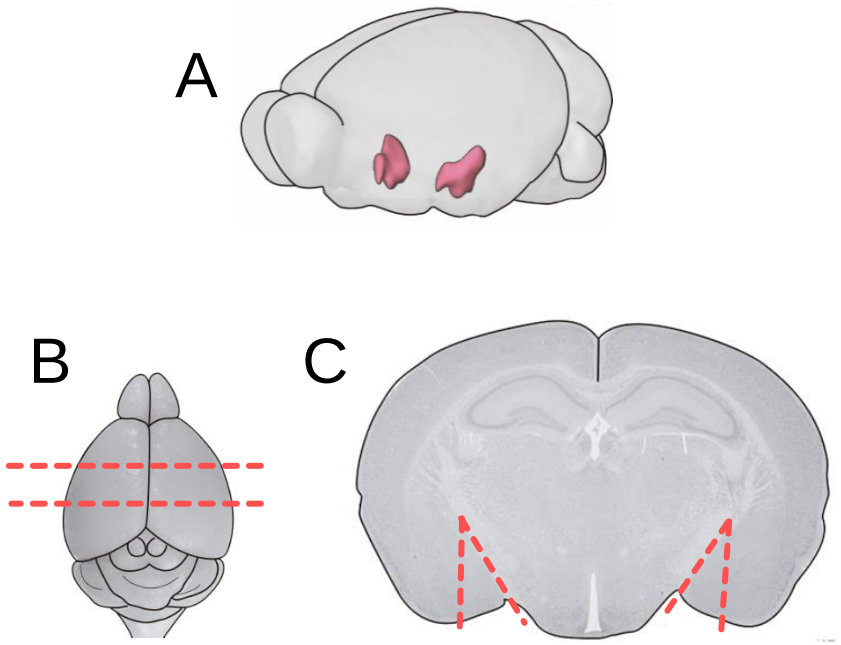

Figure 28: Representation of Me microdissection. A) Me 3D representation modified from The Brain Explorer 2 software (Allen Institute for Brain Science). B) Dorsal view of mouse brain. C) Coronal view of a mouse brain section through the Me. Modified and adapted from Paxinos & Franklin (2004). In the figures B and C, the dashed lines represent the cuts carried out for Me microextraction. Bregma levels: A-P: -0.7 mm to -2.06 mm, M-L: -2 to -2.2 mm and D-V: -4.2 mm to the surface of the brain. For abbreviations see list.

After the microdissection, the 1mm-thick brain slice was post-fixed overnight in 4% paraformaldehyde, embedded in 15% gelatine in phosphate buffer (PB) RLT, and cut in the freezing microtome in 40 micrometer–thick sections. The resulting sections were Nissl-stained to validate histologically the microdissection of the Me (FIGURE 29).

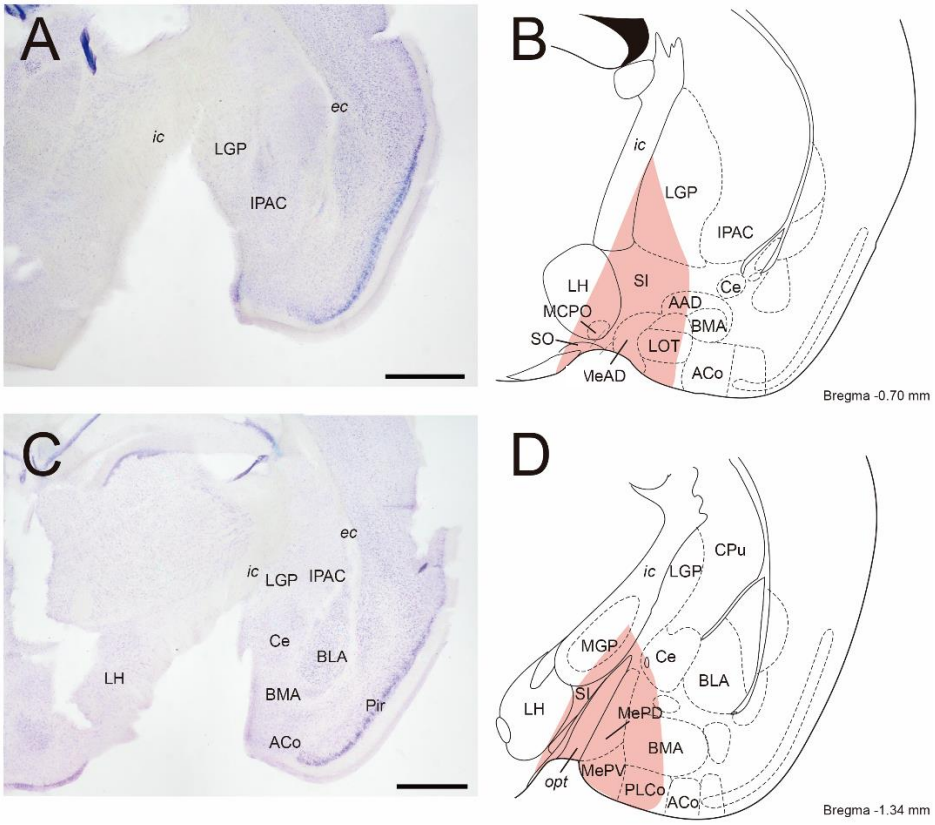

Figure 29: Example of Me microextraction showing the extent of the sample. Photomicrographs showing the rostro-caudal seizure of the microextraction (A) and C)) included in the analysis. Scale bar A-C: 1mm. B) and D) schematic reconstruction of coronal brain sections showing the extent of microextraction of photomicrographs A-C. The coloured outline represents the extent of Me extraction for individual female subject. The brain drawings are modified from Paxinos & Franklin (2004). For abbreviation see list.

RNA extraction

Total RNA from dissected Me was isolated using the RNeasy Mini kit (Qiagen, Cat# 74104). Frozen brain tissue was homogenized in β-mercaptoethanol (SIGMA, Cat# M3148) with RLT buffer (RNeasy Mini kit) according to the manufacturer's protocol (10 µl β-mercaptoethanol per 1 ml of Buffer RLT). Genomic DNA contamination was eliminated following the RNase-Free DNase Set steps (Qiagen, Cat# 79254). Total RNA was eluted from the RNeasy Mini columns with 40 µl of RNase-free water (Qiagen, Cat# 129112). The amount of total or mRNA isolated from the tissue was assessed for quality and quantified using Bioanalyzer 2100 (Agilent). Eight females (dams n=4; godmothers n=4) with the highest levels of aggression (dams) and RNA integrity number (RIN) (Mueller and Schroeder 2004) were selected for RNA-seq analysis.

Illumina sequence read mapping and analyses

RNA-seq was performed at the Genomic core facility of the Universitat de València (Secció de genómica-SCSIE). Libraries were obtained using the Illumina® TruSeq® Stranded mRNA Sample

Preparation Kit. Cluster generation and sequencing was done in a NextSeq 500 instrument using a High Output kit 1x75 bp.

Initial quality checks on the Illumina sequencing data were done using FastQC v0.11.3 (http://www.bioinformatics.babraham.ac.uk). Adaptor sequences were trimmed with Cutadapt software (version 1.8.3, Martin, 2011). Sequencing data were filtered by discarding reads of fewer than 20 nucleotides and more than 30 undetermined nucleotides.

The *Mus musculus* reference genome was obtained from Ensembl (Flicek et al. 2014). A total of 375237009 bp single-end reads were generated from the 8 RNA samples (average of 46904626 reads per sample). The processed Illumina reads were mapped to the reference genome using the Tophat alignment tool (Trapnell et al. 2009; Kim et al. 2013), version 2.0.8, which uses Bowtie2 as its underlying alignment algorithm (Langmead and Salzberg 2012).

The obtained sam files were compressed into the bam files using samtools (Morgan M, Pagès H, Obenchain V 2018). The count matrix was calculated using Rsamtools, GenomicFeatures (Lawrence et al., 2013) and GenomicAlignments (Lawrence et al. 2013) (ANNEX I).

The parameters of Tophat were set to their default values. The –GTF option was used to provide Tophat with a set of gene model annotations (note that we are using Rsamtools). Genes with a positive count for any sample were included in the study.

To analyse differential gene expression, the edgeR statistical package was used (Bioconductor version 3.0.2) (Robinson et al. 2010). To determine whether a gene was differentially expressed in dams *vs.* godmothers, a common dispersion parameter was assumed and estimated. The results obtained with this model are explained in the present study.

Additionally, another analysis with a different dispersion parameter per gene was carried out, too, but the analysis with this model did not provide reliable results (it has to be considered that samples size was small). The results of this analysis were not considered further.

The raw p-values obtained with the edgeR method were transformed to adjusted p-values by using the Benjamini-Hochberg correction in order to control the false discovery rate (FDR) (Benjamini and Hochberg 1995). Genes that were differentially expressed determined using an FDR equal or below to 0.05 are displayed in ANNEX II, TABLE 1A AND B). The genes with non-significant are shown in the ANNEX II, TABLE 1C).

Gene set analysis includes evaluation of genetic expression of genes that are grouped based on their interacting role in biological pathways (biological pathway analysis) and genes that share similar cellular functions (functional gene set analysis). Gene Ontology was used to obtain the gene set collection. The self-contained null hypothesis (Goeman and Bühlmann 2007) was tested using permutation tests. This null hypothesis establishes that the gene set considered does not contain any genes which expression levels are associated with the phenotype of interest. Statistical significance was estimated using permutation tests. The significant groups, using an FDR equal to 0.05, are displayed in (ANNEX III, TABLE 2).

Validation of the dissection

First, we performed a histological validation of the dissections by means of the analysis of the Nissl-stained sections obtained after the Me extraction (FIGURE 29). In addition, we performed a literature survey to identify genes specifically expressed in the Me (Pavlidis and Noble 2001; Brown et al. 2006; Medina et al. 2017). The same strategy was carry out with the Allen Brain Atlas (Lein et al. 2006). The genes expressed in Me that are gathered from the literature search and from the Allen Brain Atlas were compared with the list obtained in the RNA-seq (ANNEX IV).

Finally, we selected those genes with most significant p-values and some of special interest for maternal behaviour and validated their differential expression by means of Quantitative PCR (qPCR).

EXPERIMENT 2

VALIDATION OF GENES OF INTEREST SHOWING DIFFERENTIAL EXPRESSION IN DAMS AND GODMOTHERS BY MEANS OF QPCR

Animals

For this experiment, we used 22 adult female mice (*Mus musculus*) from CD1 strain (Janvier; Le Genest Saint-Isle, France). Animals were 8-12 weeks old and weighed between 25.8-48.2 g at the beginning of the experiments. The animals were randomly assigned to three groups: dams (n=7), godmothers (n=7) and virgins (n=8), and housed in cages (dams and godmother in pairs as in Experiment 1) with water and food available *ad libitum* with 12 h light: dark cycle at 22-24°C. Mice were treated according to the guidelines of the European Union Council Directive of September 22nd, 2010 (2010/63/UE). All the experimental procedures were approved by the Committee of Ethics on Animal Experimentation of the University of València.

Microdissection and RNA extraction

Animals were sacrificed by cervical dislocation and the brain was removed for Me microdissection (FIGURE 30). All of the procedures for Me microdissection and the subsequent RNA isolation were the same as those used on the Experiment 1 (See sections 2 and 3 of Experiment 1) (FIGURE 28).

The RNA concentrations were quantified with Qubit™ 3.0 Quantitation Starter Kit (Invitrogen™, Cat# Q33217). The Qubit™ RNA HS Assay Kit (included in the Starter Kit) was used for measuring RNA concentration, and calibration was performed using a two-point standard curve. The relationship between the two standards and a curve-fitting algorithm was used to calculate the concentrations of the RNA samples.

cDNA was produced in triplicate from each sample (to minimize error and ensure accurate replication of RNA pool) using SuperScript™ III Reverse Transcriptase (Thermo Fisher Scientific, Cat# 18080093) according to the manufacturer's instructions. For each sample, 132 ng of total RNA was transcribed.

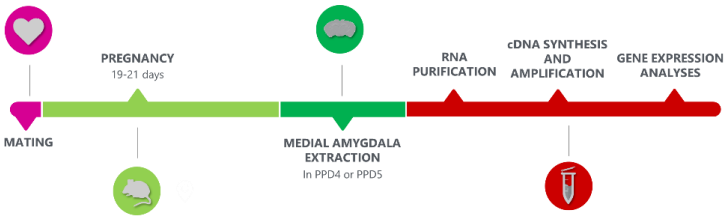

Figure 30: qPCR study timeline.

Quantitative PCR protocol

The primers used in qPCR reactions were designed using Primer3Plus software (Untergasser et al. 2007) (Laboratories Conda). Primers were designed to span an intron–exon boundary (to exclude genomic amplification) and to amplify a product between 50 and 150 bp (TABLE 2).

Table 2: Sequences of primers used for qPCR. The amplicon size is in base pairs.

GENE	FORWARD	REVERSE	AMPLICON
Prl	atcaatgactgccccacttc	ctgcaccaaactgaggatca	105
Oxt	ccatcacctacagcggatct	ccgaggtcagagccagtaag	94
Prlr	tgcttacatgctgcttgtcc	cttgtcaggggaacgacatt	94
Gal	accgagagagccttgatcct	agggtcacaaccaacaggag	112
Stat5b	gccctcaggctcactacaac	tcggtatcaaggacggagtc	58

qPCR was performed using Green™ Premix Ex Taq™ polymerase (Takara Bio Group, Cat# RR420A) in a 10 µl reaction volume, using 2 µl cDNA reaction, 0.4 µl of primers and 0.2 µl of ROX reference dye, following manufacturer's instructions. Master mixes were made for each pair of primers and cDNAs were added independently. Briefly, following an enzyme activation step for 30s at 95°C, we performed 40 cycles of 15s denaturation step at 95°C, 34s annealing at 56°C, and 15s extension at 95°C, and fluorescence data collection at the end of the denaturation step. Melt-curve analysis followed each run with ramping from 50º to 95°C, with fluorescence data collection in 0.5°C increments. Each sample, comprising cDNA from one animal, was run in triplicate.

Data analysis

Quantification was based on the number of PCR cycles (Ct) required to cross a threshold of fluorescence intensity. The results were analysed with the delta delta Ct method (ΔΔCt) which is a convenient way to analyse the relative changes in gene expression from real-time quantitative PCR experiments (Schmittgen and Livak 2008; Bustin et al. 2009). Data point was calculated for each animal as the average of the three replicates (after excluding outliers in which Ct diverged more than 0.5 from the average of the other two). The Ct data for each studied gene was normalized to the Ct values of the housekeeping gene (*Actinβ*) to obtain the ΔCt values for each animal. ΔCt indicates the difference between the number of cycles of the gene of interest and those of *Actinβ*. The ΔCT values of the two experimental groups, dams and godmothers, were normalized to the ΔCt mean of virgin's samples, giving a ΔΔCt value. This was converted into expression fold change using the $2^{-\Delta\Delta Ct}$, called relative quantification (RQ) (Goni et al. 2009; Bustin et al. 2009; Jozefczuk and Adjaye 2011).

Statistical analyses

Statistical analyses were carried out using IBM SPSS Statistics 24.0. Firstly, it was checked if the data fulfilled the conditions of ANOVA: normality (Shapiro-Wilk) and homoscedasticity (Levene's test) of the data. If the data did not follow a normal distribution a log-transformation (log [X]) was performed. Data were analysed using a one-way ANOVA with the factor GROUP. Statistically significant differences ($p \leq 0.05$) were further explored by means of post-hoc pairwise comparisons with Fisher's Least Significant Difference. When the distribution was not normal even with the logarithmic transformation the non-parametric Kruskal Wallis test was used with pairwise comparison (Dunn-Bonferroni) as post-hoc test. If the homogeneity of variance could

not be assumed, we carried out the Welch and Brown-Forsythe ANOVAs with the Games-Howell pairwise comparison post-hoc test.

RESULTS

EXPERIMENT 1

RNA- SEQUENCING (RNA-SEQ) IN THE MEDIAL AMYGDALA OF DAMS AND GODMOTHERS

Behavioural tests

This experiment was carried out to select the dams with higher levels of maternal aggression for RNA-seq studies. The comparison of the total duration of attacks showed that four of the females displayed high levels of maternal aggression (FIGURE 31 in green), whereas the other two animals showed low levels of aggressive behaviour (less than 2 seconds, FIGURE 31 in red). Therefore, the dams with higher levels of aggression and the godmothers which shared the home cage with them were selected for RNA-seq studies.

In addition to behaviour, after the RNA extraction, RIN value of these highly aggressive dams was checked to discard animals with RIN lower than 8. The results showed that all the highly aggressive dams and their respective godmothers presented RIN values above 8 (data not shown). As in the experiments described in Chapter 1, godmothers did not display aggression towards males (data not shown).

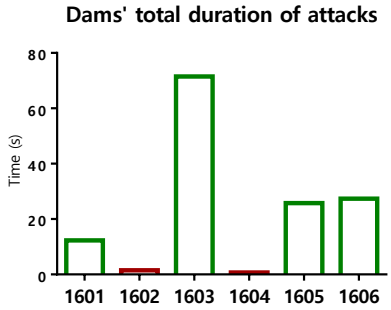

Figure 31: Dams' aggression levels. The bar chart shows the dams individual levels of aggression when they were exposed to an intruder male. In green the dams selected for RNA-seq studies, and in red the rejected animals.

Histological study

The Nissl preparations of the tissue were studied under the microscope to check the extractions. The Me was completely extracted in all the studied cases. The coordinates described above

(Material and methods: Experiment 1) ensured that all Me subdivisions (MeA, MePD and MePV) were fully included in the extractions (Example of one animal microextraction FIGURE 29).

It is important to remark that some nuclei adjacent to Me were partially microdissected in most of the cases. At rostral levels, the nearest aspects of the *substantia innominata* (SI), lateral *globus pallidus* (LGP) and internal capsule (*ic*) were affected by the incisions. In the rostral amygdala, parts of the anterior amygdaloid area, LOT, BAOT, and ACo were encompassed, to some extent, by the microdissected tissue. More caudally, parts of BMA, the central amygdala (Ce), the intraamygdaloid division of the bed nucleus of the *stria terminalis* (BSTIA), PMCo, and the amygdalohippocampal area (AHi) were also included. In addition, extra-amygdaloid structures located medial to the microdissection, such as the supraoptic nucleus (SO), *opt*, the lateral hypothalamic area (LH) and the magnocellular preoptic nucleus (MCPO) were pulled out partially in some animals.

Differential gene expression in medial amygdala

The differential gene expression analysis using edgeR, with an adjusted p value <0.05, yielded a total of 296 differentially expressed genes in the Me. From these, 197 genes were upregulated in dams as compared to godmothers, and 99 were downregulated. The full list of genes with significant differential expression between dams and godmothers is presented in TABLE 1A AND B of ANNEX II . In these tables, genes were classified depending on their Fold Change (FC), in other words, depending on how much they were upregulated or downregulated in dams with respect to godmothers.

Genes upregulated in dams

Some of the most strongly upregulated genes, according to the fold change, were related to maternal behaviour and lactation. Specifically, within these genes related with maternal behaviour, prolactin (*Prl*) and growth hormone (*Gh*) were the ones with more upregulated expression in dams with respect to godmothers. Other genes coding for peptides previously reported to be involved in maternal behaviour were also upregulated, including oxytocin (*Oxt*) and galanin (*Gal*). In addition, other genes related to *Gh* and/or *Prl* such as the growth hormone releasing hormone receptor (*Ghrhr*), the transcription factor POU domain, class 1, transcription factor 1 (*Pit-1* or *Pou1f1*) and the cytokine inducible SH2-containing protein (*Cis or Cish*) were also more expressed in dams than in godmothers (TABLE 3).

By contrast, other genes important to social and maternal behaviour such as prolactin receptor (*Prlr*), arginine vasopressin receptor 1A (*Avpr1a*), and arginine vasopressin (*Avp*) did not obtain significant values of FDR (adjp >0.05) (ANNEX II, TABLE 1A). Further, signal transducer and activator of transcription 5 (*Stat5*), which is a main factor in the intracellular signalling cascade activated by PRL, did not appear in the list of genes expressed in Me.

Moreover, some genes related with reproductive hormones or involved in the reproductive cycle were also significantly upregulated in dams. These genes included the follicle stimulating hormone beta (*Fshb*), the alpha subunit of glycoprotein hormones (*Cga*), which encodes the follicle-stimulating hormone (FSH) α subunit, the gonadotropin releasing hormone receptor (*Gnrhr*) and the gonadotropin releasing hormone 1 (*Gnrh1*) (TABLE 3).

Table 3: Overview of significant upregulated genes in dams with respect to godmothers. Genes are ordered according to their fold change (FC) in each group. Raw p-values (ANNEX II, TABLE 1A) were transformed to adjusted p-values (adjp).

Group		Gene	FC	adjp
Maternal behaviour		*Prl*	27.8	$2{,}66\text{x}10^{-188}$
		Gh	27.47	$1{,}15\ \text{x}10^{-187}$
		Ghrhr	23.59	$3{,}77\text{x}10^{-34}$
		Pou1f1	8	$2{,}21\text{x}10^{-10}$
		Oxt	1.75	$4{,}82\text{x}10^{-06}$
		Gal	1.56	$1{,}31\text{x}10^{-02}$
Reproductive hormones		*Fshb*	14.32	$2.21\text{x}10^{-10}$
		Cga	11.16	$4.04\text{x}10^{-50}$
		Gnrhr	8.51	$1.30\text{x}10^{-07}$
		Gnrh1	2.45	$3.24\text{x}10^{-02}$
Neurotransmission	*Cholinergic*	*Chrnb3*	2.81	$1{,}99\text{x}10^{-07}$
		Chrna6	2.64	$7{,}03\text{x}10^{-04}$
		Chat	2.16	$1.13\text{x}10^{-10}$
		Ngfr	1.93	$3.45\text{x}10^{-08}$
		Chrna2	1.58	$1.30\text{x}10^{-02}$
		Chrm2	1,43	$2.47\text{x}10^{-02}$
	Catecholaminergic	*Adra2b*	1.90	$1.47\text{x}10^{-02}$
		Th	1.58	$3.94\text{x}10^{-03}$
		Pomc	2.30	$2.43\text{x}10^{-11}$
		Pmch	1.86	$2.43\text{x}10^{-11}$
		Rxfp2	1.74	$4.16\text{x}10^{-02}$
	Glutamatergic	*Trpv1*	8.34	$1.29\text{x}10^{-12}$
Cell adhesion		*Siglece*	3.10	$1.87\text{x}10^{-04}$
Others		*Tbx19*	12.13	$6.24\text{x}10^{-03}$
		Pitx1	8.11	$2.73\ \text{x}10^{-14}$
		Vmn2r-ps159	7.06	$3.17\text{x}10^{-03}$
		Cis	1.47	$4.47\ \text{x}10^{-02}$

A third group of genes overexpressed in dams (ANNEX II, TABLE 1A) were related with different kinds of neurotransmission. Among them, we found several genes related with cholinergic

neurotransmission, such as the choline acetyltransferase (*Chat*), several subunits of the nicotinic receptor, including the beta polypeptide 3 (*Chrnb3*), the alpha polypeptide 6 (*Chrna6*), and the alpha polypeptide 2 (neuronal) (*Chrna2*), and the cardiac muscarinic 2 subunit (*Chrm2*). In addition, the nerve growth factor receptor (TNFR superfamily, member 16) (*Ngfr*) a p75 neurotrophin receptor, which is expressed in the cholinergic neurons of the basal telencephalon, was upregulated in dams (TABLE 3).

Another group of genes with significantly different expression in the Me of dams were the ones related with catecholaminergic pathways. Within these genes, the alpha 2b adrenergic receptor (*Adra2b*) and the tyrosine hydroxylase (*Th*) were upregulated in dams with respect to godmothers (TABLE 3)

The Me of dams also showed significant differences in the regulation of genes involved in peptidergic neurotransmission. One of these overexpressed genes in dams is the proopiomelanocortin-alpha (*Pomc*). This gene codifies for proopiomelanocortin (POMC), which is cleaved in different peptides as adrenocorticotropic hormone (ACTH). the alpha-, beta-, and gamma-melanocyte stimulating hormones (α-, β-, and γ-MSH) and β-endorphin. Also, the pro-melanin-concentrating hormone (*Pmch*) was upregulated in the Me of dams. On the other hand, relaxin/insulin-like family peptide receptor 2 (*Rxfp2*) was expressed more in dams than in godmothers (TABLE 3), however, the relaxin 3 gene (*Rln3*) did not obtained significant differences in expression between dams and godmothers (adjp >0.05) (ANNEX II, TABLE 1C).

In addition, the transient receptor potential cation channel, subfamily V, member 1 (*Trpv1*), which is involved in the glutamatergic neurotransmission, was also overexpressed in dams (see Discussion) (TABLE 3).

Genes related with cell adhesion showed significant differences between dams and godmothers in the Me. The sialic acid binding Ig-like lectin E (*Siglece*) was significantly more expressed in dams than godmothers (TABLE 3).

Finally, a surprising finding within the genes obtained in the RNA-seq was the T-box 19 (*Tbx19*) which appears to be selectively expressed in precursors of the corticoptrope/melanotrope lineages and in the rostral ventral diencephalon, which may act as a component of the POMC gene activation program; the paired-like homeodomain transcription factor 1 (*Pitx1*) which its protein acts as a transcriptional regulator involved in basal and hormone-regulated activity of PRL; the vomeronasal type 2 receptor, pseudogene 159 (*Vmn2r-ps159*) and the cytokine

inducible SH2-containing protein (*Cis or Cish*) which play a role in the regulation of activator of transcription protein-5 (STAT5) signalling. All these genes are upregulated in dams with respect to godmothers (TABLE 3).

Genes downregulated in dams

The most downregulated genes in dams compared with godmothers were inhibin Beta-C (*Inhbc*) and E (*Inhbe*) (TABLE 4). Moreover, the activating transcription factor 3 (*Atf3*) was significantly downregulated in dams. *Atf3* is a member of the mammalian activation transcription factor/cAMP responsive element-binding (CREB) protein family of transcription factors (TABLE 4).

Furthermore, it is important to highlight that some genes related with cell activation were significantly downregulated in dams. Some of these genes were the FBJ osteosarcoma oncogene (*Fos*), the FBJ osteosarcoma oncogene B (*Fosb*) (TABLE 4) and several members of the early growth response family, such as the early growth response 1 (*Egr1*), early growth response 2 (*Egr2*), early growth response 3 (*Egr3*) and early growth response 4 (*Egr4*) (TABLE 4).

Table 4: Genes most downregulated in dams in contrast with godmothers. Genes are ordered in each group according to their negative fold change (-FC). Raw p-values (ANNEX II, TABLE 1B) were transformed to adjusted p-values (adjp).

Group	Gene	-FC	adjp
Inhibins	*Inhbc*	238.86	$2.06x10^{-180}$
	Inhbe	35.51	$1.02x10^{-33}$
Transcription factors	*Atf3*	2.95	$6.01x10^{-10}$
Early-expression genes	*Egr2*	2.69	$8.89x10^{-19}$
	Fos	2.13	$9.33x10^{-09}$
	Egr4	2.11	$3.06x10^{-11}$
	Fosb	1.93	$2.67x10^{-11}$
	Egr1	1.77	$1.13x10^{-06}$
	Egr3	1.41	$3.42x10^{-02}$

Bibliographic survey

The genes obtained in the RNAseq were compared with those previously reported as expressed in the Me (according to the literature survey described in the Methods). Some of the genes that matched with the literature were overexpressed in dams with respect to godmothers, including: *Oxt*, ISL1 transcription factor, LIM/homeodomain (*Isl1*), inter-alpha trypsin inhibitor, heavy chain 3 (*Itih3*) and NK2 homeobox 1 (*Nkx2.1*).

On the other hand, *Avp*, adenylate cyclase activating polypeptide 1 (*Adcyap1*), neuritin 1 (*Nrn1*) and prostaglandin D2synthase (*Ptgs2*), glycerophosphodiester phosphodiesterase domain

containing 2 (*Gdpd2*), delta like non-canonical Notch ligand 1 (*Dlk1*), aromatase or cytochrome P450, family 19, subfamily a, polypeptide 1 (*Cyp19a1*) and neuro-oncological ventral antigen 1 (*Nova1*) concur with the bibliography as genes expressed in Me. However, these genes did not show significant differences in expression between studied groups (adjp>0.05) (TABLE 5).

Table 5: Common genes in the present Results that correspond with the bibliography survey. Genes are ordered in each group according to their fold change (FC). Raw p-values (ANNEX IV, TABLE 3) were transformed to adjusted p-values (adjp).

Group	Gene	FC	Adjp
With differential expression between groups	*Oxt*	1.75	$3.6x10^{-03}$
	Nkx2.1	1.61	$3.6x10^{-03}$
	Isl1	1.57	$7.41x10^{-03}$
	Itih3	1.40	$3.89x10^{-02}$
Without differential expression between groups	*Dlk1*	1.26	$4.51x10^{-01}$
	Avp	1.25	$5.16x10^{-01}$
	Nova1	1.22	$7.13x10^{-01}$
	Gdpd2	1.21	$8.30x10^{-01}$
	Adcyap1	0.84	$9.05x10^{-01}$
	Nrn1	0.82	$6.51x10^{-01}$
	Ptgs2	0.79	$3.73x10^{-01}$
	Cyp19a1	0.78	$9.17x10^{-01}$

Group analysis

To facilitate the global analysis of gene expression, the significantly differentially expressed genes were assigned to different functional categories using gene ontology (GO) assignments (Ashburner et al. 2000). The study of functional groups (ANNEX III, TABLE 2) gives several groups of genes with significant differential expression, among which it is important to remark the positive regulation of the Janus kinase/signal transducers and activators of transcription (JAK/STAT) cascade and the negative regulation of ERK1 and ERK2 cascade, because of the relation with the study (p<0.01).

EXPERIMENT 2

VALIDATION OF GENES OF INTEREST SHOWING DIFFERENTIAL EXPRESSION IN DAMS AND GODMOTHERS BY MEANS OF QPCR

As mentioned in the methods section, selected RNA-seq results were validated using qPCR. In addition, qPCR studies were carried out in in other genes involved in maternal behaviour which showed no differential expression in the RNA-seq studies. Thus, the expression changes among lactating females, godmothers and virgins in the Me were evaluated in 5 different genes related with maternal behaviour.

Prolactin

The study of *Prl* RQ values in the Me showed significant differences among studied groups, validating the result obtained in the RNA-Seq experiment. Since the normality tests showed that the data were not normally distributed, even if log-transformed, the non-parametric Kruskal-Wallis test was used, and it revealed significant differences between the mean ranks (p=0.007) of at least one pair of groups. The Dunn's pairwise post-hoc test showed significant differences between the group of dams and the group of virgins (p=0.005, adjusted using the Bonferroni correction) (FIGURE 32A). The difference between dams and godmothers with this analysis did not reach statistical significance (p = 0.24), and the same result was obtained comparing godmothers and virgins (p =0.7).

Since in the RNAseq experiment we could not include a group of virgin females, to run a direct comparison the RNAseq and the qPCR results we ran a statistical test comparing the expression between dams and godmothers without considering the group of virgins. The data of these two groups (dams and godmothers) followed a normal distribution so a t-test for independent samples was carried out. The t-test showed a tendency towards higher levels of *Prl* expression in dams than in godmothers (p= 0.066) (FIGURE 32B).

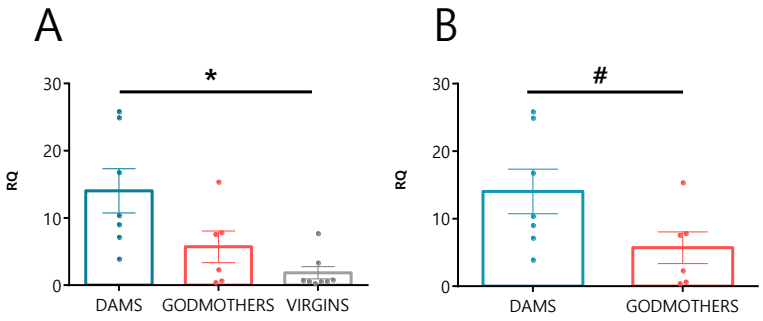

*Figure 32: Changes in Prl expression levels (RQ) between groups showed significant differences. A) A Kruskal-Wallis test revealed significant differences in expression between dams and virgins. B) The t-test between dams and godmothers showed a tendency between groups. Data are represented as mean ±SEM; *p≤0.05; #p ≈ 0.066. For abbreviations see list.*

Galanin

The analysis of the *Gal* expression using a one-way ANOVA did not show a significant effect of GROUP ($F_{2,18}$=0.705, p>0.05) (FIGURE 33).

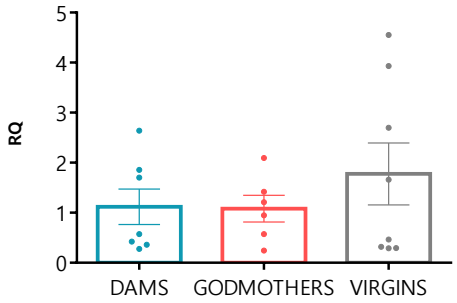

Figure 33: The three studied groups of females did not differ in Gal RQ. Dams, godmothers and virgins did not change significantly their RQ levels. Data are represented as mean ± SEM. For abbreviations see list.

Oxytocin

In the case of *Oxt*, the one-way ANOVA of the log-transformed data revealed a significant effect of the factor GROUP ($F_{2,18}$=4.065, p=0.035) and the Fisher's Least Significant Difference showed significant decrease in the group of godmothers with respect to the other two groups of females (dams p=0.022; and virgins p=0.021) (FIGURE 34).

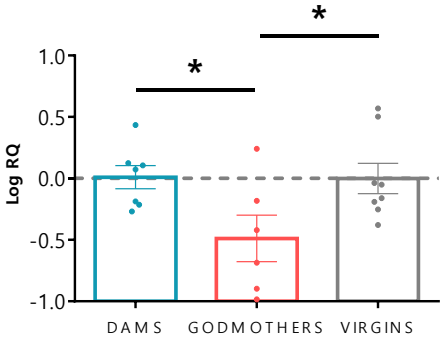

*Figure 34: Oxt showed significant differences in levels of expression (RQ) between godmothers and the rest of the groups. The one-way ANOVA revealed significant differences in expression between godmothers and dams and godmothers and virgins. RQ values are log-transformed. Data are represented as mean ±SEM; Fisher's Least Significant Difference post-hoc significance is represented; *p≤0.05. For abbreviations see list.*

Prolactin receptor

Expression levels of *Prlr* according to RQ did not show significant differences between the studied groups, according to the one-way ANOVA of the log-transformed data (factor GROUP: $F_{2,19}$=0.310, p>0.05) (FIGURE 35).

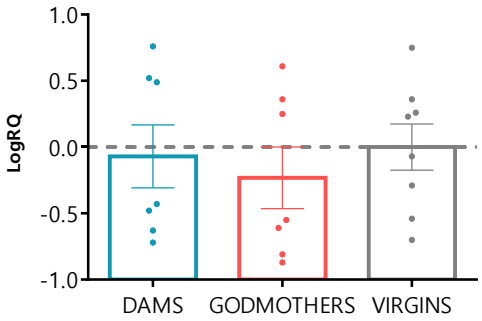

Figure 35: The three studied groups of females did not differ in Prlr RQ log-transformed data. Dams, godmothers and virgins did not change significantly their RQ levels. Data are represented as mean ± SEM. For abbreviations see list.

Signal transducer and activator of transcription 5b

The normality and homogeneity of variances of the RQ values of signal transducer and activator of transcription 5b (*Stat5b)* were checked, and the Levene's test showed that variances were not equal (p=0.028). The Welch ($F_{2,10.03}$= 4,867, p=0.033) and Brown-Forsythe ($F_{2,11.56}$= 5,817, p= 0.018) ANOVAs revealed a highly significant effect of the factor GROUP. Games-Howell post-hoc showed a significant decrease in the expression of *Stat5b* in godmothers with respect to virgins (p= 0.037) (FIGURE 36).

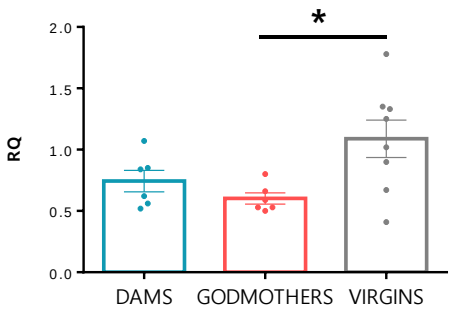

*Figure 36: Stat5b levels of expression were significantly higher in virgins than in godmothers. The one-way ANOVA revealed significant differences in expression between godmothers and virgins. Data are represented as mean ±SEM; Games-Howell post-hoc significance is represented; *p<0.05. For abbreviations see list.*

DISCUSSION

The goal of this study was to determine the changes in gene expression in the medial amygdaloid region of the female mouse brain that result from pregnancy, parturition, and postpartum maternal experience. These results show that gene expression in the Me changes during the lactation.

Specifically, we found that there are 197 genes upregulated in dams *vs* godmothers in Me and other 99 genes with higher expression in the group of godmothers compared with lactating females (summarized in TABLE 3 and TABLE 4). The differentially expressed genes in Me may have an important functional role in the display of maternal behaviour, especially in the case of maternal aggression, since godmothers do not express this behaviour (Lonstein and Gammie 2002). In addition, these genes may be related with the physiological state of the females.

OVEREXPRESSED GENES

Several of the most upregulated genes in the Me of dams are related with maternal behaviours (FIGURE 37). In this group we can find the *Prl*, which increase in dams was validated by qPCR, supporting the differences between dams and virgin females. *Prl* expression was observed previously in the hypothalamus of male and female rats (Schachter et al. 1984; Emanuele et al. 1992; Clapp et al. 1994). In addition, the expression of *Prl* was observed in other brain structures as the cerebellum, caudate, brain stem, amygdala, thalamus, cortex and hippocampus (Emanuele et al. 1992) and also in the neurohypophysis (Clapp et al. 1994). Among the structures positive for *Prl,* the degree of expression was found to be very different (Emanuele et al. 1992). Moreover, the sequence of the *Prl* mRNA expressed in the brain and that expressed in the anterior pituitary gland is identical, although this study was carried out only in male rats (Wilson et al. 1992).

Previous studies have observed an increase in *Prl* mRNA expression in the hypothalamus of pregnant and lactating rats in comparison to virgin females (Torner and Neumann 2002; Torner et al. 2002). This increase in the hypothalamus may indicate a general activation of the brain PRL system in the peripartum period to sustain its reproductive and non-reproductive functions in the CNS (Torner and Neumann 2002). The overall activation of the brain PRLergic system in dams is consistent with our observation of a significant increase in *Prl* mRNA in the Me.

The presence of *Prl* mRNA in Me suggests that this protein is being synthetized in this amygdaloid nucleus. These results are consistent with previous studies (Cabrera-Reyes et al. 2017). However, the presence of PRLergic somata has not been reported in Me (Toubeau et al. 1979a, b; Hansen et al. 1982; Harlan et al. 1989; Siaud et al. 1989; Paut-Pagano et al. 1993). By contrast, the presence of positive fibres for PRL were observed previously in this nucleus (Toubeau et al. 1979a). In addition, other authors studied the concentration of PRL in different brain regions, obtaining positive results in the extended amygdala (DeVito 1988).

Previous studies have demonstrated that mRNAs can be transported outside the cell body most probably in proximal dendrites but also in some of their branching, and possibly at synaptic contacts (Bloch et al. 1990; Alvarez et al. 2002). Also recent publications have proven that protein synthesis can be carried out in the pre and postsynaptic terminals (Hafner et al. 2019). For this reason, since it is known that mRNA can be carried far into axons by axoplasmic transport, it is likely that at least some of the extrahypothalamic *Prl* mRNA represents transcripts carried into projection fields by the transport process (Emanuele et al. 1992). This is consistent with colchicine studies which blocks axoplasmic transport, leading a significantly increased PRL protein in hypothalamus, where the majority of PRLergic somata are placed (DeVito 1988; Emanuele et al. 1988). PRL somata were also observed in extrahypothalamic regions as the BST (Siaud et al. 1989) which projects to the Me (Cádiz-Moretti et al. 2016). For all these reasons, it can be suggested that *Prl* can be transported into the terminal in Me, allowing the synthesis of PRL in this nucleus. Therefore, in next chapters we will study the presence of PRL in the Me, and compare the possible differences between lactating and virgin females.

In vitro studies suggest that the oestrogen response of the *Prl* gene requires a functional "unit" involving several factor-binding sites, the oestrogen receptor and the tissue-specific transcription factor, *Pit-1* (Nowakowski and Maurer 1994) also *Pou1f1*. Expression of *Pit-1* mRNA was detected previously by qPCR in the Pa of oestrous rats, but not of other cycling females or male rats (Torner et al. 1999). Detection of *Pit-1* mRNA in the Pa during oestrus coincides with previous suggestion that both *Pit-1* and the oestrogen receptor are required for the effect of oestrogens on *Prl* gene expression (Nowakowski and Maurer 1994; Torner et al. 1999). Our study is the first one describing the expression of *Pit-1* in Me (TABLE 3) which is upregulated in dams.

In addition, the transcription of the pituitary *Gh* gene is also dependent upon *Pit-1*, since growth hormone (GH) synthesis fails to occur in its absence (Pfaffle et al. 1992; Voss and Rosenfeld 1992). The presence of GH in the brain was previously studied by Hojvat, Baker, Kirsteins, & Lawrence, (1982) by radioimmunoassay in male and female rats and macaques and they observed the presence of the protein in the amygdala. This regulation pathway coincides with our study, where we observed an upregulation of *Prl*, *Gh* and *Pit-1* in the Me of dams with respect to godmothers. Moreover, the extra-pituitary expression in the adult mammalian CNS of GH and PRL is coordinated at mRNA and protein levels. However, a wide interindividual variation was superimposed on coordinate PRL/GH expression (Daude et al. 2016). The presence in our study of the genes (*Gh* and *Prl*) and the transcription factor (*Pit*-1) in the Me can result in an increase of the synthesis of PRL and GH. In addition, this interindividual variation in mRNA expression

was also observed in our experiments, and within each experimental group we observed females with very different levels of *Prl* expression (FIGURE 32).

These three genes (*Gh, Prl* and *Pit-1*) involved in maternal behaviour are also related with others which are also upregulated in dams as *Pitx1*, *Tbx19, Ghrhr, Fhsb and Cga* (FIGURE 37) (ANNEX II AND TABLE 1A). It has been shown before that *Pitx1* and *Tbx19* cooperate in order to transcribe *Pomc*, the two factors binding to contiguous sites within the same regulatory element in the corticoptrope/melanotrope lineages and in the rostral ventral diencephalon and in the pituitary gland (Liu et al. 2001; Bancalari et al. 2012). In addition, *Pitx1* with others transcriptional regulators are required for terminal differentiation of lactotroph cells and direct regulation of the PRL gene in the pituitary gland (Tremblay et al. 1998; Quentien et al. 2002). All these genes were not described previously in the Me of female mice. *Ghrhr, Fhsb and Cga* are discussed below.

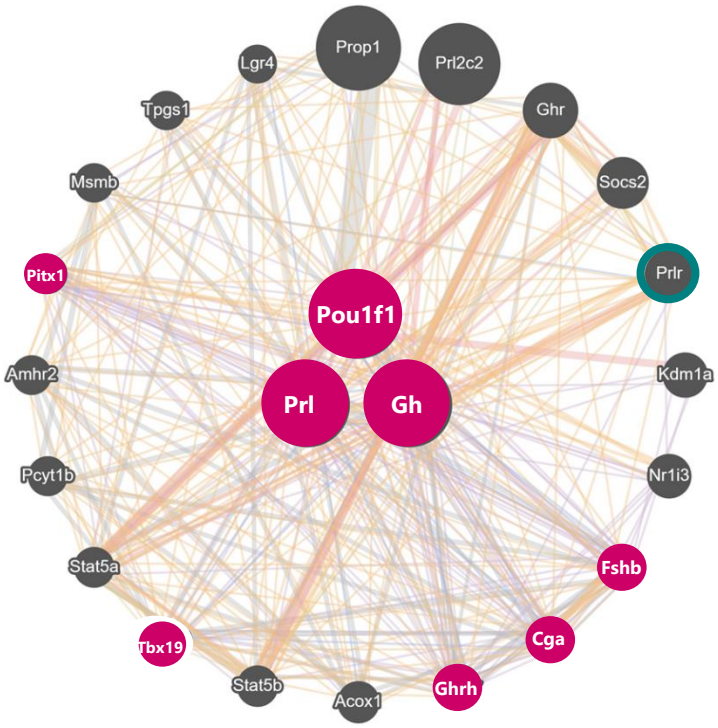

Figure 37: Overview of Pou1f1, Prl and Gh signalling intersection with other genes in Mus musculus. The graph shows with circles in pink the genes significantly upregulated in mothers with respect to godmothers and with green circles non-significant genes that appear in the list of RNA-list (see section A non-significant genes of Annex II). Graph was designed using GeneMANIA (Warde-Farley et al. 2010). For GeneMANIA network colour categories see http://pages.genemania.org/help/. For abbreviations see gene list.

PRL, after binding to its receptor, activates the signal transducer and STAT5 by phosphorylation (pSTAT5), which regulates transcription (Yip et al. 2012) (FIGURE 38). Me levels of pSTAT5 indicate an increase to PRL and GH response (Furigo et al. 2016; Salais-López et al. 2017) and it was

observed that this PRL response was higher in pregnant and lactating females compared to virgin females (Salais-López et al. 2017). This can be related to the increase of *Prl* and *Gh* mRNA observed in our study and its posterior translation to PRL and GH in Me (Toubeau et al. 1979a, b; Hojvat et al. 1982; Harlan et al. 1989; Siaud et al. 1989; Paut-Pagano et al. 1993).

Other important physiological regulation that takes place during lactation is the loss of sensitivity to PRL negative feedback in the tuberoinfundibular dopaminergic (TIDA) neurons, which is necessary to maintain hyperprolactinaemia in the mother (Freeman et al. 2000). This inhibition occurs because suckling stimulus increases hypothalamic mRNA expression of CIS (also known as CISH), a member of the Suppressor of cytokine signaling family (SOCS) of proteins, known to negatively regulate PRL signalling through JAK/STAT (FIGURE 38) (Pezet et al. 1999; Krebs and Hilton 2000). Indeed, previous studies have demonstrated that all TIDA neurons in the dorsomedial arcuate nucleus of the hypothalamus (Arc) express CIS protein, and that CIS levels in TIDA neurons are increased in lactating rats in the presence of suckling (Anderson et al. 2006b). In our results we observed an overexpression in dams of *Prl* and *Cis*, probably suggesting that the PRL negative feedback can be inhibited in the Me with the same molecular mechanism of TIDA neurons. This can also be related with the lack of upregulation of *Stat5* in our RNA-seq results. In addition, our results in qPCR (FIGURE 36) show that virgin females present a significant increase of *Stat5b* with respect to godmothers. Although the significance of this finding is uncertain, the high levels of Stat5 expression in virgins may be related with the low levels of brain and serum PRL in this physiological state. In the absence of the ligand (PRL), the expression of other elements of signalling cascade, such as STAT5b, can be upregulated.

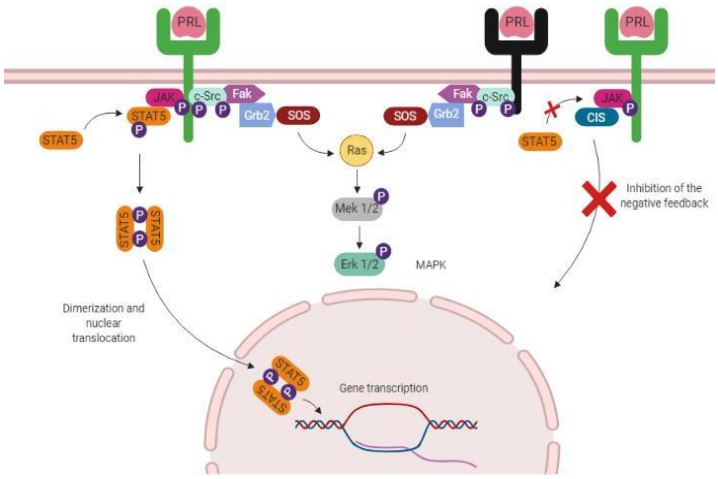

Figure 38: Diagram of the multiple signal transduction pathways mediating the action of PRL. The major pathway mediating PRL action is the JAK/ STAT5 pathway, activated by the long form of the PRLR (green) (Freeman et al. 2000; Bridges and Grattan 2019). The short form of the receptor (black) has a truncated intracellular domain that lacks the STAT binding residues but can MAPK pathway independently from

JAK/STAT pathway. The JAK/STAT pathway can be inhibited by SOCS (not shown) which inhibit JAK kinases (Krebs and Hilton 2000; Freeman et al. 2000) or CIS, which compete with STAT for docking sites on PRLR (Pezet et al. 1999). Adapted from Bridges & Grattan (2019) and Freeman et al. (2000). For abbreviations see list. The image was made with BioRender.com.

Another adaptation in dams CNS are the changes related with the neuroendocrine and behavioural stress responses. These adaptations include activation of brain oxytocyn (OXT) and PRL systems, which act to attenuate the HPA axis activity and emotional responsiveness in the peripartum period, coupled with a dampening of opioid and noradrenergic systems, which are the main excitatory inputs of the HPA axis (Freeman et al. 2000; Slattery and Neumann 2008). Related with this, in our result we also observe that *Oxt* expression is upregulated in dams with respect to godmothers in RNA-seq study (TABLE 3) and in the qPCR analysis (FIGURE 33).

Furthermore, previous studies have suggested that OXT neurons express *Prlr* mRNA and are PRL-sensitive as well, because almost all OXT neurons express pSTAT5 during lactation (Augustine et al. 2018). Indeed, phosphorylated STAT5 is expressed by almost all OXT neurones of late-pregnant and lactating rats but is almost absent from OXT neurones in virgin rats (Augustine et al. 2016). PRL can also regulate the expression level and release of OXT in lactating females (Ghosh and Sladek 1995; Augustine et al. 2018) and it is hypothesised that OXT stimulates PRL secretion by the pituitary gland triggering a positive-feedback loop (Kennett and Mckee 2012). Probably this increase in transcription of *Prl* is the reason why we observed an upregulation of *Oxt* in the Me in RNA-seq and qPCR studies in dams with respect to godmothers (FIGURE 7 and FIGURE 31 and TABLE 3). Unexpectedly, the qPCR analysis showed that the levels of *Oxt* in virgins were equivalent to those in dams. Although the significance of this finding is unknown, we hypothesize that the low levels of *Oxt* in godmothers might be due to the exposure to pups (which would produce emotional stress) without the protective effects of PRL signalling (Torner and Neumann 2002). It would be interesting to check the activation of the HPA axis in godmothers to validate this hypothesis.

However, expression levels of the PRLR are similar levels in virgin, pregnant and lactating female rats, and remain unchanged during the oestrous cycle (Sugiyama et al. 1994; Nogami et al. 2007). This can explain why we did not observe significant differences in the expression between dams and godmothers in the RNA-seq (TABLE 3) and between dams, godmothers and virgins in the qPCR study (FIGURE 34).

Regarding other genes related with PRL signalling, it has been reported that PRL regulates TRPV1 channels in sensory neurones in female rats (Patil et al. 2013), and these channels are related

with glutamatergic neurotransmission. SO neurones express TRPV1 channels and *Trpv1* mRNA is upregulated in this nucleus during lactation (Naeini et al. 2006; Augustine et al. 2016). This is consistent with the result that we obtain in the RNA-seq study, where we observe an increase in *Trpv1* mRNA in dams with respect to godmothers (TABLE 3).

Previous studies have demonstrated that galanin (GAL) (Skofitsch and Jacobowitz 1985; Melander et al. 1986) and *Gal* mRNA (Planas et al. 1994; Lein et al. 2006) are present in the Me of male rats. Immunohistochemical detection of GAL has also been described in the Me of female (and male) mice (Pérez et al. 2001). In addition, it has been demonstrated that *Gal* labelling is increased in the BST and Me of adult compared with prepubertal male rats. This increase can be related with testosterone and its metabolites (i.e. oestradiol) and probably they have an effect in the GAL pathways in these limbic regions (Planas et al. 1994). GALergic neurons seems to be a central regulatory node of social interactions with pups in parental behaviour, specifically *Gal*-expressing neurons of MPO/A are critical for the control of mouse parental behaviour and the suppression of pup-directed aggression (Wu et al. 2014) and also in pup care behaviours (Tsuneoka et al. 2013). Me shows a direct output to MPO/A (Pardo-Bellver et al. 2012) and both structures play an important role in the motivation in maternal behaviour (Numan and Insel 2003a; Chen and Hong 2018). These studies have a remarkable relation with our results where we observe in RNA-seq studies after maternal aggression tests an increase of *Gal* in Me (TABLE 3). However, when we carried out the qPCR studies without previous aggression tests, we did not observe these differences (FIGURE 32).

In addition to *Prl*, a few genes related with reproductive hormones were found to be overexpressed in dams, such as *Fshb, Cga*, which encodes the FSH α subunit, *Gnrhr* and *Gnrh1* (TABLE 3). The *Ghrhr, Fhsb and Cga* were present in the grapho, showing a close relation with *Prl, Gh and Pou1f1* (FIGURE 37). *Fshb* expression have been described in teleost fishes brain where the FSH subunits seems to be modulated by 11-ketosterone and testosterone in male pejerrey (*Odontesthes bonariensis*) (Miranda et al. 2007). It also has been described previously the presence of FSH-β in the pituitary gland of mammals (Böckers et al. 1994; Kendall et al. 1994), however, we did not find previous research carried out in mammals CNS neither the description of *Fshb* presence in Me (Lein et al. 2006). Regarding *Cga*, it has been shown mRNA and protein in the anterior lobe of the pituitary gland in sheep, mice, rat and guinea pig (Böckers et al. 1994; Japon et al. 1994; Kendall et al. 1994; Stoeckel et al. 1994) but it has been not described before the presence of mRNA in the Me of female mice. In the case of *Gnrhr,* previous studies described the presence of mRNA in several brain nuclei (Jennes et al. 1988; Albertson et al. 2008) and in

particular in the Me (Wen et al. 2011), agreeing with our results. Nevertheless, our results also suggested that the expression of these receptors is upregulated in lactating female mice and could be involved in the neural changes associated with motherhood. Regarding *Gnrh1*, previous tracer injection studies showed that injections of retrograde tracer in the amygdala mark GnRH neurons in the rostral medial septum, the caudal roots of the nervous terminalis, diagonal band, *nucleus triangularis septi, nucleus interstitialis striae terminalis*, and in the ventrolateral hypothalamus (Jennes 1987). GnRH-I neurons are found in the forebrain in olfactory bulb, along the terminal nerve, and most cells were in medial septum down to the amygdala and these cells terminate in the median eminence (ME) (Muske 1993a, b; Gore 2002). These cells positive to GnRH-I project directly to the amygdala and can have an effect on the GnRH receptors present in this region (Sanchez and Dominguez 1995). Our results can explain the fact that previous studies have reported the presence of GnRH-I and GnRH receptors in the amygdala and the upregulation in dams of these genes can be involved in maternal behaviour.

With regard to genes related to neurotransmission, our results show that dams overexpressed genes implicated in cholinergic, catecholaminergic and, to a lesser extent, glutamatergic synapses. Moreover, a number of genes related to peptidergic transmission (in addition to those directly related to maternal behaviour discussed above) showed also a significantly higher expression.

Regarding the catecholaminergic neurotransmission, PRL stimulates gene expression of tyroxine hidroxilase (TH), a rate-limiting enzyme in dopamine synthesis, in neuroendocrine dopamine neurons (Arbogast and Voogt 1991), and also modulates the phosphorylation of TH, resulting in increased dopamine synthesis (Ma et al. 2005). Dopamine synthesis and release are increased in response to acute or chronic increases in PRL levels in blood (Arbogast and Voogt 1991; Ma et al. 2005; Grattan and Kokay 2008; Grattan 2015), whereas hyperprolactinaemia results in the suppression of dopamine secretion (Arbogast and Voogt 1991; Ma et al. 2005; Grattan and Kokay 2008). Another possibility is that this *Th* expression can be related with adrenalin and noradrenalin neurotransmission because in our results of RNA-seq studies we observe an upregulation of *Th* and *Adra2b* in dams with respect to godmothers. *Adra2b* gene which codes for the presynaptic noradrenergic α2B receptor has been found to play a role in arousal-enhanced consolidation processes, influencing amygdala and hippocampus activation immediately following an emotional event (Anderson et al. 2006a; Todd et al. 2011; Mineur et al. 2018). The Me and BSTMPM of Syrian hamsters (*Mesocricetus auratus*) and prairie voles (*Microtus ochrogaster*) contain catecholaminergic cells expressing immunoreactivity against TH not found

in rats, mice, or Siberian hamsters (Asmus et al. 1992; Northcutt et al. 2007). Northcutt et al. (2007) observed that MePD contains a few TH-immunoreactive (TH-ir) cells in male and female hamsters and male meadow voles, but not rats, however they did not study their presence in mice. They observed that virgin female prairie voles had far fewer TH-ir cells in posterior BST and MePD than males. In addition, they analysed that treating ovariectomized females with testosterone substantially increased TH-ir cells in posterior BST and MePD. For this reason, they suggest that expression of TH in these sites is influenced by circulating gonadal hormones in adults, which may be related to changes in their display of social behaviours across the reproductive cycle (Northcutt et al. 2007). As they did not check the variations of TH cells populations in posterior BST and MePD in mice, maybe the presence of these neurons can be increased during lactation. However, further studies are needed in order to check the presence of this neuronal population. TH expression is influenced by gonadal hormones (Northcutt et al. 2007) and the Me is enriched neurons expressing aromatase and ESR1 (Mitra et al. 2003; Unger et al. 2015). In addition, aromatase appeared in our RNA-seq results, however it did not present significant differences between females (TABLE 5 AND TABLE 1C IN ANNEX II). These facts could explain the upregulation of *Th* in the Me of dams that we observed in the RNA-seq analysis (TABLE 2). In addition to the overexpression in *Th* we also observed an increase of *Adra2b* in dams, suggesting that all the catecholaminergic pathways may be playing an important role in parental behaviour in this nucleus. It is important to remark that no previous investigations have found TH and α2B receptor in the Me of female mice, so further studies are needed.

Concerning cholinergic neurotransmission, the superficial layer of the Me is positive for acetyl cholinesterase (Paxinos and Franklin 2004). Our RNA-seq studies have shown an increase of expression of several genes related with cholinergic neurotransmission: *Chrnb3, Chrna6*, *Chat, Ngfr, Chrna2* and *Chrm2* (TABLE 3). This kind of neurotransmission seems to be involved in the maternal pair bounding, where this behaviour is thought to be mediated in part by reorganization of the olfactory bulb (Kendrick et al. 1992; Lim and Young 2006). Previous studies in ewes have seen that the number of output neurons in the olfactory bulb, or mitral cells, increases after parturition together with increased cholinergic and noradrenergic neurotransmitter release (Kendrick et al. 1992). It is important to remark that the olfactory bulb projects to the Me (Kang et al. 2009; Gutiérrez-Castellanos et al. 2010; Cádiz-Moretti et al. 2013). Further research is needed to address the cholinergic neurotransmission role in the display of maternal behaviours.

Finally, among the overexpressed genes related with peptidergic neurotransmission, *Pomc* codifies a peptide implicated in the regulation of food intake. Neurons expressing *Pomc* were described in several nuclei including Me and BMA (Niikura et al. 2013). Stimulating POMC neurons in Arc and in the nucleus of the solitary tract suppresses feeding (Zhan et al. 2013; Wang et al. 2015). These neurons in the Arc receive inputs from the SO and Me, however the POMC neurons project mainly to the SO (Wang et al. 2015). *In situ* hybridization histochemistry in sheep demonstrated that POMC mRNA expression in the Arc decreased at parturition and increased during lactation compared to late pregnant and ovariectomized animals, and oestradiol and progesterone treatments increased POMC mRNA expression compared to ovariectomized controls (Broad et al. 1993). However, these results were not replicated in rodents (Nahi and Arbogast 2003). POMC is a complex precursor that comprises several peptidic hormones, including MSH hormones, ACTH, and β-endorphin (Navarro et al. 2015). Due to these, previous studies have observed that on days 3±5 postpartum, female rats exposed to either a male intruder or predator odour showed a more robust adrenocortical response (i.e. ACTH plasma levels) to both of these stressors when their pups were present (Deschamps et al. 2003) or when lactating resident where exposed towards a virgin or lactating intruder (Neumann et al. 2001) but in both studies the ACTH plasma levels where higher in the group of virgins. Regarding, β-endorphin studies have shown that plasma levels increase in the hypothalamus, midbrain, and amygdala by 8-10 days of gestation and remains elevated until after parturition. A decline in the β-endorphin content of the hypothalamus and amygdala was noted as early as 1-2 days postpartum and continue decreasing the posterior days (Wardlaw and Frantz 1983). In the case of MSH, the content of α-MSH in the mediobasal hypothalamus and preoptic-suprachiasmatic area compared to oestrous levels was lower during the later days of gestation and decreased further in the mediobasal hypothalamus during lactation in association with the elevated plasma PRL (Khorram et al. 1984). However, in our RNA-seq (TABLE 2) study we observed and overexpression of *Pomc* in dams with respect to godmothers. Further studies should address these contradictory results.

SUB-EXPRESSED GENES

The genes that were most upregulated in godmothers with respect to dams were the *Inhbc* and *Inhbe*. Some proteins in the inhibin family (A and B) are known to participate in the control of the oestrous cycle (Meunier et al. 1988; Woodruff et al. 1996), but the function of these specific genes in the brain is unknown, so further research is needed in order to know the role that they can play in maternal behaviour.

Other genes upregulated in godmothers are the ones related with early-expression, as *Egr2, Fos, Egr4, Fosb*, *Egr1* and *Egr3*. The increase in mRNA of these genes can be related with the exposition through the intruder male. Previous studies have seen an increase of FOS immunoreactive neurons in Me regions when females were exposed to soiled male as opposed to clean bedding (Halem et al. 1999). In addition, Egr-1 it is expressed in many brain sites after the display of sexual or maternal behaviours, including in cells that do not express *Fos* (Numan et al. 1998; Hasen and Gammie 2006).

In conclusion, RNA-seq and qPCR analyses have revealed that several genes involved in maternal behaviour are upregulated in the Me of dams, potentially playing a crucial role in the development of maternal aggression. Of those genes, we will devote the next two chapters to investigate *Prl,* because of the key role of this neuropeptide during pregnancy and lactation, and in particular to further investigate the presence of neural PRL.

CHAPTER III

SYNTHESIS OF PROLACTIN IN MEDIAL AMYGDALA

INTRODUCTION

PRL is a polypeptide hormone belonging to the type I helix-bundle protein (cytokine) family (Rand-Weaver et al. 1991), which includes also GH and other lactogenic molecules such as PL (Horseman and Yu-Lee 1994).

It is known that PRL has over 300 separate biological activities (Bole-Feysot et al. 1998), among which we found regulatory control on reproduction, immunomodulation, angiogenesis, energy metabolism, osmotic balance, and development (Freeman et al. 2000; Grattan 2001).

Although there is extensive evidence of systemic PRL being transported into the brain (Brown et al. 2016) some authors have proposed that *de novo* synthesis occurs in some nuclei of the brain in order to produce modulatory effects in several brain regions (Torner et al. 2002). Despite the fact that the role of brain PRL remains controversial, numerous reports have found presence of protein and its mRNA in brain tissue (Pochet et al. 1981; Schachter et al. 1984; DeVito et al. 1992; Clapp et al. 1994; Roselli et al. 2008). Importantly, this presence of PRL is not abolished by hypophysectomy, suggesting that this PRL has not a pituitary origin (DeVito 1988). Moreover, *de novo* PRL synthesis and release could be detected from hypothalamic fragments, in vitro (DeVito et al. 1987b, 1992), strongly suggesting local production of PRL in neurones or glial cells.

Within the modulatory roles of PRL we can find an important role in the regulation of the stress responses through the inhibition of the HPA axis (Torner and Neumann 2002; Slattery and Neumann 2008). In addition, as commented in Chapter II, PRL plays a key role in the development of maternal behaviours in order to ensure the survival and welfare of the offspring (Bridges et al. 1985; Bridges 1994; Weber and Olsson 2008). However, the exact role of central PRL in the expression of maternal behaviours is still unclear.

Consistent with the possibility of PRL being synthetized *de novo* in the brain, in the Results of Chapter II we found that *Prl* was the most upregulated gene in the Me in lactating females compared to pup-sensitized virgin females. For this reason, and given the importance of PRL in maternal behaviour, we want to confirm whether these changes observed in *Prl* mRNA are translated into protein. In order to confirm the presence of the PRL in the Me first we carried out a proteomic analysis. Then, we carried out the quantification of PRL expression in the Me with three different approaches: Western blot, immunohistochemistry and ELISA. The use of these three techniques allows us to analyse semi or quantitatively the possible changes that motherhood induces in the levels of PRL in the brain. In addition, the comparison of PRL levels

between the different group of females (dams, godmothers and pup naïve virgins) allow us to distinguish if these changes are related to hormonal changes due to pregnancy and lactation or to pup sensitization. Finally, we performed an ELISA of serum samples from these females to study whether peripheral PRL and neural PRL were correlated.

MATERIAL AND METHODS

GENERAL PROCEDURES

Animals

The experiments of this chapter were carried out using 40 adult female mice (*Mus musculus*) from the CD1 strain (Janvier; Le Genest Saint-Isle, France). The age of the animals was between 3 and 5 months at the beginning of the experiments. The females were randomly assigned to test PRL by proteomics studies, Western blot and ELISA assays, and for immunohistochemistry studies.

The animals for proteomic studies, Western blot and ELISA tests were randomly assigned to two groups: dams (n=12) and godmothers (n=10). Some of the animals were discarded for final analysis due to methodological issues. The final number of animals analysed in each experiment is shown in (TABLE 6).

Dams were mated by housing them with a stud male for 3 days. The day of birth was considered as PPD0, and in PPD2 litters were culled to 8 pups. After mating, a godmother was housed with a dam in the same cage. Therefore, as in previous chapters, godmothers were continuously exposed to pups and they shared maternal caregiving with the accompanying dams (Martín-Sánchez et al. 2015b). Animals were housed in cages with water and food available *ad libitum* with 12 h light: dark cycle at 22-24°C. Mice were treated according to the guidelines of the European Union Council Directive of September 22nd, 2010 (2010/63/UE). All the experimental procedures were approved by the Committee of Ethics on Animal Experimentation of the University Jaume I.

On the other hand, the females used in the immunohistochemistry studies were randomly assigned to three groups: dams (n=6), godmothers (n=6) and virgin pup-naïve females (n=6) (TABLE 6). All the housing conditions of these animals are explained in Chapter 1 (TABLE 6).

Table 6: Scheme that illustrates the number of animals employed in each experiment of Chapter III.

TOTAL ANIMALS	EXPERIMENT	SAMPLES	EXPERIMENTAL ANIMALS
12 DAMS 10 GODMOTHERS	Western-Blot	Me	9 Dams 9 Godmothers
	ELISA	Serum	10 Dams 9 Godmothers
		Me	10 Dams 10 Godmothers
	Proteomic assays	Me and Pituitary gland	2 Dams
6 DAMS 6 GODMOTHERS 6 VIRGINS	Immunohistochemistry		6 Dams 6 Godmothers 6 Virgins

Microdissections

Animals for proteomics (TABLE 6), ELISA and Western blot studies were sacrificed, and the Me was microdissected using the same procedures described in Chapter II (See sections 2 and 3 of Experiment 1) between 15:00 and 17:00 hours overlapping with the PRL secretion peak (in virgins) 4 hours before the light period ends (Guillou et al. 2015).

In addition, we extracted the pituitary gland of these animals. The mouse pituitary gland sits at the base of the skull in a depression of the sphenoid bone called the *sella turcica*, surrounded laterally by the trigeminal nerves and anteriorly by the optic chiasm. After removing the brain, the pituitary gland was scooped out of the sphenoid bone and stored in a plastic tube, flash-frozen in liquid nitrogen, and maintained on dry ice until storage at –80°C.

Protein extraction

Brain portions were homogenized in RIPA buffer (phosphate-buffered saline (PBS; 0.4M pH 7.4) containing 1% IGEPAL® (Cat# CA-630), 0.5% sodium deoxycholate, 0.1% sodium dodecyl sulphate (SDS), and protease inhibitors (0.01 µl per 1 µl of RIPA buffer). Thereafter, the tissue homogenates were put in ice 30 minutes and after that centrifuged at 13,200 rpm for 10 min at 4°C to eliminate large cells debris. Next, the supernatant was transferred to a fresh tube without disturbing the pellet. The supernatant was used as total protein sample. Protein concentration was determined using the Bio-Rad protein assay kit (Bio-Rad, Madrid, Spain) (FIGURE 39).

Figure 39: Timeline of the study of the PRL levels in the medial amygdala.

Outliers exclusion analysis

All the statistical analyses used in the following experiments were carried out using SPSS software package (IBM SPSS Statistics 24.0).

Tukey's hinges method was used to determine extreme values (x_i) and the boundaries of the boxes in the boxplot. The median was identified by a line inside the box. The length of the box is the interquartile range (IQR), calculated from Tukey's hinges as the difference between Q_3 (value of percentile 75) and Q_1 (value of percentile 25). Values more than three IQRs from the end of a box are labelled as extreme outliers and removed for statistical analysis ((1). Tuckey boxplots also represent out values which are values that are more than 1.5 IQRs from the end of a box, however these values were not discarded from the statistical analysis.

$$x_i \geq Q3 + 2 * 1.5(Q3 - Q1) \quad (1)$$

EXPERIMENT 1

PROTEOMICS: PROLACTIN PRESENCE IN MEDIAL AMYGDALA

Samples preparation

The proteomic analysis was performed by the proteomics facility of SCSIE at the University of Valencia. Following protein extraction, samples from two dams were selected for checking in the nucleus of interest the presence of PRL with a proteomic analysis. Pituitary gland samples of these two females were pooled to achieve 30 µg of total protein. The same was done with the samples of Me to obtain a mix with 60 µg of total protein. A 12% SDS polyacrylamide electrophoresis gel was used to separate proteins according to their mass. After that, the gel was stained with Comassie colloidal blue (FIGURE 40) to see the bands and a sample of each column was cut approximately between 25-20 KDa and between 17-12 KDa.

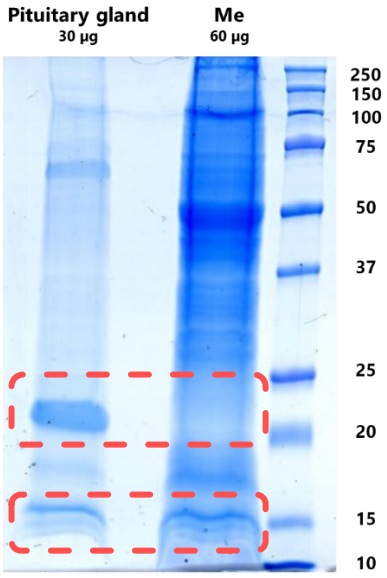

Figure 40: 12% agarose gel electrophoresis for Me and pituitary gland. The squares enclosed the samples used for liquid chromatography and tandem mass spectrometry (LC–MS/MS) analysis. For abbreviations see list.

After that, the Me and pituitary gland gel samples were reduced by 1 mM of Dithiothreitol for 20 minutes at 60ºC. The thiol groups were alkylated by 5.5 mM with Iodoacetamide for 30 minutes at room temperature in the dark. Next, 20 ng of trypsin were added, and digestion was left overnight. All the reagents were prepared in 50 mM of ammonium bicarbonate ABC. The protein digestion was stopped with 3 µl of 10 % trifluoroacetic acid in water. Samples were concentrated by rotatory evaporator at 10 µl.

Liquid chromatography and tandem mass spectrometry (LC–MS/MS) analysis

We loaded 5 µl of each sample (pituitary gland and Me) onto a trap column (NanoLC Column, 3µ C18-CL, 350 µmx0.5mm; Eksigen) and desalted with 0.1% trifluoroacetic acid at 3 µl/min during 5 min.

The peptides were then loaded onto an analytical column (LC Column, 3 µ C18-CL, 75 µm × 12 cm, Nikkyo) and equilibrated in 5% acetonitrile and 0.1% formic acid in water. Elution was carried out with a linear gradient of 5-40% of solution B (acetonitrile 99.9% and formic acid 0.1%) in 0.1% formic acid for 30 minutes a flow rate of 0.3 µl/min. Peptides were analysed in a mass spectrometer nanoESI qQTOF (5600 TripleTOF, ABSCIEX).

Eluted peptides were ionized applying 2.8 kV to the spray emitter. Analysis was carried out in a data-dependent mode. Survey MS1 scans were acquired from 350–1250 m/z for 250 ms. The quadrupole resolution was set to 'UNIT' for MS2 experiments, which were acquired 100–1500 m/z for 50 ms in 'high sensitivity' mode. The following switch criteria were used: charge: 2+ to

5+; minimum intensity; 70 counts per second (cps). Up to 50 ions were selected for fragmentation after each survey scan. Dynamic exclusion was set to 15 s. The system sensitivity was controlled with 2 fmol of 6 proteins (LC Packings).

Qualification and quantification of samples

ProteinPilot default parameters were used to generate peak list directly from 5600 TripleTof wiff files. The Paragon algorithm (Shilov et al. 2007) of ProteinPilot v 5.0 was used to search the SwissProt database (version 03-2018) with the following parameters: trypsin specificity, cys-alkylation, taxonomy restricted to human, and the search effort set to thorough.

The protein grouping was done by Pro group algorithm: A protein group in a Pro Group Report is a set of proteins that share some physical evidence. Unlike sequence alignment analyses where full length theoretical sequences are compared, the formation of protein groups in Pro Group is guided entirely by observed peptides only. Since the observed peptides are determined from experimentally acquired spectra, the grouping can be guided by usage of spectra. Then, unobserved regions of protein sequence play no role in explaining the data. The protein within each group which can explain more spectral data is that protein shown as the primary protein of the group. Only the proteins of the group for which there is individual evidence (unique peptides with enough confidence) are listed (ANNEX V, TABLE 4).

Data analysis

ANNEX V, TABLE 4 show the results of the bioinformatics analysis of the identified protein in the studied bands of the pituitary gland and Me. Only proteins showing unused ProtScore >1.3 were identified with confidence ≥ 95% (TABLE 7) and represented in the tables. According to the following equation:

$$ProtScore = -log\ (1 - (\frac{percent\ confidence}{100}) \quad (2)$$

Unused ProtScore reflects the amount of total, unique peptide evidence related to a given protein. Total ProtScore on the other hand is simply the sum of all peptide evidence related to a given protein.

Table 7: Percent confidence expressed in ProtScore units

Percent confidence	ProtScore
99%	2.0
95%	1.3
90%	1.0
66%	0.47

EXPERIMENT 2

MEDIAL AMYGDALA WESTERN BLOT

Western blot

Prolactin antibody blocking tests

Samples from the pituitary gland of two dams were used for blocking assays of the rabbit anti-mouse natural PRL (National Hormone and Peptide program, LOT# AFP-879151Rb) antibody. 3 µg of protein pooled from two pituitary glands were loaded in the gel.

The specificity of this antibody was validated by performing an antibody competition assay in Western blots of protein extract from pituitary glands, the main endocrine gland producing PRL.

The primary antibody rabbit anti-mouse natural PRL (1:1000) was incubated overnight with recombinant mouse PRL (Sigma, Cat# SRP4688) diluted in TBS-Tween (containing 0.1% Tween-20 (TBS-T)) with 5% non-fat dried milk. The recombinant PRL was added to the primary antibody incubation solution at a saturating concentration (22.753 µg/ml; corresponding to 200 times the molar equivalent of the antibody concentration used in the incubation solution). As a positive control, the same antibody solution was used without the preincubation with recombinant PRL.

In order to carry out the assay, 2 duplicates from the same pooled samples of pituitary gland were run in parallel. Proteins were separated by SDS–polyacrylamide gel gels (1.34% acrylamide stacking gel and 12% acrylamide resolving gel), transferred to a nitrocellulose membrane with 0.45 µm pore size (Bio-Rad, Cat# 1620115) using Trans-Blot® Turbo™ Transfer System apparatus (Bio-Rad) for 7 minutes. A pre-stained marker was used to identify the mass of the proteins (Precision Plus Protein™ Dual Color Standards, Bio-Rad Laboratories, Cat# 1610374). Membranes were then blocked in 5% non-fat dried milk in TBS containing 0.1% Tween-20 (TBS-T) for 1 hour. After that, the two membranes were incubated for 48 hours at 4°C. One of the membranes was incubated with the control solution (without blocking the antibody) and the other with the blocking solution. After three washes in TBS-T, the blots were incubated for 1 hour with

horseradish peroxidase–conjugated secondary antibody: Goat anti Rabbit (1:1000; Bio-Rad, Cat# 1706515) for PRL immunodetection. The labelling was developed using the ECL™ Prime Western Blotting System (ECL Plus, Amersham Bioscience, Cat# RPN2232). 400 µl of the solution A (Luminol solution) were mixed with 400 µl of the solution B (Peroxide solution) and 400 µl of that solution were diluted 1:5 in distilled water (H_2Od).

Digital images of the immunoblots were captured with ImageQuant LAS 500 chemiluminescence CCD camera (GE Healthcare, Cat# 29005063).

Differential prolactin expression

Previously, dam and godmother samples from the Me were serially diluted separately (10 µg, 20 µg, 40 µg and 60 µg) in order to determine the best amount of protein for the detection in the immunoblotting assay. According to the results obtained, the best amount of protein for the Western blot assay was 60 µg. Two replicates of each sample were used for this test. For relative quantification of PRL, 9 dams and 9 godmothers were used.

The SDS–polyacrylamide gels for electrophoresis and the transference to the membranes were carried out following the same protocol described for blocking tests. After that, each membrane was cut between 37 and 25 KDa for control detection of beta-actin (ACTB). Membranes were then blocked in 5% non-fat dried milk in TBS-T for 1 hour. After that, both parts of the membranes were incubated 48 hours at 4°C with a primary antibody: the part of the membrane corresponding to the low molecular weights was incubated with rabbit anti-mouse natural PRL diluted 1:1000 and the part of the membrane corresponding to the high molecular weights was incubated with mouse anti-ACTB monoclonal antibody (Invitrogen, Cat# MA5-15739) diluted 1:2000. Both antibodies were diluted in TBS-T with 5% non-fat dried milk. After three washes in TBS-T, the blots were incubated for 1 hour with horseradish peroxidase–conjugated secondary antibody: Goat anti Rabbit (1:1000; Bio-Rad, Cat# 1706515) for PRL immunodetection and Goat anti-Mouse (1:1000; Invitrogen, Cat# M32407) for ACTB detection. Finally, blots were developed using the ECL™ Prime Western Blotting System (ECL Plus, Amersham Bioscience, Cat# RPN2232) as explained above.

Analysis of Prolactin reactivity

Digital images of the immunoblots were captured with ImageQuant LAS 500 chemiluminescence CCD camera (GE Healthcare, Cat# 29005063). Thereafter, images were processed and analysed using Gel Analysis method of Fiji (Schindelin et al. 2012). The densitometry analysis is shown in

arbitrary units normalized to the loading control (ACTB). Finally, the data were represented as percentages.

Statistical analysis

The differences between expression levels of 60 µg of Me protein in the two groups were tested on the SPSS software package. Firstly, the presence of extreme outliers was checked. Thereafter, the normality (Kolmogorov-Smirnov test) and homogeneity of variances (Levene's test) were verified. Finally, a t-test was carried out to study the differences in PRL levels between the studied groups. If the data did not follow a normal distribution a ln-transformation (ln [X+1]) was performed.

EXPERIMENT 3

ENZYME-LINKED IMMUNOSORBENT ASSAY (ELISA)

Blood sampling

Whole blood from all of the animals was collected between 15:00 and 17:00 hours overlapping with the PRL secretion peak (in virgins) 4 hours before the light period ends (Guillou et al. 2015). After cervical dislocation, the blood was drawn with a 23G needle from the left ventricle and/or the descending aorta. A total volume of 500 µl was collected in Eppendorf tubes. The samples were left at room temperature during 30 minutes for coagulation, and after that were left a 4°C in ice. Next, the samples were centrifuged at 5000 rpm for separating the blood clot from the serum. The serum was stocked in aliquots of 50 µl and stored at -80°C.

Serum and medial amygdala prolactin measurements

Firstly, samples from Me and serum stored a -80°C were temperate in ice (n= 10 dams and n=10 godmothers). The best working dilution was determined with samples from godmothers and lactating females and was found to be the same for both groups. This dilution was 1:4 for Me samples and 1:50 for serum samples. The dilutions from serum and Me samples were assayed in duplicate for each sample. Concentrations of PRL were determined using a commercial ELISA kit (Abcam, Cat# ab100736) according to the manufacturer's instructions. The antibody employed in the kit was a biotinylated antibody specific for mouse PRL coated on a 96-well plate.

Statistical analysis

After eliminating the outliers, normality (Kolmogorov–Smirnov's test) and homoscedasticity (Levene's test) were checked. If the data did not follow a normal distribution, a ln transformation (ln [X + 1]) was carried out. Then, a t-test of independent samples was performed to study the differences in PRL levels between the studied groups.

Finally, in order to evaluate if the results from Western blot and ELISA were consistent, a Pearson's correlation test was carried out. The standardized data obtained in the Western blot and the ng of PRL observed in the ELISA of Me microdissections from the same animals were employed for Pearson's test.

EXPERIMENT 4

MEDIAL AMYGDALA IMMUNOHISTOCHEMISTRY

Animals

For the present study, we used 18 adult females (*Mus musculus*) from the CD1 strain (Janvier, Le Genest Saint-Isle, France) which were the same animals employed in Experiment 1 of Chapter 1 for behavioural tests. Animals were 8-10 weeks old and weighed between 26.8-48.5 g at the beginning of the experiments. Adult virgin females were randomly assigned to three groups: dams (n=6), godmothers (n=6) and virgin pup-naïve females (n=6). Future dams were housed each one with a stud male during four days for mating. The day of birth was considered as PPD0, and in PPD2 litters were culled to 8 pups. Animals were housed in cages with water and food available *ad libitum* with 12 h light: dark cycle at 22-24 °C. Mice were treated according to the guidelines of the European Union Council Directive of June 3rd, 2010 (6106/1/10 REV1). All the experimental procedures were approved by the Committee of Ethics on Animal Experimentation of the University of Valencia.

Histology and immunohistochemistry

Prolactin antibody blocking tests in brain tissue

Animals received an overdose of sodium pentobarbital (intraperitoneal, 100mg/kg, Eutanax, Laboratories Normon S.A. Madrid, Spain). After that, they were transcardially perfused with saline solution (0.9%) followed by 4% paraformaldehyde diluted in PB (0.1M, pH 7.6). Then, brains were carefully removed from the skulls, post-fixed for 4 hours in the same fixative and cryoprotected

until they sank in 30% sucrose in PB at 4°C. The tissue was sliced into sagittal sections in the case of the olfactory bulbs (40 μm) and into frontal sections (40 μm) in the case of the rest of the brain using a freezing microtome. In both cases, sections were collected in four parallel series.

For immunohistochemistry, we controlled the specificity of the antibody rabbit anti-mouse natural PRL (provided 1:40 by National Hormone and Peptide program, LOT# AFP-879151Rb) by a competition assay. Two kinds of PRL were tested separately: highly purified rat PRL from extracts of pituitary gland (natural PRL) (National Hormone and Peptide program, LOT# AFP7547B) (natural mice PRL was not available in any supplier) and mice recombinant PRL (Sigma, Cat# SRP4688), the same used in the western blot blocking tests (Experiment 2, point 1.1). The immunohistochemistry tests were done in series from three animals (two virgin females and one lactating female).

Next, the primary antibody rabbit anti-mouse natural PRL (1:500) was incubated overnight with highly purified rat natural PRL diluted in TBS-Tx (0.3% Triton X-100 in 0.05 M TBS, pH 7.6) with 2% NGS. The natural rat PRL was added to the primary antibody incubation solution at a saturating concentration (200 times higher than the molar equivalent of the antibody concentration used in the incubation solution which corresponds to 25.753 μg/ml) and the same was done with the mice recombinant PRL. As a positive control, the same antibody solutions were used without the preincubation with rat natural PRL and mice recombinant PRL respectively.

Secondly, tissue sections were completely washed three times for at least 10-minutes in TBS (0.05M, pH 7.6). After thawing, sections underwent an initial antigen retrieval step, consisting in a first incubation for 6 minutes citrate buffer (0.01 M, pH 6) at 80°C followed by 10 minutes in ice. These steps were repeated twice. After that, the tissue was washed again three times with TBS for 5 minutes.

In order to carry out the assay, series from each female were split in two and run in parallel for the purpose of incubating the same animal sections with and without the blocking solutions.

For the immunohistochemical detection of PRL, endogenous peroxidase was inactivated with 1% H_2O_2 TBS for 30 min at room temperature. Next, all sections were incubated in a blocking solution of TBS-Tx (0.3% Triton X-100 in 0.05 M TBS, pH 7.6) containing 3% of NGS for 2 hours at room temperature. Then, half of the series of each animal were incubated with the control solution (without the blocking of the antibody) and the other with the blocking solution 48 hours at 4°C. Then, after rinsing, all the brain sections were incubated with a biotinylated goat anti-

rabbit IgG (Vector, Cat# BA-1000) diluted 1:200 in TBS-Tx with 2% NGS for 2 hours at room temperature. After that, samples were incubated in ABC Elite (Vector, Cat#PK-6100) diluted 1:50 in TBS-Tx for 90 minutes at room temperature. Finally, the resulting peroxidase labelling was revealed with 0.025% diaminobenzidine in TB (0.1M, pH 8.0) with 0.01% H_2O_2.

Prolactin immunohistochemistry for comparative studies

In postnatal day six (PPD6) for dams, and at the same time for godmothers and pup-naïve females, animals were sacrificed, and the tissue was treated in the same way as explained in previous section. One series of each brain was processed for the detection of PRL in free-floating sections.

After that, tissue sections were washed three times for at least 10-minutes in TBS (0.05M, pH 7.6). Next, we carried out the same protocol of antigen retrieval and PRL immunodetection explained above (see previous section) (FIGURE 41).

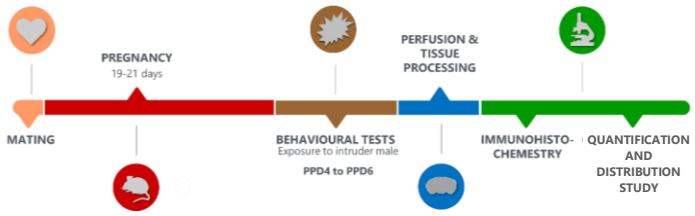

Figure 41: PRL distribution study timeline.

Image acquisition, processing and mapping

After PRL immunohistochemistry, we quantified PRL fibres in representative levels of Me subdivisions according to the stereotaxic atlas of Paxinos & Franklin (2004): MeA, Bregma -1.06 / -1.22 mm; MePD and MePV, Bregma -1,34/ -1.46 mm for both. In addition, neuroanatomical references, as *opt*, were used to reduce variability between the photomicrographs. The images of these levels were acquired in both hemispheres using a microscope Leitz DMRB (Leica AG, Germany) with a digital camera (Leica DFC495) and using a 20X objective.

After that, fibre densities were calculated using Fiji online software (Schindelin et al. 2012). To do so, a grid (available as a Fiji plugin) with 1000 μm^2 per square was superimposed after escalating the images. The number of PRL-positive fibre crossings with the grid lines was taken as a main parameter for fibre number estimation following (Menon et al. 2018). In addition, we counted the number of grid squares containing PRL-immunoreactive (PRL-ir) fibres.

Statistical analysis

First, we estimated the density of PRL-ir fibres with two measures: crossings with the grid and squares containing PRL-ir fibres. We used the average per hemisphere per animal. After eliminating the outliers, we checked the normality (Kolmogorov–Smirnov test with Lilliefors' correction) and homogeneity of variance (Levene's test). Thereafter, one-way ANOVA between groups was performed on each subnucleus. When homogeneity of variance could not be assumed, we carried out a Welch and Brown-Forsythe ANOVAs with the Games-Howell pairwise comparison post-hoc test. Statistically significant differences ($p \leq 0.05$) in the one-way ANOVA were further explored by means of post-hoc pairwise comparisons with Bonferroni's correction.

RESULTS

EXPERIMENT 1

PROTEOMICS: PROLACTIN PRESENCE IN MEDIAL AMYGDALA

The complete list of the proteins identified in the studied bands of Me and pituitary gland is provided in the ANNEX V, TABLE 4, including their unused score, UniProt accession number, protein name, species, % of sequence coverage and matched peptides (further information about the meaning of these values is provided at the bottom of the ANNEX V. Human keratins were eliminated from the list of proteins identified because it was assumed that they are due to contamination during the handling of the samples (Hodge et al. 2013).

The pituitary gland presented a total of 79 proteins in the 23 KDa band and 88 proteins in the band of 16 KDa. Moreover, we identified a total of 324 proteins in the Me in the 23KDa band and 221 in the 16 KDa region. Mouse PRL was present in all the samples except in the 16 KDa band from Me. As observed in the RNAseq study (see Chapter II), the mouse GH (also known as somatotropin), one of the genes more overexpressed in dams, was also present in the list of proteins in our samples. This protein was detected in the band of 23 KDa and 16 KDa from pituitary gland and only in the 23 KDa band from Me. Thus, proteomics analysis confirmed the presence of PRL protein in the Me.

EXPERIMENT 2

MEDIAL AMYGDALA WESTERN BLOT

Prolactin antibody blocking assays

The specificity of the antibody was tested with a competition assay, which showed that blocking the rabbit anti-mouse natural PRL (1:1000) with recombinant PRL abolished the detection of the 23 KD positive band (FIGURE 42).

Figure 42: Blocking tests showed the specificity of the antibody against PRL. The Western blot of pituitary gland showed that when the antibody against PRL was blocked with PRL (200x) the immunodetection of the PRL in the membrane was abolished.

Differential prolactin expression

In the Me of dams and godmothers, the immunoreactive band from both studied groups migrated with the band from the prestained marker of ~23 KDa (FIGURE 43A).

The t-test for independent samples of the ln-transformed data showed no significant differences between relative amounts of PRL in dams and godmothers ($t(16) = 1.269$, $p = 0.222$ FIGURE 43B). Note, however, the high variability in the PRL-ir bands in the lanes.

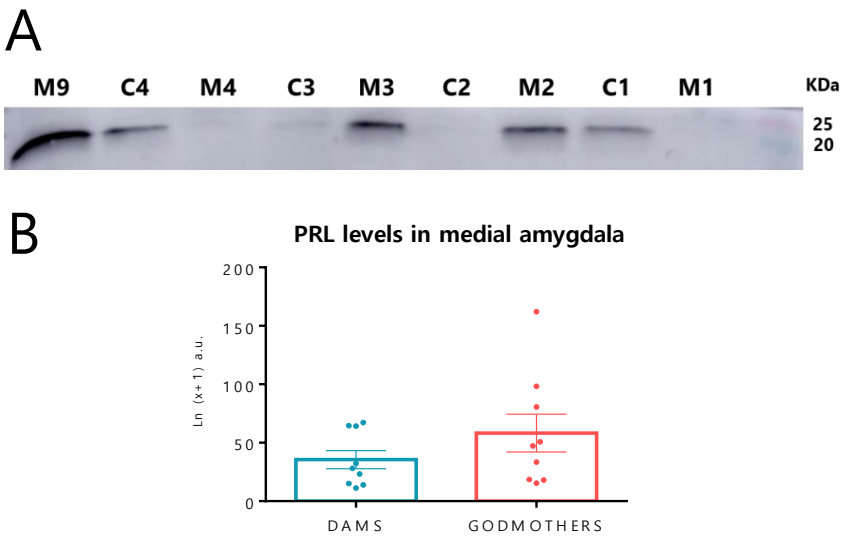

Figure 43: Western blot did not show differences in PRL levels between dams and godmothers. A) An immunoreactive for PRL band of 23 KDa was detected in Me samples. Only one membrane of the total (4 membranes) is shown in the figure. B) The t-test of independent samples of the ln-transformed data did not

present significant differences in relative amount of PRL in Me between dams (n=9) and godmothers (n=9). Data are represented as mean ± SEM. M=dam; C=Godmother. For abbreviations see list.

EXPERIMENT 3

ENZYME-LINKED IMMUNOSORBENT ASSAY (ELISA)

To confirm the results obtained in the Western blot, we carried out an ELISA assay of PRL levels in dams and godmothers from serum and Me samples.

Outlier analysis

Before the comparison between levels of PRL in dams and godmothers a Tukey outlier detection tests was carried out. The Tukey's boxplots indicated that the godmother number 6 and 5 had levels of PRL that can be consider outliers. The values observed in animal 5 were 5.39 ng/ml and in animal 6, 9.26 ng/ml. The value for Q3 obtained in the Tukey's boxplots was 0.76 ng/ml and 0.07 ng/ml for Q1. For this reason, both animals were considered outliers and they were excluded of the t-test of independent samples of the Me (FIGURE 44).

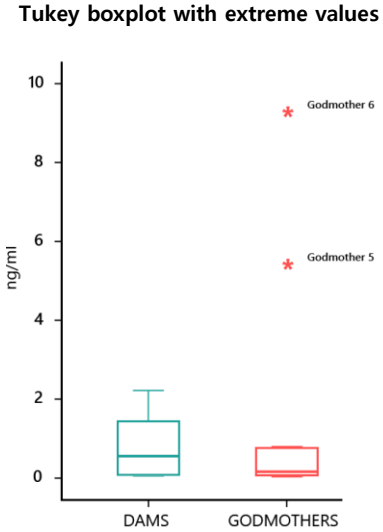

Figure 44: The Tukey boxplot results for ELISA PRL levels in dams and godmothers. The godmothers 5 and 6 were significant outliers (*) because of their extreme values.

Prolactin in serum and medial amygdala

The t-test of independent samples of ELISA assay of PRL levels in serum of the ln-transformed data showed highly significant differences between the PRL quantity in serum of PRL in dams and godmothers ($t(17) = -5.831$, $p < 0.01$ (FIGURE 45).

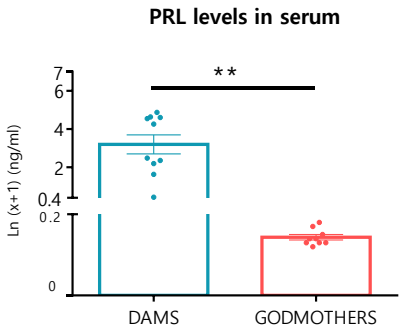

*Figure 45: ELISA assay from serum samples shown differences in PRL levels between dams and godmothers. The t-test of independent samples of the ln-transformed revealed highly significative differences in concentration of PRL in serum between dams (n=10) and godmothers (n=9). Data are represented as mean ± SEM; ** p<0.01. For abbreviations see list.*

Regarding the PRL levels in Me, the t-test of independent samples was carried out without the outliers described before. By contrast with the results obtained with Western blot, the results of the ELISA of the ln-transformed data of PRL in Me showed significant differences in the concentration of PRL in dams with respect to godmothers (t (12.37) =-2.253, p =0.043 (FIGURE 46). Thus, whereas the analysis with a semi-quantitative technique such as Western Blot failed to demonstrate significant differences in the amount of PRL in the Me, the quantitative ELISA revealed that dams have more PRL in the Me than godmothers.

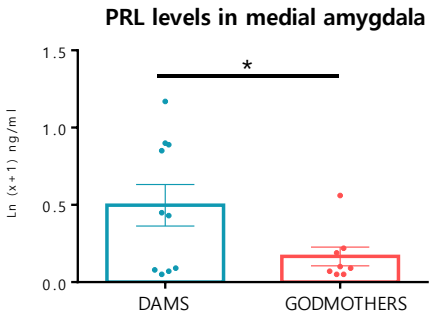

*Figure 46: ELISA assay from Me microextractions shown differences in PRL levels between dams and godmothers. The t-test of independent samples of the ln-transformed revealed significative differences in concentration of PRL in dams (n=10) with respect to godmothers (n=10). Data are represented as mean ± SEM; * p<0.05. For abbreviations see list.*

In order to know whether the levels of PRL obtained in serum correlate with those obtained in the Me of the same animals, a Pearson's correlation was run with the ln-transformed data from both samples (serum and Me). The analysis revealed lack of correlation between the levels of PRL obtained in serum and the ones obtained in the Me (r =-0.001, n =19, p=0.996) (FIGURE 47). This result further suggests that there is a central PRL source in the brain, independent of peripherally released PRL.

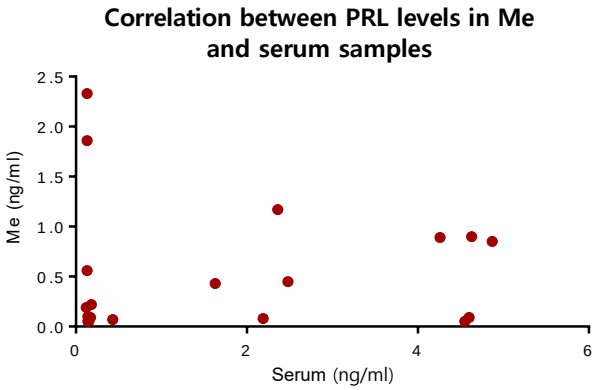

Figure 47: No significant correlation between the levels of PRL obtained in the ELISA of Me and serum. Me r =-0.001, n =19, p=0.996. For abbreviations see list.

Finally, A Pearson's correlation was run to determine the methodological consistency between the results from Western blot and the results obtained in the ELISA in Me of the same animals. This analysis showed a strong, positive and significant correlation (r =0.944, n =18, p<0.01), between the relative quantification of PRL obtained by Western blot and the amount of PRL observed in the ELISA (FIGURE 48). In addition, a positive and significant correlation is obtained without the two samples with outlier values descrived above (r =0.643, n =16, p=0.007) (data not shown).

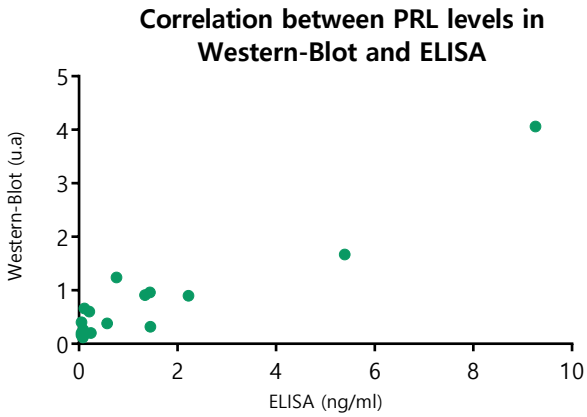

Figure 48: Positive correlation between the results obtained using Western blot and ELISA. Significant correlation between the levels of PRL obtained in the Western blot and ELISA. r =0.944, n =18, p<0.01. For abbreviations see list.

EXPERIMENT 4

MEDIAL AMYGDALA IMMUNOHISTOCHEMISTRY

Prolactin antibody blocking tests in brain tissue

Since results from previous experiments showed the presence of PRL in the Me, we sought to analyse the location of this protein in the tissue. Immunohistochemistry for PRL produced a

defined labelling in the studied brain tissue that was blocked with the rat natural PRL, but not when the antibody was incubated without the protein (FIGURE 49). However, by contrast to the result in competition assay in Western blots of protein extract from pituitary glands (Results: Experiment 2, Section 1), when the rabbit anti-mouse natural PRL antibody was pre-incubated with the mice recombinant PRL the labelling was not blocked in the immunohistochemestry.

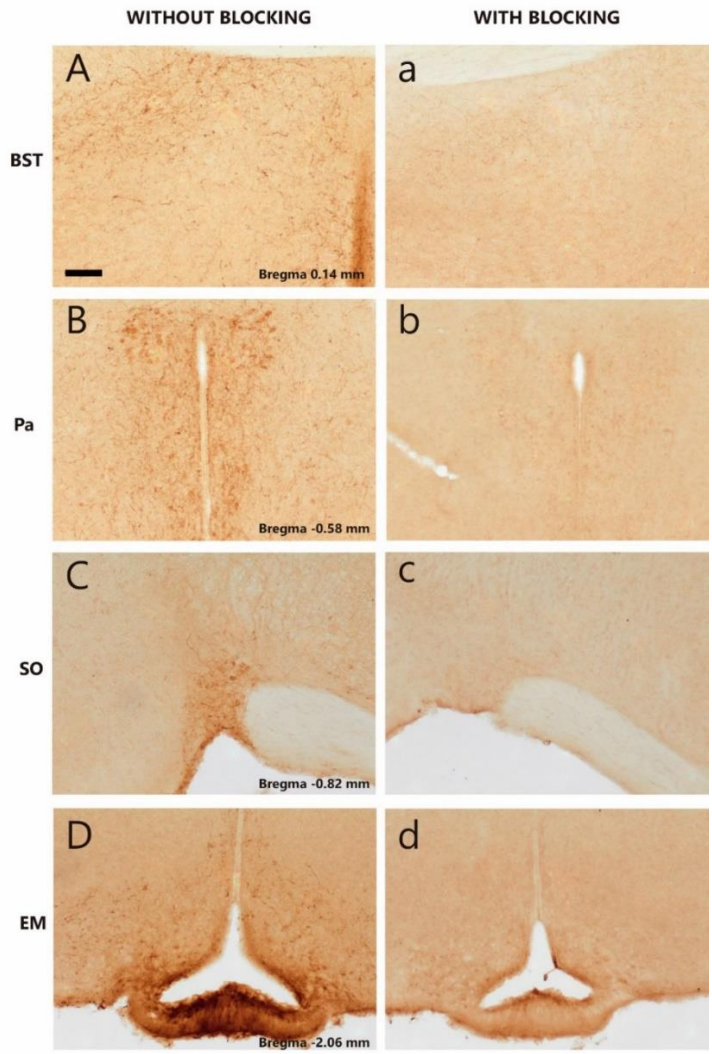

Figure 49: Blocking control of the rabbit anti-mouse natural PRL (National Hormone and Peptide program). Preincubation with mouse natural PRL virtually abolished all PRL-ir in the examined tissue (a-d), except for some faintly labelled cells and fibres), as compared to sections preincubated without the peptide (A-D). Overall, this indicates that this primary antibody specifically binds to PRL proteins, thus validating the employed primary antibody. Scale bar: 100 µm. For abbreviations see list.

In all, since blocking was successful with natural PRL, and with recombinant in Western Blot, we assumed that all the immunohistochemical procedures carried out with this antibody show a specific labelling of PRL in brain tissue (see Discussion).

Quantification of prolactin-ir innervation of the medial amygdala in dams, godmothers and virgin females

Since the ELISA revealed a significant increase in PRL in the Me of dams as compared to virgins, we hypothesise that PRL-ir fibre density might differ among virgin, godmothers and lactating females. To test this hypothesis, we estimated the number of PRL-ir fibres on each of the sampled subdivisions of the Me and performed a one-way ANOVA.

To do so, we first removed the extreme values from the data in each subdivision of Me (FIGURE 50A), and checked the normality and homogeneity of variances. Data analysis revealed no statistically significant inter-group differences in PRL-ir density of fibres in MeA ($F_{2,17}$=1.368, p>0.05) and MePD ($F_{2,16}$=0.608, p>0.05). In the case of MePV the Levene's test for homogeneity of variances showed significant differences (p=0.025), and thus Welch and Brown-Forsythe ANOVAs were used to compare the three studied groups. The Welch ANOVA ($F_{2,8.41}$=0.762, p>0.05) and Brown-Forsythe ANOVA ($F_{2,9.15}$=0.664, p>0.05) did not reveal significant differences between groups (FIGURE 50B).

After eliminating the extreme values in all the Me subdivisions for the number of squares with PRLergic fibres (FIGURE 51A) and check the normality of the data, a Levene's test for homogeneity of variances was carried out. In the case of MeA and MePD, the homogeneity of variances did not give significative values thus a one-way ANOVA was carried out. The ANOVA did not show significant values for any of the nuclei (MeA: $F_{2,17}$=0.225, p>0.05; MePD: $F_{2,16}$=0.693, p>0.05) (FIGURE 50B). Regarding MePV, Levene's test showed significant differences (p=0.012) so a Welch and Brown-Forsythe ANOVA was used to compare the three studied groups. The ANOVA, did not show any significant effect of the factor GROUP (Welch: $F_{2,7.06}$= 3.319, p=0.096; Brown-Forsythe: $F_{2,10}$=2.442, p>0.05) (FIGURE 51B). These data suggest that the increase in the amount of PRL in the Me of dams is not due to structural changes in the PRL-ir fibres.

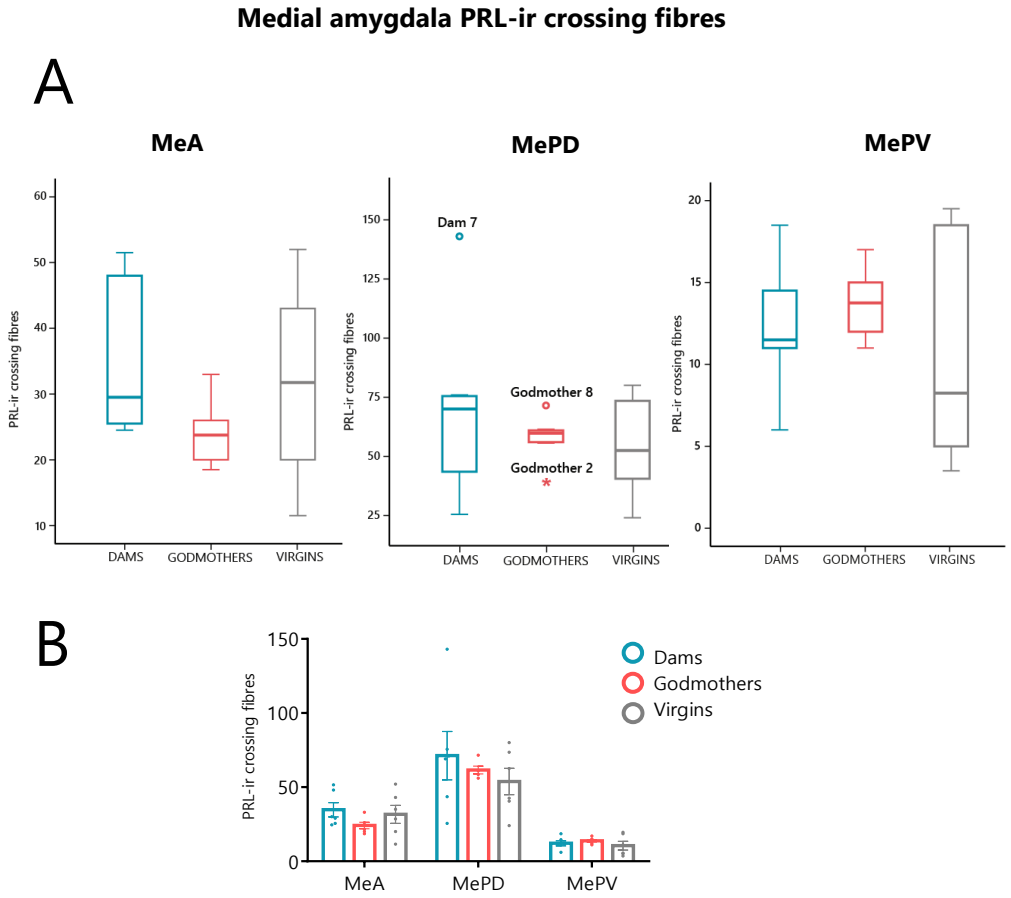

Figure 50: The quantification of Me PRL-ir crossing fibres did not shown significative differences between the studied groups. A) Tukey boxplot results for Me presented one extreme value in the group of godmothers (godmother number 2 presented 38.5 PRL-ir crossing fibres.) in MePD. B) The one-way ANOVA did not reveal significant differences in the number of positive PRL crossing fibres between godmothers, dams and virgins in the three Me subregions. Bar histograms show mean interhemispheric PRL-ir crossing fibres ±SEM. in the Tukey fences test points the extreme values (3 times the Interquartile Range); O points the out values (1.5 times the Interquartile Range). For abbreviations see list.*

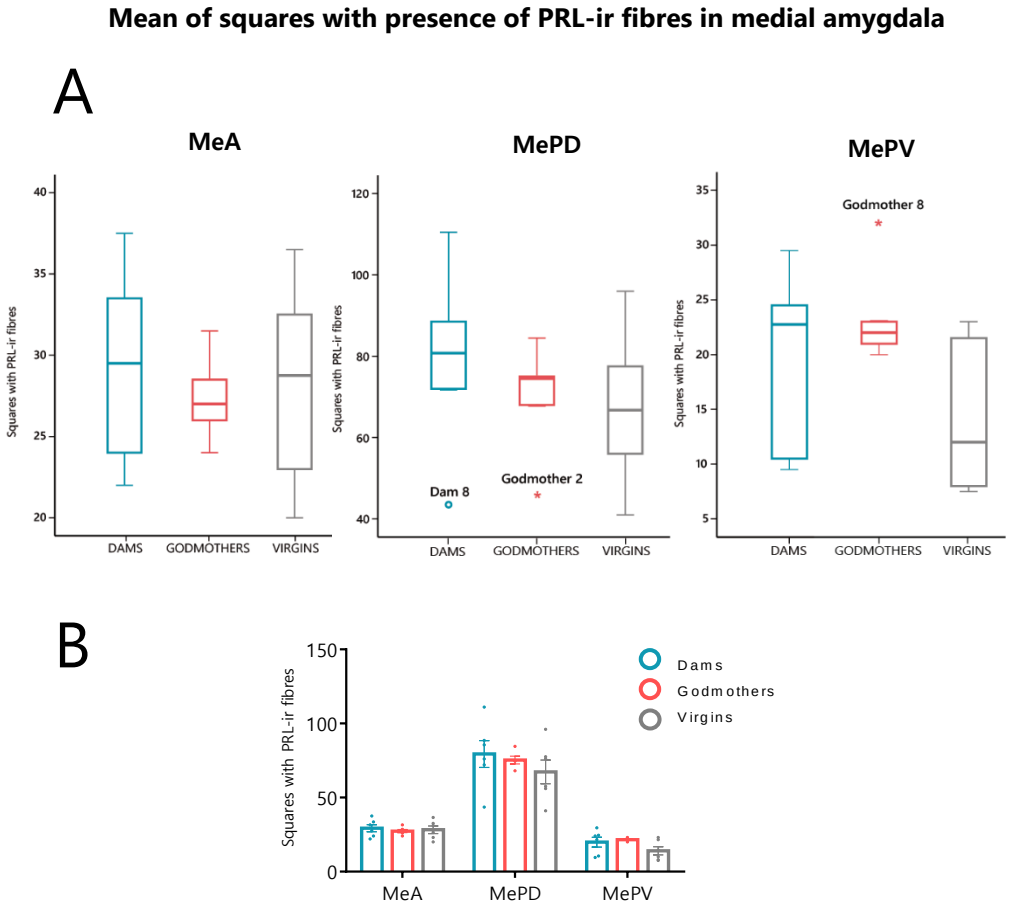

*Figure 51:The average of squares with presence of PRL-ir fibres did not shown significant differences between the studied groups. A) Tukey boxplot results for Me presented an extreme value in the group of godmothers (godmother number 2 presented a mean of 46 PRL-ir number of positive squares.) in MePD and another in MePV (godmother number 8 presented an average of 32 squares PRL-ir fibres.). B) The one-way ANOVA did not reveal significant differences between godmothers, dams and virgins in MeA, MePD and MePV. Bar histograms show mean interhemispheric PRL-ir crossing fibres ±SEM. * in the Tukey fences test points the extreme values (3 times the Interquartile Range); O points the out values (1.5 times the Interquartile Range).*

DISCUSSION

The present studies confirm the presence of PRL in the Me and, importantly, that the increase observed in *Prl* mRNA of dams in Chapter II is also observed in PRL protein levels, at least as measured by ELISA.

Firstly, we first checked the existence of PRL with different molecular weights, as previously described in the pituitary gland (Clapp et al. 1989, 1994; Torner et al. 1995; Freeman et al. 2000) and in Me (DeVito 1988). The proteomic analysis shows that both Me and pituitary gland present PRL peptides in the 23 KDa band, but the amount is higher in the latter structure (ANNEX V, TABLE 4A AND C). Also, the 16-14 KDa PRL was present in the pituitary gland only. Consistent with our results, the measurements of PRL-ir protein in CNS are, depending on the specific region, about 20,000-to 350,000-fold lower than those in pituitary gland (Emanuele et al. 1992). The amount of PRL observed in the pituitary gland approximately varies between 11 $x10^6$ pg/mg protein in male rats (Emanuele et al. 1986, 1987, 1989) and 58±15 $x10^6$ pg/mg in female rats (DeVito et al. 1987a; DeVito 1988; Devito 1989). In contrast, the female rat ventral and dorsal hypothalamus presented 25±3.6 x 10^3 pg/mg and 6 $x10^3$ pg/mg respectively and the Me 3.5±0.95 $x10^3$ pg/mg (DeVito et al. 1987a; DeVito 1988; Devito 1989). These results show that the amount of PRL present in the amygdala is much lower than in the pituitary gland (DeVito 1988) and probably the quantity of protein used for the assays was not enough to observe the 16-14 KDa PRL in Me.

Since we hypothesise that PRL exerts key functions during motherhood, and the results of Chapter 2 showed that *Prl* mRNA was significantly increased in the Me of dams as compared to virgin pup-sensitized females, we sought to confirm that this change was reflected in the protein levels. Although we were unable to detect any differences between dams and godmothers using a Western blot assay or counting manually the number of PRL-ir fibres in Me, we observed significantly higher amount of PRL in the Me of dams as compared to godmothers by performing an ELISA in the same sample. A factor that contributes to this difference between techniques is statistical, because the extreme values of two godmothers, which cannot be consider as far outs in the Western blot, were detected as such in in the ELISA (FIGURE 44). A second factor likely contributing to this difference is the nature of the technique. Thus, whereas the Western blot can be considered semiquantitative, because it estimates the amount of protein by means of optical density of the sample, relative to a housekeeping protein, the ELISA is a quantitative method, and as such is more precise. The sensitivity of the ELISA kit (Ref# ab214572; ABCAM) employed is 139 pg/ml, being able to detect very low levels of protein present in the samples. It

is also important to notice that we found a correlation between the values obtained by both techniques, giving reliability to our result. Regarding the manual counting of fibres, it is important to remark that differences in the amount of protein cannot be observed using this technique.

The increase in PRL in the Me of dams with respect to godmothers suggests that PRL levels are subjected to fluctuations caused by pregnancy, lactation and the oestrous cycle, as they are in serum PRL. Regarding neural PRL, previous studies in the cerebellum, hippocampus, hypothalamus and neocortex of dams described significant changes in expression of *Prl* during lactation in all brain regions examined, with relative high levels at PPD1 and PPD3 (Ray et al. 2016). These results point in the same directions of Chapter II results, suggesting an upregulation of *Prl* in brain mRNA levels during lactation. Thus, the increase in *Prl* mRNA together with ELISA results indicate that this rise in mRNA during lactation is being translated into protein as result of motherhood.

In the case of godmothers neural PRL, it has been reported before in virgin female mice that gene expression of *Prl* is increased in hypothalamus during metestrus (DiCarlo et al. 2017). This increase in PRL observed in female mice metestrus could explain the variations within the group of godmothers since they could be in different stages of oestrous cycle at the moment of being sacrificed. In addition, in the paraventricular nucleus (Pa) and SO, *Prl* mRNA levels appeared to be associated with the hormonal status of male and female rats. These studies observed a higher increase in *Prl* mRNA signal in cycling females than in males, with the highest value in oestrus (Torner et al. 1999). In addition, the expression of *Prl* mRNA in the Pa and SO correlates with the presence of PRL-ir in magnocellular neurons from both hypothalamic nuclei (Clapp et al. 1994; Mejía et al. 1997). Moreover, this variation observed in the group of pup-sensitized females can be related with the fact that some virgin females stop presenting ovarian cyclicity when they are exposed to pups for a certain time, suggesting that they enter in a pseudo-pregnant state in response of pups stimuli (Marinari and Moltz 1978; Erskine et al. 1980). In fact, when virgin females were exposed to pups during 9 days 83% of the females showed oestrous cycles after a exposure to an intruder male and only the 12.5% of the females showed normal oestrous cycles after 18 days of maternal experience (Erskine et al. 1980). This disruption of oestrous cycle in some of the godmothers could explain the variability observed in brain PRL levels in our experiments and probably the godmothers with highest levels of PRL in Me are in metestrus (maybe pseudopregnancy) or oestrous.

In the case of PRL levels in serum we also obtain a significative increase in dams (as expected) when we compare them with godmothers. In rodent lactating females, during pregnancy PRL levels in serum varies during early gestation, after mid gestation the levels suffer a dramatic decrease, when PL begin to rise, and right before the delivery PRL levels start to increase again (Grattan 2001; Soares 2004). In the PPD serum PRL levels decrease gradually until weaning (Broida et al. 1981; Roy and Wynne-Edwards 1995), and for these reasons it is probably that dams present some variability between them. In rats, these differences in concentration in serum PRL levels between lactating and virgin females sensitized to pups were observed previously by Stern & Siegel, (1978). They observed by radioimmunoassay that the lactating females presented significatively high levels of PRL in serum than the maternal virgin group (Stern and Siegel 1978).

On the other hand, although we obtain a strongly significant increase in PRL levels in plasma and Me of dams with respect of godmothers, the PRL levels in serum did not correlate with the levels obtained in Me in the same animals. This can be suggesting that the PRL regulation in the brain is independent or partially independent of the regulation of peripheric PRL. Previous studies have seen that concentration of PRL in the CNS does not decrease after hypophysectomy in the male rat (Emanuele et al. 1987; DeVito 1988). By contrast, in the female rat, hypophysectomy decreased, but not completely eliminated, the concentration of PRL in most of the brain regions studied (DeVito 1988). Thus, PRL levels found in the rat brain cannot simply be a reflection of vascular transport from plasma. Thus, together with the results obtained in Chapter II, it is likely that PRL is being synthetized *de novo* in the CNS, and probably playing a neuromodulatory role in the brain. Also, the small amounts of PRL found in previous studies and in our study suggest that it is unlikely that brain PRL contributes to the plasma PRL pool, but it may be playing a role in the central control of maternal behaviours.

In summary, the increase in brain PRL in dams can be related with the physiological changes of pregnancy and lactation. One of these changes related with PRL is its anxiolytic effect which is needed in the maintenance of maternal behaviour (Torner and Neumann 2002; Torner et al. 2002). Also, PRL is involved in the inhibition of HPA axis responses in lactating rats in order to inhibit the negative feedback of PRL synthesis by TIDA neurons in the arcuate nucleus (Slattery and Neumann 2008) and also modulates OXT system reactivity during lactation (Freeman et al. 2000; Grattan and Kokay 2008; Kennett and Mckee 2012; Augustine et al. 2017). For all these reasons, the increase of PRL levels in Me that are being synthetized *de novo* in the brain can be playing a neuromodulatory role related with the control of maternal behaviours.

CHAPTER IV

DISTRIBUTION OF PROLACTIN IN THE MOUSE BRAIN

INTRODUCTION

PRL from the pituitary gland can enter in the brain via specific transporters located in the membranes of the choroid plexus (Walsh et al. 1987; Brown et al. 2016). Moreover, a recent study reported that PRL transport into the mouse brain occurs mainly in the cerebral vasculature independently of the PRLR and requires a transporter that has not been identified yet (Brown et al. 2016). In addition, the results obtained in Chapters II and III indicate a synthesis of neural PRL independent from the pituitary.

Consistent with the existence of neural PRLergic circuits, as discussed in Chapter III, PRL is not decreased by hypophysectomy in any brain regions of the male rat, whereas in females the concentration is reduced significantly, but not eliminated, in hypothalamus, amygdala, thalamus, and pons-medulla (DeVito 1988; Devito 1989). In addition, previous literature (as well as our own results, see Chapter II) describes the presence of *Prl* mRNA in different species such as rodents (Schachter et al. 1984; Torner et al. 2004; Cabrera-Reyes et al. 2017), sheep (Roselli et al. 2008), reptiles (Kato et al. 2005), amphibians (Imaoka et al. 2004), birds (Chaiseha et al. 2012) and fish (Imaoka et al. 2004). Several previous studies have described PRL-ir in the brain of rats (Fuxe et al. 1977; Toubeau et al. 1979a, b; Hansen et al. 1982; Thompson 1982; Alonso et al. 1988; Harlan et al. 1989; Siaud et al. 1989; Paut-Pagano et al. 1993) and sheep (Roselli et al. 2008). All these data argue in favour of PRL synthesis by brain cells.

It is known that PRL modulates diverse physiological processes, including angiogenesis, immune response, osmoregulation, reproductive behaviour, and lactogenesis. Apart from these effects in peripheral systems, PRL plays an important role in several brain areas, and it has an effect in maternal behaviour as well as on neurogenesis, neural plasticity, and neuroprotection (Freeman et al. 2000; Grattan 2001; Cabrera-Reyes et al. 2017).

In the present study, we sought to characterise the anatomical patterns of PRL distribution and colocalization with other neuropeptides (OXT and vasopressin (AVP)) in the brain of pup-naïve virgins, pup-sensitized virgin (godmothers) and lactating female mice. To do that, we employed the immunohistochemical detection of PRL, OXT and AVP. First, we mapped the presence PRL-ir in the brain of the three female groups. We also assessed the number of immunoreactive cells in selected brain regions related with the neurosecretory system and the sociosexual brain (Newman 1999) and compared the density of PRL positive cells between the different groups of females. After that, we studied the colocalization of PLR with OXT and AVP (separately), following

previous studies of Mejía, Morales, Zetina, Martínez de la Escalera, & Clapp, (1997). These studies give us new information about neural PRL distribution in the brain of female mice, and we discuss the implications for its possible role in the regulation of maternal behaviours and in neurosecretion.

MATERIAL AND METHODS

EXPERIMENT 1

PROLACTIN DISTRIBUTION STUDY

The animals used, as well as the immunohistochemistry protocols and control specificity tests, are explained in Chapter 3 (see Material and Methods of Experiment 4). In addition, given that previous descriptions of the PRL immunohistochemical detection in the brain of rats, positive cells have shown in SO and Pa using different antibodies obtained against rat PRL (Mejía et al. 1997), we tested our antibody in sections of rat brains (kindly provided by Dr. Vicent Teruel, University of València). We obtained a labelling (FIGURE 52) that matched with the description of PRL distribution in rat brain (Toubeau et al. 1979b; DeVito 1988; Siaud et al. 1989) and was very similar to that obtained in mice (see Results).

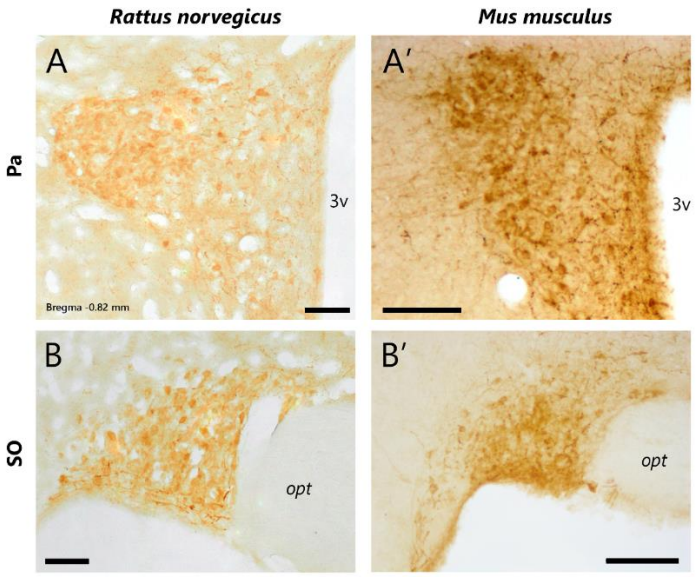

Figure 52: Comparation of PRL labelling in rat and mice in Pa and SO. The presence of labelled somata and fibres were present in the same nuclei in rat (Rattus norvegicus) (A and B) and mice (Mus musculus) (A' and B') virgin females. Scale bar: 100 µm. For abbreviations see list.

For the distribution study tissue samples were observed using an Olympus CX41RF-5 microscope and photographed with a digital Olympus XC50 camera. Figures and picture captions were

carried out using Adobe Photoshop CS6 (Adobe Systems, MountainView, CA, USA). No further changes were performed.

The Paxinos & Franklin (2004) atlas was used as a reference to draw the boundaries and divisions of the different nuclei in our sections. The distribution of PRL in the brain was mapped using one of the experimental animals (virgin M1684) as a model of the labelling pattern. On the other hand, the photomicrographs illustrating PRL distribution were taken from the lactating female M16104.

EXPERIMENT 2

DOUBLE FLUORESCENT IMMUNOHISTOCHEMISTRY

Four adult virgin females were employed to study the colocalization of OXT and AVP with PRL. Two series of each animal were used in these experiments: one for double PRL+AVP immunofluorescence and other for double PRL+OXT immunofluorescence.

Sections of the four virgin females were completely washed three times for at least 5 minutes in TBS (0.05M, pH 7.6). After that an antigen retrieval step was carried out, consisting in a first incubation for 15 minutes in citrate buffer (0.01 M, pH 6) at 90-95°C followed by 10 minutes in ice. These steps were repeated twice. Then, the tissue was washed again three times with TBS for 5 minutes.

Secondly, sodium borohydride (diluted 1% in TBS) was used as an aldehyde-blocking reagent for 30 min at room temperature. After that, sections were incubated in a blocking solution containing 3% NGS in TBS-Tx (0.3% Triton X-100 in 0.05 M TBS, pH 7.6) for 2 hours at room temperature. Next, the two series of each female were incubated for 48 hours with different antibodies: a) one of the series was incubated with a mixture of rabbit anti-mouse natural PRL (provided 1:40 by National Hormone and Peptide program, LOT# AFP-879151Rb) diluted 1:500, and mouse anti-OXT (Dr Harold Gainer, National Institutes of Health (NIH), Cat#PS38) diluted 1:200 in TBS-Tx with 2% NGS; b) the other series of the same animals was incubated with a solution of rabbit anti-mouse natural PRL diluted 1:500, and guinea pig anti-AVP (Peninsula Laboratories International, Cat#T-5048.0050) diluted 1:10000 in TBS-Tx with 2% NGS.

After rinsing, the sections were incubated with a mixture of two fluorescent secondary antibodies depending on the double immunofluorescence detection: a) the series for PRL and OXT immunodetection was incubated with Rhodamine Red-X Goat anti-Mouse (Invitrogen, Cat# R-

6393), diluted 1:250, and Alexa Fluor® 488 Goat Anti-Rabbit (Jackson ImmunoResearch, Cat# 111-545-144) diluted 1:100, in TBS-Tx with 2% NGS; b) the series for PRL and AVP double immunodetection was incubated with Rhodamine Red-X Goat Anti-Rabbit (Jackson ImmunoResearch, Cat# 111-295-003) diluted 1:100 and Alexa Fluor 488 Goat anti-Guinea Pig (Invitrogen, Cat# A-11073) diluted 1:200 in TBS-Tx with 2% NGS. Finally, sections were mounted onto gelatinized slides and cover-slipped with fluorescence mounting medium (Fluoromount, Merk).

The colocalization of OXT or AVP positive cells with PRL-ir somata was studied in SO and Pa, following Mejia et al. (1997), and also in the Me and the median eminence.

The photomicrographs showing the labelling pattern of PRL and AVP or OXT were obtained from the lactating female M1813. Images were acquired with a Leica TCS SPE confocal microscope using 20X objective. Figures were prepared using Adobe Photoshop CS6 (Adobe Systems, MountainView, CA, USA).

EXPERIMENT 3

QUANTITATIVE ANALYSIS OF PROLACTINERGIC SOMATA

The animals compared in the quantification study, the immunohistochemistry protocols and control specificity tests were the same as the ones explained in Chapter 3 (see Material and Methods of Experiment 4) and in Experiment 1 in this chapter.

Regarding the quantification, representative levels of nuclei with labelled somata were selected using the stereotaxic atlas of Paxinos & Franklin (2004). Bregma levels of the studied structures were: BSTMPM: 0.2 / -0.30 mm, the region of antero-dorsal preoptic nucleus and anterior commissural nucleus (AC/ADP): 0.2 / -0.30 mm, MPO/A: -0.2 / -0.30 mm, SO: -0.7 / -0.82 mm, Pa: -0.8 / -0.9 mm, the suprachiasmatic nucleus (SCh): -0.7 / -0.8 mm and Arc: -1.80 mm. The MPO/A is the hypothalamic region that comprises both nuclei in the atlas (medial preoptic nucleus (MPO) and MPA) (FIGURE 53) (Paxinos and Franklin 2004). Photomicrographs of these frames were obtained in both hemispheres (if it was possible) using a digital camera (Leica DFC495) attached to a microscope Leitz DMRB (Leica AG, Germany) with a 20x objective (counting frame of 330 x 441µm) with the exception of Pa and BSTPM which were photomicrographed with 10x objective (counting frame of 881 x 661µm). After that, positive cells of each photomicrograph were counted manually using Fiji (Schindelin et al. 2012) cell counter

plugin by two experimenters blind to the condition of the animals. The average of the cell counts obtained by the two experimenters was used for further calculations.

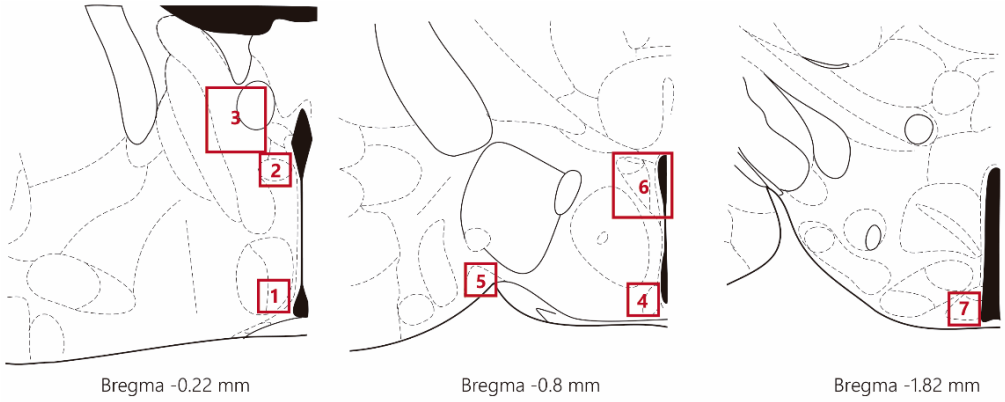

Figure 53: Anatomical location of PRL-ir somata counting frames. Schematic drawings of selected coronal sections featuring the counting frames (red) chosen for PRL-ir cells quantification: 1 MPO/A; 2 AC/ADP; 3 BSTMPM; 4 AC/ADP; 5 SO; 6 Pa; and 7 Arc. Approximate distance to Bregma enclosed for each section. For abbreviations see list.

Firstly, the average of both hemispheres was calculated for each nucleus. Statistical analysis was conducted using the SPSS software package (IBM SPSS Statistics 24.0). After eliminating the outliers (as explained in Chapter III, General procedures), normality (Shapiro-Wilk test) and homoscedasticity (Levene's test) were checked. Finally, a one-way ANOVA was performed on each nucleus to assess inter-group differences (dams, godmothers and virgin pup-naïve females) on the mean number of PRL-ir cells. The results of the ANOVA were further explored by means of post-hoc pairwise comparisons with Bonferroni's correction. When homogeneity of variance could not be assumed, we carried out the Welch and Brown-Forsythe ANOVAs with the Games-Howell pairwise comparison post-hoc test.

If the data did not follow a normal distribution, a non-parametric test for independent samples (Kruskal Wallis test) was carried out with pairwise comparison (Dunn-Bonferroni) as post-hoc test.

RESULTS

EXPERIMENT 1

PROLACTIN DISTRIBUTION STUDY

The distribution of PRL-ir structures in the brain of lactating females is described as a reference. Thereafter, we describe and analyse the differences observed in the number of labelled somata in some brain nuclei in comparison with virgin females and godmothers.

The presence of positive PRL-ir cell bodies was restricted to a few nuclei, mostly related with the sociosexual brain or with the neurosecretory system (FIGURE 54 AND FIGURE 55). Most PRL-ir cell bodies in the brain appeared in BST and the hypothalamus (TABLE 8).

Table 8: Distribution of PRL-immunoreactive cell bodies in the brain of dams, godmothers and virgin females. The distribution of PRL-ir somata was indistinguishable in the three groups of females. For abbreviation see list. ++++ very dense; +++ dense; ++ moderate; + scarce and ↓+ very scarce.

TELENCEPHALON	**AMYGDALA AND BST**		
	Vomeronasal amygdala	MeA	↓+
	BST	BSTLV	++
		BSTMA	↓+
		BSTMPM	+
		BSTMV	++
	BASAL FOREBRAIN		
	Striatum-pallidum	AL	↓+
DIENCEPHALON	**HYPOTHALAMUS**		
	Preoptic	AC/ADP	+++
		AVPe	+
		MPO/A	+
		VLPO	++
	Anterior	AH	↓+
		Pa	++++
		Pe	++++
		SCh	++
		SO	++++
	Tuberal	Arc	++
		LH	+
		TC	+

Amygdala, bed nucleus of the stria terminalis and basal forebrain

In the telencephalon, the amygdala showed a very sparse presence of PRL-ir somata, located in the most anterior parts of the MeA (FIGURE 54F and FIGURE 55G).

In the rest of the telencephalon, most of the PRL-ir neurons were in the BST. The medial part of BST showed labelled cell bodies mainly in the ventromedial division (BSTMV), BSTMPM and the anteromedial division (BSTMA) (FIGURE 54B-D and FIGURE 55A and B). BSTMV had a moderate presence of labelled perikarya close to the anterior commissure (*acp*). Regarding BSTMPM, a sparse presence of PRL-ir cell bodies was observed in this subdivision, but it is important to remark that the cell population was placed in the vomeronasal-related region of the nucleus (Scalia and Winans 1975; Cádiz-Moretti et al. 2013). In addition, a very low number of PRL-ir neurons was also present in BSTMA, which we could not observe in all the studied animals.

Finally, the lateral part of the BST showed a moderate number of labelled cells located in its ventrolateral subdivision (BSTLV), in the region close to BSTMV.

In the basal forebrain, only a few PRL-ir cell bodies were observed in the nucleus of the *ansa lenticularis* (AL) (FIGURE 54F and FIGURE 55H) (TABLE 8).

Hypothalamus

In the preoptic hypothalamus, PRL-ir cell bodies were numerous in the region between the nucleus of the anterior commissure (AC) and the antero-dorsal preoptic nucleus (ADP) (FIGURE 54E and FIGURE 55E). Another preoptic nucleus of the hypothalamus with moderate presence of PRL-ir somata was the ventrolateral preoptic nucleus (VLPO), where the somata were located mainly in the superficial regions of the nucleus (FIGURE 55C) (TABLE 8).

In addition, a few cells were observed in the anteroventral periventricular nucleus (AVPe) (FIGURE 55B and C) and in the MPO/A. In AVPe, the somata were found surrounding the nucleus, next to the third ventricle (3V) in the most anterior regions (FIGURE 55B). In the case of MPO/A, the PRL-ir cell bodies were located at most superficial regions of the nucleus close to AVPe in the rostral parts (FIGURE 55B and C) and to the periventricular hypothalamic nucleus (Pe) in the caudal ones (FIGURE 55D) (TABLE 8).

In the anterior hypothalamus, Pa, Pe and SO had the densest population of PRL positive somas in the three studied groups of females (TABLE 8). Pa showed a very dense presence of PRL-ir cells, which were mainly concentrated in the lateral magnocellular part of the nucleus, (PaLM) (FIGURE 54F and FIGURE 55E and F). In the SO (FIGURE 54G and FIGURE 55E) and Pe (FIGURE 54E and F and FIGURE 55C-F), a very high number of labelled somata were observed close to their superficial regions. In the case of Pe, PRL-ir cells were present mainly in the anterior parts of the nucleus.

In addition, SCh presented a population of PRLergic somata (TABLE 8). The labelling density was moderate compared with that observed in the Pa, Pe and SO, and the PRL-ir cell bodies were dispersed within the nucleus (FIGURE 55D and E). Finally, a few labelled somata appeared also in the AH, in its central part (FIGURE 55E and F).

In the tuberal hypothalamus, a moderate number of PRL-ir cell bodies was present in Arc (FIGURE 54I and FIGURE 55G and H), always close to the 3V. In addition, it was possible to observe scattered positive somata in the rostral parts of LH (FIGURE 54H and FIGURE 55E and F) and tuber cinereum

area (TC). In TC, the somata were only in the superficial regions, next to the boundaries of the tissue) (FIGURE 55F) (TABLE 8).

Distribution of PRL-ir fibres and terminals

The presence of PRL-ir fibres and terminals were observed mainly in the BST and hypothalamus. In addition, less dense labelling also appeared in the amygdala, the thalamus and several structures in the midbrain and brainstem.

Table 9: Distribution of PRLergic fibres in the brain of the female brain. The distribution of PRL-ir fibres were the same in the three groups of females (dams, godmothers and virgins). For abbreviation see list. ++++ very dense; +++ dense; ++ moderate; + scarce and ↓+ very scarce.

TELENCEPHALON	**OLFACTORY SYSTEM**		
	Olfactory Cortex	AOM	↓+
		AOP	↓+
		DTT/VTT	↓+
	AMYGDALA AND BST		
	Vomeronasal amygdala	MeA	+
		MePD	+
		MePV	↓+
	Basolateral complex	BLA	↓+
		BLP	↓+
		BMA	+
		BMP	↓+
	Central amygdala	CeC	↓+
		CeL	↓+
		CeM	+
	BST	BSTIA	++
		BSTLP	++
		BSTLV	+++
		BSTMA	+++
		BSTMPI	++
		BSTMPL	↓+
		BSTMPM	+++
		BSTMV	++++
	CORTEX		
	Cortex	Cg	↓+
		DP	↓+
		IL	↓+
		Prl	↓+
	SEPTUM AND BASAL FOREBRAIN		
	Lateral septal complex	LSI	↓+
		LSV	+
	Medial septum/Diagonal band	HDB	↓+
		MS	↓+
		VDB	↓+
	Striato-pallidum	Acb	↓+
		AL	++

		IPAC	+
		SI	+
		VP	+
DIENCEPHALON	**HYPOTHALAMUS**		
	Preoptic	AC/ADP	++
		AVPe	+++
		LPO	++
		MPA	+++
		MPO	+++
		VLPO	+
	Anterior	AH	+
		LA	+
		Pa	++++
		Pe	+++
		SCh	++++
		SO	+++
	Tuberal	Arc	+++
		DM	↓+
		LH	+
		MCLH	↓+
		ME	+++
		TC	++
		VMH Shell	+++
	Mammillary	LM	+
		PH	+
		PMD/PMV	++
		SuM	↓+
		VTM	+
	THALAMUS		
	CM	↓+	
	IMD	+	
	LHb	↓+	
	MD	↓+	
	MHb	+	
	PP/PIL/PoT	↓+	
	PV	+++	
	PVA/PVP	+	
	ZI	↓+	
MESENCEPHALON AND RHOMBENCEPHALON	**MIDBRAIN AND BRAINSTEM**		
	Midbrain	DpMe	↓+
		PAG	++
		SNC	+
		SNR	+
		VTA	↓+
	Brainstem	LC	↓+
		LPB	+
		MPB	↓+

Olfactory system

In the olfactory system, a few scattered PRL-ir fibres were observed, located in the anterior olfactory nucleus and *taenia tecta* (TABLE 9). In the anterior olfactory nucleus, labelling was present in its medial (AOM) and posterior (AOP) subnuclei. In the taenia tecta, labelled fibres were found in the dorsal and ventral aspect (DTT and VTT) of this structure. (FIGURE 55A). No labelling appeared in the olfactory bulbs or Pir.

Amygdala and bed nucleus of the stria terminalis

Within the amygdaloid complex, the nuclei with vomeronasal innervation showed low levels of PRLergic fibres. The MeA presented a moderate density of labelling, located next to the *opt* (FIGURE 54C and FIGURE 55E and F). In the MePD, the density of PRL-ir fibres was also moderate, and labelled fibres were observed all over the subdivision (FIGURE 54D and FIGURE 55G). By contrast, the MePV showed very sparse fibre labelling, mainly placed next to the *opt*, as in the MeA (FIGURE 54D and FIGURE 55G). No labelling was observed in the PMCo or the BAOT.

In the basolateral amygdaloid complex, a small number of fibres were observed in the anterior and posterior parts of the basolateral amygdaloid nucleus (BLA and BLP) and in BMA posterior parts of the basomedial amygdaloid nucleus (BMP) (TABLE 9). BMA showed a sparse population of PRL-ir fibres scattered in all the nucleus (FIGURE 55E-G). On the other hand, BLA (FIGURE 55E-G), BMP (FIGURE 55G) and BLP (FIGURE 55H) presented very low levels of labelled fibres.

Finally, the Ce presented a few PRL-ir fibres (TABLE 9), located mainly in the capsular (CeC) (FIGURE 55E-G) and lateral (CeL) divisions of the nucleus (FIGURE 55G). By contrast, the medial division (CeM) (FIGURE 55E-F) displayed a very sparse number of PRLergic fibres.

The nuclei composing the BST displayed the densest populations of PRL-ir fibres in the telencephalon (TABLE 9). Labelled fibres were mainly present in the BSTMV, where a very dense number of fibres were found in all the studied animals. These fibres were placed mainly next to the *acp* (FIGURE 54B and FIGURE 55B and C). BSTMA and BSTMPM also displayed dense levels of PRL-ir fibres, located mainly in the more rostral sections (FIGURE 54A and B FIGURE 55B-D). In BSTMPM, labelling appeared mainly close to the commissure. BSTLV also showed dense levels of PRL-ir fibres close to the *acp* (FIGURE 54B and FIGURE 55B and C). Regarding the rest of the posterior BST, a moderate density of PRL-ir labelled fibres were observed in its posterolateral part (BSTLP), medial postero-intermediate part (BSTMPI), and in the intraamygdaloid of the division BSTIA. In BSTLP the fibres were mainly located close to the *acp* (FIGURE 54B and FIGURE

55C). In BSTMPI, PRL-ir fibres were present in its ventral part, next to the BSTMPM (FIGURE 55D). In the case of BSTIA, labelling was centred in its ventral part (FIGURE 54A, B and D and FIGURE 55G). Finally, the medial division of the posterolateral BST (BSTMPL) showed only a few fibres close to BSTMPI (FIGURE 55D).

Basal forebrain and septal complex

In general, the immunohistochemical detection of PRL gave rise to scarce labelling in the basal cerebral hemispheres, except for the *striato-pallidum areas* (TABLE 9). Thus, a moderate density of PRL-ir fibres was observed in the AL (FIGURE 54H and FIGURE 55F) and a sparse number of labelled fibres appeared in the SI (FIGURE 55C-E), VP (FIGURE 55B-F) and interstitial nucleus of the posterior limb of the anterior commissure (IPAC). In the case of IPAC, the fibres were in the rostral part of the structure (FIGURE 55B-D), and in the VP the fibres were mainly concentrated in the region close to the *acp* and next to the BSTLV. In addition, in the core of the nucleus accumbens (AcbC) the presence of fibres was very sparse (FIGURE 54A).

In the lateral septal complex, a few PRLergic fibres appeared in the intermediate part of the lateral septal nucleus (LSI) and LSV (TABLE 9) (FIGURE 55B and C).

Finally, within the diagonal band PRL-ir fibres were very sparse (TABLE 9). Labelled fibres were found in the vertical and horizontal limbs of the diagonal band (HDB) (FIGURE 55B-D), and the medial septal nucleus (MS) (FIGURE 55B).

Cerebral cortex

In the cerebral cortex, labelling was very scarce and present only in prefrontal regions (TABLE 9), including the prelimbic cortex (PRL), the cingulate cortex (Cg), the infralimbic cortex (IL) and the dorsal peduncular cortex (DP) (FIGURE 55A).

Hypothalamus

Immunoreactivity for PRL was abundant in the four major rostro-caudal divisions of the hypothalamus, as well as in the three medio-lateral compartments (periventricular, medial and lateral) (TABLE 9).

The preoptic region displayed high levels of PRL-ir fibres in the structures surrounding the third ventricle, namely in AVPe, and the vascular organ of the lamina terminalis (VOLT) (FIGURE 54B

and FIGURE 55B). In AVPe (FIGURE 54B and FIGURE 55B) the fibres were located surrounding the boundaries of the nucleus.

The medial region of the preoptic hypothalamus also displayed widespread PRL-ir. Labelling was present in the MPA (FIGURE 54B and FIGURE 55B-D) and MPO, and as well as in dorsal preoptic structures, such as the nucleus of the anterior commissure (AC) or the antero-dorsal preoptic nucleus (ADP) (FIGURE 54E and FIGURE 55C and D). In the case of MPO, it is important to remark that the fibres were located surrounding the boundaries of the nucleus and close to Pe.

Finally, the lateral preoptic (LPO) (FIGURE 55B-D), and VLPO (FIGURE 55C) areas displayed a moderate density of scattered PRL positive fibres.

In the anterior hypothalamus (TABLE 9), the most remarkable PRL-ir group of fibres was observed in Pa (FIGURE 54F and FIGURE 55E and F), Pe (FIGURE 54E and F and FIGURE 55C-G), SO and SCh (FIGURE 55D and E), with a high density of immunostained fibres. Within Pa complex and Pe, labelled fibres were observed homogeneously within these nuclei. In SO, PRL-ir fibres were also located scattered in all the nucleus, whereas in SCh, the PRL-ir fibres were observed around the nucleus.

Additional nuclei with sparser PRL positive fibres were the AH (FIGURE 54F and FIGURE 55E and F) and the latero-anterior hypothalamic area (LA) (FIGURE 55E). LA presented fibres in the ventral area of the nuclei, in the boundaries of the tissue.

In the tuberal hypothalamus (TABLE 9), the highest density of PRL-ir fibres was observed in VMH, Arc and ME (FIGURE 54F and FIGURE 55E and F) (FIGURE 54I and FIGURE 55G and H). In the internal part of ME the fibres were thickened, and they can seem small cells or thick varicosities (Herring bodies (McMillan and Harris 2018)). By contrast, PRL-ir fibres were present in the external and internal parts. It is important to remark that a few fibres extended from Arc into the ME (FIGURE 54I and FIGURE 55G). Regarding the VMH, a dense presence of labelled fibres was observed in the shell of the nucleus (FIGURE 54I and FIGURE 55F and G).

The rest of the tuberal part of the hypothalamus displayed a moderate-to-low density and intensity of immunolabelling. TC showed a moderate number of PRLergic fibres but all of them were in the superficial region, in the boundaries of the tissue (FIGURE 55F). In addition, the lateral hypothalamus (LH) (FIGURE 54H and FIGURE 55E-G) presented a sparse number or PRL-ir fibres.

Finally, the dorsomedial hypothalamic nucleus (DM) and the magnocellular nucleus of the lateral hypothalamus (MCLH) had a very few numbers of fibres. In DM the fibres were homogeneously scattered in all the nucleus, whereas in the case of MCLH the fibres were located close to *ic* (FIGURE 55G).

In the mammillary hypothalamus, PRL-ir fibres were scarce (TABLE 9). The lateral mammillary nucleus (LM) and the ventral tuberomammillary nucleus (VTM), presented a sparse number of PRLergic fibres (FIGURE 55H), located close to the brain surface. In addition, the dorsal part of the premammillary nucleus (PMD) and PMV (FIGURE 55H) presented a sparse number or PRL-ir fibres.

Finally, the medial supramammillary nucleus (SuM), and the posterior hypothalamic area (PH) displayed very scarce immunostaining (FIGURE 55H).

Thalamus

In the thalamic complex, PRL-ir fibres were mainly observed in some midline nuclei, in the posterior intralaminar complex and in the habenula (TABLE 9). In the midline thalamus, a few labelled fibres were seen in the central medial thalamic nucleus (CM), intermediodorsal thalamic nucleus (IMD) and mediodorsal thalamic nucleus (MD), but most of the labelling was in the paraventricular thalamic nucleus (PV). There, the distribution of labelled fibres was heterogeneous, with a moderate-to-low density in the anterior and posterior divisions of the nucleus (PVA and PVP) and a high density in its intermediate part (PV) (FIGURE 54J and FIGURE 55D and G). In addition, sparse PRLergic fibres were present in the medial habenular nucleus (MHb) and very sparse in the lateral habenular nucleus (LHb) (FIGURE 55G). The zona incerta (ZI) presented a very sparse amount of PRL-ir fibres (FIGURE 55G and H). Finally, very few fibres were found in the posterior intralaminar thalamus, located in the peripeduncular nucleus (PP), the posterior intralaminar thalamic nucleus (PIL) and the triangular part of the posterior thalamic nuclear group (PoT) (FIGURE 55I).

Midbrain and brainstem

In the midbrain, PRL-ir fibres were observed mainly in the periaqueductal grey (PAG) (TABLE 9). This nucleus presented a moderate number of labelled fibres placed most of them in its dorsal part and close to the dorsal 3rd ventricle (D3V) and the aqueduct (Aq) (FIGURE 55H and I). Within the midbrain tegmentum, PRL-ir fibres were present in the ventral aspect of the deep mesencephalic area (DpMe) (FIGURE 55I). In the *substantia nigra*, both the *pars compacta* and the

pars reticulata (SNC and SNR) (FIGURE 55H and I) presented a sparse number of immunostained fibres. Finally, VTA presented few PRL-ir fibres (FIGURE 55I).

In the rhombencephalon, the parabrachial complex presented sparse PRL-ir labelling in the lateral (LPB) and the medial (MPB) subdivisions (not shown). Furthermore, the locus coeruleus (LC) showed a very few and scattered mount of PRLergic fibres (not shown) (TABLE 9).

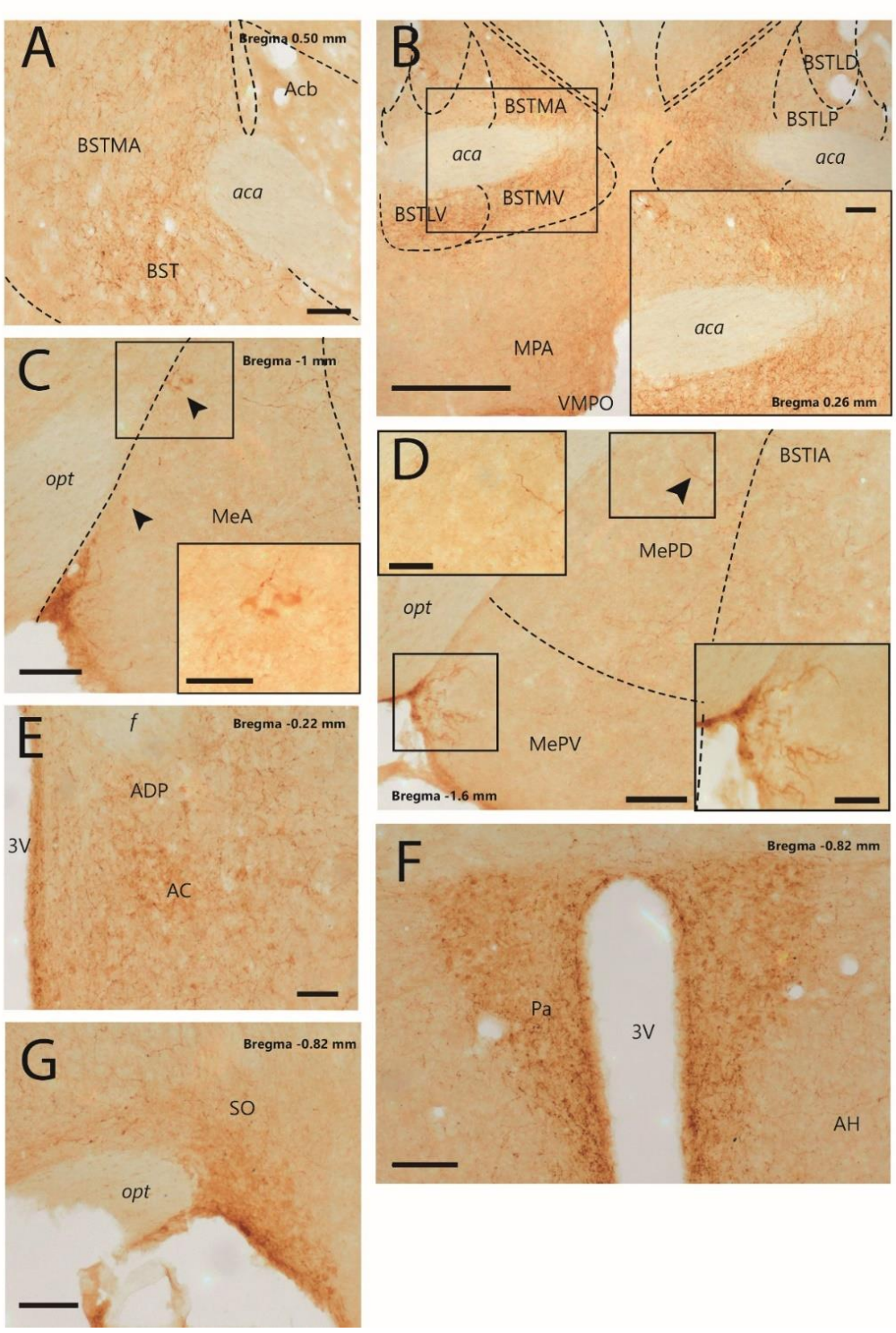

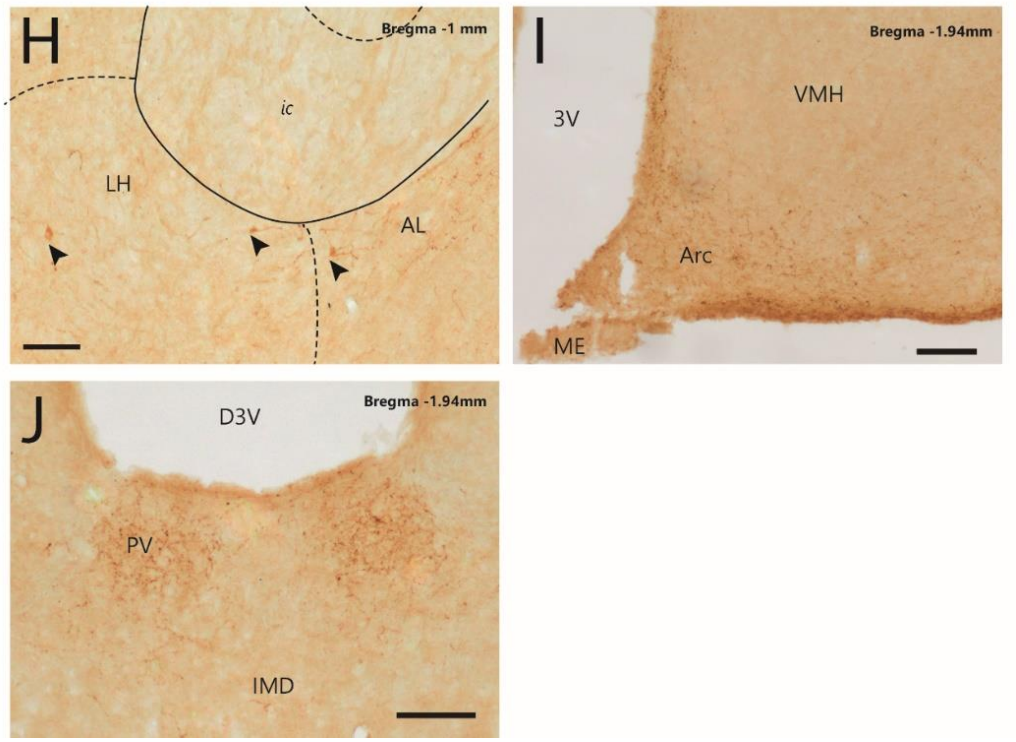

Figure 54: Photomicrographs of frontal sections through the mouse brain, illustrating the main PRL labelling in the different nuclei. A) PRLergic fibre labelling in the striato-pallidum and BST. B) Dense PRLergic labelling present in BST subdivisions. Inset in B) shows a high magnification detail of the labelled fibres. C) Presence of labelled fibres and somata in MeA. Inset in C) shows a high magnification detail of the PRL-ir neurons in the MeA. D) Positive fibres in the posterior subdivisions of Me. The insets show the localization of PRLergic fibres in MePD and MePV. E) PRL-ir somata in AC/ADP region and positive fibres and somata of the periventricular zone. F) and G) Pa and SO presented a dense population of PRL-ir fibres and somata. H) The photomicrograph shows the very scarce presence of labelled cells in LH and AL. I) The numerous PRLergic neurons and fibres are present in Arc, also ME present a dense number of positive fibres. J) Presence of dense population of labelled fibres in PV. Scale bar: A, C-I 100µm; B 500 µm; Inset A and B 100 µm; Inset C and D 50 µm. The animal represented is the dam M16104. The brain drawings are modified from Paxinos & Franklin, (2004). For abbreviations see list.

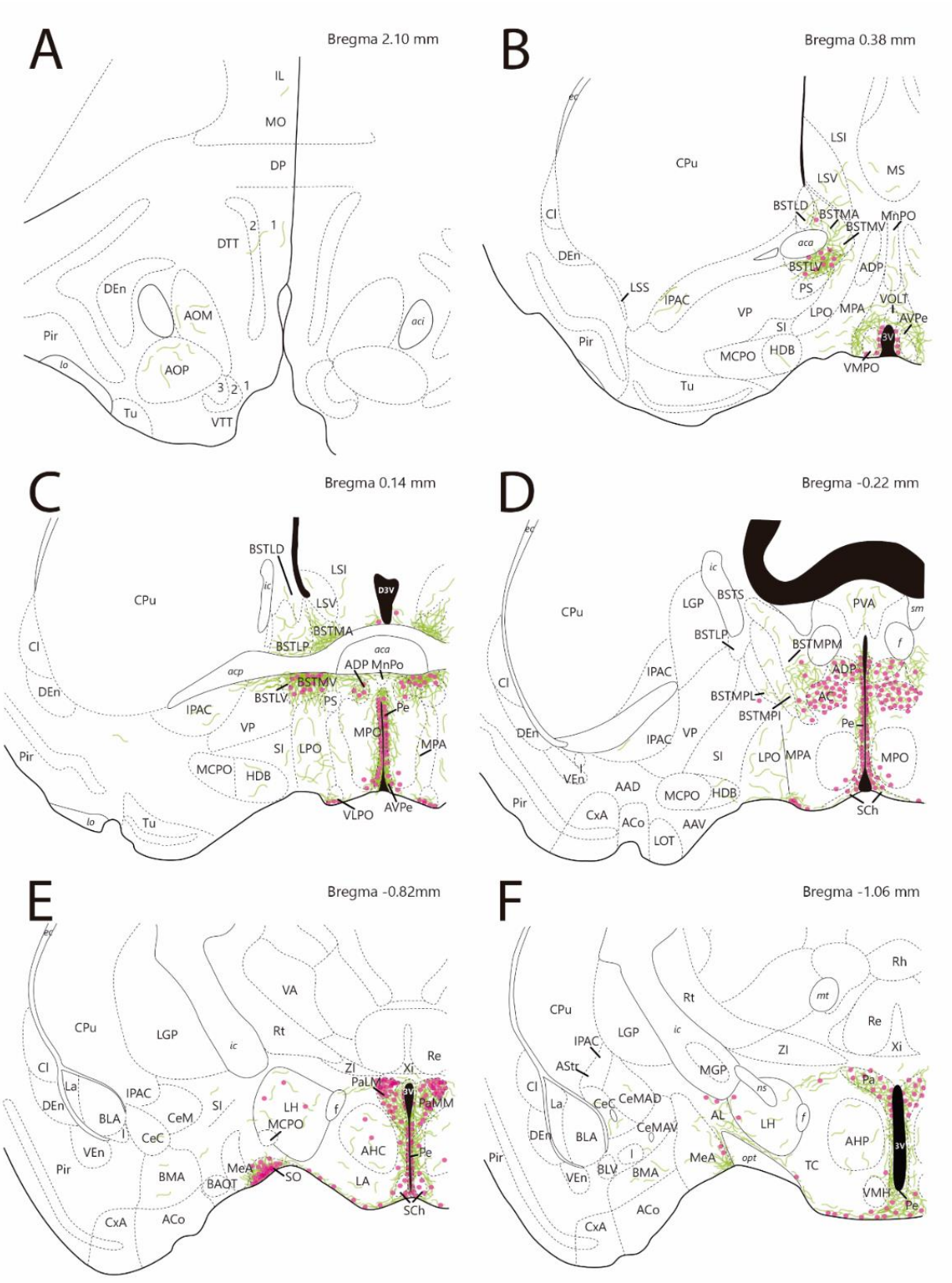
A
Bregma 2.10 mm
IL
MO
DP
DTT
2
1
DEn
AOM
aci
Pir
lo
AOP
3
2
1
Tu
VTT
B
Bregma 0.38 mm
ec
CPu
LSI
LSV
MS
Cl
BSTLD
BSTMA
MnPO
BSTMV
aca
DEn
BSTLV
ADP
LSS
IPAC
PS
VOLT
VP
LPO
MPA
AVPe
SI
3V
Pir
MCPO
HDB
VMPO
Tu
C
Bregma 0.14 mm
BSTLD
LSI
ic
D3V
CPu
LSV
BSTMA
Cl
BSTLP
aca
ADP
MnPo
acp
BSTMV
DEn
BSTLV
PS
Pe
IPAC
VP
MPO
MPA
SI
LPO
Pir
MCPO
HDB
lo
Tu
VLPO
AVPe
D
Bregma -0.22 mm
ec
ic
CPu
LGP
BSTS
PVA
sm
BSTLP
BSTMPM
f
IPAC
ADP
Cl
BSTMPL
AC
BSTMPI
DEn
Pe
IPAC
VP
SI
LPO
MPA
MPO
VEn
AAD
MCPO
HDB
Pir
CxA
ACo
AAV
SCh
LOT
E
Bregma -0.82mm
ec
VA
CPu
LGP
Rt
ic
Re
Cl
ZI
Xi
La
PaLM
3V
IPAC
PaMM
DEn
BLA
CeM
SI
LH
f
MCPO
CeC
AHC
Pe
VEn
Pir
BMA
MeA
SO
LA
BAOT
SCh
CxA
ACo
F
Rh
mt
Rt
CPu
Re
LGP
ic
IPAC
ZI
Xi
AStr
MGP
Pa
Cl
ns
La
CeC
CeMAD
AL
CeMAV
LH
f
DEn
BLA
AHP
3V
I
MeA
opt
TC
Pir
VEn
BLV
BMA
VMH
Pe
ACo
CxA

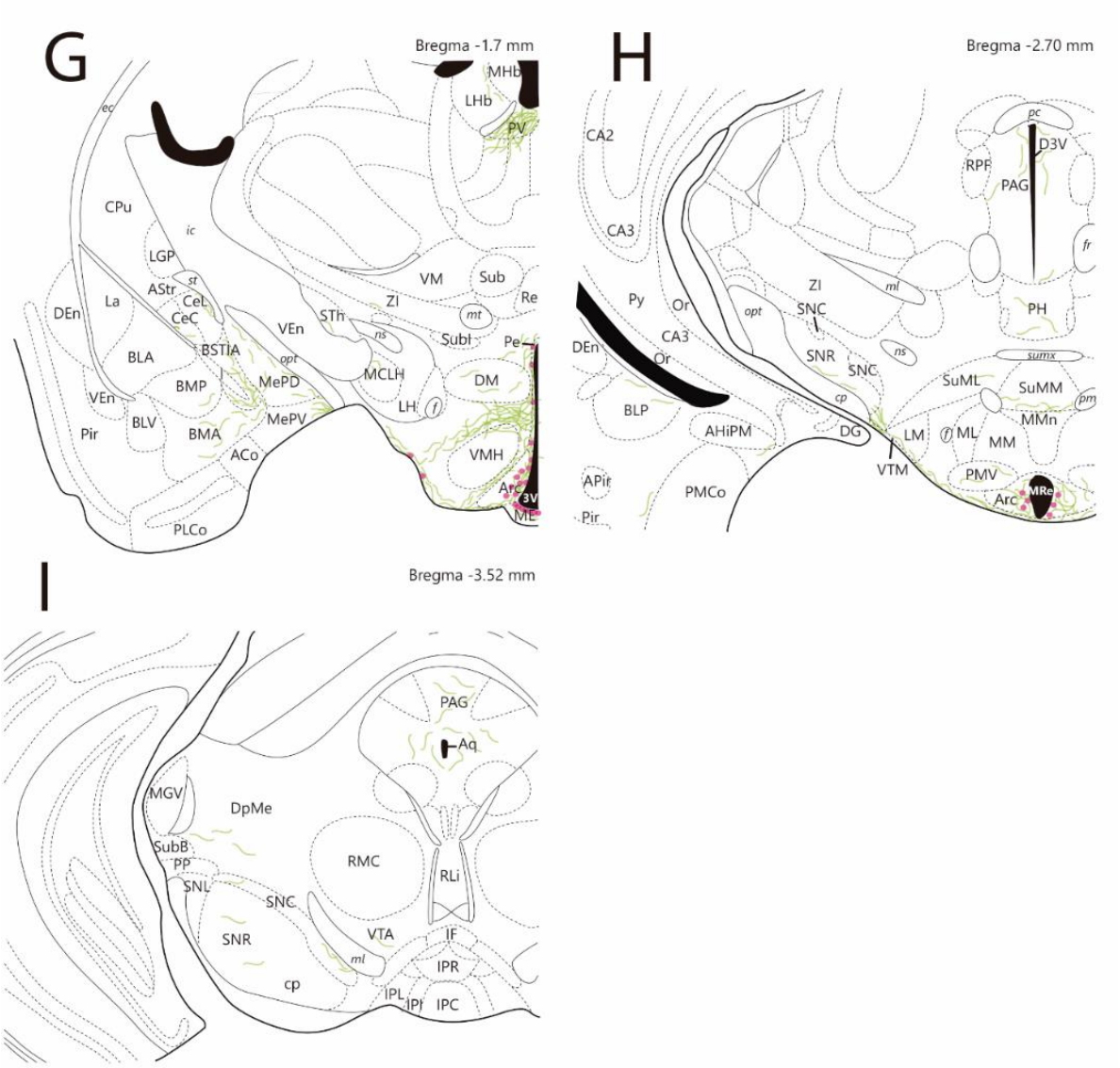

Figure 55: Semi-schematic drawings of coronal sections through the mouse brain showing the distribution of PRL-ir fibres and somata. The distribution of PRL-ir structures was the same between dams, godmothers and virgins. The animal represented is the virgin M1684. The fibres are represented in green lines and the somata in pink circles. The brain drawings are modified from Paxinos & Franklin, (2004). For abbreviations see list.

EXPERIMENT 2

DOUBLE FLUORESCENT IMMUNOHISTOCHEMISTRY

The antibody against natural mouse PRL reacted with numerous cells and fibres located in structures known by the presence of the neuropeptides AVP and OT. The results of the colocalization study showed an important degree of colocalization of PRL and AVP, and a less colocalization than with OXT.

Regarding PRL colocalization with AVP, some of the PRL-ir structures (neurons and fibres) showed colocalization with AVP in the Me (FIGURE 56C-C''), SO (FIGURE 56A-A''), Pa (FIGURE 56B-B''), and ME (FIGURE 56D-D''). It is important to remark that the labelled structures did not display a complete colocalization in fibres and somata of PRL and AVP, and it was possible to observe some structures with only PRL-ir or only AVP-ir (FIGURE 56).

In the Me, colocalization of AVP and PRL was observed only in fibres (FIGURE 56C-C''). In the MePD, colocalization was observed in fibres scattered in all the subdivision. In contrast, in the MeA and MePV double-labelling was observed mainly close to *opt* (FIGURE 56C-C'').

Regarding the SO, most of the PRL-ir cells and fibres were also stained for AVP (FIGURE 56A-A''). The presence of AVP-ir cells appeared more abundant than that of PRL-ir neurons, and it was possible to observe several somata positive for AVP only.

In the case of the Pa, PRL-ir and AVP-ir double-labelled somata were mainly present in the magnocellular part (PaLM) of the nucleus. Regarding the colocalization in fibre labelling, double-labelled fibres were observed in all Pa. However, higher levels of colocalization were observed in the lateral parts of this nucleus and in the periventricular zone (FIGURE 56B-B'').

Regarding the ME, no labelled somata for PRL or AVP were observed in the nucleus. Double-labelled fibres were present in the internal and external ME layers, with higher levels of double-labelling in the internal part (Low 2017) (FIGURE 56D-D''). It is important to remark that PRL fibres and somata were also present in the Arc but the colocalization of fibres was mainly in ME (FIGURE 56D-D''). Presence of AVP in the ME is very scarce (Otero-García et al. 2016).

On the other hand, the distribution of PRL and OXT apparently showed lower levels of colocalization than that observed for PRL and AVP. In the Me, as in the case of PRL and AVP,

double OXT and PRL-ir cells were not observed. Regarding double-labelled fibres, some of them were observed scattered within the MePD, and a few fibres showing OXT and PRL colocalization were present in MeA and MePV close to *opt* (FIGURE 57D-D'').

The region encompassing AC/ADP presented a huge OXTergic population of neurons, as described previously in Otero-García, Agustín-Pavón, Lanuza, & Martínez-García, (2016). However, the PRL-ir somata were located ventrally to the OXT-ir cells, and thus the colocalization of both neuropeptides was very low (FIGURE 57A-A''). Regarding the fibres in AC/ADP the distribution was similar as that observed with the somata, the OXT-ir fibres were mainly located dorsally to the PRL-ir fibres and double immunolabelled fibres were very scarce (FIGURE 57A-A'').

The SO was the nucleus that presented more double-immunolabelled structures (fibres and somata) for OXT and PRL. The OXT neuron population was located dorsal to the PRL-ir somata, and for this reason the colocalization was observed in the cells located in transition between the dorsal and ventral part of the SO (FIGURE 57B-B''). Regarding the fibres, their distribution was like that described for positive somata but the levels of colocalization were less than for double immunolabelled neurons (FIGURE 57B-B'').

Regarding the Pa, the OXT-ir cells and fibres appeared distributed scattered in the entire nucleus and adjacent to Pe. In contrast, PRL-ir somata, as described before, were mainly distributed in the lateral parts of the nucleus. Thus, no double labelled neuron was found in this region. However, some PRL-ir neurons in Pe were positive for both neuropeptides (FIGURE 57C-C''). The presence of PRL-ir fibres was homogeneous in all Pa and in Pe, nevertheless, the number of doubles immunolabeled fibres was very low (FIGURE 57C-C'').

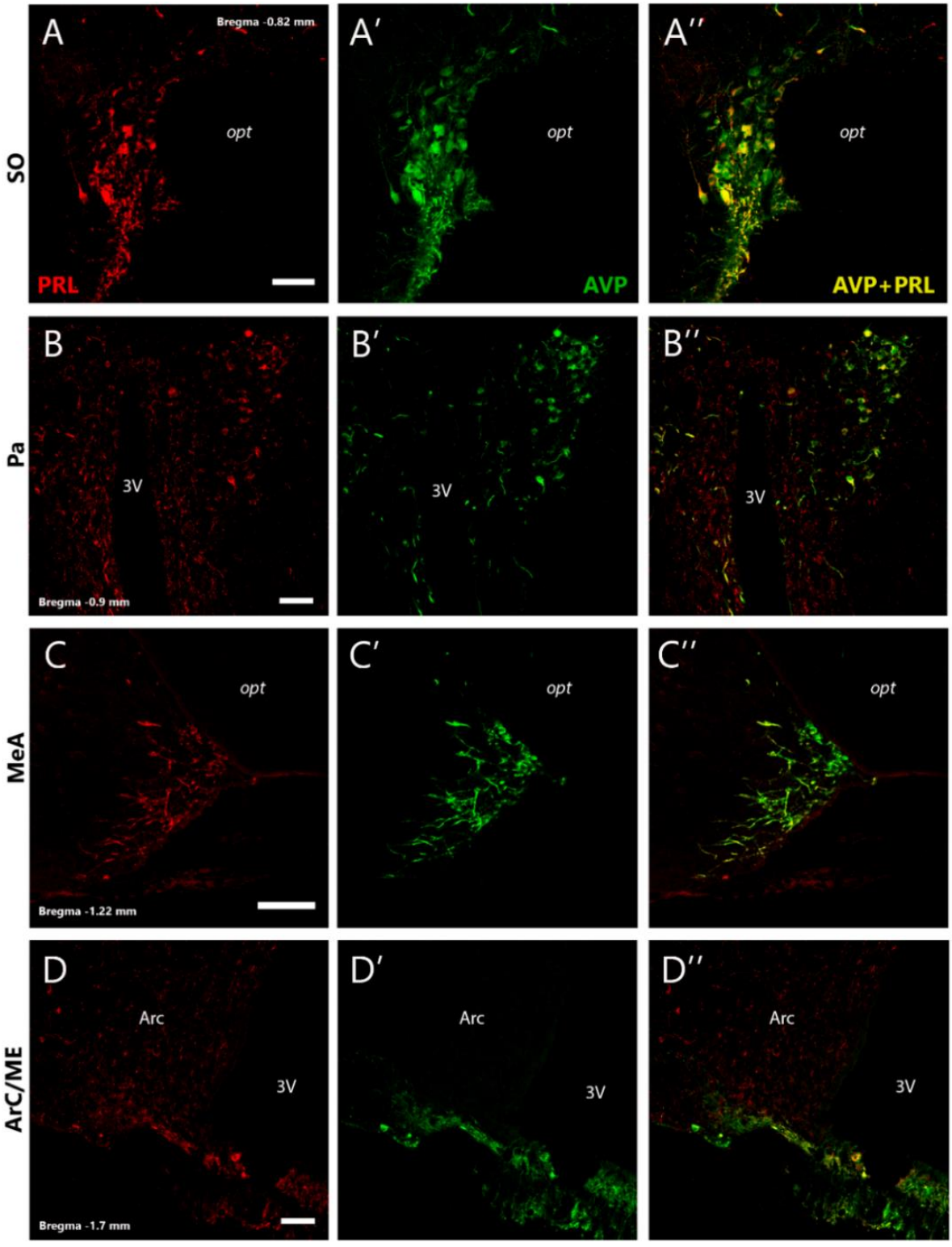

Figure 56: Distribution and colocalization of PRL and AVP immunolabelling in coronal sections of different nuclei related with the sociosexual *brain in female mouse. PRL immunolabelling is observed in red (A-D), AVP in green (A'-D') and double labelled structures in yellow (A''-D''). It is possible to observe a high level of colocalization between PRL and AVP. In the Pa the highest levels of double labelling are in the magnocellular region of the nucleus. Arc is only positive for AVP, however in the ME is possible to observe positive fibres for PRL and AVP. Scale bar: 60 µm. For abbreviations see list.*

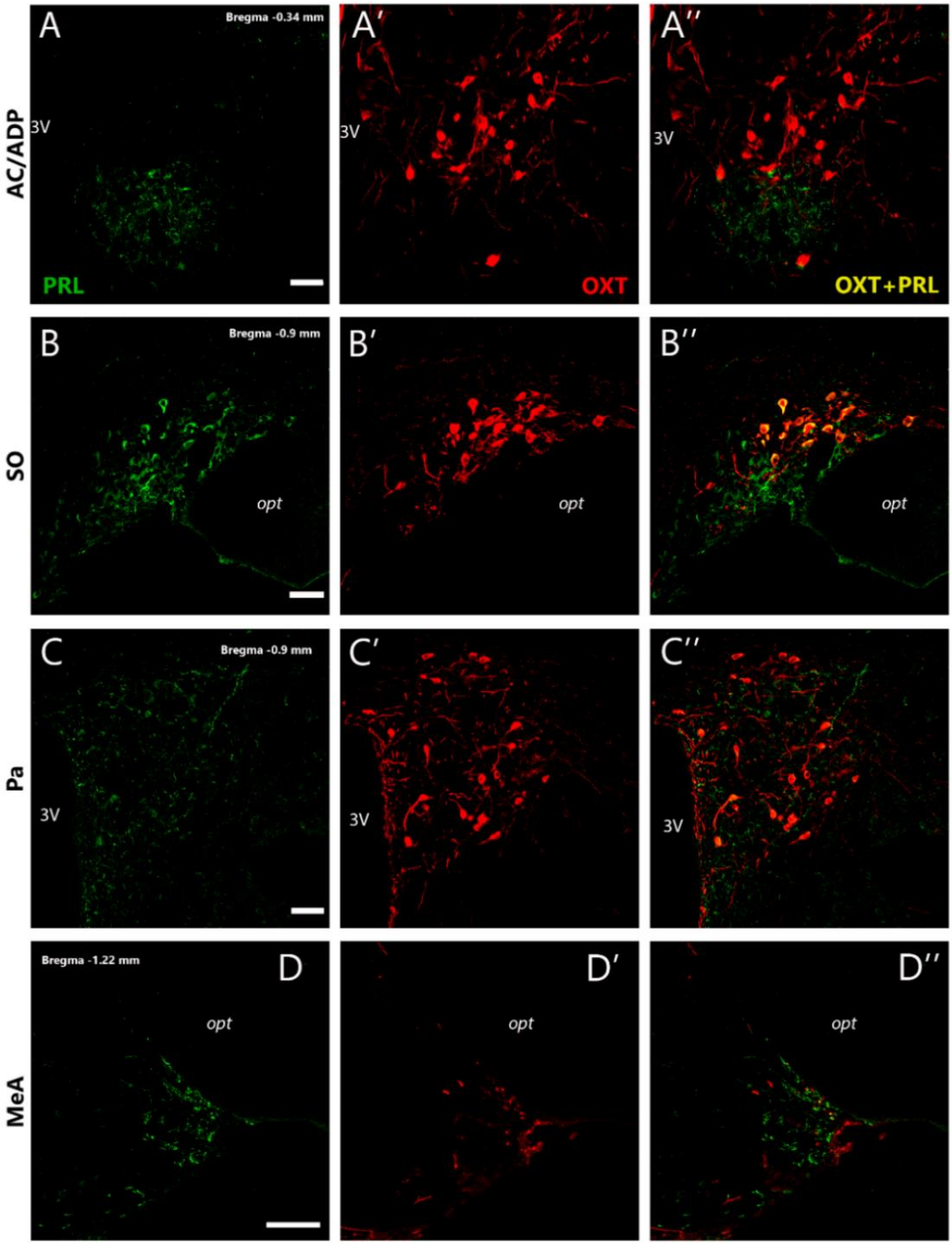

Figure 57: Representative photomicrographs of PRL and OXT distribution in different nuclei related with maternal behaviour. Labelled somata and fibres in coronal sections in female mouse brain. PRL immunolabelling is observed in green (A-D), OXT in red (A'-D') and double labelled structures in yellow (A''-D''). The levels of colocalization for both antibodies are low in AC/ADP region, Pa and MeA, however in the SO it is possible to observe higher levels of colocalization in the middle region of the nucleus. Scale bar: 60 µm. For abbreviations see list.

EXPERIMENT 3

QUANTITATIVE ANALYSIS OF PROLACTINERGIC SOMATA

The density of PRL-ir cell bodies was assessed in 7 brain regions: BSTMPM, AC/ADP, MPO, SO, Pa, SCh and Arc. These PRL-ir regions were selected according to their relevance in the context of maternal behaviour, where they play an important role as part of the sociosexual brain network (Newman 1999), and in the neurosecretory system (Watson and Qi 2012). Some of the frames used for the cell counting in each of these nuclei are depicted in (FIGURE 53) and the bregma levels are indicated in the Material and Methods section.

To assess the possible differences in the number of PRL-ir somata in virgin pup-naïve females, godmothers and lactating females, a one-way ANOVA on the data obtained in each structure was performed. Previously to the one-way ANOVA, a Tukey outlier detection tests was carried out as explained in Chapter III (General procedures).

BSTMPM

Regarding the BSTMPM, the Tukey fences test showed one extreme value (FIGURE 58A) which was eliminated for the statistical analysis. Thereafter taking out the extreme values, a non-parametric Kruskal-Wallis test did not reveal significant differences between the mean ranks of the studied groups ($p<0.05$) (FIGURE 58B).

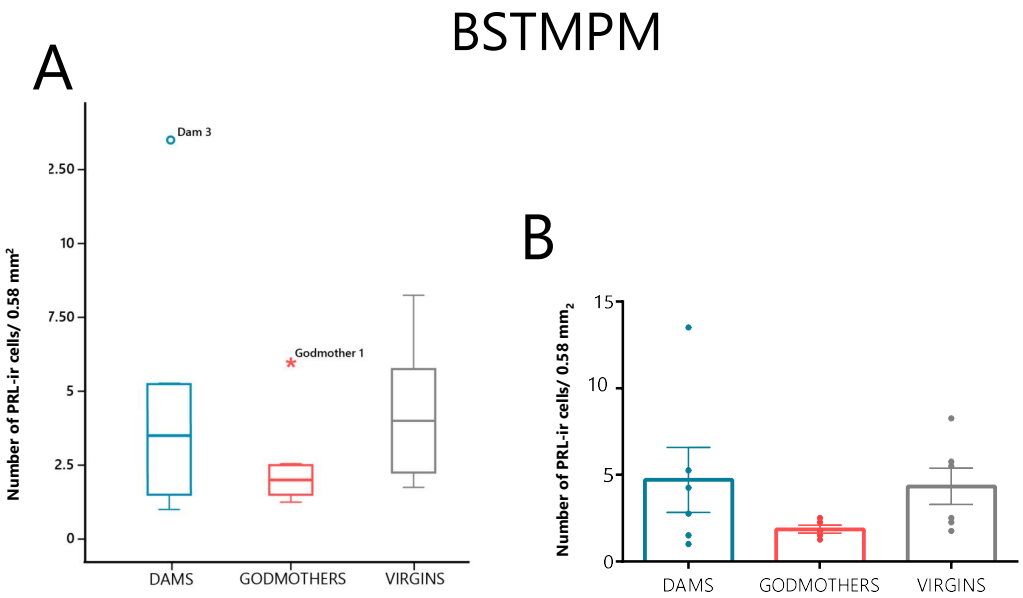

Figure 58: The density of PRL-ir cells in BSTMPM was not significantly different between the three studied groups. A) Tukey boxplot results for BSTMPM showed that Godmother 1 had an extreme value (an average of 6 PRL-ir cells). B) Kruskal-Wallis test for independent samples did not obtain significant differences between studied groups in BSTMPM data. Bar histograms show mean interhemispheric PRL-ir somata ± SEM in the

*three groups. Dams (blue; n = 6), godmothers (pink; n = 5) and virgin females (green; n = 6). * in the Tukey fences test points the far outs (3 times the Interquartile Range); **O** points the out values (1.5 times the Interquartile Range). For abbreviations see list.*

AC/ADP

In the case of the AC/ADP, after eliminating the extreme values (FIGURE 59A), data showed a normal distribution but not homoscedasticity (Levene's test, p=0.042). Therefore, Welch and Brown-Forsythe ANOVAs were used to compare the three studied groups. Data analysis revealed non statistically significant inter-group differences in the number of PRL-ir somata: Welch ANOVA ($F_{2, 8.44}$= 2.256, p>0.05) and Brown-Forsythe ANOVA ($F_{2, 10.11}$= 1.262, p>0.05) (FIGURE 59B).

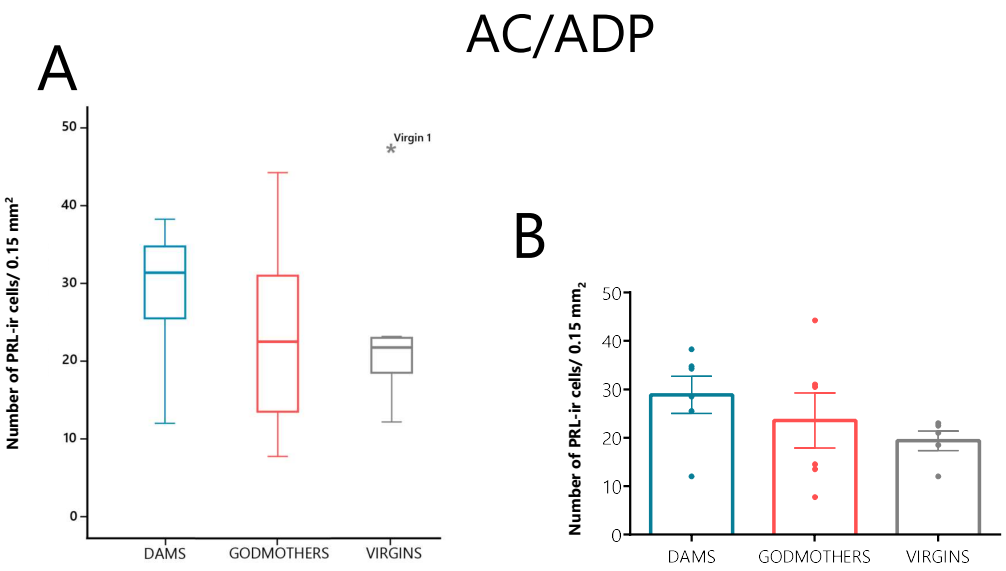

Figure 59: Quantification of PRL-ir positive cells in AC/ADP of lactating, godmothers and virgin female mice. A) Tukey boxplot results for AC/ADP in the three studied groups showed that virgin 1 had extreme value *(an average of 47 PRL-ir cells). B) Bar histograms show mean interhemispheric PRL-ir somata ± SEM in the three groups. Dams (blue; n = 6), godmothers (pink; n = 6) and virgin females (green; n = 5). Welch and Brown-Forsythe ANOVAs of independent samples was carried in AC/ADP. * in the Tukey fences test points the far outs (3 times the Interquartile Range). For abbreviations see list.*

MPO/A

In the MPO/A, after checking that the data did not present any extreme value (FIGURE 60A), and showed normality and homogeneity of variances, a one-way ANOVA for independent samples revealed a statistically significant effect of the factor GROUP ($F_{2, 17}$= 4.291, p= 0.034). Bonferroni's post-hoc showed a significant increase in the number of PRL-ir somata in dams with respect to virgins (p= 0.034) (FIGURE 60B).

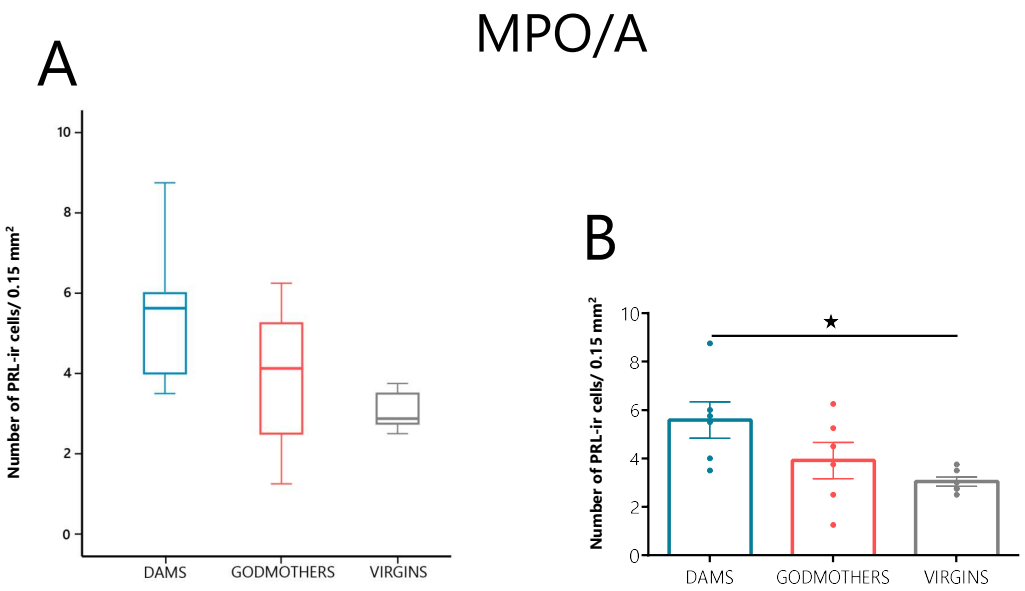

Figure 60: Quantification of PRL-ir number of somata in MPO/A showed significant differences between lactating and virgin female mice. A) Tukey boxplot results for MPO/A did not show any extreme value in the studied groups. B) Bar histograms show mean interhemispheric PRL-ir somata ± SEM in the three groups. One-way ANOVA with Bonferroni post-hoc comparisons showed significant differences between dams and virgin females. Dams (blue; n = 6), godmothers (pink; n = 6) or virgin females (green; n = 6). ★ p< 0.05. For abbreviations see list.

SO

In the SO, after removing two extreme values (FIGURE 61A), normality and homogeneity of variances were checked, the and the Levene's test showed that variances were not equal ($p<0.01$). The Welch ($F_{2,7.3}=7.705$, $p=0.017$) and Brown-Forsythe ($F_{2,\ 6.492}= 14.532$, $p= 0.004$) ANOVAs revealed a highly significant effect of the factor GROUP. Games-Howell post-hoc showed a significant increase in the number of PRL-ir somata in dams with respect to virgins ($p= 0.016$) and godmothers ($p= 0.024$) (FIGURE 61B).

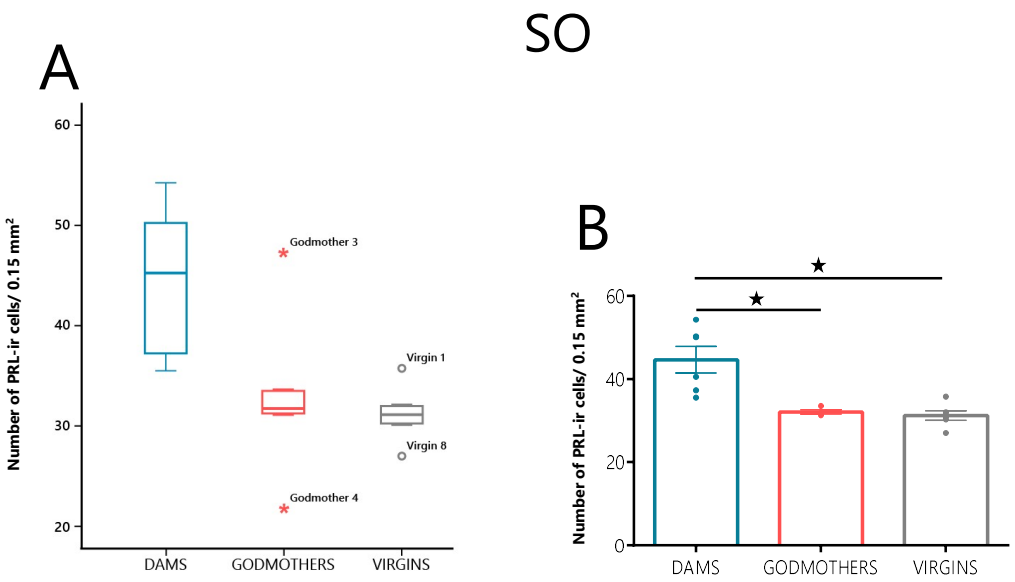

*Figure 61: SO nucleus showed significant differences in the quantification of positive PRL-ir cell between lactating female and the rest of the groups. A) Tukey boxplot results for SO presented two extreme value in the group of godmothers (Godmother 3; 47.25 PRL-ir cells average and Godmother 4; 21.75 PRL-ir cells average). B) Bar histograms show mean interhemispheric PRL-ir somata ± SEM in the three groups. Welch and Brown-Forsythe ANOVA with Games-Howell post-hoc comparisons showed significant differences between dams and the other two groups. Dams (blue; n = 6), godmothers (pink; n = 4) or virgin females (green; n = 6). * in the Tukey fences test points the far outs (3 times the Interquartile Range); O points the out values (1.5 times the Interquartile Range). ★ p< 0.05. For abbreviations see list.*

Pa

In the Pa, which probably showed the most important population of PRL-ir cells, once the extreme values were removed (FIGURE 62A), data showed normality, but not homogeneity of variances (Levene's test, p=0.004). Thus, Welch and Brown-Forsythe ANOVAs were used to study the differences between the studied groups. Data analysis revealed non statistically significant inter-group differences in PRL-ir number of somata with both tests (Brown-Forsythe ANOVA: $F_{2, 8.735} = 0.904$, p>0.05; Welch ANOVA: $F_{2, 7.18} = 2.044$, p>0.05) (FIGURE 62B).

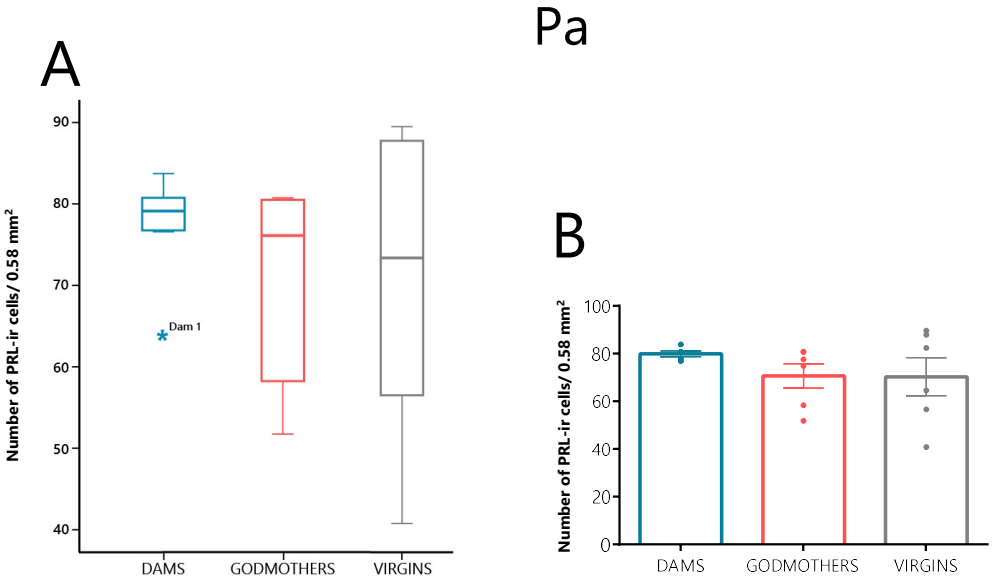

*Figure 62: The number of PRLergic cells in the Pa did not present significant differences between dams, godmothers and virgin female mice. A) Tukey fences test showed that dam 1 was an extreme value (average of 63.75 PRL-ir somata). B) Bar histograms show mean interhemispheric PRL-ir somata ± SEM in the three groups. Non-significant differences were observed in the Welch and Brown-Forsythe ANOVAs. Dams (blue; n = 5), godmothers (pink; n = 6) and virgin females (green; n = 5). * in the Tukey fences test points the extreme values (3 times the Interquartile Range). For abbreviations see list.*

SCh

In SCh, after taking out the extreme values from the data (FIGURE 63A), and checking the normality and the homogeneity of variances, a one-way ANOVA revealed a statistically significant effect of the factor GROUP ($F_{2,14}$= 4.808, p=0.029). Bonferroni's post-hoc showed a significant increase in the number of PRL-ir cells in the group of lactating females with respect of the virgins' group (p=0.047) and the comparison between dams and godmothers show a p=0.08 (FIGURE 63B).

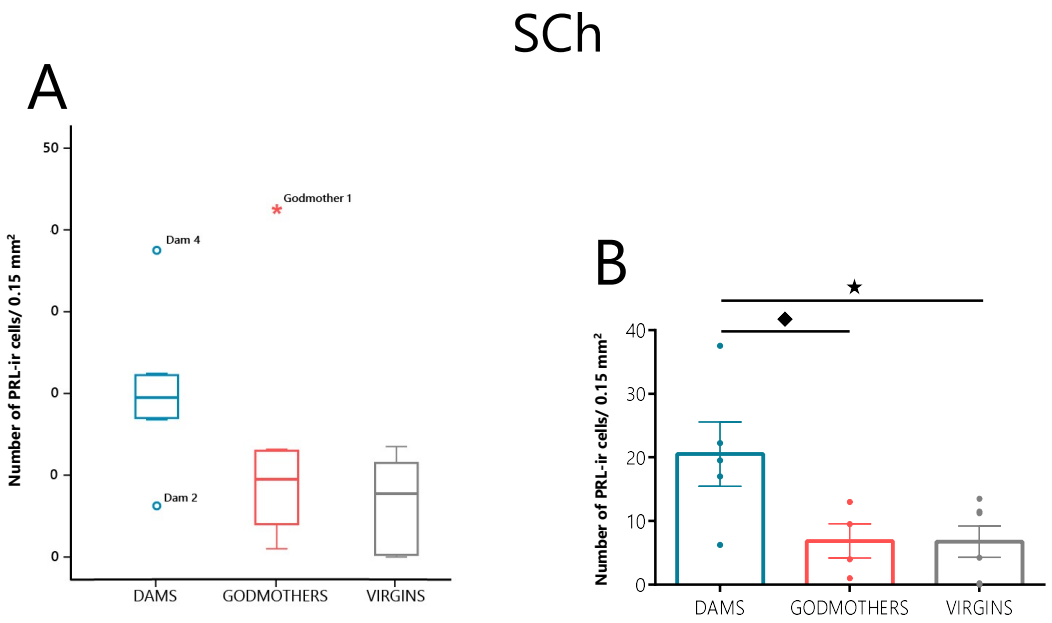

*Figure 63: SCh showed significant differences in the number of PRL-ir cell between lactating and virgin female mice. A) Tukey boxplot results for SCh presented one extreme value in the group of godmothers (Godmother 1; average of 42.5 PRL positive cells). B) Bar histograms show mean interhemispheric PRL-ir somata ± SEM in the three groups. One-way ANOVA with Bonferroni post-hoc comparisons showed significant differences between dams and virgin females and a tendency between dams and godmothers. Dams (blue; n = 6), godmothers (pink; n = 5) or virgin females (green; n = 6). * in the Tukey fences test points the far outs (3 times the Interquartile Range); **O** points the out values (1.5 times the Interquartile Range). ★ p< 0.05 ◆ p =0.08. For abbreviations see list.*

Arc

Finally, Arc did not show any extreme value. Since the normality test showed that the data were not normally distributed, a Kruskal-Wallis test was carried out. The non-parametric Kruskal-Wallis revealed no significant differences between the mean ranks of the studied groups ($p>0.05$) (FIGURE 64).

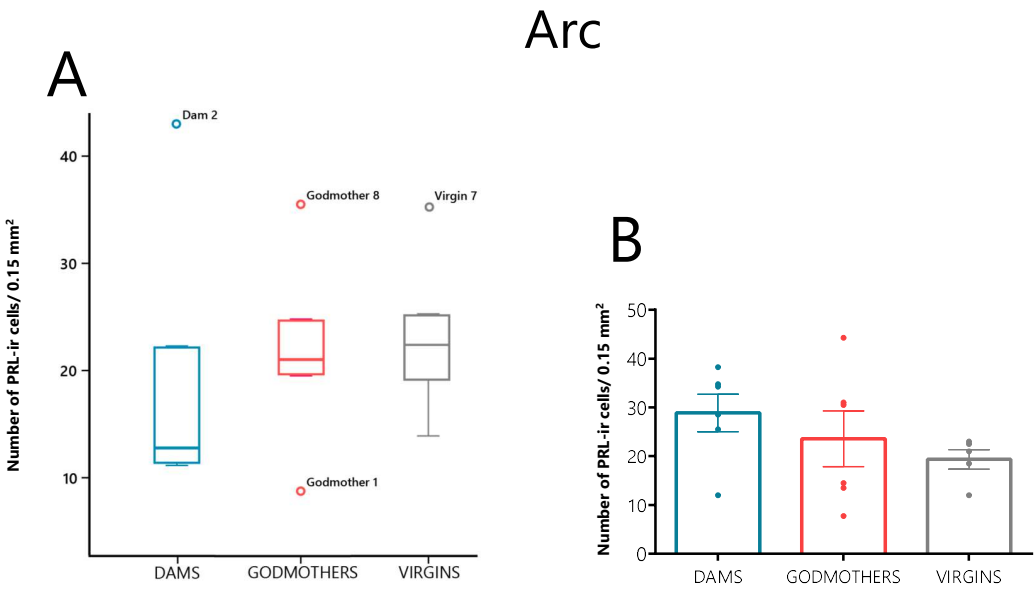

*Figure 64: Analysis of the number of prolactinergic cells in Arc did not show significant differences between dams, godmothers and virgin female mice. A) Tukey boxplot results for Arc did not show any extreme value. B) No significant results were obtained with the Kruskal-Wallis test for independent samples in Arc data. Bar histograms show mean interhemispheric PRL-ir somata ± SEM in the three groups. Dams (blue; n = 6), godmothers (pink; n = 6) and virgin females (green; n = 6). **O** in the Tukey fences test points the out values (1.5 times the Interquartile Range). For abbreviations see list.*

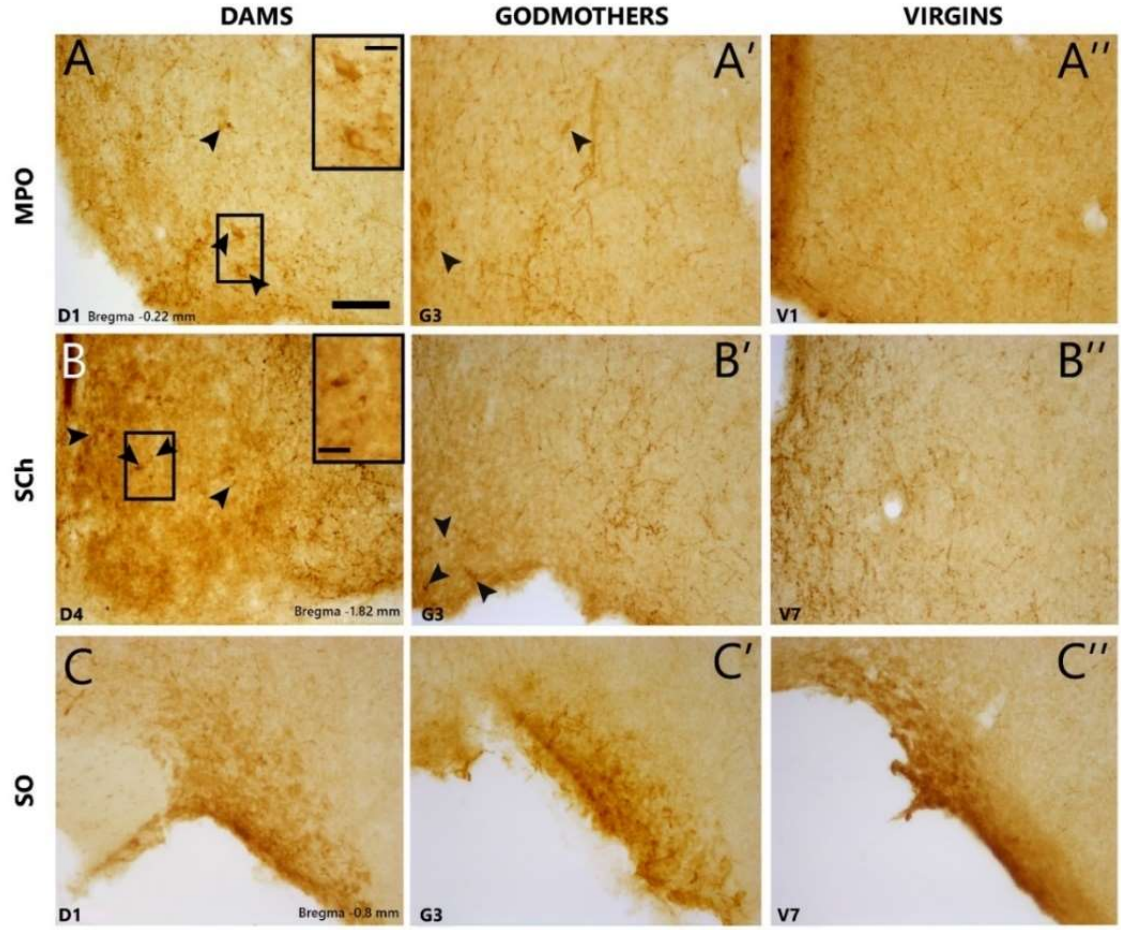

Figure 65: Representative examples of PRL somata in the nuclei with significant differences of studied female. Photomicrographs show the comparation between lactating females (D), godmothers (G) and virgins (V) in SO, SCh and MPO. The schemes represent the area and the Bregma level studied in each nucleus. Scale bar 60 µm. For abbreviations see list.

DISCUSSION

In the present study, we observed a widespread PRL innervation in the female mouse brain, suggesting the existence of important PRLergic pathways in areas related to endocrine regulation and the control of social and maternal behaviour.

To the best of our knowledge, this is the first description of the distribution of PRL-ir in the mouse brain. Regarding previous research, most available studies have been carried out in rats, and only a few of them in females (Toubeau et al. 1979b; Hansen et al. 1982; DeVito 1988) (TABLE 10). In addition, we report novel findings showing up how PRL-ir neurons change through different physiological stages in females: pup-naïve virgins, pup-sensitized virgins (godmothers) and lactating females.

NEUROANATOMY OF THE BRAIN PRLERGIC SYSTEMS

PRL neurons and the magnocellular neurosecretory system

The brain PRLergic system is originated in a few neuronal populations, present mainly in the BST and the hypothalamus (Pa, Pe and SO) (FIGURE 54 and FIGURE 55). The majority of previous studies has also indicated that the main structures with PRL-ir neurons are the SO and Pa (results in male and female rats: (Toubeau et al. 1979a, b; Hansen et al. 1982; Clapp et al. 1994; Mejía et al. 1997; Suzuki and Handa 2005) (TABLE 10). Hansen et al., (1982), (Clapp et al., (1994) and Mejía et al., (1997) also showed that somata in the Pa seem to be placed in the lateral extension of the nucleus, as observed in our results (FIGURE 54F and FIGURE 55E and F).

It is not known whether hypothalamic PRL is released in the portal system, however, Clapp et al., (1994) observed that the posterior pituitary (or neurohypophysis) was labelled only in immunohistochemistries using an antibody against the 16 KDa PRL, whereas the anterior pituitary (adenohypophysis) was labelled with antibodies against both the 23 KDa and the 16 KDa forms of PRL. Also, B. L. Hansen et al., (1982) showed labelled fibres in the posterior pituitary. The fact that hypophysectomy has no effect on the amount of immunoreactive PRL in the male hypothalamus and only diminishes (but does not abolish) the quantity of immunoreactive PRL in the female rat hypothalamus (Toubeau et al. 1979b; DeVito 1988; Harlan et al. 1989; Emanuele et al. 1992) suggests that indeed brain PRL synthesis is independent of hypophyseal PRL synthesis. Furthermore, systemic osmotic stimulation by NaCl increase PRL concentration in plasma but not within the Pa, demonstrating a pituitary release independent from that in the

brain (Torner et al. 2004). In addition, electron microscopy studies have shown that the PRL is stored in "granular" particles, matching the morphology of secretory granules (Mejía et al. 1997). In support of a PRL brain system independent of the hypophysis, several studies of mRNA expression in hypothalamus support the hypothesis that PRL could be synthetized *de novo* in the CNS (Schachter et al. 1984; Emanuele et al. 1992; Wilson et al. 1992; Clapp et al. 1994; Cabrera-Reyes et al. 2017).

Neurons in the SO and Pa projecting to the neural lobe of the hypophysis are known as magnocellular neurosecretory cells. These neurons synthesize neuropeptides, like AVP and OXT, and transport them to the neurohypophysis and to the hypothalamus-hypophysial portal system. This system is responsible for the release of these hormones to the bloodstream (Neumann and Landgraf 2012; Watson and Qi 2012; Armstrong 2015; Low 2017) (FIGURE 66).

In addition, the Pa neurons supply OXT and AVP-containing fibres to both the hypothalamus and to various extrahypothalamic areas, including the amygdala, septum, brain stem and spinal cord (Pittman et al. 1981). It is possible that the wide population of PRL-ir somata observed in the Pa and SO synthesize PRL as other neurohormones (OXT and AVP), independent of PRL synthesis in the pituitary gland. Moreover, the double labelling experiment (Experiment 2) shows that PRL colocalizes mainly with AVP in both nuclei (FIGURE 56), as Mejía et al., (1997) observed in female rats, in their case with an antibody generated against the 16 KDa form of PRL. Importantly, we found significant differences between the number of PRL-ir somata in the SO of dams and the other two groups of females (virgins and godmothers (FIGURE 61). The SO and the Pa play a role in the lactation through OXT neurotransmission in response to pup suckling (Neumann et al. 1993), and also the activity of OXT neurons in both nuclei is important for the pulsatile secretion of OXT from the neurohypophysis into blood, e.g. during the milk ejection reflex (Moos et al. 1989; Neumann et al. 1994). Moreover, elevations of FOSB during lactation occur in OXT-ir and AVP-ir neurons in the SO and the Pa (Lin et al. 1998), which is consistent with a functional role for both peptides in these regions during lactation. Also, during lactation there is a change in AVP production by magnocellular neurons in the SO (Mezey and Kiss 1991). OXT-producing neurons can also synthesize AVP in response to a special demand for the hormone and a small number of AVP-producing neurons are recruited to synthesize OXT in lactating animals as well. These data point to a hormonal regulation of the AVP and OXT precursor gene, mainly by oestrogens (Mezey and Kiss 1991). The induction of AVP and OXT synthesis through oestrogens could also stimulate the PRL synthesis in the SO, underlying the increase of PRL-ir cells in this nucleus of dams showed by our data. Moreover, some findings

demonstrate that increased levels of brain or serum PRL enhance NOS activity, and thereby stimulate OXT and AVP in males in Pa and SO (Vega et al. 2010). The presence of PRL in SO neurons and its significant increase in dams suggests that this protein may play a role like AVP and OXT in SO in relation with maternal behaviour. The results of Vega et al., (2010) and Mezey & Kiss, (1991), suggest a positive feedback between OXT, AVP and PRL in these nuclei during lactation.

Magnocellular neurons in the SO and Pa send axons that predominantly traverse the ME internal zone to end in the neural lobe of the pituitary, whereas axons of the parvocellular neurosecretory neurons project to the external layer of the ME (see below). The ME presents a wide array of blood vessels and nerve endings and is the functional link between the hypothalamus and the anterior pituitary gland (FIGURE 66).

The exchange of the hypothalamic releasing factors and the pituitary portal vessels takes place in the external zone of ME (Armstrong 2015; Low 2017). The presence of AVP and OXT in the ME was mainly observed throughout the internal layer of the ME (Kawata et al. 1983; Holmes et al. 1986; Low 2017). However, a small number of the OXT and AVP-containing nerve fibres are located in the external layer around the capillary loops (Kawata et al. 1983; Holmes et al. 1986). In our study, PRL-ir fibres colocalize with AVP in the internal and external layer of ME (FIGURE 56). The PRL-ir fibres in the external and internal layer of the ME were observed previously in different distribution studies (Hansen et al. 1982; Harlan et al. 1989; Paut-Pagano et al. 1993), however, some studies reported PRL-ir fibres mainly in the external layer (Toubeau et al. 1979a, b; Alonso et al. 1988; Siaud et al. 1989) and others in the subependymal (internal) layer (Fuxe et al. 1977). These facts suggest the possibility that PRL is present in the magnocellular and parvocellular neurosecretory system (see below).

Only a few studies have reported lack of PRLergic cells in the SO and Pa (Siaud et al. 1989; Harlan and Scammell 1991; Paut-Pagano et al. 1993), excluding the seminal work by Fuxe et al. (1977), which showed only fibre labelling, because they used immunofluorescence and, given the technical limitations available at that time, the lack of cell labelling is reasonable. The differences are probably due to the different antibodies used. In the case of Siaud et al., (1989), they used two non-commercial antisera produced against purified rat PRL, which only revealed perikarya after colchicine treatment. Harlan et al., (1989) used several antibodies, obtaining the best results with that raised against purified rat PRL by the National Hormone and Pituitary Program (NHPP). However, they showed cross-reactivity with the N-terminal fragment of POMC, and in fact the

analysis of the purified rat PRL (the antigen used to obtain the antibody) with two dimensional gel electrophoresis and immunoblot showed that the preparation contained at least four protein spots recognized by the anti-PRL antibody (see Discussion in Harlan et al., (1989), p. 19). This cross-reactivity can also explain why positive PRL immunolabelling was observed only in the anterior pituitary gland (Harlan et al. 1989; Harlan and Scammell 1991), a region with high levels of POMC (Navarro et al. 2015). Thus, careful analysis of the antibody specificity is mandatory. In the same line of reasoning, Paut-Pagano et al., (1993) used a non-commercial antiserum raised against ovine PRL, and the western blot analysis of the ovine PRL used as immunogen showed several bands.

Apart from the labelling obtained in the Pa and SO, we obtained PRL-ir in the AC, equivalent to the anterior magnocellular part of the Pa according to some authors (Swanson and Kuypers 1980) and considered as accessory neurosecretory nuclei (Peterson 1966; Armstrong et al. 1980b; Armstrong 2015). This nucleus presents magnocellular neurons, some of them containing OXT (Kiss et al. 1991; Armstrong 2015; Otero-García et al. 2016), that project to the posterior lobe by the same avenue as Pa cells, through the ME and pituitary stalk (Armstrong et al. 1980b). In spite of all these similarities with the Pa, this cell group is considered by some authors as an independent nuclei from Pa because they are topographically separated about 300-400 µm in rats (Peterson 1966; Armstrong et al. 1980b; Kiss et al. 1991; Armstrong 2015). Despite these controversies regarding the neuroanatomy, the region that comprises the AC/ADP presented a dense population of labelled PRL-ir somata in our study (FIGURE 54 and FIGURE 55) which was also observed by Hansen et al., (1982) mainly in the AC. Furthermore, our colocalization studies revealed that the OXT-ir cells were in a rostral position with respect to the PRL-ir neurons (FIGURE 57), with only a partial colocalization in the middle zone between the PRLergic and the OXTergic populations. The disagreement in the neuroanatomical boundaries can be one of the main factors explaining the lack of descriptions of this PRLergic population. The AC/ADP region is crucial for the expression of maternal behaviour in the rat, although previous reports usually include this area as the dorsal part of the preoptic region (Armstrong et al. 1980a; Paxinos and Franklin 2004; Numan and Stolzenberg 2009). Even though in the present study we did not find significant differences in the number of PRL-ir somata between dams, virgins a previous study from our group showed that STAT5 was increased in the AC/ADP region during lactation (Salais-López et al. 2017), thus suggesting that this region may have an important role in the control of maternal behaviour. Thus, we suggest that the AC/ADP can be a region with an important role in the sociosexual brain (FIGURE 66).

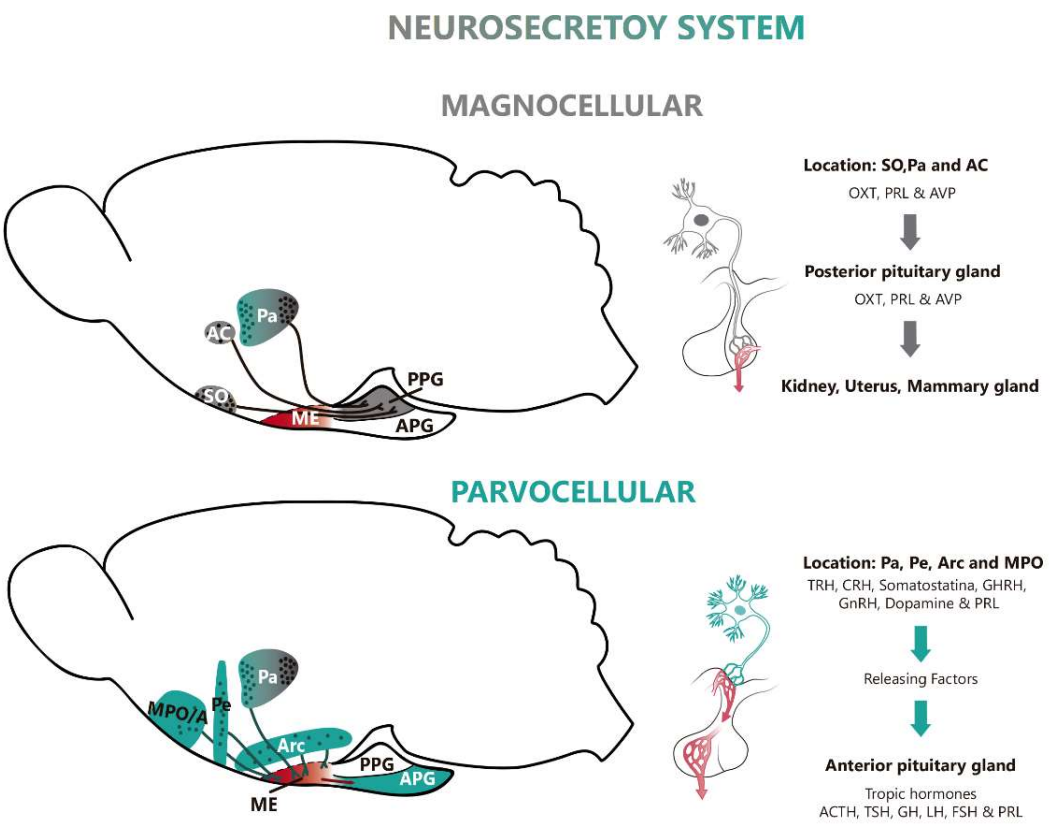

Figure 66: Schematic PRLergic neurosecretory cells in the parvocellular and magnocellular system. The magnocellular system, where OXT, AVP and probably PRL are synthetized, presents cells bodies in SO, Pa and AC, and projects to the neurohypophysis, where these neurohormones are released. The parvocellular system presents peptidergic neurons in the medial basal hypothalamus in nuclear groups including the Pe, the Pa, the MPO/A and Arc. The neuropeptides in this case are released into the hypophyseal portal system to regulate its secretion. Adapted and modified from Low (2017). For abbreviations see list.

In addition, some fibres and very few PRL-ir cells were obtained in the AH. The connections of this nucleus appear to be a subset of the connections of the MPO (Simerly 2015). AH present connections with other parts of the medial hypothalamic regions, sparse inputs from the lateral zones, and only limited inputs from telencephalic regions such as the ventral subiculum, BST and ventral part of the lateral septal nucleus (Swanson 1987). Significant projections are also directed toward the anterior Pe and Pa and a strong descending projection ends in the PAG (Swanson and Kuypers 1980; Simerly 2015).

PRL neurons in the parvocellular neurosecretory system

In addition to the SO, Pa and AC/ADP nuclei, we found an important populations of PRL-ir cells in other hypothalamic nuclei such as Pe, Arc, MPO/A, VLPO and SCh (TABLE 8). Some neurons in Pe, Arc and MPO/A, together with some parvocellular neurons of the Pa, are part of the parvocellular neurosecretory system. In contrast to the magnocellular system, parvocellular neurosecretory axons project to the ME (Wiegand and Price 1980; Armstrong 2015; Low 2017)

and play a role in the secretion of anterior lobe hormones (see above), as GH and PRL, among others (Le Tissier et al. 2012; Low 2017) (FIGURE 66).

Pe, the nucleus that surrounds the 3V, showed an important population of PRLergic cells (FIGURE 54and FIGURE 55), as showed by some of the previous reports (Hansen et al. 1982; Siaud et al. 1989). However, most papers did not observe the presence of positive somata in this region. Some authors did not differentiate it from Pa (Hansen et al. 1982), whereas others observed only positive fibres (Fuxe et al. 1977; Toubeau et al. 1979a, b; Harlan et al. 1989; Harlan and Scammell 1991; Paut-Pagano et al. 1993) (TABLE 10).

Arc is located at the base of the hypothalamus close to the ME and the pituitary gland and is intimately connected to both by neuronal and neurohemal connections. Also, Arc presents inputs and outputs to the Pa and preoptic areas, among other regions. The anatomical organization of Arc indicates that this structure plays an important neuroendocrine role and is directly involved in the regulation of PRL and GH secretion. In addition, it takes part in the regulation of oestrous cycle and sexual behaviour, sexual differentiation and stress response, among other biological functions (Chronwall 1985; Baker and Herkenham 1995). The moderate number of PRL-ir neurons observed in Arc coincide with most of the papers that have studied PRL distribution before (Toubeau et al. 1979a, b; Harlan et al. 1989; Harlan and Scammell 1991) (TABLE 10) (FIGURE 54and FIGURE 55). These PRLergic somata extended ventral to the VMH and occasionally, they were found in the lateral aspects of the median eminence. Harlan & Scammell, (1991) also pointed that the PRLergic neurons that they observed were not intensely immunostained and they remarked that this could be due to the lack of pre-treatment of the rats with colchicine. This lack of pre-treatment with colchicine (and the lack of retrieval procedures) can be the reason why some authors did not observe the PRL-ir cell in Arc (Fuxe et al. 1977; Hansen et al. 1982; Alonso et al. 1988). In the case of Siaud et al., (1989) and Paut-Pagano et al., (1993), they may have not observed labelled PRLergic neurons in Arc, probably because they used a non-commercial antisera produced against purified rat and ovine PRL (respectively). Results showed that AVP in this region did not colocalize with PRL-ir, being positive only for PRL antisera (FIGURE 56). As explained above, our results and previous studies observed the PRL-ir in the internal layer of the ME and in the posterior pituitary gland (Hansen et al. 1982; Clapp et al. 1994). Moreover, in the internal layer globular PRL-positive structures can be observed (FIGURE 54and FIGURE 55), which likely are granular aggregations of stored neurosecretory substance, called Herring bodies, in the expanded ends of the axons of the neurosecretory cells (McMillan and Harris 2018).

A group of cells in the MPO/A region is also involved in the parvocellular system (Low 2017). MPO/A is related with a variety of autonomic and behavioural functions including maternal and sexual behaviour *inter alia* (Chiba and Murata 1985; Numan and Woodside 2010; Armstrong 2015). Moreover the MPO/A efferences have been studied before and it projects to the Pa and ME indicating a role in the neurosecretion (Chiba and Murata 1985). We observed, only a scarce number of labelled somata in this region, located rostrally and close to the 3V (FIGURE 55). Just one previous article noticed the presence of PRLergic neurons in MPO/A (Hansen et al. 1982), probably because is a small cell population (Armstrong 2015). Interestingly, we found a significant increase in PRL cells in dams as compared to virgins. These results are consistent with the fact that suckling by pups induce the release of PRL within both the Pa and MPO/A but not outside these structures, and this is accompanied by a significant increase of PRL mRNA in the hypothalamus after suckling in lactating rats (Torner et al. 2004). In addition, in postpartum females, interactions of the MPO/A with the mesolimbic dopaminergic system promote voluntary maternal responses. These interactions not only regulate the onset of maternal behaviours, but also control its continuity during the postpartum period (Numan and Woodside 2010). Furthermore, indirect evidences suggest that NO release in the Pa in prairie voles (Gammie and Nelson 2000; Gammie et al. 2000) and in the MPO/A, SCh, and subparaventricular zone in mice (Gammie and Nelson 1999) may facilitate maternal aggression. Moreover, as it was mentioned before Vega et al., (2010) have proved that an increase of PRL in the brain or in the circulation promotes the activation of nNOS in the hypothalamo-neurohypophyseal system, leading to a systemic release of OXT and AVP. Therefore, the increase in PRL-ir somata in the MPO/A of dams may play a role in the increase of aggression in lactating females. These results remark the importance of these structures in the synthesis of PRL in maternal behaviours and a possible PRL regulation in the CNS independent of the systemic PRL.

PRL neurons in the SCh: circadian rhythms

Regarding SCh, this nucleus is also known to release neuropeptides and hormones into the local extracellular space, in addition to its well-known role in the regulation of circadian rhythms (Gillette and Reppert 1987). SCh, as a circadian pacemaker, drives rhythms in several downstream targets, which include brain regions implicated in sleep regulation such as VLPO and LH (Sun et al. 2001; Chou et al. 2002), both nuclei with PRL-ir somata. In addition, previous bibliography demonstrated that plasma concentrations of PRL are highest during sleep and lowest during the waking hours in humans (Parker et al. 1974; Freeman et al. 2000), and in rats it exists a similar tight relationship between sleep patterns and PRL levels (Roky et al. 1993;

Freeman et al. 2000). For all these reasons, the presence of PRLergic somata in nuclei related with circadian rhythms suggests an important role of this neurohormone in the regulation of these biological processes. The significant increase of PRL-ir somata in SCh of dams compared with virgins may be related with the alterations in the sleep-wake cycle due to the demands of maternal care.

Extrahypothalamic PRL neurons: the medial extended amygdala

Outside the hypothalamus, the BST complex presents the widest population of positive cells. These cells were mainly in BSTLV and BSTMV, ventral to the anterior commissure, but also some cells were observed in the ventral part BSTMPM. Siaud et al., (1989) pointed the existence of PRLergic cells in the BSTMPM in the same neuroanatomical position as we show in the (FIGURE 55) (see schematic representation in (Siaud et al. 1989)) after colchicine injections. However, Siaud et al., (1989) did not present in their schemes of PRL distribution BSTMV and BSTLV levels. It is important to remark that most of the papers did not report positive perikarya outside the hypothalamus (Toubeau et al. 1979a, b; Hansen et al. 1982; Harlan et al. 1989; Harlan and Scammell 1991; Paut-Pagano et al. 1993).

The BSTMPM is extensively connected with MPO/A, VMH and Me, which are involved in neuroendocrine regulation and reproductive behaviour (Moga et al. 1989; Dong and Swanson 2004), where BST PRL can play an important role. In addition, the BSTMPM is the target of direct afferents from the AOB, and therefore the processing of vomeronasal information in this structure, involved in defensive and reproductive behavioural responses (Stowers et al. 2002; Gutiérrez-Castellanos et al. 2010), can be directly modulated by PRL. In contrast, the BSTL is distinguished by its reciprocal connections with nuclei involved in central autonomic regulation (Loewy and McKellar 1980; Moga et al. 1989).

The Me presented very scarce number of PRL-ir neurons and they were not present in all the animals. These neurons were close to the *opt* and probably can be related with the shared embryological origin of Me and SO. Previous literature supports that Me is composed of a mixture of cell groups derived from the embryonic ventral pallium, the medial ganglionic eminence, the anterior peduncular area and the preopto-commissural neuroepithelium, and even from other extratelencephalic territories such as the thalamic eminence or the supraopto-paraventricular hypothalamic domain (García-López et al. 2008). This latter domain includes the SO and Pa (Puelles and Rubenstein 2003). This embryological relation between the Me and SO was proposed by Hirata et al., (2009), who described the presence in the Me of an abundant

number of nitrergic cells, apparently derived from the preoptic and/or the supraopto-paraventricular hypothalamic neuroepithelium. The presence of PRL-ir somata in Me was not described previously in the bibliography (TABLE 10).

PRLergic innervation of the extended amygdala and septum: the telencephalic nodes of the sociosexual brain network

The sociosexual brain proposed by Newman (1999) includes six major nodes: the medial extended amygdala (including Me and BST), LS, MPO/A, AH and Pa, VMH and PAG, together with other tegmental motor areas. Other authors included PM subdivisions as key nuclei for the display of specific behavioural responses, e.g. mating or aggressive/defensive behaviours (FIGURE 67) (Van Berg et al. 1983; Insel and Numan 2003).

In this framework, the densest population of PRL-ir fibres outside the hypothalamus was found in the telencephalic nodes of the sociosexual brain network i.e., the medial extended amygdala and the lateral septum (TABLE 9). The extended amygdala is composed by two poles; the caudal pole of the subpallial amygdala (Ce and Me divisions), whereas its rostral pole is represented by the BST (De Olmos and Heimer 1999; Martínez-García et al. 2008). The PRLergic innervation we observed is mainly present in the medial extended amygdala, i.e., the Me and posteromedial BST, with some fibres present also in the central extended amygdala (in the Ce and some lateral subdivisions of the BST). The PRL presence in the BST was described before by different authors (DeVito 1988; Devito 1989; Cabrera-Reyes et al. 2017). DeVito (1988) reported PRL levels in the amygdala using RIA, but the extraction of the nucleus included all the amygdala and the extended amygdala (Gispen et al. 1972). The origin of this PRLergic innervation is unknown, but among the PRLergic cell populations described above, the main candidates are the BST proper and the MPA, since the Pa and SO do not give rise to significant projections to the Me (Cádiz-Moretti et el., 2016). Our results also showed the colocalization of PRL with AVP in the Me (FIGURE 56) This suggests that the origin of the AVP-PRL innervation might be the AVPergic cells in the BST (Otero-Garcia et al. 2014), since there are no AVP-positive neurons in the area of the MPA where we find the PRLergic cell bodies.

By contrast, other authors did not find PRL-ir fibres in any amygdaloid structure (Fuxe et al. 1977; Hansen et al. 1982). Hansen et al., (1982) remarked that they were not able to observe immunoreactive nerve fibres in the brain outside the hypothalamus. This can be due to the antibody employed (Rabbit anti-ovine PRL) which was obtained by themselves. In addition the antibody was used 1:3000 for immunohistochemtries which maybe is too diluted. Regarding

Fuxe et al., (1977), as it was explained before, they used immunofluorescence and, given the technical limitations available at that time, they could miss part of the labelling.

Regarding the septum, our results have showed a scarce PRLergic innervation mainly in the lateral septum. The presence of PRL in the septum was revealed by radioimmunoassay (DeVito 1988), as well as by immunocytochemistry (Paut-Pagano et al., 1993; Siaud et al., 1989; Harlan et al., 1989; Harlan & Scammell, 1991). The lateral septum has been shown to play a role in intermale aggressive behaviour (Wong et al. 2016; Leroy et al. 2018) and in maternal aggression (Caughey et al. 2011). Therefore, it is possible that the release of PRL in the female lateral septum plays a role in the aggressive response of dams. In fact, PRL signalling through the phosphorylation of the STAT5 transcription factor is increased in the ventrolateral septum in lactating mice (Salais-López et al. 2017).

PRLergic innervation of the hypothalamic and midbrain nodes of the sociosexual brain network

The hypothalamus shows the densest PRLergic innervation in the female mouse brain. The structure is considered an essential interface between the endocrine, autonomic and somatomotor systems (Swanson and Sawchenko 1983; Armstrong 2015; Simerly 2015; Low 2017). Within the variety of behaviours in which the hypothalamus is involved, it regulates aggressive-defensive responses and the expression of appropriate sexual and maternal behaviours (Newman 1999; Bosch 2013; Simerly 2015; Low 2017). The innervation of PRL-ir fibres in the hypothalamus is abundant in all its subdivisions (preoptic, anterior, tuberal and mammillary) (TABLE 9) but the highest density of fibres was observed in nuclei related with neurosecretion (Armstrong 2015; Low 2017), as discussed above, and in the hypothalamic nodes of the sociosexual brain (Newman 1999).

The MPO/A represents the rostral node of the hypothalamic sociosexual brain network (Newman 1999), and shows the densest PRLergic innervation within the preoptic region, together with the AVPe. In addition, PRLergic fibres were also present in AC/ADP, LPO and VLPO (TABLE 9). Previous studies reported the presence of PRLergic fibres in the preoptic hypothalamus (Fuxe et al. 1977; Harlan et al. 1989; Harlan and Scammell 1991), but did not provide a detailed description of the innervated nuclei. Functional studies have implicated the MPO/A (probably including also the AC/ADP) in the initiation of motivated behaviours such as copulatory, aggressive and maternal behaviours (Chiba and Murata 1985; Simerly 2015) (Numan and Stolzenberg 2009; McHenry et al. 2017). PRL release in the MPO/A may thus affect these different motivated behaviours, and in

fact recent data have demonstrated the effect of PRL signalling in the MPO/A in maternal behaviour (Brown et al. 2017).

The anterior hypothalamus is another node of the sociosexual brain network that showed an important presence of PRLergic fibres, mainly located in the two main magnocellular neurosecretory nuclei (SO and Pa), one parvocellular neurosecretory nuclei (Pe). Paut-Pagano et al., (1993) already described PRL-ir fibres in the anterior hypothalamus, pointing to a dense labelling in the parvocellular part of the Pa, whereas in the magnocellular part the fibres were found surrounding the region. In addition, these authors also described the presence of PRL-ir fibres in the SCh, which is also consistent with our results. In agreement with Paut-Pagano et al. (1993), and with our results, Siaud et al. (1989) described dispersed elongated varicose immunoreactive fibres throughout Pe and Pa. It is important to remark that none of these two studies observed fibres in the SO (Siaud et al. 1989; Paut-Pagano et al. 1993), and it is possible that they considered fibre labelling in the SO as dendrites of PRLergic SO neurons. Our results and those of Mejía et al., (1997) showing colocalization of PRL and AVP in the SO and Pa also suggest that at least part of the PRLergic fibres are dendrites of the PRL-positive neurons. However, the dendritic release of AVP (and OXT) has been demonstrated in neurons of the SO and Pa nuclei (Ludwig and Leng 2006), and therefore PRL may also be the subject of dendritic exocytosis.

In the tuberal region of the hypothalamus the main presence of PRL-ir fibres was observed in Arc, ME and VMH (TABLE 9). Arc receives strong intra-hypothalamic inputs from the Pa and AVPe, as well as the MPO/A, among others (Swanson and Kuypers 1980; Sawchenko and Swanson 1983; Thompson and Swanson 1998; Simerly 2015). Pa, MPO/A and AVPe contained PRL-ir cells and they may be the origin of the PRLergic inputs to the Arc.

VMH is the largest cell group in the tuberal region and it is a major node of the sociosexual brain network (Newman, 1999). It is surrounded by a thick fibre capsule or "shell" that separates it from the rest of the hypothalamus (Millhouse 1973). Our results revealed a dense presence of PRLergic fibres surrounding the VMH, matching with previous descriptions of VMH shell (Millhouse 1973). Previous studies observed labelled fibres in this nucleus (Fuxe et al. 1977; Toubeau et al. 1979a, b; Hansen et al. 1982; Paut-Pagano et al. 1993) and other authors depicted PRL-ir fibres in the VMH shell in their schematic representations, even if they did not mentioned them (Harlan et al. 1989). However, other authors did not describe the presence of PRLergic fibres in this area (Alonso et al. 1988; Siaud et al. 1989).

Several structures with PRL-ir neurons have been shown to project to the VMH shell, such as BSTMPM (BSTPr in L. Swanson, (2004)) (Dong and Swanson 2004), the MPO/A (Chiba and Murata 1985; Fahrbach et al. 1989), SCh (Watts and Swanson 1987; Fahrbach et al. 1989; Simerly 2015) and a small number of neurons in the parvocellular division of the Pa (Fahrbach et al. 1989). Therefore, the PRLergic innervation of the VMH shell may be originated by these structures.

Previous studies have demonstrated an involvement of the VMH in maternal behaviour (Gunnet et al. 1981; Bridges et al. 1999; Numan and Insel 2003b). This nucleus produces a chronic inhibitory influence on maternal behaviour, and at parturition this behaviour may be induced through an inhibition of VHM, resulting in a disinhibition of neural function in brain regions involved in the display of maternal responses, such as the MPO/A (Bridges et al. 1999). These findings indicate that neurochemical changes in VMH during pregnancy and parturition can be regulating the expression of maternal behaviour through the interaction with other regions of the brain, e.g. the MPO/A (Bridges et al. 1999). In addition, VMH is involved in serum PRL surges induced by oestrogen or cervical stimulation (Gunnet et al. 1981; Pan and Gala 1985). PRL has been shown to be crucial in the onset of maternal behaviour, and it is possible that the VMH inhibits/disinhibits maternal behaviour through its interaction with the PRL system (Bridges et al. 1999).

Finally, the mammillar hypothalamus presented most of the PRL-ir fibres in premammillary region. Previously, some authors described fibres in these nuclei (Fuxe et al. 1977; Siaud et al. 1989; Paut-Pagano et al. 1993). Although the mammillar hypothalamus was not included in the network of nuclei controlling sociosexual behaviour (Newman, 1999), the major inputs to the PMV arise in sexually dimorphic forebrain regions including the MPO/A (Chiba and Murata 1985; Simerly and Swanson 1986; Cavalcante et al. 2014), the BST (mainly BSTMPM) (Dong and Swanson 2004), the Me (Pardo-Bellver et al. 2012) and the AHi (Canteras et al. 1992). The connections of the PMV are consistent with functional data that suggest a role in mediating certain aspects of reproductive behaviour and physiology (Chen and Hong 2018), and in aggressive behaviour (Van Berg et al. 1983). Van Berg et al., (1983) showed that bilateral lesions in the PMV caused a strong increase in offensive behaviour in male rats, and Motta et al., (2013) have shown that it plays a key role in maternal aggression. Therefore, a PRLergic modulation of neural activity in this nucleus will directly affect these sociosexual behaviours. The midbrain presented PRL-ir fibres mainly in the PAG, as described previously by several authors (Toubeau et al. 1979a, b; Siaud et al. 1989; Paut-Pagano et al. 1993). The PAG has been implicated in a wide variety of behavioural responses such as rage and flight responses (Marchand and Hagino

1983; Chen and Hong 2018), as well as in nursing pups and maternal aggression (Lonstein and Stern 1997). The VMH appears to be the most prominent hypothalamic source of afferents to the PAG, but it also receives direct projections from the MPO/A (Rizvi et al. 2018) and the BST complex (Dong and Swanson 2004), which can originate the PRLergic innervation. In agreement with a role of PRL in the PAG in maternal behaviour, PRL signalling through the pSTAT5 pathway is increased in this structure in lactating female mice compared with virgins (Salais-López et al. 2017). The pSTAT5 labelling in the PAG is absent in male mice (Salais-López et al. 2018).

PRLergic innervation outside the sociosexual brain network: thalamus, and brainstem

In the thalamus, PRL-ir fibres were found mainly in the central parts of PV (TABLE 8) in the midline thalamus, as previously reported (Fuxe et al. 1977; Toubeau et al. 1979a, b; Harlan et al. 1989; Siaud et al. 1989; Paut-Pagano et al. 1993). Previous studies in monkeys (*Macaca fascicularis*) (Hsu and Price 2009) and rodents (Li and Kirouac 2012; Vertes et al. 2015) have described that PV afferents arise mostly in five regions: the cortex, the amygdaloid complex (amygdala and BST), the hippocampal formation, the septum and the hypothalamus. Therefore, the PRLergic innervation of PV may be originated by the BST and/or the hypothalamic SCh, MPO/A, VMH and Arc. PV has been directly implicated in affective functions such as seeking for natural rewards or drugs, stress and anxiety, and feeding behaviour (Hsu et al. 2014; Matzeu et al. 2014). The motivation pathways are very important in maternal behaviours. Some studies have seen that during the early postpartum period, pup suckling is more rewarding than cocaine (Ferris et al. 2005). The MPO/A has been shown to be critically important for maternal motivation (Numan and Woodside 2010) and we hypothesize that the connexions between MPO/A cells and PV in the thalamus may be crucial for motivational pathways (Bridges et al. 1990; Chen and Hong 2018). Moreover, PRL facilitates the rapid onset of maternal behaviour in the rat (Bridges et al. 1985, 1990; Bridges 1996; Wansaw et al. 2008), and this may extend to a role in maternal motivation.

Finally, within the brainstem the main PRL-ir fibres were present in the parabrachial nucleus, mainly in LPB (TABLE 8). Only a few reports have described fibres in PB (Alonso et al. 1988; Harlan et al. 1989) and other represented fibres in this area (Siaud et al. 1989). This nucleus relays viscerocEptive information in its medial aspect and nociceptive information in its lateral aspect (Fulwiler and Saper 1984; Moga et al. 1990), and receives afferents from several nuclei containing

PRL-ir cells, such as the MPO/A, Pa, retrochiasmatic areas of the hypothalamus and the BST, among other nuclei (Moga et al. 1990).

METHODOLOGICAL CONCERNS

Previous studies on the distribution of PRL in the rat brain show an important degree of variability in the reported results, likely because of the different techniques, antibodies and protocols employed. On one hand, one of the most important factors contributing to this variability is the use of colchicine injections. These intraventricular injections block axonal transport, increasing the levels of protein in the cell bodies (Weisenberg et al. 1968; Woolen et al. 1975). Thus, the studies including colchicine injections show a higher number of PRL-ir somata (DeVito 1988) (TABLE 10).

On the other hand, the antibody and its concentration influence directly the obtained labelling. As explained in Experiment 4 of Chapter 3, the antibody used in the present study was rabbit anti-mouse natural PRL diluted 1:500 (from the previous 1:40 dilution provided by National Hormone and Peptide program (NHPP, LOT# AFP-879151Rb). Previous reports do not usually specify whether the antibody was made against natural or recombinant PRL. A recombinant antigen (protein) made in *Escherichia coli* or in a eukaryotic cell line can have some differences from the natural one. One of these differences is the presence of additional peptide sequences used for their purification (e.g., GST; glutathione-*S*-transferase), which cannot be completely removed and may contribute to the polyclonal pool of IgG. Secondly, recombinant proteins are often denatured because of the way they are purified and consequently the immunogenic epitopes may only be present in denatured proteins and not in proteins in their natural in vivo conformation (Ivell et al. 2014). By contrast, antibodies against "natural" peptides are made with a highly purified extract of proteins from the organism. The anti-mouse natural PRL used in this work was made in rabbits against a highly purified PRL extract from mice pituitary gland (http://www.humc.edu/hormones/material.html). Mammalian PRL has three disulphide bonds and several glycosylation and other post-translational modifications (Freeman, 2000). The antibodies generated against recombinant proteins probably lack immunoglobulins generated against the epitopes including all these post-translational modifications.

In addition, another cause for the variability in PRLergic labelling is the fixative protocols used in the perfusion. Some of the previous publications employed formalin (Fuxe et al. 1977; Suzuki and Handa 2005), others paraformaldehyde (PFA) (Harlan et al. 1989; Siaud et al. 1989; Paut-Pagano et al. 1993) and others solutions as Bouin's (Toubeau et al. 1979a, b; Hansen et al. 1982)

in different concentrations and pH (TABLE 10) . The fixation protocol is important because it affects proteins; for example, the formaldehyde mechanism of action is the formation of intra and intermolecular cross-links between side chain of lysine residues, which over time results in the formation of methylene bonds. In contrast, the Bouin's solution has coagulating as well as cross-linking effect on proteins (Howat and Wilson 2014) . Different fixation protocols result in masking different antigenic determinants (D'Amico et al. 2009; Shi et al. 2011; Ivell et al. 2014) . In fact, we applied retrieval protocols for improving the PRL labelling, and in our hands, retrieval importantly enhanced the obtained labelling.

Another possible reason for the variation in PRL labelling is the existence of several molecular forms of PRL in the hypothalamic-neurohypophyseal system (Clapp et al. 1988, 1989; Torner et al. 1995; Mejía et al. 1997) . Different PRL variants with different molecular weights can be the result of alternative splicing of the primary transcript, proteolytic cleavage and other post-translational modifications of the amino acid chain (https://www.uniprot.org/uniprot/P06879) (Freeman et al. 2000). These PRL variants have different immunoreactivity (Anthony et al. 1993; Clapp et al. 1994; Torner et al. 1995). For this reason, the diverse antibodies employed in the literature (TABLE 10) may fail to detect some of the different PRL variants, and thus affect the pattern of distribution observed.

In summary, our results mainly match with previous publications that have used a similar antibody concentration and an antibody produced in the same laboratory (NHPP) (Toubeau et al. 1979b; Hansen et al. 1982; Harlan et al. 1989; Suzuki and Handa 2005) , even that in our case the antibody was raised against mouse PRL and the rest of studies using antibodies from the same supplier have used antibodies raised against rat PRL. Also, the publications that used colchicine injections described a similar population of positive cell bodies (Toubeau et al. 1979b) (TABLE 10) .

Table 10: summary of the previous in the distribution of PRL-ir in the rat blain. When the authors use more than one antibody in the study, the asterisk (*) indicates the best antibody and with which the description of the distribution was made. Bouin-Hollande's solution contains cupric acetate, picric acid, formalin and glacial acetic acid to water. mAb: monoclonal antibody. national hormone and peptide program (NHPP) and national institute of arthritis metabolism and digestive diseases (NIAMDD) are institutes where the Dr. Parlow produces the antibodies. Prolactin (PRL) and Paraformaldehyde (PFA).

ARTICLE	PRL ANTIBODY	CONCENTRATION	ANIMALS	COLCHICINE INJECTION	FIXATION
(Alonso et al. 1988)	Rabbit anti- rat PRL (D. Grouselle) and rat PRL (NIAMDD)	1:500	Male and Female	No	PFA 0.1 M with 0.2% picric acid in PBS
(Clapp et al. 1994)	Rabbit anti-rat 16 KD PRL from 23 KDa rat PRL (NHPP) Rabbit anti-rat PRL (NHPP)	1:500	Female	No	4% PFA in PBS 0.1M pH 7.4
(Fuxe et al. 1977)	Rabbit anti-rat PRL (NIAMDD)	1:16	Male	No	formalin
(Hansen et al. 1982)	Rabbit anti-ovine PRL and ovine PRL (NIAMDD)* Rabbit anti-rat PRL (NIAMDD)	1:3000 1:200	Male and Female	No	Bouin's fluid
(Harlan et al. 1989)	Rabbit anti-rat PRL (NHPP)* Goat anti-rat PRL (M. Lieberman, University of Wisconsin) Rabbit anti-rat PRL (Arnel) Guine pig anti-ovine PRL (J. Parsons, University of Minnesota) Rabbit anti-human PRL (Accurate Chemical & Scientific Corp.)	1:1000	Female	Yes, 50 µg/ 2 µg 24-48h before sacrifice	3% neutral-buffered PFA
(Harlan and Scammell 1991)	Rabbit anti-rat PRL (NHPP) Mouse anti-rat PRL 6F11 (Mab) Mouse anti-rat PRL 17D9 (Mab)	1:1000	Female	No	3% buffered paraformaldehyde (pH 7.2)
(Mejía et al. 1997)	Rabbit anti-rat 16 KD PRL from 23 KDa rat PRL (NHPP)	1:500	Female	No	4% PFA in PBS 0.1M pH 7.4
(Paut-Pagano et al. 1993)	Rabbit anti-ovine PRL (Girod and Dubois 1976)* Rabbit anti-rat PRL (UCB)	1:20000 ¿?	Male	Yes, 50 µg/5 µl 24-36h before sacrifice	4% PFA in PBS 0.1M pH 4.5
(Siaud et al. 1989)	Rabbit anti- rat PRL (D. Grouselle) and rat PRL (NIAMDD)	1:100	Male	Yes, 50 µg/10 µl 48h before sacrifice	4% PFA 0.1 M with 0.2% picric acid in PBS
(Suzuki and Handa 2005)	Rabbit anti-rat PRL (NHPP)	1:500 (previously diluted 1:40)	Female	No	10% neutral buffered formalin
(Toubeau et al. 1979b)	Rabbit anti- rat PRL (NIAMDD)	1:400-1:800	Male and Female	Yes, 200 µg/50 µl	Bouin's fluid or Bouin-Hollande's
(Toubeau et al. 1979a)	Rabbit anti- rat PRL (NIAMDD)	1:400	Male and Female	No	Bouin's fluid

IMPLICATIONS FOR MOTHERHOOD AND FOR SOCIAL BEHAVIOUR

Our results showed a dense presence of PRLergic somata in BST, AC/ADP, Pa, SO and in the periventricular hypothalamus and Arc. Apart from Arc, all these nuclei also present OXTergic and AVPergic neurons and these colocalize with PRL. Thus, PRLergic, OXTergic and AVPergic neurons are present in the magnocellular neurosecretory system, whereas PRLergic neurons in Arc are apparently related with the parvocellular neurosecretory system (Watson and Qi 2012; Simerly 2015). This could indicate, as we propose in the FIGURE 67, that PRL is present in the magnocellular neurosecretory system, and probably released in the posterior pituitary gland, and in the parvocellular neurosecretory system, which sends its projections to the ME. The role of this direct release of neural PRL in the blood vessels of the hypothalamo-hypophysial system, probably independent of the PRL release by the pituitary lactotrophs, requires further investigation, but one possible explanation might be that brain PRL is a different molecular form, as suggested previously (Clapp et al. 1988, 1994; Anthony et al. 1993; Torner et al. 1995).

A major finding of this work is that the pattern of distribution of PRL-ir is similar in the brain of virgin, pup-sensitized and lactating females. We found, however, a higher number of PRL-ir cells in the SCh, SO and MPO/A in lactating females. These results are consistent with the increased PRL signalling through the phosphorylated (active) signal transducer and activator of transcription 5 (pSTAT5) in the MPO and SO found by (Salais-López, Lanuza, Agustín-Pavón, & Martínez-García, 2017). In this study, they reported a relatively reduced pattern of lactogenic signalling (pSTAT5-positive cells) in virgin females, in contrast to a widespread pattern in pregnant and lactating females (Salais-López, Lanuza, Agustín-Pavón, & Martínez-García, 2017), reinforcing the view that PRL plays a key role in maternity.

It is known that neuropeptides as OXT and AVP have a rather flexible mode of action: they can be released from all parts of the neuronal membrane within a particular brain region and can exert both local and more distant effects, as well as rapid and prolonged intracerebral actions. Also, these neuropeptide systems show a high degree of plasticity, as their activity can be altered by physiological or environmental stimuli (Bosch and Neumann 2012; Johnson and Young 2017).

In relation with this, a relevant question opened by the existence of brain PRL acting as neuromodulator and simultaneous pituitary PRL being incorporated into the brain by specific transporters is how the two systems are regulated. One possibility is that brain PRL may be involved in the regulation of maternal behaviour when the peripheral lactogens (PRL and PL) are

no longer required for the stimulation of maternal responsiveness. It has been observed that once maternal behaviour becomes established in female rats, it is maintained independent of pituitary regulation (Rosenblatt 1967; Erskine et al. 1980; Svare et al. 1982; Numan and Insel 2003a). We hypothesize that the regulation of maternal behaviour at this time is carried out by centrally produced PRL. Particularly important would be the influence of PRL in the motivational system, likely through the MPO/A (Numan and Woodside 2010). The results in the quantification of PRL-ir somata in the MPO/A showed significant differences between dams and virgins, with the godmothers having intermediate levels. This suggests that the PRLergic cells could have an impact in the motivational system and in the ''voluntary proactive maternal responses". In virgin females, the small number of PRL-ir somata can be a factor to fail to display maternal behaviours towards the pups. In rats, virgin females even show aversive responses against pups (Rosenblatt 1967). This is proposed to be due to the MPO/A activating the AH, VMH and the PAG, with the additional input of the Me (Numan 2006) (FIGURE 67). In contrast, during pregnancy MPO/A activity is modulated by OXT, PRL and gonadal steroids and the increase of PRLergic cells in this nucleus can play an important role in this modulation in lactating females. This modulation leads to the inhibition of the aversive pathway and the activation of the maternal pathway, integrated by VTA and its dopaminergic (DA) projection to the Acb/VP (Numan and Insel 2003b; Numan and Woodside 2010). The stimulation by pups (chemosensory, auditory, tactile cues, etc.) is needed to modulate the motivational system towards maternal behaviours (maybe recruiting the thalamic PV), and for this reason virgin females without previous exposition to pups did not display maternal behaviours (Numan and Woodside 2010; Numan 2014).

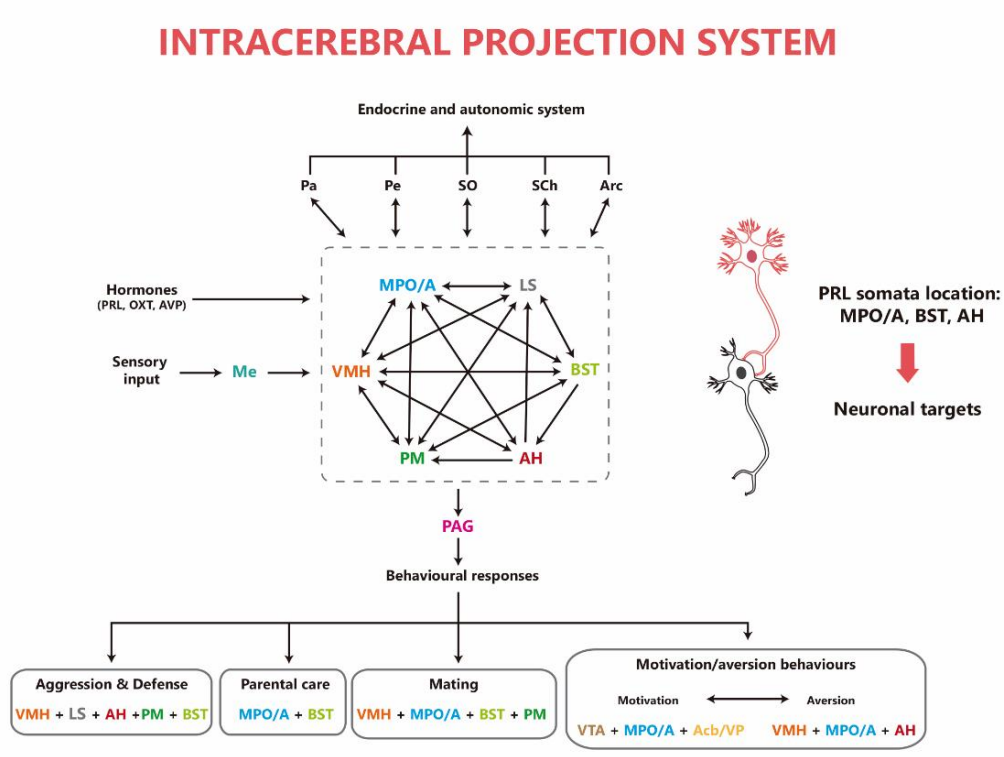

Figure 67: Schematic intracerebral connections of the PRLergic neurosecretory cells. The hypothalamic peptidergic neurons gives rise to chemical synapses on other neurons. The diagram represents a modification of the figure in Newman, (1999) which shows the connections in the SBN. The SBN is a functional brain network responsible for the expression of every social and reproductive behaviour. This system is interconnected with the nuclei of the parvocellular and magnocellular neurosecretory systems. For abbreviations see list.

It is know that the interactions of animals with pups alters both the morphological characteristics of neurons and their response to stimulation (Mezey and Kiss 1991; Modney and Hatton 1994). It is possible that long-term alterations in anatomical and biochemical processes, like those that have been identified in the synaptic connectivity in the SO of female rats (Modney and Hatton 1994; Theodosis and Poulain 2001), occur within the MPO/A because of pregnancy and lactation. These anatomical and biochemical changes in SO affect mainly the OXT system (Neumann et al. 1993; Neumann and Landgraf 2012). Previous authors have observed an increased release of OXT within the SO and Pa during parturition, and suckling is accompanied by increased electrical activity of magnocellular OXT neurons (Neumann et al. 1993).

This increase can be related with PRL synthesis in these nuclei. Previous studies have proposed a positive feedback between PRL and OXT secretion in response to suckling, mating stimuli and ovarian steroids (Lumpkin et al. 1983; Kennett and Mckee 2012). In addition previous research have reported that PRL in the brain or in the circulation promotes the activation of nNOS in the hypothalamo-neurohypophyseal system leading to the systemic release of OXT and AVP (Parker

et al. 1991). These cascade is observed also in Pa and SO (Popeski et al. 2003; Vega et al. 2010). These results suggest that a positive feedback between PRL and OXT can be also occurring in lactation in Pa and SO.

In conclusion, most of the structures where we have observed positive PRL cells and fibres are nuclei related with the sociosexual brain and especially with the display of maternal behaviours. This suggests that PRL is playing a role beyond the magnocellular and parvocellular neurosecretory systems, as a neurohormone in the intracerebral connection system (FIGURE 66 AND FIGURE 67). The presence of an increased number of PRL-ir cells in MPO/A in lactating females suggests a possible role of PRL on motivational aspects of maternal care. In addition, PRL may play a role in the emotional aspects of maternal care due to the presence of PRL-ir somata in the extended amygdala, which have a key role starting the pathways of proactive maternal behaviour (Numan and Insel 2003b; Bridges and Grattan 2019).

GENERAL DISCUSSION

The present doctoral thesis constitutes the first demonstration of the involvement of Me in the display of maternal aggression using a chemogenetic approach. Also, this work provides a comprehensive study of the gene expression changes that happen in this nucleus during pregnancy and lactation. Our results showed that PRL was the gene related with motherhood that presented the highest differential overexpression in Me in dams compared to godmothers. During maternity, PRL drives central changes to adapt the female's physiology and behaviour to the particular demands of motherhood. For this reason, we have also studied the brain distribution and possible differences in PRL expression between lactating, godmothers and virgin females. These experiments allow us to investigate the possible role of PRL in the neuronal changes related with the onset and display of maternal behaviours due to pregnancy and to exposure to pup-derived stimuli.

In Chapter I, we first describe how repeated testing increases the levels of maternal aggression in lactating females, and confirm that godmothers do not display maternal aggression even after prolonged exposure to pups and repeated testing (Martín-Sánchez et al. 2015b, a). Next, we confirmed and extended previous observations pointing out to a key role of Me in the display of maternal aggression, showing that inactivation of Me by means of DREADD technology selectively blunts the increase in aggressive behaviour displayed by dams after repeated confrontation with an intruder male.

The Me is one of the main structures showing reciprocal connections with the AOB and MOB (Scalia and Winans 1975; Pardo-Bellver et al. 2012; Cádiz-Moretti et al. 2013, 2016), and it is thus considered part of the chemosensory amygdala. The chemogenetic inhibition of this nucleus leads to a decrease in levels of maternal aggression against an intruder male, indicating a role of Me in the display of this behaviour in lactating females. This role may be related to the inability of lactating females to properly process chemosensory signals of the intruders. In this sense, lesions of Me in female mice also result in deficits in mate recognition and mating behaviour (DiBenedictis et al. 2012) and similar results have been obtained with DREADD-induced Me inhibition (McCarthy et al. 2017b). These results, together with the decrease of aggression levels observed in our studies, suggest that the Me may be tagging male-specific signals, such as *darcin*, as attractive (in non-lactating females) or aggression-inducing (in dams), and that this differential tagging would be influenced by specific hormonal changes induced by pregnancy and lactation, since godmothers never attacked male intruders.

Changes in the maternal brain would also affect the afferents to Me relaying multisensory information from pups, which is known to influence maternal aggression. In particular, the Me receives projections from the posterior intralaminar thalamic complex (Cádiz-Moretti et al. 2016), that relay suckling-induced somatosensory information (Cservenák et al. 2010, 2013). The posterior intralaminar thalamic nucleus has been shown to be sensitive to PRL, and the PRL-induced response is increased in dams (Salais-López et al. 2017). Thus, this thalamic input to Me is probably altered in dams with respect to virgin females. In addition, the posterior intralaminar thalamic complex also relays auditory (LeDoux et al. 1990) and visual cues (Doron and Ledoux 1999; Linke et al. 1999), and thus multisensory pup-derived stimuli might access Me through this pathway.

In sum, Me is a key node in processing external stimuli from intruders and probably also from pups (olfactory, auditory and suckling cues), that influence maternal aggression towards an intruder. Information from the intruder would be then sent from Me subdivisions to hypothalamic nuclei that control both aggression and mating, such as the VMH and PMV (Van Berg et al. 1983; Fahrbach et al. 1989; Numan and Insel 2003b; Pardo-Bellver et al. 2012) and AH and septal regions as LSV (Swanson and Cowan 1979; Gammie and Nelson 2001; Pardo-Bellver et al. 2012), involved mainly in aggression. In addition, Me presents a dense output to BST subnuclei (Pardo-Bellver et al. 2012) which play a role in sociosexual behaviours (Numan and Insel 2003b; Chen and Hong 2018) and also in aggression (Shaikh et al. 1986; Gammie and Nelson 2001; Padilla et al. 2016). Moreover, Me is also connected with MPO/A, a region related with the modulation of maternal behaviour (Chiba and Murata 1985; Brown et al. 2017). Previous studies have observed that many of these nuclei connected with Me display an increase of c-FOS expression in association with maternal aggression (BST, MPO/A, Pa and cortical amygdala) (Gammie and Nelson 2001). We hypothesise that the shaping of the maternal brain would shift Me outputs towards nuclei triggering aggressive responses. Changes in Me are likely mediated by hormones, including PRL, and nonapeptides (Haller 2018).

In fact, we discovered profound changes in the transcriptomic profile of the Me in Chapter II of the present thesis, by comparing the patterns of gene expression in lactating and pup-sensitized virgin females in the first days of lactation. The RNA-seq study showed many genes with differential gene expression between female groups, some of them in close relationship with maternal behaviours. Among these motherhood-related genes we found *Prl, Gh, Ghrhr, Pit-1*, *Oxt* and *Gal*. Of them, *Prl* was the one which presented the higher differential expression between the studied groups. In addition, this upregulation of *Prl* was confirmed by qPCR.

Expression of *Prl* mRNA in the CNS has been described before (Emanuele et al. 1992), especially in the Pa and SO, the major sites of OXT and AVP synthesis (Clapp et al. 1994; Torner et al. 1999, 2004). In addition, previous studies in RNA-seq have seen that the expression of *Prl* significantly changes in hypothalamus, hippocampus, neocortex, and cerebellum in lactating females as compared to virgin females, with the largest difference in expression observed in the hypothalamus (Ray et al. 2016).

Other genes upregulated in the Me of dams are related to PRL signalling. For example *Pitx1* and *Pit*-1 (Pfaffle et al. 1992; Voss and Rosenfeld 1992; Nowakowski and Maurer 1994) are transcription factors needed for the synthesis of PRL. *Cis,* a member of the suppressor of cytokine signalling family, is part of the JAK/STAT signalling pathway, playing an important role in negative feedback on the PRLR, including the long receptor isoform (Bole-Feysot et al. 1998; Pezet et al. 1999; Krebs and Hilton 2000; Nicolas et al. 2013). This gene was observed in previous microarray studies of gene expression changes in relation with motherhood (Gammie et al. 2016). Because of this negative feedback role, changes in expression of these molecules would modulate PRL effects in the maternal brain. Indeed, previous studies have demonstrated that all TIDA neurons in the dorsomedial Arc express CIS protein, and that CIS levels in TIDA neurons are increased in lactating rats in the presence of suckling (Anderson et al. 2006b). The same mechanism that occur in Arc may be happening in the Me.

Given these results and the known critical role of PRL in mammalian reproduction, we sought to explore the expression of PRL protein in Me and its possible changes with motherhood. In this sense, there is a controversy as to whether all PRL arrives to the CNS through its binding to PRL receptors in the choroid plexus, and the subsequent transport of PRL into the cerebrospinal fluid (Walsh et al. 1987; Brown et al. 2016), or whether PRL is being synthetized de novo in some nuclei of the CNS (Schachter et al. 1984; Emanuele et al. 1987, 1992; DeVito et al. 1992; Clapp et al. 1994). The results of Chapter III give support to the latter possibility, since we detected PRL in the Me by proteomics, Western blot, ELISA and immunohistochemistry assays. This result does not exclude that pituitary PRL can be also incorporated into the brain by the specific transporters in the choroid plexus.

One possibility is that the PRL synthetized in the CNS plays a role in the regulation of maternal behaviours on top of peripheric PRL. Previous studies in rats have demonstrated that, once stablished, maternal behaviour is maintained independently of pituitary regulation (Rosenblatt 1967; Erskine et al. 1980; Svare et al. 1982; Numan and Insel 2003a). In lactating females, the

onset of aggression is largely dependent on suckling by the pups (Garland and Svare 1988), which keeps high the level of pituitary PRL. However, aggression is completely normal in hypophysectomised lactating or hormone-treated sensitized virgin female rats (Erskine et al. 1980; Svare et al. 1982). These results imply that the reduction in maternal aggression observed after removal of the litter is not due to the rapid reduction in pituitary PRL that occurs at this time (Amenomori et al. 1970). In fact, this reduction in aggression after separation from the litter occurs even in hypophysectomised dams (Erskine et al. 1980). The fact that the peripheric PRL is not playing a key role in the maintenance of maternal aggression would support the existence of two roles of PRL: neuromodulatory and hormonal.

Previous authors have seen that PRL is critical in the motivational system through MPO/A. Their results show that complete deletion of PRLR from MPO/A in adults profoundly impaired maternal nursing behaviour (Brown et al. 2017). This effect is increased when the deletion of PRLR were carried out in the GABAergic neurons, which are the largest population of neurons normally activated during expression of maternal behaviour (Tsuneoka et al. 2013; Brown et al. 2017). In MePD, it is described that most of the aromatase positive cells that co-expressed GAD1, a GABAergic marker, are needed for the display of intermale aggressive behaviours (Unger et al. 2015; Chen and Hong 2018). These results suggest that PRL can have the same effect in the GABAergic neurons in Me related with maternal aggression.

It is possible that neural PRL may act by different pathways in the CNS than those of peripheral PRL. Bromocriptine treatment, which suppresses hypophyseal PRL release, showed that pSTAT5 expression in the brain was completely dependent on peripheric PRL and/or PL. Bromocriptine treatment blocked all basal pSTAT5 expression in virgin female (Brown et al. 2010) and lactating female mice (Brown et al. 2011). However, in the case of pregnant female mice bromocriptine treatment did not abolish pSTAT5 labelling (Salais-López et al. 2017), suggesting that most, if not all the pSTAT5-immunoreactive cells found in bromocriptine-treated pregnant females is due to non-hypophyseal lactogenic sources, arguably PL (Soares 2004). These results are suggesting that without peripheric PRL or PL the JAK/STAT pathway is mostly eliminated. Nevertheless, hypophysectomies did not eliminate the presence of PRL in the brain of male and female rats (DeVito 1988; Emanuele et al. 1992) or maternal behaviours as maternal aggression (Svare et al. 1982). Due to this reasons PRL synthetized de novo in the brain can be acting by other pathways different to JAK/STAT as the mitogen-activated protein (MAP) kinase cascade (ERK/MAPK) (Freeman et al. 2000).

In conclusion, neural pathways regulating the switch to a maternal brain would include the Me, which, as described in the present thesis, suffers deep transcriptomic changes during motherhood, including a strong upregulation of *Prl*. In addition, the MPO/A, connected with Me directly and via dense BST connections (Chiba and Murata 1985; Cádiz-Moretti et al. 2016), also displays significant changes during motherhood, in particular an increase in the density of PRL-ir somata. Thus, neural PRL can be acting through different nuclei of the SBN during pregnancy and lactation, allowing the development of maternal behaviours (FIGURE 68).

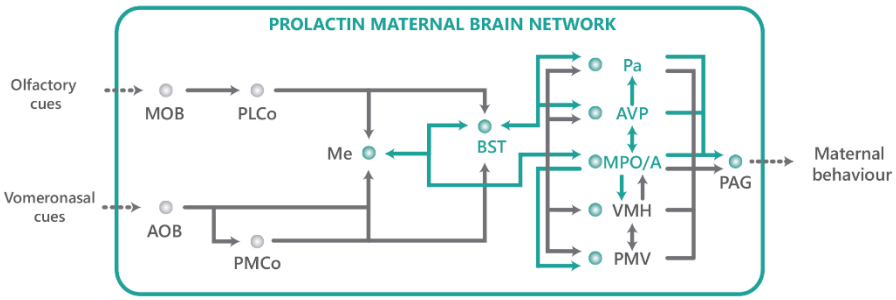

Figure 68: Representation of the PRLergic pathways involved in maternal behaviour. The scheme represents the nuclei of the maternal brain network with PRL-ir somata (letters in blue) and its connections with other nuclei involved in this behaviour (arrows and lines in blue). For abbreviations see list. Adapted from Chen and Hong (2018).

CONCLUSIONS

1. Maternal aggressiveness increases during the first third of lactation after repeated testing. This behaviour cannot be induced in pup-sensitized virgins, even when they are in continuous contact with pups (godmothers) and after extensive training.

2. Maternal aggression needs the hormonal changes that take place during pregnancy and lactation, which are probably shaping the brain and preparing it for motherhood.

3. The Me plays a key role in the display of maternal aggression in lactating females. The chemogenetic inhibition of the nucleus blocked the expected increase in maternal aggression during the second day of training.

4. Pregnancy and lactation produced gene expression changes in Me, and different patterns of expression are observed in dams and pup-sensitized virgin females. Specifically, we found 197 genes upregulated and 99 genes downregulated in dams with respect of godmothers.

5. Several of the most upregulated genes in the Me of dams are related with maternal behaviours. In this group we find *Prl*, *Oxt* and *Gal*. Other upregulated genes related to *Prl* were *Gh*, *Ghrhr*, *Pit-1* (also called *Pou1f1*) and *Cis* (also called *Cish*).

6. The presence of *Prl* mRNA in Me suggests that this protein is synthetized in this nucleus. Since there are only very scarce PRLergic somata in this nucleus, *Prl* mRNA can be transported and expressed in axon terminals.

7. The increase in *Prl* mRNA of dams is also observed in PRL protein levels, at least as measured by ELISA. The increase in PRL in the Me of dams with respect to godmothers suggests that PRL levels are subjected to fluctuations caused by pregnancy and lactation.

8. PRL levels in serum were also significantly increased in dams (as expected) compared with godmothers. However, the PRL levels in serum did not correlate with the levels obtained in Me.

9. PRL innervation has a widespread distribution in the female mouse brain, especially in areas related to endocrine regulation and the control of social and maternal

behaviour. This pattern of distribution of PRL-ir is similar in the brain of virgin, pup-sensitized females and lactating females.

10. The densest presence of PRLergic somata was found in BST, AC/ADP, Pa, SO, the periventricular hypothalamus and Arc. Apart from Arc, all these nuclei also present OXTergic and AVPergic neurons, which partially co-localized with PRL.

11. PRL-ir density changes through different physiological stages in females: pup-naïve virgins, pup-sensitized virgins (godmothers) and lactating females. Significant differences in the number of PRL-ir cells were observed in the SCh, SO and MPO/A, which was higher in lactating females.

RESUMEN EN CASTELLANO

INTRODUCCIÓN GENERAL

El cuidado parental se encuentra presente en un gran número de especies dentro del reino animal. Esto se debe a que este conjunto de comportamientos incrementa drásticamente la supervivencia de la descendencia. Estos comportamientos se pueden clasificar en maternales o paternales en función de si son llevados a cabo por un parental u otro y pueden ser desempeñados conjuntamente o únicamente por uno de los progenitores (Insel and Numan 2003; Gross 2005; Kölliker et al. 2017).

Los distintos tipos de comportamientos parentales agrupan un gran número de conductas, que abarcan desde la elección de los sitios de puesta hasta provisión de alimentos, refugio y defensa de las crías. Los comportamientos parentales son por tanto una serie de adaptaciones a los diversos cambios ecológicos que sufren los seres vivos, siendo este el motivo principal de que sean parte de las estrategias evolutivas de cada especie. Los conflictos evolutivos que surgen a consecuencia de las interacciones entre los padres y la descendencia, entre los hermanos y entre los parentales generan unas presiones selectivas sobre los cuidados parentales, es decir, cuánto hay que proporcionar, quién lo proporciona, y cómo se reparte entre los distintos individuos de la descendencia (Dulac et al. 2014; Kölliker et al. 2017). De este modo, la evolución del comportamiento parental es un proceso de coevolución, debido a que la supervivencia y el éxito reproductivo de los padres y la descendencia no se determina únicamente por sus características fenotípicas y genotípicas, sino que también son determinantes las interacciones que tienen entre ellos.

Esto tiene como resultado que en función de especie se hayan favorecido más unos comportamientos parentales que otros, aumentando así su diversidad y complejidad. Por otro lado, se ha visto que los comportamientos parentales juegan un papel muy importante en la evolución de otros comportamientos sociales como la eusocialidad (Kölliker et al. 2017) o el cuidado aloparental. Este último, es un comportamiento de cuidado de las crías por parte de un individuo conespecífico que no es el progenitor directo de estas. Esta conducta se observa en algunas especies de mamíferos incluidos los humanos (Fleming and Rosenblatt 1974; Riedman 1982). En estos casos, ciertos procesos o cambios que no están vinculados a los cambios fisiológicos que ocurren durante el embarazo y lactancia median la aparición de estos cuidados parentales.

En el caso del comportamiento maternal, que es en el que se centra esta tesis doctoral, este se puede definir como cualquier comportamiento que la hembra muestra para incrementar la supervivencia de las crías (see Jay S Rosenblatt, Mayer, & Siegel, 1985). Estos comportamientos están íntimamente relacionados con el nivel de desarrollo neonatal de las crías en el nacimiento. Según este nivel de desarrollo se puede diferenciar entre especies altriciales y precoces. En el caso de las especies altriciales, entre las que encontramos los ratones (*Mus musculus*), la descendencia es está poco desarrollada en el momento del nacimiento y son incapaces de desplazarse fuera del nido hasta que transcurren varios días o semanas (v.g. conejos, primates, cánidos, etc.) (Derrickson 1992). En estas especies los comportamientos maternales se dividen entre comportamientos dirigidos directamente a las crías y los no dirigidos directamente a las crías (Insel and Numan 2003; Gammie 2005). Dentro de los comportamientos directos encontramos el amamantamiento y la reagrupación de las crías en el nido, así como su limpieza y acicalado. Los compartimientos indirectos agrupan la construcción del nido y la defensa de las crías frente a intrusos.

En especies que viven en grupos sociales la interacción con individuos conespecíficos también puede ser un riesgo para los recién nacidos. Un ejemplo son los casos infanticidio por parte de otro individuo de la misma especie y que se puede observar en un gran número de especies de mamíferos. La muerte de las crías tiene un elevado coste para el éxito reproductivo de la madre y por este motivo las madres han desarrollado adaptaciones comportamentales para evitar estos sucesos. Por este motivo el comportamiento de defensa de las crías por parte de los progenitores es un comportamiento con un valor adaptativo muy elevado (Maestripieri 1992). La agresión maternal, es, por tanto, una respuesta de protección donde la madre lactante ataca a un intruso para mantenerlo alejado del nido. (Numan and Insel 2003a). Este comportamiento no dirigido directamente a las crías se encuentra descrito en roedores, carnívoros, pinnípedos y primates no-humanos entre otras especies (Mykytowycz and Dudzinski 1973; Harcourt 1992; Maestripieri 1992; Lonstein and Gammie 2002; Saltzman and Maestripieri 2011).

El infanticidio llevado a cabo por individuos conespecíficos puede estar relacionado con la falta de ovulación que se da durante la lactancia, esto hace que las hembras lactantes no sean receptivas a nuevos machos (Marinari and Moltz 1978). Por lo tanto, los machos intrusos se pueden beneficiar de la muerte de estas crías (con las cuales no están emparentados) al hacer que la hembra vuelva a tener ciclo estral y a si tener una oportunidad para reproducirse e incrementar su éxito reproductivo (Hrdy 1979; Labov et al. 1985; Weber and Olsson 2008).

La agresión maternal no es estable durante todo el posparto, disminuyendo la intensidad de los ataques conforme pasan los días de lactancia (B. Svare & Gandelman, (1973). Los cambios en los niveles de agresión permiten diferenciar la "fase de iniciación" donde la estimulación de los pezones al mamar es necesaria para que se dé el comportamiento de agresión maternal; la "fase intermedia de la lactancia" donde la estimulación de los pezones por parte de las crías ya no es necesaria para que se presente el comportamiento de agresión y, por último, "fase de lactación tardía" donde se observa una disminución en la agresión maternal. Los mecanismos que controlan los cambios entre las fases que dependen de los estímulos de succión de las crías para manifestar el comportamiento de agresión todavía no se han descrito. Una posible explicación es que la exposición a estímulos procedentes de las crías (v.g. somatosensoriales) puede inducir cambios neuroendocrinos o en los neurotransmisores que mantendrían la agresión maternal durante las fases independientes de la estimulación de los pezones por parte de las crías (Svare and Gandelman 1973, 1976a; Svare 1977; Lonstein and Gammie 2002).

En mamíferos y otros vertebrados, que las crías lleguen a la edad adulta requiere un gran número de adaptaciones por parte de la madre que le permitan lidiar con la maternidad. Estas adaptaciones implican una serie de cambios fisiológicos y conductuales que se originan gracias a variaciones en el cerebro durante el embarazo y que están favorecidas por las señales endocrinas que se producen en este periodo. Estos cambios se deben iniciar antes del parto y mantenerse durante el todo el postparto, requiriendo así que el sistema endocrino actúe durante el embarazo tardío y la lactancia.

Los principales cambios hormonales que ocurren durante el embarazo incluyen un incremento de los niveles circulantes de estradiol, progesterona y de hormonas lactogénicas (PRL y PL), cuyos patrones de secreción varían durante este periodo. El papel de los estrógenos y la progesterona en el comienzo y mantenimiento de la agresión maternal no está claro del todo. Sin embargo, estas hormonas deben actuar esencialmente en la periferia promoviendo el desarrollo correcto de los pezones para que las crías puedan mamar y así proporcionar a las madres la estimulación sensorial crítica para el inicio de la agresión maternal (Gandelman 1973; Svare and Gandelman 1975; Mann and Svare 1982). Por lo que respecta al papel que ejerce la PRL, se ha visto que sus niveles circulantes no están implicados ni en el inicio, ni en el mantenimiento ni en el disminución del comportamiento de agresión maternal durante la lactancia (Broida et al. 1981).

Todos estos datos sugieren que en ratones los eventos endocrinos específicos asociados con el final del embarazo pueden ser necesarios, pero no son suficientes para inducir el comportamiento de agresión maternal. De este modo, la manifestación de esta conducta agresiva en hembras de ratón parece necesitar también de la integración de estímulos multisensoriales procedentes de las crías (v.g. olfativos, auditivos, somatosensoriales, etc.) y de los cambios neuronales que ocurren durante el embarazo y el parto (Okabe et al. 2012).

Por lo que respecta a los estímulos procedentes de las crías, en roedores las señales olfativas juegan un papel clave. Esto se debe a que los roedores son animales macrosmáticos y por lo tanto sus comportamientos sociales se basan en la detección de marcas de olor. Esto también afecta a los comportamientos maternales, ya que el vínculo entre la madre y sus crías está controlado por señales quimiosensoriales (Lonstein and Gammie 2002; Wyatt 2003a; Dulac et al. 2014).

Las señales quimiosensoriales que proporcionan información sobre individuos conespecíficos se denominan feromonas (Karlson and Lüscher 1959; Wyatt 2003b). La respuesta a estas señales varía en función de una serie de factores como es el estado hormonal de los individuos o la experiencia previa. En roedores, las feromonas son detectadas por dos sistemas sensoriales principales: El sistema olfativo principal y el accesorio o vomeronasal (Wyatt 2010). El sistema olfativo principal principalmente detecta volátiles transportados por el aire, mientras que el vomeronasal parece especializado (con algunas excepciones) en la detección de productos químicos no volátiles con un valor biológico intrínseco (Krieger et al. 1999; Gutiérrez-Castellanos et al. 2010), como las feromonas sexuales. Sin embargo, a pesar de que la información olfativa y vomeronasal es detectada por dos estructuras anatómicamente separadas, ambos sistemas integran la información para permitir la generación de una imagen completa de las señales químicas presentes en el medio ambiente y así poder generar una respuesta conductual apropiada (v.g. comportamiento maternal, agresión entre machos o maternal, etc.) (Halpern and Martínez-Marcos 2003; Boehm et al. 2005; Cádiz-Moretti et al. 2013). Esta información converge en algunos núcleos amigdalinos (Gutiérrez-Castellanos et al. 2010; Cádiz-Moretti et al. 2013)

Por lo que respecta al comportamiento de agresión maternal, las señales olfativas procedentes de los intrusos (y probablemente de las crías (Okabe et al. 2013)) que recibe la madre son importantes para la manifestación de comportamientos agresivos. Se ha visto que la falta de un correcto funcionamiento del sistema olfativo en ratones (bulbectomías o mutaciones que provocan anosmia) impiden la manifestación de la agresión maternal (Gandelman et al. 1972;

Wang and Storm 2011). Esto también sucede con las alteraciones en el funcionamiento del sistema vomeronasal (Bean and Wysocki 1989; Del Punta et al. 2002; Kimchi et al. 2007; Hasen and Gammie 2009, 2011).

se ha demostrado que diferentes señales olfativas procedentes de machos que inducen comportamientos de agresión maternal: Las proteínas urinarias principales (MUPs) y moléculas de bajo peso molecular no identificadas (Chamero et al. 2007). Las MUPs aparentemente son detectadas por el VNO (Kaur et al. 2014) y su secreción presenta un claro dimorfismo sexual en el ratón de laboratorio (Hurst 1987; Hurst and Beynon 2013). Una de estas proteínas es la *darcina*, la cual se encuentra presente en la orina de machos y está implicada en la respuesta de atracción sexual de las hembras de ratón (Roberts et al. 2010). Las feromonas bajo peso molecular pueden estimular tanto por el órgano vomeronasal (VNO) como el VNO y el epitelio olfativo principal (MOE) (Chamero et al. 2007), pero es necesario realizar futuros estudios para caracterizarlas mejor y ver la relación que tienen con la manifestación del comportamiento de agresión maternal.

Por otro lado, es importante destacar que la *darcina*, aparte de estar relacionada con comportamientos de atracción en hembras sin crías, también se ha relacionado directamente con los comportamientos agresivos de hembras lactantes hacia machos intrusos (Martín-Sánchez et al. 2015b, a). Además, es importante destacar que el comportamiento de agresión maternal hacia machos intrusos no se manifiesta en hembras que no tienen crías a pesar de haber sido expuestas a ellas y mostrar el resto de comportamientos maternales (Martín-Sánchez et al. 2015b). Uno de los objetivos de esta tesis es profundizar en los cambios que pueden estar ocurriendo a nivel de sistema nervioso central (SNC) durante el embarazo y la lactancia que producen estos cambios en la respuesta comportamental de las hembras hacia las feromonas de machos, y pasar así de un comportamiento de atracción a la manifestación de conductas agresivas.

Los comportamientos sociales están controlados por el denominado cerebro sociosexual (SBN) (Newman 1999). El SBN es una red neural que se encuentra presente en gran número de especies y está altamente conservada. Esta red está compuesta por varios nodos que cumplen tres características principales: 1) se sabe que están implicados en la regulación de diversas formas de comportamiento social; 2) están interconectados recíprocamente (para permitir actuar como una red); y 3) muestran abundantes neuronas que expresan receptores de esteroides gonadales, lo que permite una expresión dimórfica de los comportamientos sociales. Además del SBN como

el circuito neuronal central del cerebro social, otros núcleos cerebrales también pueden participar en el control de comportamientos sociales concretos.

En el caso de la maternidad, los cambios adaptativos que se producen en el cerebro durante el embarazo y la lactancia y que permiten a la hembra lidiar con la nueva situación manifestando los comportamientos maternales descritos previamente, tienen lugar en los núcleos que conforman el SBN. En estos núcleos seria donde las señales endocrinas actuarían para inducir el cambio de la hembra a un cerebro maternal (Numan and Woodside 2010).

Por otro lado, como se ha comentado previamente, los ratones son animales macrosmáticos, por lo que el acoplamiento entre los sistemas de detección de señales quimiosensoriales y el SBN es de gran importancia. Por lo tanto, el VNO y el MOE permiten la entrada de información sensoriales clave a la red de estructuras neurales que controlan los comportamientos sociosexuales en roedores (Newman 1999; Insel and Numan 2003; Gutiérrez-Castellanos et al. 2010). Esta información olfativa y vomeronasal converge en algunos núcleos amigdalinos (Gutiérrez-Castellanos et al. 2010; Cádiz-Moretti et al. 2013).

El complejo amigdalino es una estructura heterogénea donde los estímulos olfativos y vomeronasales convergen en el sistema cortical/medial, principalmente en la amígdala medial (Me) (Newman 1999; Goodson 2005; Gutiérrez-Castellanos et al. 2010). La Me es un núcleo perteneciente al SBN y juega un papel clave en el control de las vías que implicadas en la manifestación de comportamientos sociosexuales en roedores (Newman 1999; Swann et al. 2009; Bergan et al. 2014). Este núcleo se subdivide en tres regiones: anterior (MeA), postero-ventral (MePV) y postero-dorsal (MePD) (Gomez and Newman 1992; Canteras et al. 1995). Estas subdivisiones se relacionan con distintos comportamientos, por ejemplo, MePD (y también la parte postero-medial de la división medial del núcleo del lecho de la estría terminal (BSTMPM)) parecen estar implicados principalmente en comportamientos reproductivos, mientras que MePV se activa cuando se manifiestan comportamientos defensivos. Ambos subnúcleos desencadenan estas respuestas conductuales a través de conexiones directas con distintos centros hipotalámicos.

El substrato neuroanatómico que controla los comportamientos de agresión maternal también comprende parte de los núcleos que conforman el SBN. Uno de estos núcleos es el VMH, que recibe proyecciones directas e indirectas de Me y BSTMPM y se ha visto que está implicado en comportamientos agresivos, especialmente la zona ventrolateral (VMHvl) (Hashikawa et al. 2017a). Las lesiones en VMHvl en hembras lactantes se ha visto que producen una reducción en

los niveles de agresión maternal pero no en el resto de cuidados maternales (Hansen 1989). VMH a su vez conecta con el núcleo gris periaqueductal (PAG), siendo el punto clave para conectar el SBN con output moto en la médula espinal (Hashikawa et al. 2017b). Además, otros núcleos hipotalámicos como la región ventral del núcleo premamilar (PMV) se ha visto que podrían ser importantes en el control del comportamiento de agresión maternal en ratones, ya que en ratas lesiones en este núcleo eliminan el comportamiento (Motta et al. 2013) y además recibe proyecciones de Me (Canteras et al. 1995; Pardo-Bellver et al. 2012).

Por lo que respecta a Me, se ha comprado mediante técnicas quimiogenéticas que MePD está implicada directamente en el comportamiento de agresión maternal (Unger et al. 2015). Además, MePD puede estar regulando la agresión a través de sus conexiones con la porción posterior del núcleo del lecho de la estría terminal (BST), ya que la estimulación de las proyecciones MePD-BST resultan en un incremento de la agresión (Padilla et al. 2016; Yamamoto et al. 2018). Sin embargo, es importante destacar que estos estos estudios únicamente se han realizado en machos y sería necesario llevarlos a cabo también en hembras lactantes para comprobar si realmente esta vía está implicada en el comportamiento de agresión maternal.

Es importante discernir si las vías de la agresión maternal y de la atracción están reguladas por los mismos circuitos o su activación depende del sexo del individuo al que se enfrenta y de su reconocimientos social como sucede en machos (Kim et al. 2015).

Estudios sobre las señales cerebrales que producen ratones anestesiados frente a diferentes estímulos muestran que las neuronas en el bulbo olfativo accesorio responden de forma similar a estímulos de machos o de hembras. Sin embargo, los registros en Me muestran una mayor activación por las señales del sexo opuesto, por lo que las neuronas en Me pueden ser excitadas o inhibidas en función de un estímulo social concreto (Li et al. 2017).

En el caso de VMHvl, este núcleo en hembras se puede dividir en dos regiones anatómicas: medial y lateral. Estas subdivisiones se activan de forma diferencial en los comportamientos de agresión y apareamiento y además muestran un patrón de expresión génica y de proyecciones axonales diferente (Hashikawa et al. 2017a). Por otro lado, otro estudio ha demostrado que las proyecciones de MePV a VMHdm y de este último a PAG son críticas para el comportamiento de lordosis mediado por feromonas (Ishii et al. 2017). Todos estos estudios sugieren que los circuitos relacionados con el apareamiento y el ataque en hembras son al menos parcialmente diferentes.

Todos estos estudios están remarcando que Me está jugando un papel crucial en el cambio entre respuestas de atracción hacia machos en hembras que no están lactando y de agresividad cuando las hembras están lactando. Hipotetizamos en base a estos estudios previos que los cambios fisiológicos u neurales que suceden durante el embarazo y la lactancia en Me están íntimamente relacionados o tienen como resultado el cambio de un comportamiento de atracción hacia las feromonas de macho a comportamientos agresivos en respuesta las mismas señales químicas.

OBJETIVOS DEL ESTUDIO Y METODOLOGÍA EMPLEADA

La presente tesis doctoral tiene como objetivo proporcionar una visión más profunda sobre la función y la regulación de Me durante la lactancia y su papel en la manifestación de los comportamientos maternales. Primero, pretendemos averiguar si Me está desempeñando un papel clave en el control de la agresión maternal. Seguidamente, nos planteamos qué cambios de expresión génica pueden estar sucediendo durante la lactancia que estén involucrados en la aparición de comportamientos agresivos hacia machos intrusos. Dado que uno de los principales cambios en la expresión génica revelados por nuestro estudio fue un aumento en la expresión de PRL, caracterizamos los circuitos PRLérgicos en el cerebro de hembras en diferentes estadios fisiológicos y los posibles cambios en estos circuitos que se pueden estar dando en las madres. Los objetivos específicos de este trabajo fueron y la metodología que se llevó a cabo para cumplirlos se detallan a continuación:

1. Caracterización del papel de Me en la expresión de la agresividad maternal. Para cumplir este objetivo inactivó este núcleo mediante una técnica quimiogenética denominada "Designer Receptors Exclusively Activated by Designer Drugs" (DREADD), en nuestro caso inhibitorios. Estos receptores son activados exclusivamente por clozapina-N-oxide (CNO) y permiten la activación o inhibición del núcleo a través de este fármaco.

2. Estudio de los cambios de expresión génica que suceden en Me y que subyacen el cambio de la respuesta comportamental de atracción hacia un macho intruso en hembras no lactantes a comportamientos agresivos en hembras lactantes. La aproximación metodológica que se llevó a cabo para conseguir este objetivo fueron técnicas de secuenciación masiva (RNA-seq y la posterior validación de

los genes de interés mediante qPCR. Posteriormente, para comprobar si la sobreexpresión del gen *Prl* se traducían en un incremento en los niveles de PRL en forma de proteína en Me, se realizaron diversas técnicas de cuantificación de proteínas (directas e indirectas): ELISA, Western blot e inmunohistoquímica.

3. Caracterización de los circuitos PRLérgicos en el cerebro de hembras y estudio de los posibles cambios que se pueden estar dando en madres. Este objetivo se llevó a cabo mediante inmunohistoquímicas frente a PRL en hembras expuestas y hembras no expuestas a crías y hembras lactantes.

RESULTADOS Y DISCUSIÓN

La presente tesis doctoral constituye la primera demostración de la implicación de Me en la manifestación del comportamiento de agresión maternal usando técnicas quimiogenéticas. A su vez, este estudio proporciona un análisis exhaustivo de los cambios de expresión génica que suceden en este núcleo a causa del embarazo y la lactancia. Nuestros resultados muestran que la PRL fue el gen relacionado con la maternidad que mostraba los niveles más altos de sobreexpresión en comparación con hembras no lactantes. Durante la maternidad, la PRL puede estar dirigiendo los cambios a nivel de sistema nervioso central (SNC) para adaptar la fisiología y el comportamiento de las hembras a las demandas de la maternidad. Por esta razón, también se realizó el estudio de los posibles cambios en la expresión de PRL entre hembras lactantes y hembras vírgenes expuestas y no expuestas a crías. Estos experimentos nos han permitido investigar el posible papel de la PRL en los cambios neurales relacionados con el comienzo y la manifestación de los comportamientos maternales debidos al embarazo y la exposición a estímulos derivados de las crías.

En el Capítulo I se describe como la exposición en días sucesivos a diferentes machos intrusos incrementa los niveles de agresión en hembras lactantes, y confirma que las comadres o hembras vírgenes expuestas a crías no muestran comportamientos de agresión a pesar de haber estado expuestas a las crías de forma prolongada (Martín-Sánchez et al. 2015b, a). Seguidamente, confirmamos y ampliamos los estudios previos que señalan que Me juega un papel clave en la manifestación de la agresión maternal. Nuestros estudios muestran que la inactivación de Me mediante DREADD se mitiga selectivamente el incremento de la agresividad mostrado por hembras lactantes tras una exposición repetida a un macho intruso.

Me es estructura que muestra una amplia conexión recíproca con el AOB y el MOB (Scalia and Winans 1975; Pardo-Bellver et al. 2012; Cádiz-Moretti et al. 2013, 2016), considerándose así parte de la amígdala quimiosensorial. La inactivación quimiogenética de este núcleo da como resultado una disminución de los niveles de agresión maternal hacia machos intrusos, implicando a este núcleo directamente en la manifestación del comportamiento en hembras lactantes. El papel que juega Me puede estar relacionado con la incapacidad de las hembras lactantes para procesar correctamente las señales quimiosensoriales de los intrusos. Esto se relaciona con estudios previos que indican que lesiones en Me en hembras de ratón da como resultado déficits en el reconocimiento de machos y en el comportamiento de apareamiento (DiBenedictis et al. 2012) y se obtuvieron resultados similares cuando se inactive Me mediante DREADD. Los resultados obtenidos en este capítulo junto con las investigaciones previas sugieren que Me puede estar clasificando las señales específicas de machos, como la *darcina*, como atractivas (en el caso de hembras no lactantes) o como aversivas (en el caso de hembras lactantes). Esta clasificación podría estar influenciada por cambios hormonales concretos inducidos por el embarazo y la lactancia debido a que las comadres nunca atacan a los machos intrusos.

En resumen, Me es un núcleo clave en el procesamiento de estímulos externos de intrusos y probablemente también de las crías (olfativos, auditivos y de succión durante el amamantamiento), que influencian la agresión maternal hacia un intruso. La información proveniente del intruso seria enviada desde los sistemas olfativos hasta las subdivisiones de Me y de ahí a los núcleos hipotalámicos que controlan por un lado la agresión y por otro las conductas sexuales, como VMH y PMV (Van Berg et al. 1983; Fahrbach et al. 1989; Numan and Insel 2003b; Pardo-Bellver et al. 2012) entre otras estructuras. Además, Me presenta una proyección a los diferentes subnúcleos de BST (Pardo-Bellver et al. 2012) que podría estar jugando un papel en el control de los comportamientos sociosexuales (Numan and Insel 2003b; Chen and Hong 2018) y también en el de agresión (Shaikh et al. 1986; Gammie and Nelson 2001; Padilla et al. 2016). Por otro lado, Me está conectado a su vez con la región preóptica medial (MPO/A) que está implicada en la modulación del comportamiento materna l(Chiba and Murata 1985; Brown et al. 2017). Por estos motivos hipotetizamos que la adaptación de cerebro maternal probablemente está induciendo cambios en la señalización a través de Me hacia los núcleos relacionados con respuestas agresivas. Además estos cambios en Me seguramente estén mediados por hormonas, incluida la PRL y los diferentes nonapéptidos (Haller 2018).

De hecho, hemos observado grandes cambios en el perfil transcriptómico de Me en el Capítulo II de esta tesis, comparando los patrones de expresión en hembras lactantes y hembras vírgenes expuestas a crías durante los primeros días postparto. El estudio de RNA-seq mostró un gran número de genes con cambios de expresión génica entre los grupos de hembras y algunos de ellos íntimamente relacionados con el comportamiento maternal. Entre estos genes relacionados con la maternidad encontramos *Prl, Gh, Ghrhr, Pit-1*, *Oxt* y *Gal* (para las abreviaturas ir a la lista de genes). *Prl* fue el gen que mostró las diferencias más significativas entre los grupos de hembras y estas diferencias fueron comprobadas mediante qPCR. La expresión de *Prl* en el CNS ya había sido descrita previamente (Emanuele et al. 1992), especialmente en el núcleo paraventricular hipotalámico (Pa) y en el núcleo supraóptico (SO), que también son los núcleos con mayor síntesis de oxitocina (OXT) y vasopresina (AVP) (Clapp et al. 1994; Torner et al. 1999, 2004). Es importante remarcar que estudios previos de RNA-seq han mostrados cambios significativos en la expresión de *Prl* en el hipotálamo, hipocampo, neocórtex y cerebelo de hembras lactantes en comparación con hembras vírgenes (Ray et al. 2016).

A parte de genes relacionados con la maternidad se encontraron otros implicados en la señalización de PRL como *Pitx1* and *Pit*-1 (Pfaffle et al. 1992; Voss and Rosenfeld 1992; Nowakowski and Maurer 1994) and *Cis* (Bole-Feysot et al. 1998; Pezet et al. 1999; Krebs and Hilton 2000; Nicolas et al. 2013).

Los resultados obtenidos junto con el conocido papel que desempeña la PRL en la reproducción de mamíferos, decidimos centrarnos en el estudio de la expresión de esta proteína en Me y los posibles cambios que podía estar sufriendo a consecuencia de la maternidad. En este sentido, existe una controversia sobre si toda la PRL que se encuentra en CNS llega a través de su unión a los receptores de PRL en el plexo coroideo, y el posterior transporte mediante el líquido cefalorraquídeo (Walsh et al. 1987; Brown et al. 2016) o por el contrario la PRL se está sintetizando *de novo* en algunos núcleos del SNC (Schachter et al. 1984; Emanuele et al. 1987, 1992; DeVito et al. 1992; Clapp et al. 1994). Los resultados de Capitulo III apoyan la última hipotaxis debido a que se detecta PRL en Me mediante técnicas proteómicas, Western blot, ELISA e inmunohistoquímica. Estos resultados no excluyen el hecho de que PRL de origen pituitario también pueda ser incorporada al SNC por trasportadores específicos en el plexo coroideo.

Una posibilidad es que la PRL sintetizada en el SNC juegue un papel en la regulación de los comportamientos maternales encabezando la PRL periférica. Estudios precios en ratas han

demostrado que una vez se establecen los comportamientos maternales, estos se mantienen de forma independiente a la regulación de la pituitaria (Rosenblatt 1967; Erskine et al. 1980; Svare et al. 1982; Numan and Insel 2003a). En hembras lactantes, el comienzo de la agresión maternal es dependiente de la estimulación de los pezones durante el amamantamiento de las crías (Garland and Svare 1988), la cual mantiene también altos los niveles de PRL hipofisaria. Sin embargo, la agresión se presenta igual en hembras lactantes hipofisectomizadas o ratas hembra vírgenes sensibilizadas mediante hormonas (Erskine et al. 1980; Svare et al. 1982). Estos resultados implican que la reducción en los niveles de agresión al quitar las crías no se debe a la rápida disminución de PRL hipofisaria (Amenomori et al. 1970) que también se observa en hembras hipofisectomizadas (Erskine et al. 1980). De hecho, que la PRL periférica no esté jugando un papel clase en el mantenimiento de la agresión maternal apoyaría la existencia de dos funciones para la PRL: una neuromoduladora y otra hormonal.

Es posible que la PRL neural esté actuando por vías diferentes en el SNC a la PRL hipofisiaria. Los tratamientos con bromocriptina, los cuales suprimen la liberación de PRL hipofisaria, mostrando que la fosforilación de STAT5 (pSTAT5) en el cerebro es completamente dependiente de esta PRL periférica y/o de los PL. El tratamiento con bromocriptina bloquea toda la expresión basal de pSTAT5 en hembras vírgenes (Brown et al. 2010) y en hembras lactantes (Brown et al. 2011). Sin embargo, en el caso de hembras preñadas de ratón el tratamiento con bromocriptina no elimina el marcaje de pSTAT5 (Salais-López et al. 2017), sugiriendo que la mayor parte, sino todo el marcaje frente a pSTAT5 observado en esas hembras tratadas con bromocriptina es debido a un origen lactogénico no hipofisario, probablemente por PL (Soares 2004). Estos resultados están sugiriendo que sin PRL periférica o PL la vía JAK/STAT (a través de la cual señaliza la PRL) se elimina. Sin embargo, una hipofisectomía no elimina la presencia de PRL en el cerebro de ratas hembra y machos (DeVito 1988; Emanuele et al. 1992) o los comportamientos maternales como el de agresión (Svare et al. 1982). Debido a estas razones, la PRL sintetizada de novo en el cerebro podría estar actuando a través de otras cascadas de activación diferentes a JAK/STAT como la ERK/MAPK (Freeman et al. 2000).

En conclusión, las vías neuronales que regulan el cambio hacia un cerebro maternal incluirían a Me, la cual, tal y como se describe en esta tesis, estaría sufriendo grandes cambios de expresión génica durante la maternidad, incluyendo una elevada sobrexpresión de *Prl*. Además, la región preóptica medial del hipotálamo (MPO/A) al estar conectado con Me directamente e indirectamente a través de las conexiones con BST (Chiba and Murata 1985; Cádiz-Moretti et al. 2016) también estaría sufriendo cambios durante la maternidad, que implicarían un incremento

de somas PRLérgicos como se observa en el Capítulo IV. Por este motivo, la PRL neural podría estar actuando a través de diferentes núcleos del SBN durante el embarazo y la lactancia, permitiendo así el desarrollo de los comportamientos maternale.

CONCLUSIONES

1. La exposición repetida a machos intrusos incrementa la agresión maternal durante el primer tercio de la lactancia. Este comportamiento no se puede inducir en hembras vírgenes expuestas a crías a pesar de que el contacto con ellas sea continuado (comadres) y se les exponga de forma repetida a machos intrusos.

2. Los cambios hormonales que suceden durante el embarazo y la lactancia son necesarios para que se produzca el comportamiento de agresión maternal. Estos cambios hormonales probablemente estén adaptando y preparando el cerebro de las hembras para la maternidad.

3. La amígdala medial (Me) juega un papel esencial en la manifestación del comportamiento de agresión maternal en hembras lactantes. La inhibición quimiogenética de este núcleo bloquea el incremento esperado en los niveles de agresión después de exponer a las hembras por segundo día consecutivo a machos intrusos.

4. El embarazo y la lactancia inducen cambios de expresión génica en Me, así como patrones de expresión que son diferentes entre hembras lactantes y hembras vírgenes expuestas a crías. Específicamente, encontramos 197 genes sobre expresados y 99 genes que reducen su expresión en madres respecto a comadres.

5. Entre los genes que se encuentran sobre expresados en el grupo de hembras lactantes algunos están participan en la regulación del comportamiento maternal. En este grupo de genes encontramos la *Prl*, *Oxt* and *Gal*. También se observan dentro del conjunto de genes sobre expresados algunos relacionados con la *Prl*, como *Gh*, *Ghrhr*, *Pit-1* (también conocido por *Pou1f1*) y *Cis* (llamado también *Cish*).

6. La presencia de ARNm de *Prl* en Me sugiere que esta proteína se está sintetizando en este núcleo. Debido a que la presencia de somas PRLérgicos es muy escasa en

este núcleo, el ARNm de *Prl* puede estar siendo transportado y expresado en los terminales axónicos.

7. El incremento observado en ARNm de *Prl* en madres también se aprecia en los niveles de proteína, al menos cuando estas mediciones se realizan mediante un ELISA. El incremento de PRL en Me obtenido en hembras lactantes respecto a las comadres sugiere que los niveles de PRL están sujetos a fluctuaciones causadas por el embarazo y la lactancia.

8. Los niveles de PRL presente en el suero de hembras lactantes también se incrementan significativamente, tal y como se esperaba, cuando se comparan con los de hembras vírgenes expuestas a crías. Sin embargo, los niveles de PRL en suero no correlacionan con los niveles obtenidos en Me.

9. La inervación de PRL presenta una amplia distribución en el cerebro de hembra de ratón, especialmente en áreas relacionadas con la regulación endocrina y el control de los comportamientos sociales y maternales. Este patrón de distribución neural de PRL-ir es similar en hembras vírgenes, hembras vírgenes expuestas a crías y en hembras lactantes.

10. BST, AC/ADP, Pa, SO, el hipotálamo periventricular y Arc presentan la población más densa de somas PRLérgicos. Todos estos núcleos, a excepción de Arc, también presentan somas OXTérgicos y AVPérgicos los cuales colocalizan parcialmente con PRL.

11. La densidad de la PRL-ir varía en función el estado fisiológico de las hembras: vírgenes, comadres y lactantes. Existen diferencias significativas en el número de células PRL-ir en SCh, SO and MPO/A, siendo mayor en el caso de las madres.

ANNEXES

ANNEX I

The following code details the pipeline in "R" used to obtain the count matrix from the sequence reads with the tools *Bowtie2*, *Rsamtools*, *GenomicFeatures* and *GenomicAlignments*.

*** Short read alignment using bowtie2**

```
bowtie2 -x Mus_musculus/Ensembl/GRCm38/Sequence/Bowtie2Index/genome -U C1_S2.fastq.gz -
S C1_S2.sam

bowtie2 -x Mus_musculus/Ensembl/GRCm38/Sequence/Bowtie2Index/genome -U C6_S3.fastq.gz -
S C6_S3.sam

bowtie2 -x Mus_musculus/Ensembl/GRCm38/Sequence/Bowtie2Index/genome -U C8_S8.fastq.gz -
S C8_S8.sam

bowtie2 -x Mus_musculus/Ensembl/GRCm38/Sequence/Bowtie2Index/genome -U C9_S5.fastq.gz -
S C9_S5.sam

bowtie2 -x Mus_musculus/Ensembl/GRCm38/Sequence/Bowtie2Index/genome -U M1_S7.fastq.gz -
S M1_S7.sam

bowtie2 -x Mus_musculus/Ensembl/GRCm38/Sequence/Bowtie2Index/genome -U M6_S4.fastq.gz -
S M6_S4.sam

bowtie2 -x Mus_musculus/Ensembl/GRCm38/Sequence/Bowtie2Index/genome -U M8_S6.fastq.gz -
S M8_S6.sam

bowtie2 -x Mus_musculus/Ensembl/GRCm38/Sequence/Bowtie2Index/genome -U M9_S1.fastq.gz -
S M9_S1.sam
```

*** From sam to bam using samtools and sorting the reads**

```
samtools view -bS C1_S2.sam | samtools sort - C1_S2

samtools view -bS C6_S3.sam | samtools sort - C6_S3

samtools view -bS C8_S8.sam | samtools sort - C8_S8

samtools view -bS C9_S5.sam | samtools sort - C9_S5

samtools view -bS M1_S7.sam | samtools sort - M1_S7

samtools view -bS M6_S4.sam | samtools sort - M6_S4

samtools view -bS M8_S6.sam | samtools sort - M8_S6

samtools view -bS M9_S1.sam | samtools sort - M9_S1
```

*** Using Rsamtools for counting the reads aligned.**

```
** Creating files with the names of the bam files.
```

Some samples are single and other samples are pair-ended.

We create the file BamFiles.txt with the following content.

```
C1_S2.bam
C6_S3.bam
C8_S8.bam
C9_S5.bam
M1_S7.bam
M6_S4.bam
M8_S6.bam
M9_S1.bam
** Executing R code
library(Rsamtools)
library(GenomicFeatures)
library(GenomicAlignments)
gtfFile = "Mus_musculus/Ensembl/GRCm38/Annotation/Genes/genes.gtf"
txdb = makeTxDbFromGFF(gtfFile, format="gtf")
genes = exonsBy(txdb, by="gene")
dirActualData =  paste(getwd(),"/",sep="")
sampleTableSingle = read.table("BamFiles.txt")
fls = paste(dirActualData,sampleTableSingle[,1],sep="")
bamLst = BamFileList(fls, index=character(),yieldSize=100000,obeyQname=TRUE)
EL16 = summarizeOverlaps(features = genes,read=bamLst,
      mode="Union",
      singleEnd=TRUE,
      ignore.strand=TRUE,
      fragments=FALSE)
metadatos = read.csv("EL16coldata.csv",header=TRUE,sep =";")
metadatos[,"treatment"] = factor(metadatos[,"treatment"],levels=1:2,
labels=c("M","L"))
metadatos[,"strain"] = factor(metadatos[,"strain"],levels=1:4,
```

```
              labels=c("daf-2(e1370);daf-16(mu86);Punc-119::gfp","daf-2(e1370);Punc-
119::gfp",
                    "pmec-4::gfp","Punc-119::gfp"))


colData(EL16) = DataFrame(metadatos)

colnames(EL16) = colData(EL16)[,"run"]

save(EL16,file="EL16.rda")
```

Tenemos un objeto SummarizedExperiment::RangedSummarizedExperiment

ANNEX II

Table 1: Differentially expressed genes between dams and godmothers in the Me. The logFC (log base 2 fold-change) is the measure for differential gene expression between dams in respect of godmothers; positive values (A) indicate that gene is over-expressed in dams in comparation with godmothers and negative values (B) indicate an upregulation in godmothers and the last table show the genes without significant differences between groups (C)., FDR adjusted p<0,05, Raw p-values (rawp) obtained were transformed to adjusted p-values (adjp), FC: fold-change. For abbreviations see list.

A. GENES UPREGULATED IN DAMS COMPARED TO GODMOTHERS

Gene	ENSEMBL	logFC	FC	rawp	adjp
Fc receptor-like 5	ENSMUSG00000048031	5.87	58.49	2.52E-09	8.73E-07
chemokine (C-X-C motif) ligand 9	ENSMUSG00000029417	4.9	29.86	7.70E-05	8.16E-03
prolactin	ENSMUSG00000021342	4.8	27.86	1.30E-192	2.66E-188
growth hormone	ENSMUSG00000020713	4.78	27.47	1.13E-191	1.15E-187
POU domain, class 1, transcription factor 1	ENSMUSG00000004842	4.56	23.59	1.29E-37	3.77E-34
protease, serine 22	ENSMUSG00000045027	4.3	19.70	4.77E-45	1.95E-41
methionine adenosyltransferase I, alpha	ENSMUSG00000037798	3.92	15.14	4.93E-06	7.58E-04
sine oculis-related homeobox 6	ENSMUSG00000021099	3.85	14.42	2.12E-32	4.81E-29
follicle stimulating hormone beta	ENSMUSG00000027120	3.84	14.32	3.78E-13	2.21E-10
RIKEN cDNA D830030K20 gene	ENSMUSG00000096039	3.6	12.13	5.87E-25	1.20E-21
T-box 19	ENSMUSG00000026572	3.6	12.13	5.61E-05	6.24E-03
matrix metallopeptidase 8	ENSMUSG00000005800	3.59	12.04	5.25E-04	3.95E-02
epithelial splicing regulatory protein 1	ENSMUSG00000040728	3.51	11.39	1.40E-20	2.05E-17
glycoprotein hormones, alpha subunit	ENSMUSG00000028298	3.48	11.16	7.90E-54	4.04E-50
RIKEN cDNA A930006I01 gene	ENSMUSG00000087278	3.18	9.06	6.35E-04	4.48E-02
gonadotropin releasing hormone receptor	ENSMUSG00000029255	3.09	8.51	3.17E-10	1.30E-07
transient receptor potential cation channel, subfamily V, member 1	ENSMUSG00000005952	3.06	8.34	1.33E-15	1.29E-12
histocompatibility 2, class II antigen E alpha, pseudogene	ENSMUSG00000036322	3.05	8.28	2.74E-07	6.23E-05
POU domain, class 4, transcription factor 1	ENSMUSG00000048349	3.04	8.22	2.71E-09	9.24E-07
paired-like homeodomain transcription factor 1	ENSMUSG00000021506	3.02	8.11	2.54E-17	2.73E-14
growth hormone releasing hormone receptor	ENSMUSG00000004654	3	8.00	3.78E-13	2.21E-10
predicted gene 12290	ENSMUSG00000087622	2.98	7.89	1.11E-13	7.07E-11
G protein-coupled receptor 174	ENSMUSG00000073008	2.92	7.57	4.89E-11	2.27E-08
vomeronasal 2, receptor, pseudogene 159	ENSMUSG00000057021	2.82	7.06	2.64E-05	3.17E-03
predicted gene 10408	ENSMUSG00000072739	2.69	6.45	8.49E-08	2.07E-05
RIKEN cDNA 4932435O22 gene	ENSMUSG00000062391	2.55	5.86	1.70E-04	1.61E-02
RAB25, member RAS oncogene family	ENSMUSG00000008601	2.5	5.66	5.17E-08	1.35E-05
nuclear RNA export factor 3	ENSMUSG00000057000	2.49	5.62	5.31E-12	2.65E-09
predicted gene 2244	ENSMUSG00000092036	2.45	5.46	4.35E-08	1.17E-05
claudin 8	ENSMUSG00000050520	2.44	5.43	4.36E-06	6.87E-04
myosin XV	ENSMUSG00000042678	2.43	5.39	1.85E-18	2.10E-15
NIPA-like domain containing 1	ENSMUSG00000067219	2.42	5.35	4.37E-06	6.87E-04
transmembrane protein 184a	ENSMUSG00000036687	2.37	5.17	9.20E-09	2.85E-06
uncharacterized LOC102632821	ENSMUSG00000086495	2.09	4.26	3.51E-06	5.83E-04
epithelial cell adhesion molecule	ENSMUSG00000045394	2.04	4.11	4.81E-21	7.57E-18
maelstrom spermatogenic transposon silencer	ENSMUSG00000040629	1.99	3.97	4.19E-06	6.71E-04
synaptonemal complex protein 1	ENSMUSG00000027855	1.97	3.92	1.15E-06	2.26E-04
CWC22 spliceosome-associated protein	ENSMUSG00000027014	1.94	3.84	6.31E-40	2.15E-36
basic helix-loop-helix family, member a15	ENSMUSG00000052271	1.93	3.81	3.81E-10	1.53E-07

paired-like homeodomain transcription factor 2	ENSMUSG00000028023	1.87	3.66	1.71E-14	1.59E-11
predicted gene 3278	ENSMUSG00000091185	1.84	3.58	1.74E-05	2.22E-03
ets homologous factor	ENSMUSG00000012350	1.8	3.48	2.54E-06	4.32E-04
X-linked lymphocyte-regulated 4C	ENSMUSG00000031362	1.78	3.43	1.72E-05	2.21E-03
FGGY carbohydrate kinase domain containing	ENSMUSG00000028573	1.73	3.32	6.12E-23	1.14E-19
HEPACAM family member 2	ENSMUSG00000044156	1.73	3.32	6.06E-12	2.95E-09
S100 calcium binding protein A9 (calgranulin B)	ENSMUSG00000056071	1.71	3.27	1.15E-06	2.26E-04
protease, serine 56	ENSMUSG00000036480	1.67	3.18	1.52E-06	2.78E-04
X-linked lymphocyte-regulated 4B	ENSMUSG00000067768	1.67	3.18	7.16E-06	1.02E-03
sialic acid binding Ig-like lectin E	ENSMUSG00000030474	1.63	3.10	9.04E-07	1.87E-04
guanine nucleotide binding protein (G protein), beta 3	ENSMUSG00000023439	1.58	2.99	4.20E-06	6.71E-04
solute carrier family 47, member 2	ENSMUSG00000069855	1.58	2.99	7.39E-05	7.92E-03
NLR family, pyrin domain containing 4F	ENSMUSG00000032999	1.55	2.93	2.36E-04	2.11E-02
chemokine (C-C motif) receptor 1	ENSMUSG00000025804	1.54	2.91	1.49E-07	3.55E-05
predicted gene 5741	ENSMUSG00000095845	1.52	2.87	2.33E-05	2.85E-03
cholinergic receptor, nicotinic, beta polypeptide 3	ENSMUSG00000031492	1.49	2.81	5.26E-10	1.99E-07
expressed sequence AI606473	ENSMUSG00000093738	1.47	2.77	7.89E-14	5.20E-11
cholinergic receptor, nicotinic, alpha polypeptide 6	ENSMUSG00000031491	1.4	2.64	4.50E-06	7.03E-04
acyl-Coenzyme A oxidase 2, branched chain	ENSMUSG00000021751	1.4	2.64	4.58E-04	3.51E-02
RIKEN cDNA 2610028E06 gene	ENSMUSG00000085562	1.39	2.62	1.39E-05	1.84E-03
neurogenic differentiation 4	ENSMUSG00000048015	1.38	2.60	5.47E-08	1.42E-05
G protein-coupled receptor 15	ENSMUSG00000047293	1.38	2.60	6.28E-07	1.37E-04
RIKEN cDNA G530011O06 gene	ENSMUSG00000072844	1.37	2.58	3.13E-16	3.20E-13
RUN and FYVE domain containing 4	ENSMUSG00000061815	1.36	2.57	5.24E-06	7.93E-04
S100 calcium binding protein A8 (calgranulin A)	ENSMUSG00000056054	1.36	2.57	4.58E-04	3.51E-02
uncharacterized LOC102635948	ENSMUSG00000086742	1.35	2.55	5.66E-04	4.15E-02
N-acetyltransferase 8 (GCN5-related) family member 2	ENSMUSG00000033634	1.33	2.51	2.95E-10	1.23E-07
protein tyrosine phosphatase, non-receptor type 7	ENSMUSG00000031506	1.33	2.51	8.01E-05	8.45E-03
ethanolamine phosphate phospholyase	ENSMUSG00000019232	1.32	2.50	9.15E-20	1.25E-16
gonadotropin releasing hormone 1	ENSMUSG00000015812	1.29	2.45	4.13E-04	3.24E-02
RIKEN cDNA 1700001K19 gene	ENSMUSG00000056508	1.25	2.38	1.64E-05	2.13E-03
solute carrier family 4, sodium bicarbonate cotransporter, member 5	ENSMUSG00000068323	1.23	2.35	5.47E-11	2.49E-08
carbonic anhydrase 9	ENSMUSG00000028463	1.23	2.35	3.98E-06	6.52E-04
mab-21-like 2 (C. elegans)	ENSMUSG00000057777	1.22	2.33	1.65E-04	1.58E-02
pro-opiomelanocortin-alpha	ENSMUSG00000020660	1.2	2.30	2.73E-14	2.43E-11
LIM homeobox protein 8	ENSMUSG00000096225	1.2	2.30	4.26E-14	3.11E-11
neurotrophic tyrosine kinase, receptor, type 1	ENSMUSG00000028072	1.2	2.30	3.73E-12	1.91E-09
gastrulation brain homeobox 2	ENSMUSG00000034486	1.19	2.28	1.66E-06	3.01E-04
membrane frizzled-related protein	ENSMUSG00000034739	1.18	2.27	2.93E-10	1.23E-07
beta-1,4-N-acetyl-galactosaminyl transferase 3	ENSMUSG00000041372	1.18	2.27	5.90E-05	6.52E-03
sine oculis-related homeobox 1	ENSMUSG00000051367	1.14	2.20	8.46E-07	1.78E-04
choline acetyltransferase	ENSMUSG00000021919	1.11	2.16	1.82E-13	1.13E-10
solute carrier family 18 (vesicular monoamine), member 3	ENSMUSG00000100241	1.11	2.16	9.86E-13	5.45E-10
LARGE xylosyl- and glucuronyltransferase 2	ENSMUSG00000040434	1.11	2.16	4.56E-05	5.27E-03
solute carrier family 5 (choline transporter), member 7	ENSMUSG00000023945	1.1	2.14	3.41E-14	2.79E-11
solute carrier family 17, member 9	ENSMUSG00000023393	1.1	2.14	2.11E-04	1.94E-02
N-acetyltransferase 8 (GCN5-related) family member 4	ENSMUSG00000068299	1.09	2.13	3.93E-13	2.23E-10
peptidyl arginine deiminase, type IV	ENSMUSG00000025330	1.09	2.13	1.85E-08	5.40E-06
glycerophosphodiester phosphodiesterase domain containing 3	ENSMUSG00000030703	1.09	2.13	3.69E-06	6.08E-04

CD4 antigen	ENSMUSG00000023274	1.08	2.11	3.96E-08	1.09E-05
tandem C2 domains, nuclear	ENSMUSG00000021187	1.07	2.10	3.05E-04	2.55E-02
transthyretin	ENSMUSG00000061808	1.06	2.08	3.60E-14	2.83E-11
interferon inducible GTPase 1	ENSMUSG00000054072	1.05	2.07	1.78E-07	4.14E-05
chemokine (C-C motif) receptor 6	ENSMUSG00000040899	1.01	2.01	2.73E-07	6.23E-05
complement component 1, s subcomponent 1	ENSMUSG00000038521	1.01	2.01	5.58E-05	6.23E-03
transmembrane protein 52	ENSMUSG00000023153	0.989	1.98	3.81E-04	3.06E-02
calcyphosphine 2	ENSMUSG00000035694	0.985	1.98	3.59E-04	2.90E-02
RIKEN cDNA A730020M07 gene	ENSMUSG00000044522	0.98	1.97	2.46E-04	2.16E-02
midline 1	ENSMUSG00000035299	0.961	1.95	7.01E-11	3.12E-08
nerve growth factor receptor (TNFR superfamily, member 16)	ENSMUSG00000000120	0.947	1.93	7.93E-11	3.45E-08
gastrulation brain homeobox 1	ENSMUSG00000067724	0.942	1.92	1.08E-08	3.30E-06
cDNA sequence BC006965	ENSMUSG00000041674	0.941	1.92	1.20E-06	2.33E-04
transmembrane protein 72	ENSMUSG00000048108	0.938	1.92	5.04E-06	7.69E-04
predicted gene, 19461	ENSMUSG00000101693	0.936	1.91	2.16E-04	1.98E-02
solute carrier family 26, member 7	ENSMUSG00000040569	0.934	1.91	7.01E-09	2.28E-06
histocompatibility 2, class II antigen E beta	ENSMUSG00000060586	0.933	1.91	7.59E-05	8.09E-03
solute carrier family 10 (sodium/bile acid cotransporter family), member 4	ENSMUSG00000029219	0.926	1.90	4.68E-10	1.84E-07
adrenergic receptor, alpha 2b	ENSMUSG00000058620	0.926	1.90	1.53E-04	1.47E-02
predicted gene 5868	ENSMUSG00000060204	0.92	1.89	3.33E-05	3.94E-03
SKI family transcriptional corepressor 1	ENSMUSG00000022245	0.917	1.89	4.55E-05	5.27E-03
SET and MYND domain containing 1	ENSMUSG00000055027	0.909	1.88	1.33E-08	3.99E-06
pro-melanin-concentrating hormone	ENSMUSG00000035383	0.898	1.86	8.56E-07	1.79E-04
potassium voltage-gated channel, Isk-related subfamily, gene 2	ENSMUSG00000039672	0.897	1.86	1.11E-05	1.54E-03
zinc finger protein 605	ENSMUSG00000023284	0.884	1.85	5.52E-10	2.05E-07
thyroid stimulating hormone, beta subunit	ENSMUSG00000027857	0.884	1.85	9.70E-07	1.96E-04
phenazine biosynthesis-like protein domain containing 2	ENSMUSG00000020072	0.884	1.85	1.28E-05	1.72E-03
zinc finger protein 459	ENSMUSG00000055560	0.88	1.84	2.04E-06	3.60E-04
F-box and WD-40 domain protein 10	ENSMUSG00000090173	0.875	1.83	4.06E-04	3.21E-02
glyceraldehyde-3-phosphate dehydrogenase, spermatogenic	ENSMUSG00000061099	0.86	1.82	1.43E-06	2.68E-04
membrane protein, palmitoylated 7 (MAGUK p55 subfamily member 7)	ENSMUSG00000057440	0.854	1.81	3.55E-07	7.89E-05
collagen, type VIII, alpha 1	ENSMUSG00000068196	0.853	1.81	6.42E-08	1.60E-05
MINDY lysine 48 deubiquitinase 4B, pseudogene	ENSMUSG00000101860	0.852	1.81	1.95E-05	2.42E-03
IQ motif containing G	ENSMUSG00000035578	0.835	1.78	5.71E-08	1.46E-05
sodium channel, type IV, beta	ENSMUSG00000046480	0.831	1.78	4.33E-09	1.43E-06
dynein light chain Tctex-type 1A	ENSMUSG00000092074	0.816	1.76	1.74E-07	4.09E-05
vitamin D (1,25-dihydroxyvitamin D3) receptor	ENSMUSG00000022479	0.805	1.75	1.06E-06	2.14E-04
oxytocin	ENSMUSG00000027301	0.801	1.74	1.63E-08	4.82E-06
relaxin/insulin-like family peptide receptor 2	ENSMUSG00000053368	0.801	1.74	5.74E-04	4.16E-02
RIKEN cDNA 4632428C04 gene	ENSMUSG00000097184	0.796	1.74	6.75E-04	4.71E-02
periostin, osteoblast specific factor	ENSMUSG00000027750	0.791	1.73	2.61E-06	4.41E-04
erythroid differentiation regulator 1	ENSMUSG00000096768	0.789	1.73	2.14E-08	6.17E-06
claudin 9	ENSMUSG00000066720	0.786	1.72	5.81E-04	4.17E-02
aquaporin 1	ENSMUSG00000004655	0.77	1.71	2.85E-04	2.43E-02
hedgehog interacting protein-like 1	ENSMUSG00000021260	0.769	1.70	4.96E-07	1.09E-04
folate receptor 1 (adult)	ENSMUSG00000001827	0.761	1.69	1.20E-05	1.63E-03
interleukin 31 receptor A	ENSMUSG00000050377	0.759	1.69	3.83E-04	3.06E-02
mitogen-activated protein kinase 13	ENSMUSG00000004864	0.745	1.68	5.62E-04	4.13E-02
dynein light chain Tctex-type 1B	ENSMUSG00000096255	0.743	1.67	7.71E-07	1.64E-04
collagen, type XI, alpha 1	ENSMUSG00000027966	0.736	1.67	1.49E-06	2.75E-04
phospholipase A2, group V	ENSMUSG00000041193	0.734	1.66	1.31E-04	1.30E-02

protein tyrosine phosphatase, receptor type, V	ENSMUSG00000097993	0.728	1.66	5.22E-05	5.86E-03
ADAMTS-like 3	ENSMUSG00000070469	0.716	1.64	6.91E-06	9.95E-04
V-set and immunoglobulin domain containing 2	ENSMUSG00000001943	0.712	1.64	1.99E-06	3.54E-04
functional intergenic repeating RNA element	ENSMUSG00000085396	0.705	1.63	1.23E-06	2.37E-04
guanylate binding protein 4	ENSMUSG00000079363	0.697	1.62	1.10E-04	1.12E-02
T cell specific GTPase 1	ENSMUSG00000078922	0.696	1.62	5.77E-04	4.16E-02
predicted gene 14204	ENSMUSG00000086496	0.692	1.62	9.62E-07	1.96E-04
nudix (nucleoside diphosphate linked moiety X)-type motif 19	ENSMUSG00000034875	0.689	1.61	1.32E-06	2.49E-04
NK2 homeobox 1	ENSMUSG00000001496	0.687	1.61	3.01E-05	3.60E-03
carbonic anhydrase 3	ENSMUSG00000027559	0.685	1.61	4.05E-04	3.21E-02
cilia and flagella associated protein 126	ENSMUSG00000026649	0.682	1.60	2.26E-05	2.79E-03
phytanoyl-CoA dioxygenase domain containing 1	ENSMUSG00000079484	0.681	1.60	2.23E-04	2.01E-02
zinc finger protein 951	ENSMUSG00000072774	0.678	1.60	2.98E-04	2.52E-02
transmembrane protein 181A	ENSMUSG00000038141	0.674	1.60	1.47E-06	2.73E-04
ring finger protein 207	ENSMUSG00000058498	0.672	1.59	9.13E-06	1.27E-03
synaptotagmin II	ENSMUSG00000026452	0.664	1.58	2.50E-06	4.32E-04
ribonuclease L (2', 5'-oligoisoadenylate synthetase-dependent)	ENSMUSG00000066800	0.662	1.58	5.40E-06	8.13E-04
tyrosine hydroxylase	ENSMUSG00000000214	0.662	1.58	3.33E-05	3.94E-03
interferon-induced protein with tetratricopeptide repeats 3	ENSMUSG00000074896	0.661	1.58	1.37E-05	1.82E-03
cholinergic receptor, nicotinic, alpha polypeptide 2 (neuronal)	ENSMUSG00000022041	0.66	1.58	1.31E-04	1.30E-02
solute carrier family 9, subfamily B (NHA2, cation proton antiporter 2), member 2	ENSMUSG00000037994	0.659	1.58	1.85E-05	2.31E-03
aldo-keto reductase family 1, member E1	ENSMUSG00000045410	0.658	1.58	5.96E-06	8.77E-04
immunoglobulin-like domain containing receptor 1	ENSMUSG00000022900	0.655	1.57	2.72E-04	2.34E-02
1 transcription factor, LIM/homeodomain	ENSMUSG00000042258	0.652	1.57	6.81E-05	7.41E-03
alkylglycerol monooxygenase	ENSMUSG00000050103	0.649	1.57	5.06E-05	5.71E-03
RIKEN cDNA 2700038G22 gene	ENSMUSG00000097180	0.648	1.57	3.52E-04	2.87E-02
kelch-like 1	ENSMUSG00000022076	0.645	1.56	1.15E-05	1.56E-03
perilipin 4	ENSMUSG00000002831	0.643	1.56	2.41E-05	2.94E-03
galanin	ENSMUSG00000024907	0.641	1.56	1.33E-04	1.31E-02
ubiquitin-associated protein 1-like	ENSMUSG00000086228	0.632	1.55	3.04E-04	2.55E-02
potassium voltage-gated channel, subfamily G, member 4	ENSMUSG00000045246	0.626	1.54	2.41E-04	2.14E-02
cadherin 19, type 2	ENSMUSG00000047216	0.613	1.53	4.62E-05	5.31E-03
ectonucleoside triphosphate diphosphohydrolase 2	ENSMUSG00000015085	0.595	1.51	6.05E-05	6.65E-03
G protein-coupled receptor 179	ENSMUSG00000070337	0.59	1.51	1.28E-04	1.28E-02
Ras association (RalGDS/AF-6) domain family member 4	ENSMUSG00000042129	0.578	1.49	6.86E-05	7.43E-03
hephaestin	ENSMUSG00000031209	0.578	1.49	7.22E-05	7.77E-03
dynein light chain Tctex-type 1C	ENSMUSG00000000579	0.576	1.49	9.73E-05	1.01E-02
ankyrin repeat and SOCS box-containing 4	ENSMUSG00000042607	0.573	1.49	4.09E-04	3.21E-02
lipopolysaccharide binding protein	ENSMUSG00000016024	0.571	1.49	2.22E-04	2.01E-02
proline rich membrane anchor 1	ENSMUSG00000041669	0.57	1.48	6.96E-04	4.83E-02
arachidonate 8-lipoxygenase	ENSMUSG00000020891	0.569	1.48	2.73E-04	2.34E-02
epsin 3	ENSMUSG00000010080	0.568	1.48	5.71E-04	4.16E-02
prostaglandin I2 (prostacyclin) synthase	ENSMUSG00000017969	0.566	1.48	5.28E-04	3.96E-02
CD36 molecule	ENSMUSG00000002944	0.565	1.48	1.44E-04	1.39E-02
coronin 6	ENSMUSG00000020836	0.564	1.48	1.07E-04	1.09E-02
tetraspanin 11	ENSMUSG00000030351	0.564	1.48	7.00E-04	4.83E-02
xanthine dehydrogenase	ENSMUSG00000024066	0.563	1.48	3.42E-04	2.83E-02
RIKEN cDNA 1500015A07 gene	ENSMUSG00000098702	0.554	1.47	9.20E-05	9.65E-03
cytokine inducible SH2-containing protein	ENSMUSG00000032578	0.554	1.47	6.32E-04	4.47E-02
Sec24 related gene family, member D (S. cerevisiae)	ENSMUSG00000039234	0.547	1.46	1.27E-04	1.27E-02

alpha-2-macroglobulin	ENSMUSG00000030111	0.536	1.45	2.32E-04	2.09E-02
secreted acidic cysteine rich glycoprotein	ENSMUSG00000018593	0.534	1.45	1.17E-04	1.18E-02
phospholipase A2, group III	ENSMUSG00000034579	0.523	1.44	4.92E-04	3.73E-02
cholinergic receptor, muscarinic 2, cardiac	ENSMUSG00000045613	0.519	1.43	2.91E-04	2.47E-02
transcription factor 7 like 2, T cell specific, HMG box	ENSMUSG00000024985	0.508	1.42	5.88E-04	4.19E-02
putative homeodomain transcription factor 1	ENSMUSG00000058388	0.507	1.42	3.45E-04	2.84E-02
collagen, type VI, alpha 1	ENSMUSG00000001119	0.496	1.41	3.78E-04	3.04E-02
inter-alpha trypsin inhibitor, heavy chain 3	ENSMUSG00000006522	0.484	1.40	5.15E-04	3.89E-02

B. GENES DOWNREGULATED IN DAMS COMPARED TO GODMOTHERS

Gene	ENSEMBL	logFC	-FC	rawp	adjp
inhibin beta-C	ENSMUSG00000025405	-7.9	238.86	3.01E-184	2.06E-180
inhibin beta-E	ENSMUSG00000047492	-5.15	35.51	4.00E-37	1.02E-33
ST8 alpha-N-acetyl-neuraminide alpha-2,8-sialyltransferase 3, opposite strand	ENSMUSG00000086128	-2.87	7.31	4.57E-14	3.22E-11
RIKEN cDNA F830045P16 gene	ENSMUSG00000043727	-2.74	6.68	4.52E-08	1.20E-05
keratin 5	ENSMUSG00000061527	-2.73	6.63	5.76E-06	8.57E-04
signal-regulatory protein beta 1A	ENSMUSG00000095788	-1.98	3.94	1.08E-07	2.61E-05
CD300 molecule like family member F	ENSMUSG00000047798	-1.78	3.43	1.75E-06	3.14E-04
TNNI3 interacting kinase	ENSMUSG00000040086	-1.58	2.99	1.18E-04	1.19E-02
WD repeat domain 49	ENSMUSG00000104301	-1.58	2.99	2.51E-04	2.19E-02
activating transcription factor 3	ENSMUSG00000026628	-1.56	2.95	1.12E-12	6.01E-10
triggering receptor expressed on myeloid cells-like 2	ENSMUSG00000071068	-1.44	2.71	7.43E-06	1.05E-03
early growth response 2	ENSMUSG00000037868	-1.43	2.69	5.21E-22	8.89E-19
expressed sequence AA465934	ENSMUSG00000093483	-1.43	2.69	1.11E-18	1.34E-15
ring finger protein 151	ENSMUSG00000008482	-1.42	2.68	8.75E-06	1.23E-03
zinc finger protein 979	ENSMUSG00000066000	-1.34	2.53	8.48E-10	3.10E-07
C-type lectin domain family 9, member a	ENSMUSG00000046080	-1.28	2.43	1.39E-04	1.36E-02
nuclear receptor subfamily 4, group A, member 1	ENSMUSG00000023034	-1.25	2.38	8.37E-19	1.07E-15
oligodendrocyte transcription factor 3	ENSMUSG00000045591	-1.22	2.33	1.56E-09	5.48E-07
C-type lectin domain family 10, member A	ENSMUSG00000000318	-1.22	2.33	2.39E-08	6.79E-06
matrilin 1, cartilage matrix protein	ENSMUSG00000040533	-1.2	2.30	3.46E-04	2.84E-02
cartilage oligomeric matrix protein	ENSMUSG00000031849	-1.13	2.19	4.92E-04	3.73E-02
cytochrome P450, family 4, subfamily x, polypeptide 1, opposite strand	ENSMUSG00000086896	-1.11	2.16	3.36E-07	7.55E-05
FBJ osteosarcoma oncogene B	ENSMUSG00000003545	-1.09	2.13	3.13E-14	2.67E-11
early growth response 4	ENSMUSG00000071341	-1.08	2.11	4.04E-14	3.06E-11
RIKEN cDNA E030013I19 gene	ENSMUSG00000086843	-1.07	2.10	6.08E-08	1.53E-05
CD209f antigen	ENSMUSG00000051906	-1.07	2.10	7.46E-06	1.05E-03
activity regulated cytoskeletal-associated protein	ENSMUSG00000022602	-1.06	2.08	4.99E-14	3.40E-11
nuclear receptor subfamily 4, group A, member 3	ENSMUSG00000028341	-0.99	1.98	2.98E-12	1.57E-09
thrombospondin 4	ENSMUSG00000021702	-0.96	1.94	4.16E-06	6.71E-04
Scl/Tal1 interrupting locus	ENSMUSG00000028718	-0.95	1.94	5.76E-04	4.16E-02
apolipoprotein L domain containing 1	ENSMUSG00000090698	-0.95	1.93	4.98E-10	1.92E-07
FBJ osteosarcoma oncogene	ENSMUSG00000021250	-0.95	1.93	1.96E-11	9.33E-09
PR domain containing 13	ENSMUSG00000040478	-0.94	1.92	1.05E-04	1.08E-02
MORN repeat containing 2	ENSMUSG00000045257	-0.93	1.90	9.04E-09	2.84E-06
t-complex-associated testis expressed 2	ENSMUSG00000038347	-0.86	1.83	4.21E-08	1.15E-05
histidine triad nucleotide binding protein 2	ENSMUSG00000028470	-0.87	1.83	7.24E-09	2.31E-06
jun B proto-oncogene	ENSMUSG00000052837	-0.86	1.81	1.14E-09	4.07E-07
netrin 5	ENSMUSG00000070564	-0.84	1.79	5.78E-06	8.57E-04
early growth response 1	ENSMUSG00000038418	-0.83	1.77	3.36E-09	1.13E-06

collagen, type X, alpha 1	ENSMUSG00000039462	-0.82	1.76	4.71E-04	3.59E-02
solute carrier family 22 (organic cation transporter), member 2	ENSMUSG00000040966	-0.80	1.74	1.81E-05	2.27E-03
Ras-related associated with diabetes	ENSMUSG00000031880	-0.80	1.74	6.62E-08	1.63E-05
tumor necrosis factor receptor superfamily, member 25	ENSMUSG00000024793	-0.80	1.74	6.81E-06	9.88E-04
predicted gene 9602	ENSMUSG00000090539	-0.79	1.73	1.80E-04	1.69E-02
fos-like antigen 2	ENSMUSG00000029135	-0.78	1.72	2.65E-08	7.43E-06
transmembrane protein 203	ENSMUSG00000078201	-0.78	1.72	6.97E-07	1.50E-04
predicted gene 10069	ENSMUSG00000059659	-0.74	1.66	3.01E-06	5.05E-04
suprabasin	ENSMUSG00000046056	-0.72	1.65	1.50E-05	1.96E-03
activity-dependent neuroprotective protein	ENSMUSG00000051149	-0.71	1.64	4.17E-04	3.25E-02
CD6 antigen	ENSMUSG00000024670	-0.71	1.63	5.50E-04	4.06E-02
lymphocyte-activation gene 3	ENSMUSG00000030124	-0.69	1.61	1.43E-05	1.87E-03
TCDD-inducible poly(ADP-ribose) polymerase	ENSMUSG00000034640	-0.69	1.61	1.28E-06	2.45E-04
SCAN domain-containing 1	ENSMUSG00000046229	-0.69	1.61	2.52E-06	4.32E-04
geminin coiled-coil domain containing	ENSMUSG00000068428	-0.68	1.61	5.45E-04	4.06E-02
dentin matrix protein 1	ENSMUSG00000029307	-0.68	1.60	1.76E-05	2.24E-03
salt inducible kinase 1	ENSMUSG00000024042	-0.67	1.59	2.17E-06	3.79E-04
CCAAT/enhancer binding protein (C/EBP), beta	ENSMUSG00000056501	-0.67	1.59	2.12E-04	1.95E-02
C-type lectin domain family 18, member A	ENSMUSG00000033633	-0.66	1.58	3.39E-04	2.82E-02
ribosomal protein L21	ENSMUSG00000041453	-0.66	1.58	4.66E-06	7.22E-04
solute carrier family 37 (glycerol-3-phosphate transporter), member 1	ENSMUSG00000024036	-0.66	1.57	6.09E-06	8.90E-04
predicted gene 266	ENSMUSG00000010529	-0.65	1.57	2.47E-05	2.99E-03
protein interacting with cyclin A1	ENSMUSG00000044122	-0.65	1.57	1.15E-05	1.56E-03
heparan sulfate (glucosamine) 3-O-sulfotransferase 3B1	ENSMUSG00000070407	-0.64	1.55	5.49E-04	4.06E-02
G protein-coupled receptor 182	ENSMUSG00000058396	-0.63	1.54	6.24E-05	6.82E-03
radial spoke head 1 homolog (Chlamydomonas)	ENSMUSG00000024033	-0.63	1.54	1.79E-05	2.25E-03
dual specificity phosphatase 1	ENSMUSG00000024190	-0.62	1.53	1.34E-05	1.79E-03
Kruppel-like factor 2 (lung)	ENSMUSG00000055148	-0.62	1.53	4.70E-05	5.37E-03
serine (or cysteine) peptidase inhibitor, clade A, member 3M	ENSMUSG00000079012	-0.61	1.52	2.43E-04	2.15E-02
sphingosine kinase 1	ENSMUSG00000061878	-0.61	1.52	3.57E-05	4.20E-03
predicted gene 5796	ENSMUSG00000096775	-0.6	1.52	1.51E-04	1.46E-02
growth arrest and DNA-damage-inducible 45 beta	ENSMUSG00000015312	-0.59	1.51	4.81E-05	5.46E-03
nuclear receptor subfamily 4, group A, member 2	ENSMUSG00000026826	-0.58	1.50	4.45E-05	5.20E-03
coiled-coil domain containing 42	ENSMUSG00000045915	-0.58	1.50	2.36E-04	2.11E-02
alpha takusan-like	ENSMUSG00000079396	-0.58	1.50	1.39E-04	1.36E-02
guanine nucleotide binding protein (G protein), gamma 13	ENSMUSG00000025739	-0.58	1.50	1.73E-04	1.64E-02
myosin binding protein C, slow-type	ENSMUSG00000020061	-0.58	1.49	2.10E-04	1.94E-02
AT rich interactive domain 5A (MRF1-like)	ENSMUSG00000037447	-0.57	1.48	9.33E-05	9.73E-03
dual specificity phosphatase 5	ENSMUSG00000034765	-0.57	1.48	1.85E-04	1.73E-02
predicted gene 2897	ENSMUSG00000079410	-0.56	1.48	1.96E-04	1.82E-02
RIKEN cDNA 2810001G20 gene	ENSMUSG00000087497	-0.56	1.48	2.52E-04	2.19E-02
GRP1 (general receptor for phosphoinositides 1)-associated scaffold protein	ENSMUSG00000000531	-0.55	1.47	1.01E-04	1.04E-02
chordin-like 1	ENSMUSG00000031283	-0.55	1.46	2.77E-04	2.37E-02
olfactomedin-like 2A	ENSMUSG00000046618	-0.55	1.46	2.57E-04	2.23E-02
sulfotransferase family, cytosolic, 2B, member 1	ENSMUSG00000003271	-0.54	1.46	5.90E-04	4.19E-02
LYR motif containing 7	ENSMUSG00000020268	-0.53	1.45	3.87E-04	3.08E-02
ADP-ribosylation factor-like 4D	ENSMUSG00000034936	-0.53	1.44	2.46E-04	2.16E-02
poliovirus receptor	ENSMUSG00000040511	-0.53	1.44	6.53E-04	4.58E-02
solute carrier family 13 (sodium-dependent dicarboxylate transporter), member 3	ENSMUSG00000018459	-0.53	1.44	1.74E-04	1.64E-02

RAS-like, family 10, member A	ENSMUSG00000034209	-0.53	1.44	3.27E-04	2.73E-02
T cell activation Rho GTPase activating protein	ENSMUSG00000033450	-0.52	1.44	3.52E-04	2.87E-02
elongin BC and polycomb repressive complex 2 associated protein	ENSMUSG00000043439	-0.51	1.42	3.56E-04	2.89E-02
keratin 9	ENSMUSG00000051617	-0.51	1.42	5.77E-04	4.16E-02
nucleoporin 35	ENSMUSG00000026999	-0.51	1.42	5.87E-04	4.19E-02
immediate early response 5-like	ENSMUSG00000089762	-0.50	1.42	4.24E-04	3.30E-02
endothelin 3	ENSMUSG00000027524	-0.50	1.42	6.89E-04	4.79E-02
B cell translocation gene 2, anti-proliferative	ENSMUSG00000020423	-0.50	1.41	4.33E-04	3.36E-02
early growth response 3	ENSMUSG00000033730	-0.50	1.41	4.43E-04	3.42E-02
serum/glucocorticoid regulated kinase 1	ENSMUSG00000019970	-0.49	1.40	5.50E-04	4.06E-02
RIKEN cDNA 1810037I17 gene	ENSMUSG00000054091	-0.48	1.40	6.39E-04	4.49E-02

C. NON-SIGNIFICANT GENES

Gene	ENSEMBL	logFC	FC	rawp	adjp
lin-28 homolog A (C. elegans)	ENSMUSG00000050966	22.01	4.46	2.16E-03	1.14E-01
olfactory receptor 1392	ENSMUSG00000101750	22.01	4.46	2.16E-03	1.14E-01
predicted gene. 21188	ENSMUSG00000095609	21.71	4.44	4.23E-03	1.82E-01
keratin associated protein 26-1	ENSMUSG00000071471	16.22	4.02	1.64E-02	4.34E-01
killer cell lectin-like receptor subfamily A. member 14. pseudogene	ENSMUSG00000072721	16.00	4.00	3.23E-02	6.32E-01
RIKEN cDNA 1700021F07 gene	ENSMUSG00000027518	14.32	3.84	3.23E-02	6.32E-01
myosin. light chain 10. regulatory	ENSMUSG00000005474	12.47	3.64	3.23E-02	6.32E-01
histocompatibility 2. M region locus 2	ENSMUSG00000016283	12.47	3.64	3.23E-02	6.32E-01
tripartite motif-containing 60	ENSMUSG00000053490	12.47	3.64	3.23E-02	6.32E-01
fibroblast growth factor 6	ENSMUSG00000000183	12.38	3.63	6.39E-02	8.78E-01
family with sequence similarity 89. member B	ENSMUSG00000024939	12.38	3.63	6.39E-02	8.78E-01
aldo-keto reductase family 1. member B7	ENSMUSG00000052131	12.38	3.63	6.39E-02	8.78E-01
microRNA 181c	ENSMUSG00000065483	12.38	3.63	6.39E-02	8.78E-01
microRNA 695	ENSMUSG00000076216	12.38	3.63	6.39E-02	8.78E-01
macrophage receptor with collagenous structure	ENSMUSG00000026390	12.30	3.62	6.39E-02	8.78E-01
killer cell lectin-like receptor subfamily A. member 9	ENSMUSG00000033024	12.30	3.62	6.39E-02	8.78E-01
interleukin 1 receptor antagonist	ENSMUSG00000026981	10.56	3.40	6.39E-02	8.78E-01
RIKEN cDNA 9230104L09 gene	ENSMUSG00000027446	10.56	3.40	6.39E-02	8.78E-01
C-type lectin domain family 4. member e	ENSMUSG00000030142	10.56	3.40	6.39E-02	8.78E-01
killer cell lectin-like receptor subfamily C. member 1	ENSMUSG00000030167	10.56	3.40	6.39E-02	8.78E-01
RIKEN cDNA 4930528P14 gene	ENSMUSG00000087309	10.56	3.40	6.39E-02	8.78E-01
RIKEN cDNA 1700122O11 gene	ENSMUSG00000094928	10.56	3.40	6.39E-02	8.78E-01
poly(A) binding protein. cytoplasmic 6	ENSMUSG00000046173	10.48	3.39	6.39E-02	8.78E-01
solute carrier family 22. member 29	ENSMUSG00000075044	8.82	3.14	3.87E-03	1.71E-01
predicted gene. 36079	ENSMUSG00000095029	8.17	3.03	1.27E-02	3.80E-01
histone cluster 1. H4b	ENSMUSG00000069266	7.67	2.94	7.03E-03	2.52E-01
lysophosphatidylcholine acyltransferase 2B	ENSMUSG00000033794	7.16	2.84	7.03E-03	2.52E-01
predicted gene 4847	ENSMUSG00000051081	7.16	2.84	7.03E-03	2.52E-01
RIKEN cDNA 4933400C23 gene	ENSMUSG00000101734	7.01	2.81	2.29E-02	5.23E-01
microRNA 5119	ENSMUSG00000093176	6.77	2.76	9.21E-04	6.19E-02
transmembrane and immunoglobulin domain containing 3	ENSMUSG00000074344	6.50	2.70	4.12E-02	7.12E-01
vomeronasal 2. receptor 57	ENSMUSG00000066537	5.90	2.56	2.29E-02	5.23E-01
RIKEN cDNA 1700011M02 gene	ENSMUSG00000079476	5.86	2.55	2.29E-02	5.23E-01
cytochrome P450. family 2. subfamily d. polypeptide 10	ENSMUSG00000094806	5.86	2.55	2.29E-02	5.23E-01
predicted gene 3143	ENSMUSG00000105153	5.86	2.55	2.29E-02	5.23E-01
predicted gene. 26544	ENSMUSG00000097362	5.82	2.54	4.10E-02	7.12E-01
trichohyalin-like 1	ENSMUSG00000027908	5.78	2.53	7.28E-02	9.21E-01

pluripotency associated transcript 21	ENSMUSG00000086807	5.28	2.40	4.10E-02	7.12E-01
RIKEN cDNA 3830403N18 gene	ENSMUSG00000031125	5.24	2.39	5.28E-03	2.09E-01
predicted gene 3043	ENSMUSG00000090364	5.21	2.38	2.02E-03	1.11E-01
keratin 16	ENSMUSG00000053797	5.17	2.37	7.28E-02	9.21E-01
myogenic differentiation 1	ENSMUSG00000009471	4.63	2.21	7.28E-02	9.21E-01
microRNA 135a-2	ENSMUSG00000065524	4.63	2.21	7.28E-02	9.21E-01
signal-regulatory protein beta 1B	ENSMUSG00000095028	4.63	2.21	7.28E-02	9.21E-01
cholinergic receptor. nicotinic. alpha polypeptide 9	ENSMUSG00000029205	4.56	2.19	7.03E-03	2.52E-01
predicted gene. 26641	ENSMUSG00000097045	4.50	2.17	1.44E-02	4.06E-01
HEAT repeat containing 9	ENSMUSG00000018925	4.50	2.17	3.43E-02	6.49E-01
phospholipase A2. group IVD	ENSMUSG00000070719	4.38	2.13	5.16E-03	2.08E-01
zinc finger and SCAN domain containing 10	ENSMUSG00000023902	4.32	2.11	1.88E-03	1.06E-01
hydroxysteroid (17-beta) dehydrogenase 13	ENSMUSG00000034528	4.20	2.07	4.12E-02	7.12E-01
predicted gene 15413	ENSMUSG00000053049	4.20	2.07	4.12E-02	7.12E-01
microRNA 7030	ENSMUSG00000099254	4.00	2.00	2.36E-02	5.30E-01
RIKEN cDNA 4930471M09 gene	ENSMUSG00000097693	3.86	1.95	2.29E-02	5.23E-01
predicted gene 8094	ENSMUSG00000091733	3.84	1.94	2.01E-03	1.11E-01
snoRNA DQ267101	ENSMUSG00000064496	3.84	1.94	2.29E-02	5.23E-01
HRAS-like suppressor family. member 5	ENSMUSG00000024973	3.84	1.94	6.88E-02	9.05E-01
T-box 22	ENSMUSG00000031241	3.81	1.93	4.10E-02	7.12E-01
nephrosis 1 homolog. nephrin. opposite strand	ENSMUSG00000087009	3.53	1.82	1.43E-02	4.05E-01
predicted gene 5547	ENSMUSG00000104835	3.51	1.81	1.43E-02	4.05E-01
family with sequence similarity 209	ENSMUSG00000027505	3.48	1.80	4.10E-02	7.12E-01
coagulation factor II	ENSMUSG00000027249	3.43	1.78	3.29E-03	1.55E-01
GATA binding protein 3	ENSMUSG00000015619	3.39	1.76	5.28E-03	2.09E-01
RIKEN cDNA 1810062G17 gene	ENSMUSG00000027713	3.36	1.75	2.18E-02	5.15E-01
microRNA 8116	ENSMUSG00000099145	3.27	1.71	3.74E-03	1.67E-01
free fatty acid receptor 2	ENSMUSG00000051314	3.27	1.71	6.13E-02	8.73E-01
outer dense fiber of sperm tails 4	ENSMUSG00000032921	3.14	1.65	1.75E-02	4.52E-01
predicted gene 4832	ENSMUSG00000058869	3.14	1.65	4.10E-02	7.12E-01
urocanase domain containing 1	ENSMUSG00000034456	3.12	1.64	7.28E-02	9.21E-01
zygote arrest 1	ENSMUSG00000063935	3.10	1.63	1.69E-03	1.00E-01
DnaJ heat shock protein family (Hsp40) member C22	ENSMUSG00000038009	3.10	1.63	1.48E-02	4.12E-01
cathelicidin antimicrobial peptide	ENSMUSG00000038357	3.03	1.60	6.13E-02	8.73E-01
distal-less homeobox 3	ENSMUSG00000001510	3.01	1.59	4.92E-03	2.02E-01
ADP-ribosyltransferase 4	ENSMUSG00000030217	3.01	1.59	4.60E-02	7.55E-01
vomeronasal 2. receptor 54	ENSMUSG00000096593	3.01	1.59	6.13E-02	8.73E-01
interleukin 6	ENSMUSG00000025746	2.99	1.58	6.88E-02	9.05E-01
cysteine-rich secretory protein 1	ENSMUSG00000025431	2.95	1.56	2.36E-02	5.30E-01
carcinoembryonic antigen-related cell adhesion molecule 15	ENSMUSG00000078795	2.89	1.53	1.35E-02	3.94E-01
chemokine (C-X-C motif) receptor 2	ENSMUSG00000026180	2.87	1.52	2.64E-02	5.65E-01
RIKEN cDNA 4933424M12 gene	ENSMUSG00000087289	2.87	1.52	8.55E-02	9.84E-01
glutathione peroxidase 6	ENSMUSG00000004341	2.83	1.50	6.83E-03	2.50E-01
urotensin 2	ENSMUSG00000028963	2.83	1.50	7.12E-02	9.17E-01
solute carrier family 5 (iodide transporter). member 8	ENSMUSG00000020062	2.77	1.47	1.22E-03	7.84E-02
claudin 4	ENSMUSG00000047501	2.77	1.47	5.34E-02	8.14E-01
chitinase-like 6	ENSMUSG00000027902	2.77	1.47	7.28E-02	9.21E-01
RIKEN cDNA 4930558K02 gene	ENSMUSG00000086277	2.73	1.45	4.60E-02	7.55E-01
phospholipid scramblase family. member 5	ENSMUSG00000095654	2.73	1.45	6.88E-02	9.05E-01
peptidyl arginine deiminase. type I	ENSMUSG00000025329	2.71	1.44	6.93E-02	9.05E-01
predicted gene 8271	ENSMUSG00000079380	2.69	1.43	3.44E-03	1.61E-01
predicted gene. 26685	ENSMUSG00000097281	2.58	1.37	3.43E-02	6.49E-01
coagulation factor X	ENSMUSG00000031444	2.58	1.37	6.93E-02	9.05E-01
coiled-coil domain containing 192	ENSMUSG00000058925	2.57	1.36	1.00E-02	3.25E-01
RIKEN cDNA 1700057G04 gene	ENSMUSG00000074139	2.57	1.36	3.43E-02	6.49E-01

relaxin 3	ENSMUSG00000045232	2.57	1.36	4.60E-02	7.55E-01
small nucleolar RNA. H/ACA box 62	ENSMUSG00000064925	2.57	1.36	5.84E-02	8.57E-01
vomeronasal 1 receptor 32	ENSMUSG00000062905	2.55	1.35	8.22E-02	9.72E-01
2'-5' oligoadenylate synthetase-like 1	ENSMUSG00000041827	2.50	1.32	3.09E-03	1.49E-01
predicted gene 8127	ENSMUSG00000090713	2.50	1.32	1.72E-02	4.47E-01
potassium channel. subfamily V. member 2	ENSMUSG00000047298	2.50	1.32	5.95E-02	8.64E-01
inducible T cell co-stimulator	ENSMUSG00000026009	2.45	1.29	1.18E-02	3.65E-01
CD27 antigen	ENSMUSG00000030336	2.41	1.27	1.23E-03	7.87E-02
RIKEN cDNA 1700030A11 gene	ENSMUSG00000085333	2.41	1.27	4.16E-02	7.13E-01
RIKEN cDNA 4930593C16 gene	ENSMUSG00000086365	2.41	1.27	4.99E-02	7.85E-01
RIKEN cDNA C430042M11 gene	ENSMUSG00000097254	2.39	1.26	2.00E-03	1.11E-01
small nucleolar RNA. C/D box 89	ENSMUSG00000077704	2.39	1.26	3.40E-02	6.49E-01
lactotransferrin	ENSMUSG00000032496	2.38	1.25	1.28E-02	3.82E-01
RIKEN cDNA 2010016I18 gene	ENSMUSG00000091575	2.38	1.25	2.12E-02	5.11E-01
predicted gene 5415	ENSMUSG00000091318	2.36	1.24	1.97E-02	4.89E-01
tubby-like protein 2	ENSMUSG00000023467	2.35	1.23	4.39E-03	1.87E-01
expressed sequence AI662270	ENSMUSG00000087107	2.35	1.23	6.64E-03	2.46E-01
RIKEN cDNA 4930407G08 gene	ENSMUSG00000086713	2.35	1.23	6.13E-02	8.73E-01
placenta expressed transcript 1. opposite strand	ENSMUSG00000101304	2.33	1.22	1.34E-02	3.92E-01
forkhead box O6. opposite strand	ENSMUSG00000084929	2.30	1.20	2.39E-03	1.25E-01
RIKEN cDNA A730018C14 gene	ENSMUSG00000047828	2.30	1.20	1.16E-02	3.61E-01
protein phosphatase 1. regulatory subunit 3A	ENSMUSG00000042717	2.30	1.20	8.55E-02	9.84E-01
transmembrane protease. serine 2	ENSMUSG00000000385	2.28	1.19	3.53E-02	6.59E-01
kelch-like 31	ENSMUSG00000044938	2.28	1.19	6.93E-02	9.05E-01
shugoshin 1	ENSMUSG00000023940	2.27	1.18	6.32E-03	2.37E-01
small nucleolar RNA. C/D box 53	ENSMUSG00000092887	2.25	1.17	3.02E-02	6.10E-01
RIKEN cDNA 4930511M06 gene	ENSMUSG00000086607	2.23	1.16	3.55E-02	6.61E-01
predicted gene 6588	ENSMUSG00000072722	2.22	1.15	4.91E-02	7.79E-01
killer cell lectin-like receptor. subfamily D. member 1	ENSMUSG00000030165	2.22	1.15	8.07E-02	9.67E-01
pluripotency associated transcript 14	ENSMUSG00000086454	2.20	1.14	1.57E-03	9.46E-02
pyruvate kinase liver and red blood cell	ENSMUSG00000041237	2.20	1.14	9.02E-03	3.06E-01
predicted gene 16208	ENSMUSG00000085464	2.20	1.14	3.38E-02	6.47E-01
glutathione S-transferase. alpha 2 (Yc2)	ENSMUSG00000057933	2.20	1.14	5.95E-02	8.64E-01
RIKEN cDNA 4930538E20 gene	ENSMUSG00000085516	2.19	1.13	1.82E-02	4.62E-01
predicted gene 5464	ENSMUSG00000075553	2.19	1.13	2.16E-02	5.13E-01
UL16 binding protein 1	ENSMUSG00000079685	2.19	1.13	2.97E-02	6.06E-01
metastasis associated in colon cancer 1	ENSMUSG00000041886	2.19	1.13	6.93E-02	9.05E-01
unc-93 homolog A2	ENSMUSG00000056133	2.17	1.12	5.65E-02	8.43E-01
predicted gene. 17660	ENSMUSG00000091034	2.17	1.12	6.93E-02	9.05E-01
interleukin 23. alpha subunit p19	ENSMUSG00000025383	2.16	1.11	7.63E-03	2.69E-01
erythroferrone	ENSMUSG00000047443	2.16	1.11	3.01E-02	6.10E-01
apolipoprotein B	ENSMUSG00000020609	2.14	1.10	1.02E-02	3.28E-01
nonagouti	ENSMUSG00000084897	2.14	1.10	7.63E-02	9.45E-01
solute carrier family 4. sodium bicarbonate cotransporter. member 9	ENSMUSG00000024485	2.13	1.09	2.46E-02	5.46E-01
regulatory factor X 8	ENSMUSG00000057173	2.11	1.08	4.94E-03	2.02E-01
tetratricopeptide repeat domain 36	ENSMUSG00000039438	2.11	1.08	2.18E-02	5.15E-01
microRNA 466i	ENSMUSG00000080574	2.11	1.08	8.55E-02	9.84E-01
CD300E molecule	ENSMUSG00000048498	2.08	1.06	4.16E-02	7.13E-01
family with sequence similarity 83. member E	ENSMUSG00000054161	2.08	1.06	8.42E-02	9.80E-01
claudin 34C2	ENSMUSG00000095474	2.07	1.05	2.29E-03	1.21E-01
transmembrane protein 30B	ENSMUSG00000034435	2.07	1.05	2.60E-03	1.32E-01
synaptotagmin-like 3	ENSMUSG00000041831	2.07	1.05	2.56E-02	5.56E-01
cytochrome P450. family 4. subfamily a. polypeptide 12B	ENSMUSG00000078597	2.06	1.04	1.00E-02	3.25E-01
predicted gene 42788	ENSMUSG00000107388	2.06	1.04	2.89E-02	5.96E-01
integrin beta 6	ENSMUSG00000026971	2.04	1.03	4.22E-02	7.19E-01

beta-1.4-N-acetyl-galactosaminyl transferase 2	ENSMUSG00000013418	2.03	1.02	2.79E-02	5.86E-01
cytochrome P450. family 2. subfamily r. polypeptide 1	ENSMUSG00000030670	1.99	0.99	3.13E-02	6.24E-01
predicted gene. 26670	ENSMUSG00000097416	1.99	0.99	7.12E-02	9.17E-01
C-type lectin domain family 12. member a	ENSMUSG00000053063	1.99	0.99	2.06E-03	1.12E-01
EF-hand calcium binding domain 8	ENSMUSG00000044083	1.98	0.99	6.47E-03	2.40E-01
Nik related kinase	ENSMUSG00000052854	1.98	0.99	1.81E-02	4.62E-01
microRNA 149	ENSMUSG00000065470	1.98	0.99	2.18E-02	5.15E-01
fetuin beta	ENSMUSG00000022871	1.98	0.98	9.63E-03	3.20E-01
tyrosinase-related protein 1	ENSMUSG00000005994	1.96	0.97	3.74E-03	1.67E-01
RIKEN cDNA 4732471J01 gene	ENSMUSG00000053714	1.96	0.97	8.07E-02	9.67E-01
tyrosine kinase. non-receptor. 1	ENSMUSG00000001583	1.95	0.96	4.75E-02	7.66E-01
SH3-binding domain kinase family. member 2	ENSMUSG00000030433	1.94	0.95	1.03E-02	3.31E-01
cytochrome c oxidase subunit 8B	ENSMUSG00000025488	1.93	0.95	5.80E-03	2.23E-01
epoxide hydrolase 3	ENSMUSG00000037577	1.92	0.94	9.80E-03	3.23E-01
transmembrane protein 150B	ENSMUSG00000046456	1.92	0.94	8.79E-03	3.00E-01
HEAT repeat containing 4	ENSMUSG00000090843	1.90	0.93	6.93E-02	9.05E-01
predicted gene 8050	ENSMUSG00000091814	1.89	0.92	2.89E-02	5.96E-01
RIKEN cDNA A230004M16 gene	ENSMUSG00000087306	1.87	0.91	3.55E-02	6.61E-01
indoleamine 2.3-dioxygenase 1	ENSMUSG00000031551	1.86	0.90	1.19E-03	7.73E-02
olfactory receptor 558	ENSMUSG00000070423	1.86	0.89	1.36E-02	3.95E-01
chemokine (C-X-C motif) receptor 5	ENSMUSG00000047880	1.86	0.89	6.06E-03	2.29E-01
uncharacterized LOC102634389	ENSMUSG00000078648	1.85	0.89	3.67E-02	6.75E-01
killer cell lectin-like receptor family I member 1	ENSMUSG00000067610	1.85	0.89	2.89E-02	5.96E-01
glial cell line derived neurotrophic factor	ENSMUSG00000022144	1.84	0.88	1.24E-03	7.87E-02
RIKEN cDNA 4833417C18 gene	ENSMUSG00000086015	1.84	0.88	1.92E-03	1.07E-01
homeobox A1	ENSMUSG00000029844	1.84	0.88	6.30E-02	8.78E-01
predicted gene 16287	ENSMUSG00000073739	1.83	0.87	1.88E-03	1.06E-01
dynein. axonemal. heavy chain 14	ENSMUSG00000047369	1.83	0.87	1.59E-02	4.29E-01
predicted gene. 17634	ENSMUSG00000097482	1.83	0.87	3.50E-02	6.55E-01
prostaglandin-endoperoxide synthase 2. opposite strand	ENSMUSG00000097028	1.83	0.87	6.81E-02	9.05E-01
HAUS augmin-like complex. subunit 5	ENSMUSG00000078762	1.82	0.86	2.06E-03	1.12E-01
predicted gene 807	ENSMUSG00000097848	1.82	0.86	3.50E-02	6.55E-01
collagen. type IV. alpha 3	ENSMUSG00000079465	1.82	0.86	2.78E-03	1.39E-01
ubiquitin carboxy-terminal hydrolase L1. opposite strand	ENSMUSG00000087601	1.81	0.85	8.66E-03	2.97E-01
tripartite motif-containing 6	ENSMUSG00000072244	1.81	0.85	3.24E-03	1.54E-01
solute carrier family 1 (glutamate transporter). member 7	ENSMUSG00000008932	1.81	0.85	5.84E-02	8.57E-01
insulinoma-associated 2	ENSMUSG00000045440	1.80	0.85	3.50E-03	1.62E-01
vertebrae development associated	ENSMUSG00000071235	1.79	0.84	6.81E-02	9.05E-01
mesothelin-like	ENSMUSG00000041062	1.79	0.84	4.14E-02	7.13E-01
FGR proto-oncogene. Src family tyrosine kinase	ENSMUSG00000028874	1.79	0.84	5.28E-02	8.10E-01
T-box 4	ENSMUSG00000000094	1.79	0.84	4.50E-02	7.46E-01
microRNA 23b	ENSMUSG00000065599	1.79	0.84	3.95E-02	7.06E-01
RIKEN cDNA B230323A14 gene	ENSMUSG00000097623	1.77	0.83	2.00E-03	1.11E-01
FUN14 domain containing 2 pseudogene	ENSMUSG00000074619	1.77	0.83	8.71E-02	9.89E-01
USH1 protein network component harmonin	ENSMUSG00000030838	1.77	0.82	3.43E-03	1.61E-01
predicted gene 21976	ENSMUSG00000096330	1.77	0.82	2.79E-02	5.86E-01
luteinizing hormone/choriogonadotropin receptor	ENSMUSG00000024107	1.77	0.82	4.34E-02	7.31E-01
NLR family. apoptosis inhibitory protein 1	ENSMUSG00000021640	1.76	0.82	4.35E-03	1.86E-01
maestro heat-like repeat family member 3	ENSMUSG00000087230	1.76	0.82	3.00E-02	6.08E-01
RIKEN cDNA 1810009A15 gene	ENSMUSG00000071653	1.76	0.81	1.58E-02	4.28E-01
solute carrier family 43. member 1	ENSMUSG00000027075	1.75	0.81	2.67E-02	5.70E-01
RIKEN cDNA 2310016G11 gene	ENSMUSG00000070574	1.75	0.81	8.03E-02	9.66E-01
retinal pigment epithelium derived rhodopsin homolog	ENSMUSG00000028012	1.75	0.80	1.82E-02	4.63E-01
expressed sequence AU040972	ENSMUSG00000091523	1.74	0.80	6.82E-02	9.05E-01

amylase 2a3	ENSMUSG00000093931	1.74	0.80	7.63E-02	9.45E-01
nodal	ENSMUSG00000037171	1.73	0.79	5.85E-03	2.25E-01
testicular cell adhesion molecule 1	ENSMUSG00000020712	1.73	0.79	8.03E-02	9.66E-01
NADPH oxidase 4	ENSMUSG00000030562	1.73	0.79	7.00E-03	2.52E-01
polyamine modulated factor 1 binding protein 1	ENSMUSG00000031727	1.72	0.79	8.42E-02	9.80E-01
predicted gene 10030	ENSMUSG00000057802	1.72	0.78	1.82E-02	4.63E-01
RIKEN cDNA 6720483E21 gene	ENSMUSG00000097934	1.71	0.78	7.20E-03	2.56E-01
R-spondin 4	ENSMUSG00000032852	1.71	0.78	1.47E-02	4.09E-01
tripartite motif-containing 43A	ENSMUSG00000090693	1.71	0.78	1.97E-03	1.10E-01
adhesion G protein-coupled receptor G3	ENSMUSG00000060470	1.70	0.77	5.88E-02	8.58E-01
Purkinje cell protein 2 (L7)	ENSMUSG00000004630	1.70	0.77	9.94E-03	3.25E-01
serine (or cysteine) peptidase inhibitor. clade B. member 6c	ENSMUSG00000052180	1.70	0.77	4.03E-02	7.11E-01
Rh blood group. D antigen	ENSMUSG00000028825	1.70	0.77	4.01E-02	7.10E-01
angiopoietin-like 8	ENSMUSG00000047822	1.69	0.76	8.71E-02	9.89E-01
RIKEN cDNA 1300017J02 gene	ENSMUSG00000033688	1.69	0.76	3.11E-02	6.23E-01
transmembrane protein 71	ENSMUSG00000036944	1.69	0.76	4.01E-02	7.10E-01
cDNA sequence BC016548	ENSMUSG00000070794	1.69	0.75	6.82E-02	9.05E-01
sushi-repeat-containing protein	ENSMUSG00000090084	1.68	0.75	8.41E-02	9.80E-01
WAP four-disulfide core domain 2	ENSMUSG00000017723	1.67	0.74	6.40E-03	2.39E-01
transmembrane protein 190	ENSMUSG00000013091	1.67	0.74	4.01E-02	7.10E-01
angiopoietin 4	ENSMUSG00000027460	1.67	0.74	7.63E-02	9.45E-01
solute carrier family 9 (sodium/hydrogen exchanger). member 3	ENSMUSG00000036123	1.67	0.74	5.00E-02	7.86E-01
ripply transcriptional repressor 3	ENSMUSG00000022941	1.67	0.74	8.69E-02	9.89E-01
acid phosphatase. prostate	ENSMUSG00000032561	1.67	0.74	5.43E-03	2.13E-01
calpain 8	ENSMUSG00000038599	1.66	0.74	5.38E-02	8.17E-01
insulin-like growth factor 2 mRNA binding protein 2	ENSMUSG00000033581	1.66	0.73	4.12E-03	1.79E-01
RIKEN cDNA 9330158H04 gene	ENSMUSG00000073154	1.66	0.73	2.57E-03	1.32E-01
BTB and CNC homology 2. opposite strand	ENSMUSG00000086150	1.66	0.73	8.03E-02	9.66E-01
predicted gene 4951	ENSMUSG00000073555	1.65	0.72	5.76E-02	8.51E-01
RIKEN cDNA B230319C09 gene	ENSMUSG00000051844	1.65	0.72	1.74E-02	4.51E-01
ureidopropionase. beta	ENSMUSG00000033427	1.65	0.72	4.29E-02	7.25E-01
predicted gene 11190	ENSMUSG00000055045	1.64	0.72	8.12E-02	9.71E-01
predicted gene. 17597	ENSMUSG00000097613	1.64	0.72	1.82E-03	1.04E-01
placenta expressed transcript 1	ENSMUSG00000032068	1.64	0.72	2.86E-02	5.94E-01
REC114 meiotic recombination protein	ENSMUSG00000074269	1.64	0.71	2.96E-02	6.06E-01
RIKEN cDNA 1700003D09 gene	ENSMUSG00000085944	1.64	0.71	7.82E-02	9.59E-01
glycerol-3-phosphate acyltransferase 2. mitochondrial	ENSMUSG00000046338	1.63	0.71	9.82E-03	3.23E-01
desmoglein 1 alpha	ENSMUSG00000069441	1.63	0.70	4.77E-02	7.67E-01
Indian hedgehog	ENSMUSG00000006538	1.63	0.70	2.09E-02	5.07E-01
cytochrome c. testis	ENSMUSG00000056436	1.62	0.70	8.03E-02	9.66E-01
tenomodulin	ENSMUSG00000031250	1.61	0.68	1.40E-02	4.01E-01
lysyl oxidase-like 2	ENSMUSG00000034205	1.61	0.68	3.71E-03	1.67E-01
heat shock factor binding protein 1-like 1	ENSMUSG00000078963	1.61	0.68	7.31E-03	2.59E-01
3-oxoacid CoA transferase 2B	ENSMUSG00000076438	1.61	0.68	6.81E-02	9.05E-01
acyl-CoA wax alcohol acyltransferase 2	ENSMUSG00000031220	1.60	0.68	2.85E-02	5.93E-01
BRCA1 interacting protein C-terminal helicase 1	ENSMUSG00000034329	1.60	0.68	5.76E-02	8.51E-01
serine/threonine/tyrosine interacting-like 1	ENSMUSG00000019178	1.60	0.68	5.32E-02	8.13E-01
RIKEN cDNA A230001M10 gene	ENSMUSG00000105891	1.59	0.67	9.98E-04	6.67E-02
chemokine (C-X-C motif) ligand 5	ENSMUSG00000029371	1.59	0.67	2.60E-03	1.32E-01
lysyl oxidase	ENSMUSG00000024529	1.59	0.67	1.39E-03	8.72E-02
keratin 25	ENSMUSG00000035831	1.59	0.67	8.20E-02	9.72E-01
tumor necrosis factor (ligand) superfamily. member 9	ENSMUSG00000035678	1.58	0.66	3.70E-03	1.67E-01
RIKEN cDNA A930006K02 gene	ENSMUSG00000084866	1.58	0.66	7.22E-03	2.57E-01
complement component 1. r subcomponent B	ENSMUSG00000098470	1.58	0.66	3.03E-02	6.10E-01

LIM homeobox protein 3	ENSMUSG00000026934	1.58	0.66	3.24E-03	1.54E-01
dopamine receptor D3	ENSMUSG00000022705	1.58	0.66	5.22E-03	2.09E-01
FXYD domain-containing ion transport regulator 3	ENSMUSG00000057092	1.58	0.66	1.45E-02	4.07E-01
predicted gene 10421	ENSMUSG00000099907	1.57	0.65	2.05E-03	1.12E-01
guanylate-binding protein 8	ENSMUSG00000034438	1.56	0.64	1.71E-02	4.46E-01
predicted gene 12108	ENSMUSG00000086386	1.56	0.64	2.82E-02	5.91E-01
phospholipase A2 receptor 1	ENSMUSG00000054580	1.56	0.64	4.80E-02	7.69E-01
paired immunoglobin-like type 2 receptor alpha	ENSMUSG00000046245	1.56	0.64	3.34E-02	6.42E-01
tumor protein p53 pathway corepressor 1	ENSMUSG00000085912	1.56	0.64	1.13E-02	3.57E-01
fibroblast activation protein	ENSMUSG00000000392	1.56	0.64	4.77E-02	7.67E-01
predicted gene 27199	ENSMUSG00000098649	1.55	0.64	3.27E-02	6.34E-01
uncharacterized LOC102631780	ENSMUSG00000097233	1.55	0.64	1.41E-03	8.79E-02
isopentenyl-diphosphate delta isomerase 2	ENSMUSG00000033520	1.55	0.63	3.62E-02	6.70E-01
RIKEN cDNA 1700109H08 gene	ENSMUSG00000008307	1.54	0.63	1.22E-03	7.84E-02
ATP-binding cassette. sub-family C (CFTR/MRP). member 12	ENSMUSG00000036872	1.54	0.63	4.49E-03	1.88E-01
RIKEN cDNA B230206L02 gene	ENSMUSG00000086003	1.54	0.62	4.96E-02	7.84E-01
predicted gene 10109	ENSMUSG00000062073	1.54	0.62	8.00E-02	9.66E-01
von Willebrand factor A domain containing 7	ENSMUSG00000007030	1.54	0.62	3.54E-02	6.61E-01
collectin sub-family member 11	ENSMUSG00000036655	1.54	0.62	8.20E-02	9.72E-01
protein phosphatase 1J	ENSMUSG00000002228	1.54	0.62	3.17E-02	6.30E-01
predicted gene 16223	ENSMUSG00000067285	1.54	0.62	6.52E-02	8.86E-01
major facilitator superfamily domain containing 7A	ENSMUSG00000029490	1.54	0.62	3.69E-03	1.67E-01
RIKEN cDNA 3425401B19 gene	ENSMUSG00000071540	1.53	0.62	5.19E-02	8.04E-01
KDEL (Lys-Asp-Glu-Leu) endoplasmic reticulum protein retention receptor 3	ENSMUSG00000010830	1.53	0.62	9.36E-03	3.13E-01
six transmembrane epithelial antigen of the prostate 1	ENSMUSG00000015652	1.53	0.62	6.65E-02	8.95E-01
2'-5' oligoadenylate synthetase 1A	ENSMUSG00000052776	1.53	0.61	2.84E-02	5.93E-01
adhesion G protein-coupled receptor F2	ENSMUSG00000057899	1.53	0.61	5.88E-02	8.58E-01
cholinergic receptor. nicotinic. beta polypeptide 4	ENSMUSG00000035200	1.52	0.61	8.39E-03	2.89E-01
melanocortin 2 receptor accessory protein	ENSMUSG00000039956	1.52	0.60	6.77E-02	9.03E-01
protein tyrosine phosphatase. receptor type. H	ENSMUSG00000035429	1.52	0.60	9.65E-03	3.20E-01
Rho GTPase activating protein 40	ENSMUSG00000074625	1.51	0.60	2.20E-02	5.16E-01
epidermal growth factor	ENSMUSG00000028017	1.51	0.60	1.46E-03	9.01E-02
stabilin 2	ENSMUSG00000035459	1.51	0.60	5.96E-03	2.27E-01
X-linked lymphocyte-regulated 3C	ENSMUSG00000058147	1.51	0.60	6.68E-03	2.47E-01
membrane anchored junction protein	ENSMUSG00000024786	1.51	0.60	3.24E-02	6.32E-01
interleukin 11	ENSMUSG00000004371	1.51	0.60	8.69E-02	9.89E-01
RIKEN cDNA 1700071M16 gene	ENSMUSG00000090307	1.51	0.59	2.68E-03	1.35E-01
ubiquitination factor E4B. opposite strand 3	ENSMUSG00000085286	1.51	0.59	7.91E-02	9.62E-01
solute carrier family 17 (sodium-dependent inorganic phosphate cotransporter). member 8	ENSMUSG00000019935	1.51	0.59	1.09E-03	7.22E-02
cyclic nucleotide gated channel alpha 3	ENSMUSG00000026114	1.51	0.59	1.35E-03	8.48E-02
hemolytic complement	ENSMUSG00000026874	1.51	0.59	6.65E-02	8.95E-01
H19. imprinted maternally expressed transcript	ENSMUSG00000000031	1.51	0.59	7.31E-02	9.22E-01
nitric oxide synthase 2. inducible	ENSMUSG00000020826	1.51	0.59	6.43E-02	8.80E-01
predicted gene. 17399	ENSMUSG00000097402	1.50	0.59	2.91E-02	5.98E-01
eva-1 homolog C (C. elegans)	ENSMUSG00000039903	1.50	0.59	2.96E-03	1.44E-01
schlafen 8	ENSMUSG00000035208	1.50	0.59	7.66E-03	2.69E-01
atypical chemokine receptor 2	ENSMUSG00000044534	1.50	0.59	9.36E-03	3.13E-01
spermatogenesis associated 4	ENSMUSG00000031518	1.50	0.58	8.58E-02	9.84E-01
CD300 molecule like family member D5	ENSMUSG00000089722	1.49	0.58	4.99E-02	7.85E-01
aryl-hydrocarbon receptor repressor	ENSMUSG00000021575	1.49	0.58	6.42E-03	2.39E-01
kinesin family member 18B	ENSMUSG00000051378	1.49	0.58	4.02E-02	7.11E-01
Sp110 nuclear body protein	ENSMUSG00000070034	1.49	0.58	4.39E-02	7.36E-01
small nucleolar RNA. H/ACA box 31	ENSMUSG00000065147	1.49	0.57	6.29E-02	8.78E-01

RIKEN cDNA A330015K06 gene	ENSMUSG00000104093	1.49	0.57	2.36E-02	5.30E-01
proline-rich transmembrane protein 2	ENSMUSG00000045114	1.49	0.57	1.33E-02	3.90E-01
serine (or cysteine) peptidase inhibitor. clade A (alpha-1 antiproteinase. antitrypsin). member 9	ENSMUSG00000058260	1.48	0.57	1.88E-03	1.06E-01
ISG15 ubiquitin-like modifier	ENSMUSG00000035692	1.48	0.57	2.72E-03	1.37E-01
formyl peptide receptor 2	ENSMUSG00000052270	1.48	0.57	2.36E-02	5.30E-01
secreted frizzled-related protein 4	ENSMUSG00000021319	1.48	0.57	2.95E-03	1.44E-01
complement component 1. r subcomponent A	ENSMUSG00000055172	1.48	0.57	6.89E-03	2.51E-01
predicted gene 11110	ENSMUSG00000079414	1.48	0.57	6.89E-03	2.51E-01
RIKEN cDNA D930048N14 gene	ENSMUSG00000052563	1.48	0.56	3.02E-03	1.46E-01
collagen. type IV. alpha 4	ENSMUSG00000067158	1.47	0.56	1.50E-02	4.16E-01
coiled-coil domain containing 152	ENSMUSG00000091119	1.47	0.56	6.72E-02	9.01E-01
DEAD (Asp-Glu-Ala-Asp) box polypeptide 60	ENSMUSG00000037921	1.47	0.56	1.06E-02	3.38E-01
transient receptor potential cation channel. subfamily A. member 1	ENSMUSG00000032769	1.47	0.55	1.26E-02	3.78E-01
arginine vasopressin receptor 1A	ENSMUSG00000020123	1.47	0.55	5.11E-03	2.07E-01
WD repeat domain 86	ENSMUSG00000055235	1.47	0.55	1.02E-02	3.29E-01
noncompact myelin associated protein	ENSMUSG00000043924	1.47	0.55	1.41E-02	4.03E-01
predicted gene 6034	ENSMUSG00000073407	1.47	0.55	1.72E-02	4.47E-01
predicted gene 5532	ENSMUSG00000073535	1.47	0.55	4.69E-02	7.60E-01
vanin 1	ENSMUSG00000037440	1.47	0.55	6.52E-02	8.86E-01
lipin 3	ENSMUSG00000027412	1.46	0.55	2.55E-02	5.55E-01
RIKEN cDNA 6030407O03 gene	ENSMUSG00000100301	1.46	0.55	1.83E-02	4.64E-01
carboxylesterase 1D	ENSMUSG00000056973	1.46	0.54	3.70E-02	6.78E-01
kallikrein related-peptidase 6	ENSMUSG00000050063	1.46	0.54	1.65E-03	9.82E-02
cation channel sperm associated auxiliary subunit delta	ENSMUSG00000040828	1.45	0.54	4.64E-02	7.58E-01
RIKEN cDNA 4930431P03 gene	ENSMUSG00000075042	1.45	0.54	6.14E-02	8.74E-01
RIKEN cDNA 4833423E24 gene	ENSMUSG00000075217	1.45	0.54	2.59E-03	1.32E-01
interferon induced protein with tetratricopeptide repeats 1B like 2	ENSMUSG00000067297	1.45	0.54	4.54E-03	1.89E-01
phosphatidylcholine transfer protein	ENSMUSG00000020553	1.45	0.54	1.81E-02	4.62E-01
anoctamin 7	ENSMUSG00000034107	1.45	0.54	8.58E-02	9.84E-01
beaded filament structural protein 2. phakinin	ENSMUSG00000032556	1.45	0.54	1.59E-02	4.29E-01
apolipoprotein A-I	ENSMUSG00000032083	1.45	0.54	3.39E-02	6.49E-01
RIKEN cDNA 4930447C04 gene	ENSMUSG00000021098	1.45	0.54	8.82E-04	5.97E-02
microfibrillar-associated protein 2	ENSMUSG00000060572	1.45	0.54	3.02E-03	1.46E-01
PR domain containing 9	ENSMUSG00000051977	1.45	0.54	2.51E-03	1.29E-01
BCLl2-like 15	ENSMUSG00000044165	1.45	0.53	4.52E-02	7.47E-01
chondroadherin	ENSMUSG00000039084	1.45	0.53	7.31E-02	9.22E-01
GATA binding protein 2	ENSMUSG00000015053	1.44	0.53	9.10E-04	6.14E-02
brachyury 2	ENSMUSG00000058159	1.44	0.53	3.71E-02	6.79E-01
hypocretin	ENSMUSG00000045471	1.44	0.53	2.85E-02	5.93E-01
Iroquois homeobox 2	ENSMUSG00000001504	1.44	0.53	3.82E-02	6.93E-01
LIM homeobox transcription factor 1 beta	ENSMUSG00000038765	1.44	0.53	8.23E-02	9.72E-01
small regulatory polypeptide of amino acid response	ENSMUSG00000028475	1.44	0.52	3.42E-02	6.49E-01
RIKEN cDNA 2700046A07 gene	ENSMUSG00000041789	1.43	0.52	5.64E-02	8.42E-01
tripartite motif-containing 12C	ENSMUSG00000057143	1.43	0.52	3.83E-03	1.70E-01
cyclin A2	ENSMUSG00000027715	1.43	0.52	8.97E-03	3.05E-01
protease. serine 30	ENSMUSG00000024124	1.43	0.52	1.60E-02	4.29E-01
arachidonate 5-lipoxygenase	ENSMUSG00000025701	1.43	0.52	1.63E-02	4.33E-01
T-box 1	ENSMUSG00000009097	1.43	0.52	3.89E-02	7.00E-01
proline rich 32	ENSMUSG00000037086	1.43	0.52	5.47E-02	8.26E-01
peptidylprolyl isomerase (cyclophilin)-like 6	ENSMUSG00000078451	1.43	0.52	1.90E-03	1.07E-01
fibronectin type III domain containing 8	ENSMUSG00000018844	1.43	0.52	2.86E-03	1.41E-01
leucine rich repeat containing 29	ENSMUSG00000041679	1.43	0.52	6.90E-03	2.51E-01
predicted gene 12992	ENSMUSG00000085667	1.43	0.52	1.42E-02	4.04E-01
prokineticin receptor 1	ENSMUSG00000049409	1.43	0.52	4.62E-02	7.58E-01

orthodenticle homeobox 2	ENSMUSG00000021848	1.43	0.52	4.91E-03	2.01E-01
leucine rich repeat and Ig domain containing 4	ENSMUSG00000044505	1.43	0.52	1.08E-02	3.43E-01
WD40 repeat domain 95	ENSMUSG00000029658	1.43	0.51	6.52E-02	8.86E-01
RIKEN cDNA 9130019P16 gene	ENSMUSG00000073067	1.43	0.51	7.87E-02	9.62E-01
tudor domain containing 6	ENSMUSG00000040140	1.43	0.51	1.56E-03	9.46E-02
testis derived transcript	ENSMUSG00000029552	1.43	0.51	2.09E-03	1.13E-01
collagen. type VII. alpha 1	ENSMUSG00000025650	1.43	0.51	5.02E-03	2.05E-01
killer cell lectin-like receptor subfamily G. member 1	ENSMUSG00000030114	1.42	0.51	1.10E-02	3.48E-01
RIKEN cDNA 4930522L14 gene	ENSMUSG00000072762	1.42	0.51	4.62E-03	1.93E-01
pleckstrin homology domain containing. family N member 1	ENSMUSG00000078485	1.42	0.51	1.55E-03	9.43E-02
dopamine receptor D5	ENSMUSG00000039358	1.42	0.51	4.11E-03	1.79E-01
calpastatin	ENSMUSG00000021585	1.42	0.51	1.82E-03	1.04E-01
forkhead box B2	ENSMUSG00000056829	1.42	0.51	5.86E-02	8.58E-01
dynein light chain Tctex-type 1F	ENSMUSG00000095677	1.42	0.50	1.69E-03	1.00E-01
atypical chemokine receptor 4	ENSMUSG00000079355	1.42	0.50	2.18E-02	5.15E-01
RIKEN cDNA B230217O12 gene	ENSMUSG00000097785	1.42	0.50	2.04E-03	1.12E-01
polyamine oxidase (exo-N4-amino)	ENSMUSG00000025464	1.42	0.50	4.46E-03	1.88E-01
SH2 domain containing 6	ENSMUSG00000052631	1.42	0.50	4.78E-02	7.68E-01
gremlin 1. DAN family BMP antagonist	ENSMUSG00000074934	1.42	0.50	9.63E-04	6.46E-02
chloride intracellular channel 3	ENSMUSG00000015093	1.42	0.50	1.54E-02	4.21E-01
collagen. type VIII. alpha 2	ENSMUSG00000056174	1.42	0.50	8.80E-04	5.97E-02
RIKEN cDNA 5830444B04 gene	ENSMUSG00000084803	1.42	0.50	2.84E-02	5.93E-01
RIKEN cDNA 9530059O14 gene	ENSMUSG00000097736	1.42	0.50	4.79E-02	7.68E-01
histocompatibility 2. Q region locus 10	ENSMUSG00000067235	1.41	0.50	5.33E-03	2.09E-01
guanine nucleotide binding protein (G protein). gamma 8	ENSMUSG00000063594	1.41	0.50	7.17E-02	9.19E-01
collagen. type III. alpha 1	ENSMUSG00000026043	1.41	0.50	2.00E-03	1.11E-01
interferon lambda receptor 1	ENSMUSG00000062157	1.41	0.50	4.00E-02	7.10E-01
pyrroline-5-carboxylate reductase 1	ENSMUSG00000025140	1.41	0.50	6.12E-03	2.31E-01
arylalkylamine N-acetyltransferase	ENSMUSG00000020804	1.41	0.50	1.69E-02	4.43E-01
predicted gene 6445	ENSMUSG00000100141	1.41	0.50	2.99E-02	6.08E-01
hemoglobin. theta 1B	ENSMUSG00000073063	1.41	0.50	6.24E-02	8.78E-01
keratin 8	ENSMUSG00000049382	1.41	0.50	2.04E-02	5.00E-01
kelch-like 30	ENSMUSG00000026308	1.41	0.50	7.01E-02	9.11E-01
Ly6/Plaur domain containing 3	ENSMUSG00000057454	1.41	0.49	3.72E-02	6.81E-01
solute carrier family 27 (fatty acid transporter). member 6	ENSMUSG00000024600	1.41	0.49	8.08E-02	9.68E-01
claudin 2	ENSMUSG00000047230	1.41	0.49	3.46E-03	1.61E-01
crumbs family member 3	ENSMUSG00000044279	1.41	0.49	5.43E-02	8.23E-01
myopalladin	ENSMUSG00000020067	1.41	0.49	8.44E-02	9.80E-01
coiled-coil domain containing 38	ENSMUSG00000036168	1.41	0.49	3.22E-02	6.32E-01
solute carrier family 25 (mitochondrial carrier. adenine nucleotide translocator). member 13	ENSMUSG00000015112	1.40	0.49	4.80E-03	1.98E-01
RIKEN cDNA D630039A03 gene	ENSMUSG00000052117	1.40	0.49	7.15E-02	9.19E-01
solute carrier family 26. member 11	ENSMUSG00000039908	1.40	0.49	1.70E-03	1.00E-01
pipecolic acid oxidase	ENSMUSG00000017453	1.40	0.49	3.19E-03	1.52E-01
calpain 9	ENSMUSG00000031981	1.40	0.49	6.07E-02	8.69E-01
solute carrier family 47. member 1	ENSMUSG00000010122	1.40	0.48	1.83E-03	1.05E-01
solute carrier family 25. member 45	ENSMUSG00000024818	1.40	0.48	3.60E-03	1.65E-01
RIKEN cDNA 6430550D23 gene	ENSMUSG00000074646	1.40	0.48	1.61E-02	4.29E-01
lipase. member O2	ENSMUSG00000087303	1.40	0.48	4.80E-02	7.69E-01
2'-5' oligoadenylate synthetase 1C	ENSMUSG00000001166	1.40	0.48	5.88E-02	8.58E-01
centrin 4	ENSMUSG00000045031	1.40	0.48	1.71E-03	1.00E-01
mab-21-like 1 (C. elegans)	ENSMUSG00000056947	1.40	0.48	2.31E-03	1.21E-01
bone morphogenetic protein 2	ENSMUSG00000027358	1.40	0.48	3.73E-03	1.67E-01
cysteinyl leukotriene receptor 1	ENSMUSG00000052821	1.40	0.48	1.83E-02	4.64E-01
Fanconi anemia. complementation group C	ENSMUSG00000021461	1.40	0.48	3.53E-03	1.63E-01

trafficking regulator of GLUT4 (SLC2A4) 1	ENSMUSG00000046275	1.40	0.48	8.17E-02	9.72E-01
RIKEN cDNA 1110015O18 gene	ENSMUSG00000098659	1.39	0.48	2.80E-03	1.39E-01
Sp7 transcription factor 7	ENSMUSG00000060284	1.39	0.48	5.91E-03	2.26E-01
membrane protein. palmitoylated 4 (MAGUK p55 subfamily member 4)	ENSMUSG00000079550	1.39	0.48	2.02E-02	4.99E-01
Emx2 opposite strand/antisense transcript (non-protein coding)	ENSMUSG00000087095	1.39	0.48	4.05E-03	1.77E-01
paired related homeobox 2	ENSMUSG00000039476	1.39	0.48	3.00E-02	6.08E-01
RIKEN cDNA 4933404O12 gene	ENSMUSG00000097908	1.39	0.48	7.49E-04	5.12E-02
cholinergic receptor. nicotinic. alpha polypeptide 3	ENSMUSG00000032303	1.39	0.48	5.92E-03	2.26E-01
heat shock protein 1-like	ENSMUSG00000007033	1.39	0.48	1.75E-02	4.52E-01
Rho guanine nucleotide exchange factor (GEF) 15	ENSMUSG00000052921	1.39	0.48	1.07E-03	7.12E-02
shisa family member 3	ENSMUSG00000050010	1.39	0.48	1.28E-02	3.81E-01
carbonic anhydrase 13	ENSMUSG00000027555	1.39	0.47	4.18E-03	1.81E-01
3-hydroxybutyrate dehydrogenase. type 2	ENSMUSG00000028167	1.39	0.47	1.02E-02	3.30E-01
predicted gene 10814	ENSMUSG00000097404	1.39	0.47	7.16E-02	9.19E-01
solute carrier family 39 (metal ion transporter). member 5	ENSMUSG00000039878	1.39	0.47	7.92E-02	9.62E-01
zinc finger protein 947	ENSMUSG00000063383	1.39	0.47	2.93E-02	6.00E-01
C-type lectin domain family 2. member d	ENSMUSG00000030157	1.39	0.47	4.85E-03	2.00E-01
nexilin	ENSMUSG00000039103	1.39	0.47	1.00E-02	3.25E-01
G protein-coupled receptor 149	ENSMUSG00000043441	1.38	0.47	2.43E-03	1.26E-01
signal peptide. CUB domain. EGF-like 2	ENSMUSG00000007279	1.38	0.47	1.23E-02	3.73E-01
amine oxidase. copper containing 3	ENSMUSG00000019326	1.38	0.47	4.90E-02	7.78E-01
claudin 34C1	ENSMUSG00000079450	1.38	0.47	6.75E-03	2.48E-01
DENN/MADD domain containing 2D	ENSMUSG00000027901	1.38	0.47	3.91E-02	7.02E-01
NLR family. CARD domain containing 5	ENSMUSG00000074151	1.38	0.47	3.35E-02	6.43E-01
RAB37. member RAS oncogene family	ENSMUSG00000020732	1.38	0.47	1.09E-02	3.45E-01
adenosine A2a receptor	ENSMUSG00000020178	1.38	0.46	1.53E-03	9.36E-02
endothelin 1	ENSMUSG00000021367	1.38	0.46	1.22E-02	3.72E-01
transglutaminase 3. E polypeptide	ENSMUSG00000027401	1.38	0.46	1.16E-02	3.63E-01
RIKEN cDNA 5430416N02 gene	ENSMUSG00000097772	1.38	0.46	8.52E-03	2.93E-01
maestro heat-like repeat family member 7	ENSMUSG00000047502	1.38	0.46	2.06E-03	1.12E-01
collagen. type XXVII. alpha 1	ENSMUSG00000045672	1.38	0.46	2.13E-03	1.14E-01
wingless-type MMTV integration site family. member 3	ENSMUSG00000000125	1.38	0.46	2.03E-02	5.00E-01
interferon-induced protein 44	ENSMUSG00000028037	1.38	0.46	5.67E-02	8.43E-01
ST8 alpha-N-acetyl-neuraminide alpha-2.8-sialyltransferase 6	ENSMUSG00000003418	1.37	0.46	2.95E-03	1.44E-01
X-linked lymphocyte-regulated 3B	ENSMUSG00000073125	1.37	0.46	1.15E-02	3.60E-01
serine/threonine/tyrosine interaction protein	ENSMUSG00000053205	1.37	0.46	6.91E-02	9.05E-01
phosphoinositide-interacting regulator of transient receptor potential channels	ENSMUSG00000048070	1.37	0.46	4.42E-03	1.88E-01
tachykinin receptor 3	ENSMUSG00000028172	1.37	0.46	1.49E-03	9.20E-02
zinc finger protein 457	ENSMUSG00000055341	1.37	0.46	1.18E-02	3.65E-01
fyn-related kinase	ENSMUSG00000019779	1.37	0.46	3.69E-02	6.78E-01
RIKEN cDNA 4930581F22 gene	ENSMUSG00000070315	1.37	0.46	5.16E-03	2.08E-01
potassium inwardly-rectifying channel. subfamily J. member 5	ENSMUSG00000032034	1.37	0.46	1.19E-02	3.66E-01
regulator of G-protein signaling 11	ENSMUSG00000024186	1.37	0.46	1.63E-03	9.76E-02
predicted gene 13293	ENSMUSG00000086006	1.37	0.46	1.06E-02	3.38E-01
collagen. type XXIV. alpha 1	ENSMUSG00000028197	1.37	0.46	1.38E-02	3.97E-01
myosin. light polypeptide 1	ENSMUSG00000061816	1.37	0.46	7.87E-02	9.62E-01
sterile alpha motif domain containing 3	ENSMUSG00000051354	1.37	0.45	1.42E-02	4.05E-01
pancreatic lipase	ENSMUSG00000046008	1.37	0.45	7.48E-02	9.34E-01
tudor domain containing 9	ENSMUSG00000054003	1.37	0.45	8.68E-02	9.89E-01
predicted gene 5577	ENSMUSG00000084950	1.37	0.45	3.57E-03	1.64E-01
small nucleolar RNA. C/D box 22	ENSMUSG00000065087	1.37	0.45	6.02E-02	8.68E-01
RIKEN cDNA A830036E02 gene	ENSMUSG00000084890	1.37	0.45	3.01E-03	1.46E-01

X-linked lymphocyte-regulated 3A	ENSMUSG00000057836	1.37	0.45	1.31E-02	3.86E-01
adenosine deaminase	ENSMUSG00000017697	1.37	0.45	6.58E-02	8.92E-01
acetyl-Coenzyme A acyltransferase 1A	ENSMUSG00000036138	1.37	0.45	1.40E-03	8.72E-02
uncharacterized LOC102637720	ENSMUSG00000090235	1.37	0.45	8.39E-02	9.80E-01
RIKEN cDNA C530005A16 gene	ENSMUSG00000085408	1.36	0.45	3.46E-03	1.61E-01
WD repeat domain 63	ENSMUSG00000043020	1.36	0.45	1.59E-02	4.29E-01
vaccinia related kinase 2	ENSMUSG00000064090	1.36	0.45	3.90E-02	7.01E-01
zinc finger protein 953	ENSMUSG00000098905	1.36	0.45	4.09E-02	7.12E-01
RIKEN cDNA 1700024F13 gene	ENSMUSG00000097709	1.36	0.45	6.50E-02	8.86E-01
oviductal glycoprotein 1	ENSMUSG00000074340	1.36	0.45	8.70E-03	2.98E-01
TRAF-interacting protein with forkhead-associated domain. family member B	ENSMUSG00000049625	1.36	0.45	1.04E-02	3.34E-01
ankyrin repeat domain 23	ENSMUSG00000067653	1.36	0.45	5.64E-02	8.42E-01
prolactin receptor	ENSMUSG00000005268	1.36	0.44	1.58E-03	9.48E-02
histocompatibility 2. Q region locus 7	ENSMUSG00000060550	1.36	0.44	1.23E-02	3.73E-01
androglobin	ENSMUSG00000050994	1.36	0.44	1.51E-02	4.17E-01
estrogen-related receptor gamma	ENSMUSG00000026610	1.36	0.44	1.78E-03	1.03E-01
cytochrome P450. family 2. subfamily j. polypeptide 12	ENSMUSG00000081225	1.36	0.44	2.20E-02	5.15E-01
SLIT and NTRK-like family. member 6	ENSMUSG00000045871	1.36	0.44	5.30E-03	2.09E-01
dopamine receptor D2	ENSMUSG00000032259	1.36	0.44	3.70E-03	1.67E-01
interferon. alpha-inducible protein 27 like 2A	ENSMUSG00000079017	1.36	0.44	6.13E-02	8.73E-01
sphingosine-1-phosphate phosphotase 2	ENSMUSG00000032908	1.35	0.44	2.51E-03	1.29E-01
sterile alpha motif domain containing 5	ENSMUSG00000060487	1.35	0.44	3.66E-03	1.66E-01
serine (or cysteine) peptidase inhibitor. clade B. member 1b	ENSMUSG00000051029	1.35	0.44	1.08E-02	3.43E-01
lecithin-retinol acyltransferase (phosphatidylcholine-retinol-O-acyltransferase)	ENSMUSG00000028003	1.35	0.44	1.32E-02	3.90E-01
interleukin 17 receptor B	ENSMUSG00000015966	1.35	0.44	1.35E-02	3.93E-01
G protein-coupled receptor 157	ENSMUSG00000047875	1.35	0.44	1.39E-02	4.00E-01
SH3 domain containing ring finger 2	ENSMUSG00000057719	1.35	0.44	1.43E-02	4.05E-01
sushi domain containing 3	ENSMUSG00000021384	1.35	0.44	4.99E-02	7.85E-01
angiotensinogen (serpin peptidase inhibitor. clade A. member 8)	ENSMUSG00000031980	1.35	0.44	1.71E-03	1.00E-01
solute carrier family 36 (proton/amino acid symporter). member 2	ENSMUSG00000020264	1.35	0.44	6.41E-03	2.39E-01
bone marrow stromal cell antigen 2	ENSMUSG00000046718	1.35	0.44	1.96E-02	4.87E-01
tripartite motif-containing 68	ENSMUSG00000073968	1.35	0.44	9.61E-03	3.20E-01
complement component 3	ENSMUSG00000024164	1.35	0.43	9.36E-03	3.13E-01
interferon-induced protein with tetratricopeptide repeats 1	ENSMUSG00000034459	1.35	0.43	1.66E-02	4.38E-01
fibrinogen C domain containing 1	ENSMUSG00000026841	1.35	0.43	1.91E-03	1.07E-01
tetratricopeptide repeat domain 39A	ENSMUSG00000028555	1.35	0.43	6.77E-03	2.48E-01
synaptotagmin-like 5	ENSMUSG00000054453	1.35	0.43	4.46E-03	1.88E-01
acyl-Coenzyme A dehydrogenase family. member 12	ENSMUSG00000042647	1.35	0.43	1.24E-02	3.73E-01
predicted gene 15663	ENSMUSG00000085282	1.34	0.43	4.04E-03	1.77E-01
proprotein convertase subtilisin/kexin type 4	ENSMUSG00000020131	1.34	0.43	4.34E-03	1.86E-01
collagen. type XIV. alpha 1	ENSMUSG00000022371	1.34	0.43	1.89E-02	4.73E-01
predicted gene 3636	ENSMUSG00000091754	1.34	0.43	2.28E-02	5.23E-01
RIKEN cDNA 4930444P10 gene	ENSMUSG00000067795	1.34	0.43	7.25E-02	9.21E-01
RNA-binding region (RNP1. RRM) containing 3	ENSMUSG00000027981	1.34	0.43	2.70E-03	1.36E-01
zinc finger protein 36	ENSMUSG00000044786	1.34	0.43	7.51E-03	2.65E-01
SCO-spondin	ENSMUSG00000029797	1.34	0.43	2.03E-02	5.00E-01
tumor necrosis factor receptor superfamily. member 18	ENSMUSG00000041954	1.34	0.42	2.36E-02	5.30E-01
T cell specific GTPase 2	ENSMUSG00000078921	1.34	0.42	3.79E-02	6.92E-01
klotho	ENSMUSG00000058488	1.34	0.42	2.82E-03	1.40E-01
troponin T2. cardiac	ENSMUSG00000026414	1.34	0.42	5.19E-03	2.08E-01
G-protein coupled receptor 88	ENSMUSG00000068696	1.34	0.42	2.58E-03	1.32E-01

interferon induced protein with tetratricpeptide repeats 1B like 1	ENSMUSG00000079339	1.34	0.42	6.38E-03	2.38E-01
G protein-coupled receptor 21	ENSMUSG00000053164	1.34	0.42	3.91E-02	7.02E-01
armadillo-like helical domain containing 1	ENSMUSG00000060268	1.34	0.42	4.66E-02	7.58E-01
solute carrier family 16 (monocarboxylic acid transporters). member 8	ENSMUSG00000032988	1.34	0.42	5.24E-02	8.09E-01
collagen. type XVI. alpha 1	ENSMUSG00000040690	1.34	0.42	3.89E-03	1.72E-01
RIKEN cDNA E130311K13 gene	ENSMUSG00000048581	1.34	0.42	4.43E-03	1.88E-01
transforming growth factor. beta receptor III-like	ENSMUSG00000089736	1.34	0.42	1.63E-02	4.33E-01
butyrylcholinesterase	ENSMUSG00000027792	1.34	0.42	5.20E-03	2.08E-01
adenosine A2b receptor	ENSMUSG00000018500	1.33	0.42	5.54E-03	2.16E-01
neurotensin	ENSMUSG00000019890	1.33	0.42	3.87E-03	1.71E-01
amylase 1. salivary	ENSMUSG00000074264	1.33	0.42	4.01E-03	1.75E-01
transmembrane channel-like gene family 4	ENSMUSG00000019734	1.33	0.42	1.60E-02	4.29E-01
fucosyltransferase 4	ENSMUSG00000049307	1.33	0.42	4.66E-02	7.58E-01
non-SMC condensin I complex. subunit H	ENSMUSG00000034906	1.33	0.41	4.01E-02	7.10E-01
HtrA serine peptidase 3	ENSMUSG00000029096	1.33	0.41	6.71E-03	2.47E-01
phosphatidylinositol-4-phosphate 5-kinase-like 1	ENSMUSG00000046854	1.33	0.41	1.07E-02	3.39E-01
signal transducing adaptor family member 2	ENSMUSG00000038781	1.33	0.41	3.81E-02	6.93E-01
RIKEN cDNA 1810024B03 gene	ENSMUSG00000044145	1.33	0.41	3.88E-02	7.00E-01
RAD54 like (S. cerevisiae)	ENSMUSG00000028702	1.33	0.41	6.40E-02	8.78E-01
Eph receptor A8	ENSMUSG00000028661	1.33	0.41	1.22E-02	3.72E-01
tRNA methyltransferase 13	ENSMUSG00000033439	1.33	0.41	9.84E-03	3.23E-01
T-box 3	ENSMUSG00000018604	1.33	0.41	1.83E-02	4.63E-01
kinesin light chain 3	ENSMUSG00000040714	1.33	0.41	3.61E-02	6.68E-01
early B cell factor 4	ENSMUSG00000053552	1.33	0.41	5.23E-03	2.09E-01
protein kinase. membrane associated tyrosine/threonine 1	ENSMUSG00000023908	1.33	0.41	1.61E-02	4.29E-01
RIKEN cDNA 9930012K11 gene	ENSMUSG00000044551	1.33	0.41	1.71E-02	4.47E-01
proline rich 22	ENSMUSG00000090273	1.33	0.41	7.84E-02	9.60E-01
RAS p21 protein activator 4	ENSMUSG00000004952	1.33	0.41	1.16E-02	3.61E-01
growth factor receptor bound protein 7	ENSMUSG00000019312	1.33	0.41	1.92E-02	4.81E-01
potassium voltage-gated channel. subfamily H (eag-related). member 8	ENSMUSG00000035580	1.33	0.41	3.15E-02	6.27E-01
CD14 antigen	ENSMUSG00000051439	1.33	0.41	3.60E-02	6.67E-01
CD59b antigen	ENSMUSG00000068686	1.33	0.41	2.50E-02	5.51E-01
RIKEN cDNA 1700040D17 gene	ENSMUSG00000097515	1.33	0.41	3.64E-02	6.72E-01
chemokine (C-X-C motif) ligand 10	ENSMUSG00000034855	1.33	0.41	8.33E-02	9.79E-01
thymidylate synthase	ENSMUSG00000025747	1.32	0.41	5.22E-02	8.08E-01
thymidine kinase 1	ENSMUSG00000025574	1.32	0.41	5.71E-02	8.47E-01
retbindin	ENSMUSG00000048617	1.32	0.40	2.11E-02	5.11E-01
neutrophil cytosolic factor 2	ENSMUSG00000026480	1.32	0.40	2.90E-02	5.98E-01
solute carrier family 35. member G1	ENSMUSG00000044026	1.32	0.40	2.15E-02	5.13E-01
purinergic receptor P2Y. G-protein coupled. 14	ENSMUSG00000036381	1.32	0.40	2.48E-02	5.49E-01
solute carrier family 6. member 16	ENSMUSG00000094152	1.32	0.40	2.87E-02	5.94E-01
zinc finger. B-box domain containing	ENSMUSG00000034151	1.32	0.40	5.84E-02	8.57E-01
spindlin family. member 4	ENSMUSG00000071722	1.32	0.40	2.99E-02	6.08E-01
B9 protein domain 1. opposite strand	ENSMUSG00000060808	1.32	0.40	8.47E-02	9.82E-01
synapse differentiation inducing 1 like	ENSMUSG00000071234	1.32	0.40	6.06E-03	2.29E-01
myelocytomatosis oncogene	ENSMUSG00000022346	1.32	0.40	9.16E-03	3.10E-01
RIKEN cDNA 1500015O10 gene	ENSMUSG00000026051	1.32	0.40	2.57E-02	5.58E-01
thyroid stimulating hormone receptor	ENSMUSG00000020963	1.32	0.40	4.79E-02	7.68E-01
interferon regulatory factor 7	ENSMUSG00000025498	1.32	0.40	4.88E-02	7.77E-01
testis-specific serine kinase 4	ENSMUSG00000007591	1.32	0.40	7.21E-02	9.20E-01
actinin alpha 2	ENSMUSG00000052374	1.32	0.40	6.26E-03	2.35E-01
cadherin-related family member 1	ENSMUSG00000021803	1.32	0.40	8.76E-03	2.99E-01
cytochrome P450. family 4. subfamily f. polypeptide 17	ENSMUSG00000091586	1.32	0.40	1.39E-02	4.00E-01
two pore segment channel 2	ENSMUSG00000048677	1.32	0.40	2.15E-02	5.13E-01

ankyrin repeat domain 37	ENSMUSG00000050914	1.32	0.40	2.19E-02	5.15E-01
cytochrome P450. family 2. subfamily s. polypeptide 1	ENSMUSG00000040703	1.32	0.40	1.45E-02	4.06E-01
telomere repeat binding bouquet formation protein 1	ENSMUSG00000052616	1.32	0.40	8.23E-02	9.72E-01
lymphocyte antigen 75	ENSMUSG00000026980	1.31	0.39	3.13E-02	6.24E-01
synaptotagmin-like 4	ENSMUSG00000031255	1.31	0.39	9.78E-03	3.23E-01
a disintegrin-like and metallopeptidase (reprolysin type) with thrombospondin type 1 motif. 6	ENSMUSG00000046169	1.31	0.39	1.66E-02	4.38E-01
cDNA sequence BC030867	ENSMUSG00000034773	1.31	0.39	6.83E-02	9.05E-01
six transmembrane epithelial antigen of prostate 2	ENSMUSG00000015653	1.31	0.39	5.96E-03	2.27E-01
G patch domain and ankyrin repeats 1	ENSMUSG00000092417	1.31	0.39	1.17E-02	3.64E-01
family with sequence similarity 131. member C	ENSMUSG00000006218	1.31	0.39	2.35E-02	5.30E-01
calcium channel. voltage-dependent. alpha 2/delta subunit 2	ENSMUSG00000010066	1.31	0.39	5.27E-03	2.09E-01
hypoxia inducible factor 3. alpha subunit	ENSMUSG00000004328	1.31	0.39	1.23E-02	3.73E-01
cerebellin 3 precursor protein	ENSMUSG00000040380	1.31	0.39	1.61E-02	4.29E-01
zinc finger protein 738	ENSMUSG00000048280	1.31	0.39	6.36E-03	2.38E-01
tumor necrosis factor receptor superfamily. member 11b (osteoprotegerin)	ENSMUSG00000063727	1.31	0.39	2.16E-02	5.14E-01
membrane bound O-acyltransferase domain containing 4	ENSMUSG00000071113	1.31	0.39	4.46E-02	7.42E-01
lipoma HMGIC fusion partner-like 5	ENSMUSG00000062252	1.31	0.39	1.36E-02	3.96E-01
annexin A1	ENSMUSG00000024659	1.31	0.39	2.99E-02	6.08E-01
RIKEN cDNA C130060K24 gene	ENSMUSG00000029917	1.31	0.39	4.80E-02	7.69E-01
basonuclin 2	ENSMUSG00000028487	1.31	0.39	7.08E-02	9.15E-01
protein disulfide isomerase associated 5	ENSMUSG00000022844	1.31	0.39	4.14E-02	7.13E-01
potassium voltage-gated channel. Isk-related subfamily. gene 4	ENSMUSG00000047330	1.31	0.39	5.16E-02	8.03E-01
major facilitator superfamily domain containing 3	ENSMUSG00000019080	1.30	0.38	1.46E-02	4.09E-01
vomeronasal 2. receptor 87	ENSMUSG00000091511	1.30	0.38	4.70E-02	7.60E-01
transforming growth factor. beta induced	ENSMUSG00000035493	1.30	0.38	1.55E-02	4.21E-01
aspartylglucosaminidase	ENSMUSG00000031521	1.30	0.38	2.00E-02	4.95E-01
dipeptidylpeptidase 4	ENSMUSG00000035000	1.30	0.38	8.28E-02	9.76E-01
CD47 antigen (Rh-related antigen. integrin-associated signal transducer)	ENSMUSG00000055447	1.30	0.38	6.05E-03	2.29E-01
small nucleolar RNA host gene 11	ENSMUSG00000044349	1.30	0.38	5.94E-03	2.27E-01
adenylosuccinate synthetase like 1	ENSMUSG00000011148	1.30	0.38	1.17E-02	3.64E-01
sulfotransferase family 1A. phenol-preferring. member 1	ENSMUSG00000030711	1.30	0.38	1.18E-02	3.65E-01
cut-like homeobox 2	ENSMUSG00000042589	1.30	0.38	7.50E-03	2.65E-01
mutated in colorectal cancers	ENSMUSG00000071856	1.30	0.38	8.32E-03	2.88E-01
TOG array regulator of axonemal microtubules 2	ENSMUSG00000045761	1.30	0.38	9.32E-03	3.13E-01
collagen. type V. alpha 1	ENSMUSG00000026837	1.30	0.38	9.66E-03	3.20E-01
immunoglobulin superfamily. member 10	ENSMUSG00000036334	1.30	0.38	1.06E-02	3.39E-01
RIKEN cDNA 1700029J07 gene	ENSMUSG00000071103	1.30	0.38	1.62E-02	4.32E-01
nicotinamide riboside kinase 1	ENSMUSG00000037847	1.30	0.38	1.97E-02	4.89E-01
RAR-related orphan receptor gamma	ENSMUSG00000028150	1.30	0.38	4.10E-02	7.12E-01
apolipoprotein O-like	ENSMUSG00000025525	1.30	0.38	4.13E-02	7.13E-01
tripartite motif-containing 34A	ENSMUSG00000056144	1.30	0.38	8.29E-02	9.76E-01
chloride intracellular channel 5	ENSMUSG00000023959	1.30	0.37	1.31E-02	3.88E-01
cytochrome P450. family 4. subfamily f. polypeptide 14	ENSMUSG00000024292	1.30	0.37	1.51E-02	4.17E-01
serine/arginine-rich protein specific kinase 3	ENSMUSG00000002007	1.30	0.37	2.22E-02	5.17E-01
kielin/chordin-like protein	ENSMUSG00000059022	1.30	0.37	5.53E-02	8.30E-01
heparan sulfate (glucosamine) 3-O-sulfotransferase 5	ENSMUSG00000044499	1.29	0.37	1.40E-02	4.01E-01
XIAP associated factor 1	ENSMUSG00000040483	1.29	0.37	5.53E-02	8.30E-01
growth arrest specific 5	ENSMUSG00000053332	1.29	0.37	1.11E-02	3.49E-01

cyclic nucleotide binding domain containing 2	ENSMUSG00000038085	1.29	0.37	2.45E-02	5.43E-01
telomerase reverse transcriptase	ENSMUSG00000021611	1.29	0.37	2.15E-02	5.13E-01
nei like 2 (E. coli)	ENSMUSG00000035121	1.29	0.37	5.82E-02	8.57E-01
tuftelin 1	ENSMUSG00000005968	1.29	0.37	2.63E-02	5.65E-01
collagen. type V. alpha 3	ENSMUSG00000004098	1.29	0.37	3.31E-02	6.38E-01
RIKEN cDNA B430212C06 gene	ENSMUSG00000046415	1.29	0.37	5.38E-02	8.17E-01
ret proto-oncogene	ENSMUSG00000030110	1.29	0.37	1.25E-02	3.75E-01
acid phosphatase 5. tartrate resistant	ENSMUSG00000001348	1.29	0.37	6.74E-02	9.01E-01
RIKEN cDNA A330074K22 gene	ENSMUSG00000097960	1.29	0.37	1.22E-02	3.72E-01
nidogen 1	ENSMUSG00000005397	1.29	0.37	1.23E-02	3.73E-01
protein kinase C. eta	ENSMUSG00000021108	1.29	0.37	2.68E-02	5.70E-01
IZUMO family member 4	ENSMUSG00000055862	1.29	0.36	1.32E-02	3.90E-01
solute carrier family 35. member D3	ENSMUSG00000050473	1.29	0.36	1.69E-02	4.42E-01
coiled-coil domain containing 36	ENSMUSG00000047220	1.29	0.36	3.11E-02	6.23E-01
galactosidase. beta 1-like	ENSMUSG00000026200	1.28	0.36	1.57E-02	4.27E-01
MYCBP associated protein	ENSMUSG00000039110	1.28	0.36	2.86E-02	5.94E-01
zinc finger protein 946	ENSMUSG00000071266	1.28	0.36	1.22E-02	3.72E-01
zinc finger protein 57	ENSMUSG00000036036	1.28	0.36	1.25E-02	3.76E-01
chemokine (C-C motif) ligand 28	ENSMUSG00000074715	1.28	0.36	1.35E-02	3.93E-01
zwilch kinetochore protein	ENSMUSG00000032400	1.28	0.36	3.99E-02	7.10E-01
DNA segment. Chr 7. ERATO Doi 443. expressed	ENSMUSG00000030994	1.28	0.36	4.27E-02	7.23E-01
RIKEN cDNA B230307C23 gene	ENSMUSG00000080717	1.28	0.36	4.61E-02	7.56E-01
S100 calcium binding protein A11	ENSMUSG00000027907	1.28	0.36	4.79E-02	7.68E-01
RIKEN cDNA 4933439C10 gene	ENSMUSG00000072893	1.28	0.36	1.47E-02	4.09E-01
diacylglycerol kinase kappa	ENSMUSG00000062393	1.28	0.36	1.38E-02	3.99E-01
tetraspanin 2	ENSMUSG00000027858	1.28	0.36	1.09E-02	3.45E-01
KN motif and ankyrin repeat domains 4	ENSMUSG00000035407	1.28	0.36	1.93E-02	4.81E-01
phospholamban	ENSMUSG00000038583	1.28	0.36	7.92E-02	9.62E-01
ATP-binding cassette. sub-family C (CFTR/MRP). member 9	ENSMUSG00000030249	1.28	0.35	1.73E-02	4.50E-01
transferrin receptor	ENSMUSG00000022797	1.28	0.35	1.14E-02	3.59E-01
fatty acid 2-hydroxylase	ENSMUSG00000033579	1.28	0.35	1.31E-02	3.86E-01
uncoupling protein 3 (mitochondrial. proton carrier)	ENSMUSG00000032942	1.28	0.35	2.65E-02	5.65E-01
Rho guanine nucleotide exchange factor (GEF) 19	ENSMUSG00000028919	1.28	0.35	1.88E-02	4.73E-01
RIKEN cDNA 0610040B10 gene	ENSMUSG00000089889	1.28	0.35	6.54E-02	8.88E-01
Ndufa4. mitochondrial complex associated like 2	ENSMUSG00000040280	1.28	0.35	7.37E-02	9.26E-01
matrix metallopeptidase 2	ENSMUSG00000031740	1.27	0.35	3.26E-02	6.33E-01
opioid receptor. kappa 1	ENSMUSG00000025905	1.27	0.35	1.54E-02	4.21E-01
EF-hand calcium binding domain 12	ENSMUSG00000030321	1.27	0.35	1.90E-02	4.75E-01
chloride intracellular channel 6	ENSMUSG00000022949	1.27	0.35	1.54E-02	4.21E-01
death-associated protein	ENSMUSG00000039168	1.27	0.35	2.12E-02	5.11E-01
protease. serine 41	ENSMUSG00000024114	1.27	0.35	2.28E-02	5.23E-01
CD180 antigen	ENSMUSG00000021624	1.27	0.35	4.67E-02	7.58E-01
WD repeat domain 62	ENSMUSG00000037020	1.27	0.35	7.51E-02	9.36E-01
PDZ and pleckstrin homology domains 1	ENSMUSG00000024227	1.27	0.35	8.22E-02	9.72E-01
prominin 1	ENSMUSG00000029086	1.27	0.34	1.85E-02	4.66E-01
src homology 2 domain-containing transforming protein B	ENSMUSG00000044813	1.27	0.34	2.61E-02	5.63E-01
solute carrier family 1 (neutral amino acid transporter). member 5	ENSMUSG00000001918	1.27	0.34	4.97E-02	7.85E-01
polypeptide N-acetylgalactosaminyltransferase 6	ENSMUSG00000037280	1.27	0.34	2.23E-02	5.18E-01
butyrobetaine (gamma). 2-oxoglutarate dioxygenase 1 (gamma-butyrobetaine hydroxylase)	ENSMUSG00000041660	1.27	0.34	2.60E-02	5.62E-01
regulator of G-protein signaling like 1	ENSMUSG00000042641	1.27	0.34	6.41E-02	8.79E-01
G protein-coupled receptor 15-like	ENSMUSG00000031212	1.27	0.34	2.14E-02	5.13E-01
cingulin	ENSMUSG00000068876	1.27	0.34	2.18E-02	5.15E-01

euchromatic histone methyltransferase 1	ENSMUSG00000036893	1.27	0.34	1.46E-02	4.09E-01
leucine rich repeat containing 10B	ENSMUSG00000090291	1.27	0.34	2.12E-02	5.12E-01
anoctamin 5	ENSMUSG00000055489	1.27	0.34	3.13E-02	6.24E-01
Rhesus blood group-associated C glycoprotein	ENSMUSG00000030549	1.27	0.34	3.26E-02	6.33E-01
torsin family 4. member A	ENSMUSG00000059555	1.27	0.34	4.02E-02	7.11E-01
predicted gene 14164	ENSMUSG00000068062	1.27	0.34	4.07E-02	7.12E-01
solute carrier family 16 (monocarboxylic acid transporters). member 3	ENSMUSG00000025161	1.27	0.34	5.94E-02	8.64E-01
RNA binding motif. single stranded interacting protein	ENSMUSG00000039607	1.26	0.34	1.58E-02	4.28E-01
WD repeat and SOCS box-containing 1	ENSMUSG00000017677	1.26	0.34	1.52E-02	4.19E-01
forkhead box P2	ENSMUSG00000029563	1.26	0.34	1.75E-02	4.52E-01
microsomal glutathione S-transferase 1	ENSMUSG00000008540	1.26	0.34	2.13E-02	5.13E-01
enkurin. TRPC channel interacting protein	ENSMUSG00000026679	1.26	0.34	4.53E-02	7.48E-01
unc-13 homolog C	ENSMUSG00000062151	1.26	0.34	1.51E-02	4.17E-01
transient receptor potential cation channel. subfamily C. member 3	ENSMUSG00000027716	1.26	0.34	2.35E-02	5.30E-01
oligodendrocytic myelin paranodal and inner loop protein	ENSMUSG00000050121	1.26	0.34	2.45E-02	5.43E-01
transmembrane serine protease 7	ENSMUSG00000033177	1.26	0.34	7.89E-02	9.62E-01
calmegin	ENSMUSG00000002190	1.26	0.34	2.63E-02	5.65E-01
histocompatibility 2. T region locus 10	ENSMUSG00000079491	1.26	0.34	2.71E-02	5.74E-01
TAR RNA binding protein 1	ENSMUSG00000090290	1.26	0.34	2.76E-02	5.81E-01
SEC16 homolog B (S. cerevisiae)	ENSMUSG00000026589	1.26	0.34	6.51E-02	8.86E-01
L-3-hydroxyproline dehydratase (trans-)	ENSMUSG00000019718	1.26	0.34	3.50E-02	6.55E-01
RIKEN cDNA 4632427E13 gene	ENSMUSG00000074024	1.26	0.34	3.70E-02	6.78E-01
perilipin 5	ENSMUSG00000011305	1.26	0.34	4.22E-02	7.19E-01
MDS1 and EVI1 complex locus	ENSMUSG00000027684	1.26	0.34	4.96E-02	7.84E-01
F-box protein 5	ENSMUSG00000019773	1.26	0.34	6.50E-02	8.86E-01
hypocretin (orexin) receptor 2	ENSMUSG00000032360	1.26	0.33	3.01E-02	6.10E-01
C-type lectin domain family 3. member b	ENSMUSG00000025784	1.26	0.33	3.67E-02	6.76E-01
membrane metallo endopeptidase	ENSMUSG00000027820	1.26	0.33	2.26E-02	5.23E-01
harbinger transposase derived 1	ENSMUSG00000027243	1.26	0.33	2.76E-02	5.81E-01
roundabout guidance receptor 3	ENSMUSG00000032128	1.26	0.33	3.43E-02	6.49E-01
delta like non-canonical Notch ligand 1	ENSMUSG00000040856	1.26	0.33	1.74E-02	4.51E-01
mohawk homeobox	ENSMUSG00000061013	1.26	0.33	3.76E-02	6.85E-01
phospholipase A2. group IVA (cytosolic. calcium-dependent)	ENSMUSG00000056220	1.26	0.33	5.07E-02	7.94E-01
F-box protein 17	ENSMUSG00000030598	1.26	0.33	8.20E-02	9.72E-01
myelin-associated glycoprotein	ENSMUSG00000036634	1.26	0.33	1.78E-02	4.59E-01
mitogen-activated protein kinase kinase kinase kinase 2	ENSMUSG00000024948	1.26	0.33	1.87E-02	4.70E-01
purinergic receptor P2Y. G-protein coupled 13	ENSMUSG00000036362	1.26	0.33	2.29E-02	5.23E-01
centrosomal protein 89	ENSMUSG00000023072	1.26	0.33	2.59E-02	5.61E-01
nidogen 2	ENSMUSG00000021806	1.26	0.33	3.57E-02	6.63E-01
aryl hydrocarbon receptor nuclear translocator-like 2	ENSMUSG00000040187	1.26	0.33	4.13E-02	7.13E-01
interleukin 3 receptor. alpha chain	ENSMUSG00000068758	1.26	0.33	7.15E-02	9.19E-01
N-deacetylase/N-sulfotransferase (heparin glucosaminyl) 4	ENSMUSG00000027971	1.26	0.33	2.07E-02	5.03E-01
MALT1 paracaspase	ENSMUSG00000032688	1.25	0.33	3.21E-02	6.32E-01
nudix (nucleoside diphosphate linked moiety X)-type motif 12	ENSMUSG00000024228	1.25	0.33	3.28E-02	6.34E-01
collagen. type VI. alpha 4	ENSMUSG00000032572	1.25	0.33	6.35E-02	8.78E-01
collagen. type XVIII. alpha 1	ENSMUSG00000001435	1.25	0.33	2.29E-02	5.23E-01
slingshot protein phosphatase 1	ENSMUSG00000042121	1.25	0.33	2.05E-02	5.01E-01
DNA segment. Chr 3. ERATO Doi 751. expressed	ENSMUSG00000025766	1.25	0.33	2.15E-02	5.13E-01
amyloid beta (A4) precursor protein-binding. family B. member 1 interacting protein	ENSMUSG00000026786	1.25	0.33	3.53E-02	6.59E-01
RIKEN cDNA C330013E15 gene	ENSMUSG00000097093	1.25	0.33	8.72E-02	9.89E-01
collagen. type V. alpha 2	ENSMUSG00000026042	1.25	0.32	3.16E-02	6.27E-01

BarH-like homeobox 2	ENSMUSG00000032033	1.25	0.32	3.45E-02	6.50E-01
NCK-associated protein 1	ENSMUSG00000027002	1.25	0.32	1.96E-02	4.88E-01
zinc finger protein 599	ENSMUSG00000062794	1.25	0.32	3.63E-02	6.70E-01
coiled-coil domain containing 180	ENSMUSG00000035539	1.25	0.32	4.10E-02	7.12E-01
superoxide dismutase 2. mitochondrial	ENSMUSG00000006818	1.25	0.32	2.02E-02	4.99E-01
NK6 homeobox 2	ENSMUSG00000041309	1.25	0.32	2.44E-02	5.43E-01
zonadhesin	ENSMUSG00000079173	1.25	0.32	6.26E-02	8.78E-01
GIPC PDZ domain containing family. member 2	ENSMUSG00000039131	1.25	0.32	8.14E-02	9.72E-01
PATJ. crumbs cell polarity complex component	ENSMUSG00000061859	1.25	0.32	2.53E-02	5.53E-01
hyaluronan and proteoglycan link protein 2	ENSMUSG00000004894	1.25	0.32	2.61E-02	5.63E-01
collagen. type VI. alpha 2	ENSMUSG00000020241	1.25	0.32	2.35E-02	5.30E-01
LY6/PLAUR domain containing 6	ENSMUSG00000050447	1.25	0.32	2.53E-02	5.53E-01
regulator of G-protein signaling 9	ENSMUSG00000020599	1.25	0.32	2.56E-02	5.56E-01
a disintegrin-like and metallopeptidase (reprolysin type) with thrombospondin type 1 motif. 10	ENSMUSG00000024299	1.25	0.32	2.57E-02	5.57E-01
CD59a antigen	ENSMUSG00000032679	1.25	0.32	2.83E-02	5.93E-01
Slc2a4 regulator. pseudogene	ENSMUSG00000085028	1.25	0.32	3.30E-02	6.37E-01
RIKEN cDNA 1810022K09 gene	ENSMUSG00000078784	1.25	0.32	3.46E-02	6.51E-01
arginine vasopressin	ENSMUSG00000037727	1.25	0.32	2.21E-02	5.16E-01
nescient helix loop helix 2	ENSMUSG00000048540	1.25	0.32	5.67E-02	8.43E-01
RIKEN cDNA 2700046G09 gene	ENSMUSG00000097787	1.25	0.32	6.73E-02	9.01E-01
family with sequence similarity 205. member A1	ENSMUSG00000078721	1.25	0.32	7.05E-02	9.13E-01
coagulation factor V	ENSMUSG00000026579	1.25	0.32	4.06E-02	7.12E-01
SEC14-like lipid binding 5	ENSMUSG00000091712	1.25	0.32	4.54E-02	7.49E-01
zinc finger protein 990	ENSMUSG00000078503	1.25	0.32	5.50E-02	8.29E-01
EF-hand domain (C-terminal) containing 1	ENSMUSG00000041809	1.25	0.32	8.53E-02	9.84E-01
leukocyte receptor cluster (LRC) member 8	ENSMUSG00000035545	1.24	0.32	2.29E-02	5.23E-01
pre B cell leukemia homeobox 3	ENSMUSG00000038718	1.24	0.32	2.54E-02	5.53E-01
X-ray repair complementing defective repair in Chinese hamster cells 2	ENSMUSG00000028933	1.24	0.32	3.25E-02	6.33E-01
elastin	ENSMUSG00000029675	1.24	0.32	4.66E-02	7.58E-01
cyclic nucleotide gated channel beta 1	ENSMUSG00000031789	1.24	0.32	6.21E-02	8.78E-01
solute carrier family 26. member 8	ENSMUSG00000036196	1.24	0.32	8.00E-02	9.66E-01
solute carrier family 25. member 51	ENSMUSG00000045973	1.24	0.32	2.36E-02	5.30E-01
protein phosphatase 1. regulatory subunit 3B	ENSMUSG00000046794	1.24	0.32	5.54E-02	8.32E-01
aldehyde dehydrogenase 1 family. member B1	ENSMUSG00000035561	1.24	0.31	3.42E-02	6.49E-01
caprin family member 2	ENSMUSG00000030309	1.24	0.31	3.45E-02	6.50E-01
predicted gene 15328	ENSMUSG00000086095	1.24	0.31	8.05E-02	9.67E-01
RIKEN cDNA 9330179D12 gene	ENSMUSG00000097166	1.24	0.31	8.12E-02	9.71E-01
RIKEN cDNA 6230400D17 gene	ENSMUSG00000097577	1.24	0.31	8.72E-02	9.89E-01
N-acylsphingosine amidohydrolase 2	ENSMUSG00000024887	1.24	0.31	2.99E-02	6.08E-01
NIMA (never in mitosis gene a)-related expressed kinase 8	ENSMUSG00000017405	1.24	0.31	6.07E-02	8.69E-01
URB1 ribosome biogenesis 1 homolog (S. cerevisiae)	ENSMUSG00000039929	1.24	0.31	3.31E-02	6.38E-01
PDZ domain containing 7	ENSMUSG00000074818	1.24	0.31	4.28E-02	7.25E-01
sphingomyelin synthase 2	ENSMUSG00000050931	1.24	0.31	4.32E-02	7.27E-01
retinol binding protein 4. plasma	ENSMUSG00000024990	1.24	0.31	5.44E-02	8.23E-01
solute carrier family 16 (monocarboxylic acid transporters). member 9	ENSMUSG00000037762	1.24	0.31	6.41E-02	8.79E-01
secreted frizzled-related sequence protein 5	ENSMUSG00000018822	1.24	0.31	4.51E-02	7.47E-01
capping protein regulator and myosin 1 linker 3	ENSMUSG00000022211	1.24	0.31	2.69E-02	5.72E-01
DENN/MADD domain containing 6B	ENSMUSG00000015377	1.24	0.31	2.84E-02	5.93E-01
hyperpolarization-activated. cyclic nucleotide-gated K+ 3	ENSMUSG00000028051	1.24	0.31	2.92E-02	6.00E-01
RIKEN cDNA A530058N18 gene	ENSMUSG00000087694	1.24	0.31	4.08E-02	7.12E-01
male germ cell-associated kinase	ENSMUSG00000021363	1.24	0.31	4.84E-02	7.73E-01
cytotoxic granule-associated RNA binding protein 1	ENSMUSG00000071337	1.24	0.31	2.66E-02	5.68E-01

HPS3. biogenesis of lysosomal organelles complex 2 subunit 1	ENSMUSG00000027615	1.24	0.31	3.25E-02	6.33E-01
tetratricopeptide repeat domain 9	ENSMUSG00000042734	1.24	0.31	3.16E-02	6.27E-01
family with sequence similarity 205. member A3	ENSMUSG00000093996	1.24	0.31	6.03E-02	8.68E-01
predicted gene 15612	ENSMUSG00000085828	1.24	0.31	8.51E-02	9.84E-01
transcription termination factor. RNA polymerase II	ENSMUSG00000033222	1.24	0.31	8.22E-02	9.72E-01
maternally expressed 3	ENSMUSG00000021268	1.24	0.31	2.75E-02	5.80E-01
galanin receptor 1	ENSMUSG00000024553	1.24	0.31	4.17E-02	7.13E-01
prenyl (solanesyl) diphosphate synthase. subunit 1	ENSMUSG00000026784	1.24	0.31	4.23E-02	7.20E-01
zinc finger protein 647	ENSMUSG00000054967	1.24	0.31	6.34E-02	8.78E-01
glutamate receptor. ionotropic. NMDA1 (zeta 1). opposite strand	ENSMUSG00000085830	1.24	0.31	6.61E-02	8.94E-01
vesicle-associated membrane protein 1	ENSMUSG00000030337	1.23	0.30	2.87E-02	5.94E-01
predicted gene 867	ENSMUSG00000050157	1.23	0.30	7.74E-02	9.55E-01
chloride channel. voltage-sensitive 1	ENSMUSG00000029862	1.23	0.30	7.90E-02	9.62E-01
myosin XVIIIb	ENSMUSG00000072720	1.23	0.30	6.03E-02	8.68E-01
ciliary rootlet coiled-coil. rootletin family member 2	ENSMUSG00000084989	1.23	0.30	3.33E-02	6.41E-01
stimulated by retinoic acid gene 6	ENSMUSG00000032327	1.23	0.30	5.15E-02	8.03E-01
THAP domain containing 6	ENSMUSG00000102644	1.23	0.30	6.64E-02	8.95E-01
collagen. type IV. alpha 2	ENSMUSG00000031503	1.23	0.30	3.13E-02	6.24E-01
MOB kinase activator 3B	ENSMUSG00000073910	1.23	0.30	4.63E-02	7.58E-01
piezo-type mechanosensitive ion channel component 2	ENSMUSG00000041482	1.23	0.30	4.94E-02	7.83E-01
interferon gamma induced GTPase	ENSMUSG00000078853	1.23	0.30	7.44E-02	9.31E-01
adenosine deaminase. tRNA-specific 1	ENSMUSG00000031949	1.23	0.30	4.17E-02	7.14E-01
galactose-1-phosphate uridyl transferase	ENSMUSG00000036073	1.23	0.30	5.32E-02	8.13E-01
protocadherin gamma subfamily A. 1	ENSMUSG00000103144	1.23	0.30	5.48E-02	8.27E-01
collagen. type XI. alpha 2	ENSMUSG00000024330	1.23	0.30	4.18E-02	7.14E-01
trafficking protein. kinesin binding 2	ENSMUSG00000026028	1.23	0.30	3.28E-02	6.35E-01
acid phosphatase 6. lysophosphatidic	ENSMUSG00000028093	1.23	0.30	4.43E-02	7.40E-01
cysteine and tyrosine-rich protein 1	ENSMUSG00000041134	1.23	0.30	5.17E-02	8.03E-01
cDNA sequence BC030500	ENSMUSG00000049946	1.23	0.30	4.06E-02	7.12E-01
membrane integral NOTCH2 associated receptor 1	ENSMUSG00000039313	1.23	0.30	4.24E-02	7.21E-01
retinoic acid receptor responder (tazarotene induced) 2	ENSMUSG00000009281	1.23	0.29	4.85E-02	7.74E-01
sterile alpha motif domain containing 11	ENSMUSG00000096351	1.23	0.29	6.14E-02	8.74E-01
sideroflexin 2	ENSMUSG00000025036	1.23	0.29	5.36E-02	8.17E-01
zinc finger protein 51	ENSMUSG00000023892	1.23	0.29	5.92E-02	8.64E-01
hemicentin 2	ENSMUSG00000055632	1.23	0.29	6.31E-02	8.78E-01
tumor necrosis factor (ligand) superfamily. member 10	ENSMUSG00000039304	1.23	0.29	8.25E-02	9.73E-01
tubulin-specific chaperone E	ENSMUSG00000039233	1.22	0.29	4.12E-02	7.12E-01
limb region 1 like	ENSMUSG00000022999	1.22	0.29	5.87E-02	8.58E-01
histocompatibility 2. Q region locus 2	ENSMUSG00000091705	1.22	0.29	6.40E-02	8.78E-01
parvalbumin	ENSMUSG00000005716	1.22	0.29	4.89E-02	7.78E-01
protein phosphatase 1. regulatory inhibitor subunit 1B	ENSMUSG00000061718	1.22	0.29	3.83E-02	6.94E-01
pitrilysin metallepetidase 1	ENSMUSG00000021193	1.22	0.29	4.04E-02	7.12E-01
RIKEN cDNA 2300009A05 gene	ENSMUSG00000032403	1.22	0.29	5.74E-02	8.49E-01
poly (ADP-ribose) polymerase family. member 3	ENSMUSG00000023249	1.22	0.29	6.75E-02	9.01E-01
family with sequence similarity 210. member B	ENSMUSG00000027495	1.22	0.29	4.17E-02	7.13E-01
ATP-binding cassette. sub-family A (ABC1). member 7	ENSMUSG00000035722	1.22	0.29	4.43E-02	7.40E-01
dysferlin	ENSMUSG00000033788	1.22	0.29	6.68E-02	8.98E-01
myelin oligodendrocyte glycoprotein	ENSMUSG00000076439	1.22	0.29	4.29E-02	7.25E-01
a disintegrin-like and metallopeptidase (reprolysin type) with thrombospondin type 1 motif. 20	ENSMUSG00000022449	1.22	0.29	4.75E-02	7.66E-01

transmembrane protein 117	ENSMUSG00000063296	1.22	0.29	5.52E-02	8.30E-01
FCH and double SH3 domains 1	ENSMUSG00000038524	1.22	0.29	5.94E-02	8.64E-01
3-hydroxy-3-methylglutaryl-Coenzyme A synthase 2	ENSMUSG00000027875	1.22	0.29	4.21E-02	7.19E-01
family with sequence similarity 221. member A	ENSMUSG00000047115	1.22	0.29	8.36E-02	9.80E-01
myelin and lymphocyte protein. T cell differentiation protein	ENSMUSG00000027375	1.22	0.28	4.09E-02	7.12E-01
neuro-oncological ventral antigen 1	ENSMUSG00000021047	1.22	0.28	4.14E-02	7.13E-01
Fras1 related extracellular matrix protein 1	ENSMUSG00000059049	1.22	0.28	5.30E-02	8.11E-01
RIKEN cDNA A730046J19 gene	ENSMUSG00000085139	1.22	0.28	7.00E-02	9.10E-01
family with sequence similarity 114. member A1	ENSMUSG00000029185	1.22	0.28	6.21E-02	8.78E-01
UBX domain protein 10	ENSMUSG00000043621	1.22	0.28	6.65E-02	8.95E-01
collagen. type IV. alpha 1	ENSMUSG00000031502	1.22	0.28	4.43E-02	7.40E-01
SLIT-ROBO Rho GTPase activating protein 1	ENSMUSG00000020121	1.22	0.28	4.68E-02	7.58E-01
glycerophosphodiester phosphodiesterase domain containing 2	ENSMUSG00000019359	1.21	0.28	5.52E-02	8.30E-01
coiled-coil domain containing 8	ENSMUSG00000041117	1.21	0.28	7.02E-02	9.11E-01
potassium channel tetramerisation domain containing 9	ENSMUSG00000034327	1.21	0.28	5.83E-02	8.57E-01
retinoblastoma binding protein 8. endonuclease	ENSMUSG00000041238	1.21	0.28	8.76E-02	9.91E-01
sema domain. immunoglobulin domain (Ig). short basic domain. secreted. (semaphorin) 3C	ENSMUSG00000028780	1.21	0.28	5.11E-02	7.97E-01
DEP domain containing MTOR-interacting protein	ENSMUSG00000022419	1.21	0.28	5.23E-02	8.09E-01
dystrophia myotonica-protein kinase	ENSMUSG00000030409	1.21	0.28	5.25E-02	8.09E-01
CDC42 effector protein (Rho GTPase binding) 2	ENSMUSG00000045664	1.21	0.28	6.72E-02	9.01E-01
olfactomedin 3	ENSMUSG00000027965	1.21	0.28	4.89E-02	7.78E-01
ring finger protein 38	ENSMUSG00000035696	1.21	0.28	5.02E-02	7.88E-01
ankyrin repeat domain 24	ENSMUSG00000054708	1.21	0.28	5.07E-02	7.94E-01
diphthamine biosynethesis 7	ENSMUSG00000026975	1.21	0.28	5.25E-02	8.09E-01
methylenetetrahydrofolate dehydrogenase (NADP+ dependent) 2-like	ENSMUSG00000029376	1.21	0.28	6.61E-02	8.94E-01
PERP. TP53 apoptosis effector	ENSMUSG00000019851	1.21	0.28	6.79E-02	9.05E-01
CD93 antigen	ENSMUSG00000027435	1.21	0.28	7.20E-02	9.20E-01
migration and invasion inhibitory protein	ENSMUSG00000029022	1.21	0.28	7.39E-02	9.26E-01
castor zinc finger 1	ENSMUSG00000028977	1.21	0.28	8.57E-02	9.84E-01
cadherin-related family member 4	ENSMUSG00000032595	1.21	0.27	8.53E-02	9.84E-01
sema domain. immunoglobulin domain (Ig). short basic domain. secreted. (semaphorin) 3F	ENSMUSG00000034684	1.21	0.27	6.24E-02	8.78E-01
regulator of microtubule dynamics 1	ENSMUSG00000028229	1.21	0.27	7.00E-02	9.10E-01
MORN repeat containing 1	ENSMUSG00000029049	1.21	0.27	8.23E-02	9.72E-01
ras responsive element binding protein 1	ENSMUSG00000039087	1.21	0.27	5.01E-02	7.86E-01
endothelin converting enzyme-like 1	ENSMUSG00000026247	1.21	0.27	5.08E-02	7.94E-01
arrestin domain containing 1	ENSMUSG00000026972	1.21	0.27	6.81E-02	9.05E-01
damage specific DNA binding protein 2	ENSMUSG00000002109	1.21	0.27	8.68E-02	9.89E-01
acetylcholinesterase	ENSMUSG00000023328	1.21	0.27	5.08E-02	7.94E-01
cytochrome c oxidase subunit 7B	ENSMUSG00000031231	1.21	0.27	5.16E-02	8.03E-01
glutathione reductase	ENSMUSG00000031584	1.21	0.27	5.27E-02	8.10E-01
lysine methyltransferase 5C	ENSMUSG00000059851	1.21	0.27	6.37E-02	8.78E-01
TatD DNase domain containing 3	ENSMUSG00000026632	1.21	0.27	6.87E-02	9.05E-01
cerebral endothelial cell adhesion molecule	ENSMUSG00000039787	1.21	0.27	7.79E-02	9.57E-01
interferon-induced protein with tetratricopeptide repeats 3B	ENSMUSG00000062488	1.21	0.27	8.01E-02	9.66E-01
phosphoglucomutase 2	ENSMUSG00000025791	1.21	0.27	5.34E-02	8.14E-01
UDP galactosyltransferase 8A	ENSMUSG00000032854	1.21	0.27	5.39E-02	8.19E-01
molybdenum cofactor synthesis 2	ENSMUSG00000015536	1.21	0.27	5.82E-02	8.57E-01
sperm acrosome associated 6	ENSMUSG00000080316	1.20	0.27	5.96E-02	8.64E-01
zinc finger protein 783	ENSMUSG00000072653	1.20	0.27	6.03E-02	8.68E-01
kinase insert domain protein receptor	ENSMUSG00000062960	1.20	0.27	6.05E-02	8.69E-01
X-linked myotubular myopathy gene 1	ENSMUSG00000031337	1.20	0.27	7.90E-02	9.62E-01
glutathione peroxidase 8 (putative)	ENSMUSG00000021760	1.20	0.27	8.68E-02	9.89E-01

RUN and FYVE domain-containing 2	ENSMUSG00000020070	1.20	0.27	5.40E-02	8.19E-01
Mir124-1 host gene (non-protein coding)	ENSMUSG00000097545	1.20	0.27	5.47E-02	8.26E-01
von Willebrand factor C domain-containing protein 2-like	ENSMUSG00000045648	1.20	0.27	6.28E-02	8.78E-01
G patch domain containing 1	ENSMUSG00000063808	1.20	0.27	6.22E-02	8.78E-01
GULP. engulfment adaptor PTB domain containing 1	ENSMUSG00000056870	1.20	0.27	7.88E-02	9.62E-01
TBC1 domain family. member 19	ENSMUSG00000039178	1.20	0.27	5.95E-02	8.64E-01
T cell. immune regulator 1. ATPase. H+ transporting. lysosomal V0 protein A3	ENSMUSG00000001750	1.20	0.27	6.75E-02	9.01E-01
ELOVL family member 7. elongation of long chain fatty acids (yeast)	ENSMUSG00000021696	1.20	0.27	6.73E-02	9.01E-01
RAD1 checkpoint DNA exonuclease	ENSMUSG00000022248	1.20	0.27	7.75E-02	9.55E-01
cerebellar degeneration-related 2	ENSMUSG00000030878	1.20	0.27	7.24E-02	9.21E-01
zinc finger. MYM-type 6	ENSMUSG00000042408	1.20	0.27	5.85E-02	8.57E-01
cilia and flagella associated protein 65	ENSMUSG00000047021	1.20	0.27	6.60E-02	8.93E-01
methyltransferase like 25	ENSMUSG00000036009	1.20	0.27	8.37E-02	9.80E-01
G protein-coupled receptor 101	ENSMUSG00000036357	1.20	0.26	5.70E-02	8.45E-01
ciliary rootlet coiled-coil. rootletin	ENSMUSG00000040860	1.20	0.26	5.99E-02	8.67E-01
RIKEN cDNA A330023F24 gene	ENSMUSG00000096929	1.20	0.26	6.26E-02	8.78E-01
mitochondrial ribosomal protein L35	ENSMUSG00000052962	1.20	0.26	6.44E-02	8.80E-01
RAS. guanyl releasing protein 2	ENSMUSG00000032946	1.20	0.26	6.52E-02	8.86E-01
leucine rich repeat containing 55	ENSMUSG00000075224	1.20	0.26	6.88E-02	9.05E-01
gap junction protein. beta 1	ENSMUSG00000047797	1.20	0.26	7.48E-02	9.34E-01
signal peptide. CUB domain. EGF-like 3	ENSMUSG00000038677	1.20	0.26	7.52E-02	9.37E-01
follistatin-like 5	ENSMUSG00000034098	1.20	0.26	5.96E-02	8.64E-01
RIKEN cDNA 3110039I08 gene	ENSMUSG00000074415	1.20	0.26	6.12E-02	8.73E-01
TRAF3 interacting protein 2	ENSMUSG00000019842	1.20	0.26	8.46E-02	9.82E-01
regulator of G-protein signalling 22	ENSMUSG00000037627	1.20	0.26	6.01E-02	8.67E-01
miRNA containing gene	ENSMUSG00000097391	1.20	0.26	6.64E-02	8.95E-01
ATPase. class VI. type 11B	ENSMUSG00000037400	1.20	0.26	6.12E-02	8.73E-01
lipoma HMGIC fusion partner-like 3	ENSMUSG00000106379	1.20	0.26	6.16E-02	8.75E-01
isochorismatase domain containing 1	ENSMUSG00000024601	1.20	0.26	6.36E-02	8.78E-01
tachykinin receptor 1	ENSMUSG00000030043	1.20	0.26	6.41E-02	8.79E-01
methyl-CpG binding domain protein 1	ENSMUSG00000024561	1.20	0.26	6.71E-02	9.01E-01
polymerase (RNA) I polypeptide B	ENSMUSG00000027395	1.20	0.26	7.08E-02	9.15E-01
predicted gene 14169	ENSMUSG00000086118	1.20	0.26	7.92E-02	9.62E-01
procollagen lysine. 2-oxoglutarate 5-dioxygenase 2	ENSMUSG00000032374	1.20	0.26	8.38E-02	9.80E-01
solute carrier family 26 (sulfate transporter). member 2	ENSMUSG00000034320	1.20	0.26	7.21E-02	9.20E-01
family with sequence similarity 177. member A	ENSMUSG00000095595	1.20	0.26	7.31E-02	9.22E-01
UV stimulated scaffold protein A	ENSMUSG00000037355	1.20	0.26	7.46E-02	9.33E-01
regulator of telomere elongation helicase 1	ENSMUSG00000038685	1.20	0.26	7.58E-02	9.43E-01
family with sequence similarity 107. member A	ENSMUSG00000021750	1.19	0.26	6.37E-02	8.78E-01
Rho guanine nucleotide exchange factor (GEF) 40	ENSMUSG00000004562	1.19	0.26	6.86E-02	9.05E-01
centrosomal protein 295	ENSMUSG00000046111	1.19	0.26	7.27E-02	9.21E-01
melanoma associated antigen (mutated) 1-like 1	ENSMUSG00000042515	1.19	0.26	7.93E-02	9.62E-01
FERM domain containing 3	ENSMUSG00000049122	1.19	0.26	8.67E-02	9.89E-01
chemokine (C-X-C motif) ligand 12	ENSMUSG00000061353	1.19	0.26	6.61E-02	8.94E-01
serine/threonine kinase 19	ENSMUSG00000061207	1.19	0.26	6.96E-02	9.08E-01
synaptopodin 2	ENSMUSG00000050315	1.19	0.26	7.38E-02	9.26E-01
vascular endothelial growth factor D	ENSMUSG00000031380	1.19	0.26	7.77E-02	9.57E-01
asparagine-linked glycosylation 6 (alpha-1.3.-glucosyltransferase)	ENSMUSG00000073792	1.19	0.26	7.79E-02	9.57E-01
predicted gene 11681	ENSMUSG00000075437	1.19	0.26	7.92E-02	9.62E-01
glutamate receptor interacting protein 2	ENSMUSG00000030098	1.19	0.25	7.32E-02	9.22E-01
potassium voltage-gated channel. shaker-related subfamily. beta member 3	ENSMUSG00000018470	1.19	0.25	7.78E-02	9.57E-01

ribosomal protein S6 kinase. polypeptide 2	ENSMUSG00000024830	1.19	0.25	7.82E-02	9.59E-01
family with sequence similarity 214. member A	ENSMUSG00000034858	1.19	0.25	6.98E-02	9.09E-01
small integral membrane protein 17	ENSMUSG00000093536	1.19	0.25	7.38E-02	9.26E-01
cilia and flagella associated protein 44	ENSMUSG00000071550	1.19	0.25	7.36E-02	9.26E-01
cofilin 2. muscle	ENSMUSG00000062929	1.19	0.25	7.20E-02	9.20E-01
zinc finger. CCHC domain containing 7	ENSMUSG00000035649	1.19	0.25	7.60E-02	9.44E-01
WD repeat domain 66	ENSMUSG00000029442	1.19	0.25	8.38E-02	9.80E-01
PNN interacting serine/arginine-rich	ENSMUSG00000028248	1.19	0.25	7.20E-02	9.20E-01
formin binding protein 4	ENSMUSG00000008200	1.19	0.25	7.47E-02	9.34E-01
cadherin 11 pseudogene	ENSMUSG00000071793	1.19	0.25	8.19E-02	9.72E-01
choroideremia-like	ENSMUSG00000078185	1.19	0.25	8.23E-02	9.72E-01
ankyrin repeat domain 34B	ENSMUSG00000045034	1.19	0.25	7.88E-02	9.62E-01
chimerin 2	ENSMUSG00000004633	1.19	0.25	8.07E-02	9.67E-01
zinc finger protein of the cerebellum 1	ENSMUSG00000032368	1.19	0.25	8.23E-02	9.72E-01
transmembrane protein 63a	ENSMUSG00000026519	1.19	0.25	8.36E-02	9.80E-01
sigma non-opioid intracellular receptor 1	ENSMUSG00000036078	1.19	0.25	8.51E-02	9.84E-01
A kinase (PRKA) anchor protein 8	ENSMUSG00000024045	1.19	0.25	7.74E-02	9.55E-01
PAX3 and PAX7 binding protein 1	ENSMUSG00000022974	1.19	0.25	8.14E-02	9.72E-01
CDK5 and Abl enzyme substrate 2	ENSMUSG00000038990	1.19	0.25	8.15E-02	9.72E-01
A kinase (PRKA) anchor protein 8-like	ENSMUSG00000002625	1.18	0.24	7.97E-02	9.65E-01
CXXC finger 4	ENSMUSG00000044365	1.18	0.24	8.39E-02	9.80E-01
tripartite motif-containing 39	ENSMUSG00000045409	1.18	0.24	8.55E-02	9.84E-01
serine/arginine-rich splicing factor 5	ENSMUSG00000021134	1.18	0.24	8.25E-02	9.73E-01
ectonucleotide pyrophosphatase/phosphodiesterase 2	ENSMUSG00000022425	1.18	0.24	8.30E-02	9.76E-01
proteolipid protein (myelin) 1	ENSMUSG00000031425	1.18	0.24	8.29E-02	9.76E-01
aldehyde dehydrogenase family 3. subfamily A2	ENSMUSG00000010025	1.18	0.24	8.75E-02	9.91E-01
synaptoporin	ENSMUSG00000056296	-0.24	0.85	8.44E-02	9.80E-01
transmembrane protein 198	ENSMUSG00000051703	-0.24	0.85	8.59E-02	9.84E-01
reticulon 4 receptor-like 1	ENSMUSG00000045287	-0.24	0.85	8.42E-02	9.80E-01
ribosomal protein, large P2	ENSMUSG00000025508	-0.24	0.85	8.59E-02	9.84E-01
leucine rich repeat containing 73	ENSMUSG00000071073	-0.24	0.85	8.66E-02	9.89E-01
transmembrane protein 121B	ENSMUSG00000094626	-0.24	0.85	8.42E-02	9.80E-01
guanosine monophosphate reductase	ENSMUSG00000000253	-0.24	0.84	8.33E-02	9.79E-01
APC membrane recruitment 2	ENSMUSG00000021986	-0.24	0.84	8.59E-02	9.84E-01
serum response factor	ENSMUSG00000015605	-0.24	0.84	8.00E-02	9.66E-01
metallothionein 1	ENSMUSG00000031765	-0.25	0.84	7.74E-02	9.55E-01
lysozyme 2	ENSMUSG00000069516	-0.25	0.84	8.51E-02	9.84E-01
NMDA receptor synaptonuclear signaling and neuronal migration factor	ENSMUSG00000006476	-0.25	0.84	7.59E-02	9.44E-01
leucine rich repeat and Ig domain containing 1	ENSMUSG00000049556	-0.25	0.84	7.48E-02	9.34E-01
LIM homeobox protein 2	ENSMUSG00000000247	-0.25	0.84	7.79E-02	9.57E-01
phosphotriesterase related	ENSMUSG00000026730	-0.25	0.84	7.30E-02	9.22E-01
DnaJ heat shock protein family (Hsp40) member B5	ENSMUSG00000036052	-0.25	0.84	7.36E-02	9.26E-01
glycerol-3-phosphate dehydrogenase 1 (soluble)	ENSMUSG00000023019	-0.25	0.84	7.58E-02	9.43E-01
solute carrier family 6 (neurotransmitter transporter), member 20A	ENSMUSG00000036814	-0.25	0.84	7.94E-02	9.62E-01
PARK2 co-regulated	ENSMUSG00000037196	-0.25	0.84	8.07E-02	9.67E-01
Rab interacting lysosomal protein-like 2	ENSMUSG00000029401	-0.25	0.84	8.47E-02	9.82E-01
protein phosphatase 1, regulatory subunit 35	ENSMUSG00000029725	-0.25	0.84	8.63E-02	9.87E-01
vascular cell adhesion molecule 1	ENSMUSG00000027962	-0.25	0.84	7.39E-02	9.26E-01
somatostatin receptor 3	ENSMUSG00000044933	-0.25	0.84	7.84E-02	9.60E-01
neurogranin	ENSMUSG00000053310	-0.25	0.84	6.74E-02	9.01E-01
heat shock protein 8	ENSMUSG00000041548	-0.25	0.84	7.23E-02	9.21E-01
interleukin 17 receptor D	ENSMUSG00000040717	-0.25	0.84	8.45E-02	9.82E-01
Fraser extracellular matrix complex subunit 1	ENSMUSG00000034687	-0.26	0.84	6.98E-02	9.09E-01
adenylate cyclase activating polypeptide 1	ENSMUSG00000024256	-0.26	0.84	6.87E-02	9.05E-01

N(alpha)-acetyltransferase 38, NatC auxiliary subunit	ENSMUSG00000059278	-0.26	0.84	7.72E-02	9.55E-01
RIKEN cDNA 1110065P20 gene	ENSMUSG00000078570	-0.26	0.84	8.16E-02	9.72E-01
ArfGAP with GTPase domain, ankyrin repeat and PH domain 2	ENSMUSG00000025422	-0.26	0.84	6.16E-02	8.75E-01
mevalonate (diphospho) decarboxylase	ENSMUSG00000006517	-0.26	0.84	7.21E-02	9.20E-01
abhydrolase domain containing 17A	ENSMUSG00000003346	-0.26	0.84	6.20E-02	8.78E-01
pyruvate dehydrogenase kinase, isoenzyme 4	ENSMUSG00000019577	-0.26	0.84	7.15E-02	9.19E-01
PR domain containing 16	ENSMUSG00000039410	-0.26	0.84	7.73E-02	9.55E-01
ribosomal protein L35	ENSMUSG00000062997	-0.26	0.84	7.88E-02	9.62E-01
cadherin, EGF LAG seven-pass G-type receptor 1	ENSMUSG00000016028	-0.26	0.84	8.60E-02	9.84E-01
family with sequence similarity 171, member A2	ENSMUSG00000034685	-0.26	0.83	6.06E-02	8.69E-01
RNA binding motif protein 12 B2	ENSMUSG00000052137	-0.26	0.83	6.82E-02	9.05E-01
retinol binding protein 1, cellular	ENSMUSG00000046402	-0.26	0.83	7.07E-02	9.15E-01
a disintegrin-like and metallopeptidase (reprolysin type) with thrombospondin type 1 motif, 9	ENSMUSG00000030022	-0.26	0.83	7.98E-02	9.65E-01
tetraspanin 18	ENSMUSG00000027217	-0.26	0.83	8.40E-02	9.80E-01
transducer of ERBB2, 2	ENSMUSG00000048546	-0.26	0.83	6.27E-02	8.78E-01
mex3 RNA binding family member D	ENSMUSG00000048696	-0.26	0.83	6.43E-02	8.80E-01
atypical chemokine receptor 3	ENSMUSG00000044337	-0.26	0.83	6.94E-02	9.06E-01
vacuolar protein sorting 37B	ENSMUSG00000066278	-0.26	0.83	7.13E-02	9.19E-01
Sec31 homolog A (S. cerevisiae)	ENSMUSG00000035325	-0.27	0.83	5.69E-02	8.44E-01
actin, alpha 1, skeletal muscle	ENSMUSG00000031972	-0.27	0.83	8.01E-02	9.66E-01
NHS-like 1	ENSMUSG00000039835	-0.27	0.83	5.72E-02	8.47E-01
regulator of G-protein signaling 14	ENSMUSG00000052087	-0.27	0.83	5.81E-02	8.57E-01
dishevelled-binding antagonist of beta-catenin 2	ENSMUSG00000048826	-0.27	0.83	5.93E-02	8.64E-01
adrenergic receptor, beta 1	ENSMUSG00000035283	-0.27	0.83	6.05E-02	8.69E-01
endonuclease G	ENSMUSG00000015337	-0.27	0.83	8.09E-02	9.68E-01
vexin	ENSMUSG00000067879	-0.27	0.83	5.31E-02	8.13E-01
sosondowah ankyrin repeat domain family member A	ENSMUSG00000044352	-0.27	0.83	5.17E-02	8.03E-01
glycosyltransferase 8 domain containing 2	ENSMUSG00000020251	-0.27	0.83	7.06E-02	9.13E-01
solute carrier family 5 (sodium iodide symporter), member 5	ENSMUSG00000000792	-0.27	0.83	5.98E-02	8.66E-01
regulator of G-protein signaling 16	ENSMUSG00000026475	-0.27	0.83	6.18E-02	8.77E-01
histocompatibility 2, T region locus 23	ENSMUSG00000067212	-0.27	0.83	7.19E-02	9.20E-01
family with sequence similarity 180, member A	ENSMUSG00000047420	-0.27	0.83	7.83E-02	9.60E-01
palmdelphin	ENSMUSG00000033377	-0.27	0.83	6.03E-02	8.68E-01
heat shock protein 1	ENSMUSG00000004951	-0.27	0.83	7.95E-02	9.63E-01
neurogenic differentiation 6	ENSMUSG00000037984	-0.27	0.83	6.85E-02	9.05E-01
SERTA domain containing 1	ENSMUSG00000008384	-0.28	0.83	6.40E-02	8.78E-01
RNA, 7SK, nuclear	ENSMUSG00000065037	-0.28	0.83	6.36E-02	8.78E-01
glutamate receptor, ionotropic, NMDA2A (epsilon 1)	ENSMUSG00000059003	-0.28	0.83	4.69E-02	7.60E-01
phosphoglycolate phosphatase	ENSMUSG00000043445	-0.28	0.83	4.88E-02	7.77E-01
integrin alpha 4	ENSMUSG00000027009	-0.28	0.83	5.43E-02	8.23E-01
interferon-induced protein with tetratricopeptide repeats 2	ENSMUSG00000045932	-0.28	0.83	5.45E-02	8.25E-01
RIKEN cDNA 2900079G21 gene	ENSMUSG00000087038	-0.28	0.83	8.35E-02	9.80E-01
pleiotrophin	ENSMUSG00000029838	-0.28	0.82	4.46E-02	7.42E-01
candidate tumor suppressor in ovarian cancer 2	ENSMUSG00000038268	-0.28	0.82	5.60E-02	8.39E-01
glyoxalase 1	ENSMUSG00000024026	-0.28	0.82	4.41E-02	7.40E-01
solute carrier family 5 (inositol transporters), member 3	ENSMUSG00000089774	-0.28	0.82	4.50E-02	7.46E-01
polymerase (RNA) I polypeptide D	ENSMUSG00000029642	-0.28	0.82	4.95E-02	7.83E-01
COBW domain containing 1	ENSMUSG00000024878	-0.28	0.82	5.99E-02	8.67E-01
FK506 binding protein 10	ENSMUSG00000001555	-0.28	0.82	6.58E-02	8.92E-01
protein tyrosine phosphatase, receptor type, C	ENSMUSG00000026395	-0.28	0.82	7.00E-02	9.10E-01
EGF-like and EMI domain containing 1	ENSMUSG00000063600	-0.28	0.82	8.15E-02	9.72E-01

tropomyosin 3, gamma	ENSMUSG00000027940	-0.28	0.82	4.37E-02	7.34E-01
DNA-damage-inducible transcript 4-like	ENSMUSG00000046818	-0.28	0.82	5.52E-02	8.30E-01
cerebellin 2 precursor protein	ENSMUSG00000024647	-0.28	0.82	4.28E-02	7.25E-01
ribosomal protein S2	ENSMUSG00000044533	-0.28	0.82	4.44E-02	7.41E-01
alkB homolog 6	ENSMUSG00000042831	-0.28	0.82	4.46E-02	7.42E-01
follistatin-like 4	ENSMUSG00000036264	-0.28	0.82	4.84E-02	7.73E-01
aquaporin 11	ENSMUSG00000042797	-0.28	0.82	5.25E-02	8.09E-01
dishevelled-binding antagonist of beta-catenin 3	ENSMUSG00000078794	-0.29	0.82	3.92E-02	7.02E-01
four jointed box 1	ENSMUSG00000075012	-0.29	0.82	4.02E-02	7.11E-01
predicted gene 13889	ENSMUSG00000087006	-0.29	0.82	4.54E-02	7.49E-01
dynein, axonemal, heavy chain 5	ENSMUSG00000022262	-0.29	0.82	5.24E-02	8.09E-01
empty spiracles homeobox 1	ENSMUSG00000033726	-0.29	0.82	5.63E-02	8.42E-01
protocadherin alpha 10	ENSMUSG00000007440	-0.29	0.82	7.04E-02	9.12E-01
intercellular adhesion molecule 5, telencephalin	ENSMUSG00000032174	-0.29	0.82	3.82E-02	6.93E-01
Ly6/Plaur domain containing 1	ENSMUSG00000026344	-0.29	0.82	3.71E-02	6.79E-01
S-phase kinase-associated protein 2 (p45)	ENSMUSG00000054115	-0.29	0.82	5.55E-02	8.32E-01
RIKEN cDNA B230216N24 gene	ENSMUSG00000089706	-0.29	0.82	6.69E-02	8.98E-01
RIKEN cDNA 2900097C17 gene	ENSMUSG00000102869	-0.29	0.82	3.66E-02	6.75E-01
family with sequence similarity 131, member A	ENSMUSG00000050821	-0.29	0.82	3.57E-02	6.63E-01
proviral integration site 3	ENSMUSG00000035828	-0.29	0.82	3.85E-02	6.95E-01
cytochrome c oxidase assembly protein 11, copper chaperone	ENSMUSG00000020544	-0.29	0.82	7.75E-02	9.55E-01
a disintegrin-like and metallopeptidase (reprolysin type) with thrombospondin type 1 motif, 1	ENSMUSG00000022893	-0.29	0.82	4.45E-02	7.41E-01
zinc finger protein 568	ENSMUSG00000074221	-0.29	0.82	6.00E-02	8.67E-01
neuritin 1	ENSMUSG00000039114	-0.29	0.82	3.46E-02	6.51E-01
tribbles pseudokinase 1	ENSMUSG00000032501	-0.29	0.82	3.94E-02	7.05E-01
proprotein convertase subtilisin/kexin type 1 inhibitor	ENSMUSG00000039278	-0.30	0.82	3.28E-02	6.34E-01
FXYD domain-containing ion transport regulator 7	ENSMUSG00000036578	-0.30	0.82	3.64E-02	6.72E-01
solute carrier family 6 (neurotransmitter transporter), member 20B	ENSMUSG00000025243	-0.30	0.82	6.65E-02	8.95E-01
coiled-coil-helix-coiled-coil-helix domain containing 2, pseudogene	ENSMUSG00000094320	-0.30	0.81	3.67E-02	6.76E-01
dual specificity phosphatase 14	ENSMUSG00000018648	-0.30	0.81	3.42E-02	6.49E-01
neuronal pentraxin receptor	ENSMUSG00000022421	-0.30	0.81	2.97E-02	6.06E-01
mitogen-activated protein kinase kinase kinase 14	ENSMUSG00000020941	-0.30	0.81	4.66E-02	7.58E-01
translocator protein	ENSMUSG00000041736	-0.30	0.81	6.08E-02	8.69E-01
C1q-like 3	ENSMUSG00000049630	-0.30	0.81	3.05E-02	6.13E-01
reticulon 4 receptor	ENSMUSG00000043811	-0.30	0.81	3.18E-02	6.30E-01
C2 calcium-dependent domain containing 4C	ENSMUSG00000045912	-0.30	0.81	3.04E-02	6.12E-01
growth arrest and DNA-damage-inducible 45 gamma	ENSMUSG00000021453	-0.30	0.81	3.53E-02	6.59E-01
ribonuclease H2, subunit C	ENSMUSG00000024925	-0.30	0.81	3.73E-02	6.81E-01
phosphodiesterase 5A, cGMP-specific	ENSMUSG00000053965	-0.30	0.81	3.97E-02	7.07E-01
isthmin 1, angiogenesis inhibitor	ENSMUSG00000074766	-0.30	0.81	4.75E-02	7.66E-01
predicted gene 3500	ENSMUSG00000096003	-0.30	0.81	5.69E-02	8.45E-01
cyclin F	ENSMUSG00000072082	-0.30	0.81	6.19E-02	8.78E-01
tumor suppressor candidate 1	ENSMUSG00000054000	-0.31	0.81	3.88E-02	7.00E-01
immunoglobulin-like and fibronectin type III domain containing 1	ENSMUSG00000051985	-0.31	0.81	3.12E-02	6.24E-01
nuclear factor of kappa light polypeptide gene enhancer in B cells inhibitor, delta	ENSMUSG00000036931	-0.31	0.81	7.33E-02	9.23E-01
sin3 associated polypeptide	ENSMUSG00000031609	-0.31	0.81	4.75E-02	7.66E-01
deiodinase, iodothyronine, type II	ENSMUSG00000007682	-0.31	0.81	2.72E-02	5.75E-01
denticleless E3 ubiquitin protein ligase	ENSMUSG00000037474	-0.31	0.81	4.28E-02	7.25E-01
suppressor APC domain containing 2	ENSMUSG00000026955	-0.31	0.81	6.90E-02	9.05E-01
bone morphogenetic protein 7	ENSMUSG00000008999	-0.31	0.80	2.52E-02	5.53E-01

cystathionase (cystathionine gamma-lyase)	ENSMUSG00000028179	-0.31	0.80	4.66E-02	7.58E-01
cellular retinoic acid binding protein II	ENSMUSG00000004885	-0.31	0.80	3.85E-02	6.95E-01
H1 histone family, member X	ENSMUSG00000044927	-0.32	0.80	2.80E-02	5.88E-01
procollagen C-endopeptidase enhancer protein	ENSMUSG00000029718	-0.32	0.80	3.04E-02	6.12E-01
kirre like nephrin family adhesion molecule 3	ENSMUSG00000032036	-0.32	0.80	2.30E-02	5.23E-01
cytochrome P450, family 4, subfamily f, polypeptide 16	ENSMUSG00000048440	-0.32	0.80	6.83E-02	9.05E-01
reprimo-like	ENSMUSG00000046215	-0.32	0.80	2.40E-02	5.35E-01
coiled-coil domain containing 85C	ENSMUSG00000084883	-0.32	0.80	2.63E-02	5.65E-01
connective tissue growth factor	ENSMUSG00000019997	-0.32	0.80	2.71E-02	5.74E-01
fatty acid binding protein 7, brain	ENSMUSG00000019874	-0.32	0.80	2.31E-02	5.25E-01
dynein regulatory complex subunit 1	ENSMUSG00000073102	-0.32	0.80	2.54E-02	5.53E-01
complement component 1, q subcomponent-like 2	ENSMUSG00000036907	-0.32	0.80	2.67E-02	5.70E-01
phospholipid scramblase 2	ENSMUSG00000032372	-0.32	0.80	3.92E-02	7.03E-01
MRV integration site 1	ENSMUSG00000005611	-0.32	0.80	3.41E-02	6.49E-01
heat shock protein 2	ENSMUSG00000059970	-0.32	0.80	2.14E-02	5.13E-01
G protein-coupled receptor 27	ENSMUSG00000072875	-0.32	0.80	2.72E-02	5.75E-01
insulin receptor substrate 2	ENSMUSG00000038894	-0.32	0.80	2.04E-02	5.00E-01
RAS-like, family 2, locus 9	ENSMUSG00000083649	-0.32	0.80	8.49E-02	9.83E-01
protocadherin beta 2	ENSMUSG00000051599	-0.33	0.80	4.52E-02	7.47E-01
inositol 1,4,5-trisphosphate 3-kinase A	ENSMUSG00000027296	-0.33	0.80	1.81E-02	4.62E-01
thyroid hormone responsive	ENSMUSG00000035686	-0.33	0.80	2.09E-02	5.08E-01
transmembrane protein 252	ENSMUSG00000048572	-0.33	0.80	6.93E-02	9.05E-01
dendrin	ENSMUSG00000059213	-0.33	0.80	1.69E-02	4.43E-01
nuclear receptor subfamily 2, group F, member 6	ENSMUSG00000002393	-0.33	0.80	2.14E-02	5.13E-01
odd-skipped related transcription factor 1	ENSMUSG00000048387	-0.33	0.80	4.85E-02	7.74E-01
CCAAT/enhancer binding protein (C/EBP), alpha	ENSMUSG00000034957	-0.33	0.79	2.50E-02	5.50E-01
prospero homeobox 1	ENSMUSG00000010175	-0.33	0.79	1.94E-02	4.85E-01
ATP synthase, H+ transporting, mitochondrial F1 complex, epsilon subunit	ENSMUSG00000016252	-0.33	0.79	1.67E-02	4.38E-01
immediate early response 5	ENSMUSG00000056708	-0.33	0.79	1.77E-02	4.56E-01
dishevelled-binding antagonist of beta-catenin 1	ENSMUSG00000044548	-0.33	0.79	2.48E-02	5.49E-01
shisa family member 2	ENSMUSG00000044461	-0.33	0.79	2.87E-02	5.94E-01
scleraxis	ENSMUSG00000034161	-0.34	0.79	6.66E-02	8.96E-01
protein FAM205A-like	ENSMUSG00000095779	-0.34	0.79	2.18E-02	5.15E-01
opticin	ENSMUSG00000010311	-0.34	0.79	3.95E-02	7.06E-01
carbonyl reductase 2	ENSMUSG00000025150	-0.34	0.79	8.63E-02	9.87E-01
solute carrier family 22 (organic anion transporter), member 6	ENSMUSG00000024650	-0.34	0.79	1.80E-02	4.61E-01
cell migration inducing protein, hyaluronan binding	ENSMUSG00000052353	-0.34	0.79	2.05E-02	5.01E-01
protocadherin beta 15	ENSMUSG00000047033	-0.34	0.79	3.48E-02	6.54E-01
MAS1 oncogene	ENSMUSG00000068037	-0.34	0.79	1.95E-02	4.85E-01
olfactomedin-like 2B	ENSMUSG00000038463	-0.34	0.79	3.25E-02	6.33E-01
zinc finger protein 607A	ENSMUSG00000020420	-0.34	0.79	6.50E-02	8.86E-01
jun D proto-oncogene	ENSMUSG00000071076	-0.34	0.79	1.47E-02	4.09E-01
FAST kinase domains 3	ENSMUSG00000021532	-0.34	0.79	2.37E-02	5.30E-01
clarin 1	ENSMUSG00000043850	-0.34	0.79	5.56E-02	8.34E-01
solute carrier family 6 (neurotransmitter transporter, GABA), member 13	ENSMUSG00000030108	-0.34	0.79	1.65E-02	4.36E-01
potassium voltage-gated channel, subfamily G, member 2	ENSMUSG00000059852	-0.34	0.79	2.04E-02	5.00E-01
glycoprotein Ib, beta polypeptide	ENSMUSG00000050761	-0.34	0.79	2.23E-02	5.18E-01
metallothionein 2	ENSMUSG00000031762	-0.34	0.79	1.50E-02	4.15E-01
aristaless-like homeobox 4	ENSMUSG00000040310	-0.34	0.79	3.52E-02	6.59E-01
wingless-type MMTV integration site family, member 5B	ENSMUSG00000030170	-0.34	0.79	4.45E-02	7.42E-01
leucine-rich repeat-containing G protein-coupled receptor 6	ENSMUSG00000042793	-0.34	0.79	7.50E-02	9.35E-01

somatostatin receptor 4	ENSMUSG00000037014	-0.34	0.79	2.30E-02	5.23E-01
Rho guanine nucleotide exchange factor (GEF) 33	ENSMUSG00000054901	-0.34	0.79	7.74E-02	9.55E-01
prostaglandin D2 synthase (brain)	ENSMUSG00000015090	-0.35	0.79	1.23E-02	3.73E-01
neurturin	ENSMUSG00000039481	-0.35	0.79	6.08E-02	8.69E-01
heat shock protein 1B	ENSMUSG00000090877	-0.35	0.79	1.43E-02	4.05E-01
transient receptor potential cation channel, subfamily V, member 2	ENSMUSG00000018507	-0.35	0.79	1.57E-02	4.28E-01
predicted gene 3667	ENSMUSG00000090691	-0.35	0.79	3.02E-02	6.10E-01
leucine rich repeat neuronal 4	ENSMUSG00000043110	-0.35	0.79	4.73E-02	7.64E-01
solute carrier family 17 (sodium-dependent inorganic phosphate cotransporter), member 7	ENSMUSG00000070570	-0.35	0.79	1.18E-02	3.65E-01
regulator of cell cycle	ENSMUSG00000022018	-0.35	0.79	1.61E-02	4.30E-01
R-spondin 2	ENSMUSG00000051920	-0.35	0.79	2.44E-02	5.43E-01
ATP-binding cassette, sub-family A (ABC1), member 8a	ENSMUSG00000041828	-0.35	0.78	1.59E-02	4.29E-01
amnionless	ENSMUSG00000021278	-0.35	0.78	3.16E-02	6.27E-01
zinc finger protein 697	ENSMUSG00000050064	-0.35	0.78	1.54E-02	4.21E-01
cyclin-dependent kinase inhibitor 1C (P57)	ENSMUSG00000037664	-0.35	0.78	1.60E-02	4.29E-01
Fc receptor, IgG, low affinity IIb	ENSMUSG00000026656	-0.35	0.78	2.54E-02	5.53E-01
kirre like nephrin family adhesion molecule 2	ENSMUSG00000036915	-0.35	0.78	2.30E-02	5.23E-01
5-hydroxytryptamine (serotonin) receptor 3A	ENSMUSG00000032269	-0.36	0.78	2.23E-02	5.18E-01
zinc finger protein 69	ENSMUSG00000064141	-0.36	0.78	5.29E-02	8.10E-01
ADP-ribosylation factor-like 5B	ENSMUSG00000017418	-0.36	0.78	1.19E-02	3.66E-01
heat shock protein 1A	ENSMUSG00000091971	-0.36	0.78	1.28E-02	3.81E-01
adenylate cyclase 1	ENSMUSG00000020431	-0.36	0.78	9.29E-03	3.13E-01
F-box and leucine-rich repeat protein 15	ENSMUSG00000025226	-0.36	0.78	1.39E-02	4.00E-01
period circadian clock 1	ENSMUSG00000020893	-0.36	0.78	9.49E-03	3.17E-01
cyclin dependent kinase inhibitor 2C	ENSMUSG00000028551	-0.36	0.78	7.21E-02	9.20E-01
pleckstrin homology domain containing, family F (with FYVE domain) member 1	ENSMUSG00000074170	-0.36	0.78	2.21E-02	5.16E-01
cartilage intermediate layer protein 2	ENSMUSG00000044006	-0.37	0.78	2.15E-02	5.13E-01
cytochrome P450, family 19, subfamily a, polypeptide 1	ENSMUSG00000032274	-0.37	0.78	7.11E-02	9.17E-01
basic helix-loop-helix family, member e22	ENSMUSG00000025128	-0.37	0.78	8.71E-03	2.98E-01
RAS, dexamethasone-induced 1	ENSMUSG00000049892	-0.37	0.78	1.41E-02	4.03E-01
Kruppel-like factor 10	ENSMUSG00000037465	-0.37	0.77	9.34E-03	3.13E-01
popeye domain containing 3	ENSMUSG00000019848	-0.37	0.77	3.41E-02	6.49E-01
dual specificity phosphatase 4	ENSMUSG00000031530	-0.37	0.77	9.72E-03	3.21E-01
dual-specificity tyrosine-(Y)-phosphorylation regulated kinase 3	ENSMUSG00000016526	-0.37	0.77	1.29E-02	3.83E-01
polypeptide N-acetylgalactosaminyltransferase 3	ENSMUSG00000026994	-0.37	0.77	4.67E-02	7.58E-01
Rho GTPase activating protein 15	ENSMUSG00000049744	-0.37	0.77	1.34E-02	3.92E-01
solute carrier family 30 (zinc transporter), member 2	ENSMUSG00000028836	-0.37	0.77	2.52E-02	5.53E-01
MAS-related GPR, member F	ENSMUSG00000031070	-0.37	0.77	2.92E-02	6.00E-01
paralemmin 3	ENSMUSG00000047986	-0.37	0.77	1.84E-02	4.64E-01
inka box actin regulator 2	ENSMUSG00000048458	-0.37	0.77	7.67E-03	2.69E-01
proline rich 7 (synaptic)	ENSMUSG00000034686	-0.37	0.77	8.36E-03	2.89E-01
NFU1 iron-sulfur cluster scaffold	ENSMUSG00000029993	-0.37	0.77	9.51E-03	3.17E-01
uncharacterized LOC105245673	ENSMUSG00000096869	-0.38	0.77	6.89E-02	9.05E-01
peptidoglycan recognition protein 1	ENSMUSG00000030413	-0.38	0.77	2.05E-02	5.01E-01
DnaJ heat shock protein family (Hsp40) member B1	ENSMUSG00000005483	-0.38	0.77	6.71E-03	2.47E-01
tetratricopeptide repeat domain 9B	ENSMUSG00000007944	-0.38	0.77	6.72E-03	2.47E-01
gem nuclear organelle associated protein 6	ENSMUSG00000055760	-0.38	0.77	2.71E-02	5.74E-01
wingless-type MMTV integration site family, member 6	ENSMUSG00000033227	-0.38	0.77	1.78E-02	4.59E-01
nuclear factor of kappa light polypeptide gene enhancer in B cells inhibitor, alpha	ENSMUSG00000021025	-0.38	0.77	7.62E-03	2.69E-01

carboxypeptidase X 1 (M14 family)	ENSMUSG00000027408	-0.38	0.77	9.95E-03	3.25E-01
predicted gene 1976	ENSMUSG00000066057	-0.39	0.77	6.13E-03	2.31E-01
RIKEN cDNA A330009N23 gene	ENSMUSG00000097915	-0.39	0.77	8.86E-03	3.02E-01
tryptophan 2,3-dioxygenase	ENSMUSG00000028011	-0.39	0.77	7.41E-02	9.27E-01
predicted gene 3095	ENSMUSG00000091756	-0.39	0.76	1.30E-02	3.86E-01
cholecystokinin	ENSMUSG00000032532	-0.39	0.76	5.19E-03	2.08E-01
DNA-damage-inducible transcript 4	ENSMUSG00000020108	-0.39	0.76	5.56E-03	2.17E-01
bone morphogenetic protein 6	ENSMUSG00000039004	-0.39	0.76	7.03E-03	2.52E-01
parvin, gamma	ENSMUSG00000022439	-0.39	0.76	7.00E-03	2.52E-01
neurogenic differentiation 1	ENSMUSG00000034701	-0.39	0.76	7.80E-03	2.72E-01
coiled-coil domain containing 103	ENSMUSG00000020930	-0.39	0.76	2.64E-02	5.65E-01
dual specificity phosphatase 6	ENSMUSG00000019960	-0.39	0.76	5.08E-03	2.06E-01
Ngfi-A binding protein 2	ENSMUSG00000025402	-0.39	0.76	5.74E-03	2.22E-01
zinc finger protein 189	ENSMUSG00000039634	-0.39	0.76	7.73E-03	2.70E-01
signal-regulatory protein beta 1-like	ENSMUSG00000074677	-0.39	0.76	6.22E-02	8.78E-01
coiled-coil domain containing 85B	ENSMUSG00000095098	-0.40	0.76	4.64E-03	1.93E-01
aldehyde dehydrogenase family 1, subfamily A2	ENSMUSG00000013584	-0.40	0.76	5.32E-03	2.09E-01
immediate early response 2	ENSMUSG00000053560	-0.40	0.76	7.71E-03	2.70E-01
WAP, follistatin/kazal, immunoglobulin, kunitz and netrin domain containing 2	ENSMUSG00000044177	-0.40	0.76	7.16E-03	2.56E-01
zinc finger E-box binding homeobox 2, opposite strand	ENSMUSG00000052248	-0.40	0.76	7.89E-02	9.62E-01
SLAM family member 9	ENSMUSG00000026548	-0.40	0.76	5.97E-02	8.65E-01
G protein-coupled receptor 1	ENSMUSG00000046856	-0.40	0.76	3.33E-02	6.41E-01
folate receptor 2 (fetal)	ENSMUSG00000032725	-0.40	0.76	4.42E-02	7.40E-01
SET binding factor 1	ENSMUSG00000036529	-0.41	0.76	3.52E-03	1.63E-01
neurogenic differentiation 2	ENSMUSG00000038255	-0.41	0.76	4.12E-03	1.79E-01
anti-Mullerian hormone	ENSMUSG00000035262	-0.41	0.76	7.69E-02	9.52E-01
forkhead box D2, opposite strand	ENSMUSG00000085399	-0.41	0.75	4.37E-02	7.35E-01
protein FAM205A-like	ENSMUSG00000084010	-0.41	0.75	7.94E-03	2.76E-01
hydrogen voltage-gated channel 1	ENSMUSG00000064267	-0.41	0.75	3.08E-02	6.19E-01
solute carrier family 13 (sodium/sulfate symporters), member 4	ENSMUSG00000029843	-0.41	0.75	3.50E-03	1.62E-01
ADP-ribosylation factor-like 11	ENSMUSG00000043157	-0.41	0.75	8.06E-02	9.67E-01
vasoactive intestinal polypeptide	ENSMUSG00000019772	-0.41	0.75	3.97E-03	1.74E-01
predicted gene 3383	ENSMUSG00000096629	-0.41	0.75	1.17E-02	3.64E-01
biogenesis of lysosomal organelles complex-1, subunit 1	ENSMUSG00000090247	-0.42	0.75	1.46E-02	4.09E-01
fibroblast growth factor 7	ENSMUSG00000027208	-0.42	0.75	7.17E-02	9.19E-01
solute carrier family 30 (zinc transporter), member 3	ENSMUSG00000029151	-0.42	0.75	2.72E-03	1.36E-01
von Willebrand factor A domain containing 3B	ENSMUSG00000050122	-0.42	0.75	8.37E-02	9.80E-01
predicted gene 1673	ENSMUSG00000070858	-0.42	0.75	3.63E-03	1.66E-01
secretory blood group 1	ENSMUSG00000040364	-0.42	0.75	8.23E-02	9.72E-01
protein phosphatase 1, regulatory subunit 3G	ENSMUSG00000050423	-0.42	0.75	3.91E-03	1.72E-01
RAB5 interacting factor	ENSMUSG00000027637	-0.42	0.75	4.48E-03	1.88E-01
Y box protein 1 pseudogene	ENSMUSG00000044141	-0.42	0.75	2.62E-02	5.64E-01
SPARC related modular calcium binding 2	ENSMUSG00000023886	-0.42	0.75	5.13E-03	2.08E-01
somatostatin receptor 2	ENSMUSG00000047904	-0.43	0.74	2.70E-03	1.36E-01
empty spiracles homeobox 2	ENSMUSG00000043969	-0.43	0.74	3.97E-03	1.74E-01
coiled-coil domain containing 114	ENSMUSG00000040189	-0.43	0.74	7.41E-03	2.63E-01
protease, serine 50	ENSMUSG00000048752	-0.43	0.74	1.57E-02	4.27E-01
CD48 antigen	ENSMUSG00000015355	-0.43	0.74	7.11E-02	9.17E-01
transcription factor AP-2, gamma	ENSMUSG00000028640	-0.43	0.74	3.58E-02	6.64E-01
predicted gene, 20754	ENSMUSG00000103428	-0.43	0.74	3.26E-02	6.33E-01
transcription factor AP-2 beta	ENSMUSG00000025927	-0.43	0.74	2.39E-02	5.34E-01
heparan sulfate (glucosamine) 3-O-sulfotransferase 6	ENSMUSG00000039628	-0.43	0.74	6.57E-02	8.91E-01
kelch-like 40	ENSMUSG00000074001	-0.43	0.74	1.14E-02	3.57E-01

cAMP responsive element binding protein 3-like 3	ENSMUSG00000035041	-0.43	0.74	4.60E-02	7.55E-01
predicted gene 3317	ENSMUSG00000095912	-0.43	0.74	5.66E-02	8.43E-01
RIKEN cDNA 1700001L19 gene	ENSMUSG00000021534	-0.43	0.74	3.15E-03	1.51E-01
potassium channel, subfamily K, member 12	ENSMUSG00000050138	-0.43	0.74	4.47E-03	1.88E-01
frequently rearranged in advanced T cell lymphomas 2	ENSMUSG00000047604	-0.43	0.74	4.71E-03	1.96E-01
family with sequence similarity 160, member A1	ENSMUSG00000051000	-0.43	0.74	5.54E-03	2.16E-01
serine hydroxymethyltransferase 1 (soluble)	ENSMUSG00000020534	-0.43	0.74	1.24E-02	3.75E-01
hydrocarboxylic acid receptor 1	ENSMUSG00000049241	-0.44	0.74	5.64E-03	2.19E-01
RAB42, member RAS oncogene family	ENSMUSG00000089687	-0.44	0.74	3.23E-02	6.32E-01
rhomboid like 1	ENSMUSG00000025735	-0.44	0.74	4.67E-02	7.58E-01
nuclear factor, interleukin 3, regulated	ENSMUSG00000056749	-0.44	0.74	2.90E-03	1.43E-01
chymotrypsin-like elastase family, member 1	ENSMUSG00000023031	-0.44	0.74	2.50E-02	5.50E-01
jun proto-oncogene	ENSMUSG00000052684	-0.44	0.74	1.63E-03	9.76E-02
solute carrier family 22 (organic anion transporter), member 8	ENSMUSG00000063796	-0.44	0.74	1.73E-03	1.01E-01
dual specificity phosphatase 27 (putative)	ENSMUSG00000026564	-0.44	0.74	2.21E-02	5.16E-01
loricrin	ENSMUSG00000043165	-0.44	0.74	3.53E-03	1.63E-01
DEP domain containing 7	ENSMUSG00000027173	-0.44	0.74	2.11E-02	5.11E-01
glucagon-like peptide 2 receptor	ENSMUSG00000049928	-0.44	0.74	4.49E-02	7.45E-01
frizzled-related protein	ENSMUSG00000027004	-0.45	0.73	2.40E-03	1.25E-01
sorbin and SH3 domain containing 2, opposite strand	ENSMUSG00000085440	-0.45	0.73	3.41E-02	6.49E-01
four and a half LIM domains 3	ENSMUSG00000032643	-0.45	0.73	4.26E-02	7.22E-01
GINS complex subunit 2 (Psf2 homolog)	ENSMUSG00000031821	-0.45	0.73	3.44E-02	6.50E-01
protease, serine 12 neurotrypsin (motopsin)	ENSMUSG00000027978	-0.45	0.73	2.80E-03	1.39E-01
adrenergic receptor, alpha 1d	ENSMUSG00000027335	-0.45	0.73	3.35E-03	1.57E-01
C1q and tumor necrosis factor related protein 4	ENSMUSG00000040794	-0.45	0.73	1.10E-03	7.22E-02
PR domain containing 8	ENSMUSG00000035456	-0.46	0.73	1.71E-03	1.00E-01
zinc finger protein 771	ENSMUSG00000054716	-0.46	0.73	1.30E-03	8.19E-02
histocompatibility 2, M region locus 5	ENSMUSG00000024459	-0.46	0.73	2.16E-02	5.13E-01
hes family bHLH transcription factor 7	ENSMUSG00000023781	-0.46	0.73	5.19E-02	8.04E-01
brain derived neurotrophic factor	ENSMUSG00000048482	-0.46	0.73	1.22E-03	7.84E-02
neuronal pentraxin 2	ENSMUSG00000059991	-0.46	0.73	1.12E-03	7.33E-02
triggering receptor expressed on myeloid cells 2	ENSMUSG00000023992	-0.46	0.73	1.54E-03	9.40E-02
basic helix-loop-helix family, member a9	ENSMUSG00000044243	-0.46	0.73	1.33E-02	3.91E-01
defensin beta 1	ENSMUSG00000044748	-0.46	0.73	4.23E-02	7.20E-01
RAS-like, family 11, member A	ENSMUSG00000029641	-0.46	0.73	4.43E-03	1.88E-01
guanylate cyclase 2g	ENSMUSG00000055523	-0.47	0.72	2.05E-03	1.12E-01
predicted gene 6345	ENSMUSG00000096964	-0.47	0.72	6.34E-02	8.78E-01
tumor necrosis factor (ligand) superfamily, member 13	ENSMUSG00000089669	-0.47	0.72	5.17E-02	8.03E-01
cysteine rich protein 61	ENSMUSG00000028195	-0.47	0.72	1.53E-03	9.36E-02
RIKEN cDNA 1700067K01 gene	ENSMUSG00000046408	-0.47	0.72	3.27E-02	6.34E-01
RIKEN cDNA 1700022N22 gene	ENSMUSG00000097523	-0.47	0.72	8.16E-02	9.72E-01
testis expressed gene 15	ENSMUSG00000009628	-0.47	0.72	3.59E-03	1.65E-01
predicted gene, 16701	ENSMUSG00000102548	-0.47	0.72	7.03E-02	9.12E-01
prostaglandin-endoperoxide synthase 2	ENSMUSG00000032487	-0.47	0.72	1.22E-03	7.84E-02
mitochondrial ribosomal protein S34	ENSMUSG00000038880	-0.47	0.72	1.86E-03	1.06E-01
reticulon 4 receptor-like 2	ENSMUSG00000050896	-0.47	0.72	1.08E-03	7.17E-02
abnormal spindle microtubule assembly	ENSMUSG00000033952	-0.47	0.72	6.74E-02	9.01E-01
RIKEN cDNA 5830418P13 gene	ENSMUSG00000086236	-0.48	0.72	1.67E-02	4.38E-01
major facilitator superfamily domain containing 13B	ENSMUSG00000030877	-0.48	0.72	6.27E-02	8.78E-01
serine (or cysteine) peptidase inhibitor, clade E, member 1	ENSMUSG00000037411	-0.48	0.72	4.48E-03	1.88E-01
ring finger protein 39	ENSMUSG00000036492	-0.48	0.71	1.82E-02	4.63E-01
RRS1 ribosome biogenesis regulator homolog pseudogene	ENSMUSG00000048106	-0.49	0.71	7.28E-04	5.01E-02
PDZ domain containing 3	ENSMUSG00000032105	-0.49	0.71	1.73E-02	4.50E-01

neuralized E3 ubiquitin protein ligase 3	ENSMUSG00000047180	-0.49	0.71	2.45E-02	5.44E-01
Fanconi anemia, complementation group I	ENSMUSG00000039187	-0.49	0.71	6.20E-02	8.78E-01
fibroblast growth factor binding protein 1	ENSMUSG00000048373	-0.49	0.71	2.07E-03	1.12E-01
membrane-spanning 4-domains, subfamily A, member 7	ENSMUSG00000024672	-0.49	0.71	8.56E-02	9.84E-01
coagulation factor II (thrombin) receptor-like 1	ENSMUSG00000021678	-0.50	0.71	4.51E-02	7.47E-01
CCAAT/enhancer binding protein (C/EBP), delta	ENSMUSG00000071637	-0.50	0.71	3.02E-03	1.46E-01
PDZ and LIM domain 1 (elfin)	ENSMUSG00000055044	-0.50	0.71	5.24E-03	2.09E-01
transient receptor potential cation channel, subfamily C, member 6	ENSMUSG00000031997	-0.50	0.71	1.28E-03	8.13E-02
predicted gene 3696	ENSMUSG00000092167	-0.50	0.71	1.10E-03	7.22E-02
leucine rich repeat containing 46	ENSMUSG00000020878	-0.50	0.71	3.81E-02	6.93E-01
Iroquois homeobox 6	ENSMUSG00000031738	-0.51	0.70	7.83E-02	9.60E-01
zinc finger protein 976	ENSMUSG00000092335	-0.51	0.70	6.50E-02	8.86E-01
solute carrier family 23 (nucleobase transporters), member 3	ENSMUSG00000026205	-0.51	0.70	2.36E-02	5.30E-01
predicted gene 16434	ENSMUSG00000095015	-0.51	0.70	1.20E-02	3.68E-01
small nuclear ribonucleoprotein polypeptide F	ENSMUSG00000020018	-0.51	0.70	5.85E-03	2.25E-01
melanocortin 5 receptor	ENSMUSG00000007480	-0.51	0.70	3.81E-02	6.93E-01
histone cluster 1, H2ba	ENSMUSG00000050799	-0.51	0.70	7.29E-02	9.22E-01
antigen identified by monoclonal antibody Ki 67	ENSMUSG00000031004	-0.52	0.70	7.71E-03	2.70E-01
glutamate rich 5	ENSMUSG00000044726	-0.52	0.70	2.36E-02	5.30E-01
nudix (nucleoside diphosphate linked moiety X)-type motif 6	ENSMUSG00000050174	-0.52	0.70	6.07E-02	8.69E-01
kinocilin	ENSMUSG00000073774	-0.52	0.70	7.92E-03	2.75E-01
fibroblast growth factor 5	ENSMUSG00000029337	-0.52	0.70	9.92E-03	3.25E-01
mitochondrial translational initiation factor 3	ENSMUSG00000016510	-0.53	0.69	1.37E-02	3.97E-01
predicted gene 7361	ENSMUSG00000059645	-0.53	0.69	2.32E-02	5.25E-01
calcium release activated channel regulator 2A	ENSMUSG00000061414	-0.53	0.69	2.61E-02	5.63E-01
proline/serine-rich coiled-coil 1	ENSMUSG00000068744	-0.54	0.69	1.44E-03	8.95E-02
notum palmitoleoyl-protein carboxylesterase	ENSMUSG00000042988	-0.54	0.69	3.26E-03	1.54E-01
thiosulfate sulfurtransferase (rhodanese)-like domain containing 1	ENSMUSG00000103711	-0.54	0.69	3.89E-02	7.00E-01
uncharacterized LOC108168187	ENSMUSG00000090627	-0.54	0.69	2.07E-02	5.04E-01
elastin microfibril interfacer 3	ENSMUSG00000050700	-0.55	0.68	5.85E-02	8.57E-01
retinal degeneration 3	ENSMUSG00000049353	-0.55	0.68	2.19E-02	5.15E-01
general transcription factor IIA, 1-like	ENSMUSG00000024154	-0.55	0.68	8.15E-02	9.72E-01
zinc finger protein 984	ENSMUSG00000078495	-0.55	0.68	2.33E-03	1.22E-01
titin-cap	ENSMUSG00000007877	-0.57	0.68	2.28E-02	5.23E-01
predicted gene 7854	ENSMUSG00000085720	-0.57	0.68	8.58E-02	9.84E-01
CFAP97 domain containing 2	ENSMUSG00000090336	-0.57	0.67	1.53E-02	4.21E-01
frequently rearranged in advanced T cell lymphomas	ENSMUSG00000067199	-0.58	0.67	1.78E-03	1.03E-01
aldehyde oxidase 3	ENSMUSG00000064294	-0.58	0.67	1.71E-03	1.00E-01
olfactory marker protein	ENSMUSG00000074006	-0.58	0.67	4.38E-02	7.36E-01
lymphocyte antigen 6 complex, locus G6F	ENSMUSG00000034923	-0.59	0.67	5.27E-02	8.10E-01
MORN repeat containing 5	ENSMUSG00000026894	-0.59	0.67	4.64E-02	7.58E-01
collagen, type II, alpha 1	ENSMUSG00000022483	-0.59	0.66	1.69E-02	4.43E-01
cation channel sperm associated auxiliary subunit gamma 2	ENSMUSG00000049123	-0.60	0.66	5.30E-03	2.09E-01
RIKEN cDNA 9130024F11 gene	ENSMUSG00000087022	-0.60	0.66	1.40E-02	4.01E-01
aldehyde dehydrogenase family 1, subfamily A3	ENSMUSG00000015134	-0.60	0.66	2.94E-03	1.44E-01
RIKEN cDNA 1110002E22 gene	ENSMUSG00000090066	-0.60	0.66	3.64E-03	1.66E-01
solute carrier family 25, member 41	ENSMUSG00000011486	-0.60	0.66	5.67E-02	8.43E-01
CD209a antigen	ENSMUSG00000031494	-0.61	0.65	1.54E-02	4.21E-01
E2F transcription factor 8	ENSMUSG00000046179	-0.61	0.65	3.97E-02	7.07E-01
RIKEN cDNA 4933417O13 gene	ENSMUSG00000101360	-0.61	0.65	2.36E-02	5.30E-01
melanotransferrin	ENSMUSG00000022780	-0.62	0.65	2.74E-02	5.79E-01
vomeronasal 2, receptor 29	ENSMUSG00000095730	-0.62	0.65	3.02E-02	6.10E-01
trans-acting transcription factor 5	ENSMUSG00000075304	-0.62	0.65	4.57E-02	7.53E-01

Fc fragment of IgG binding protein	ENSMUSG00000047730	-0.63	0.65	8.75E-02	9.91E-01
tripartite motif-containing 63	ENSMUSG00000028834	-0.64	0.64	5.24E-02	8.09E-01
integrin alpha L	ENSMUSG00000030830	-0.64	0.64	2.84E-02	5.93E-01
CD209b antigen	ENSMUSG00000065987	-0.64	0.64	1.01E-02	3.26E-01
leucine rich melanocyte differentiation associated	ENSMUSG00000063458	-0.65	0.64	1.14E-02	3.58E-01
ALK and LTK ligand 2	ENSMUSG00000054204	-0.65	0.64	1.33E-03	8.36E-02
interleukin 12a	ENSMUSG00000027776	-0.66	0.64	2.39E-02	5.34E-01
tudor domain containing 12	ENSMUSG00000030491	-0.66	0.63	2.20E-02	5.16E-01
KH domain containing 3, subcortical maternal complex member	ENSMUSG00000092622	-0.66	0.63	2.02E-02	4.99E-01
pentraxin 4	ENSMUSG00000044172	-0.66	0.63	1.81E-02	4.62E-01
lysozyme-like 4	ENSMUSG00000032530	-0.67	0.63	5.58E-02	8.36E-01
B cell translocation gene 1, anti-proliferative, pseudogene 1	ENSMUSG00000068173	-0.67	0.63	5.17E-02	8.03E-01
NLR family, pyrin domain containing 10	ENSMUSG00000049709	-0.67	0.63	5.28E-02	8.10E-01
doublesex and mab-3 related transcription factor 2	ENSMUSG00000048138	-0.67	0.63	1.77E-03	1.03E-01
predicted gene 6337	ENSMUSG00000091882	-0.68	0.63	3.84E-02	6.95E-01
uncharacterized LOC105246847	ENSMUSG00000085196	-0.68	0.63	4.16E-02	7.13E-01
apolipoprotein F	ENSMUSG00000047631	-0.68	0.63	3.43E-02	6.49E-01
RIKEN cDNA 1700061G19 gene	ENSMUSG00000024209	-0.68	0.62	1.33E-02	3.90E-01
long non-protein coding RNA, Trp53 induced transcript	ENSMUSG00000044471	-0.68	0.62	2.85E-02	5.93E-01
predicted gene 6583	ENSMUSG00000051503	-0.68	0.62	8.71E-02	9.89E-01
zinc finger protein 980	ENSMUSG00000058186	-0.69	0.62	1.20E-02	3.68E-01
RIKEN cDNA 2310001H17 gene	ENSMUSG00000097354	-0.70	0.62	3.76E-02	6.85E-01
RIKEN cDNA A930001A20 gene	ENSMUSG00000098008	-0.70	0.62	5.17E-02	8.03E-01
secretin receptor	ENSMUSG00000026387	-0.71	0.61	1.48E-02	4.11E-01
retinal pigment epithelium 65	ENSMUSG00000028174	-0.71	0.61	1.16E-03	7.59E-02
heat shock protein family, member 7 (cardiovascular)	ENSMUSG00000006221	-0.71	0.61	8.20E-02	9.72E-01
NADP+ dependent oxidoreductase domain containing 1	ENSMUSG00000072919	-0.71	0.61	3.27E-03	1.54E-01
RIKEN cDNA A330069E16 gene	ENSMUSG00000097868	-0.72	0.61	3.16E-03	1.51E-01
S100 calcium binding protein A3	ENSMUSG00000001021	-0.72	0.61	4.29E-02	7.25E-01
histone cluster 2, H4	ENSMUSG00000091405	-0.72	0.61	2.60E-03	1.32E-01
axonemal dynein light chain domain containing 1	ENSMUSG00000026601	-0.72	0.61	8.69E-02	9.89E-01
Ly6/Plaur domain containing 2	ENSMUSG00000022595	-0.73	0.60	4.50E-03	1.88E-01
X-prolyl aminopeptidase (aminopeptidase P) 2, membrane-bound	ENSMUSG00000037005	-0.73	0.60	2.22E-02	5.18E-01
B cell leukemia/lymphoma 3	ENSMUSG00000053175	-0.74	0.60	1.26E-02	3.76E-01
basic leucine zipper transcription factor, ATF-like	ENSMUSG00000034266	-0.74	0.60	5.28E-02	8.10E-01
serine/threonine/tyrosine kinase 1	ENSMUSG00000032899	-0.74	0.60	8.26E-04	5.63E-02
NADPH oxidase 1	ENSMUSG00000031257	-0.75	0.59	5.00E-02	7.86E-01
C-type lectin domain family 1, member b	ENSMUSG00000030159	-0.75	0.59	8.60E-02	9.84E-01
NLR family, apoptosis inhibitory protein 6	ENSMUSG00000078942	-0.75	0.59	2.33E-03	1.22E-01
cathepsin E	ENSMUSG00000004552	-0.76	0.59	4.31E-02	7.27E-01
RIKEN cDNA 2310007B03 gene	ENSMUSG00000034159	-0.76	0.59	5.67E-02	8.43E-01
uncharacterized LOC105242449	ENSMUSG00000094811	-0.77	0.59	1.65E-02	4.36E-01
predicted gene 6904	ENSMUSG00000090881	-0.77	0.59	7.63E-02	9.45E-01
zinc finger protein 819	ENSMUSG00000055102	-0.77	0.59	2.13E-02	5.13E-01
zinc finger protein 985	ENSMUSG00000065999	-0.78	0.58	5.32E-03	2.09E-01
bestrophin 1	ENSMUSG00000037418	-0.78	0.58	5.70E-03	2.21E-01
iodotyrosine deiodinase	ENSMUSG00000019762	-0.79	0.58	2.86E-02	5.94E-01
RIKEN cDNA 1700123K08 gene	ENSMUSG00000029526	-0.79	0.58	2.04E-02	5.00E-01
Williams Beuren syndrome chromosome region 25 (human)	ENSMUSG00000054909	-0.80	0.57	3.11E-02	6.23E-01
RIKEN cDNA 1500015L24 gene	ENSMUSG00000094732	-0.81	0.57	5.38E-02	8.17E-01

establishment of sister chromatid cohesion N-acetyltransferase 2	ENSMUSG00000022034	-0.82	0.57	6.82E-02	9.05E-01
tigger transposable element derived 4	ENSMUSG00000047819	-0.82	0.57	5.28E-02	8.10E-01
lymphocyte antigen 9	ENSMUSG00000004707	-0.83	0.56	4.75E-03	1.97E-01
otopetrin 3	ENSMUSG00000018862	-0.83	0.56	4.65E-02	7.58E-01
lymphocyte antigen 6 complex, locus G6E	ENSMUSG00000013766	-0.83	0.56	1.23E-02	3.73E-01
RIKEN cDNA 4933413J09 gene	ENSMUSG00000021874	-0.85	0.55	8.42E-02	9.80E-01
CD209g antigen	ENSMUSG00000079168	-0.85	0.55	2.49E-02	5.49E-01
microRNA 3091	ENSMUSG00000092827	-0.85	0.55	5.09E-02	7.95E-01
predicted gene 13483	ENSMUSG00000085862	-0.86	0.55	1.81E-02	4.62E-01
predicted gene, 21663	ENSMUSG00000104824	-0.86	0.55	3.95E-02	7.06E-01
growth differentiation factor 6	ENSMUSG00000051279	-0.86	0.55	7.40E-02	9.27E-01
adhesion G protein-coupled receptor G5	ENSMUSG00000061577	-0.86	0.55	2.53E-02	5.53E-01
solute carrier organic anion transporter family, member 1a6	ENSMUSG00000079262	-0.89	0.54	2.97E-02	6.06E-01
mucin 19	ENSMUSG00000044021	-0.89	0.54	6.22E-02	8.78E-01
RIKEN cDNA A630072M18 gene	ENSMUSG00000101013	-0.91	0.53	9.57E-03	3.19E-01
terminal nucleotidyltransferase 5B	ENSMUSG00000046694	-0.92	0.53	2.19E-02	5.15E-01
protein tyrosine phosphatase, non-receptor type 22 (lymphoid)	ENSMUSG00000027843	-0.92	0.53	3.10E-03	1.49E-01
cDNA sequence BC051537	ENSMUSG00000098197	-0.92	0.53	4.91E-02	7.79E-01
polypeptide N-acetylgalactosaminyltransferase 2	ENSMUSG00000089704	-0.93	0.53	1.98E-03	1.10E-01
predicted gene 10451	ENSMUSG00000073000	-0.93	0.53	5.64E-02	8.42E-01
keratin 31	ENSMUSG00000048981	-0.94	0.52	2.53E-02	5.53E-01
NLR family, pyrin domain containing 12	ENSMUSG00000078817	-0.96	0.52	8.54E-02	9.84E-01
RIKEN cDNA B430306N03 gene	ENSMUSG00000043740	-0.96	0.51	5.67E-03	2.20E-01
keratin 7	ENSMUSG00000023039	-0.96	0.51	7.63E-02	9.45E-01
ventricular zone expressed PH domain-containing 1	ENSMUSG00000027831	-0.97	0.51	4.29E-03	1.84E-01
transmembrane protease, serine 11B	ENSMUSG00000035861	-0.97	0.51	5.84E-02	8.57E-01
sperm motility kinase 4A	ENSMUSG00000079711	-0.98	0.51	8.07E-02	9.67E-01
RIKEN cDNA 1700016A09 gene	ENSMUSG00000102737	-0.98	0.51	2.29E-03	1.21E-01
predicted gene 16551	ENSMUSG00000066477	-0.99	0.50	1.60E-02	4.29E-01
carcinoembryonic antigen-related cell adhesion molecule 18	ENSMUSG00000030472	-0.99	0.50	7.00E-02	9.10E-01
butyrophilin-like 2	ENSMUSG00000024340	-0.99	0.50	3.50E-02	6.55E-01
RIKEN cDNA 1700125H20 gene	ENSMUSG00000018479	-1.00	0.50	2.97E-02	6.06E-01
basic helix-loop-helix family, member e23	ENSMUSG00000045493	-1.01	0.50	7.16E-02	9.19E-01
cytochrome P450, family 2, subfamily j, polypeptide 8	ENSMUSG00000082932	-1.03	0.49	5.84E-02	8.57E-01
killer cell immunoglobulin-like receptor, three domains, long cytoplasmic tail, 1	ENSMUSG00000031424	-1.04	0.49	8.71E-02	9.89E-01
thymosin beta 15b like	ENSMUSG00000072955	-1.05	0.48	2.83E-03	1.40E-01
ATPase, H+/K+ transporting, nongastric, alpha polypeptide	ENSMUSG00000022229	-1.05	0.48	8.68E-03	2.98E-01
regulator of G-protein signalling 9 binding protein	ENSMUSG00000056043	-1.05	0.48	2.04E-02	5.00E-01
transketolase-like 1	ENSMUSG00000031397	-1.06	0.48	5.03E-03	2.05E-01
tripartite motif-containing 75	ENSMUSG00000071089	-1.06	0.48	1.60E-02	4.29E-01
achaete-scute family bHLH transcription factor 5	ENSMUSG00000097918	-1.06	0.48	4.20E-02	7.18E-01
HtrA serine peptidase 4	ENSMUSG00000037406	-1.07	0.48	3.77E-03	1.68E-01
claudin 20	ENSMUSG00000091530	-1.08	0.47	5.77E-03	2.22E-01
zona pellucida like domain containing 1	ENSMUSG00000064310	-1.08	0.47	1.00E-02	3.25E-01
regulator of G-protein signaling 18	ENSMUSG00000026357	-1.09	0.47	1.87E-02	4.70E-01
interleukin 20 receptor beta	ENSMUSG00000044244	-1.10	0.47	1.26E-03	8.01E-02
RIKEN cDNA C130026I21 gene	ENSMUSG00000052477	-1.10	0.47	1.34E-02	3.92E-01
RIKEN cDNA 4930447F24 gene	ENSMUSG00000102224	-1.11	0.46	1.57E-03	9.46E-02
chloride channel accessory 3A2	ENSMUSG00000028262	-1.11	0.46	1.00E-02	3.25E-01
microRNA 106b	ENSMUSG00000065514	-1.11	0.46	4.99E-02	7.85E-01
predicted gene 9920	ENSMUSG00000053749	-1.12	0.46	4.16E-02	7.13E-01

Fancd2 opposite strand	ENSMUSG00000033963	-1.14	0.45	4.01E-02	7.10E-01
olfactory receptor 1564	ENSMUSG00000096169	-1.16	0.45	8.42E-02	9.80E-01
opsin 1 (cone pigments), short-wave-sensitive (color blindness, tritan)	ENSMUSG00000058831	-1.17	0.44	4.99E-02	7.85E-01
olfactory receptor 1417	ENSMUSG00000048292	-1.18	0.44	2.55E-02	5.55E-01
spermatogenesis associated 25	ENSMUSG00000017767	-1.18	0.44	4.16E-02	7.13E-01
7S RNA 1	ENSMUSG00000099021	-1.19	0.44	8.55E-02	9.84E-01
spermatogenesis associated 31 subfamily D, member 1A	ENSMUSG00000050876	-1.28	0.41	5.84E-02	8.57E-01
transketolase-like 2	ENSMUSG00000025519	-1.29	0.41	1.22E-03	7.84E-02
KH domain containing 1C	ENSMUSG00000041722	-1.29	0.41	3.95E-02	7.06E-01
amphiregulin	ENSMUSG00000029378	-1.31	0.40	6.93E-02	9.05E-01
tyrosine aminotransferase	ENSMUSG00000001670	-1.32	0.40	3.38E-02	6.47E-01
uncoupling protein 1 (mitochondrial, proton carrier)	ENSMUSG00000031710	-1.34	0.40	5.34E-02	8.14E-01
ribosomal protein L39-like	ENSMUSG00000039209	-1.34	0.40	6.93E-02	9.05E-01
olfactory receptor 690	ENSMUSG00000050266	-1.39	0.38	1.03E-02	3.31E-01
CD22 antigen	ENSMUSG00000030577	-1.42	0.37	9.16E-03	3.10E-01
tubulin, alpha 3A	ENSMUSG00000067702	-1.43	0.37	4.93E-02	7.81E-01
cyclin B1, pseudogene	ENSMUSG00000048574	-1.46	0.36	6.83E-03	2.50E-01
CD244 molecule A	ENSMUSG00000004709	-1.46	0.36	7.16E-03	2.56E-01
olfactory receptor 691	ENSMUSG00000043948	-1.47	0.36	4.60E-02	7.55E-01
ubiquitin-conjugating enzyme E2U (putative)	ENSMUSG00000069733	-1.47	0.36	8.55E-02	9.84E-01
PTK6 protein tyrosine kinase 6	ENSMUSG00000038751	-1.49	0.36	1.37E-02	3.97E-01
keratocan	ENSMUSG00000019932	-1.50	0.35	2.12E-02	5.11E-01
predicted gene 10855	ENSMUSG00000075538	-1.59	0.33	4.12E-02	7.12E-01
RAB11 family interacting protein 4 (class II), opposite strand 1	ENSMUSG00000087434	-1.61	0.33	8.22E-02	9.72E-01
myosin VIIB	ENSMUSG00000024388	-1.62	0.33	3.43E-02	6.49E-01
CD163 molecule-like 1	ENSMUSG00000025461	-1.64	0.32	2.64E-02	5.65E-01
RIKEN cDNA 4631405J19 gene	ENSMUSG00000075027	-1.68	0.31	2.51E-03	1.29E-01
syncytin b	ENSMUSG00000047977	-1.73	0.30	4.10E-02	7.12E-01
RIKEN cDNA 1700020N18 gene	ENSMUSG00000100253	-1.78	0.29	7.44E-04	5.11E-02
G protein-coupled receptor 82	ENSMUSG00000047678	-1.83	0.28	1.88E-03	1.06E-01
zona pellucida 3 receptor	ENSMUSG00000042554	-1.84	0.28	4.12E-02	7.12E-01
CD3 antigen, gamma polypeptide	ENSMUSG00000002033	-1.89	0.27	7.28E-02	9.21E-01
urotensin 2B	ENSMUSG00000056423	-1.91	0.27	2.29E-02	5.23E-01
RIKEN cDNA 4930550L24 gene	ENSMUSG00000046180	-1.91	0.27	6.88E-02	9.05E-01
ATPase, H+ transporting, lysosomal V1 subunit E2	ENSMUSG00000053375	-1.92	0.26	3.43E-02	6.49E-01
microRNA 1192	ENSMUSG00000080626	-2.05	0.24	6.88E-02	9.05E-01
a disintegrin and metallopeptidase domain 18	ENSMUSG00000031552	-2.07	0.24	3.82E-02	6.93E-01
S100 calcium binding protein A5	ENSMUSG00000001023	-2.09	0.23	8.37E-03	2.89E-01
BPI fold containing family A, member 1	ENSMUSG00000027483	-2.16	0.22	1.43E-02	4.05E-01
olfactory receptor 1349	ENSMUSG00000048067	-2.19	0.22	4.85E-03	2.00E-01
T-box 3, opposite strand 2	ENSMUSG00000086847	-2.23	0.21	3.87E-03	1.71E-01
microRNA 8102	ENSMUSG00000098919	-2.27	0.21	1.44E-02	4.06E-01
cytochrome P450, family 2, subfamily g, polypeptide 1	ENSMUSG00000049685	-2.32	0.20	4.12E-02	7.12E-01
tetraspanin 10	ENSMUSG00000039691	-2.34	0.20	7.03E-03	2.52E-01
tescalcin-like	ENSMUSG00000055826	-2.39	0.19	3.16E-03	1.51E-01
flavin containing monooxygenase 6	ENSMUSG00000095576	-2.44	0.18	7.28E-02	9.21E-01
microRNA 3473e	ENSMUSG00000099301	-2.44	0.18	7.28E-02	9.21E-01
predicted gene 11437	ENSMUSG00000051452	-2.45	0.18	4.10E-02	7.12E-01
RIKEN cDNA 4932413F04 gene	ENSMUSG00000099616	-2.46	0.18	1.43E-02	4.05E-01
carbonic anhydrase 6	ENSMUSG00000028972	-2.78	0.15	4.10E-02	7.12E-01
Hoxa adjacent long noncoding RNA 1	ENSMUSG00000085412	-2.93	0.13	2.16E-03	1.14E-01
keratin associated protein 7-1	ENSMUSG00000056706	-2.94	0.13	2.16E-03	1.14E-01
FK506 binding protein 6	ENSMUSG00000040013	-3.19	0.11	2.12E-03	1.14E-01
small nucleolar RNA, H/ACA box 21	ENSMUSG00000064901	-3.25	0.11	6.39E-02	8.78E-01

H2A histone family, member B3	ENSMUSG00000083616	-3.25	0.11	6.39E-02	8.78E-01
tubulin polymerization-promoting protein family member 2	ENSMUSG00000008813	-3.53	0.09	6.39E-02	8.78E-01
aldo-keto reductase family 1, member C-like	ENSMUSG00000025955	-3.53	0.09	6.39E-02	8.78E-01
KH domain containing 1A	ENSMUSG00000067750	-3.53	0.09	6.39E-02	8.78E-01
RIKEN cDNA 4930455B14 gene	ENSMUSG00000097898	-3.54	0.09	3.23E-02	6.32E-01
lysozyme-like 6	ENSMUSG00000020945	-3.54	0.09	6.39E-02	8.78E-01
4short chain dehydrogenase/reductase family 9C, member 7	ENSMUSG00000040127	-3.76	0.07	6.39E-02	8.78E-01
tryptase beta 2	ENSMUSG00000033825	-3.77	0.07	3.23E-02	6.32E-01
predicted gene 8267	ENSMUSG00000091923	-3.77	0.07	3.23E-02	6.32E-01
lipase, member I	ENSMUSG00000032948	-3.96	0.06	3.23E-02	6.32E-01
RIKEN cDNA 4930579F01 gene	ENSMUSG00000012042	-3.97	0.06	3.23E-02	6.32E-01
microRNA 6937	ENSMUSG00000098579	-3.97	0.06	3.23E-02	6.32E-01
olfactomedin 5	ENSMUSG00000044265	-4.33	0.05	4.23E-03	1.82E-01

ANNEX III

Table 2: Study of significant functional groups expressed in dams. The significantly differentially expressed genes were assigned to different functional categories using GO assignments, GO: Gene ontology; Raw p-values (rawp) obtained were transformed to adjusted p-values (adjp). For abbreviations see list.

Group name	GO	statistic	rawp	adjp
negative regulation of ERK1 and ERK2 cascade	GO:0070373	8.87e-07	0.0	0.0
positive regulation of receptor internalization	GO:0002092	1.50e-03	0.0	0.0
regulation of JAK/STAT cascade	GO:0007262	1.50e-03	0.0	0.0
positive regulation of cerebellar granule cell precursor proliferation	GO:0021940	1.50e-03	0.0	0.0
positive regulation of canonical Wnt signaling pathway	GO:0035413	1.50e-03	0.0	0.0
Wnt signaling pathway involved in dorsal/ventral axis specification	GO:0044332	1.50e-03	0.0	0.0
regulation of peptidyl-tyrosine phosphorylation	GO:0050730	1.50e-03	0.0	0.0
regulation of protein transport	GO:0051223	1.50e-03	0.0	0.0
embryonic retina morphogenesis in camera-type eye	GO:0060059	1.50e-03	0.0	0.0
regulation of calcium ion import	GO:0090279	1.50e-03	0.0	0.0
negative regulation of cholesterol efflux	GO:0090370	1.50e-03	0.0	0.0
positive regulation of hyaluronan biosynthetic process	GO:1900127	1.50e-03	0.0	0.0
regulation of protein localization to cell surface	GO:2000008	1.50e-03	0.0	0.0
very long-chain fatty acid metabolic process	GO:0000038	1.52e-03	0.0	0.0
fatty acid beta-oxidation	GO:0006635	1.52e-03	0.0	0.0
bile acid metabolic process	GO:0008206	1.52e-03	0.0	0.0
regulation of systemic arterial blood pressure by circulatory renin-angiotensin	GO:0001991	1.84e-03	0.0	0.0
cellular sodium ion homeostasis	GO:0006883	1.84e-03	0.0	0.0
positive regulation of cholesterol esterification	GO:0010873	1.84e-03	0.0	0.0
peristalsis	GO:0030432	1.84e-03	0.0	0.0
positive regulation of fatty acid biosynthetic process	GO:0045723	1.84e-03	0.0	0.0
regulation of cardiac conduction	GO:1903779	1.84e-03	0.0	0.0
regulation of chemokine production	GO:0032642	2.64e-03	0.0	0.0
protein O-linked glycosylation	GO:0006493	3.13e-03	0.0	0.0
glycolipid biosynthetic process	GO:0009247	3.13e-03	0.0	0.0
carbohydrate biosynthetic process	GO:0016051	3.13e-03	0.0	0.0
regulation of fibroblast growth factor receptor signaling pathway	GO:0040036	5.16e-03	0.0	0.0
natural killer cell activation involved in immune response	GO:0002323	7.18e-03	0.0	0.0
positive regulation of interferon-gamma secretion	GO:1902715	7.18e-03	0.0	0.0
nuclear-transcribed mRNA poly(A) tail shortening	GO:0000289	8.33e-03	0.0	0.0
regulation of tumor necrosis factor production	GO:0032680	8.33e-03	0.0	0.0
negative regulation of viral transcription	GO:0032897	8.33e-03	0.0	0.0
negative regulation of inflammatory response	GO:0050728	8.33e-03	0.0	0.0
positive regulation of nuclear-transcribed mRNA poly(A) tail shortening	GO:0060213	8.33e-03	0.0	0.0
positive regulation of mRNA catabolic process	GO:0061014	8.33e-03	0.0	0.0
3'-UTR-mediated mRNA stabilization	GO:0070935	8.33e-03	0.0	0.0
B cell apoptotic process	GO:0001783	9.44e-03	0.0	0.0
positive regulation of mesenchymal cell proliferation	GO:0002053	9.44e-03	0.0	0.0
positive regulation of B cell apoptotic process	GO:0002904	9.44e-03	0.0	0.0
amino acid transport	GO:0006865	9.44e-03	0.0	0.0
cellular iron ion homeostasis	GO:0006879	9.44e-03	0.0	0.0
cellular response to interferon-alpha	GO:0035457	9.44e-03	0.0	0.0
pigmentation	GO:0043473	9.44e-03	0.0	0.0
canonical Wnt signaling pathway involved in negative regulation of apoptotic process	GO:0044336	9.44e-03	0.0	0.0
detection of mechanical stimulus involved in sensory perception of sound	GO:0050910	9.44e-03	0.0	0.0

positive regulation of oxidative phosphorylation	GO:1903862	9.44e-03	0.0	0.0
positive regulation of DNA biosynthetic process	GO:2000573	9.44e-03	0.0	0.0
positive regulation of ATP biosynthetic process	GO:2001171	9.44e-03	0.0	0.0
tissue regeneration	GO:0042246	1.12e-02	0.0	0.0
bone mineralization	GO:0030282	1.40e-02	0.0	0.0
positive regulation of BMP signaling pathway	GO:0030513	1.40e-02	0.0	0.0
positive regulation of smoothened signaling pathway	GO:0045880	2.10e-02	0.0	0.0
embryonic placenta development	GO:0001892	2.51e-02	0.0	0.0
transcription by RNA polymerase I	GO:0006360	2.51e-02	0.0	0.0
myeloid cell differentiation	GO:0030099	2.51e-02	0.0	0.0
granulocyte differentiation	GO:0030851	2.51e-02	0.0	0.0
fat cell differentiation	GO:0045444	2.51e-02	0.0	0.0
positive regulation of fat cell differentiation	GO:0045600	2.51e-02	0.0	0.0
positive regulation of osteoblast differentiation	GO:0045669	2.51e-02	0.0	0.0
negative regulation of cell cycle	GO:0045786	2.51e-02	0.0	0.0
positive regulation of transcription by RNA polymerase III	GO:0045945	2.51e-02	0.0	0.0
cell maturation	GO:0048469	2.51e-02	0.0	0.0
brown fat cell differentiation	GO:0050873	2.51e-02	0.0	0.0
cellular response to lithium ion	GO:0071285	2.51e-02	0.0	0.0
cellular response to organic cyclic compound	GO:0071407	2.51e-02	0.0	0.0
positive regulation of DNA-templated transcription. initiation	GO:2000144	2.51e-02	0.0	0.0
developmental growth	GO:0048589	4.29e-02	0.0	0.0
female sex differentiation	GO:0046660	5.69e-02	0.0	0.0
cellular aldehyde metabolic process	GO:0006081	9.05e-02	0.0	0.0
positive regulation of epidermal growth factor-activated receptor activity	GO:0045741	1.04e-01	0.0	0.0
histone H3-K4 demethylation	GO:0034720	1.29e-01	0.0	0.0
protection from non-homologous end joining at telomere	GO:0031848	1.30e-01	0.0	0.0
acylglycerol catabolic process	GO:0046464	1.34e-01	0.0	0.0
cellular phosphate ion homeostasis	GO:0030643	1.40e-01	0.0	0.0
phosphate ion homeostasis	GO:0055062	1.40e-01	0.0	0.0
chemosensory behavior	GO:0007635	1.51e-01	0.0	0.0
positive regulation of T cell mediated cytotoxicity	GO:0001916	1.71e-01	0.0	0.0
cation transport	GO:0006812	1.71e-01	0.0	0.0
vesicle budding from membrane	GO:0006900	1.71e-01	0.0	0.0
plasma membrane organization	GO:0007009	1.71e-01	0.0	0.0
response to mechanical stimulus	GO:0009612	1.71e-01	0.0	0.0
gene expression	GO:0010467	1.71e-01	0.0	0.0
positive regulation of glutamate secretion	GO:0014049	1.71e-01	0.0	0.0
positive regulation of gamma-aminobutyric acid secretion	GO:0014054	1.71e-01	0.0	0.0
synaptic vesicle exocytosis	GO:0016079	1.71e-01	0.0	0.0
phospholipid scrambling	GO:0017121	1.71e-01	0.0	0.0
cytolysis	GO:0019835	1.71e-01	0.0	0.0
collagen metabolic process	GO:0032963	1.71e-01	0.0	0.0
T cell proliferation	GO:0042098	1.71e-01	0.0	0.0
ceramide biosynthetic process	GO:0046513	1.71e-01	0.0	0.0
pore complex assembly	GO:0046931	1.71e-01	0.0	0.0
membrane depolarization	GO:0051899	1.71e-01	0.0	0.0
positive regulation of mitochondrial depolarization	GO:0051901	1.71e-01	0.0	0.0
cellular response to dsRNA	GO:0071359	1.71e-01	0.0	0.0
cation transmembrane transport	GO:0098655	1.71e-01	0.0	0.0
female meiosis I	GO:0007144	1.77e-01	0.0	0.0
cellular response to heat	GO:0034605	2.00e-01	0.0	0.0
regulation of protein heterodimerization activity	GO:0043497	2.00e-01	0.0	0.0
embryonic process involved in female pregnancy	GO:0060136	2.00e-01	0.0	0.0
cellular response to copper ion	GO:0071280	2.00e-01	0.0	0.0
cellular response to estradiol stimulus	GO:0071392	2.00e-01	0.0	0.0

negative regulation of inclusion body assembly	GO:0090084	2.00e-01	0.0	0.0
positive regulation of inclusion body assembly	GO:0090261	2.00e-01	0.0	0.0
cellular response to angiotensin	GO:1904385	2.00e-01	0.0	0.0
protein localization to phagophore assembly site	GO:0034497	2.40e-01	0.0	0.0
muscle organ morphogenesis	GO:0048644	2.52e-01	0.0	0.0
muscle tissue morphogenesis	GO:0060415	2.52e-01	0.0	0.0
glycoprotein metabolic process	GO:0009100	2.62e-01	0.0	0.0
regulation of exit from mitosis	GO:0007096	2.86e-01	0.0	0.0
protein localization to kinetochore	GO:0034501	2.86e-01	0.0	0.0
regulation of stress-activated MAPK cascade	GO:0032872	3.42e-01	0.0	0.0
cell motility	GO:0048870	3.42e-01	0.0	0.0
trachea formation	GO:0060440	3.42e-01	0.0	0.0
placenta blood vessel development	GO:0060674	3.42e-01	0.0	0.0
labyrinthine layer development	GO:0060711	3.42e-01	0.0	0.0
negative regulation of hypoxia-induced intrinsic apoptotic signaling pathway	GO:1903298	3.42e-01	0.0	0.0
regulation of early endosome to late endosome transport	GO:2000641	3.42e-01	0.0	0.0
negative regulation of RNA polymerase II regulatory region sequence-specific DNA binding	GO:1903026	3.66e-01	0.0	0.0
glycerol-3-phosphate metabolic process	GO:0006072	3.95e-01	0.0	0.0
NADH metabolic process	GO:0006734	3.95e-01	0.0	0.0
NAD metabolic process	GO:0019674	3.95e-01	0.0	0.0
vasculature development	GO:0001944	4.86e-01	0.0	0.0
regulation of cysteine-type endopeptidase activity involved in apoptotic process	GO:0043281	4.86e-01	0.0	0.0
histone exchange	GO:0043486	4.86e-01	0.0	0.0
ribosome assembly	GO:0042255	5.15e-01	0.0	0.0
regulation of cytosolic calcium ion concentration	GO:0051480	5.41e-01	0.0	0.0
regulation of potassium ion transmembrane transporter activity	GO:1901016	5.41e-01	0.0	0.0
phospholipase C-activating dopamine receptor signaling pathway	GO:0060158	5.45e-01	0.0	0.0
regulation of macroautophagy	GO:0016241	5.81e-01	0.0	0.0
negative regulation of macrophage differentiation	GO:0045650	5.81e-01	0.0	0.0
regulation of stem cell division	GO:2000035	5.81e-01	0.0	0.0

ANNEX IV

Table 3: Common genes in the present our that correspond with the bibliography survey. Genes are ordered in each group according to their fold change (FC). Raw p-values were transformed to adjusted p-values (adjp). For abbreviations see list.

Name	Description	Aliases	ENSEMBL
(Brown et al.. 2006)			
Oxt	oxytocin	OT. Oxy	ENSMUSG00000027301
Nkx2-1	NK2 homeobox 1	AV026640. Nkx2.1. T/EBP. Titf1. Ttf-1	ENSMUSG00000001496
Adcyap1	adenylate cyclase activating polypeptide 1	PACAP	ENSMUSG00000024256
Avp	arginine vasopressin	Vp. Vsp	ENSMUSG00000037727
(Pavlidis & Noble. 2001)			
Ptgds	prostaglandin D2synthase	21kDa. L-PGDS. PGD2. PGDS. PGDS2. Ptgs3	ENSMUSG00000015090
(Medina et al.. 2017)			
Isl1	ISL1 transcription factor. LIM/homeodomain		ENSMUSG00000042258
Nkx2-1	NK2 homeobox 1	AV026640. Nkx2.1. T/EBP. Titf1. Ttf-1	ENSMUSG00000001496
(Lein et al.. 2006)			
Itih3	inter-alpha trypsin inhibitor. heavychain 3	AW108094. ITI-HC3. Intin3. Itih-3	ENSMUSG00000006522
Gdpd2	glycerophosphodiester phosphodiesterase domain containing 2	9130017L10Rik. Gde3. Obdpf	ENSMUSG00000019359
Nova1	neuro-oncological ventral antigen 1	9430099M15Rik. G630039L02. Nova-1	ENSMUSG00000021047
Nrn1	neuritin 1	0710008J23Rik. Cpg15. Nrn	ENSMUSG00000039114
Dlk1	delta like non-canonical Notch ligand 1	AW742678. DLK-1. Dlkl. FA1. Ly107. Peg9. SCP1. ZOG. pG2. pref-1	ENSMUSG00000040856
(Unger et al. 2015)			
Cyp19a1	cytochrome P450, family 19, subfamily a, polypeptide 1	Aromatase, ArKO, Cyp19, Int-5, Int5, p450arom	ENSMUSG00000032274

ANNEX V

Table 4: Protein summary obtained from pituitary gland and Me in the 23 KDa and 16 KDa bands with ProteinPilot v 5.0. The Proteins detected table lists the winner protein for each group, sorted by Unused ProtScore. A) and B) proteins detected in the bands of pituitary gland and C) and D) in the Me. For abbreviation see the protein summary interpretation after the tables. For abbreviations see list.

A. PITUITARY GLAND 23 KDA BAND

PROTEIN	ACCESSION	SPECIES	UNUSED	TOTAL	% COV	% COV (50)	% COV (95)	PEPTIDES (95%)
Somatotropin	sp|P06880|SOMA_MOUSE	MOUSE	84.38	84.38	89.81	87.04	84.26	145
Prolactin	**sp|P06879|PRL_MOUSE**	**MOUSE**	**22.64**	**22.64**	**50.44**	**50.44**	**50.44**	**16**
Peroxiredoxin-1	sp|P35700|PRDX1_MOUSE	MOUSE	12.68	12.68	57.29	46.23	37.19	8
Peroxiredoxin-2	sp|Q61171|PRDX2_MOUSE	MOUSE	11.93	11.93	56.57	35.35	31.82	7
Chromogranin-A	sp|P26339|CMGA_MOUSE	MOUSE	11.89	11.89	33.05	29.81	28.51	12
Phosphatidylethanolamine-binding protein 1	sp|P70296|PEBP1_MOUSE	MOUSE	10.68	10.68	77.01	72.73	51.87	5
Sorcin	sp|Q6P069|SORCN_MOUSE	MOUSE	9.28	9.28	43.94	37.88	30.3	5
Hemoglobin subunit beta-1	sp|P02088|HBB1_MOUSE	MOUSE	8.33	8.33	47.62	34.69	28.57	4
Polyubiquitin	sp|P62976|UBIQP_CRIGR	CRIGR	8.27	8.27	65.35	63.37	55.17	4
Ras-related protein Rab-2A	sp|Q90965|RAB2A_CHICK	CHICK	8.02	8.02	31.6	24.06	24.06	4
Transforming protein RhoA	sp|Q9QUI0|RHOA_MOUSE	MOUSE	8	8	24.35	24.35	24.35	4
Transmembrane emp24 domain-containing protein 10	sp|Q9D1D4|TMEDA_MOUSE	MOUSE	7.89	7.89	25.57	22.37	22.37	5
Ras-related protein Rab-7a	sp|Q5R9Y4|RAB7A_PONAB	PONAB	7.07	7.07	44.93	31.88	27.05	4
Chromobox protein homolog 3	sp|Q5R6X7|CBX3_PONAB	PONAB	6.09	6.09	30.05	22.95	22.95	4
60S ribosomal protein L23a	sp|Q24JY1|RL23A_BOVIN	BOVIN	6.07	6.07	35.26	21.79	21.79	3
Glycoprotein hormones alpha chain	sp|Q9ERG4|GLHA_MASCO	MASCO	6	6	37.5	25	25	3
Glucosamine 6-phosphate N-acetyltransferase	sp|Q9JK38|GNA1_MOUSE	MOUSE	6	6	23.37	23.37	23.37	3
Programmed cell death protein 6	sp|P12815|PDCD6_MOUSE	MOUSE	5.89	5.89	35.08	29.32	26.18	3
Cell division control protein 42 homolog	sp|Q90694|CDC42_CHICK	CHICK	5.89	5.89	30.89	19.9	19.9	3
Proopiomelanocortin	sp|P01193|COLI_MOUSE	MOUSE	5.65	5.65	30.64	30.21	27.23	4
Trypsin	sp|P00761|TRYP_PIG	PIG	5.46	5.46	34.2	34.2	25.11	18
Ferritin light chain 1	sp|P29391|FRIL1_MOUSE	MOUSE	4.69	4.69	32.79	25.68	25.68	3
Ferritin heavy chain	sp|P09528|FRIH_MOUSE	MOUSE	4.59	4.59	59.34	30.22	26.37	4

Histone H2A type 1-C	sp|Q93077|H2A1C_HUMAN	HUMAN	4.43	4.43	35.38	26.92	21.54	2
Ras-related C3 botulinum toxin substrate 1	sp|Q6RUV5|RAC1_RAT	RAT	4.26	4.26	35.42	29.17	12.5	2
Mitochondrial import receptor subunit TOM22 homolog	sp|Q9CPQ3|TOM22_MOUSE	MOUSE	4.19	4.19	33.8	33.8	33.8	3
N(4)-(beta-N-acetylglucosaminyl)-L-asparaginase	sp|Q64191|ASPG_MOUSE	MOUSE	4.04	4.04	16.47	8.382	8.382	2
Lymphocyte antigen 6H	sp|Q9WUC3|LY6H_MOUSE	MOUSE	4.03	4.03	28.06	17.27	17.27	3
60S ribosomal protein L24	sp|Q8BP67|RL24_MOUSE	MOUSE	4.01	4.01	19.11	13.38	13.38	3
60S ribosomal protein L11	sp|Q9CXW4|RL11_MOUSE	MOUSE	4	4	17.42	12.92	12.92	2
Parathymosin	sp|Q9D0J8|PTMS_MOUSE	MOUSE	4	4	22.77	22.77	22.77	2
Cysteine and glycine-rich protein 1	sp|Q5RCT4|CSRP1_PONAB	PONAB	4	4	7.772	7.772	7.772	2
Glutathione peroxidase 3	sp|P46412|GPX3_MOUSE	MOUSE	4	4	11.95	11.95	11.95	2
COP9 signalosome complex subunit 8	sp|Q8VBV7|CSN8_MOUSE	MOUSE	3.47	3.47	21.05	14.83	14.83	2
ADP-ribosylation factor-like protein 3	sp|Q9WUL7|ARL3_MOUSE	MOUSE	3.36	3.49	20.88	20.88	17.58	2
Glutathione peroxidase 1	sp|P11352|GPX1_MOUSE	MOUSE	3.3	3.3	44.28	36.82	15.42	2
60S ribosomal protein L12	sp|P35979|RL12_MOUSE	MOUSE	2.86	2.86	21.82	15.15	15.15	3
CD81 antigen	sp|P35762|CD81_MOUSE	MOUSE	2.8	2.8	19.07	19.07	19.07	2
Ras-related protein Rap-1b	sp|Q9YH37|RAP1B_CYPCA	CYPCA	2.59	2.59	26.63	12.5	12.5	2
Histone H4	sp|Q9U7D0|H4_MASBA	MASBA	2.55	2.55	16.67	16.67	16.67	2
Peptidyl-prolyl cis-trans isomerase B	sp|P24369|PPIB_MOUSE	MOUSE	2.35	2.35	15.74	9.722	6.019	1
Lactoylglutathione lyase	sp|Q9CPU0|LGUL_MOUSE	MOUSE	2.35	2.35	14.13	14.13	9.239	1
Peptidyl-prolyl cis-trans isomerase FKBP11	sp|Q9D1M7|FKB11_MOUSE	MOUSE	2.14	2.14	23.38	19.4	4.975	1
60S ribosomal protein L26	sp|P61257|RL26_BOVIN	BOVIN	2.03	2.03	27.59	6.207	6.207	1
Vasopressin-neurophysin 2-copeptin	sp|P01185|NEU2_HUMAN	HUMAN	2.02	2.02	27.44	14.02	14.02	1
Beta-casein	sp|Q9TSI0|CASB_BUBBU	BUBBU	2.02	2.02	11.61	8.482	8.482	1
Keratin, type II cytoskeletal 6B	sp|P04259|K2C6B_HUMAN	HUMAN	2.01	29.71	48.23	28.37	24.82	16
Somatotropin	sp|P34005|SOMA_CHEMY	CHEMY	2.01	10.54	50.79	24.61	17.8	15
Peptidyl-prolyl cis-trans isomerase A	sp|Q9TTC6|PPIA_RABIT	RABIT	2.01	2.01	34.15	16.46	16.46	2
Signal peptidase complex subunit 3	sp|Q568Z4|SPCS3_RAT	RAT	2.01	2.01	15	8.333	8.333	1
Keratin, type II cytoskeletal 6A	sp|P02538|K2C6A_HUMAN	HUMAN	2	27.96	44.86	26.06	22.52	15
Pregnancy zone protein	sp|P20742|PZP_HUMAN	HUMAN	2	2	2.901	1.417	1.417	1
Metalloproteinase inhibitor 2	sp|Q9WUC6|TIMP2_CAVPO	CAVPO	2	2	6.818	6.818	6.818	1
Ras-related protein Rab-18	sp|Q9NP72|RAB18_HUMAN	HUMAN	2	2	10.19	7.282	7.282	1
Dual specificity protein phosphatase 3	sp|Q9D7X3|DUS3_MOUSE	MOUSE	2	2	16.22	7.027	7.027	1
Tubulin polymerization-promoting protein family member 3	sp|Q9CRB6|TPPP3_MOUSE	MOUSE	2	2	13.07	7.955	7.955	1
Cytochrome b5 type B	sp|Q9CQX2|CYB5B_MOUSE	MOUSE	2	2	39.04	23.29	23.29	1
40S ribosomal protein S7	sp|Q90YR7|RS7_ICTPU	ICTPU	2	2	6.701	6.186	6.186	1

UPF0598 protein C8orf82 homolog	sp|Q8VE95|CH082_MOUSE	MOUSE	2	2	13.76	8.257	8.257	1
Transgelin-2	sp|Q9WVA4|TAGL2_MOUSE	MOUSE	2	2	7.035	7.035	7.035	1
Vesicle-associated membrane protein 2	sp|Q9N0Y0|VAMP2_MACMU	MACMU	2	2	20.69	20.69	20.69	1
Ras-related protein Rab-1B	sp|Q9H0U4|RAB1B_HUMAN	HUMAN	2	2	7.96	7.96	7.96	1
Eukaryotic translation initiation factor 5A-2	sp|Q9GZV4|IF5A2_HUMAN	HUMAN	2	2	7.843	7.843	7.843	1
NADH dehydrogenase [ubiquinone] 1 beta subcomplex subunit 10	sp|Q9DCS9|NDUBA_MOUSE	MOUSE	2	2	10.8	10.8	10.8	1
39S ribosomal protein L12, mitochondrial	sp|Q9DB15|RM12_MOUSE	MOUSE	2	2	6.965	6.965	6.965	1
FXYD domain-containing ion transport regulator 6	sp|Q9D164|FXYD6_MOUSE	MOUSE	2	2	26.6	26.6	26.6	1
60S ribosomal protein L17	sp|Q9CPR4|RL17_MOUSE	MOUSE	2	2	5.435	5.435	5.435	1
Calcineurin B homologous protein 1	sp|Q99653|CHP1_HUMAN	HUMAN	2	2	6.154	6.154	6.154	1
Galectin-related protein	sp|Q8VED9|LEGL_MOUSE	MOUSE	2	2	6.395	6.395	6.395	1
Cellular nucleic acid-binding protein	sp|Q5R5R5|CNBP_PONAB	PONAB	2	2	8.475	8.475	8.475	1
Transmembrane protein 109	sp|Q3UBX0|TM109_MOUSE	MOUSE	2	2	4.938	4.938	4.938	1
60S acidic ribosomal protein P1	sp|P47955|RLA1_MOUSE	MOUSE	2	2	14.04	14.04	14.04	1
60S ribosomal protein L21	sp|P20280|RL21_RAT	RAT	2	2	9.375	9.375	9.375	1
Alpha-S1-casein	sp|P02662|CASA1_BOVIN	BOVIN	2	2	5.607	5.607	5.607	1
Protein JTB	sp|O88824|JTB_MOUSE	MOUSE	2	2	8.904	8.904	8.904	1
60S ribosomal protein L18a	sp|Q3T003|RL18A_BOVIN	BOVIN	1.64	1.64	10.8	7.386	7.386	1
Neuronal calcium sensor 1	sp|Q8BNY6|NCS1_MOUSE	MOUSE	1.57	1.57	9.474	9.474	9.474	1
Transmembrane emp24 domain-containing protein 2	sp|Q9R0Q3|TMED2_MOUSE	MOUSE	1.49	1.49	13.93	10.95	4.478	1
Clusterin	sp|Q06890|CLUS_MOUSE	MOUSE	1.47	1.49	2.679	2.679	2.679	1

B. PITUITARY GLAND 16 KDA BAND

PROTEIN	ACCESSION	SPECIES	UNUSED	TOTAL	% COV	% COV (50)	% COV (95)	PEPTIDES (95%)
Hemoglobin subunit beta-1	sp|P02088|HBB1_MOUSE	MOUSE	48.33	48.33	95.24	95.24	84.35	57
Hemoglobin subunit alpha	sp|P01942|HBA_MOUSE	MOUSE	20.27	20.27	62.68	58.45	58.45	23
Profilin-1	sp|P62963|PROF1_RAT	RAT	17.49	17.49	67.14	67.14	67.14	10
Histone H4	sp|Q7KQD1|H4_CHAVR	CHAVR	16.22	16.22	59.22	58.25	53.4	10
Ubiquitin-60S ribosomal protein L40	sp|P68205|RL40_OPHHA	OPHHA	14.23	14.23	60.94	55.47	50.78	12
2-iminobutanoate/2-iminopropanoate deaminase	sp|P52760|RIDA_MOUSE	MOUSE	14.21	14.21	65.19	65.19	60	7
10 kDa heat shock protein, mitochondrial	sp|Q64433|CH10_MOUSE	MOUSE	13.7	13.7	74.51	73.53	61.76	7

Oxytocin-neurophysin 1	sp|P35454|NEU1_MOUSE	MOUSE	12.63	12.63	72.8	72.8	72.8	10
Hemoglobin subunit beta-2	sp|P02089|HBB2_MOUSE	MOUSE	12.1	43.06	84.35	84.35	84.35	46
ATP synthase subunit e, mitochondrial	sp|Q06185|ATP5I_MOUSE	MOUSE	10.31	10.31	78.87	76.06	64.79	6
Somatotropin	sp|P06880|SOMA_MOUSE	MOUSE	10.02	10.02	44.91	36.11	23.15	6
Pancreatic trypsin inhibitor	sp|P00974|BPT1_BOVIN	BOVIN	9.84	9.84	46	42	29	9
Dynein light chain 2, cytoplasmic	sp|Q9D0M5|DYL2_MOUSE	MOUSE	9.6	9.6	65.17	52.81	52.81	6
Cytochrome c oxidase subunit 5A, mitochondrial	sp|P12787|COX5A_MOUSE	MOUSE	8.79	8.79	36.99	31.51	26.71	5
D-dopachrome decarboxylase	sp|O35215|DOPD_MOUSE	MOUSE	8.32	8.32	88.98	69.49	53.39	4
Glutaredoxin-related protein 5, mitochondrial	sp|Q80Y14|GLRX5_MOUSE	MOUSE	8.01	8.01	46.71	39.47	39.47	4
Glutaredoxin-1	sp|Q9QUH0|GLRX1_MOUSE	MOUSE	8	8	51.4	49.53	39.25	4
ATP synthase subunit g, mitochondrial	sp|Q9CPQ8|ATP5L_MOUSE	MOUSE	8	8	42.72	42.72	42.72	5
40S ribosomal protein S21	sp|Q9CQR2|RS21_MOUSE	MOUSE	7.72	7.72	71.08	59.04	59.04	6
Vasopressin-neurophysin 2-copeptin	sp|P35455|NEU2_MOUSE	MOUSE	7.32	11.68	53.57	53.57	52.98	11
Trypsin	sp|P00761|TRYP_PIG	PIG	7.04	7.04	39.39	33.77	33.77	17
Acylphosphatase-1	sp|P56376|ACYP1_MOUSE	MOUSE	6.72	6.72	46.46	46.46	46.46	4
Thioredoxin	sp|P10639|THIO_MOUSE	MOUSE	6.14	6.14	40	22.86	22.86	3
Hemoglobin subunit delta	sp|P13558|HBD_TARSY	TARSY	6.02	11.39	36.73	22.45	22.45	12
Cathepsin D	sp|P18242|CATD_MOUSE	MOUSE	6.01	6.01	19.51	12.2	12.2	3
Dermcidin	sp|P81605|DCD_HUMAN	HUMAN	6	6	29.09	22.73	22.73	3
Peptidyl-prolyl cis-trans isomerase FKBP1A	sp|P62943|FKB1A_RABIT	RABIT	5.96	6	41.67	41.67	41.67	5
NADH dehydrogenase [ubiquinone] 1 alpha subcomplex subunit 2	sp|Q9CQ75|NDUA2_MOUSE	MOUSE	5.91	5.91	53.54	41.41	34.34	3
Profilin-2	sp|Q9JJV2|PROF2_MOUSE	MOUSE	5.82	5.82	36.43	25	25	4
Small nuclear ribonucleoprotein E	sp|Q7ZUG0|RUXE_DANRE	DANRE	5.68	5.68	29.35	29.35	29.35	4
Upregulated during skeletal muscle growth protein 5	sp|Q78IK2|USMG5_MOUSE	MOUSE	5.59	5.59	44.83	44.83	44.83	3
Cytochrome c oxidase subunit NDUFA4	sp|Q62425|NDUA4_MOUSE	MOUSE	5.56	5.56	56.1	47.56	37.8	3
Serum albumin	sp|P02768|ALBU_HUMAN	HUMAN	5.34	5.34	15.76	8.867	5.255	3
Dolichyl-diphosphooligosaccharide--protein glycosyltransferase subunit DAD1	sp|Q5RBB4|DAD1_PONAB	PONAB	4.81	4.81	26.55	26.55	26.55	3
Macrophage migration inhibitory factor	sp|P34884|MIF_MOUSE	MOUSE	4.58	4.58	23.48	23.48	17.39	6
Acyl-CoA-binding protein	sp|P31786|ACBP_MOUSE	MOUSE	4.46	4.46	60.92	42.53	33.33	2
Proopiomelanocortin	sp|P01193|COLI_MOUSE	MOUSE	4.37	4.37	23.4	22.13	17.87	4
Protein S100-A11	sp|Q6B345|S10AB_RAT	RAT	4.26	4.26	21.43	21.43	21.43	2
Cytochrome c, somatic	sp|P62898|CYC_RAT	RAT	4.09	4.09	41.9	21.9	21.9	2
Histone H2B type 1-L	sp|Q99880|H2B1L_HUMAN	HUMAN	4.03	4.03	41.27	20.63	20.63	3
Vesicle-associated membrane protein 2	sp|Q9N0Y0|VAMP2_MACMU	MACMU	4.02	4.02	20.69	20.69	20.69	2

Cytochrome c oxidase subunit 6B1	sp|P56391|CX6B1_MOUSE	MOUSE	4.01	4.01	43.02	24.42	24.42	2
Dynein light chain roadblock-type 1	sp|Q3T140|DLRB1_BOVIN	BOVIN	4	4	51.04	29.17	29.17	2
NADH dehydrogenase [ubiquinone] iron-sulfur protein 6, mitochondrial	sp|P52503|NDUS6_MOUSE	MOUSE	4	4	30.17	21.55	21.55	2
Signal recognition particle 9 kDa protein	sp|P49962|SRP09_MOUSE	MOUSE	4	4	23.26	23.26	23.26	2
Cytochrome c oxidase subunit 6C	sp|Q9CPQ1|COX6C_MOUSE	MOUSE	3.66	3.66	35.53	35.53	26.32	2
Hemoglobin subunit beta	sp|P11758|HBB_MYOVE	MYOVE	3.46	17.63	58.22	43.15	43.15	15
Hornerin	sp|Q86YZ3|HORN_HUMAN	HUMAN	3.37	3.37	10.74	7.158	4.351	2
Ubiquitin-fold modifier 1	sp|Q803Y4|UFM1_DANRE	DANRE	3.12	3.12	25.56	25.56	25.56	2
Cytochrome b-c1 complex subunit 9	sp|Q8R1I1|QCR9_MOUSE	MOUSE	3.03	3.03	50	37.5	37.5	2
40S ribosomal protein S28	sp|Q6QAT1|RS28_PIG	PIG	2.86	2.86	30.43	30.43	30.43	2
Cytochrome c oxidase subunit 7A2, mitochondrial	sp|P48771|CX7A2_MOUSE	MOUSE	2.62	2.62	39.76	37.35	21.69	2
Ragulator complex protein LAMTOR2	sp|Q9Y2Q5|LTOR2_HUMAN	HUMAN	2.58	2.58	30.4	23.2	23.2	2
NEDD8	sp|Q71UE8|NEDD8_RAT	RAT	2.19	2.19	39.51	39.51	23.46	1
Dolichol-phosphate mannosyltransferase subunit 3	sp|Q9D1Q4|DPM3_MOUSE	MOUSE	2.19	2.19	23.91	23.91	10.87	1
Secretogranin-1	sp|P16014|SCG1_MOUSE	MOUSE	2.16	2.16	3.397	3.397	1.773	1
ATP synthase protein 8	sp|P03930|ATP8_MOUSE	MOUSE	2.15	2.15	26.87	26.87	14.93	1
Cytochrome b-c1 complex subunit 8	sp|Q9CQ69|QCR8_MOUSE	MOUSE	2.02	2.02	36.59	15.85	15.85	1
Protein transport protein Sec61 subunit beta	sp|Q9CQS8|SC61B_MOUSE	MOUSE	2.01	2.01	38.54	21.88	10.42	1
Protein S100-A8	sp|P05109|S10A8_HUMAN	HUMAN	2.01	2.01	36.56	11.83	11.83	1
NADH dehydrogenase [ubiquinone] 1 alpha subcomplex subunit 5	sp|Q9CPP6|NDUA5_MOUSE	MOUSE	2.01	2.01	19.83	13.79	13.79	1
Hemoglobin subunit beta	sp|B3EWD0|HBB_SPEBE	SPEBE	2	11.51	46.58	40.41	40.41	15
Myelin basic protein	sp|P04370|MBP_MOUSE	MOUSE	2	2	17.6	8.8	4.8	1
Alpha-2-macroglobulin	sp|Q5R4N8|A2MG_PONAB	PONAB	2	2	2.714	1.425	1.425	1
Myotrophin	sp|P62775|MTPN_RAT	RAT	2	2	33.9	14.41	14.41	1
Lysozyme C	sp|P37712|LYSC_CAMDR	CAMDR	2	2	18.46	9.231	9.231	1
Protein S100-A10	sp|P08207|S10AA_MOUSE	MOUSE	2	2	31.96	10.31	10.31	1
U6 snRNA-associated Sm-like protein LSm2	sp|Q9Y333|LSM2_HUMAN	HUMAN	2	2	21.05	20	20	1
PHD finger-like domain-containing protein 5A	sp|Q9VMC8|PHF5A_DROME	DROME	2	2	18.92	11.71	11.71	1
40S ribosomal protein S29	sp|Q5R9J0|RS29_PONAB	PONAB	2	2	33.93	14.29	14.29	1
Acylphosphatase-2	sp|P07033|ACYP2_BOVIN	BOVIN	2	2	20.2	13.13	13.13	1
Prolactin	**sp|P06879|PRL_MOUSE**	**MOUSE**	**2**	**2**	**8.85**	**4.425**	**4.425**	**1**
Prefoldin subunit 1	sp|O60925|PFD1_HUMAN	HUMAN	2	2	15.57	9.016	9.016	1
Mitochondrial import inner membrane translocase subunit Tim13	sp|Q9Y5L4|TIM13_HUMAN	HUMAN	2	2	14.74	14.74	14.74	1

Mitochondrial import inner membrane translocase subunit TIM14	sp|Q9CQV7|TIM14_MOUSE	MOUSE	2	2	12.07	12.07	12.07	1
Transmembrane protein 14C	sp|Q9CQN6|TM14C_MOUSE	MOUSE	2	2	9.649	9.649	9.649	1
Peroxiredoxin-2	sp|Q61171|PRDX2_MOUSE	MOUSE	2	2	8.081	8.081	8.081	1
Costars family protein ABRACL	sp|Q4KML4|ABRAL_MOUSE	MOUSE	2	2	11.11	11.11	11.11	1
6.8 kDa mitochondrial proteolipid	sp|P56379|68MP_MOUSE	MOUSE	2	2	20.69	20.69	20.69	1
Beta-2-microglobulin	sp|P07151|B2MG_RAT	RAT	2	2	7.563	7.563	7.563	1
Protein S100-A9	sp|P06702|S10A9_HUMAN	HUMAN	2	2	11.4	11.4	11.4	1
Fatty acid-binding protein, adipocyte	sp|P04117|FABP4_MOUSE	MOUSE	2	2	9.848	9.848	9.848	1
Hemoglobin subunit alpha	sp|P01944|HBA_ONDZI	ONDZI	1.8	10.08	53.19	38.3	38.3	9
Protein kish-A	sp|Q9CR64|KISHA_MOUSE	MOUSE	1.68	1.68	12.5	12.5	12.5	1
Myosin light chain 6B	sp|Q8CI43|MYL6B_MOUSE	MOUSE	1.66	1.68	6.28	6.28	6.28	1
ATP synthase subunit f, mitochondrial	sp|P56135|ATPK_MOUSE	MOUSE	1.66	1.66	43.18	26.14	26.14	2
Immediate early response 3-interacting protein 1 1	sp|Q9Y5U9|IR3IP_HUMAN	HUMAN	1.54	1.54	34.15	24.39	24.39	1
Small nuclear ribonucleoprotein G	sp|Q3ZBL0|RUXG_BOVIN	BOVIN	1.46	1.46	36.84	17.11	17.11	1

C. MEDIAL AMYGDALA 23 KDA BAND

PROTEIN	ACCESSION	SPECIES	UNUSED	TOTAL	% COV	% COV (50)	% COV (95)	PEPTIDES (95%)
Ras-related protein Rab-2A	sp|P53994|RAB2A_MOUSE	MOUSE	27.97	27.97	68.87	68.87	62.74	18
Ras-related protein Rab-7a	sp|P51150|RAB7A_MOUSE	MOUSE	27.86	27.86	83.09	78.74	68.6	19
ATP synthase subunit O, mitochondrial	sp|Q9DB20|ATPO_MOUSE	MOUSE	27.77	27.77	74.65	69.01	65.73	28
Ras-related protein Rap-1A	sp|P62836|RAP1A_RAT	RAT	25.78	25.78	53.26	53.26	53.26	16
Proteasome subunit beta type-5	sp|O55234|PSB5_MOUSE	MOUSE	25.22	25.22	60.23	52.65	48.11	15
Transgelin-3	sp|Q9R1Q8|TAGL3_MOUSE	MOUSE	24.46	24.46	84.42	76.88	73.37	20
Somatotropin	sp|P06880|SOMA_MOUSE	MOUSE	23.67	23.67	72.69	72.69	63.43	22
Protein/nucleic acid deglycase DJ-1	sp|Q99LX0|PARK7_MOUSE	MOUSE	22.88	22.88	69.31	68.78	64.55	19
Phosphatidylethanolamine-binding protein 1	sp|P70296|PEBP1_MOUSE	MOUSE	22.66	22.66	93.05	87.17	73.26	20
Ras-related C3 botulinum toxin substrate 1	sp|Q6RUV5|RAC1_RAT	RAT	22.52	22.52	60.94	60.94	54.69	16
ATP synthase subunit d, mitochondrial	sp|Q9DCX2|ATP5H_MOUSE	MOUSE	21.98	21.98	84.47	79.5	70.81	13
Myelin basic protein	sp|P02688|MBP_RAT	RAT	21.94	21.94	63.59	51.28	47.18	17
Ras-related protein Rab-1A	sp|Q6NYB7|RAB1A_RAT	RAT	21.58	21.58	80.98	76.1	55.12	14
Transforming protein RhoA	sp|Q9QUI0|RHOA_MOUSE	MOUSE	19.56	19.56	73.06	63.73	55.44	14

NADH dehydrogenase [ubiquinone] flavoprotein 2, mitochondrial	sp|Q9D6J6|NDUV2_MOUSE	MOUSE	19.2	19.2	59.68	51.61	48.79	11
Ras-related protein Rab-11B	sp|Q3MHP2|RB11B_BOVIN	BOVIN	18.59	18.59	52.29	52.29	48.62	11
40S ribosomal protein S9	sp|Q6ZWN5|RS9_MOUSE	MOUSE	18.08	18.08	59.28	41.75	27.84	9
Thioredoxin-dependent peroxide reductase, mitochondrial	sp|P20108|PRDX3_MOUSE	MOUSE	17.89	17.89	50.19	41.63	41.63	12
Tubulin alpha-1A chain	sp|Q71U36|TBA1A_HUMAN	HUMAN	17.68	17.68	38.58	30.6	25.28	10
Visinin-like protein 1	sp|Q5RD22|VISL1_PONAB	PONAB	17.19	17.19	71.73	59.16	49.21	9
NADH dehydrogenase [ubiquinone] 1 beta subcomplex subunit 10	sp|Q9DCS9|NDUBA_MOUSE	MOUSE	16.11	16.11	59.09	51.7	51.7	11
Ras-related protein Rab-18	sp|Q9NP72|RAB18_HUMAN	HUMAN	16.09	16.09	64.08	51.94	48.06	11
Superoxide dismutase [Mn], mitochondrial	sp|P09671|SODM_MOUSE	MOUSE	16.02	16.02	41.89	41.89	38.74	8
Peroxiredoxin-2	sp|Q61171|PRDX2_MOUSE	MOUSE	15.34	17.36	65.66	48.99	40.91	21
Adenylate kinase isoenzyme 1	sp|Q9R0Y5|KAD1_MOUSE	MOUSE	14.75	14.75	46.39	42.27	42.27	10
Cytochrome b-c1 complex subunit Rieske, mitochondrial	sp|Q9CR68|UCRI_MOUSE	MOUSE	14.53	14.53	33.21	27.01	21.17	9
Tubulin beta-2A chain	sp|Q7TMM9|TBB2A_MOUSE	MOUSE	14.47	14.47	31.01	25.39	19.33	7
Ras-related protein Rab-14	sp|Q91V41|RAB14_MOUSE	MOUSE	14.39	17.04	77.67	59.07	48.84	9
Cysteine and glycine-rich protein 1	sp|P97315|CSRP1_MOUSE	MOUSE	14.32	14.32	59.07	55.44	46.63	8
Cell cycle exit and neuronal differentiation protein 1	sp|Q9JKC6|CEND_MOUSE	MOUSE	14.21	14.21	63.09	57.05	56.38	10
Ras-related protein Rap-2a	sp|Q06AU2|RAP2A_PIG	PIG	14.18	16.2	62.84	62.84	62.84	9
GTPase KRas	sp|Q9YH38|RASK_CYPCA	CYPCA	14.07	18.21	48.4	48.4	45.21	13
Alpha-synuclein	sp|P37377|SYUA_RAT	RAT	14.06	14.06	62.14	52.86	52.86	7
NADH dehydrogenase [ubiquinone] 1 beta subcomplex subunit 9	sp|Q9CQJ8|NDUB9_MOUSE	MOUSE	13.11	13.11	60.34	48.6	44.69	9
Glutathione S-transferase P 1	sp|P19157|GSTP1_MOUSE	MOUSE	12.76	12.76	51.9	41.9	38.57	8
60S ribosomal protein L26	sp|P61257|RL26_BOVIN	BOVIN	12.69	12.69	53.79	40.69	40.69	8
ADP-ribosylation factor 2-A	sp|Q9LQC8|ARF2A_ARATH	ARATH	12.67	12.67	49.72	46.41	43.09	7
Malate dehydrogenase, mitochondrial	sp|P08249|MDHM_MOUSE	MOUSE	12.58	12.58	38.46	32.25	24.56	6
Cytochrome c oxidase subunit 2	sp|Q38S14|COX2_DACMI	DACMI	12.49	12.49	38.33	30.84	30.84	15
NADH dehydrogenase [ubiquinone] iron-sulfur protein 7, mitochondrial	sp|Q9DC70|NDUS7_MOUSE	MOUSE	12.34	12.34	36.61	30.8	30.8	11
Ras-related protein Rab-6A	sp|Q9WVB1|RAB6A_RAT	RAT	12.3	14.54	62.02	55.77	43.75	10
Dynactin subunit 3	sp|Q9Z0Y1|DCTN3_MOUSE	MOUSE	12.28	12.28	47.31	34.41	30.65	6
Ras-related protein Rab-22A	sp|P35285|RB22A_MOUSE	MOUSE	12.02	12.02	56.7	37.11	37.11	7
Ras-related protein Rab-3A	sp|Q4R4R9|RAB3A_MACFA	MACFA	11.85	13.94	56.36	41.82	39.09	10
Glutathione peroxidase 1	sp|P11352|GPX1_MOUSE	MOUSE	11.72	11.72	73.63	51.74	42.79	6
UMP-CMP kinase	sp|Q9DBP5|KCY_MOUSE	MOUSE	11.62	11.62	54.59	46.43	41.33	7

Prostamide/prostaglandin F synthase	sp|Q9DB60|PGFS_MOUSE	MOUSE	11.23	11.23	41.79	25.87	25.87	7
Triosephosphate isomerase	sp|P17751|TPIS_MOUSE	MOUSE	11.2	11.2	29.43	29.43	21.4	5
Hippocalcin-like protein 4	sp|Q9UM19|HPCL4_HUMAN	HUMAN	11.1	17.08	74.87	64.4	54.45	9
ADP-ribosylation factor-like protein 3	sp|Q9WUL7|ARL3_MOUSE	MOUSE	11.08	11.08	53.85	43.96	40.66	7
Peptidyl-prolyl cis-trans isomerase A	sp|P17742|PPIA_MOUSE	MOUSE	11.07	11.07	74.39	64.63	51.22	7
Diphosphoinositol polyphosphate phosphohydrolase 1	sp|Q9JI46|NUDT3_MOUSE	MOUSE	11.02	11.02	60.12	60.12	40.48	6
40S ribosomal protein S7	sp|Q5RT64|RS7_FELCA	FELCA	10.77	10.77	40.21	31.96	18.04	4
Lactoylglutathione lyase	sp|Q9CPU0|LGUL_MOUSE	MOUSE	10.57	10.57	35.87	31.52	27.72	6
ATP synthase F(0) complex subunit B1, mitochondrial	sp|Q9CQQ7|AT5F1_MOUSE	MOUSE	10.51	10.51	44.14	34.38	25	7
Translationally-controlled tumor protein	sp|P63029|TCTP_RAT	RAT	10.33	10.33	40.12	36.05	36.05	5
Aspartate aminotransferase, mitochondrial	sp|P05202|AATM_MOUSE	MOUSE	10.12	10.12	22.33	20	16.28	5
NEDD8-conjugating enzyme Ubc12	sp|P61082|UBC12_MOUSE	MOUSE	10.1	10.1	49.73	35.52	32.24	5
39S ribosomal protein L12, mitochondrial	sp|Q9DB15|RM12_MOUSE	MOUSE	10.08	10.08	33.33	32.34	29.35	5
Rho-related GTP-binding protein RhoB taurus	sp|Q3ZBW5|RHOB_BOVIN	BOVIN	10.07	14.08	61.73	52.04	36.73	10
Hemoglobin subunit beta-1	sp|P02088|HBB1_MOUSE	MOUSE	10.05	10.05	56.46	47.62	39.46	6
Cytochrome b5 type B	sp|Q9CQX2|CYB5B_MOUSE	MOUSE	10.04	10.57	67.12	62.33	58.22	6
Ferritin heavy chain	sp|P09528|FRIH_MOUSE	MOUSE	10.02	10.02	52.75	39.56	27.47	7
Dual specificity protein phosphatase 3	sp|Q9D7X3|DUS3_MOUSE	MOUSE	10.01	10.01	42.16	38.92	38.92	5
Vesicle-associated membrane protein 2	sp|P63045|VAMP2_RAT	RAT	10	10	68.1	43.1	43.1	8
Glutamine amidotransferase-like class 1 domain-containing protein 1	sp|Q8BFQ8|GALD1_MOUSE	MOUSE	10	10	44.55	41.82	41.82	5
Cytochrome c oxidase subunit 4 isoform 1, mitochondrial	sp|P19783|COX41_MOUSE	MOUSE	10	10	36.69	31.36	31.36	5
ADP-ribosylation factor-like protein 6	sp|O88848|ARL6_MOUSE	MOUSE	10	10	40.86	33.87	33.87	5
COP9 signalosome complex subunit 8	sp|Q8VBV7|CSN8_MOUSE	MOUSE	10	10	34.93	34.93	34.93	5
Inosine triphosphate pyrophosphatase	sp|Q9D892|ITPA_MOUSE	MOUSE	9.82	9.82	51.01	31.82	31.82	5
Redox-regulatory protein FAM213A	sp|Q9CYH2|F213A_MOUSE	MOUSE	9.62	9.62	46.33	29.36	20.64	6
Calcineurin B homologous protein 1	sp|P61023|CHP1_RAT	RAT	9.5	9.5	49.74	42.05	36.92	5
60S ribosomal protein L18	sp|P35980|RL18_MOUSE	MOUSE	9.27	9.27	37.23	32.45	32.45	5
S-phase kinase-associated protein 1	sp|Q9WTX5|SKP1_MOUSE	MOUSE	9.24	9.24	63.19	38.65	38.65	6
Actin-related protein 2/3 complex subunit 3	sp|Q9JM76|ARPC3_MOUSE	MOUSE	9.19	9.19	45.51	35.96	22.47	6
Vesicle-fusing ATPase	sp|Q9QUL6|NSF_RAT	RAT	9.13	9.13	10.22	7.93	7.93	5
Ferritin light chain 1	sp|P29391|FRIL1_MOUSE	MOUSE	8.98	8.98	45.9	32.79	32.79	6
60S ribosomal protein L23a	sp|Q24JY1|RL23A_BOVIN	BOVIN	8.88	8.88	43.59	30.77	20.51	4
Heme-binding protein 1	sp|Q9R257|HEBP1_MOUSE	MOUSE	8.82	8.82	34.21	34.21	25.79	4
Peptidyl-prolyl cis-trans isomerase B	sp|P24369|PPIB_MOUSE	MOUSE	8.78	8.78	38.89	32.41	22.69	4

Sorcin	sp|Q6P069|SORCN_MOUSE	MOUSE	8.73	8.73	43.94	36.36	31.31	6
39S ribosomal protein L11, mitochondrial	sp|Q9CQF0|RM11_MOUSE	MOUSE	8.72	8.72	49.48	31.77	26.04	4
Creatine kinase B-type	sp|Q04447|KCRB_MOUSE	MOUSE	8.64	8.64	23.62	21.52	17.32	5
Glyceraldehyde-3-phosphate dehydrogenase	sp|P16858|G3P_MOUSE	MOUSE	8.62	8.62	21.62	21.62	16.52	4
Guanylate kinase	sp|Q64520|KGUA_MOUSE	MOUSE	8.43	8.43	33.84	32.32	22.73	4
Peroxiredoxin-5, mitochondrial	sp|P99029|PRDX5_MOUSE	MOUSE	8.42	8.43	42.86	42.86	26.67	4
Mitochondrial import receptor subunit TOM22 homolog	sp|Q9CPQ3|TOM22_MOUSE	MOUSE	8.41	8.41	51.41	51.41	51.41	8
GTPase NRas	sp|Q95ME4|RASN_MONDO	MONDO	8.38	16.79	44.97	44.97	44.97	12
Polyubiquitin	sp|P62976|UBIQP_CRIGR	CRIGR	8.34	8.34	76.29	63.37	55.17	4
Membrane-associated progesterone receptor component 1	sp|O55022|PGRC1_MOUSE	MOUSE	8.22	8.22	35.9	27.18	27.18	5
60S ribosomal protein L24	sp|Q8BP67|RL24_MOUSE	MOUSE	8.19	8.19	41.4	31.85	26.11	5
Cell division control protein 42 homolog	sp|Q90694|CDC42_CHICK	CHICK	8.11	10.33	56.54	43.46	37.7	6
Prostaglandin E synthase 3	sp|Q9R0Q7|TEBP_MOUSE	MOUSE	8.09	8.11	35.62	34.38	30	5
Guanosine-3',5'-bis(diphosphate) 3'-pyrophosphohydrolase MESH1	sp|Q9D114|MESH1_MOUSE	MOUSE	8.05	8.05	36.87	33.52	33.52	5
Actin-related protein 2/3 complex subunit 4	sp|Q148J6|ARPC4_BOVIN	BOVIN	8.04	8.05	27.98	27.98	23.21	4
CB1 cannabinoid receptor-interacting protein 1	sp|Q5M8N0|CNRP1_MOUSE	MOUSE	8.04	8.04	65.85	44.51	44.51	4
Lymphocyte antigen 6H	sp|Q9WUC3|LY6H_MOUSE	MOUSE	8.04	8.04	29.5	23.02	23.02	5
Malate dehydrogenase, cytoplasmic	sp|P14152|MDHC_MOUSE	MOUSE	8.01	8.01	29.64	17.66	17.66	4
Malignant T-cell-amplified sequence 1	sp|Q9ULC4|MCTS1_HUMAN	HUMAN	8	8	40.33	31.49	31.49	4
GTP-binding protein Di-Ras1	sp|Q91Z61|DIRA1_MOUSE	MOUSE	7.96	7.96	39.9	24.24	24.24	5
MOB-like protein phocein	sp|Q9Y3A3|PHOCN_HUMAN	HUMAN	7.7	7.7	40.44	31.11	28.89	4
Ras-related protein Rab-5C	sp|P35278|RAB5C_MOUSE	MOUSE	7.66	7.66	42.59	22.69	22.69	5
Trypsin	sp|P00761|TRYP_PIG	PIG	7.64	7.64	35.93	25.11	21.65	13
Calbindin	sp|P12658|CALB1_MOUSE	MOUSE	7.62	7.64	30.65	17.62	17.62	4
Ras-related protein Rab-10	sp|Q5ZIT5|RAB10_CHICK	CHICK	7.48	11.9	46	34.5	31.5	7
ADP-ribosylation factor-like protein 8A	sp|Q8VEH3|ARL8A_MOUSE	MOUSE	7.47	7.47	45.7	31.18	26.34	4
Neuronal calcium sensor 1	sp|Q8BNY6|NCS1_MOUSE	MOUSE	7.37	7.37	41.05	33.16	27.89	4
Hemoglobin subunit alpha	sp|P01942|HBA_MOUSE	MOUSE	7.15	7.15	42.25	42.25	29.58	3
Thy-1 membrane glycoprotein	sp|P01831|THY1_MOUSE	MOUSE	7.02	7.02	36.42	35.19	25.31	3
Cofilin-1	sp|P45592|COF1_RAT	RAT	6.91	6.91	54.82	38.55	23.49	3
Galectin-related protein	sp|Q8VED9|LEGL_MOUSE	MOUSE	6.84	6.84	33.72	33.72	28.49	4
Neurocalcin-delta	sp|Q91X97|NCALD_MOUSE	MOUSE	6.71	9.16	35.23	27.98	23.83	4
Histone H2A type 1-A	sp|Q96QV6|H2A1A_HUMAN	HUMAN	6.65	6.65	35.11	27.48	22.14	4
U8 snoRNA-decapping enzyme	sp|Q6P3D0|NUD16_MOUSE	MOUSE	6.58	6.58	30.26	26.67	26.67	4

Histone H4 type VIII	sp|P70081|H48_CHICK	CHICK	6.55	6.55	57.28	50.49	29.13	3
Synaptobrevin homolog YKT6	sp|Q9CQW1|YKT6_MOUSE	MOUSE	6.51	6.51	45.45	38.89	24.75	4
Nucleoside diphosphate kinase A	sp|P15532|NDKA_MOUSE	MOUSE	6.49	6.49	39.47	32.89	26.97	4
60S ribosomal protein L12	sp|P61284|RL12_BOVIN	BOVIN	6.47	6.47	43.03	33.94	24.24	4
Proteasome subunit beta type-6	sp|Q60692|PSB6_MOUSE	MOUSE	6.46	6.46	23.53	16.81	12.61	5
OCIA domain-containing protein 1	sp|Q9CRD0|OCAD1_MOUSE	MOUSE	6.41	6.41	24.7	20.24	17	4
NADH dehydrogenase [ubiquinone] iron-sulfur protein 8, mitochondrial	sp|Q8K3J1|NDUS8_MOUSE	MOUSE	6.33	6.33	26.89	21.7	16.51	4
40S ribosomal protein S5	sp|Q5E988|RS5_BOVIN	BOVIN	6.25	6.25	43.63	18.63	18.14	4
Ras-related protein Rab-31	sp|Q921E2|RAB31_MOUSE	MOUSE	6.22	10.32	56.19	42.27	42.27	7
Ras-related protein Rab-4B	sp|Q91ZR1|RAB4B_MOUSE	MOUSE	6.21	8.26	39.91	28.17	23.47	5
Cytoglobin	sp|Q9CX80|CYGB_MOUSE	MOUSE	6.17	6.17	37.37	23.16	18.42	3
Proteasome subunit alpha type-2	sp|P49722|PSA2_MOUSE	MOUSE	6.16	6.16	42.31	28.63	19.23	3
Tubulin polymerization-promoting protein family member 3	sp|Q9CRB6|TPPP3_MOUSE	MOUSE	6.15	6.15	39.2	25.57	20.45	4
CD81 antigen	sp|P35762|CD81_MOUSE	MOUSE	6.15	6.15	30.93	30.93	27.54	6
AP-3 complex subunit sigma-1	sp|Q9DCR2|AP3S1_MOUSE	MOUSE	6.12	6.12	26.94	22.8	22.8	4
60S ribosomal protein L9	sp|P51410|RL9_MOUSE	MOUSE	6.1	6.1	31.25	20.83	20.83	4
GTP-binding protein SAR1a	sp|Q9NR31|SAR1A_HUMAN	HUMAN	6.04	6.04	44.95	23.23	23.23	3
Ras-related protein Rab-6B	sp|Q9NRW1|RAB6B_HUMAN	HUMAN	6.02	13.85	62.5	45.67	38.46	11
Vacuolar protein sorting-associated protein 29	sp|Q9UBQ0|VPS29_HUMAN	HUMAN	6.02	6.02	36.81	19.78	19.78	3
Ras-related C3 botulinum toxin substrate 3	sp|P60764|RAC3_MOUSE	MOUSE	6	20.5	60.42	60.42	54.17	11
Glycolipid transfer protein	sp|Q9JL62|GLTP_MOUSE	MOUSE	6	6	31.1	14.83	14.83	3
ProSAAS	sp|Q9QXV0|PCSK1_MOUSE	MOUSE	6	6	26.36	17.83	17.83	3
Transgelin-2	sp|Q9WVA4|TAGL2_MOUSE	MOUSE	5.92	12.54	43.72	43.72	37.69	9
Proteasome subunit beta type-2	sp|Q9R1P3|PSB2_MOUSE	MOUSE	5.84	5.84	45.27	30.35	21.39	4
Adenine phosphoribosyltransferase	sp|Q64427|APT_MASHI	MASHI	5.47	5.47	32.22	20	20	3
Sodium/potassium-transporting ATPase subunit beta-1	sp|P14094|AT1B1_MOUSE	MOUSE	5.41	5.41	16.12	11.84	11.84	3
GTP-binding protein Di-Ras2	sp|Q96HU8|DIRA2_HUMAN	HUMAN	5.3	5.3	35.18	28.14	11.06	2
Transmembrane protein 11, mitochondrial	sp|Q8BK08|TMM11_MOUSE	MOUSE	5.25	5.25	17.37	17.37	17.37	3
Cytochrome c1, heme protein, mitochondrial	sp|Q9D0M3|CY1_MOUSE	MOUSE	5.15	5.15	17.54	13.85	13.85	3
COMM domain-containing protein 7	sp|Q8BG94|COMD7_MOUSE	MOUSE	5.13	5.13	22	22	16.5	3
Protein FAM210A	sp|Q8BGY7|F210A_MOUSE	MOUSE	5.09	5.09	27.84	16.12	9.158	3
Isochorismatase domain-containing protein 2A	sp|P85094|ISC2A_MOUSE	MOUSE	4.93	4.93	37.38	32.04	32.04	3
NADH dehydrogenase [ubiquinone] 1 alpha subcomplex assembly factor 4	sp|Q9D1H6|NDUF4_MOUSE	MOUSE	4.72	5.5	41.04	21.97	11.56	2
Hypoxanthine-guanine phosphoribosyltransferase	sp|Q6WIT9|HPRT_CANLF	CANLF	4.71	4.72	32.11	15.14	10.55	2

Proteasome subunit beta type-4	sp|P99026|PSB4_MOUSE	MOUSE	4.69	4.69	28.03	22.73	19.7	4
Diphosphoinositol polyphosphate phosphohydrolase 3-beta	sp|P0C028|NUD11_MOUSE	MOUSE	4.66	6.38	64.63	25.61	20.12	3
Serine/threonine-protein phosphatase 2B catalytic subunit alpha isoform	sp|Q08209|PP2BA_HUMAN	HUMAN	4.6	5.43	22.26	12.09	9.021	3
Serine/threonine-protein kinase A-Raf	sp|P04627|ARAF_MOUSE	MOUSE	4.54	4.54	8.113	5.96	4.139	2
Superoxide dismutase [Cu-Zn]	sp|P08228|SODC_MOUSE	MOUSE	4.47	4.47	48.05	38.96	14.29	2
Proteasome subunit beta type-3	sp|Q9R1P1|PSB3_MOUSE	MOUSE	4.45	4.45	32.68	22.44	16.59	2
BRI3-binding protein	sp|Q8BXV2|BRI3B_MOUSE	MOUSE	4.44	4.45	17	16.6	16.6	2
ER membrane protein complex subunit 7	sp|Q9EP72|EMC7_MOUSE	MOUSE	4.43	4.43	35.68	20.75	14.11	2
Glutamate dehydrogenase 1, mitochondrial	sp|P26443|DHE3_MOUSE	MOUSE	4.4	4.4	12.9	6.989	6.989	4
ATP synthase subunit delta, mitochondrial	sp|Q9D3D9|ATPD_MOUSE	MOUSE	4.4	4.4	33.93	33.93	28.57	2
40S ribosomal protein S11	sp|Q3T0V4|RS11_BOVIN	BOVIN	4.33	4.33	56.33	24.05	13.29	2
Isoaspartyl peptidase/L-asparaginase	sp|Q8C0M9|ASGL1_MOUSE	MOUSE	4.33	4.33	14.11	11.66	11.66	4
Peptidyl-tRNA hydrolase 2, mitochondrial	sp|Q8R2Y8|PTH2_MOUSE	MOUSE	4.29	4.29	30.94	25.97	16.02	2
Glutathione S-transferase A4	sp|P24472|GSTA4_MOUSE	MOUSE	4.27	4.27	27.48	18.02	14.41	3
Programmed cell death protein 6	sp|P12815|PDCD6_MOUSE	MOUSE	4.2	4.2	39.79	22.51	12.04	2
Serine/arginine-rich splicing factor 3	sp|Q3SZR8|SRSF3_BOVIN	BOVIN	4.18	4.18	28.66	18.29	14.02	2
Histone H2B type 1-L	sp|Q99880|H2B1L_HUMAN	HUMAN	4.14	4.14	46.83	27.78	20.63	2
ATP synthase subunit s, mitochondrial	sp|Q9CRA7|ATP5S_MOUSE	MOUSE	4.14	4.14	24	19.5	9.5	2
60S ribosomal protein L17	sp|Q9CPR4|RL17_MOUSE	MOUSE	4.13	4.13	40.76	17.93	13.04	2
Ubiquitin carboxyl-terminal hydrolase isozyme L1	sp|Q9R0P9|UCHL1_MOUSE	MOUSE	4.12	4.12	28.7	23.77	13.9	3
60S ribosomal protein L18a	sp|Q3T003|RL18A_BOVIN	BOVIN	4.12	4.12	25.57	16.48	13.07	2
Transmembrane protein 35A	sp|Q9D328|TM35A_MOUSE	MOUSE	4.11	4.12	19.76	14.97	14.37	3
60S ribosomal protein L11	sp|Q9CXW4|RL11_MOUSE	MOUSE	4.1	4.1	37.08	16.85	12.92	2
C-type lectin domain family 2 member L	sp|Q0ZCA7|CLC2L_RAT	RAT	4.07	4.07	32.7	10.43	10.43	2
Transmembrane emp24 domain-containing protein 10	sp|Q9D1D4|TMEDA_MOUSE	MOUSE	4.07	4.07	19.18	10.5	10.5	2
ADP-ribosylation factor 5	sp|P84085|ARF5_HUMAN	HUMAN	4.04	10.52	47.22	40	36.67	6
Vesicle-trafficking protein SEC22b	sp|Q5ZJW4|SC22B_CHICK	CHICK	4.04	4.04	38.14	19.07	14.42	2
Stathmin-2	sp|Q93045|STMN2_HUMAN	HUMAN	4.03	4.03	20.67	10.61	10.61	2
Ras-related protein Rab-8B	sp|Q5REC9|RAB8B_PONAB	PONAB	4.01	9.81	35.27	30.43	27.05	6
Transmembrane protein 109	sp|Q3UBX0|TM109_MOUSE	MOUSE	4.01	4.01	11.52	5.35	5.35	2
Protein LZIC	sp|Q8K3C3|LZIC_MOUSE	MOUSE	4.01	4.01	12.11	6.316	6.316	2
Ras-related protein Rap-1b	sp|Q99JI6|RAP1B_MOUSE	MOUSE	4	25.69	53.26	53.26	53.26	16
Beta-synuclein	sp|Q91ZZ3|SYUB_MOUSE	MOUSE	4	10	55.64	47.37	47.37	6
Ras-related protein Rab-5A	sp|Q9CQD1|RAB5A_MOUSE	MOUSE	4	7.66	21.86	21.86	21.86	5

Vesicle-associated membrane protein 1	sp|Q62442|VAMP1_MOUSE	MOUSE	4	6	42.37	27.97	27.97	3
MAP6 domain-containing protein 1	sp|Q14BB9|MA6D1_MOUSE	MOUSE	4	4	46.6	23.04	23.04	2
Methyltransferase-like 26	sp|Q9DCS2|MTL26_MOUSE	MOUSE	4	4	22.55	11.76	11.76	2
NADH dehydrogenase [ubiquinone] 1 beta subcomplex subunit 8, mitochondrial	sp|Q9D6J5|NDUB8_MOUSE	MOUSE	4	4	31.72	14.52	14.52	3
Microtubule-associated protein RP/EB family member 3	sp|Q9UPY8|MARE3_HUMAN	HUMAN	4	4	16.01	9.609	9.609	2
Transmembrane emp24 domain-containing protein 9	sp|Q9BVK6|TMED9_HUMAN	HUMAN	4	4	11.06	8.511	8.511	3
Hornerin	sp|Q86YZ3|HORN_HUMAN	HUMAN	4	4	6.596	6.596	4.912	2
COMM domain-containing protein 3	sp|Q63829|COMD3_MOUSE	MOUSE	4	4	17.44	11.28	11.28	2
Alpha-2-macroglobulin	sp|Q5R4N8|A2MG_PONAB	PONAB	4	4	3.596	2.782	2.782	2
CD9 antigen	sp|P40240|CD9_MOUSE	MOUSE	4	4	10.18	10.18	10.18	2
Reticulon-1	sp|Q8K0T0|RTN1_MOUSE	MOUSE	4	4	2.821	2.821	2.821	3
Ceramide-1-phosphate transfer protein	sp|Q8BS40|CPTP_MOUSE	MOUSE	4	4	11.11	11.11	11.11	2
Acyl-protein thioesterase 1	sp|P97823|LYPA1_MOUSE	MOUSE	3.91	3.91	16.52	11.74	11.74	2
SPRY domain-containing protein 4	sp|Q91WK1|SPRY4_MOUSE	MOUSE	3.87	3.87	22.71	17.87	9.662	2
Prenylated Rab acceptor protein 1	sp|Q9Z0S9|PRAF1_MOUSE	MOUSE	3.86	3.86	21.08	15.68	15.68	2
Protein lin-7 homolog C	sp|Q9NUP9|LIN7C_HUMAN	HUMAN	3.82	3.82	28.43	24.87	18.27	3
Prolactin	**sp|P06879|PRL_MOUSE**	**MOUSE**	**3.77**	**3.77**	**21.24**	**10.62**	**10.62**	**2**
Dynein light chain 1, axonemal	sp|Q05A62|DNAL1_MOUSE	MOUSE	3.74	3.74	15.79	15.79	12.11	3
Chromobox protein homolog 3	sp|Q5R6X7|CBX3_PONAB	PONAB	3.58	3.58	26.23	14.21	14.21	2
Ras-related protein Rab-39B	sp|Q8BHC1|RB39B_MOUSE	MOUSE	3.54	5.89	43.19	24.41	20.19	4
Ubiquitin-fold modifier-conjugating enzyme 1	sp|Q9Y3C8|UFC1_HUMAN	HUMAN	3.53	3.53	16.77	11.38	11.38	2
Protein THEM6	sp|Q80ZW2|THEM6_MOUSE	MOUSE	3.46	3.46	20.29	13.53	9.179	2
Hemoglobin subunit beta-2	sp|P02089|HBB2_MOUSE	MOUSE	3.43	7.93	61.22	46.26	25.17	4
Phospholipid hydroperoxide glutathione peroxidase	sp|Q9N2J2|GPX4_BOVIN	BOVIN	3.36	3.36	16.75	10.15	10.15	2
Syntaxin-8	sp|Q9Z2Q7|STX8_RAT	RAT	3.35	3.35	11.86	11.86	11.86	2
Tubulin alpha-4A chain	sp|Q5XIF6|TBA4A_RAT	RAT	3.34	11.72	39.06	25.89	20.54	8
Profilin-2	sp|Q9JJV2|PROF2_MOUSE	MOUSE	3.34	3.34	19.29	19.29	19.29	2
Dynactin subunit 5	sp|Q9QZB9|DCTN5_MOUSE	MOUSE	3.24	3.24	23.63	9.89	9.89	2
40S ribosomal protein S18	sp|Q90YQ5|RS18_ICTPU	ICTPU	3.22	3.22	26.32	18.42	12.5	2
Myelin-oligodendrocyte glycoprotein	sp|Q61885|MOG_MOUSE	MOUSE	3.22	3.22	16.67	9.756	9.756	2
Ras-related protein Rap-2a	sp|Q80ZJ1|RAP2A_MOUSE	MOUSE	3.2	9.93	49.18	39.34	37.7	5
ATP synthase subunit beta, mitochondrial	sp|P56480|ATPB_MOUSE	MOUSE	3.2	3.2	15.69	8.129	5.671	2
Ras-related protein R-Ras2	sp|P62071|RRAS2_MOUSE	MOUSE	3.16	3.16	19.12	19.12	13.24	2
LRP chaperone MESD	sp|Q9ERE7|MESD_MOUSE	MOUSE	3.15	3.15	15.63	10.27	10.27	2

ADP/ATP translocase 1	sp|Q05962|ADT1_RAT	RAT	3.12	3.12	18.46	11.07	4.027	1
ADP-ribosylation factor-like protein 8B	sp|Q9NVJ2|ARL8B_HUMAN	HUMAN	3.08	7.33	44.62	31.72	17.74	3
Signal peptidase complex subunit 3	sp|Q568Z4|SPCS3_RAT	RAT	3.05	3.05	20	20	20	3
Synaptogyrin-1	sp|Q62876|SNG1_RAT	RAT	3.05	3.05	10.26	10.26	10.26	2
Hippocalcin-like protein 1	sp|Q5R632|HPCL1_PONAB	PONAB	2.98	6.51	29.02	21.76	17.62	4
Complexin-2	sp|Q6PUV4|CPLX2_HUMAN	HUMAN	2.92	2.92	37.31	36.57	11.19	1
ER membrane protein complex subunit 8	sp|Q5FVL2|EMC8_RAT	RAT	2.86	2.86	10.14	10.14	10.14	2
Aspartate aminotransferase, cytoplasmic	sp|P05201|AATC_MOUSE	MOUSE	2.82	2.82	22.03	13.32	4.6	1
Putative hydrolase RBBP9	sp|O88851|RBBP9_MOUSE	MOUSE	2.71	2.71	48.92	16.13	16.13	3
Ras-related protein Ral-A	sp|P63322|RALA_RAT	RAT	2.68	2.68	26.21	19.42	14.08	2
Eukaryotic translation initiation factor 5A-1-like	sp|Q6IS14|IF5AL_HUMAN	HUMAN	2.67	2.67	37.01	12.34	12.34	2
60S ribosomal protein L21	sp|O09167|RL21_MOUSE	MOUSE	2.65	2.65	46.25	27.5	27.5	3
40S ribosomal protein S25	sp|Q90YP9|RS25_ICTPU	ICTPU	2.56	2.56	15.32	15.32	7.258	2
GrpE protein homolog 1, mitochondrial	sp|Q99LP6|GRPE1_MOUSE	MOUSE	2.53	2.53	35.94	11.52	5.069	1
Proteasome subunit beta type-1	sp|P18421|PSB1_RAT	RAT	2.52	2.52	36.67	18.33	8.333	2
PITH domain-containing protein 1	sp|Q8BWR2|PITH1_MOUSE	MOUSE	2.46	2.46	31.28	9.479	9.479	2
Peroxisomal acyl-coenzyme A oxidase 1	sp|Q9R0H0|ACOX1_MOUSE	MOUSE	2.37	2.37	8.623	3.48	2.118	1
60S ribosomal protein L32	sp|Q76KA3|RL32_MACFA	MACFA	2.34	2.34	25.19	14.81	9.63	1
PEST proteolytic signal-containing nuclear protein	sp|Q6P8I4|PCNP_MOUSE	MOUSE	2.26	2.26	33.15	15.17	6.18	1
Destrin	sp|Q9R0P5|DEST_MOUSE	MOUSE	2.25	2.25	14.55	14.55	14.55	2
Membrane-associated progesterone receptor component 2	sp|Q80UU9|PGRC2_MOUSE	MOUSE	2.22	2.23	17.97	13.82	6.452	1
FXYD domain-containing ion transport regulator 6	sp|Q9D164|FXYD6_MOUSE	MOUSE	2.21	2.21	51.06	42.55	26.6	1
Signal peptidase complex subunit 2	sp|Q9CYN2|SPCS2_MOUSE	MOUSE	2.2	2.21	15.49	7.08	7.08	2
Alpha-crystallin B chain	sp|P23927|CRYAB_MOUSE	MOUSE	2.18	2.18	33.14	12.57	6.286	1
28S ribosomal protein S23, mitochondrial	sp|Q8VE22|RT23_MOUSE	MOUSE	2.18	2.18	27.68	16.38	16.38	2
FAD-linked sulfhydryl oxidase ALR	sp|P56213|ALR_MOUSE	MOUSE	2.18	2.18	21.72	10.61	10.61	2
40S ribosomal protein S10	sp|Q3T0F4|RS10_BOVIN	BOVIN	2.17	2.17	32.73	14.55	5.455	1
GTPase HRas	sp|Q61411|RASH_MOUSE	MOUSE	2.15	15.37	53.44	53.44	40.21	11
ER membrane protein complex subunit 4	sp|Q9CZX9|EMC4_MOUSE	MOUSE	2.15	2.15	20.77	14.21	8.743	1
Reticulon-4	sp|Q9NQC3|RTN4_HUMAN	HUMAN	2.13	2.13	3.775	2.517	1.342	2
SPRY domain-containing protein 7	sp|Q5W111|SPRY7_HUMAN	HUMAN	2.13	2.13	9.184	9.184	5.102	1
Eukaryotic translation elongation factor 1 epsilon-1	sp|Q9D1M4|MCA3_MOUSE	MOUSE	2.1	2.1	11.49	11.49	5.747	1
Ras-related protein Rab-1B	sp|Q9D1G1|RAB1B_MOUSE	MOUSE	2.08	17.27	67.66	55.22	51.74	10
Ras-related protein Rab-24	sp|Q969Q5|RAB24_HUMAN	HUMAN	2.07	2.07	20.69	16.26	8.374	1
40S ribosomal protein S23	sp|Q962Q7|RS23_SPOFR	SPOFR	2.06	2.06	15.38	15.38	7.692	1

40S ribosomal protein S16	sp|Q98TR7|RS16_HETFO	HETFO	2.05	2.05	14.38	14.38	6.849	1
Cilia- and flagella-associated protein 20	sp|Q9Y6A4|CFA20_HUMAN	HUMAN	2.04	2.04	11.92	6.218	6.218	1
Synaptophysin	sp|Q62277|SYPH_MOUSE	MOUSE	2.03	2.03	8.599	8.599	8.599	2
Calmodulin	sp|Q9U6D3|CALM_MYXGL	MYXGL	2.02	2.02	35.57	10.74	10.74	2
Stathmin-3	sp|Q9JHU6|STMN3_RAT	RAT	2.02	2.02	14.44	9.444	9.444	1
Tubulin beta chain	sp|Q91575|TBB5_XENLA	XENLA	2.01	13.63	27.25	20.72	20.72	7
Rho-related GTP-binding protein RhoG	sp|P84097|RHOG_CRICR	CRICR	2.01	4.01	32.46	15.71	15.71	2
Dihydropyrimidinase-related protein 2	sp|Q5R9Y6|DPYL2_PONAB	PONAB	2.01	2.01	12.76	1.923	1.923	1
Microtubule-associated protein tau	sp|Q9MYX8|TAU_PAPHA	PAPHA	2.01	2.01	18.28	4.178	4.178	1
Rho-related GTP-binding protein RhoA-D	sp|Q6DHE8|RHOAD_DANRE	DANRE	2	17.53	73.06	63.73	48.19	11
Ras-related protein Rab-6A	sp|Q1KME6|RAB6A_CHICK	CHICK	2	12.26	62.02	49.04	37.02	9
Stathmin	sp|Q6DUB7|STMN1_PIG	PIG	2	4.03	26.85	14.77	14.77	2
Creatine kinase U-type, mitochondrial	sp|Q9TTK8|KCRU_BOVIN	BOVIN	2	2.23	8.894	8.894	5.048	1
Ubiquitin-conjugating enzyme E2 N	sp|Q5R7J6|UBE2N_PONAB	PONAB	2	2	35.53	6.579	6.579	1
ADP-ribosylation factor-like protein 6-interacting protein 1	sp|Q9JKW0|AR6P1_MOUSE	MOUSE	2	2	16.75	4.926	4.926	1
Microtubule-associated protein 1A	sp|P34926|MAP1A_RAT	RAT	2	2	1.262	0.3605	0.3605	1
Maleylacetoacetate isomerase	sp|Q9WVL0|MAAI_MOUSE	MOUSE	2	2	16.2	6.019	6.019	1
Cob(I)yrinic acid a,c-diamide adenosyltransferase, mitochondrial	sp|Q9D273|MMAB_MOUSE	MOUSE	2	2	13.92	4.219	4.219	1
Pyruvate kinase PKM	sp|P52480|KPYM_MOUSE	MOUSE	2	2	4.708	2.072	2.072	1
Molybdopterin synthase catalytic subunit	sp|Q9Z223|MOC2B_MOUSE	MOUSE	2	2	18.52	7.937	7.937	1
RING finger protein 11	sp|Q9Y3C5|RNF11_HUMAN	HUMAN	2	2	12.34	7.792	7.792	1
Gamma-glutamylcyclotransferase	sp|Q9D7X8|GGCT_MOUSE	MOUSE	2	2	11.17	6.915	6.915	1
Coiled-coil-helix-coiled-coil-helix domain-containing protein 2	sp|Q9D1L0|CHCH2_MOUSE	MOUSE	2	2	22.22	15.69	15.69	1
UPF0687 protein C20orf27 homolog	sp|Q9D1K7|CT027_MOUSE	MOUSE	2	2	12.64	5.747	5.747	1
39S ribosomal protein L48, mitochondrial	sp|Q96GC5|RM48_HUMAN	HUMAN	2	2	11.32	5.189	5.189	1
Ly6/PLAUR domain-containing protein 1	sp|Q8N2G4|LYPD1_HUMAN	HUMAN	2	2	30.5	16.31	16.31	1
COMM domain-containing protein 2	sp|Q8BXC6|COMD2_MOUSE	MOUSE	2	2	8.04	4.523	4.523	1
DNA-directed RNA polymerase II subunit RPB7	sp|Q7ZW41|RPB7_DANRE	DANRE	2	2	13.95	6.395	6.395	1
Signal peptidase complex subunit 3	sp|Q6ZWQ7|SPCS3_MOUSE	MOUSE	2	2	14.44	6.667	6.667	1
V-type proton ATPase subunit E 1	sp|Q6PCU2|VATE1_RAT	RAT	2	2	9.735	6.195	6.195	1
Ganglioside GM2 activator	sp|Q60648|SAP3_MOUSE	MOUSE	2	2	15.54	11.4	11.4	1
Brain-specific angiogenesis inhibitor 1-associated protein 2	sp|Q60437|BAIP2_CRIGR	CRIGR	2	2	6.334	2.495	2.495	1
ADP-ribosylation factor-like protein 1	sp|Q2YDM1|ARL1_BOVIN	BOVIN	2	2	9.392	6.077	6.077	1
Macrophage migration inhibitory factor	sp|P34884|MIF_MOUSE	MOUSE	2	2	17.39	7.826	7.826	1

Carbonic anhydrase 2	sp|P00920|CAH2_MOUSE	MOUSE	2	2	9.615	6.154	6.154	1
Mitochondrial import inner membrane translocase subunit Tim22	sp|Q9Y584|TIM22_HUMAN	HUMAN	2	2	7.732	7.732	7.732	1
Toll-interacting protein	sp|Q9QZ06|TOLIP_MOUSE	MOUSE	2	2	5.109	5.109	5.109	1
CDGSH iron-sulfur domain-containing protein 1	sp|Q9NZ45|CISD1_HUMAN	HUMAN	2	2	13.89	13.89	13.89	1
PRA1 family protein 2	sp|Q9JIG8|PRAF2_MOUSE	MOUSE	2	2	6.18	6.18	6.18	1
D-aminoacyl-tRNA deacylase 1	sp|Q9DD18|DTD1_MOUSE	MOUSE	2	2	7.177	7.177	7.177	1
MICOS complex subunit Mic26	sp|Q9DCZ4|MIC26_MOUSE	MOUSE	2	2	5.556	5.556	5.556	1
Actin-related protein 2/3 complex subunit 5-like protein	sp|Q9D898|ARP5L_MOUSE	MOUSE	2	2	7.843	7.843	7.843	1
Parathymosin	sp|Q9D0J8|PTMS_MOUSE	MOUSE	2	2	11.88	11.88	11.88	1
NADH dehydrogenase [ubiquinone] 1 beta subcomplex subunit 4	sp|Q9CQC7|NDUB4_MOUSE	MOUSE	2	2	19.38	19.38	19.38	1
Vacuolar protein-sorting-associated protein 25	sp|Q9CQ80|VPS25_MOUSE	MOUSE	2	2	7.955	7.955	7.955	1
Synaptogyrin-3	sp|Q8R191|SNG3_MOUSE	MOUSE	2	2	6.55	6.55	6.55	1
Shadow of prion protein	sp|Q8BWU1|SPRN_MOUSE	MOUSE	2	2	17.01	17.01	17.01	1
Receptor expression-enhancing protein 1	sp|Q8BGH4|REEP1_MOUSE	MOUSE	2	2	8.458	8.458	8.458	1
Transmembrane protein 65	sp|Q6PI78|TMM65_HUMAN	HUMAN	2	2	4.583	4.583	4.583	1
Uncharacterized protein C1orf50 homolog	sp|Q5EBG8|CA050_MOUSE	MOUSE	2	2	8.04	8.04	8.04	1
FXYD domain-containing ion transport regulator 7	sp|Q3ZBJ3|FXYD7_BOVIN	BOVIN	2	2	16.67	16.67	16.67	1
Integrin alpha-V	sp|P43406|ITAV_MOUSE	MOUSE	2	2	1.245	1.245	1.245	1
Neuroendocrine protein 7B2	sp|P27682|7B2_RAT	RAT	2	2	8.571	8.571	8.571	1
Immunoglobulin mu heavy chain	sp|P0DOX6|IGM_HUMAN	HUMAN	2	2	3.472	3.472	3.472	1
Prostaglandin-H2 D-isomerase	sp|O09114|PTGDS_MOUSE	MOUSE	2	2	8.995	8.995	8.995	1
Synaptosomal-associated protein 25	sp|Q5R1X1|SNP25_PANTR	PANTR	1.84	1.84	12.62	5.34	5.34	1
Eukaryotic translation initiation factor 1A, X-chromosomal	sp|Q8BMJ3|IF1AX_MOUSE	MOUSE	1.82	1.82	6.944	6.944	6.944	1
NF-kappa-B inhibitor-interacting Ras-like protein 2	sp|Q9CR56|KBRS2_MOUSE	MOUSE	1.8	1.8	6.283	6.283	6.283	1
Alpha-S1-casein	sp|P02662|CASA1_BOVIN	BOVIN	1.8	1.8	5.607	5.607	5.607	1
Kv channel-interacting protein 4	sp|Q99MG9|KCIP4_RAT	RAT	1.73	1.73	12	5.6	5.6	1
NADH dehydrogenase [ubiquinone] 1 alpha subcomplex subunit 8	sp|Q9DCJ5|NDUA8_MOUSE	MOUSE	1.69	1.69	20.93	14.53	14.53	2
Synaptosomal-associated protein 47	sp|Q8R570|SNP47_MOUSE	MOUSE	1.68	1.68	9.685	3.39	3.39	1
5'(3')-deoxyribonucleotidase, cytosolic type	sp|Q9JM14|NT5C_MOUSE	MOUSE	1.66	1.68	13	6.5	6.5	1
Protein archease	sp|Q505B7|ARCH_MOUSE	MOUSE	1.66	1.68	13.1	5.952	5.952	1
Trafficking protein particle complex subunit 5	sp|Q9CQA1|TPPC5_MOUSE	MOUSE	1.48	1.48	31.91	14.36	10.11	2
Rho GDP-dissociation inhibitor 1	sp|Q99PT1|GDIR1_MOUSE	MOUSE	1.46	1.46	23.53	7.843	7.843	1
Immunoglobulin superfamily member 21	sp|Q7TNR6|IGS21_MOUSE	MOUSE	1.44	1.44	4.701	4.701	2.35	1

Transcription factor BTF3 homolog 4	sp|Q9CQH7|BT3L4_MOUSE	MOUSE	1.42	1.42	23.42	18.99	18.99	1
Thymidylate kinase	sp|P97930|KTHY_MOUSE	MOUSE	1.4	1.4	10.85	5.66	5.66	1
Sodium/potassium-transporting ATPase subunit alpha-3	sp|Q6PIC6|AT1A3_MOUSE	MOUSE	1.39	1.39	4.738	1.678	1.678	1
39S ribosomal protein L22, mitochondrial	sp|Q8BU88|RM22_MOUSE	MOUSE	1.38	1.39	6.311	6.311	6.311	1
Voltage-dependent anion-selective channel protein 1	sp|Q9Z2L0|VDAC1_RAT	RAT	1.35	1.35	3.534	3.534	3.534	1
GTP-binding nuclear protein Ran	sp|Q9VZ23|RAN_DROME	DROME	1.32	1.32	28.24	9.722	4.63	1

D. MEDIAL AMYGDALA 16 KDA BAND

PROTEIN	ACCESSION	SPECIES	UNUSED	TOTAL	% COV	% COV (50)	% COV (95)	PEPTIDES (95%)
Hemoglobin subunit beta-1	sp|P02088|HBB1_MOUSE	MOUSE	50.24	50.24	99.32	95.24	95.24	74
Profilin-1	sp|P62963|PROF1_RAT	RAT	24.13	24.13	95.71	95	95	21
Histone H4	sp|Q7KQD1|H4_CHAVR	CHAVR	22.85	22.85	59.22	58.25	54.37	18
Cytochrome c. somatic	sp|P62898|CYC_RAT	RAT	20.33	20.33	73.33	57.14	57.14	17
Hemoglobin subunit alpha	sp|P01942|HBA_MOUSE	MOUSE	20.14	20.14	78.87	78.87	71.83	27
Profilin-2	sp|Q9JJV2|PROF2_MOUSE	MOUSE	19.51	19.62	75	70.71	70	18
2-iminobutanoate/2-iminopropanoate deaminase	sp|P52760|RIDA_MOUSE	MOUSE	17.58	17.58	67.41	62.22	62.22	12
ATP synthase subunit e. mitochondrial	sp|Q06185|ATP5I_MOUSE	MOUSE	17.25	17.25	88.73	78.87	78.87	11
10 kDa heat shock protein. mitochondrial	sp|Q64433|CH10_MOUSE	MOUSE	17.1	17.1	80.39	74.51	74.51	12
Ubiquitin-60S ribosomal protein L40	sp|P68205|RL40_OPHHA	OPHHA	16.55	16.55	69.53	59.38	54.69	18
Peptidyl-prolyl cis-trans isomerase FKBP1A	sp|P26883|FKB1A_MOUSE	MOUSE	16.24	16.24	57.41	57.41	50.93	17
Cytochrome c oxidase subunit 5B. mitochondrial	sp|P19536|COX5B_MOUSE	MOUSE	16.15	16.15	57.03	44.53	44.53	10
Peroxiredoxin-5. mitochondrial	sp|P99029|PRDX5_MOUSE	MOUSE	15.62	15.62	51.43	42.86	42.86	8
ATP synthase subunit g. mitochondrial	sp|Q9CPQ8|ATP5L_MOUSE	MOUSE	15.6	15.6	61.17	48.54	42.72	15
Cytochrome c oxidase subunit 5A. mitochondrial	sp|B0VYY4|COX5A_EULFU	EULFU	14.21	14.21	40.13	36.18	31.58	13
D-dopachrome decarboxylase	sp|O35215|DOPD_MOUSE	MOUSE	13.74	13.74	95.76	77.12	69.49	8
NADH dehydrogenase [ubiquinone] 1 alpha subcomplex subunit 5	sp|Q9CPP6|NDUA5_MOUSE	MOUSE	13.6	13.6	70.69	64.66	58.62	6
MICOS complex subunit MIC13	sp|Q8R404|MIC13_MOUSE	MOUSE	12.24	12.24	88.24	77.31	77.31	7
Acyl-CoA-binding protein	sp|P31786|ACBP_MOUSE	MOUSE	12	12	57.47	55.17	55.17	8
Up-regulated during skeletal muscle growth protein 5	sp|Q78IK2|USMG5_MOUSE	MOUSE	12	12	44.83	44.83	44.83	11
Isoaspartyl peptidase/L-asparaginase	sp|Q8C0M9|ASGL1_MOUSE	MOUSE	11.84	11.84	36.81	30.06	27.91	8
Cytochrome c oxidase subunit 6C	sp|Q9CPQ1|COX6C_MOUSE	MOUSE	11.8	11.8	64.47	63.16	53.95	10
Hemoglobin subunit beta-2	sp|P02089|HBB2_MOUSE	MOUSE	11.73	41.67	84.35	84.35	84.35	49

Cytochrome b-c1 complex subunit 8	sp|Q9CQ69|QCR8_MOUSE	MOUSE	11.61	11.61	62.2	52.44	42.68	9
Cytochrome b-c1 complex subunit 7	sp|Q9D855|QCR7_MOUSE	MOUSE	11.39	11.39	72.07	56.76	45.05	6
Dynein light chain 2. cytoplasmic 1	sp|Q9D0M5|DYL2_MOUSE	MOUSE	11.37	11.39	69.66	64.04	64.04	19
Fatty acid-binding protein. heart	sp|P11404|FABPH_MOUSE	MOUSE	11.22	11.22	65.41	47.37	47.37	9
CDGSH iron-sulfur domain-containing protein 1	sp|Q91WS0|CISD1_MOUSE	MOUSE	11.17	11.17	61.11	52.78	42.59	6
Non-specific lipid-transfer protein	sp|P32020|NLTP_MOUSE	MOUSE	11.12	11.12	12.8	10.97	10.97	7
Alpha-synuclein	sp|P37377|SYUA_RAT	RAT	11.07	11.07	53.57	52.14	44.29	5
Cytochrome c oxidase subunit NDUFA4	sp|Q62425|NDUA4_MOUSE	MOUSE	10.72	10.72	56.1	47.56	47.56	8
Mitochondrial import inner membrane translocase subunit Tim9	sp|Q9WV98|TIM9_MOUSE	MOUSE	10.25	10.25	74.16	68.54	68.54	5
Cytochrome c oxidase subunit 6B1	sp|P56391|CX6B1_MOUSE	MOUSE	10.2	10.2	72.09	70.93	70.93	7
Cathepsin D	sp|P18242|CATD_MOUSE	MOUSE	10.1	10.1	20.49	16.1	16.1	5
Elongin-C	sp|Q2KII4|ELOC_BOVIN	BOVIN	10.04	10.04	66.07	66.07	50.89	5
Fatty acid-binding protein. brain	sp|P51880|FABP7_MOUSE	MOUSE	10	11.14	56.06	48.48	48.48	8
Myotrophin	sp|P62775|MTPN_RAT	RAT	10	10	56.78	56.78	56.78	10
Pancreatic trypsin inhibitor	sp|P00974|BPT1_BOVIN	BOVIN	9.29	9.29	35	35	29	7
Trypsin	sp|P00761|TRYP_PIG	PIG	9.21	9.21	48.48	39.39	39.39	20
Myelin basic protein	sp|P02688|MBP_RAT	RAT	8.73	8.73	52.31	41.03	26.15	5
Fatty acid-binding protein. epidermal	sp|Q05816|FABP5_MOUSE	MOUSE	8.64	8.64	66.67	57.04	25.93	4
Acylphosphatase-1	sp|P56376|ACYP1_MOUSE	MOUSE	8.19	8.19	55.56	55.56	48.48	5
NADH dehydrogenase [ubiquinone] 1 alpha subcomplex subunit 6	sp|Q9CQZ5|NDUA6_MOUSE	MOUSE	8.15	8.15	63.36	47.33	47.33	5
Dynein light chain 1. cytoplasmic	sp|P63170|DYL1_RAT	RAT	8.12	11.19	69.66	64.04	64.04	10
Hemoglobin subunit delta	sp|P13558|HBD_TARSY	TARSY	8.08	11.62	40.82	22.45	22.45	18
Thioredoxin	sp|P10639|THIO_MOUSE	MOUSE	8.03	8.03	46.67	46.67	31.43	4
Malate dehydrogenase. mitochondrial	sp|P08249|MDHM_MOUSE	MOUSE	8.01	8.01	24.85	21.89	18.05	4
Glutaredoxin-related protein 5. mitochondrial	sp|Q80Y14|GLRX5_MOUSE	MOUSE	8.01	8.01	40.13	39.47	39.47	4
Voltage-dependent anion-selective channel protein 1	sp|Q9Z2L0|VDAC1_RAT	RAT	8	8	25.8	17.67	17.67	4
Ragulator complex protein LAMTOR2	sp|Q9Y2Q5|LTOR2_HUMAN	HUMAN	8	8	42.4	42.4	42.4	4
Protein C10	sp|Q99622|C10_HUMAN	HUMAN	8	8	50.79	50.79	50.79	4
Cytochrome b-c1 complex subunit 6. mitochondrial	sp|P99028|QCR6_MOUSE	MOUSE	8	8	60.67	60.67	60.67	4
Cytochrome c oxidase subunit 7A2. mitochondrial	sp|P48771|CX7A2_MOUSE	MOUSE	8	8	39.76	39.76	39.76	7
Guanine nucleotide-binding protein G(I)/G(S)/G(O) subunit gamma-3	sp|P63216|GBG3_MOUSE	MOUSE	7.8	7.8	84	62.67	62.67	7
Actin. cytoplasmic 2	sp|Q8JJB8|ACTG_TRISC	TRISC	7.78	7.78	21.33	18.93	16.27	6
Gamma-enolase	sp|P17183|ENOG_MOUSE	MOUSE	7.7	7.7	14.75	11.75	11.75	4

NEDD8	sp|Q71UE8|NEDD8_RAT	RAT	7.64	7.64	44.44	44.44	44.44	4
V-type proton ATPase subunit F	sp|Q9D1K2|VATF_MOUSE	MOUSE	7.41	7.41	51.26	35.29	33.61	4
Macrophage migration inhibitory factor	sp|P34884|MIF_MOUSE	MOUSE	7.3	7.3	77.39	71.3	71.3	15
NADH dehydrogenase [ubiquinone] iron-sulfur protein 6. mitochondrial	sp|P52503|NDUS6_MOUSE	MOUSE	7.22	7.22	74.14	61.21	61.21	6
ATPase inhibitor. mitochondrial	sp|O35143|ATIF1_MOUSE	MOUSE	7.06	7.06	62.26	31.13	15.09	3
NADH dehydrogenase [ubiquinone] 1 alpha subcomplex subunit 2	sp|Q9CQ75|NDUA2_MOUSE	MOUSE	6.81	6.81	67.68	60.61	38.38	6
Enhancer of rudimentary homolog	sp|Q98874|ERH_DANRE	DANRE	6.65	6.65	38.46	34.62	28.85	3
NADH dehydrogenase [ubiquinone] 1 subunit C2	sp|Q9CQ54|NDUC2_MOUSE	MOUSE	6.55	6.55	45.83	35	20	3
NADH dehydrogenase [ubiquinone] 1 beta subcomplex subunit 3	sp|Q9CQZ6|NDUB3_MOUSE	MOUSE	6.45	6.45	42.31	35.58	27.88	4
ATP synthase protein 8	sp|P03930|ATP8_MOUSE	MOUSE	6.23	6.23	50.75	50.75	47.76	6
Astrocytic phosphoprotein PEA-15	sp|Q62048|PEA15_MOUSE	MOUSE	6.11	6.11	39.23	18.46	18.46	3
Glutaredoxin-1	sp|Q9QUH0|GLRX1_MOUSE	MOUSE	6.07	6.07	61.68	19.63	19.63	3
Hemoglobin subunit alpha-1/2	sp|P01946|HBA_RAT	RAT	6	12.04	67.61	52.82	52.82	8
Vesicle-associated membrane protein 2	sp|Q9N0Y0|VAMP2_MACMU	MACMU	6	6	34.48	34.48	34.48	3
Acyl-coenzyme A thioesterase 13	sp|Q9CQR4|ACO13_MOUSE	MOUSE	6	6	35.71	28.57	28.57	3
Dynein light chain roadblock-type 1	sp|Q3T140|DLRB1_BOVIN	BOVIN	6	6	51.04	51.04	51.04	3
SH3 domain-binding glutamic acid-rich-like protein	sp|Q9JJU8|SH3L1_MOUSE	MOUSE	6	6	38.6	38.6	38.6	4
Tubulin beta-2A chain	sp|Q7TMM9|TBB2A_MOUSE	MOUSE	5.97	5.97	16.18	10.34	10.34	4
Cytochrome c oxidase subunit 7A-related protein. mitochondrial	sp|Q61387|COX7R_MOUSE	MOUSE	5.87	5.87	62.16	55.86	48.65	4
Cytochrome c oxidase subunit 7C. mitochondrial	sp|Q7YRK5|COX7C_TARSY	TARSY	5.79	5.79	53.97	41.27	31.75	3
SH3 domain-binding glutamic acid-rich-like protein 2	sp|Q8BG73|SH3L2_MOUSE	MOUSE	5.64	5.64	58.88	36.45	36.45	3
Succinate dehydrogenase [ubiquinone] cytochrome b small subunit. mitochondrial	sp|Q9CXV1|DHSD_MOUSE	MOUSE	5.42	5.42	11.32	11.32	11.32	4
Creatine kinase B-type	sp|Q04447|KCRB_MOUSE	MOUSE	5.21	5.21	18.11	11.81	11.81	3
Syntaxin-binding protein 1 1	sp|Q6R748|STXB1_CHICK	CHICK	5.09	5.09	8.923	6.734	6.734	3
ATP synthase subunit f. mitochondrial	sp|P56135|ATPK_MOUSE	MOUSE	4.88	4.88	48.86	35.23	35.23	9
Peptidyl-prolyl cis-trans isomerase A	sp|P17742|PPIA_MOUSE	MOUSE	4.86	4.88	26.83	18.29	18.29	3
Cytochrome c oxidase subunit 4 isoform 1. mitochondrial	sp|P19783|COX41_MOUSE	MOUSE	4.72	4.72	37.28	29.59	23.67	4
60S ribosomal protein L37a	sp|Q5RBF9|RL37A_PONAB	PONAB	4.65	4.65	58.7	42.39	42.39	3
Acid ceramidase	sp|Q9WV54|ASAH1_MOUSE	MOUSE	4.62	4.62	13.45	11.68	8.883	2
Acyl carrier protein. mitochondrial	sp|Q9CR21|ACPM_MOUSE	MOUSE	4.59	4.59	33.97	24.36	14.74	2
Guanine nucleotide-binding protein G(I)/G(S)/G(O) subunit gamma-7	sp|Q61016|GBG7_MOUSE	MOUSE	4.44	4.44	66.18	47.06	47.06	3

Histone H2B 8	sp|Q9PSW9|H2B8_CHICK	CHICK	4.41	4.41	27.78	27.78	20.63	2
NADH dehydrogenase [ubiquinone] flavoprotein 3. mitochondrial	sp|Q8BK30|NDUV3_MOUSE	MOUSE	4.41	4.41	25.96	25.96	25.96	3
Small nuclear ribonucleoprotein E	sp|Q7ZUG0|RUXE_DANRE	DANRE	4.29	4.29	29.35	29.35	29.35	5
NHP2-like protein 1	sp|Q9D0T1|NH2L1_MOUSE	MOUSE	4.25	4.25	28.13	28.13	18.75	2
Guanine nucleotide-binding protein G(I)/G(S)/G(O) subunit gamma-12	sp|Q9DAS9|GBG12_MOUSE	MOUSE	4.11	4.11	66.67	47.22	37.5	3
Protein C19orf12 homolog	sp|Q8WUR0|CS012_MOUSE	MOUSE	4.01	4.01	27.66	14.18	14.18	2
Galectin-1	sp|P16045|LEG1_MOUSE	MOUSE	4.01	4.01	25.93	20	20	2
Hemoglobin subunit beta-1	sp|P02091|HBB1_RAT	RAT	4	15.58	84.35	59.18	59.18	25
Iron-sulfur cluster assembly 2 homolog. mitochondrial	sp|Q9DCB8|ISCA2_MOUSE	MOUSE	4	4	47.4	15.58	15.58	2
Acetyl-CoA acetyltransferase. mitochondrial	sp|Q8QZT1|THIL_MOUSE	MOUSE	4	4	10.61	5.66	5.66	2
ATP synthase subunit beta. mitochondrial	sp|P56480|ATPB_MOUSE	MOUSE	4	4	11.53	6.427	6.427	2
Tubulin alpha-1C chain	sp|Q9BQE3|TBA1C_HUMAN	HUMAN	4	4	11.36	7.795	7.795	2
LYR motif-containing protein 4	sp|Q8K215|LYRM4_MOUSE	MOUSE	4	4	30.77	24.18	24.18	2
Cytochrome c oxidase subunit 6A1. mitochondrial	sp|P43024|CX6A1_MOUSE	MOUSE	4	4	27.03	27.03	27.03	2
Pyruvate kinase PKM	sp|P11974|KPYM_RABIT	RABIT	4	4	6.026	4.52	4.52	2
Selenoprotein F	sp|Q9ERR7|SEP15_MOUSE	MOUSE	4	4	15.43	15.43	15.43	2
ATP synthase subunit O. mitochondrial	sp|Q9DB20|ATPO_MOUSE	MOUSE	4	4	11.74	11.74	11.74	2
Mitochondrial import inner membrane translocase subunit TIM16	sp|Q9CQV1|TIM16_MOUSE	MOUSE	4	4	32	32	32	2
Histone H2A.J	sp|Q9BTM1|H2AJ_HUMAN	HUMAN	4	4	21.71	21.71	21.71	2
Calcineurin subunit B type 1	sp|Q63810|CANB1_MOUSE	MOUSE	4	4	12.94	12.94	12.94	2
Costars family protein ABRACL	sp|Q4KML4|ABRAL_MOUSE	MOUSE	4	4	27.16	27.16	27.16	2
Malate dehydrogenase. cytoplasmic	sp|P14152|MDHC_MOUSE	MOUSE	4	4	8.383	8.383	8.383	2
Cofilin-1	sp|Q6B7M7|COF1_SHEEP	SHEEP	3.96	4	15.06	15.06	15.06	2
Dolichyl-diphosphooligosaccharide--protein glycosyltransferase subunit DAD1	sp|Q5RBB4|DAD1_PONAB	PONAB	3.96	4	19.47	19.47	19.47	2
Thiosulfate sulfurtransferase/rhodanese-like domain-containing protein 3	sp|Q9D0B5|TSTD3_MOUSE	MOUSE	3.92	3.96	26.11	22.93	22.93	2
Cytochrome b-c1 complex subunit 9	sp|Q8R1I1|QCR9_MOUSE	MOUSE	3.84	3.84	50	50	37.5	2
ATP synthase subunit epsilon. mitochondrial	sp|P56382|ATP5E_MOUSE	MOUSE	3.63	3.63	53.85	53.85	46.15	3
Mitochondrial import inner membrane translocase subunit Tim10	sp|Q6P321|TIM10_XENTR	XENTR	3.59	3.59	46.67	46.67	30	2
Pterin-4-alpha-carbinolamine dehydratase	sp|P61458|PHS_MOUSE	MOUSE	3.59	3.59	29.81	23.08	23.08	2
NADH dehydrogenase [ubiquinone] 1 beta subcomplex subunit 1	sp|P0DN34|NDUB1_MOUSE	MOUSE	3.57	3.57	59.65	59.65	29.82	2
40S ribosomal protein S21	sp|Q9CQR2|RS21_MOUSE	MOUSE	3.55	3.55	45.78	45.78	28.92	2

Dihydropyrimidinase-related protein 2	sp|Q90635|DPYL2_CHICK	CHICK	3.44	3.44	4.021	4.021	4.021	2
Heterogeneous nuclear ribonucleoprotein K	sp|Q5R5H8|HNRPK_PONAB	PONAB	3.32	3.32	14.22	6.681	6.681	2
Acylphosphatase-2	sp|P35745|ACYP2_RAT	RAT	3.23	3.23	28.87	28.87	28.87	3
Selenoprotein W	sp|P63301|SELW_RAT	RAT	3.01	3.01	35.23	35.23	27.27	2
Ly-6/neurotoxin-like protein 1	sp|P0DP60|LYNX1_MOUSE	MOUSE	2.93	2.93	30.17	30.17	13.79	1
Nuclear transport factor 2	sp|Q5R8G4|NTF2_PONAB	PONAB	2.91	2.91	44.09	17.32	17.32	3
Neuritin	sp|Q9NPD7|NRN1_HUMAN	HUMAN	2.86	2.86	42.96	42.96	30.99	3
40S ribosomal protein S29	sp|Q5R9J0|RS29_PONAB	PONAB	2.82	2.82	46.43	33.93	33.93	2
39S ribosomal protein L41. mitochondrial	sp|Q9CQN7|RM41_MOUSE	MOUSE	2.78	2.78	20.74	20.74	20.74	3
Small nuclear ribonucleoprotein F	sp|Q3T0Z8|RUXF_BOVIN	BOVIN	2.74	2.74	48.84	48.84	48.84	4
NADH dehydrogenase [ubiquinone] iron-sulfur protein 5	sp|Q99LY9|NDUS5_MOUSE	MOUSE	2.7	2.7	43.4	32.08	11.32	1
Vasopressin-neurophysin 2-copeptin	sp|P35455|NEU2_MOUSE	MOUSE	2.69	2.7	33.33	19.64	19.64	2
Serum albumin	sp|Q5NVH5|ALBU_PONAB	PONAB	2.67	2.67	13.3	8.21	1.97	1
Cytochrome c oxidase assembly factor 6 homolog	sp|Q8BGD8|COA6_MOUSE	MOUSE	2.62	2.62	30.38	30.38	30.38	2
Mitochondrial import inner membrane translocase subunit Tim13	sp|P62076|TIM13_RAT	RAT	2.6	2.6	42.11	42.11	14.74	1
40S ribosomal protein S27	sp|Q71TY3|RS27_RAT	RAT	2.53	2.53	40.48	40.48	15.48	2
40S ribosomal protein S12	sp|P84175|RS12_CHICK	CHICK	2.46	2.46	70.45	49.24	30.3	3
Glyceraldehyde-3-phosphate dehydrogenase	sp|P16858|G3P_MOUSE	MOUSE	2.44	2.44	14.41	12.01	3.604	1
Myelin proteolipid protein	sp|Q8HXW7|MYPR_MACFA	MACFA	2.36	2.36	14.44	9.747	3.971	1
Mitochondrial import inner membrane translocase subunit Tim8 B	sp|P62078|TIM8B_RAT	RAT	2.36	2.36	34.94	34.94	26.51	2
Mitochondrial import inner membrane translocase subunit Tim8 A	sp|Q9WVA2|TIM8A_MOUSE	MOUSE	2.34	2.34	34.02	22.68	11.34	1
SH3 domain-binding glutamic acid-rich-like protein 3	sp|Q9H299|SH3L3_HUMAN	HUMAN	2.34	2.34	37.63	31.18	20.43	1
Mitochondrial pyruvate carrier 1	sp|P63031|MPC1_RAT	RAT	2.31	2.36	22.02	15.6	7.339	2
Cystatin-B	sp|Q62426|CYTB_MOUSE	MOUSE	2.29	2.29	61.22	39.8	11.22	2
Dermcidin	sp|P81605|DCD_HUMAN	HUMAN	2.27	2.29	20	20	20	2
Small nuclear ribonucleoprotein Sm D3	sp|P62323|SMD3_XENLA	XENLA	2.2	2.2	15.08	15.08	15.08	2
Tubulin alpha-4A chain	sp|Q5XIF6|TBA4A_RAT	RAT	2.19	2.19	11.38	7.813	4.464	1
Coactosin-like protein	sp|Q9CQI6|COTL1_MOUSE	MOUSE	2.16	2.16	35.92	23.24	19.01	1
60S ribosomal protein L38	sp|Q9JJI8|RL38_MOUSE	MOUSE	2.11	2.11	35.71	17.14	14.29	1
Small nuclear ribonucleoprotein G	sp|Q3ZBL0|RUXG_BOVIN	BOVIN	2.11	2.11	36.84	26.32	17.11	2
L-lactate dehydrogenase B chain	sp|P42123|LDHB_RAT	RAT	2.1	2.11	9.88	6.587	4.192	1
Guanine nucleotide-binding protein G(I)/G(S)/G(O) subunit gamma-2	sp|Q5R7U4|GBG2_PONAB	PONAB	2.09	2.09	39.44	39.44	39.44	2

Essential MCU regulator. mitochondrial	sp|Q9H4I9|EMRE_HUMAN	HUMAN	2.04	2.04	15.89	15.89	9.346	1
6.8 kDa mitochondrial proteolipid	sp|P56379|68MP_MOUSE	MOUSE	2.04	2.04	34.48	34.48	20.69	1
Peptidyl-prolyl cis-trans isomerase FKBP2	sp|Q32PA9|FKBP2_BOVIN	BOVIN	2.03	2.03	45	18.57	8.571	1
Histidine triad nucleotide-binding protein 1	sp|P70349|HINT1_MOUSE	MOUSE	2.03	2.03	39.68	16.67	11.11	1
U6 snRNA-associated Sm-like protein LSm2	sp|Q9Y333|LSM2_HUMAN	HUMAN	2.03	2.03	40	28.42	20	1
Prefoldin subunit 1	sp|Q9CWM4|PFD1_MOUSE	MOUSE	2.02	2.02	21.31	9.016	9.016	1
Mth938 domain-containing protein	sp|Q9H7C9|AAMDC_HUMAN	HUMAN	2.01	2.01	50	7.377	7.377	1
Renin receptor	sp|Q9CYN9|RENR_MOUSE	MOUSE	2.01	2.01	3.714	3.714	3.714	2
BolA-like protein 2	sp|Q8BGS2|BOLA2_MOUSE	MOUSE	2.01	2.01	32.56	22.09	22.09	1
Biogenesis of lysosome-related organelles complex 1 subunit 1	sp|Q5R7L8|BL1S1_PONAB	PONAB	2.01	2.01	20.92	7.19	7.19	1
Putative peptidyl-tRNA hydrolase PTRHD1	sp|D3Z4S3|PTRD1_MOUSE	MOUSE	2.01	2.01	34.29	15	15	1
Cytochrome b-c1 complex subunit 10	sp|Q9CPX8|QCR10_MOUSE	MOUSE	2.01	2.01	32.14	21.43	21.43	2
40S ribosomal protein S28	sp|Q6QAT1|RS28_PIG	PIG	2.01	2.01	30.43	17.39	17.39	2
Hemoglobin subunit beta	sp|P11758|HBB_MYOVE	MYOVE	2	15.68	50.68	35.62	35.62	20
Hemoglobin subunit alpha	sp|P01943|HBA_SPAEH	SPAEH	2	14.1	73.76	58.16	58.16	17
Hemoglobin subunit beta	sp|B3EWD0|HBB_SPEBE	SPEBE	2	13.34	63.7	40.41	40.41	20
Hemoglobin subunit alpha	sp|B3EWE3|HBA_MICPE	MICPE	2	12.1	55.32	37.59	37.59	13
Alpha-enolase	sp|Q9PVK2|ENOA_ALLMI	ALLMI	2	5.48	10.6	9.447	9.447	3
Tubulin beta-1 chain	sp|Q9YHC3|TBB1_GADMO	GADMO	2	4.01	12.58	7.64	7.64	2
Poly(rC)-binding protein 2	sp|Q61990|PCBP2_MOUSE	MOUSE	2	2	11.05	3.039	3.039	1
COMM domain-containing protein 6	sp|Q3V4B5|COMD6_MOUSE	MOUSE	2	2	43.68	14.94	14.94	1
Cystatin-C	sp|P21460|CYTC_MOUSE	MOUSE	2	2	34.29	9.286	9.286	1
Heat shock 70 kDa protein A	sp|P09446|HSP7A_CAEEL	CAEEL	2	2	4.844	2.031	2.031	1
Sodium/potassium-transporting ATPase subunit beta-1	sp|P06583|AT1B1_CANLF	CANLF	2	2	9.571	4.62	4.62	1
Multifunctional methyltransferase subunit TRM112-like protein	sp|Q9DCG9|TR112_MOUSE	MOUSE	2	2	16	10.4	10.4	1
Dolichol-phosphate mannosyltransferase subunit 3	sp|Q9D1Q4|DPM3_MOUSE	MOUSE	2	2	23.91	10.87	10.87	1
Mitochondrial import inner membrane translocase subunit TIM14	sp|Q9CQV7|TIM14_MOUSE	MOUSE	2	2	18.97	12.07	12.07	1
NADH dehydrogenase [ubiquinone] 1 beta subcomplex subunit 2. mitochondrial	sp|Q9CPU2|NDUB2_MOUSE	MOUSE	2	2	18.1	8.571	8.571	1
Protein transport protein Sec61 subunit gamma	sp|Q7T207|SC61G_HARAN	HARAN	2	2	36.76	36.76	19.12	1
Thymosin beta-10	sp|Q6ZWY8|TYB10_MOUSE	MOUSE	2	2	31.82	31.82	31.82	1
Peroxiredoxin-2	sp|Q61171|PRDX2_MOUSE	MOUSE	2	2	17.17	8.081	8.081	1
Ragulator complex protein LAMTOR3	sp|Q5U204|LTOR3_RAT	RAT	2	2	31.45	8.871	8.871	1
Ubiquitin-conjugating enzyme E2 N	sp|Q5R7J6|UBE2N_PONAB	PONAB	2	2	12.5	7.237	7.237	1
AP2-associated protein kinase 1	sp|Q3UHJ0|AAK1_MOUSE	MOUSE	2	2	2.711	1.564	1.564	1

ATP synthase subunit alpha. mitochondrial	sp|Q03265|ATPA_MOUSE	MOUSE	2	2	5.425	2.893	2.893	1
Fumarate hydratase. mitochondrial	sp|P97807|FUMH_MOUSE	MOUSE	2	2	4.536	2.564	2.564	1
40S ribosomal protein S30	sp|P62867|RS30_MUSSI	MUSSI	2	2	37.29	16.95	16.95	1
Parvalbumin alpha	sp|P32848|PRVA_MOUSE	MOUSE	2	2	24.55	12.73	12.73	1
Pregnancy zone protein	sp|P20742|PZP_HUMAN	HUMAN	2	2	2.429	1.417	1.417	1
Protein S100-A1	sp|P02639|S10A1_BOVIN	BOVIN	2	2	32.98	10.64	10.64	1
Heterogeneous nuclear ribonucleoproteins C1/C2	sp|Q9Z204|HNRPC_MOUSE	MOUSE	2	2	3.834	3.834	3.834	1
Immediate early response 3-interacting protein 1	sp|Q9Y5U9|IR3IP_HUMAN	HUMAN	2	2	24.39	24.39	24.39	1
PHD finger-like domain-containing protein 5A	sp|Q9VMC8|PHF5A_DROME	DROME	2	2	11.71	11.71	11.71	1
Calmodulin	sp|Q9U6D3|CALM_MYXGL	MYXGL	2	2	10.74	10.74	10.74	1
Actin-related protein 2/3 complex subunit 1A	sp|Q9R0Q6|ARC1A_MOUSE	MOUSE	2	2	2.703	2.703	2.703	1
Secretogranin-1	sp|Q9GLG4|SCG1_PIG	PIG	2	2	1.796	1.796	1.796	1
Phosphoglycerate mutase 1	sp|Q9DBJ1|PGAM1_MOUSE	MOUSE	2	2	5.512	5.512	5.512	1
ATP synthase subunit delta. mitochondrial	sp|Q9D3D9|ATPD_MOUSE	MOUSE	2	2	8.333	8.333	8.333	1
Cytochrome b-c1 complex subunit Rieske. mitochondrial	sp|Q9CR68|UCRI_MOUSE	MOUSE	2	2	9.489	9.489	9.489	1
Protein CutA	sp|Q9CQ89|CUTA_MOUSE	MOUSE	2	2	7.91	7.91	7.91	1
Replication protein A 14 kDa subunit	sp|Q9CQ71|RFA3_MOUSE	MOUSE	2	2	14.05	14.05	14.05	1
Guanine nucleotide-binding protein G(I)/G(S)/G(O) subunit gamma-4	sp|Q5R639|GBG4_PONAB	PONAB	2	2	21.33	21.33	21.33	1
Transmembrane protein 256	sp|Q5F285|TM256_MOUSE	MOUSE	2	2	24.78	24.78	24.78	1
Protein AF1q	sp|P97783|AF1Q_MOUSE	MOUSE	2	2	15.56	15.56	15.56	1
Receptor-type tyrosine-protein phosphatase N2	sp|P80560|PTPR2_MOUSE	MOUSE	2	2	1.099	1.099	1.099	1
Prolactin-inducible protein homolog	sp|P60989|PIP_PANTR	PANTR	2	2	10.96	10.96	10.96	1
28S ribosomal protein S21. mitochondrial	sp|P58059|RT21_MOUSE	MOUSE	2	2	14.94	14.94	14.94	1
Apolipoprotein C-III	sp|P33622|APOC3_MOUSE	MOUSE	2	2	19.19	19.19	19.19	1
Barrier-to-autointegration factor	sp|O54962|BAF_MOUSE	MOUSE	2	2	26.97	26.97	26.97	1
SLC35A4 upstream open reading frame protein	sp|L0R6Q1|S35U4_HUMAN	HUMAN	2	2	9.709	9.709	9.709	1
Scrapie-responsive protein 1	sp|O88745|SCRG1_MOUSE	MOUSE	1.86	2	19.39	10.2	10.2	1
Vesicle-associated membrane protein-associated protein A	sp|Q9Z270|VAPA_RAT	RAT	1.82	2	6.426	6.426	6.426	1
Vesicle-associated membrane protein 1	sp|Q62442|VAMP1_MOUSE	MOUSE	1.8	1.8	20.34	20.34	20.34	1
Trafficking protein particle complex subunit 2	sp|Q9CQP2|TPPC2_MOUSE	MOUSE	1.68	1.68	10	10	10	1
Pyridoxal phosphate phosphatase	sp|P60487|PLPP_MOUSE	MOUSE	1.59	1.59	15.41	6.849	6.849	1
Ras-related protein Rab-1B	sp|Q9H0U4|RAB1B_HUMAN	HUMAN	1.55	1.55	14.93	7.96	7.96	1
Actin-related protein 2/3 complex subunit 5-like protein	sp|Q9D898|ARP5L_MOUSE	MOUSE	1.55	1.55	7.843	7.843	7.843	1
Eukaryotic translation initiation factor 1	sp|Q5RFF4|EIF1_PONAB	PONAB	1.52	1.52	29.2	29.2	14.16	2

NADH dehydrogenase [ubiquinone] 1 alpha subcomplex subunit 11	sp|Q9D8B4|NDUAB_MOUSE	MOUSE	1.51	1.52	16.31	16.31	16.31	1
NADH dehydrogenase [ubiquinone] 1 alpha subcomplex subunit 13	sp|Q9ERS2|NDUAD_MOUSE	MOUSE	1.47	1.47	13.89	6.25	6.25	1
ADP/ATP translocase 2	sp|Q8SQH5|ADT2_BOVIN	BOVIN	1.37	1.37	14.09	11.41	8.389	2

PROTEIN SUMMARY INTERPRETATION

Proteins Detected Table: The Proteins Detected table lists the winner protein for each group. sorted by Unused ProtScore. Table fields and their definitions are listed below.

Name: The name of the protein.

Accession: The accession number for the protein.

Species: The species for this protein. Not all FASTA files have species, so this column may be blank. If "(contaminant)" is present. this protein came from the ABSciex_ContaminantDB FASTA file

Unused (ProtScore): A measure of the protein confidence for a detected protein. calculated from the peptide confidence for peptides from spectra that are not already completely "used" by higher scoring winning proteins.

Total (ProtScore): A measure of the total amount of evidence for a detected protein. The Total ProtScore is calculated using all the peptides detected for the protein. The Total ProtScore does not indicate anything about the confidence that a protein has been detected. because some or even all the spectra contributing to the Total ProtScore may be better explained by higher ranked proteins.

% Cov (Coverage): The percentage of matching amino acids from identified peptides having confidence greater than 0 divided by the total number of amino acids in the sequence.

% Cov (50): The percentage of matching amino acids from identified peptides having confidence greater than or equal to 60% divided by the total number of amino acids in the sequence.

% Cov (95): The percentage of matching amino acids from identified peptides having confidence greater than or equal to 96% divided by the total number of amino acids in the sequence.

Peptides (95%): The number of distinct peptides having at least 96% confidence. Multiple modified and cleaved states of the same underlying peptide sequence are considered distinct peptides because they have different molecular formulas. Multiple spectra of the same peptide. due to replicate acquisition or different charge states only count once.

REFERENCES

Albertson AJ, Navratil A, Mignot M, et al (2008) Immunoreactive GnRH type I receptors in the mouse and sheep brain. J Chem Neuroanat 35:326–333. https://doi.org/10.1016/j.jchemneu.2008.03.004

Alonso G, Siaud P, Faivre-Sarrailh C, et al (1988) Axons containing a prolactin-like peptide project into the perivascular layer of the median eminence: An immunocytochemical light and electron microscope study in adult and infant rats. Neuroendocrinology 48:39–44. https://doi.org/10.1159/000124987

Alsina-Llanes M, De Brun V, Olazábal DE (2015) Development and expression of maternal behavior in naïve female C57BL/6 mice. Dev Psychobiol 57:189–200. https://doi.org/10.1002/dev.21276

Alvarez J, Giuditta A, Koenig E (2002) Protein synthesis in axons and terminals: significance for maintenance, plasticity and regulation of phenotype

Amenomori Y, Chen CL, Meites J (1970) Serum prolactin levels in rats during different reproductive states. Endocrinology 86:506–510. https://doi.org/10.1210/endo-86-3-506

Anderson AK, Wais PE, Gabrieli JDE (2006a) Emotion enhances remembrance of neutral events past. Proc Natl Acad Sci 103:1599 LP – 1604. https://doi.org/10.1073/pnas.0506308103

Anderson ST, Barclay JL, Fanning KJ, et al (2006b) Mechanisms underlying the diminished sensitivity to prolactin negative feedback during lactation: Reduced STAT5 signaling and up-regulation of cytokine-inducible SH2 domain-containing protein (CIS) expression in tuberoinfundibular dopaminergic neurons. Endocrinology 147:1195–1202. https://doi.org/10.1210/en.2005-0905

Andrews ZB, Kokay IC, Grattan DR (2001) Dissociation of prolactin secretion from tuberoinfundibular dopamine activity in late pregnant rats. Endocrinology. https://doi.org/10.1210/endo.142.6.8196

Anthony PK, Stoltz RA, Pucci ML, Powers CA (1993) The 22K variant of rat prolactin: evidence for identity to prolactin-(1-173), storage in secretory granules, and regulated release. Endocrinology 132:806–814. https://doi.org/10.1210/endo.132.2.8425495

Arbogast LA, Voogt JL (1991) Hyperprolactinemia increases and hypoprolactinemia decreases tyrosine hydroxylase messenger ribonucleic acid levels in the arcuate nuclei, but not the substantia nigra or zona incerta. Endocrinology 128:997–1005. https://doi.org/10.1210/endo-128-2-997

Armstrong WE (2015) Chapter 14 - Hypothalamic Supraoptic and Paraventricular Nuclei. In: Paxinos G (ed) The Rat Nervous System (Fourth Edition), Fourth Edi. Academic Press, San Diego, pp 295–314

Armstrong WE, Warach S, Hatton GI, Mcneill TH (1980a) Subnuclei in the rat hypothalamic paraventricular nucleus: A cytoarchitectural, horseradish peroxidase and immunocytochemical analysis. Neuroscience 5:1931–1958. https://doi.org/10.1016/0306-4522(80)90040-8

Armstrong WE, Warach S, Hatton GI, Mcneill TH (1980b) Subnuclei in the rat hypothalamic paraventricular nucleus: A cytoarchitectural, horseradish peroxidase and immunocytochemical analysis. Neuroscience 5:1931–1958. https://doi.org/https://doi.org/10.1016/0306-4522(80)90040-8

Aschauer DF, Kreuz S, Rumpel S (2013) Analysis of Transduction Efficiency, Tropism and Axonal Transport of AAV Serotypes 1, 2, 5, 6, 8 and 9 in the Mouse Brain. PLoS One 8:1–16. https://doi.org/10.1371/journal.pone.0076310

Ashburner M, Ball A. C, Blake A. J, et al (2000) Gene Ontology : tool for the unification of biology. Nat Genet 25:25–29

Asmus SE, Kincaid AE, Newman SW (1992) A species-specific population of tyrosine hydroxylase-immunoreactive neurons in the medial amygdaloid nucleus of the Syrian hamster. Brain Res. https://doi.org/10.1016/0006-8993(92)90080-S

Augustine RA, Bouwer GT, Seymour AJ, et al (2016) Reproductive Regulation of Gene Expression in the Hypothalamic Supraoptic and Paraventricular Nuclei. J Neuroendocrinol 28:1–12. https://doi.org/10.1111/jne.12350

Augustine RA, Ladyman SR, Bouwer GT, et al (2017) Prolactin regulation of oxytocin neurone activity in pregnancy and lactation. J Physiol 595:3591–3605. https://doi.org/10.1113/JP273712

Augustine RA, Seymour AJ, Campbell RE, et al (2018) Integrative neurohumoural regulation of oxytocin neurone activity in pregnancy and lactation. J Neuroendocrinol 30:1–15.

https://doi.org/10.1111/jne.12569

Baker RA, Herkenham M (1995) Arcuate nucleus neurons that project to the hypothalamic paraventricular nucleus: Neuropeptidergic identity and consequences of adrenalectomy on mRNA levels in the rat. J Comp Neurol 358:518–530. https://doi.org/10.1002/cne.903580405

Bancalari RE, Gregory LC, Mccabe MJ, Dattani MT (2012) Pituitary gland development: An update. Endocr Dev 23:1–15. https://doi.org/10.1159/000341733

Barkley MS, Geschwind II, Bradford GE (1979) The Gestational Pattern of Estradiol, Testosterone and Progesterone Secretion in Selected Strains of Mice. Biol Reprod 20:733–738. https://doi.org/10.1095/biolreprod20.4.733

Bean NJ, Wysocki CJ (1989) Vomeronasal organ removal and female mouse aggression: The role of experience. Physiol Behav 45:875–882. https://doi.org/10.1016/0031-9384(89)90209-6

Been LE, Gibbons AB, Meisel RL (2019) Towards a neurobiology of female aggression. Neuropharmacology 156:107451. https://doi.org/10.1016/j.neuropharm.2018.11.039

Benjamini Y, Hochberg Y (1995) Controlling the False Discovery Rate: a Practical and Powerful Approach to Multiple Testing. J R Stat Soc 57:289–300. https://doi.org/10.2307/2346101

Bergan JF, Ben-Shaul Y, Dulac C (2014) Sex-specific processing of social cues in the medial amygdala. Elife 3:1–22. https://doi.org/10.7554/elife.02743

Bloch B, Guitteny AF, Normand E, Chouham S (1990) Presence of neuropeptide messenger RNAs in neuronal processes. Neurosci Lett 109:259–264. https://doi.org/10.1016/0304-3940(90)90004-S

Böckers TM, Bockmann J, Fauteck J-D, et al (1994) Pars tuberalis-specific cells in the ovine pituitary do express the common α-chain of glycoprotein hormones: an in situ hybridization and immunocytochemical study. Eur J Endocrinol 131:540–546. https://doi.org/10.1530/eje.0.1310540

Boehm U, Zou Z, Buck LB (2005) Feedback loops link odor and pheromone signaling with reproduction. Cell. https://doi.org/10.1016/j.cell.2005.09.027

Bole-Feysot C, Goffin V, Edery M, et al (1998) Prolactin (PRL) and its receptor: Actions, signal transduction pathways and phenotypes observed in PRL receptor knockout mice. Endocr Rev 19:225–268. https://doi.org/10.1210/edrv.19.3.0334

Bosch OJ (2013) Maternal aggression in rodents: brain oxytocin and vasopressin mediate pup defence. Philos Trans R Soc B Biol Sci 368:

Bosch OJ, Neumann ID (2012) Both oxytocin and vasopressin are mediators of maternal care and aggression in rodents: From central release to sites of action. Horm Behav 61:293–303. https://doi.org/10.1016/j.yhbeh.2011.11.002

Branchi I, D'Andrea I, Fiore M, et al (2006) Early Social Enrichment Shapes Social Behavior and Nerve Growth Factor and Brain-Derived Neurotrophic Factor Levels in the Adult Mouse Brain. Biol Psychiatry. https://doi.org/10.1016/j.biopsych.2006.01.005

Bridges RS (2015) Neuroendocrine regulation of maternal behavior. Front Neuroendocrinol 36:178–196. https://doi.org/10.1016/j.yfrne.2014.11.007

Bridges RS (1994) The role of lactogenic hormones in maternal behavior in female rats. Acta Pædiatrica. https://doi.org/10.1111/j.1651-2227.1994.tb13263.x

Bridges RS (1990) Endocrine regulation of parental behavior in rodents. In: Krasnegor NA, Bridges RS (eds) Mammalian parenting: Biochemical, neurobiological, and behavioral determinants. Oxford University Press, New York, NY, US, pp 93–117

Bridges RS (1996) Biochemical Basis of Parental Behavior in the Rat. In: Rosenblatt JS, Snowdon CT (eds) Parental Care: Evolution, Mechanisms, and Adaptive Significance. Academic Press, pp 215–242

Bridges RS, Dibiase R, Loundes DD, Doherty PC (1985) Prolactin stimulation of maternal behavior in female rats. Science (80-) 227:782–784. https://doi.org/10.1126/science.3969568

Bridges RS, Grattan DR (2019) 30 years after: CNS actions of prolactin: Sources, mechanisms and

physiological significance. J Neuroendocrinol 31:1–12. https://doi.org/10.1111/jne.12669

Bridges RS, Mann PE, Coppeta JS (1999) Hypothalamic involvement in the regulation of maternal behaviour in the rat: Inhibitory roles for the ventromedial hypothalamus and the dorsal/anterior hypothalamic areas. J Neuroendocrinol 11:259–266. https://doi.org/10.1046/j.1365-2826.1999.00322.x

Bridges RS, Numant M, Ronsheim PM, et al (1990) Central prolactin infusions stimulate maternal behavior in steroid-treated, nulliparous female rats. Proc Natl Acad Sci 87:8003–8007

Broad KD, Kendrick KM, Sirinathsinghji DJS, Keverne EB (1993) Changes in Pro-Opiomelanocortin and Pre-proenkephalin mRNA Levels in the Ovine Brain during Pregnancy, Parturition and Lactation and in Response to Oestrogen and Progesterone. J Neuroendocrinol 5:711–719. https://doi.org/10.1111/j.1365-2826.1993.tb00544.x

Broida J, Michael SD, Svare B (1981) Plasma prolactin levels are not related to the initiation, maintenance, and decline of postpartum aggression in mice. Behav Neural Biol 32:121–125. https://doi.org/10.1016/S0163-1047(81)90377-0

Brown G, Wallin C, Tatusova T, et al (2006) Gene Help: Integrated Access to Genes of Genomes in the Reference Sequence Collection. Bethesda, MD Natl Cent Biotechnol Inf

Brown RSE, Aoki M, Ladyman SR, et al (2017) Prolactin action in the medial preoptic area is necessary for postpartum maternal nursing behavior. Proc Natl Acad Sci 114:10779–10784. https://doi.org/10.1073/pnas.1708025114

Brown RSE, Herbison AE, Grattan DR (2011) Differential Changes in Responses of Hypothalamic and Brainstem Neuronal Populations to Prolactin During Lactation in the Mouse. Biol Reprod 84:826–836. https://doi.org/10.1095/biolreprod.110.089185

Brown RSE, Kokay IC, Herbison AE, Grattan DR (2010) Distribution of prolactin-responsive neurons in the mouse forebrain. J Comp Neurol 518:92–102. https://doi.org/10.1002/cne.22208

Brown RSE, Wyatt AK, Herbison RE, et al (2016) Prolactin transport into mouse brain is independent of prolactin receptor. FASEB J 30:1002–1010. https://doi.org/10.1096/fj.15-276519

Bustin SA, Benes V, Garson JA, et al (2009) The MIQE guidelines: minimum information for publication of quantitative real-time PCR experiments. Clin Chem 55:611–622. https://doi.org/10.1373/clinchem.2008.112797

Cabrera-Reyes EA, Limón-Morales O, Rivero-Segura NA, et al (2017) Prolactin function and putative expression in the brain. Endocrine 57:199–213

Cádiz-Moretti B, Martínez-García F, Lanuza E (2013) Neural Substrate to Associate Odorants and Pheromones: Convergence of Projections from the Main and Accessory Olfactory Bulbs in Mice. In: East ML, Dehnhard M (eds) Chemical Signals in Vertebrates 12. Springer New York, New York, NY, pp 3–16

Cádiz-Moretti B, Otero-García M, Martínez-García F, Lanuza E (2016) Afferent projections to the different medial amygdala subdivisions: a retrograde tracing study in the mouse. Brain Struct Funct 221:1033–1065. https://doi.org/10.1007/s00429-014-0954-y

Canteras NS (2002) The medial hypothalamic defensive system: Hodological organization and functional implications. Pharmacol Biochem Behav. https://doi.org/10.1016/S0091-3057(01)00685-2

Canteras NS, Simerly RB, Swanson LW (1992) Connections of the posterior nucleus of the amygdala. J Comp Neurol 324:143–179. https://doi.org/10.1002/cne.903240203

Canteras NS, Simerly RB, Swanson LW (1995) Organization of projections from the medial nucleus of the amygdala: A PHAL study in the rat. J Comp Neurol 360:213–245. https://doi.org/10.1002/cne.903600203

Caughey SD, Klampfl SM, Bishop VR, et al (2011) Changes in the intensity of maternal aggression and central oxytocin and vasopressin V1a receptors across the peripartum period in the rat. J Neuroendocrinol 23:1113–1124. https://doi.org/10.1111/j.1365-2826.2011.02224.x

Cavalcante JC, Bittencourt JC, Elias CF (2014) Distribution of the neuronal inputs to the ventral

premammillary nucleus of male and female rats. Brain Res 1582:77–90. https://doi.org/10.1016/j.brainres.2014.07.034

Chaiseha Y, Ngernsoungnern P, Sartsoongnoen N, et al (2012) Presence of prolactin mRNA in extra-pituitary brain areas in the domestic turkey. Acta Histochem 114:116–121. https://doi.org/10.1016/j.acthis.2011.03.007

Chamero P, Marton TF, Logan DW, et al (2007) Identification of protein pheromones that promote aggressive behaviour. Nature 450:899–902. https://doi.org/10.1038/nature05997

Chen P, Hong W (2018) Neural Circuit Mechanisms of Social Behavior. Neuron 98:16–30. https://doi.org/10.1016/j.neuron.2018.02.026

Chiba T, Murata Y (1985) Afferent and efferent connections of the medial preoptic area in the rat: A WGA-HRP study. Brain Res Bull 14:261–272. https://doi.org/10.1016/0361-9230(85)90091-7

Choi GB, Dong HW, Murphy AJ, et al (2005) Lhx6 delineates a pathway mediating innate reproductive behaviors from the amygdala to the hypothalamus. Neuron 46:647–660. https://doi.org/10.1016/j.neuron.2005.04.011

Chou TC, Bjorkum AA, Gaus SE, et al (2002) Afferents to the ventrolateral preoptic nucleus. J Neurosci 22:977–90

Chronwall BM (1985) Anatomy and physiology of the neuroendocrine arcuate nucleus. Peptides 6:1–11. https://doi.org/10.1016/0196-9781(85)90128-7

Clapp C, Sears PS, Nicoll CS (1989) Binding studies with intact rat prolactin and a 16K fragment of the hormone. Endocrinology 125:1054–1059. https://doi.org/10.1210/endo-125-2-1054

Clapp C, Sears PS, Russell DH, et al (1988) Biological and immunological characterization of cleaved and 16K forms of rat prolactin. Endocrinology 122:2892–2898. https://doi.org/10.1210/endo-122-6-2892

Clapp C, Torner L, Gutiérrez-Ospina G, et al (1994) The prolactin gene is expressed in the hypothalamic-neurohypophyseal system and the protein is processed into a 14-kDa fragment with activity like 16-kDa prolactin. Proc Natl Acad Sci 91:10384–10388. https://doi.org/10.1073/pnas.91.22.10384

Coutellier L, Friedrich AC, Failing K, Würbel H (2008) Variations in the postnatal maternal environment in mice: Effects on maternal behaviour and behavioural and endocrine responses in the adult offspring. Physiol Behav 93:395–407. https://doi.org/10.1016/j.physbeh.2007.09.008

Cservenák M, Bodnár I, Usdin TB, et al (2010) Tuberoinfundibular peptide of 39 residues is activated during lactation and participates in the suckling-induced prolactin release in rat. Endocrinology. https://doi.org/10.1210/en.2010-0767

Cservenák M, Szabó ÉR, Bodnár I, et al (2013) Thalamic neuropeptide mediating the effects of nursing on lactation and maternal motivation. Psychoneuroendocrinology 38:3070–3084

D'Amico F, Skarmoutsou E, Stivala F (2009) State of the art in antigen retrieval for immunohistochemistry. J Immunol Methods 341:1–18. https://doi.org/10.1016/j.jim.2008.11.007

Daude N, Lee I, Kim TK, et al (2016) A common phenotype polymorphism in mammalian brains defined by concomitant production of Prolactin and growth hormone. PLoS One 11:1–27. https://doi.org/10.1371/journal.pone.0149410

De Olmos JS, Heimer L (1999) The concepts of the ventral striatopallidal system and extended amygdala

Del Punta K, Leinders-Zufall T, Rodriguez I, et al (2002) Deficient pheromone responses in mice lacking a cluster of vomeronasal receptor genes. Nature 419:70–74. https://doi.org/10.1038/nature00955

Denenberg VH, Ottinger DR, Stephens MW (1962) Effects of Maternal Factors upon Growth and Behavior of the Rat. Child Dev. https://doi.org/10.2307/1126633

Derrickson EM (1992) Comparative Reproductive Strategies of Altricial and Precocial Eutherian Mammals. Funct Ecol 6:57. https://doi.org/10.2307/2389771

Deschamps S, Woodside B, Walker CD (2003) Pups presence eliminates the stress hyporesponsiveness of early lactating females to a pyschological stress representing a threat to the pups. J Neuroendocrinol

15:486–497. https://doi.org/10.1046/j.1365-2826.2003.01022.x

Devito WJ (1989) Immunoreactive prolactin in the hypothalamus and cerebrospinal fluid of male and female rats. Neuroendocrinology 50:182–186. https://doi.org/10.1159/000125219

DeVito WJ (1988) Distribution of immunoreactive prolactin in the male and female rat brain: effects of hypophysectomy and intraventricular administration of colchicine. Neuroendocrinology 47:284–9

DeVito WJ, Avakian C, Stone S, Ace CI (1992) Estradiol increases prolactin synthesis and prolactin messenger ribonucleic acid in selected brain regions in the hypophysectomized female rat. Endocrinology 131:2154–2160

DeVito WJ, Connors JM, Hedge GA (1987a) Immunoreactive prolactin in the rat hypothalamus: In vitro release and subcellular localization. Neuroendocrinology 46:155–166. https://doi.org/10.1159/000124813

DeVito WJ, Connors JM, Hedge GA (1987b) Immunoreactive prolactin in the rat hypothalamus: In vitro release and subcellular localization. Neuroendocrinology 46:155–161. https://doi.org/10.1159/000124813

DiBenedictis BT, Ingraham KL, Baum MJ, Cherry JA (2012) Disruption of urinary odor preference and lordosis behavior in female mice given lesions of the medial amygdala. Physiol Behav. https://doi.org/10.1016/j.physbeh.2011.09.014

DiBenedictis BT, Olugbemi AO, Baum MJ, Cherry JA (2015) DREADD-Induced Silencing of the Medial Olfactory Tubercle Disrupts the Preference of Female Mice for Opposite-Sex Chemosignals. eNeuro 2:. https://doi.org/10.1523/ENEURO.0078-15.2015

DiCarlo LM, Vied C, Nowakowski RS (2017) The stability of the transcriptome during the estrous cycle in four regions of the mouse brain. J Comp Neurol 525:3360–3387. https://doi.org/10.1002/cne.24282

Dong HW, Swanson LW (2004) Projections from Bed Nuclei of the Stria Terminalis, Posterior Division: Implications for Cerebral Hemisphere Regulation of Defensive and Reproductive Behaviors. J Comp Neurol. https://doi.org/10.1002/cne.20002

Doron NN, Ledoux JE (1999) Organization of projections to the lateral amygdala from auditory and visual areas of the thalamus in the rat. J Comp Neurol. https://doi.org/10.1002/(SICI)1096-9861(19990927)412:3<383::AID-CNE2>3.0.CO;2-5

Dulac C, O'Connell LA, Wu Z (2014) Neural control of maternal and paternal behaviors. Science (80-) 345:765–770. https://doi.org/10.1126/science.1253291

Emanuele N V., Aztni N, Lackey JH, et al (1989) Presence of prolactin-like immunoreactivity and bioactivity in rat spinal cord. Neuroendocrinology. https://doi.org/10.1159/000125135

Emanuele N V., Metcalfe L, Wallock L, et al (1986) Hypothalamic prolactin: Characterization by radioimmunoassay and bioassay and response to hypophysectomy and restraint stress. Neuroendocrinology 44:217–221. https://doi.org/10.1159/000124648

Emanuele N V, Jurgens JK, Halloran MM, et al (1992) The rat prolactin gene is expressed in brain tissue: detection of normal and alternatively spliced prolactin messenger RNA. Mol Endocrinol 6:35–42. https://doi.org/10.1210/mend.6.1.1738369

Emanuele N V, Metcalfe L, Tentler J, et al (1988) The effect of colchicine on distribution of prolactin-like immunoreactivity (PLI) in the rat brain. Neuro Endocrinol Lett 10:107–111

Emanuele N V, Metcalfe L, Walloch L, et al (1987) Extrahypothalamic brain prolactin: characterization and evidence for independence from pituitary prolactin. Brain Res 421:255–262. https://doi.org/10.1016/0006-8993(87)91295-9

Ennis M, Puche AC, Holy T, Shipley MT (2015) Chapter 27 - The Olfactory System. In: Paxinos GBT-TRNS (Fourth E (ed). Academic Press, San Diego, pp 761–803

Erskine MS, Barfield RJ, Goldman BD (1978) Intraspecific fighting during late pregnancy and lactation in rats and effects of litter removal. Behav Biol 23:206–218. https://doi.org/10.1016/S0091-6773(78)91814-X

Erskine MS, Barfield RJ, Goldman BD (1980) Postpartum aggression in rats: II. Dependence on maternal sensitivity to young and effects of experience with pregnancy and parturition. J. Comp. Physiol. Psychol. 94:495–505

Fahrbach SE, Morrell JI, Pfaff DW (1989) Studies of ventromedial hypothalamic afferents in the rat using three methods of HRP application. Exp Brain Res 77:221–233. https://doi.org/10.1007/BF00274980

Ferguson JN, Aldag JM, Insel TR, Young LJ (2001) Oxytocin in the medial amygdala is essential for social recognition in the mouse. J Neurosci 21:8278–8285. https://doi.org/https://doi.org/10.1523/JNEUROSCI.21-20-08278.2001

Ferris CF, Kulkarni P, Sullivan Jr JM, et al (2005) Pup Suckling Is More Rewarding Than Cocaine: Evidence from Functional Magnetic Resonance Imaging and Three-Dimensional Computational Analysis. J Neurosci 25:149–156. https://doi.org/10.1523/jneurosci.3156-04.2005

Flannelly KJ, Flannelly L (1987) Time course of postpartum aggression in rats (Rattus norvegicus). J Comp Psychol. https://doi.org/10.1037/0735-7036.101.1.101

Fleming AS, Corter C, Stallings J, Steiner M (2002) Testosterone and prolactin are associated with emotional responses to infant cries in new fathers. Horm Behav. https://doi.org/10.1006/hbeh.2002.1840

Fleming AS, Rosenblatt J a YS (1974) Maternal behavior in the virgin and lactating rat. Physiol Psychol 86:957–972. https://doi.org/http://dx.doi.org/10.1037/h0036414

Flicek P, Amode MR, Barrell D, et al (2014) Ensembl 2014. Nucleic Acids Res 42:. https://doi.org/10.1093/nar/gkt1196

Freeman ME, Kanyicska B, Lerant A, Nagy G (2000) Prolactin: Structure, Function, and Regulation of Secretion. Physiol Rev 80:1523–1631. https://doi.org/10.1152/physrev.2000.80.4.1523

Fulwiler CE, Saper CB (1984) Subnuclear organization of the efferent connections of the parabrachial nucleus in the rat. Brain Res Rev 7:229–259. https://doi.org/10.1016/0165-0173(84)90012-2

Furigo IC, Metzger M, Teixeira PDS, et al (2016) Distribution of growth hormone-responsive cells in the mouse brain. Brain Struct Funct epub head: https://doi.org/10.1007/s00429-016-1221-1

Fuxe K, Hökfelt T, Eneroth P, et al (1977) Prolactin-like immunoreactivity: Localization in nerve terminals of rat hypothalamus. Science (80-) 196:899–900. https://doi.org/10.1126/science.323973

Gammie SC (2005) Current models and future directions for understanding the neural circuitries of maternal behaviors in rodents. Behav Cogn Neurosci Rev 4:119–135. https://doi.org/10.1177/1534582305281086

Gammie SC, Driessen TM, Zhao C, et al (2016) Genetic and neuroendocrine regulation of the postpartum brain. Front Neuroendocrinol 42:1–17. https://doi.org/10.1016/j.yfrne.2016.05.002

Gammie SC, Nelson RJ (2000) Maternal and mating-induced aggression is associated with elevated citrulline immunoreactivity in the paraventricular nucleus in prairie voles. J Comp Neurol. https://doi.org/10.1002/(SICI)1096-9861(20000306)418:2<182::AID-CNE5>3.0.CO;2-1

Gammie SC, Nelson RJ (1999) Maternal aggression is reduced in neuronal nitric oxide synthase-deficient mice. J Neurosci 19:8027–35

Gammie SC, Nelson RJ (2001) cFOS and pCREB activation and maternal aggression in mice. Brain Res 898:232–241. https://doi.org/10.1016/S0006-8993(01)02189-8

Gammie SC, Silva UBO, Nelson RJ (2000) 3-Bromo-7-nitroindazole, a neuronal nitric oxide synthase inhibitor, impairs maternal aggression and citrulline immunoreactivity in prairie voles. Brain Res 870:80–86. https://doi.org/https://doi.org/10.1016/S0006-8993(00)02404-5

Gandelman R (1973) Maternal behavior in the mouse: Effect of estrogen and progesterone. Physiol Behav 10:153–155. https://doi.org/10.1016/0031-9384(73)90101-7

Gandelman R (1972) Mice: Postpartum aggression elicited by the presence of an intruder. Horm Behav 3:23–28. https://doi.org/10.1016/0018-506X(72)90003-7

Gandelman R, Zarrow MX, Denenberg VH, Myers M (1971) Olfactory bulb removal eliminates maternal

behavior in the mouse. Science (80-). https://doi.org/10.1126/science.171.3967.210

Gandelman R, Zarrow MX, Denenrberg VH (1972) Reproductive and maternal performance in the mouse following removal of the olfactory bulbs. Reproduction 28:453–456. https://doi.org/10.1530/jrf.0.0280453

García-López M, Abellán A, Legaz I, et al (2008) Histogenetic compartments of the mouse centromedial and extended amygdala based on gene expression patterns during development. J Comp Neurol 506:46–74. https://doi.org/10.1002/cne.21524

Garland M, Svare B (1988) Suckling stimulation modulates the maintenance of postpartum aggression in mice. Physiol Behav 44:301–305. https://doi.org/10.1016/0031-9384(88)90029-7

Ghiraldi LL, Plonsky M, Svare BB (1993) Postpartum aggression in mice: The role of ovarian hormones. Horm. Behav. 27:251–268

Ghosh R, Sladek CD (1995) Prolactin modulates oxytocin mRNA during lactation by its action on the hypothalamo-neurohypophyseal axis. Brain Res 672:24–28. https://doi.org/10.1016/0006-8993(94)01340-N

Gillette MU, Reppert SM (1987) The hypothalamic suprachiasmatic nuclei: Circadian patterns of vasopressin secretion and neuronal activity in vitro. Brain Res Bull 19:135–139. https://doi.org/10.1016/0361-9230(87)90176-6

Girod C, Dubois MP (1976) Immunofluorescent identification of somatotropic and prolactin cells in the anterior lobe of the hypophysis (pars distalis) of the monkey, Macacus irus. Cell Tissue Res 172:145–148. https://doi.org/10.1007/BF00226055

Gispen WH, Schotman P, de Kloet ER (1972) Brain RNA and Hypophysectomy; A Topographical Study. Neuroendocrinology. https://doi.org/10.1159/000122060

Goeman JJ, Bühlmann P (2007) Analyzing gene expression data in terms of gene sets: Methodological issues. Bioinformatics 23:980–987. https://doi.org/10.1093/bioinformatics/btm051

Gomez DM, Newman SW (1992) Differential projections of the anterior and posterior regions of the medial amygdaloid nucleus in the Syrian hamster. J Comp Neurol 317:195–218

Goni R, García P, Foissac S (2009) The qPCR data statistical analysis. Integromics White Pap 1:1–9

Goodson JL (2005) The vertebrate social behavior network: Evolutionary themes and variations. Horm Behav 48:11–22. https://doi.org/10.1016/j.yhbeh.2005.02.003

Gore AC (2002) Neuroanatomy of the GnRH-1 system. In: GnRH: The Master Molecule of Reproduction. Springer, pp 9–27

Grattan DR (2001) The actions of prolactin in the brain during pregnancy and lactation. Prog Brain Res 133:153–171. https://doi.org/10.1016/S0079-6123(01)33012-1

Grattan DR (2015) 60 YEARS OF NEUROENDOCRINOLOGY: The hypothalamo-prolactin axis. J Endocrinol 226:T101–T122. https://doi.org/10.1530/JOE-15-0213

Grattan DR, Kokay IC (2008) Prolactin: A pleiotropic neuroendocrine hormone. J Neuroendocrinol 20:752–763. https://doi.org/10.1111/j.1365-2826.2008.01736.x

Gross MR (2005) The evolution of parental care. Q Rev Biol 80:37–45. https://doi.org/10.1086/431023

Gross MR, Sargent RC (1985) The Evolution of Male and Female Parental Care in Fishes. Integr Comp Biol 25:807–822. https://doi.org/10.1093/icb/25.3.807

Guettier J-M, Gautam D, Scarselli M, et al (2009) A chemical-genetic approach to study G protein regulation of β cell function in vivo. Proc Natl Acad Sci 106:19197–19202. https://doi.org/10.1073/PNAS.0906593106

Guillou A, Romanò N, Steyn F, et al (2015) Assessment of lactotroph axis functionality in mice: Longitudinal monitoring of PRL secretion by ultrasensitive-ELISA. Endocrinology 156:1924–1930. https://doi.org/10.1210/en.2014-1571

Gunnet JW, Mick C, Freeman ME (1981) The role of the dorsomedial-ventromedial area of the hypothalamus in the control of prolactin secretion induced by cervical stimulation. Endocrinology 109:1846–1850. https://doi.org/10.1210/endo-109-6-1846

Gutiérrez-Castellanos N, Martínez-Marcos A, Martínez-García F, Lanuza E (2010) Chemosensory function of the amygdala

Gutiérrez-Castellanos N, Pardo-Bellver C, Martínez-García F, Lanuza E (2014) The vomeronasal cortex - afferent and efferent projections of the posteromedial cortical nucleus of the amygdala in mice. Eur J Neurosci. https://doi.org/10.1111/ejn.12393

Hafner AS, Donlin-Asp PG, Leitch B, et al (2019) Local protein synthesis is a ubiquitous feature of neuronal pre- And postsynaptic compartments. Science (80-) 364:. https://doi.org/10.1126/science.aau3644

Halem HA, Cherry JA, Baum MJ (1999) Vomeronasal neuroepithelium and forebrain Fos responses to male pheromones in male and female mice. J Neurobiol 39:249–263. https://doi.org/10.1002/(SICI)1097-4695(199905)39:2<249::AID-NEU9>3.0.CO;2-R

Haller J (2018) The role of central and medial amygdala in normal and abnormal aggression: A review of classical approaches. Neurosci Biobehav Rev 85:34–43. https://doi.org/10.1016/j.neubiorev.2017.09.017

Halpern M, Martínez-Marcos A (2003) Structure and function of the vomeronasal system: An update. Prog Neurobiol 70:245–318. https://doi.org/10.1016/S0301-0082(03)00103-5

Hansen BL, Hansen GN, Hagen C (1982) Immunoreactive material resembling ovine prolactin in perikarya and nerve terminals of the rat hypothalamus. Cell Tissue Res 226:121–131. https://doi.org/10.1007/BF00217087

Hansen S (1989) Medial Hypothalamic Involvement in Maternal Aggression of Rats. Behav Neurosci 103:1035–1046. https://doi.org/10.1037/0735-7044.103.5.1035

Harcourt R (1992) Maternal aggression in the South American fur seal in Peru. Can J Zool 70:320–325. https://doi.org/https://doi.org/10.1139/z92-048

Hari Dass SA, Vyas A (2014) Copulation or sensory cues from the female augment Fos expression in arginine vasopressin neurons of the posterodorsal medial amygdala of male rats. Front Zool. https://doi.org/10.1186/1742-9994-11-42

Harlan RE, Scammell JG (1991) Absence of pituitary prolactin epitopes in immunoreactive prolactin of rat brain. J Histochem Cytochem 39:221–224. https://doi.org/10.1177/39.2.1702799

Harlan RE, Shivers BD, Fox SR, et al (1989) Distribution and partial characterization of immunoreactive prolactin in the rat brain. Neuroendocrinology 49:7–22

Hasen NS, Gammie SC (2009) Trpc2 gene impacts on maternal aggression, accessory olfactory bulb anatomy and brain activity. Genes, Brain Behav. https://doi.org/10.1111/j.1601-183X.2009.00511.x

Hasen NS, Gammie SC (2011) Trpc2-deficient lactating mice exhibit altered brain and behavioral responses to bedding stimuli. Behav Brain Res 217:347–353. https://doi.org/10.1016/j.bbr.2010.11.002

Hasen NS, Gammie SC (2005) Differential fos activation in virgin and lactating mice in response to an intruder. Physiol Behav 84:681–695. https://doi.org/10.1016/j.physbeh.2005.02.010

Hasen NS, Gammie SC (2006) Maternal aggression: New insights from Egr-1. Brain Res 1108:147–156. https://doi.org/10.1016/j.brainres.2006.06.007

Hashikawa K, Hashikawa Y, Tremblay R, et al (2017a) Esr1+ cells in the ventromedial hypothalamus control female aggression. Nat Neurosci 20:1580–1590. https://doi.org/10.1038/nn.4644

Hashikawa Y, Hashikawa K, Falkner AL, Lin D (2017b) Ventromedial Hypothalamus and the Generation of Aggression. Front Syst Neurosci 11:1–13. https://doi.org/10.3389/fnsys.2017.00094

Hedricks C, Daniels CE (1981) Agonistic behavior between pregnant mice and male intruders. Behav Neural Biol 31:236–241. https://doi.org/10.1016/S0163-1047(81)91249-8

Hirata T, Li P, Lanuza GM, et al (2009) Identification of distinct telencephalic progenitor pools for neuronal

diversity in the amygdala. Nat Neurosci. https://doi.org/10.1038/nn.2241

Hodge K, Have S Ten, Hutton L, Lamond AI (2013) Cleaning up the masses: Exclusion lists to reduce contamination with HPLC-MS/MS. J Proteomics 88:92–103. https://doi.org/10.1016/j.jprot.2013.02.023

Hojvat S, Baker G, Kirsteins L, Lawrence AM (1982) Growth hormone (GH) immunoreactivity in the rodent and primate CNS: Distribution, characterization and presence posthypophysectomy. Brain Res 239:543–557. https://doi.org/10.1016/0006-8993(82)90529-7

Holmes MC, Antoni FA, Aguilera G, Catt KJ (1986) Magnocellular axons in passage through the median eminence release vasopressin. Nature 319:326–329. https://doi.org/10.1038/319326a0

Hong W, Kim DW, Anderson DJ (2014) Antagonistic control of social versus repetitive self-grooming behaviors by separable amygdala neuronal subsets. Cell 158:1348–1361. https://doi.org/http://dx.doi.org/10.1016/j.cell.2014.07.049

Horseman ND, Yu-Lee LY (1994) Transcriptional regulation by the helix bundle peptide hormones: Growth hormone, prolactin, and hematopoietic cytokines. Endocr Rev 15:627–649. https://doi.org/10.1210/edrv-15-5-627

Howat WJ, Wilson BA (2014) Tissue fixation and the effect of molecular fixatives on downstream staining procedures. Methods 70:12–19. https://doi.org/10.1016/j.ymeth.2014.01.022

Hrdy SB (1979) Infanticide among animals: A review, classification, and examination of the implications for the reproductive strategies of females. Ethol Sociobiol. https://doi.org/10.1016/0162-3095(79)90004-9

Hsu DT, Kirouac GJ, Zubieta J-K, Bhatnagar S (2014) Contributions of the paraventricular thalamic nucleus in the regulation of stress, motivation, and mood. Front Behav Neurosci. https://doi.org/10.3389/fnbeh.2014.00073

Hsu DT, Price JL (2009) Paraventricular thalamic nucleus: Subcortical connections and innervation by serotonin, orexin, and corticotropin-releasing hormone in Macaque monkeys. J Comp Neurol 512:825–848. https://doi.org/10.1002/cne.21934

Hurst JL (1987) The functions of urine marking in a free-living population of house mice, Mus domesticus Rutty. Anim Behav 35:1433–1442. https://doi.org/10.1016/S0003-3472(87)80016-7

Hurst JL, Beynon RJ (2013) Rodent Urinary Proteins: Genetic Identity Signals and Pheromones BT - Chemical Signals in Vertebrates 12. In: East ML, Dehnhard M (eds) Chemical Signals in Vertebrates 12. Springer New York, New York, NY, pp 117–133

Imaoka T, Matsuda M, Mori T (2004) Extrapituitary Expression of the Prolactin Gene in the Goldfish, African Clawed Frog and Mouse. Zoolog Sci 17:791–796. https://doi.org/10.2108/zsj.17.791

Insel TR, Numan M (2003) The Neurobiology of Parental Behaviour

Ishii KK, Osakada T, Mori H, et al (2017) A Labeled-Line Neural Circuit for Pheromone-Mediated Sexual Behaviors in Mice. Neuron 95:123-137.e8. https://doi.org/10.1016/j.neuron.2017.05.038

Ismail N, Garas P, Blaustein JD (2011) Long-term effects of pubertal stressors on female sexual receptivity and estrogen receptor-α expression in CD-1 female mice. Horm Behav 59:565–571. https://doi.org/https://doi.org/10.1016/j.yhbeh.2011.02.010

Ivell R, Teerds K, Hoffman GE (2014) Proper application of antibodies for immunohistochemical detection: Antibody crimes and how to prevent them. Endocrinology 155:676–687. https://doi.org/10.1210/en.2013-1971

Japon MA, Rubinstein M, Low MJ (1994) In situ hybridization analysis of anterior pituitary hormone gene expression during fetal mouse development. J Histochem Cytochem 42:1117–1125. https://doi.org/10.1177/42.8.8027530

Jennes L (1987) Sites of origin of gonadotropin releasing hormone containing projections to the amygdala and the interpenduncular nucleus. Brain Res 404:339–344. https://doi.org/10.1016/0006-8993(87)91391-6

Jennes L, Dalati B, Michael Conn P (1988) Distribution of gonadrotropin releasing hormone agonist binding sites in the rat central nervous system. Brain Res 452:156–164. https://doi.org/10.1016/0006-8993(88)90020-0

Johnson Z V., Young LJ (2017) Oxytocin and vasopressin neural networks: Implications for social behavioral diversity and translational neuroscience. Neurosci Biobehav Rev 76:87–98. https://doi.org/10.1016/j.neubiorev.2017.01.034

Jozefczuk J, Adjaye J (2011) Chapter Six - Quantitative Real-Time PCR-Based Analysis of Gene Expression

Kaitz M, Good A, Rokem AM (1987) Mothers ' Recognition of Their Newborns by Olfactory Cues. Dev Psychobiol 20:587–591. https://doi.org/https://doi.org/10.1002/dev.420200604

Kang N, Baum MJ, Cherry JA (2009) A direct main olfactory bulb projection to the "vomeronasal" amygdala in female mice selectively responds to volatile pheromones from males. Eur J Neurosci. https://doi.org/10.1111/j.1460-9568.2009.06638.x

Karlson P, Lüscher M (1959) 'Pheromones': a new term for a class of biologically active substances. Nature 183:55–56

Kato K, Ikemoto T, Park MK (2005) Identification of the reptilian prolactin and its receptor cDNAs in the leopard gecko, Eublepharis macularius. Gene 346:267–276. https://doi.org/10.1016/j.gene.2004.11.016

Kaur AW, Ackels T, Kuo TH, et al (2014) Murine pheromone proteins constitute a context-dependent combinatorial code governing multiple social behaviors. Cell. https://doi.org/10.1016/j.cell.2014.02.025

Kawata M, Hashimoto K, Takahara J, Sano Y (1983) Differences in the distributional pattern of CRF-, oxytocin-, and vasopressin-immunoreactive nerve fibers in the median eminence of the rat. Cell Tissue Res 230:247–258

Keller M, Baum MJ, Brock O, et al (2009) The main and the accessory olfactory systems interact in the control of mate recognition and sexual behavior. Behav Brain Res 200:268–276. https://doi.org/10.1016/j.bbr.2009.01.020

Kelly PA, Tsushima T, Shiu RPC, Friesen HG (1976) Lactogenic and growth hormone-like activities in pregnancy determined by radioreceptor assays. Endocrinology. https://doi.org/10.1210/endo-99-3-765

Kendall SK, Gordon DF, Birkmeier TS, et al (1994) Enhancer-mediated high level expression of mouse pituitary glycoprotein hormone α-subunit transgene in thyrotropes, gonadotropes, and developing pituitary gland. Mol Endocrinol 8:1420–1433. https://doi.org/10.1210/me.8.10.1420

Kendrick KM, Levy F, Keverne EB (1992) Changes in the sensory processing of olfactory signals induced by birth in sleep. Science (80-) 256:833 LP – 836. https://doi.org/10.1126/science.256.5058.833

Kennett JE, Mckee DT (2012) Oxytocin: An Emerging Regulator of Prolactin Secretion in the Female Rat. J Neuroendocrinol 24:403–412. https://doi.org/10.1111/j.1365-2826.2011.02263.x

Khorram O, DePalatis LR, McCann SM (1984) Changes in Hypothalamic and Pituitary Content of Immunoreactive α-Melanocyte-Stimulating Hormone during the Gestational and Postpartum Periods in the Rat. Proc Soc Exp Biol Med 177:318–326. https://doi.org/10.3181/00379727-177-41950

Kim D, Pertea G, Trapnell C, et al (2013) TopHat2: Accurate alignment of transcriptomes in the presence of insertions, deletions and gene fusions. Genome Biol 14:. https://doi.org/10.1186/gb-2013-14-4-r36

Kim Y, Venkataraju KU, Pradhan K, et al (2015) Mapping social behavior-induced brain activation at cellular resolution in the mouse. Cell Rep 10:292–305. https://doi.org/10.1016/j.celrep.2014.12.014

Kimchi T, Xu J, Dulac C (2007) A functional circuit underlying male sexual behaviour in the female mouse brain. Nature 448:1009–1014. https://doi.org/10.1038/nature06089

Kiss JZ, Martos J, Palkovits M (1991) Hypothalamic paraventricular nucleus: A quantitative analysis of cytoarchitectonic subdivisions in the rat. J Comp Neurol 313:563–573. https://doi.org/10.1002/cne.903130403

Kölliker M, Smiseth PT, Royle NJ. (2017) Evolution of parental care. In: Baum DA, Futuyma DJ, Hoekstra HE, et al. (eds) The Princeton Guide to Evolution. Princeton University Press, pp 663–670

Kolunie JM, Stern JM (1995) Maternal aggression in rats: Effects of olfactory bulbectomy, ZnSO4-induced anosmia, and vomeronasal organ removal. Horm Behav. https://doi.org/10.1006/hbeh.1995.1285

Koolhaas JM, Van Den Brink THC, Roozendaal B, Boorsma F (1990) Medial amygdala and aggressive behavior: Interaction between testosterone and vasopressin. Aggress Behav 16:223–229. https://doi.org/10.1002/1098-2337(1990)16:3/4<223::AID-AB2480160308>3.0.CO;2-#

Krebs DL, Hilton DJ (2000) SOCS: physiological suppressors of cytokine signaling. J Cell Sci 113:2813–2819

Krieger J, Schmitt A, Löbel D, et al (1999) Selective activation of G protein subtypes in the vomeronasal organ upon stimulation with urine-derived compounds. J Biol Chem. https://doi.org/10.1074/jbc.274.8.4655

Labov JB, Huck UW, Elwood RW, Brooks RJ (1985) Current Problems in the Study of Infanticidal Behavior of Rodents. Q Rev Biol. https://doi.org/10.1086/414170

Langmead B, Salzberg SL (2012) Fast gapped-read alignment with Bowtie 2. Nat Methods 9:357–359. https://doi.org/10.1038/nmeth.1923

Lanuza E, Martín-Sánchez A, Marco-Manclús P, et al (2014) Sex pheromones are not always attractive: Changes induced by learning and illness in mice. Anim Behav. https://doi.org/10.1016/j.anbehav.2014.08.011

Lawrence M, Huber W, Pagès H, et al (2013) Software for Computing and Annotating Genomic Ranges. PLoS Comput Biol. https://doi.org/10.1371/journal.pcbi.1003118

Le Tissier PR, Hodson DJ, Lafont C, et al (2012) Anterior pituitary cell networks. Front Neuroendocrinol 33:252–266. https://doi.org/10.1016/j.yfrne.2012.08.002

LeDoux JE, Farb C, Ruggiero DA (1990) Topographic organization of neurons in the acoustic thalamus that project to the amygdala. J Neurosci

Lee H, Kim DW, Remedios R, et al (2014) Scalable control of mounting and attack by Esr1+ neurons in the ventromedial hypothalamus. Nature 509:627–632. https://doi.org/10.1038/nature13169

Legrand R (1970) Successful aggression as the reinforcer for runway behavior of mice. Psychon Sci 20:303–305. https://doi.org/10.3758/BF03329080

Lein ES, Hawrylycz MJ, Ao N, et al (2006) Genome-wide atlas of gene expression in the adult mouse brain. Nature 445:168

Lepri JJ, Wysocki CJ, Vandenbergh JG (1985) Mouse vomeronasal organ: effects on chemosignal production and maternal behavior. Physiol Behav 35:809–814. https://doi.org/10.1016/0031-9384(85)90416-0

Leroy F, Park J, Asok A, et al (2018) A circuit from hippocampal CA2 to lateral septum disinhibits social aggression. Nature 564:213–218. https://doi.org/10.1038/s41586-018-0772-0

Lévy F, Keller M (2009) Olfactory mediation of maternal behavior in selected mammalian species. Behav. Brain Res. 200:336–345

Lévy F, Keller M, Poindron P (2004) Olfactory regulation of maternal behavior in mammals. Horm Behav 46:284–302. https://doi.org/10.1016/j.yhbeh.2004.02.005

Li CI, Maglinao TL, Takahashi LK (2004) Medial Amygdala Modulation of Predator Odor-Induced Unconditioned Fear in the Rat. Behav Neurosci. https://doi.org/10.1037/0735-7044.118.2.324

Li S, Kirouac GJ (2012) Sources of inputs to the anterior and posterior aspects of the paraventricular nucleus of the thalamus. Brain Struct Funct 217:257–273. https://doi.org/10.1007/s00429-011-0360-7

Li Y, Mathis A, Grewe BF, et al (2017) Neuronal Representation of Social Information in the Medial Amygdala of Awake Behaving Mice. Cell 171:1176-1190.e17. https://doi.org/10.1016/j.cell.2017.10.015

Lim MM, Young LJ (2006) Neuropeptidergic regulation of affiliative behavior and social bonding in animals. Horm Behav 50:506–517. https://doi.org/10.1016/j.yhbeh.2006.06.028

Lin D, Boyle MP, Dollar P, et al (2011) Functional identification of an aggression locus in the mouse hypothalamus. Nature 470:221–227. https://doi.org/10.1038/nature09736

Lin SH, Miyata S, Weng W, et al (1998) Comparison of the expression of two immediate early gene proteins, FosB and Fos in the rat preoptic area, hypothalamus and brainstem during pregnancy, parturition and lactation. Neurosci Res. https://doi.org/10.1016/S0168-0102(98)00100-X

Linke R, De Lima AD, Schwegler H, Pape HC (1999) Direct synaptic connections of axons from superior colliculus with identified thalamo-amygdaloid projection neurons in the rat: Possible substrates of a subcortical visual pathway to the amygdala. J Comp Neurol. https://doi.org/10.1002/(SICI)1096-9861(19990111)403:2<158::AID-CNE2>3.0.CO;2-6

Linzer DIH, Fisher SJ (1999) The placenta and the prolactin family of hormones: Regulation of the physiology of pregnancy. Mol. Endocrinol.

Liu J, Lin C, Gleiberman A, et al (2001) Tbx19, a tissue-selective regulator of POMC gene expression. Proc Natl Acad Sci U S A 98:8674–8679. https://doi.org/10.1073/pnas.141234898

Loewy AD, McKellar S (1980) The neuroanatomical basis of central cardiovascular control. Fed Proc

Lonstein JS, De Vries GJ (2000) Maternal behaviour in lactating rats stimulates c-fos in glutamate decarboxylase-synthesizing neurons of the medial preoptic area, ventral bed nucleus of the stria terminalis, and ventrocaudal periaqueductal gray. Neuroscience 100:557–568. https://doi.org/10.1016/S0306-4522(00)00287-6

Lonstein JS, Gammie SC (2002) Sensory, hormonal, and neural control of maternal aggression in laboratory rodents. Neurosci Biobehav Rev 26:869–888. https://doi.org/10.1016/S0149-7634(02)00087-8

Lonstein JS, Simmons DA, Stern JM (1998) Functions of the caudal periaqueductal gray in lactating rats: Kyphosis, lordosis, maternal aggression, and fearfulness. Behav Neurosci. https://doi.org/10.1037/0735-7044.112.6.1502

Lonstein JS, Stern JM (1997) Role of the midbrain periaqueductal gray in maternal nurturance and aggression: c-fos and electrolytic lesion studies in lactating rats. J Neurosci 17:3364–78

Low MJ (2017) Chapter 7 - Neuroendocrinology. In: Melmed S, Polonsky KS, Larsen PR, Kronenberg HM (eds) Williams Textbook of Endocrinology (Thirteenth Edition), Thirteenth. Philadelphia, pp 109–175

Ludwig M, Leng G (2006) Dendritic peptide release and peptide-dependent behaviours. Nat Rev Neurosci 7:126–36. https://doi.org/10.1038/nrn1845

Lumpkin MD, Samson WK, Mc cann SM (1983) Hypothalamic and pituitary sites of action of oxytocin to alter prolactin secretion in the rat. Endocrinology 112:1711–1717. https://doi.org/10.1210/endo-112-5-1711

Ma FY, Grattan DR, Goffin V, Bunn SJ (2005) Prolactin-regulated tyrosine hydroxylase activity and messenger ribonucleic acid expression in mediobasal hypothalamic cultures: The differential role of specific protein kinases. Endocrinology 146:93–102. https://doi.org/10.1210/en.2004-0800

MacLaren DAA, Browne RW, Shaw JK, et al (2016) Clozapine N-Oxide Administration Produces Behavioral Effects in Long-Evans Rats: Implications for Designing DREADD Experiments. eNeuro 3:. https://doi.org/10.1523/ENEURO.0219-16.2016

Macrí S, Mason GJ, Würbel H (2004) Dissociation in the effects of neonatal maternal separations on maternal care and the offspring's HPA and fear responses in rats. Eur J Neurosci 20:1017–1024. https://doi.org/10.1111/j.1460-9568.2004.03541.x

Maestripieri D (1992) Functional aspects of maternal aggression in mammals. Can J Zool 70:1069–1077. https://doi.org/10.1139/z92-150

Mahler S V., Vazey EM, Beckley JT, et al (2014) Designer receptors show role for ventral pallidum input to ventral tegmental area in cocaine seeking. Nat Neurosci 17:577–585. https://doi.org/10.1038/nn.3664

Mann MA, Konen C, Svare B (1984) The role of progesterone in pregnancy-induced aggression in mice. Horm Behav 18:140–160. https://doi.org/10.1016/0018-506X(84)90039-4

Mann MA, Svare B (1982) Factors influencing pregnancy-induced aggression in mice. Behav Neural Biol 36:242–258. https://doi.org/10.1016/S0163-1047(82)90867-6

Maras PM, Petrulis A (2010) Anatomical connections between the anterior and posterodorsal sub-regions of the medial amygdala: integration of odor and hormone signals. Neuroscience 170:610–622

Marchand JE, Hagino N (1983) Afferents to the periaqueductal gray in the rat. A horseradish peroxidase study. Neuroscience 9:95–106. https://doi.org/10.1016/0306-4522(83)90049-0

Marinari KT, Moltz H (1978) Serum prolactin levels and vaginal cyclicity in concaveated and lactating female rats. Physiol Behav 21:525–528. https://doi.org/https://doi.org/10.1016/0031-9384(78)90124-5

Martín-Sánchez A, McLean L, Beynon RJ, et al (2015a) From sexual attraction to maternal aggression: when pheromones change their behavioural significance. Horm. Behav. 68:65–76

Martín-Sánchez A, Valera-Marín G, Hernández-Martínez A, et al (2015b) Wired for motherhood: induction of maternal care but not maternal aggression in virgin female CD1 mice. Front Behav Neurosci 9:1–12. https://doi.org/10.3389/fnbeh.2015.00197

Martin M (2011) Cutadapt removes adapter sequences from high-throughput sequencing reads. EMBnet.journal. https://doi.org/10.14806/ej.17.1.200

Martínez-García F, Lanuza E (2018) Evolution of vertebrate survival circuits. Curr Opin Behav Sci 24:113–123. https://doi.org/10.1016/j.cobeha.2018.06.012

Martínez-García F, Martínez-Ricós J, Agustín-Pavón C, et al (2009) Refining the dual olfactory hypothesis: Pheromone reward and odour experience. Behav Brain Res. https://doi.org/10.1016/j.bbr.2008.10.002

Martinez-Garcia F, Novejarque A, Lanuza E (2009) Evolution of the Amygdala in Vertebrates. In: Kaas JH (ed) Evolutionary Neuroscience, 1st edn. Academic Press, Elsevier, pp 313–392

Martínez-García F, Novejarque A, Lanuza E (2008) Two interconnected functional systems in the amygdala of amniote vertebrates. Brain Res. Bull.

Martinez-Marcos A (2009) On the organization of olfactory and vomeronasal cortices. Prog. Neurobiol.

Martínez-Ricós J, Agustín-Pavón C, Lanuza E, Martínez-García F (2008) Role of the vomeronasal system in intersexual attraction in female mice. Neuroscience. https://doi.org/10.1016/j.neuroscience.2008.02.002

Martínez-Ricós J, Agustín-Pavón C, Lanuza E, Martínez-García F (2007) Intraspecific communication through chemical signals in female mice: Reinforcing properties of involatile male sexual pheromones. Chem Senses. https://doi.org/10.1093/chemse/bjl039

Matzeu A, Zamora-Martinez ER, Martin-Fardon R (2014) The paraventricular nucleus of the thalamus is recruited by both natural rewards and drugs of abuse: recent evidence of a pivotal role for orexin/hypocretin signaling in this thalamic nucleus in drug-seeking behavior. Front Behav Neurosci 8:1–9. https://doi.org/10.3389/fnbeh.2014.00117

McCarthy EA, Kunkhyen T, Korzan WJ, et al (2017a) A comparison of the effects of male pheromone priming and optogenetic inhibition of accessory olfactory bulb forebrain inputs on the sexual behavior of estrous female mice. Horm Behav 89:104–112. https://doi.org/https://doi.org/10.1016/j.yhbeh.2016.12.011

McCarthy EA, Maqsudlu A, Bass M, et al (2017b) DREADD-induced silencing of the medial amygdala reduces the preference for male pheromones and the expression of lordosis in estrous female mice. Eur J Neurosci 46:2035–2046. https://doi.org/10.1111/ejn.13636

McHenry JA, Otis JM, Rossi MA, et al (2017) Hormonal gain control of a medial preoptic area social reward circuit. Nat Neurosci 20:449–458. https://doi.org/10.1038/nn.4487

McMillan DB, Harris RJ (2018) Endocrine Organs. In: An Atlas of Comparative Vertebrate Histology. pp 479–509

Meaney MJ (2001) Maternal Care, Gene Expression, and the Transmission of Individual Differences in Stress Reactivity Across Generations. Annu Rev Neurosci. https://doi.org/10.1146/annurev.neuro.24.1.1161

Medina L, Abellán A, Vicario A, et al (2017) The Amygdala. In: Evolution of Nervous Systems, vol.1. pp 427–478

Meisel RL, Mullins AJ (2006) Sexual experience in female rodents: Cellular mechanisms and functional consequences. Brain Res 1126:56–65. https://doi.org/10.1016/j.brainres.2006.08.050

Meisel RL, Sterner MR (1990) Progesterone inhibition of sexual behavior is accompanied by an activation of aggression in female Syrian hamsters. Physiol Behav. https://doi.org/10.1016/0031-9384(90)90102-A

Mejía S, Morales MA, Zetina ME, et al (1997) Immunoreactive Prolactin Forms Colocalize with Vasopressin in Neurons of the Hypothalamic Paraventricular and Supraoptic Nuclei. Neuroendocrinology 66:151–159. https://doi.org/10.1159/000127233

Melander T, Hökfelt T, Rökaeus A (1986) Distribution of galaninlike immunoreactivity in the rat central nervous system. J Comp Neurol 248:475–517. https://doi.org/10.1002/cne.902480404

Menon R, Grund T, Zoicas I, et al (2018) Oxytocin Signaling in the Lateral Septum Prevents Social Fear during Lactation. Curr Biol. https://doi.org/10.1016/j.cub.2018.02.044

Meunier H, Cajander SB, Roberts VJ, et al (1988) Rapid changes in the expression of inhibin α-, βA-, and βB-subunits in ovarian cell types during the rat estrous cycle. Mol Endocrinol 2:1352–1363. https://doi.org/10.1210/mend-2-12-1352

Mezey É, Kiss JZ (1991) Coexpression of vasopressin and oxytocin in hypothalamic supraoptic neurons of lactating rats. Endocrinology 129:1814–1820. https://doi.org/10.1210/endo-129-4-1814

Millhouse EO (1973) The Organization of the Ventromedial Hypothalamic Nucleus. Brain Res 55:71–87. https://doi.org/10.1016/0006-8993(73)90489-7

Mineur YS, Cahuzac EL, Mose TN, et al (2018) Interaction between noradrenergic and cholinergic signaling in amygdala regulates anxiety- and depression-related behaviors in mice. Neuropsychopharmacology 43:2118–2125. https://doi.org/10.1038/s41386-018-0024-x

Mintz M, Rüedi-Bettschen D, Feldon J, Pryce CR (2005) Early social and physical deprivation leads to reduced social motivation in adulthood in Wistar rats. Behav Brain Res. https://doi.org/10.1016/j.bbr.2004.08.017

Miranda LA, Strüssmann CA, Guilgur LG, et al (2007) Cloning of FSH-β, LH-β and glycoprotein hormone α subunits in pejerrey Odontesthes bonariensis (Valenciennes): Expression profile and relationship with GnRH expression and plasma sex steroid levels in male fish. J Fish Biol 71:1571–1589. https://doi.org/10.1111/j.1095-8649.2007.01621.x

Mitra SW, Hoskin E, Yudkovitz J, et al (2003) Immunolocalization of estrogen receptor β in the mouse brain: Comparison with estrogen receptor α. Endocrinology 144:2055–2067. https://doi.org/10.1210/en.2002-221069

Modney BK, Hatton GI (1994) Maternal behaviors: evidence that they feed back to alter brain morphology and function. Acta Paediatr 83:29–32. https://doi.org/10.1111/j.1651-2227.1994.tb13262.x

Moga MM, Herbert H, Hurley KM, et al (1990) Organization of cortical, basal forebrain, and hypothalamic afferents to the parabrachial nucleus in the rat. J Comp Neurol 295:624–661. https://doi.org/10.1002/cne.902950408

Moga MM, Saper CB, Gray TS (1989) Bed Nucleus of the Stria Termin &: and Projection to the Parabrachial Nucleus i n the Rat. 332:

Moncho-Bogani J, Lanuza E, Hernández A, et al (2002) Attractive properties of sexual pheromones in mice: Innate or learned? Physiol Behav 77:167–176. https://doi.org/10.1016/S0031-9384(02)00842-9

Moncho-Bogani J, Martinez-Garcia F, Novejarque A, Lanuza E (2005) Attraction to sexual pheromones and associated odorants in female mice involves activation of the reward system and basolateral amygdala. Eur J Neurosci 21:2186–2198. https://doi.org/10.1111/j.1460-9568.2005.04036.x

Moos F, Poulain DA, Rodriguez F, et al (1989) Release of oxytocin within the supraoptic nucleus during the milk ejection reflex in rats. Exp Brain Res 76:593–602. https://doi.org/10.1016/0022-460X(90)90652-

G

Morgan HD, Watchus JA, Milgram NW, Fleming AS (1999) The long lasting effects of electrical simulation of the medial preoptic area and medial amygdala on maternal behavior in female rats. Behav Brain Res. https://doi.org/10.1016/S0166-4328(98)00070-9

Morgan M, Pagès H, Obenchain V HN (2018) Rsamtools: Binary alignment (BAM), FASTA, variant call (BCF), and tabix file import.

Motta SC, Guimaraes CC, Furigo IC, et al (2013) Ventral premammillary nucleus as a critical sensory relay to the maternal aggression network. Proc Natl Acad Sci 110:14438–14443. https://doi.org/10.1073/pnas.1305581110

Mueller O, Schroeder A (2004) RNA Integrity Number (RIN) – Standardization of RNA Quality Control Application. Nano. https://doi.org/10.1101/gr.189621.115.7

Muske LE (1993a) Evolution of Gonadotropin-Releasing Hormone (GnRH) Neuronal Systems (Part 1 of 2). Brain Behav Evol 42:215–223. https://doi.org/10.1159/000114156

Muske LE (1993b) Evolution of Gonadotropin-Releasing Hormone (GnRH) Neuronal Systems (Part 2 of 2). Brain Behav Evol 42:224–230. https://doi.org/10.1159/000316219

Mychasiuk R, Zahir S, Schmold N, et al (2012) Parental enrichment and offspring development: Modifications to brain, behavior and the epigenome. Behav Brain Res 228:294–298. https://doi.org/10.1016/j.bbr.2011.11.036

Mykytowycz R, Dudzinski ML (1973) Aggressive and Protective Behaviour of Adult Rabbits Oryctolagus Cuniculus (L.) Towards Juveniles. Behaviour 43:97–120. https://doi.org/10.1163/156853973X00490

Naeini RS, Witty MF, Séguéla P, Bourque CW (2006) An N-terminal variant of Trpv1 channel is required for osmosensory transduction. Nat Neurosci 9:93–98. https://doi.org/10.1038/nn1614

Nahi F, Arbogast LA (2003) Prolactin modulates hypothalamic preproenkephalin, but not proopiomelanocortin, gene expression during lactation. Endocrine 20:115–122. https://doi.org/10.1385/ENDO:20:1-2:115

Navarro S, Soletto L, Puchol S, et al (2015) 60 YEARS OF POMC: POMC: an evolutionary perspective. J Mol Endocrinol 56:T113–T118. https://doi.org/10.1530/jme-15-0288

Neumann I, Koehler E, Landgraf R, Summy-Long J (1994) An oxytocin receptor antagonist infused into the supraoptic nucleus attenuates intranuclear and peripheral release of oxytocin during suckling in conscious rats. Endocrinology 134:141–148. https://doi.org/10.1210/endo.134.1.8275928

Neumann ID, Landgraf R (2012) Balance of brain oxytocin and vasopressin: Implications for anxiety, depression, and social behaviors. Trends Neurosci 35:649–659. https://doi.org/10.1016/j.tins.2012.08.004

Neumann ID, Russell JA, Landgraf R (1993) Oxytocin and vasopressin release within the supraoptic and paraventricular nuclei of pregnant, parturient and lactating rats: A microdialysis study. Neuroscience 53:65–75. https://doi.org/https://doi.org/10.1016/0306-4522(93)90285-N

Neumann ID, Toschi N, Ohl F, et al (2001) Maternal defence as an emotional stressor in female rats: Correlation of neuroendocrine and behavioural parameters and involvement of brain oxytocin. Eur J Neurosci 13:1016–1024. https://doi.org/10.1046/j.0953-816X.2001.01460.x

Newman S (1999) The medial extended amygdala in male reproductive behavior. Ann N Y Acad Sci 877:242–257. https://doi.org/10.1111/j.1749-6632.1999.tb09271.x

Nicolas CS, Amici M, Bortolotto ZA, et al (2013) The role of JAK-STAT signaling within the CNS. Jak-Stat 2:e22925. https://doi.org/10.4161/jkst.22925

Niikura K, Zhou Y, Ho A, Kreek MJ (2013) Proopiomelanocortin (POMC) expression and conditioned place aversion during protracted withdrawal from chronic intermittent escalating-dose heroin in POMC-EGFP promoter transgenic mice. Neuroscience 236:220–232. https://doi.org/10.1016/j.neuroscience.2012.12.071

Nogami H, Hoshino R, Ogasawara K, et al (2007) Region-specific expression and hormonal regulation of the first exon variants of rat prolactin receptor mRNA in rat brain and anterior pituitary gland. J Neuroendocrinol 19:583–593. https://doi.org/10.1111/j.1365-2826.2007.01565.x

Noirot E (1972) The Onset of Maternal Behavior in Rats, Hamsters, and Mice A Selective Review. Adv Study Behav 4:107–145. https://doi.org/10.1016/S0065-3454(08)60008-X

Noirot E, Goyens J, Buhot MC (1975) Aggressive behavior of pregnant mice toward males. Horm Behav 6:9–17. https://doi.org/10.1016/0018-506X(75)90018-5

Northcutt K V, Wang Z, Lonstein JS (2007) Sex and species differences in tyrosine hydroxylase-synthesizing cells of the rodent olfactory extended amygdala. J Comp Neurol 500:103–115. https://doi.org/10.1002/cne.21148

Novotny M V., Ma W, Wiesler D, Žídek L (1999) Positive identification of the puberty-accelerating pheromone of the house mouse: The volatile ligands associating with the major urinary protein. Proc R Soc B Biol Sci 266:2017–2022. https://doi.org/10.1098/rspb.1999.0880

Nowakowski BE, Maurer RA (1994) Multiple Pit-1-binding sites facilitate estrogen responsiveness of the prolactin gene. Mol Endocrinol 8:1742–1749. https://doi.org/10.1210/mend.8.12.7708061

Numan M (2014) Neurobiology of social behavior: toward an understanding of the prosocial and antisocial brain. Academic Press

Numan M (2006) Hypothalamic neural circuits regulating maternal responsiveness toward infants. Behav Cogn Neurosci Rev 5:163–190. https://doi.org/10.1177/1534582306288790

Numan M, Insel TR (2003a) Hormonal and Nonhormonal Basis of Maternal Behavior. In: The Neurobiology of Parental Behavior. Springer New York, New York, NY, pp 8–41

Numan M, Insel TR (2003b) Neuroanatomy of Maternal Behavior. In: The Neurobiology of Parental Behavior. Springer, New York, NY, pp 107–189

Numan M, Numan MJ, Marzella SR, Palumbo A (1998) Expression of c-fos, fos B, and egr-1 in the medial preoptic area and bed nucleus of the stria terminalis during maternal behavior in rats. 348–352

Numan M, Stolzenberg DS (2009) Medial preoptic area interactions with dopamine neural systems in the control of the onset and maintenance of maternal behavior in rats. Front Neuroendocrinol 30:46–64. https://doi.org/10.1016/j.yfrne.2008.10.002

Numan M, Stolzenberg DS (2008) Chapter 1 - Hypothalamic Interaction with the Mesolimbic Dopamine System and the Regulation of Maternal Responsiveness. In: Bridges RSBT-N of the PB (ed). Academic Press, San Diego, pp 1–22

Numan M, Woodside B (2010) Maternity: Neural Mechanisms, Motivational Processes, and Physiological Adaptations. Behav Neurosci 124:715–741. https://doi.org/10.1037/a0021548

Okabe S, Nagasawa M, Mogi K, Kikusui T (2012) The importance of mother-infant communication for social bond formation in mammals. Anim Sci J 83:446–452. https://doi.org/10.1111/j.1740-0929.2012.01014.x

Okabe S, Nagaswa M, Koto M, et al (2013) Pup odor and ultrasonic vocalizations synergistically stimulate maternal attention in mice. Behav Neurosci 127:432–438. https://doi.org/10.1037/a0032395

Otero-García M, Agustín-Pavón C, Lanuza E, Martínez-García F (2016) Distribution of oxytocin and co-localization with arginine vasopressin in the brain of mice. Brain Struct Funct 221:3445–3473. https://doi.org/10.1007/s00429-015-1111-y

Otero-Garcia M, Martin-Sanchez A, Fortes-Marco L, et al (2014) Extending the socio-sexual brain: Arginine-vasopressin immunoreactive circuits in the telencephalon of mice. Brain Struct Funct. https://doi.org/10.1007/s00429-013-0553-3

Padilla SL, Qiu J, Soden ME, et al (2016) Agouti-related peptide neural circuits mediate adaptive behaviors in the starved state. Nat Neurosci 19:734–741. https://doi.org/10.1038/nn.4274

Pan J-T, Gala RR (1985) Central Nervous System Regions Involved in the Estrogen-Induced Afternoon

Prolactin Surge. I. Lesion Studies*. Endocrinology 117:382–387. https://doi.org/10.1210/endo-117-1-382

Pardo-Bellver C, Cádiz-Moretti B, Novejarque A, et al (2012) Differential efferent projections of the anterior, posteroventral, and posterodorsal subdivisions of the medial amygdala in mice. Front Neuroanat. https://doi.org/10.3389/fnana.2012.00033

Parker DC, Rossman LG, Vanderlaan EF (1974) Relation of sleep-entrained human prolactin release to REM-NonREM cycles. J Clin Endocrinol Metab. https://doi.org/10.1210/jcem-38-4-646

Parker SL, Armstrong WE, Sladek CD, et al (1991) Prolactin stimulates the release of oxytocin in lactating rats: Evidence for a physiological role via an action at the neural lobe. Neuroendocrinology 53:503–510. https://doi.org/10.1159/000125764

Parmigiani S, Brain PF (1983) Effects of residence, aggressive experience and intruder familiarity on attack shown by male mice. Behav Processes 8:45–57. https://doi.org/https://doi.org/10.1016/0376-6357(83)90042-6

Parmigiani S, Brain PF, Mainardi D, Brunoni V (1988) Different patterns of biting attack employed by lactating female mice (Mus domesticus) in encounters with male and female conspecific intruders. J Comp Psychol 102:287–293. https://doi.org/10.1037/0735-7036.102.3.287

Parmigiani S, Francesco Ferrari P, Palanza P (1998) An evolutionary approach to behavioral pharmacology: Using drugs to understand proximate and ultimate mechanisms of different forms of aggression in mice. Neurosci Biobehav Rev 23:143–153. https://doi.org/10.1016/S0149-7634(98)00016-5

Patil MJ, Ruparel SB, Henry MA, Akopian AN (2013) Prolactin regulates TRPV1, TRPA1, and TRPM8 in sensory neurons in a sex-dependent manner: Contribution of prolactin receptor to inflammatory pain. Am J Physiol Metab 305:E1154–E1164. https://doi.org/10.1152/ajpendo.00187.2013

Paul L, Gronek J, Politch J (1980) Maternal aggression in mice: Protection of young is a by-product of attacks at the home site. Aggress Behav 6:19–29. https://doi.org/10.1002/1098-2337(1980)6:1<19::AID-AB2480060104>3.0.CO;2-9

Paut-Pagano L, Roky R, Valatx JL, et al (1993) Anatomical Distribution of Prolactin-Like Immunoreactivity in the Rat Brain. Neuroendocrinology 58:682–695. https://doi.org/10.1159/000126609

Pavlidis P, Noble WS (2001) Analysis of strain and regional variation in gene expression in mouse brain. Genome Biol 2:RESEARCH0042. https://doi.org/10.1186/gb-2001-2-10-research0042

Paxinos G, Franklin KBJ (2004) Mouse Brain in Stereotaxic Coordinates

Pérez SE, Wynick D, Steiner RA, Mufson EJ (2001) Distribution of galaninergic immunoreactivity in the brain of the mouse. J Comp Neurol 434:158–185. https://doi.org/10.1002/cne.1171

Peterson PR (1966) Magnocellular neurosecretory centers in the rat hypothalamus. J Comp Neurol 128:181–189. https://doi.org/10.1002/cne.901280205

Petrovich GD, Canteras NS, Swanson LW (2001) Combinatorial amygdalar inputs to hippocampal domains and hypothalamic behavior systems. Brain Res Rev 38:247–289. https://doi.org/https://doi.org/10.1016/S0165-0173(01)00080-7

Pezet A, Favre H, Kelly PA, Edery M (1999) Inhibition and restoration of prolactin signal transduction by suppressors of cytokine signaling. J Biol Chem 274:24497–24502. https://doi.org/10.1074/jbc.274.35.24497

Pfaffle RW, DiMattia GE, Parkst JS, et al (1992) Mutation of the POU-specific domain of Pit-1 and hypopituitarism without pituitary hypoplasia. Science (80-) 257:1118–1121. https://doi.org/10.1126/science.257.5073.1118

Phelan MM, McLean L, Armstrong SD, et al (2014) The Structure, Stability and Pheromone Binding of the Male Mouse Protein Sex Pheromone Darcin. PLoS One 9:e108415

Pittman QJ, Blume HW, Renaud LP (1981) Connections of the hypothalamic paraventricular necleus with the neurohypophysis, median eminence, amygdala, lateral septum and midbrain periaqueductal gray: An electrophysiological study in the rat. Brain Res 215:15–28. https://doi.org/10.1016/0006-

8993(81)90488-1

Planas B, Kolb PE, Raskind MA, Miller MA (1994) Activation of galanin pathways across puberty in the male rat: Galanin gene expression in the bed nucleus of the stria terminalis and medial amygdala. Neuroscience 63:851–858. https://doi.org/10.1016/0306-4522(94)90529-0

Pochet R, Brocas H, Vassart G, et al (1981) Radioautographic localization of prolactin messenger RNA on histological sections by in situ hybridization. Brain Res 211:433–438. https://doi.org/10.1016/0006-8993(81)90969-0

Popeski N, Amir S, Diorio J, Woodside B (2003) Prolactin and oxytocin interaction in the paraventricular and supraoptic nuclei: Effects on oxytocin mRNA and nitric oxide synthase. J Neuroendocrinol 15:687–696. https://doi.org/10.1046/j.1365-2826.2003.01048.x

Porter RH, Cernoch JM, Mclaughlin FJ (1983) Maternal Recognition of Neonates Through Olfactory Cues. Physiol Behav 30:151–154. https://doi.org/https://doi.org/10.1016/0031-9384(83)90051-3

Pro-Sistiaga P, Mohedano-Moriano A, Ubeda-Bañon I, et al (2007) Convergence of olfactory and vomeronasal projections in the rat basal telencephalon. J Comp Neurol 504:346–362. https://doi.org/10.1002/cne.21455

Puelles L, Rubenstein JLR (2003) Forebrain gene expression domains and the evolving prosomeric model. Trends Neurosci. https://doi.org/10.1016/S0166-2236(03)00234-0

Quentien MH, Manfroid I, Moncet D, et al (2002) Pitx factors are involved in basal and hormone-regulated activity of the human prolactin promoter. J Biol Chem 277:44408–44416. https://doi.org/10.1074/jbc.M207824200

Rand-Weaver M, Noso T, Kawauchi H, Muramoto K (1991) Isolation and Characterization of Somatolactin, a New Protein Related to Growth Hormone and Prolactin from Atlantic Cod (Gadus morhua) Pituitary Glands. Biochemistry 30:1509–1515. https://doi.org/10.1021/bi00220a010

Ray RS, Corcoran AE, Brust RD, et al (2011) Impaired respiratory and body temperature control upon acute serotonergic neuron inhibition. Science (80-) 333:637–642. https://doi.org/10.1126/science.1205295

Ray S, Tzeng R-Y, DiCarlo LM, et al (2016) An Examination of Dynamic Gene Expression Changes in the Mouse Brain During Pregnancy and the Postpartum Period. G3 Genes, Genomes, Genet 6:221–233. https://doi.org/10.1534/g3.115.020982

Remedios R, Kennedy A, Zelikowsky M, et al (2017) Social behaviour shapes hypothalamic neural ensemble representations of conspecific sex. Nature 550:388–392. https://doi.org/10.1038/nature23885

Riedman ML (1982) The Evolution of Alloparental Care and Adoption in Mammals and Birds. Q Rev Biol 57:405–435

Rizvi T, Murphy A, Ennis M, et al (2018) Medial preoptic area afferents to periaqueductal gray medullo-output neurons: a combined Fos and tract tracing study. J Neurosci 16:333–344. https://doi.org/10.1523/jneurosci.16-01-00333.1996

Roberts SA, Davidson AJ, McLean L, et al (2012) Pheromonal induction of spatial learning in mice. Science (80-) 338:1462–1465. https://doi.org/10.1126/science.1225638

Roberts SA, Simpson DM, Armstrong SD, et al (2010) Darcin: A male pheromone that stimulates female memory and sexual attraction to an individual male's odour. BMC Biol 8:. https://doi.org/10.1186/1741-7007-8-75

Robinson MD, McCarthy DJ, Smyth GK (2010) edgeR: a Bioconductor package for differential expression analysis of digital gene expression data. Bioinformatics 26:139–140. https://doi.org/10.1093/bioinformatics/btp616

Roky R, Valatx JL, Jouvet M (1993) Effect of prolactin on the sleep-wake cycle in the rat. Neurosci Lett. https://doi.org/10.1016/0304-3940(93)90453-R

Roselli CE, Bocklandt S, Stadelman HL, et al (2008) Prolactin expression in the sheep brain. Neuroendocrinology 87:206–215. https://doi.org/10.1159/000114643

Rosenblatt JS (1967) Nonhormonal Basis of Maternal Behavior in the Rat. Science (80-) 156:1512–1513. https://doi.org/10.1126/science.156.3781.1512

Rosenblatt JS, Mayer AD, Siegel HI (1985) Maternal behavior among the nonprimate mammals. In: Reproduction. Springer, Boston, MA, pp 229–298

Roy BN, Wynne-Edwards KE (1995) Progesterone, Estradiol, and Prolactin Involvement in Lactation, Including Lactation Following a Postpartum Mating, in the Djungarian Hamster (Phodopus Campbelli). Biol Reprod 52:855–863. https://doi.org/10.1095/biolreprod52.4.855

Salais-López H, Agustín-Pavón C, Lanuza E, Martínez-García F (2018) The maternal hormone in the male brain: Sexually dimorphic distribution of prolactin signalling in the mouse brain. PLoS One 13:1–21. https://doi.org/10.1371/journal.pone.0208960

Salais-López H, Lanuza E, Agustín-Pavón C, Martínez-García F (2017) Tuning the brain for motherhood: prolactin-like central signalling in virgin, pregnant, and lactating female mice. Brain Struct Funct 222:895–921. https://doi.org/10.1007/s00429-016-1254-5

Saltzman W, Maestripieri D (2011) The neuroendocrinology of primate maternal behavior. Prog Neuro-Psychopharmacology Biol Psychiatry 35:1192–1204. https://doi.org/10.1016/j.pnpbp.2010.09.017

Sanchez MA, Dominguez R (1995) Differential effects of unilateral lesions in the medial amygdala on spontaneous and induced ovulation. Brain Res Bull 38:313–317. https://doi.org/10.1016/0361-9230(95)00094-U

Sano K, Tsuda MC, Musatov S, et al (2013) Differential effects of site-specific knockdown of estrogen receptor α in the medial amygdala, medial pre-optic area, and ventromedial nucleus of the hypothalamus on sexual and aggressive behavior of male mice. Eur J Neurosci. https://doi.org/10.1111/ejn.12131

Sasaki K, Suzuki M, Mieda M, et al (2011) Pharmacogenetic modulation of orexin neurons alters sleep/wakefulness states in mice. PLoS One 6:. https://doi.org/10.1371/journal.pone.0020360

Sawchenko PE, Swanson LW (1983) The Organization and Biochemical Specificity of Afferent Projections to the Paraventricular and Supraoptic Nuclei. Prog Brain Res. https://doi.org/10.1016/S0079-6123(08)64371-X

Scalia F, Winans SS (1975) The differential projections of the olfactory bulb and accessory olfactory bulb in mammals. J Comp Neurol 161:31–55. https://doi.org/10.1002/cne.901610105

Schachter BS, Durgerian S, Harlan RE, et al (1984) PROLACTIN mRNA EXISTS IN RAT HYPOTHALAMUS. Endocrinology 114:1947–1949. https://doi.org/10.1210/endo-114-5-1947

Schindelin J, Arganda-Carreras I, Frise E, et al (2012) Fiji: an open-source platform for biological-image analysis. Nat Methods. https://doi.org/10.1038/nmeth.2019

Schmittgen TD, Livak KJ (2008) Analyzing real-time PCR data by the comparative CTmethod. Nat Protoc 3:1101–1108. https://doi.org/10.1038/nprot.2008.73

Shaikh MB, Brutus M, Siegel HE, Siegel A (1986) Regulation of feline aggression by the bed nucleus of stria terminalis. Brain Res Bull. https://doi.org/10.1016/0361-9230(86)90031-6

Shi S-R, Cote RJ, Taylor CR (2011) Antigen Retrieval Techniques. J Histochem Cytochem 49:931–937. https://doi.org/10.1177/002215540104900801

Shilov I V., Seymour SL, Patel AA, et al (2007) The Paragon Algorithm, a Next Generation Search Engine That Uses Sequence Temperature Values and Feature Probabilities to Identify Peptides from Tandem Mass Spectra. Mol Cell Proteomics 6:1638–1655. https://doi.org/10.1074/mcp.T600050-MCP200

Siaud P, Manzoni O, Balmefrezol M, et al (1989) The organization of prolactin-like-immunoreactive neurons in the rat central nervous system - Light- and electron-microscopic immunocytochemical studies. Cell Tissue Res 255:107–115. https://doi.org/10.1007/BF00229071

Simerly RB (2002) Wired for Reproduction: Organization and Development of Sexually Dimorphic Circuits in the Mammalian Forebrain. Annu Rev Neurosci. https://doi.org/10.1146/annurev.neuro.25.112701.142745

Simerly RB (2015) Organization of the Hypothalamus, Fourth Edi. Elsevier Inc.

Simerly RB, Swanson LW (1986) The organization of neural inputs to the medial preoptic nucleus of the rat. J Comp Neurol 246:312–342. https://doi.org/10.1002/cne.902460304

Skofitsch G, Jacobowitz DM (1985) Immunohistochemical mapping of galanin-like neurons in the rat central nervous system. Peptides 6:509–546. https://doi.org/10.1016/0196-9781(85)90118-4

Slattery DA, Neumann ID (2008) No stress please! Mechanisms of stress hyporesponsiveness of the maternal brain. J Physiol 586:377–385. https://doi.org/10.1113/jphysiol.2007.145896

Smith KS, Bucci DJ, Luikart BW, Mahler S V (2016) DREADDS: Use and application in behavioral neuroscience. Behav Neurosci 130:137–55. https://doi.org/10.1037/bne0000135

Soares MJ (2004) The prolactin and growth hormone families: Pregnancy-specific hormones/cytokines at the maternal-fetal interface. Reprod Biol Endocrinol 2:1–15. https://doi.org/10.1186/1477-7827-2-51

Soares MJ, Müller H, Orwig KE, et al (1998) The Uteroplacental Prolactin Family and Pregnancy. Biol Reprod. https://doi.org/10.1095/biolreprod58.2.273

Southard JN, Talamantes F (1991) Placental prolactin-like proteins in rodents: Variations on a structural theme. Mol Cell Endocrinol. https://doi.org/10.1016/0303-7207(91)90084-6

St. John RD, Corning PA (1973) Maternal aggression in mice. Behav Biol 9:635–639. https://doi.org/10.1016/S0091-6773(73)80058-6

Stern JM, Siegel HI (1978) Prolactin Release in Lactating, Primiparous and Multiparous Thelectomized and Maternal Virgin Rats Exposed to Pup Stimuli. Biol Reprod 19:177–182. https://doi.org/10.1095/biolreprod19.1.177

Stoeckel ME, Hindelang C, Klein MJ, et al (1994) Expression of the α-subunit of glycoprotein hormones in the pars tuberalis-specific glandular cells in rat, mouse and guinea-pig. Cell Tissue Res 278:617–624. https://doi.org/10.1007/BF00331382

Stowers L, Holy TE, Meister M, et al (2002) Loss of sex discrimination and male-male aggression in mice deficient for TRP2. Science (80-). https://doi.org/10.1126/science.1069259

Sugiyama T, Minoura H, Kawabe N, et al (1994) Preferential expression of long form prolactin receptor mRNA in the rat brain during the oestrous cycle, pregnancy and lactation: Hormones involved in its gene expression. J Endocrinol 141:325–333. https://doi.org/10.1677/joe.0.1410325

Sun X, Whitefield S, Rusak B, Semba K (2001) Electrophysiological analysis of suprachiasmatic nucleus projections to the ventrolateral preoptic area in the rat. Eur J Neurosci 14:1257–1274. https://doi.org/10.1046/j.0953-816X.2001.0001755.x

Suzuki S, Handa RJ (2005) Estrogen receptor-β, but not estrogen receptor-α, is expressed in prolactin neurons of the female rat paraventricular and supraoptic nuclei: Comparison with other neuropeptides. J Comp Neurol 484:28–42. https://doi.org/10.1002/cne.20457

Svare B, Gandelman R (1976a) A longitudinal analysis of maternal aggression in Rockland-Swiss albino mice. Dev Psychobiol 9:437–446. https://doi.org/10.1002/dev.420090506

Svare B, Gandelman R (1973) Postpartum aggression in mice: Experiential and environmental factors. Horm Behav 4:323–334. https://doi.org/10.1016/0018-506X(73)90032-9

Svare B, Gandelman R (1976b) Postpartum aggression in mice: The influence of suckling stimulation. Horm Behav 7:407–416. https://doi.org/10.1016/0018-506X(76)90012-X

Svare B, Gandelman R (1975) Postpartum aggression in mice: Inhibitory effect of estrogen. Physiol Behav 14:31–35. https://doi.org/10.1016/0031-9384(75)90137-7

Svare B, Mann MA, Broida J, Michael SD (1982) Maternal aggression exhibited by hypophysectomized parturient mice. Horm Behav 16:455–461. https://doi.org/10.1016/0018-506X(82)90052-6

Svare BB (1977) Maternal aggression in mice: Influence of the young. Biobehav Rev 1:151–164. https://doi.org/10.1016/0147-7552(77)90004-3

Swann J, Fabre-Nys C, Barton R (2009) Hormonal and pheromonal modulation of the extended amygdala: implications for social behavior

Swanson L (2004) Brain maps: structure of the rat brain. Gulf Professional Publishing

Swanson L (1987) The hypothalamus. In: Bjorklund A, Hokfelt T, Swanson LW (eds) Handbook of Chemical Neuroanatomy Integrated Systems of the CNS, Part I: Vol. 5: Integrated Systems of the CNS. Amsterdam: Elsevier, pp 1–124

Swanson LW, Cowan WM (1979) The connections of the septal region in the rat. J Comp Neurol 186:621–655. https://doi.org/10.1002/cne.901860408

Swanson LW, Kuypers HGJM (1980) The paraventricular nucleus of the hypothalamus: Cytoarchitectonic subdivisions and organization of projections to the pituitary, dorsal vagal complex, and spinal cord as demonstrated by retrograde fluorescence double-labeling methods. J Comp Neurol 194:555–570. https://doi.org/10.1002/cne.901940306

Swanson LW, Sawchenko PE (1983) Hypothalamic Integration: Organization of the Paraventricular and Supraoptic Nuclei. Annu Rev Neurosci 6:269–324. https://doi.org/10.1146/annurev.ne.06.030183.001413

Takahashi LK, Lisk RD (1985) Estrogen action in anterior and ventromedial hypothalamus and the modulation of heterosexual behavior in female golden hamsters. Physiol Behav. https://doi.org/10.1016/0031-9384(85)90111-8

Tellegen A, Horn JM (1972) Primary aggressive motivation in three inbred strains of mice. J Comp Physiol Psychol 78:297–304. https://doi.org/10.1037/h0032192

Tellegen A, Horn JM, Legrand RG (1969) Opportunity for aggression as a reinforcer in mice. Psychon Sci 14:104–105. https://doi.org/10.3758/BF03332727

Terkel J, Rosenblatt JS (1968) Maternal Behavior Induced By Maternal Blood Plasma Injected Into Virgin Rats. J Comp Physiol Psychol 65:479–482. https://doi.org/10.1016/S0021-9940(07)65740-1

Theodosis DT, Poulain DABT-P in BR (2001) Chapter 3 Maternity leads to morphological synaptic plasticity in the oxytocin system. In: The Maternal Brain. Elsevier, pp 49–58

Thompson ML, Edwards DA (1971) Experiential and strain determinants of the estrogen-progesterone induction of sexual receptivity in spayed female mice. Horm Behav 2:299–305. https://doi.org/https://doi.org/10.1016/0018-506X(71)90004-3

Thompson RH, Swanson LW (1998) Organization of inputs to the dorsomedial nucleus of the hypothalamus: A reexamination with Fluorogold and PHAL in the rat. Brain Res Rev. https://doi.org/10.1016/S0165-0173(98)00010-1

Thompson SA (1982) Localization of immunoreactive prolactin in ependyma and circumventricular organs of rat brain. Cell Tissue Res 225:79–93. https://doi.org/10.1007/BF00216220

Todd RM, Palombo DJ, Levine B, Anderson AK (2011) Genetic differences in emotionally enhanced memory. Neuropsychologia 49:734–744. https://doi.org/10.1016/j.neuropsychologia.2010.11.010

Torner L, Maloumby R, Nava G, et al (2004) In vivo release and gene upregulation of brain prolactin in response to physiological stimuli. Eur J Neurosci 19:1601–1608. https://doi.org/10.1111/j.1460-9568.2004.03264.x

Torner L, Mejía S, López-Gómez FJ, et al (1995) A 14-kilodalton prolactin-like fragment is secreted by the hypothalamo-neurohypophyseal system of the rat. Endocrinology 136:5454–5460

Torner L, Nava G, Dueñas Z, et al (1999) Changes in the expression of neurohypophyseal prolactins during the estrous cycle and after estrogen treatment. J Endocrinol 161:423–432. https://doi.org/10.1677/joe.0.1610423

Torner L, Neumann ID (2002) The brain prolactin system: Involvement in stress response adaptations in lactation. Stress 5:249–257. https://doi.org/10.1080/1025389021000048638

Torner L, Toschi N, Nava G, et al (2002) Increased hypothalamic expression of prolactin in lactation:

Involvement in behavioural and neuroendocrine stress responses. Eur J Neurosci 15:1381–1389. https://doi.org/10.1046/j.1460-9568.2002.01965.x

Toubeau G, Desclin J, Parmentier M, Pasteels JL (1979a) Compared localizations of prolactin-like and adrenocorticotropin immunoreactivities within the brain of the rat. Neuroendocrinology 29:374–384. https://doi.org/10.1159/000122948

Toubeau G, Desclin J, Parmentier M, Pasteels JL (1979b) Cellular localization of a prolactin-like antigen in the rat brain. J Endocrinol 83:261–266

Trapnell C, Pachter L, Salzberg SL (2009) TopHat: Discovering splice junctions with RNA-Seq. Bioinformatics 25:1105–1111. https://doi.org/10.1093/bioinformatics/btp120

Tremblay JJ, Lanctot C, Drouin J (1998) The pan-pituitary activator of transcription, Ptx1 (pituitary homeobox 1), acts in synergy with SF-1 and Pit1 and is an upstream regulator of the Lim-homeodomain gene Lim3/Lhx3. Mol Endocrinol 12:428–441. https://doi.org/10.1210/mend.12.3.0073

Tsuneoka Y, Maruyama T, Yoshida S, et al (2013) Functional, anatomical, and neurochemical differentiation of medial preoptic area subregions in relation to maternal behavior in the mouse. J Comp Neurol 521:1633–1663. https://doi.org/10.1002/cne.23251

Unger EK, Burke KJJ, Yang CF, et al (2015) Medial amygdalar aromatase neurons regulate aggression in both sexes. Cell Rep 10:453–462. https://doi.org/10.1016/j.celrep.2014.12.040

Untergasser A, Nijveen H, Rao X, et al (2007) Primer3Plus, an enhanced web interface to Primer3. Nucleic Acids Res. https://doi.org/10.1093/nar/gkm306

Urban DJ, Roth BL (2014) DREADDs (Designer Receptors Exclusively Activated by Designer Drugs): Chemogenetic Tools with Therapeutic Utility. Annu Rev Pharmacol Toxicol 55:399–417. https://doi.org/10.1146/annurev-pharmtox-010814-124803

Vaiserman A (2015) Epidemiologic evidence for association between adverse environmental exposures in early life and epigenetic variation: a potential link to disease susceptibility? Clin. Epigenetics

Van Berg MJ Den, Horst GJ Ter, Koolhaas JM (1983) The nucleus premammillaris ventralis (PMV) and aggressive behavior in the rat. Aggress Behav 9:41–47. https://doi.org/10.1002/1098-2337(1983)9:1<41::AID-AB2480090106>3.0.CO;2-9

Vandenbergh JG (1973) Effects of central and peripheral anosmia on reproduction of female mice. Physiol Behav 10:257–261. https://doi.org/10.1016/0031-9384(73)90307-7

Vega C, Moreno-Carranza B, Zamorano M, et al (2010) Prolactin promotes oxytocin and vasopressin release by activating neuronal nitric oxide synthase in the supraoptic and paraventricular nuclei. Am J Physiol Integr Comp Physiol 299:R1701–R1708. https://doi.org/10.1152/ajpregu.00575.2010

Vertes RP, Linley SB, Hoover WB (2015) Limbic circuitry of the midline thalamus. Neurosci Biobehav Rev 54:89–107. https://doi.org/https://doi.org/10.1016/j.neubiorev.2015.01.014

Voss JW, Rosenfeld MG (1992) Anterior pituitary development: Short tales from dwarf mice. Cell 70:527–530. https://doi.org/https://doi.org/10.1016/0092-8674(92)90422-9

Walsh RJ, Slaby FJ, Posner BI (1987) A receptor-mediated mechanism for the transport of prolactin from blood to cerebrospinal fluid. Endocrinology. https://doi.org/10.1210/endo-120-5-1846

Wang D, He X, Zhao Z, et al (2015) Whole-brain mapping of the direct inputs and axonal projections of POMC and AgRP neurons. Front Neuroanat 9:1–17. https://doi.org/10.3389/fnana.2015.00040

Wang Y, He Z, Zhao C, Li L (2013) Medial amygdala lesions modify aggressive behavior and immediate early gene expression in oxytocin and vasopressin neurons during intermale exposure. Behav Brain Res 245:42–49. https://doi.org/10.1016/j.bbr.2013.02.002

Wang Z, Storm DR (2011) Maternal behavior is impaired in female mice lacking type 3 adenylyl cyclase. Neuropsychopharmacology 36:772–781. https://doi.org/10.1038/npp.2010.211

Wansaw MP, Pereira M, Morrell JI (2008) Characterization of maternal motivation in the lactating rat: Contrasts between early and late postpartum responses. Horm Behav 54:294–301.

https://doi.org/10.1016/j.yhbeh.2008.03.005

Warde-Farley D, Donaldson SL, Comes O, et al (2010) The GeneMANIA prediction server: Biological network integration for gene prioritization and predicting gene function. Nucleic Acids Res 38:214–220. https://doi.org/10.1093/nar/gkq537

Wardlaw SL, Frantz AG (1983) Brain β-endorphin during Pregnancy, Parturition, and the Postpartum Period. Endocrinology 113:1664–1668. https://doi.org/https://doi.org/10.1210/endo-113-5-1664

Watson C, Qi Y (2012) Neurosecretory Nuclei of the Hypothalamus and Preoptic Area. Mouse Nerv Syst 520–527. https://doi.org/10.1016/B978-0-12-369497-3.10018-4

Watts AG, Swanson LW (1987) Efferent projections of the suprachiasmatic nucleus: II. Studies using retrograde transport of fluorescent dyes and simultaneous peptide immunohistochemistry in the rat. J Comp Neurol 258:230–252. https://doi.org/10.1002/cne.902580205

Weaver ICG, Cervoni N, Champagne FA, et al (2004) Epigenetic programming by maternal behavior. Nat Neurosci 7:847–854. https://doi.org/10.1038/nn1276

Weber EM, Olsson IAS (2008) Maternal behaviour in Mus musculus sp.: An ethological review. Appl Anim Behav Sci 114:1–22. https://doi.org/10.1016/j.applanim.2008.06.006

Weisenberg RC, Borisy GG, Taylor EW (1968) The Colchicine-Binding Protein of Mammalian Brain and Its Relation to Microtubules. Biochemistry 7:4466–4479. https://doi.org/10.1021/bi00852a043

Weiss J, Pyrski M, Jacobi E, et al (2011) Loss-of-function mutations in sodium channel Na v 1.7 cause anosmia. Nature 472:186–192. https://doi.org/10.1038/nature09975

Wen S, Götze IN, Mai O, et al (2011) Genetic identification of GnRH receptor neurons: A new model for studying neural circuits underlying reproductive physiology in the mouse brain. Endocrinology 152:1515–1526. https://doi.org/10.1210/en.2010-1208

Wiegand SJ, Price JL (1980) Cells of origin of the afferent fibers to the median eminence in the rat. J Comp Neurol 192:1–19. https://doi.org/10.1002/cne.901920102

Wilson DM 3rd, Emanuele N V, Jurgens JK, Kelley MR (1992) Prolactin message in brain and pituitary of adult male rats is identical: PCR cloning and sequencing of hypothalamic prolactin cDNA from intact and hypophysectomized adult male rats. Endocrinology 131:2488–2490. https://doi.org/10.1210/endo.131.5.1339346

Wolff JO (1985) Maternal aggression as a deterrent to infanticide in Peromyscus leucopus and P. maniculatus. Anim Behav. https://doi.org/10.1016/S0003-3472(85)80125-1

Wolff JO (1993) Why Are Female Small Mammals Territorial? Oikos 68:364–370. https://doi.org/10.2307/3544853

Wolff PR, Powell AJ (1984) Urine patterns in mice: An analysis of male/female counter-marking. Anim Behav 32:1185–1191. https://doi.org/10.1016/S0003-3472(84)80235-3

Wong LC, Wang L, D'Amour JA, et al (2016) Effective Modulation of Male Aggression through Lateral Septum to Medial Hypothalamus Projection. Curr Biol 26:593–604. https://doi.org/10.1016/j.cub.2015.12.065

Woodruff TK, Besecke LM, Groome N, et al (1996) Inhibin A and inhibin B are inversely correlated to follicle-stimulating hormone, yet are discordant during the follicular phase of the rat estrous cycle, and inhibin A is expressed in a sexually dimorphic manner. Endocrinology 137:5463–5467. https://doi.org/10.1210/endo.137.12.8940372

Woodson J, Niemeyer A, Bergan J (2017) Untangling the Neural Circuits for Sexual Behavior. Neuron 95:1–2. https://doi.org/10.1016/j.neuron.2017.06.035

Woolen GF, Kopin IJ, Axelrod J (1975) Effects of Colchicine and Vinblastine on Axonal Transport and Transmitter Release in Sympathetic Nerves. Ann N Y Acad Sci 253:528–534. https://doi.org/10.1111/j.1749-6632.1975.tb19226.x

Wu Z, Autry AE, Bergan JF, et al (2014) Galanin neurons in the medial preoptic area govern parental

behaviour. Nature 509:325–330. https://doi.org/10.1038/nature13307

Wyatt TD (2010) Pheromones and signature mixtures: Defining species-wide signals and variable cues for identity in both invertebrates and vertebrates. J Comp Physiol A Neuroethol Sensory, Neural, Behav Physiol 196:685–700. https://doi.org/10.1007/s00359-010-0564-y

Wyatt TD (2003a) Animals in a chemical world. In: Pheromones and animal behaviour: communication by smell and taste. Cambridge University Press, pp 1–22

Wyatt TD (2003b) Pheromones and animal behaviour: communication by smell and taste. Cambridge university press

Xu F, Schaefer M, Kida I, et al (2005) Simultaneous activation of mouse main and accessory olfactory bulbs by odors or pheromones. J Comp Neurol. https://doi.org/10.1002/cne.20652

Yamaguchi M, Ogren L, Endo H, et al (1992) Production of mouse placental lactogen-I and placental lactogen-II by the same giant cell. Endocrinology. https://doi.org/10.1210/endo.131.4.1396305

Yamamoto R, Ahmed N, Ito T, et al (2018) Optogenetic study of anterior bnst and basomedial amygdala projections to the ventromedial hypothalamus. eNeuro 5:1–12. https://doi.org/10.1523/ENEURO.0204-18.2018

Yip SH, Eguchi R, Grattan DR, Bunn SJ (2012) Prolactin Signalling in the Mouse Hypothalamus is Primarily Mediated by Signal Transducer and Activator of Transcription Factor 5b but not 5a. J Neuroendocrinol. https://doi.org/10.1111/j.1365-2826.2012.02357.x

Zarrow MX, Gandelman R, Denenberg VH (1971) Lack of nest building and maternal behavior in the mouse following olfactory bulb removal. Horm Behav. https://doi.org/10.1016/0018-506X(71)90020-1

Zhan C, Zhou J, Feng Q, et al (2013) Acute and Long-Term Suppression of Feeding Behavior by POMC Neurons in the Brainstem and Hypothalamus, Respectively. J Neurosci. https://doi.org/10.1523/jneurosci.2742-12.2013

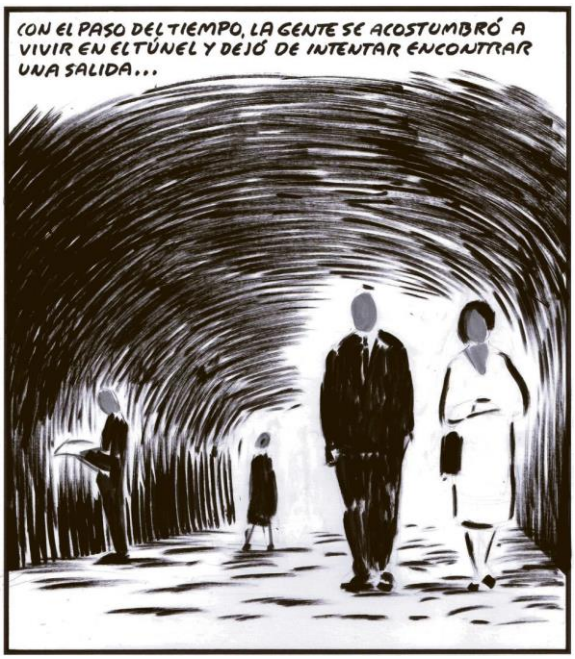
CON EL PASO DEL TIEMPO, LA GENTE SE ACOSTUMBRÓ A VIVIR EN EL TÚNEL Y DEJÓ DE INTENTAR ENCONTRAR UNA SALIDA...

El Roto